OIL FAMILIES AND THEIR INFERRED SOURCE ROCKS FROM THE NIGER DELTA BASIN

Onoriode ESEGBUE

B.Sc. Geology
M.Sc. Petroleum Geochemistry
M.Sc. Petroleum Geology and Sedimentology

A thesis submitted to the Newcastle University in partial fulfilment of the requirements for the award of the degree of Doctor of Philosophy in Petroleum Geochemistry in the Faculty of Science, Agriculture and Engineering

School of Civil Engineering and Geosciences, Newcastle University
Newcastle upon Tyne, NE1 7RU
United Kingdom.

January 2016.

DECLARATION

I hereby certify that this work is my own, except where otherwise acknowledged and that this work has not been submitted previously for a degree at this, or any other university.

…….

Onoriode ESEGBUE

ABSTRACT

The Niger Delta Basin is one of the world's most prolific hydrocarbon provinces, yet the origin of the vast amounts of oil and gas found in numerous sub-basins across the Delta remains contested. Two principal mixed Type II/III kerogen source rocks, from the Miocene and Eocene, respectively, are often reported to be the origins of the Tertiary reservoired oils of the Delta, although contributions from a deeper Cretaceous source have also been suggested but not proven to date. The current poor understanding of the petroleum systems of the Niger Delta is mainly as a result of non-availability of mature source rock samples and variability in fluid types (oil/gas/condensates) from the various sub-basins in the delta, even from those in close proximity to each other.

A total of 50 source rock samples from 6 exploration wells across different parts of the basin were subjected to geochemical analyses, including TOC and Rock Eval screening analyses, and 180 oil samples from more than 40 oil fields in the Niger Delta were analysed for their saturated, and aromatic hydrocarbons, resins and asphaltene (SARA) contents. Gas chromatography (GC), GC-mass spectrometry (GC-MS) and GC isotope-ratio mass spectrometry (GC-IRMS) was carried out on selected samples. Unravelling the history of the potentially mixed oils from the Delta was undertaken using several geochemical approaches on the different components/molecular weight ranges of each hydrocarbon fraction.

The interpreted thermal maturity and source depositional environments of those hydrocarbons show significant variations depending on the components analysed, and allows no clear correlation to a single source rock but rather implies extensive mixed contributions. These observations give rise to questions on whether the Niger Delta hydrocarbons were mainly sourced from an early/marginally mature source as indicated by hopane and sterane biomarkers, or a peak mature source as indicated by aromatic steroids, or even from the thermal cracking of either earlier generated hydrocarbons or kerogen cracking within deep seated source rocks. The studied source rock samples were of relatively low thermal maturity, with mainly Type III kerogens with some Type II influence, deposited in deltaic/marine environments.

Diamondoid hydrocarbon parameters were used for the first time on these Tertiary reservoir hosted oils to investigate source, thermal maturity and mixing effects and to allow cross-correlations of these oils. The diamondoid abundances and distributions support the hypothesis of co-sourcing of oil from a thermally cracked, sub-delta, Type II marine source which was then mixed with oils of relatively lower maturities in the Tertiary reservoirs. Statistical principal component analyses (PCA) of diamondoid correlation parameters indicate that the

suspected highly mature, deep sourced oils are from the same genetic family and not related to the studied source rocks. Furthermore, PCA of gasoline range and aromatic hydrocarbon indicate mixed sources, with the central Niger Delta region showing more contributions from terrigenous sources, while the other regions have more marine contributions. Compound specific carbon and hydrogen stable isotope analyses of *n*-alkanes of molecular weight greater than $nC_{21,}$ show some correlation between the source rocks and the oil samples, but these correlations cannot be established in the lighter hydrocarbons. However, potential source rock cuttings samples from wells BA-1, BA-SW and EA show good correlations with the produced oil samples based on the hopane and sterane biomarker distributions, however the studied source rocks are thermally immature.

Two broad oil families can be identified amongst the samples analysed in this study:

- Family A comprises highly cracked oil from a Type II marine shale and based on geochemical results, this oil contributes up to about 90% of the oil accumulations in some fields.
- Family B is a Type II/III marine shale sourced oil from the Akata Formation which has contributed a lower percentage to the accumulations than the Family A oils,

The Central delta oils are mostly biodegraded whereas the Southern delta oils are least biodegraded and there exists an interplay of multiple charge episodes, complex reservoir architecture and several other controls, such as maturity and fill-spill episodes on the current biodegradation levels of oils in the basin. The relative abundance of an unknown C_{29} triterpane and a parameter based on unidentified seco-oleananes (seen in *m/z* 193 mass chromatograms) can be useful indicators of biodegradation level in highly biodegraded oil samples. Multiple sourcing of oil samples from the basin makes migration distance studies uncertain using the parameters measured, but it appears likely that the Western and Eastern Delta oils have migrated over relatively longer distances than the Southern Delta oils.

Biomarker contamination during migration appears to be an important process in this complex geological setting and as such geochemical interpretation would potentially yield erroneous interpretations based on any such standalone routine analyses. Future geochemical interpretations should treat the Niger Delta oils as potentially mixtures of oils of variable maturities from different sources, often with the most important source biomarkers depleted because of the extent of thermal cracking.

ACKNOWLEDGMENTS

I am grateful to God for seeing me through my studies hitch free and for preserving my life all through these years. More than just a routine tradition, I will like to say thank you to my Supervisor, Dr David M. Jones for his effort towards securing samples for this research work and valued input which has made this research a success. Drs. Sadat Kolonic and Pim van Bergen are highly acknowledged for the role they played during samples acquisition from shell and the constant correspondence that has made the project come out more refined, working with them over the years has made me a better geochemist.

I will also like to say thank you to the Petroleum Geochemistry academic team; Dr Geoff Abbott, Prof. Tom Wagner, Dr Helen Talbot, Dr Martin Cook for all their help throughout the years of my studies and not forgetting Dr Neil Gray for all his input and useful discussion on statistics. Unreserved acknowledgment goes to Berni Bowler, Paul Donohoe and Philip Green for all the thought provoking discussions and analytical assistance rendered during this research and also Mrs Yvonne Hall for always having a way of making complex organisation look very simple for both staff and students in Geosciences. My utmost gratitude goes to PTDF for funding my MSc and PhD studies in the UK; I would not have been able to do this without sponsorship.

I am also indebted to my Mum and siblings for their constant prayers and always looking out for me while trying to stay in touch. I will not forget the numerous families which have helped through the time of my studies – my inlaws: the Muoboghares, the Osevwes, the Usehs, the Ohimors, the Agbidis, the Okonyes, the Ighodaros, the Eshiets, the Davis and Pastor Sam and the Member of Glory Chapel and also Pastor Clive and Sally and the members of Andrew Bowie's Cell group of International Harvest Church Newcastle. A big thank you also to the other PTDF scholars in Newcastle University for always displaying oneness and continued support.

My unreserved appreciation goes to my lovely wife Akpevwe for all her prayers, support and all the time spent lonely while I am away in school trying to put this research work together and also to my children for all the times daddy was not around because he had to pursue his academic aspiration.

DEDICATION

I dedicate this thesis to the memory of my dad and sister - late Mr Napoleon Esegbue and late Ms Josephine Esegbue, for their love and guidance towards me while they were alive.

''The logical answer might not always be right one but a show of our limited knowledge''.

Onos 2015

TABLE OF CONTENTS

LIST OF TABLES

LIST OF FIGURES

CHAPTER ONE

INTRODUCTION

1.0 General introduction

The world energy demand is increasing continually and Africa has been a player in meeting this demand, with countries including Nigeria, Algeria, Angola, Libya and Egypt steadily increasing their average daily output yearly, and the continent is currently ranked as the third largest exporter of oil after the Middle East and South America, with the Niger Delta as the most important petroliferous basin in Africa (Li *et al.*, 2007). Investment in exploration and production of hydrocarbon in Africa has been massive especially in offshore basins and predictions show that investment in the West Africa sub region will exceed those of the Gulf of Mexico and the North Sea in the near future (Wang, 2007).

The Niger Delta Basin is located in the Southern part of Nigeria between latitudes 4° 00"N to 6° 00"N and longitudes 3° 00"N to 9° 00"N (Figure 1.1), and occupies an area of about 300,000 km^2 with a sediment thickness of about 2 km at the flank of the basin (Tuttle *et al*., 1999) and 12 km at the basin centre (Kaplan *et al*., 1994; Kulke, 1995). The basin has six depobelts that are structurally controlled by regional growth faults, and it holds approximately 2.3% of the world oil and gas reserves (79.5 billion barrel of oil and 127.2 trillion cubic feet of gas), which makes it the twelfth largest oil province in the world (Tuttle *et al.*, 1999; Sonibare *et al*., 2008; Liu *et al*., 2008). However, despite more than 55 years of oil production in the Niger Delta (Figure 1.2), there are still many controversies in defining the petroleum system (Samuel *et al*., 2009) and especially in the source rock/rocks that generated these huge oil reserves in the basin (Lambert & Ibe, 1984; Ekweozor & Daukoru, 1984; Ejedavwe *et al*., 1984; Haack *et al*., 2000).

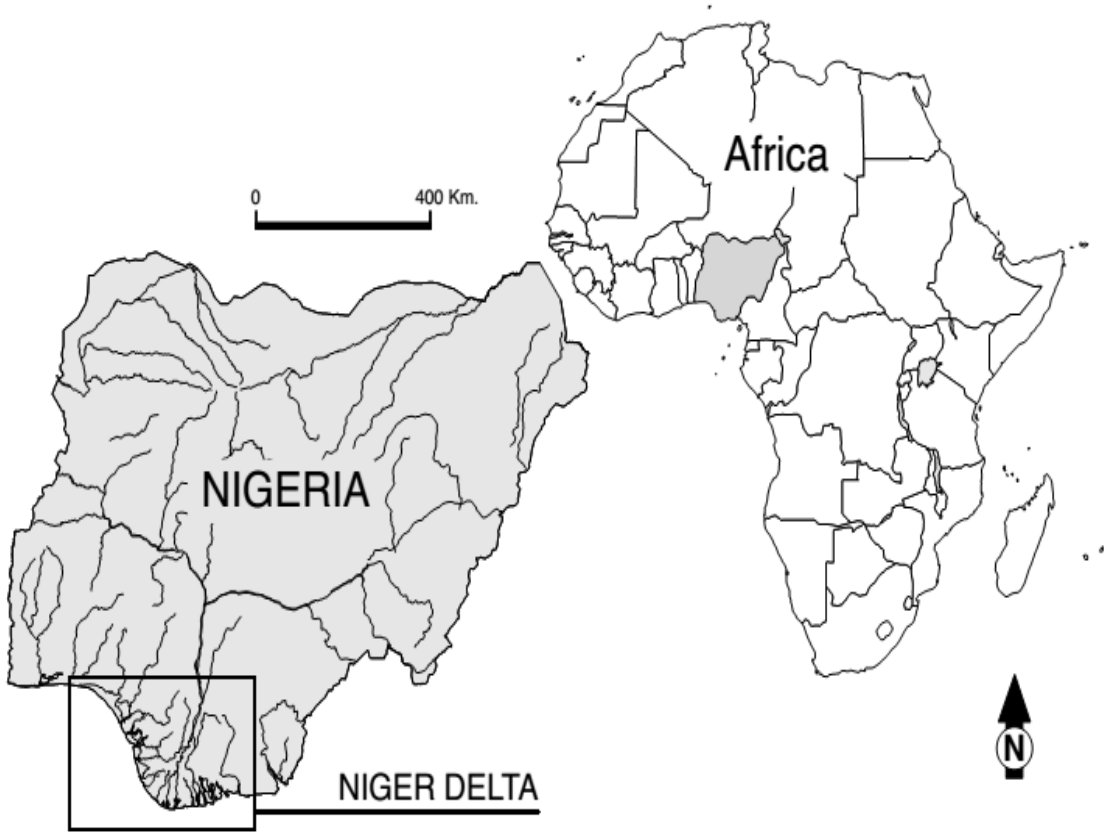

Figure 1.1: Map of Nigeria showing the location of Niger Delta (Haack *et al*., 2000).

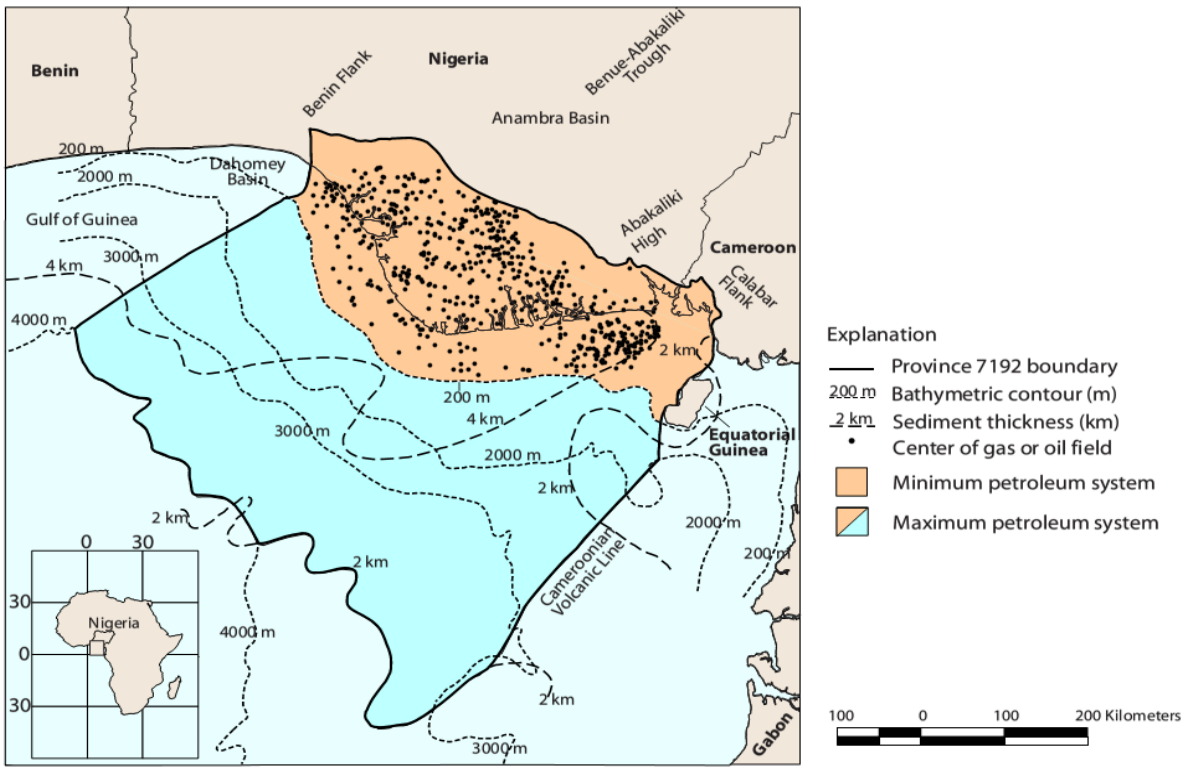

Figure 1.2: Map of Niger Delta showing several oil/gas fields and possible maximum petroleum systems in deep offshore (bathymetry 4 km) with 2 km sediment thickness (Tuttle *et al*., 1999).

Hydrocarbon exploration in the basin started at around 1937 and today about 5,000 wells have been drilled in the various oil fields (Reijers *et al*., 2011) but exploration in the basin is shifting offshore as most operators tend to avoid drilling deeper because of over-pressure as a result of the under-compacted sediments of the Akata Formation. Offshore exploration around the world has shown that active petroleum systems often occur in major deltas that build on passive margins (Morgan, 2003; Samuel *et al*., 2009). The shift into offshore exploration in the Niger Delta in the last two decades has witnessed the discovery of and production from several giant offshore fields which include Agbami, Bonga, Akpo, Erha, Akparo etc., (Bilotti & Shaw, 2005; Samuel *et al*., 2008; Reijers, 2011). Despite increasing focus on the offshore part of the basin, there has been little understanding of the petroleum system and especially of the source of the vast amount of hydrocarbons (Lambert & Ibe, 1984; Ekweozor & Daukoru, 1984; Ejedavwe *et al*., 1984; Haack *et al*., 2000; Fadahunsi *et al*., 2004).

1.1 Niger Delta Basin tectonic history

Rifting along the West African margin started in the Late Jurassic and did not stop until the Middle Cretaceous (Lehner & De Ruiter, 1977). This rifting lead to the formation of the Niger Delta Basin from the breakup of South American plate from the African plate (Whiteman, 1982), which was mainly controlled by the failed arm of a rift triple junction (RRF) that formed the Benue Trough (Tuttle *et al*., 1999) and this event was associated with the South Atlantic sea opening (Figure 1.3). This tectonic framework along the West African Margin was responsible for the formation of several fracture zones that form notable trenches and ridges in the Atlantic Ocean (Tuttle *et al*., 1999).

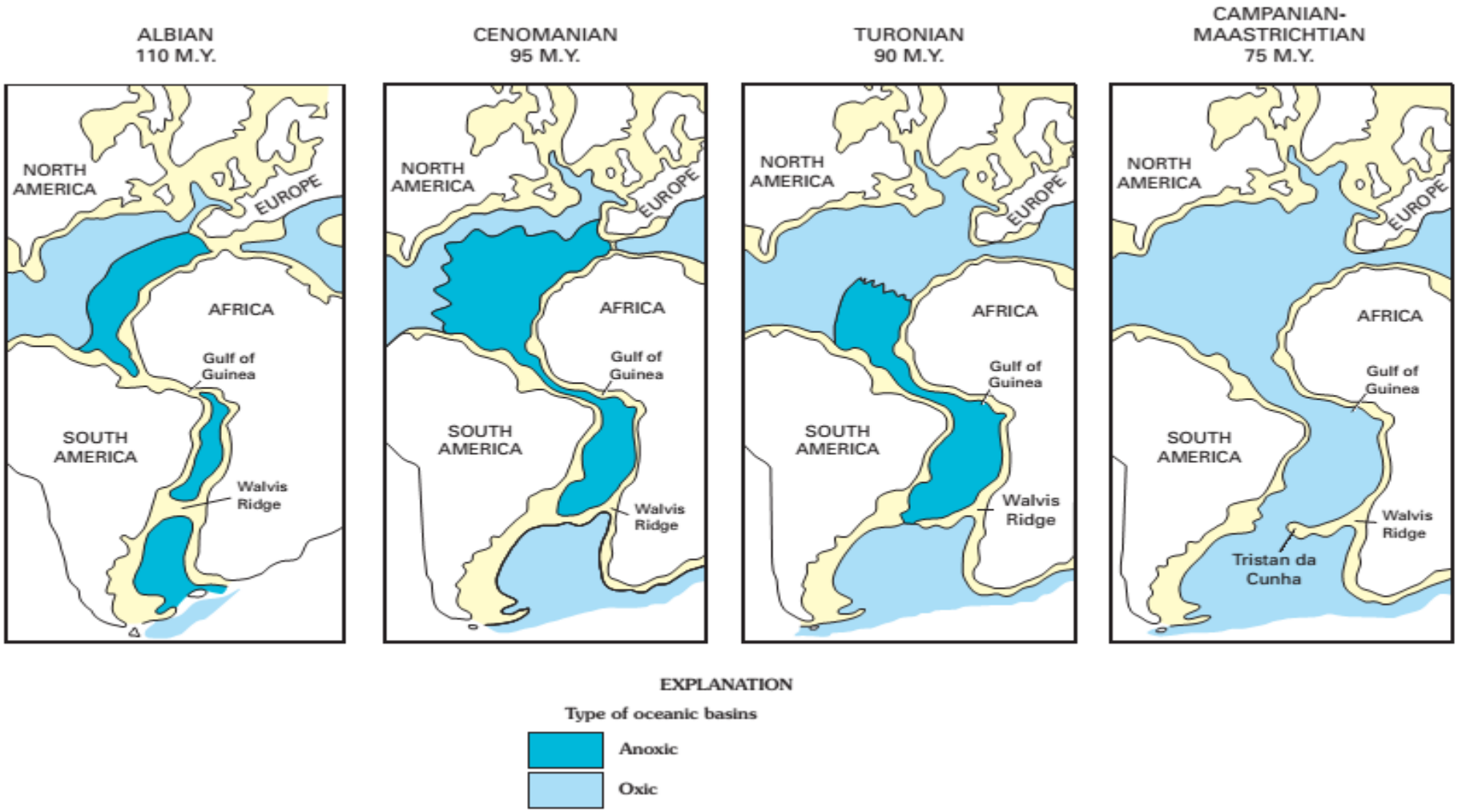

Figure 1.3: Paleogeographic map of the Africa and South America breakup showing relative oxygenation of the basins during the Cretaceous (Brownfield & Charpentier, 2006).

The formation of shale diapirs occurred as a result of excessive overburden weight of the Agbada Formation on the over-pressured and under-compacted Akata Formation and clays on the delta slope with continual progradation, thus the delta slope became unstable due to the mobile Akata Formation not finding suitable support basin-ward (Tuttle *et al*., 1999). The complex gravity tectonics in this basin came to an end with the deposition of the Benin Formation on depobelts in the delta and this was marked with the formation of shale diapirs, growth faults, rollover anticlines, antithetic faults, etc. (Evamy *et al*., 1978; Tuttle *et al*., 1999).

1.2 Stratigraphy and depositional sequence

Three major stratigraphic units are present in the Niger Delta and these are the Akata , Agbada and Benin Formations (Tuttle *et al*., 1999; Haack et al., 2000), although there is a strong indication of a Cretaceous shale that lies unconformable on the basement complex (Figure 1.4), however, the distribution is generally unknown (Tuttle *et al*., 1999). However, recently Geoexpro was able to show that a regional Cretaceous shale exists on the basement complex with thicknesses of about 2 km in the offshore part of the basin (Figure 1.5), based on 18secs two way travel time (TWT) seismic measurements (Bellingham *et al*., 2014). The Cretaceous shales have so far not been drilled in the Niger Delta region mostly because they are beneath the over pressured formation and the thick overburden pile above them (Reijers, 2011).

The lateral equivalent of these Cretaceous shales and Akata Formation in the adjacent Anambra Basin (located at the northeast of the Niger Delta) were deposited in the Albian to Palaeocene when the shoreline was concave (Hospers, 1965) which resulted in tidal dominated and river dominated sedimentation during transgression and regression (Reijers, 2011). These Cretaceous shale equivalents in the Anambra basin include; Asu River shales

(Albian-Cenomanian); Eze-Uku/ Awgu shales (Cenomanian to Santonian); Nkporo shales (Campanian-Maastrichtian) etc., (Nwanchukwu, 1972; Reijers *et al*., 2011).

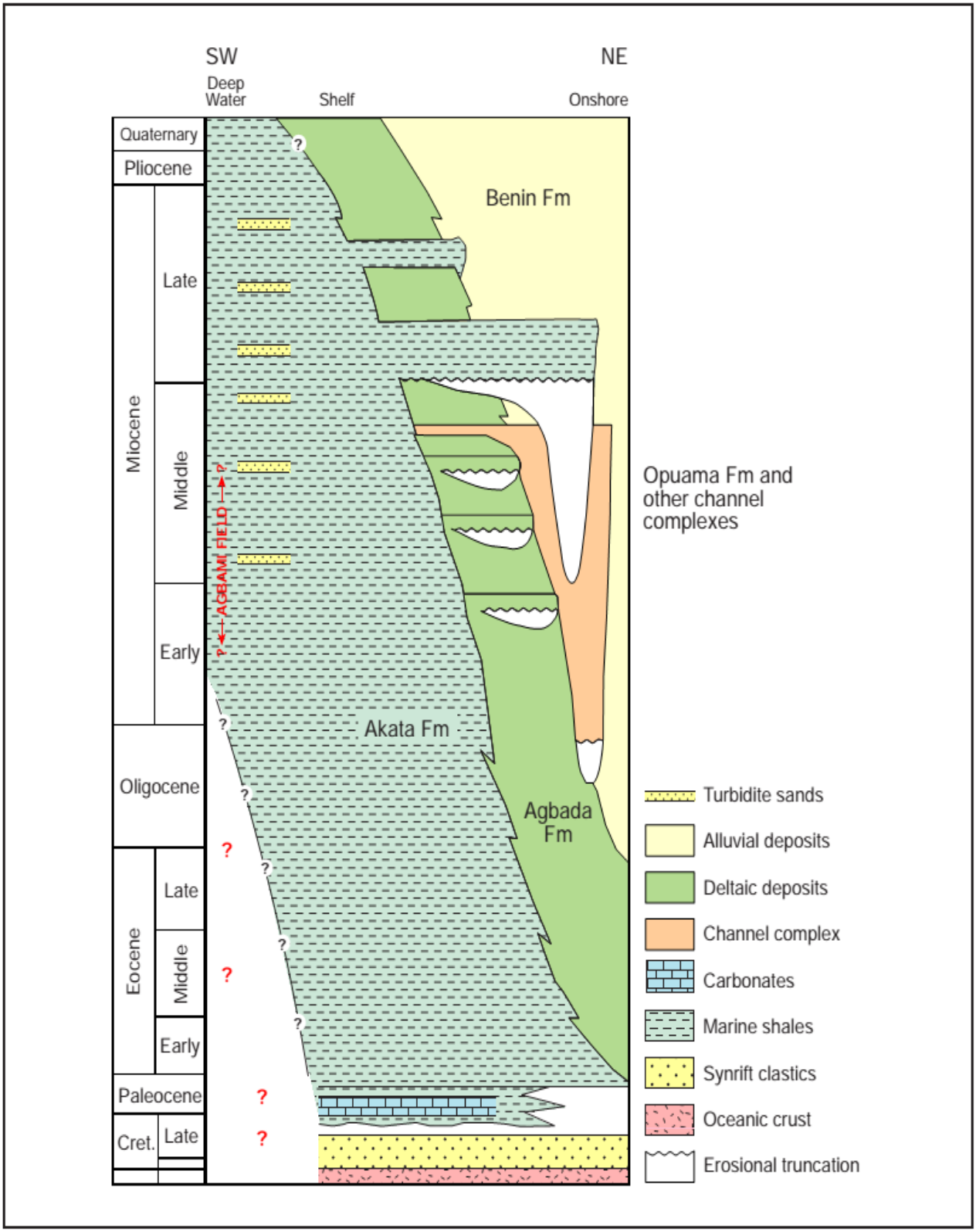

Figure 1.4: Regional stratigraphy of the Niger Delta Basin showing the three major stratigraphic units present in the delta (Akata, Agbada and Benin Formations). Note the possible occurrence of an unknown Cretaceous formation (Corredor *et al*., 2005).

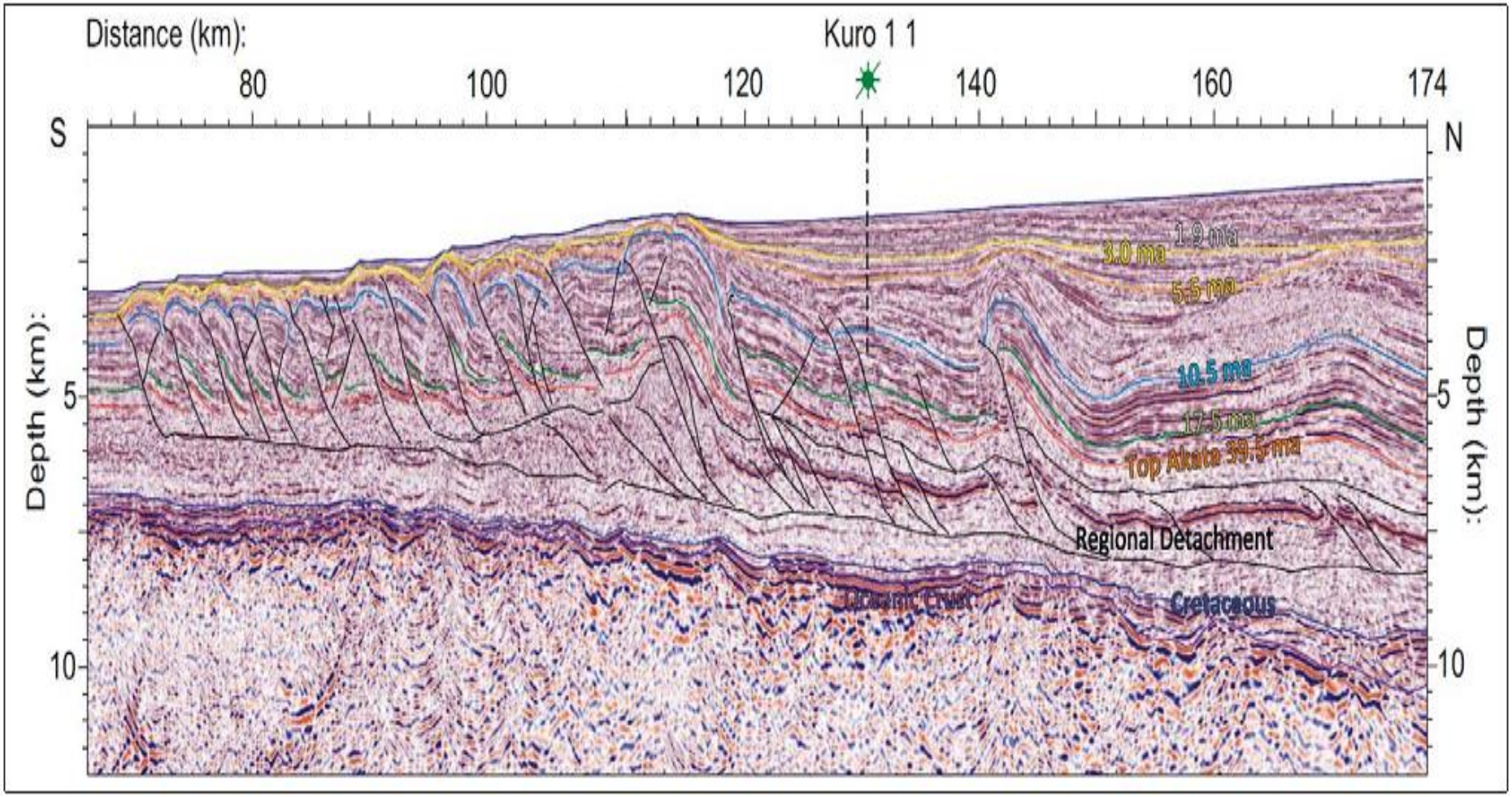

Figure 1.5: Regional 2D seismic section offshore (outer fold and thrust belt) Niger Delta showing the Cretaceous and severe brittle deformation through the Akata Formation (Bellingham *et al*., 2014).

The Imo shale formation was deposited in the Anambra Basin during a major transgression in the Palaeocene period and this marked the onset of the deposition of the under-compacted and over-pressured Akata Formation in the Niger Delta (Short & Stauble, 1967; Tuttle *et al*., 1999; Reijers *et al*., 2011). Sedimentation in the Niger Delta switched to wave dominated from the Eocene because of the change in the coastline shape and this marked the onset of progradation of the paralic delta which resulted in the delta shape becoming more convex towards the sea (Burke, 1972; Tuttle *et al*., 1999). The diachronous Akata Formation is composed of thick marine shale across the delta with some turbidite in the deep offshore and with the possibility of localised occurrences of clay and silt (Avbovbo, 1978; Doust & Omatsola, 1990; Tuttle *et al*., 1999). This formation was believed to have been developed during a lowstand characterised by low oxygen supply and reduced energy conditions (Stacher, 1995). The over-pressured and under-compacted nature of this formation makes it difficult to drill, but its thickness has been estimated at about 7 km in the basin centre and this thins towards the deep offshore (Doust & Omatsola, 1990).

The overlying paralic Agbada Formation was deposited during the Eocene, but continued until Recent because of the diachronous nature of the basin (Short & Stauble, 1967; Tuttle *et al*., 1999), with thickness up to 3.7 km in some areas, this formation is typically characterised by fluvio-deltaic depositional signatures (Tuttle *et al*., 1999). The sandstone to shale bed ratio of the Agbada Formation decreases with increase in age i.e. the lower potion is made up of about 50/50 percentage whereas the younger sequences are mostly sandstones with very little intercalations of shale (Short & Stauble, 1967).

The Benin Formation which is the youngest formation in the delta was deposited from the Eocene to Recent times and thicknesses generally average about 2 km (Avbovbo, 1986). The Benin Formation sediments were deposited in a largely continental environment with a lot of braided and meandering river systems channelling through the delta (Obaje, 2009).

1.3 Source Rocks

Various possible scenarios exist when trying to constrain the source rocks of the Niger Delta Basin, with possibilities ranging from proven to speculative. The major problem in constraining the main source rocks of the basin is that the major encountered formation during drilling (Agbada Formation), although thick, has generally very low TOC and HI values and therefore has a low possibility of having been the major or only source of the world class oil reserves in the basin. Several authors have written about the source rocks in the basin (e.g. Short & Stauble, 1967; Evamy *et al*., 1978; Ekweozor *et al*., 1979; Ekweozor & Okoye, 1980; Bustin 1984; Doust & Omatsola, 1990; Ekweozor & Daukore, 1994; Haack *et al*., 2000; Eneogwe & Ekundayo, 2003; Akinlau *et al*., 2006; Samuel *et al*., 2009; Lehne & Dieckmann, 2010) with most of them having variable levels of uncertainty about them because the Tertiary reservoired oils correlate poorly with the Tertiary source rocks encountered during drilling in the basin (Samuel *et al*., 2009).

The various possible sources of the Niger Delta hydrocarbons as pointed out by most authors include one or a combination of: a) Marine shales of the Agbada Formation, b) Marine shales of the Akata Formation, c) Inferred Cretaceous marine shale (Sub-delta)? d) Inferred Lower Cretaceous lacustrine formation (Sub-delta)?

The transgressive shales in the paralic Agbada Formation have some intervals with high generative potential (Ekweozor & Okoye, 1980; Nwachukwu & Chukura, 1986). However, these shales are too immature in most parts of the formation to generate hydrocarbons and their thicknesses are low (Evamy *et al*., 1978; Ekweozor & Okoye, 1980; Stacher, 1995), although a thermal maturity model by Lambert & Ibe (1984) indicated that some of the source rocks of the Agbada Formation are thermally mature enough to have generated the oil and gas in the basin. Bustin (1988) showed that their TOC contents increase with age (0.9 to 2.2 wt%) and concluded that the shales of the paralic Agbada formation are of low potential, but the poor generative potential of these shales might have been compensated

for by their huge volume and excellent migration pathways as a result of the complex structuration in the basin.

The geochemical results reported vary, with several authors giving a wide range of results for the, mostly immature, samples studied. For example, TOC values reported include 0.9 to 2.2 wt% (Bustin, 1988); 2.3 to 2.5 wt% from two wells (Udo & Ekweozor, 1988); 0.4 to 14.4 wt% in onshore and offshore (Ekweozor & Okoye, 1980); up to 5.2 wt% in the western part of the basin (Nwachukwu & Chukura, 1986); 0.21 to 4.22 wt% (Akinlau & Torto, 2011). However, Doust & Omatsola (1990) pointed out that the beds with high TOC contents were always very thin and usually insignificant based on their studies on core samples from different wells in the basin. HI values are also highly variable e.g. 50 to 160 HC/g rock, with an average value of 90 mgHC/g rock (Bustin, 1988); an average of 232 mgHC/g rock (Udo *et al*., 1988); 38 to 239 mgHC/g rock (Akinlau & Torto, 2011), which shows that they have potential to generate gas and some oil (Baskin, 1997).

The marine shale of the Akata Formation is deeply buried in the central part of the delta and should be in the thermal maturity oil window (Stacher *et al*., 1995) and has thickness that makes it a possible contender for the source of the Tertiary reservoired oil in the delta (Stacher *et al*., 1995; Tuttle *et al*., 1999) with TOC of between 2 – 8 wt% in Pologbere and Awa-zombe wells (Erdem 2015. Personal communication). However, Lambert & Ibe (1984) believed that the over-pressure and under-compacted nature of this formation would reduce the migration efficiency to around 12%, thereby reducing the overall expulsion of generated hydrocarbon from this formation to a minimum (Lambert & Ibe, 1984).

Some authors argue in favour of multiple contributory sources to the world class hydrocarbon reserves in the delta, with Evamy *et al*, (1978) basing their argument on the organic matter type and organic matter contents of both formations, whereas Ekweozor *et al*., (1979) believed that the oil in the Eastern Delta are from the shales of the Agbada Formation while those in the Western Delta are co-sourced from both formations based on

αβ-hopane and oleanane compositions of oils. From maturation models, Ejedawe *et al*., (1984) infer that the Central Delta oil were sourced from the paralic Agbada Formation while the gas was sourced from the Akata Formation, whereas Doust & Omatsola (1990) based their argument on sequence stratigraphy and inferred that the source of the hydrocarbons in the basin are from the lower coastal plain (delta offlap sequence), which implies that the bulk of the onshore hydrocarbons were sourced from the paralic Agbada Formation, whereas those from the offshore were sourced from the delta slope and turbidite fans of the over-pressured and the under-compacted marine Akata Formation.

A marine Cretaceous shale beneath the Tertiary Niger Delta has been proposed as a possible source of the reservoired oil in the delta (Frost, 1997; Haack *et al*., 2000) although this has not been proven because samples from this age are not available as exploration wells in the delta are not drilled deep enough to penetrate them (Tuttle *et al*., 1997). It is also not proven that migration pathways exist within the Akata shales for hydrocarbons generated in the underlying formations to have migrate through (Tuttle et al., 1997). However, Bellingham *et al*., (2014) was able to show some pre-stacked and depth migrated regional seismic sections of 18ses TWT with severe brittle deformation through the Akata Formation (Figure 1.5), that could serve as a good migration route for the hydrocarbons generated in the Cretaceous Formations. The Gulf of Mexico model where older rocks sourced the oil and gas in the basin has been invoked by Haack *et al*., (2000) and was supported by the model developed by Samuel *et al*. (2007; 2009), but it should be noted that there is no conclusive geochemical data to prove this (Tuttle *et al*., 1997).

Although a Cretaceous source for the Niger Delta Basin oil is hypothetical and not yet proven (Frost, 1997; Haack *et al*., 2000; Samuel *et al*., 2007; 2009), other basins along the West African margin have proven Cretaceous source rocks that are related to their hydrocarbon discoveries in most fields (Brownfield & Charpentier, 2006) and these basins started developing the same time as the Niger Delta, i.e. during the Late Jurassic after the

separation of the South American plate from the African plate (Whiteman, 1982). The Cretaceous source rocks from some important West African margin (Africa + South America) basins include:

1. Marine marls of the Douala Basin (Brownfield & Charpentier, 2006).
2. Marine marls and shales of the Iabe Formation in Central and Southern Congo Basin (Brownfield & Charpentier, 2006).
3. Lacustrine and marine source rocks of the Bucomazi Formation in offshore Lower Congo (Pasley *et al*., 1986; McHargue, 1990).
4. Lacustrine source rocks of the Pointe Noire marl in Northern Congo Basin (Baudouy & Legorjus, 1991).
5. Lacustrine source rocks of the Kissenda and Melania Formation in offshore Southern Garbon (Teisserence & Villemine, 1990).
6. Lacustrine carbonates of Lagoa Feia Formation in Campos Basin (Coward *et al*., 1999; Schieflbein *et al*., 1999).
7. Lacustrine shales of Guaratiba Formation in Santos Basin (Coward *et al*., 1999; Schieflbein et al., 1999).
8. Limestones and dark shale of Itaipe Formation in Alamda Camamu sub-basin (Coward *et al*., 1999; Schieflbein *et al*., 1999).

A relevant question therefore is, why are there no proven Cretaceous source rocks in the Niger Delta Basin?

1.4 Reservoir rocks

The oil and gas reserves in the Niger Delta basin are mostly reservoired in the sandstones and sands of the paralic Agbada Formation with the characteristics of individual fields dependent on burial depth and depositional environment (Tuttle *et al*., 1997), as well as age ranging between Eocene to Pliocene (Evamy *et al*., 1978); the most important fields are

related to point bars and barrier bars (Kulke, 1995) with reservoir thickness increases where there is multiple stacking of sand facies (Doust & Omatsola; 1990). Although Evamy *et al*., (1978) puts the reservoir thicknesses as 15 to 45 m, Edward & Santogrossi (1990) point out that most reservoirs are up to 100 m thick with porosities of 40% possible at shallow reservoirs, but generally around 15% at 3 km sediment thickness and permeabilities of up to 2 Darcy. The Agbada formation sandstones are highly porous and permeable, and therefore serve as excellent reservoirs and so the major risk during exploration is the seal (Doust & Omatsola, 1989).

The lateral extent of reservoirs in this delta is seen to be highly variable and dependent on the growth fault with thicknesses greater in the down-thrown blocks (Weber & Daukore, 1975; Tuttle, 1999). The fluvial sands tend to be very coarse while the barrier bars are well sorted, with high reservoir quality as they are poorly cemented with generally very low reduction in porosity with depth increase (Kulke, 1995; Tuttle, 1999). Turbidites and deep sea channel sands are the most important reservoirs in the offshore Niger Delta and these regions of the delta have mostly been influenced by gravity flow (Beka & Oti, 1995) and submarine water fans (Burke, 1972).

1.5 Structures and trap definition

Deposition of the Akata/Agbada/Benin Formations that make up the Tertiary Niger Delta occurred in 5/6 offlap cycles, with each cycle having a width of 30/60 km and progrades southwards into the sea; each of these cycles is called a depobelt (Stacher, 1995; Tuttle *et al*., 1999). These depobelts are controlled by the regional syn-sedimentary growth faults which are developed by rapid changes in rates of subsidence and sediment supply/sediment loading (Doust & Omatsola, 1990).

When the rate of sediment supply is more than crustal subsidence (accommodation), there is always the formation of a new depobelt seaward (Doust & Omatsola, 1990). Each of the

5/6 depobelts in the Niger Delta (Figure 1.6) is marked by a regional growth fault trending from north to south and a counter regional fault trending from south to north (Evamy *et al*., 1978; Doust & Omatsola, 1990). The depobelts include:

1. Northern depobelt
2. Greater Ughelli depobelt
3. Central swamp depobelt
4. Costal swamp depobelt
5. Shallow offshore depobelt
6. Deep offshore depobelt

} Offshore depobelts

The age of the depobelts increase from inland offshore, with the distal depobelts the most structurally complex as a result of gravity tectonics (Doust & Omatsola, 1990). Structural traps are the most common in the basin (Tuttle *et al*., 1999) and most are syn-sedimentary in nature, restricted mainly to the paralic Agbada Formation (Stacher, 1995) and with structural complexity increasing in a north-southern trend as a result of the overpressure in the Akata Formation (Tuttle *et al*., 1999).

Stratigraphic traps play an important role on the flanks of the delta and most are pockets of sands in incised valley and diapiric structures (Beka & Oti, 1995). The most common structural traps in the delta include: multiple growth faults, rollover anticlines, collapsed crest structures and antithetic faults (Figure 1.7), with seal units formed from interbedded shales in the paralic Agbada Formation (Doust & Omatsola, 1990). Seals in this formation can be as a result of clay smearing in faults; juxtaposition of sands against clay along fault line and up-dip shale seals (Doust & Omatsola, 1990), whereas on Niger Delta flank, clay field submarine canyons and incised valley serves as seals (Doust & Omatsola, 1990).

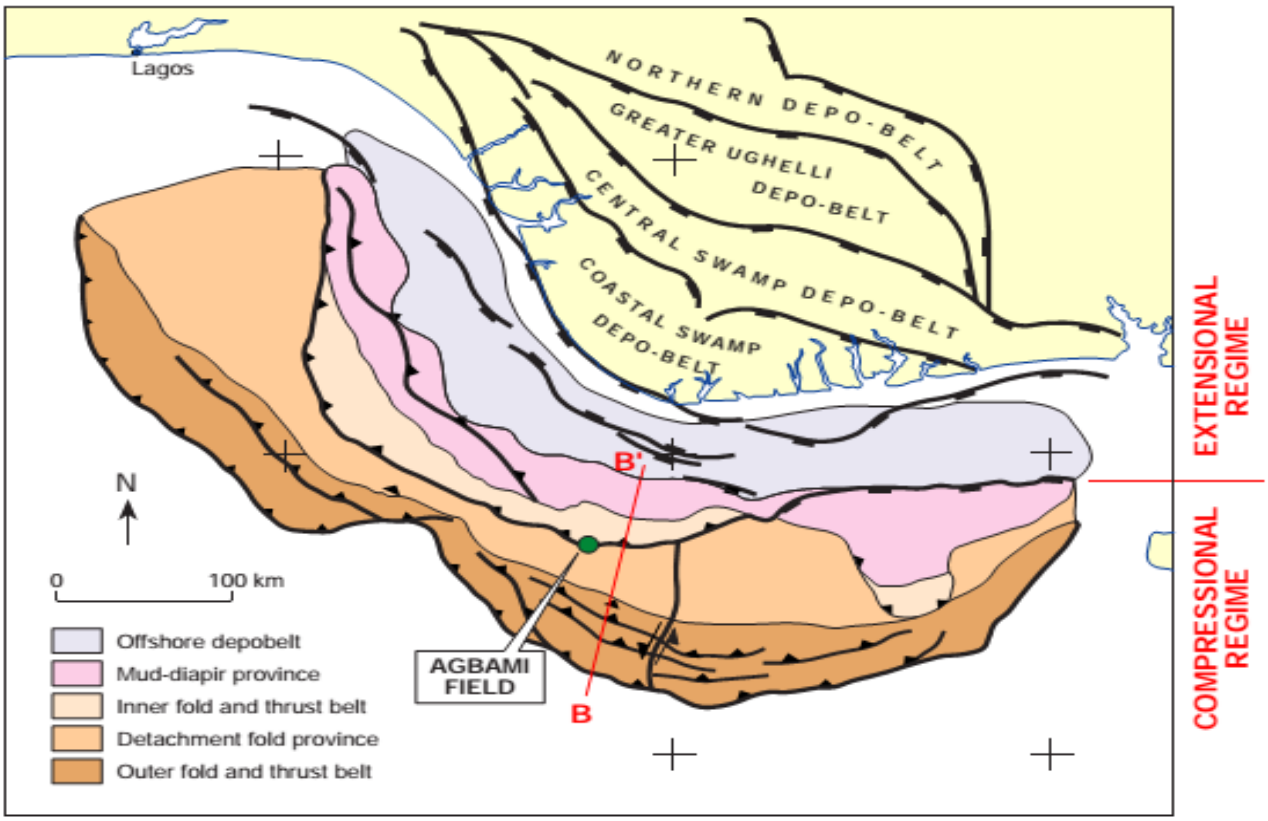

Figure 1.6: Map of Niger Delta showing the major depobelts. Note the extensional regime onshore and compressional regime offshore (Corredor *et al*., 2005).

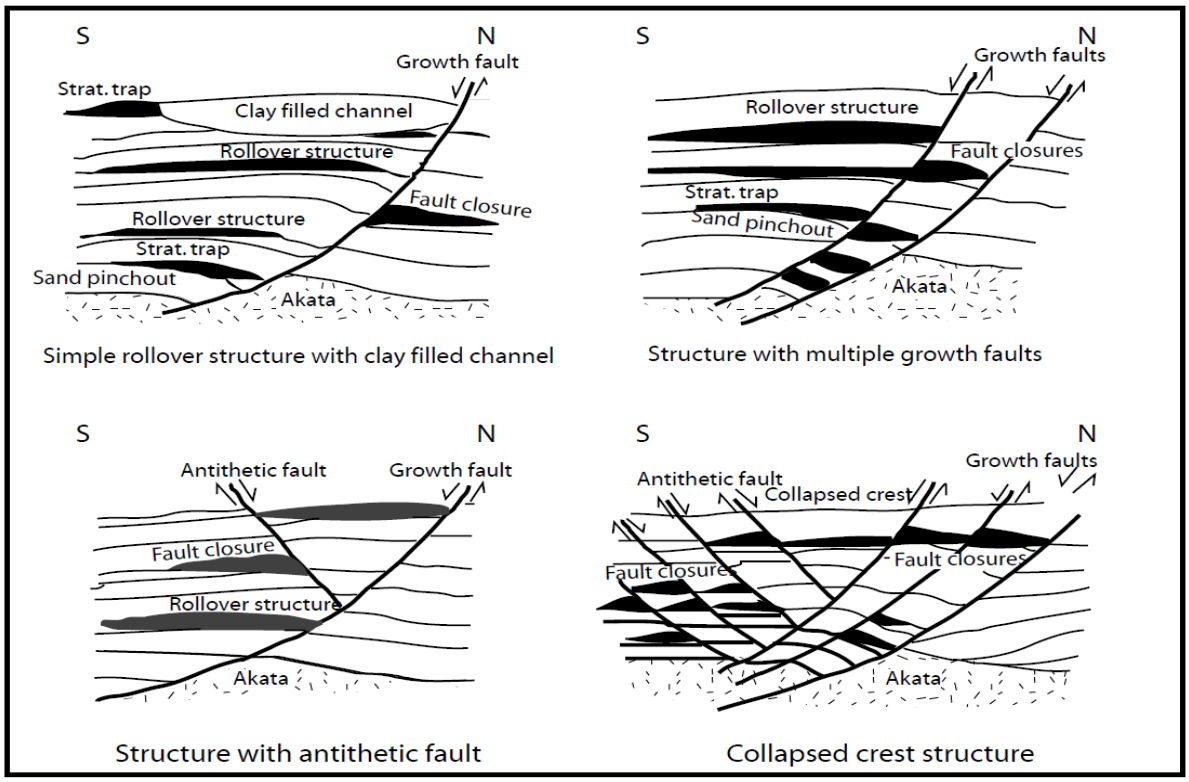

Figure 1.7: Hydrocarbon trapping mechanism and principal structures in the Niger Delta (Doust & Omatsola, 1989).

1.6 Review of hydrocarbon geochemistry

During any exploration activity, there is always interest not only to know the source of the hydrocarbons in any reservoir/field but also to have information on the thermal maturity of those oil samples, since this knowledge helps the petroleum geochemist with decisions on the production and development of a field.

There have been huge controversies on the source of the hydrocarbons in the Niger Delta over the years, possibly because of mixed signatures (Type II + II/III + III) expected from a paralic source depositional environment and the huge oil/gas/condensate reserves which often have marginally mature biomarker signatures (Frost, 1997; Haack *et al*., 2000; Samuel *et al*., 2007; 2009; Sonibare *et al*., 2008). However, all petroleum are potentially mixtures of either different maturity oils from the same source rock or from different source rocks (Wilhelms & Larter, 2004).

1.6.1 Source environment of deposition

Determination of source rock depositional environment helps to determine the probable kerogen type that will be present in the source rock, as lacustrine environment mostly yields Type I kerogen, marine environment yields Type II kerogen and terrigenous deposition environment mostly yields Type III kerogen (Peters *et al*., 2005). There are several parameters which are routinely used to decipher source deposition environment and these includes; Pr/Ph, oleanane index, C_{30} sterane, Sulphur content, cH/bcC_7, cP/bcC_7, b/bcC_7, and stable hydrogen isotope (δD).

The Pr/Ph ratio helps indicate the source depositional environment of an oil (Didyk *et al*., 1978) however there are various other sources for pristane and phytane (e.g. ten Haven *et al*., 1987; Volkman & Maxwell, 1986; Goossens *et al*., 1984) but the ratio is still very useful in oil source depositional environment interpretation (Peters *et al*., 2005). Pr/*n*C_{17} and Ph/*n*C_{18} are also very useful in indicating redox condition but they are affected by

biodegradation (Peters et al., 2005). The oleanane index helps indicate higher plant (angiosperm) input in any deposition environment, with their preservation increasing to a maximum when they are deposited in a marine setting (Ekweozor and Telnaes, 1990) but very high oleanane index can also indicate oil window mature as the ratio is known to be dependent on thermal maturity (Ekweozor and Telnaes, 1990).

The C_{30} regular steranes are known to only be contributed by marine algae, without any terrestrial source, they help to place a tighter constrain on environment with suspected marine influence (Moldowan, 1984; Moldowan *et al*., 1990). Hydrocarbon sourced from terrestrial materials are usually deposited in oxic settings with <1% sulphur content and those from marine environment are usually deposited in anoxic settings with >1% sulphur content and kerogen with bounded sulphur tend to have a lower temperature of expulsion because of the C-S bond (Orr, 1986).

The methylcyclohexyls (cH/bcC_7), ethylcyclopentyls (cP/bcC_7) and branched heptanes (b/bcC_7) are not only useful as correlation parameters (Mango, 1997; Odden *et al*., 1998), but also help to discriminate between source rocks but with possible overlaps between the various fields (ten Haven, 1996). The abundances of benzene and toluene have been used as a separating factor between terrigenous sources and marine sources, as source rocks deposited in marine environment are known to be depleted in their toluene and benzene concentration compared to those of terrigenous origin (Leythaeuser *et al*., 1979a; 1979b; Odden *et al*., 1998).

Stable hydrogen isotope (δD) compositions of hydrocarbons reflect their precursors and environment of deposition but δD might be altered by thermal maturation (Dawson *et al*., 2005; Radke *et al*., 2005; Pedentchouk *et al*., 2006). Organic matter of marine derived sediments have δD values of approximate $-150^0/_{00}$ if no alteration has taken place (Smith & Epstein, 1970; Santos & Hayes, 1999) and the hydrocarbons sourced from them tend to retain this value (Dawson *et al*., 2007).

The ternary plot of C_{27}-C_{28}-C_{29} C-ring monoaromatic steroids has been shown to distinguish oils of terrigenous, marine and lacustrine sources (Moldowan *et al*., 1985) but with possible overlap. This plot has a clear relationship with the sterane ternary plot of Huang and Meinschein (1979), but the C-ring monoaromatic steroids may be derived from early diagenesis of sterols and have been shown to be a better precursor tracers of source than the sterane ternary plot (Peters *et al*., 2005).

1.6.2 Thermal maturity, cracking and reservoir mixing

Hydrocarbon thermal maturity parameters are based on the relative abundances of a stable isomer to another isomer which is relatively unstable, where it is observed that the less stable isomers will be destroyed preferentially to the more stable ones with increase in thermal stress (Peters *et al*., 2005). It has been noted over the years that the maturity parameters used are influenced to some extent by source/organo-facies, depositional environment conditions, biodegradation and mixing. Apart from the stated influences on various maturity parameters, it has been well documented that various maturity parameters have a limited maturity range (window) where they can be applied and in which their results are valid. Most of the common biomarker thermal maturity parameters normally reaches equilibrium before or within peak oil generation (e.g. C_{29} ββ/ββ+αα sterane, C_{29} 20S/20S+20R sterane, 18β/β+α oleanane, C_{30} βα/βα+αβ, C_{32} 22S/ 22S+22R), whereas others can be used in peak and late oil window but are not useful in the gas window (eg dia/dia+reg steranes, tric/tri+17α-hopane, Ts/Ts+Tm, TA(1)/TA(1+11), MA(1)/MA(1+11) and most are generally not linear compared with vitrinite reflectance (Peters *et al*., 2005).

Cracking of kerogen and petroleum either in the source or in the reservoir is thought to follow first order, or multiple first order, reactions (Burnham & Braun, 1990; Horsfield *et al*., 1992; Peters & Fowler, 2002) but the kinetic parameters used for various studies are hugely varied (Waples 2000) and the influence of reservoir water and clay minerals in these

process is not very well understood (Mango *et al*., 1994). Therefore, the backward predictive model of oil deadline temperature for any basin remain unachievable (Quigley & Mackenzie, 1988; BeMent 1996) and the evidence from high temperature reservoirs shows that liquid hydrocarbon have a wide range of existence temperatures (Waples 2000).

Diamondoids which are thermally stable hydrocarbons and which also have high resistance to biodegradation (e.g. diamantanes) have been shown to help resolve mixing and cracking extent in an oilfield (Dahl *et al*., 1999) and detection of highly mature oil and condensates mixed with low mature oil can help indicate the existence of new petroleum plays (Peters and Fowler, 2002).

The heptane value (HeptRat) and isoheptane value (IsoheptRat) suggested by Thompson (1979; 1983) as a measure of maturity is based on the behaviour of the acyclic alkanes relative to the cycloalkanes, with changes in thermal maturity (Phillippi 1975; Thompson 1979; 1983). Thompson (1979) proposed that polycylic alkanes are cracked to form cyclohexanes and cyclopentanes and with further increases in temperature form acyclic alkanes. These maturity ratios are shown to be very useful but can be dependent on source facies, especially in the oils of the Norwegian offshore (Odden *et al*., 1998) and suggestions has been made to cross check results with those from a mature source rock (ten Haven, 1996; Odden *et al*., 1998). Biodegraded oils have very low IsoheptRat and HeptRat values ($\leq$18 HeptRat) and those with very high values are generally of very high thermal maturity and may have been cracked (Thompson 1983) but low HeptRat (as low as 12) can also be as a result of low maturity (Peters *et al*., 2005) and the use of the parameters should be restricted to oil samples that have not undergone reservoir fractionation and phase separation (Thompson, 1987).

Most aromatic hydrocarbon maturity ratios although source dependent are valid into the late oil window even when alkane biomarkers are destroyed due to high thermal maturity

(Peters *et al*., 2005) and the methylphenanthrene index (MPI) is very significant because of its high range of validity i.e. from 0.6 to 1.7% mean vitrinite reflectance (Radke *et al*., 1982; 1988) and the ratio has been well calibrated to vitrinite reflectance (Radke & Welte 1983; Radke *et al*., 1986).

Several aromatic thermal maturity ratios have been proposed but some come with drawbacks which limit their use; among those ratios is the methylnaphthalene ratio (MNR) which is particularly valid in samples of greater than 0.9% vitrinite reflectance (Radke *et al*., 1982), also the dimethylnephthalene ratio (DMNR) is not valid at low maturity but can be used in samples between 1.0 and 1.5% vitrinite reflectance (Radke *et al*., 1984), and the methylphenanthrene ratio (MPR) which is not valid at low maturity but can be used in samples between 1.0 and 1.7% vitrinite reflectance (Radke *et al*., 1984). The TAS (20+21)/total [which is defined as C_{20} + C_{21} triaromatics relative to total triaromatics] has a wider valid range of 0.5 to 1.5% vitrinite reflectance, however it is highly dependent on source rock facies and comparison of results can often only be made for samples from the same source rock (Mackenzie 1984; Beach *et al*., 1989). Methylated naphthalenes have been used as maturity parameters over the years (Alexander *et al*., 1985; Radke *et al*., 1986, 1990, 1994; Bastow *et al*; 1998; van Aarssen, *et al*., 1999) and their distributions in crude oils have been used as maturity indicators, with the ratios of trimethylnaphthalenes (TMN), tetramethylnaphthalenes (TeMN) and pentamethylnaphthalenes (PMN) having strong correlations with other thermal maturity parameter like Ts/Ts+Tm (van Aarssen, *et al*., 1999). Apart from thermal maturity, those ratios have been shown to indicate mixing and biodegradation (van Aarssen, *et al*., 1999).

1.6.3 Secondary Migration

Effective secondary migration of hydrocarbons between the source rock and the reservoir is an essential component of the petroleum system. A positive correlation between the source and the reservoir can be proven if the direction and distance of migration can be

established and this may also aid the discovery of new fields and accumulations, which often lie along the migration pathway (Larter *et al*., 1996).

Carbazoles and benzocarbazoles have been used as molecular migration tracers, especially with respect to distance and directions (Li *et al*., 1995; Later *et al.*, 1996; Liu *et al*., 1997; Bennett *et al*., 2002) but these compounds have shown to also be affected by source rock maturity (Li *et al*., 1997; Clegg *et al*., 1998; Bechtel *et al*., 2013) and biodegradation (Huang *et al*., 2003).

The chemical components of petroleum are often strongly related to the source rocks from which they are generated (Tissot & Welte 1984; Peters *et al*., 2005) but sometimes these relationships are difficult to establish, mostly because of processes occurring in-reservoir or along the migration pathway. These processes includes thermal cracking (Horsfield *et al*., 1992; Dahl *et al*., 1999); biodegradation (Connan, 1984; Horstad *et al*., 1991; Peters *et al*., 1996; Head *et al*., 2003; Larter *et al*., 2003; Aitken *et al*., 2004; Bennett *et al*., 2013); migration/phase/evaporative fractionation (Thompson, 1987; 1988; Dzou & Huges, 1993; Curial & Bromley, 1996); water washing (Lafargue & Barker, 1988; Palmer, 1993; de Hemptinne *et al*., 2001); deasphalting (Wilhelms & Larter 1994); and thermochemical/bacterial sulphate reduction (Peters & Fowler, 2002; Worden & Smalley, 1996) etc.

The NH-shielded alkylcarbazole isomers are often enriched in oils compared to the NH-unshielded isomers, while the reverse is true for bitumen extracts from source rocks (Bennett *et al*., 2002). The proposed use of alkylcarbazoles and benzocarbazoles as relative migration distance indicators is related to the differences in physio-chemical properties of the isomer within these two groups of compounds (Larter *et al*., 1996). For the benzocarbazoles, the concentrations of the benzo[a]carbazole isomer decreases preferentially to that of the benzo[c]carbazole isomer, with increasing migration distance (Larter *et al*., 1996; 2000). The benzocarbazole ratio

(benzo[a]carbazole/benzo[a]carbazole+benzo[c]carbazole) has been shown to be very useful in the determination of the relative migration distance of crude oil in several studies (Li *et al*., 1995; 1997; Larter *et al*., 1996; Clegg *et al*., 1998; Bennett *et al*., 2002; Huang *et al*., 2003; Bechtel *et al*., 2013). However the concentration of benzocarbazoles can be affected by source facies (Clegg *et al*., 1997), thermal maturity of the source rock (Clegg *et al*., 1998; Larter *et al*., 2000, Bennett *et al*., 2002) and biodegradation (Zhang *et al*., 1999; Huang *et al*., 2002; 2003). Larter *et al.* (2000) propose the use of benzocarbazole ratios only for petroleum systems that have same source rock, with oil generated within same thermal maturity and must have travelled over a relatively long migration distances.

1.6.4 Biodegradation

There are still very large conventional hydrocarbon reserves in the Middle East, Russia, Nigeria etc., but a huge percentage of the world's reserves are biodegraded with most biodegraded oils being present in Venezuela and Canada (Head *et al*., 2003). Biodegradation reduces the economic value of oil (Aitken *et al*., 2004) and usually occurs when microorganisms selectively feeds on components of oil (Connan, 1984, Larter *et al*., 2003, Bennett *et al*., 2013).

Biodegradation of hydrocarbons in the reservoir is possible when one or more of the following conditions are met:

1. Presence of water and nutrients (Jobson *et al*., 1972; Jones *et al*., 2008)
2. The reservoir must be permeable and porous (Brooks *et al*., 1998)
3. There must be microorganisms in the reservoir (Jones *et al*., 2008)
4. The reservoir must not be "paleopasteurised" (Wilhelms *et al*., 2000)
5. Salinity of formation waters must be lower than 10% (Peters *et al*., 2005)
6. There must be low H_2S concentrations in the reservoir (Peters *et al*., 2005)

Several studies over the years have tried to explain biodegradation of hydrocarbon as a quasi-stepwise quantitative or qualitative process, but usually based on the selective removal of a component relative to other components with various author proposing various scales (Volkman, *et al*., 1983; Connan, 1984; Peters & Moldowan 1993; Wenger *et al*., 2000; Peters *et al*., 2005; Larter *et al*., 2012). However, biodegradation is a complex process (Larter *et al.*, 2003; 2006; Bennett, 2008) with several other physiochemical factors in play and components been removed at different rates (Peters & Moldowan, 1991) because of the prevailing physiochemical conditions.

The molecular composition of aliphatic and aromatic hydrocarbon fractions has long been the basis for classifying the level of biodegradation of any oil based on the comparative susceptibility of compounds to biodegradation (e.g. Volkman *et al*., 1984). In the first instance the Peters & Moldowan (1993) PM scale considered the qualitative approach by assessing which compound was attacked and subsequently removed, but the Manco scale (MN2) assigned a number to the degradation stage, with a higher number (weight) assigned to compounds that are highly stable (e.g. steranes) and a lower number (weight) assigned to compounds that are relatively susceptible to biodegradation (e.g. low molecular weight *n*-alkanes), and with the possibility of 5 levels (0 to 4) for each compound class (Larter *et al*., 2012).

Biodegradation of hydrocarbons is possible under both aerobic and anaerobic conditions (Boll *et al*., 2002; Aitken *et al*., 2004) with both conditions following different pathways (Bekins *et al*., 2005; Jones *et al*., 2008) but the rate of biodegradation will be faster for surface oil spills under aerobic conditions than in deep anaerobic reservoirs (Larter *et al*., 2000).

The physical properties of any reservoired oil (viscosity, API gravity, pour point etc.) is mostly dependent on the properties of the charge and the rate of charging and

biodegradation level (Larter *et al*., 2012). The oil properties therefore depend on a complex interplay of the existing physical and chemical conditions in any reservoir (e.g. Head *et al*., 2003, Larter *et al*., 2003), thereby complicating the simplistic approach to biodegraded oil ranking (Larter *et al*., 2012).

1.6.5 Evaporative fractionation

Crude oils that have their light ends (C_6-C_{14}) missing but have relatively high concentrations of low molecular weight aromatic hydrocarbon components (benzene, toluene, xylene) and also relatively high concentrations of cycloalkanes are thought to have undergone separation migration (Silverman 1965), which is also known as evaporative fractionation (Thompson 1987), migration fractionation (Dzou & Hughes, 1993), phase fractionation (van Graas *et al*., 2000), gas washing (Loosh *et al*., 2002).

Fractionation is a commonly recognised feature in most basins/ fields and have been known to occur in offshore Indonesia (Schoell *et al*., 1985), Gulf of Mexico (Thompson, 1987), Eugene island (Meulbroek *et al*., 1998), Offshore Taiwan (Dzou & Hughes, 1993), North Sea (Larter & Mills, 1991) etc., and there is always a possibility of fractionation in a basin when there is a free gas phase that can migrate through an hydrocarbon reservoir (Meulbroek *et al*., 1998).

There is a high possibility of oils from the same source to have different compositions due to migration and remigration of gas through oil (gas washing) in different reservoirs with different pressure, volume, temperature (PVT) conditions and at different rates (e.g. van Grass *et al.*, 2000). These compositional variation in hydrocarbons from the same source will have effect on isotopic and molecular parameters used in correlation studies and if care is not taken it can lead to wrong interpretations of the parameters measured from them (Dzou & Hughes, 1993). The economic importance of a fractionated hydrocarbon residue

will be much less than that which is unfractionated, since the former has lost much of its light ends which are usually more economically valuable (Losh & Cathles, 2010).

Fractionation occurs when an oil is continually washed with a free gas phase thereby removing/mobilizing/dissolving its light end *n*-alkanes in the process, but leaving behind its light end aromatics (which are less volatile than the equivalent carbon numbered *n*-alkanes), in its residue and this can be a continual process (Thompson 1987; van Graas *et al*., 2000; Loosh *et al*., 2002; Schoell *et al*., 1985; Meulbroek *et al*., 1998; Dzou & Hughes, 1993; Larter & Mills, 1991)

1.6.6 Water washing

Water washing is a common phenomenon that often occurs with biodegradation in oil reservoirs and leads to compositional changes in hydrocarbons but the effect of water washing alone may be difficult to quantify (Cubitt *et al*., 1995; Leythaeuser *et al*., 1989). Water washing usually occurs when water is in constant contact with oil (de Hemptinne *et al*., 2001) as in the case of hydrodynamic trap (e.g. Lafargue & Thiez, 1996) and the effect might be negligible over a short time however, but over a longer time scale components that are more soluble in water (e.g. toluene and benzene) will continually be preferentially dissolved in water leaving behind the insoluble fractions (Lafargue & Thiez, 1996, Mango 1997).

The effect of water washing is dependent on the rate of flow of water and the height of the oil column (Lafargue & Thiez, 1996). Fast flowing water will continually dissolve more light aromatic compounds as it washes through the reservoir because the saturation of light aromatic compounds in the mobile water will remain low and the higher the height of the oil leg the more the leaching effect and compositional variation within the reservoir (Lafargue & Thiez, 1996).

1.6.7 Correlation

An important role of geochemistry in petroleum exploration is the establishment of relationships between oils or oils and their source rocks. However, several potential pitfalls exist in any correlation studies, with the possibility of arriving at incorrect conclusions. Peters *et al*., (2005, 447pp), noted that a positive correlation does not always mean that samples are related, but a negative correlation shows strong evidence of a lack of relationship between samples. Some correlation studies have been carried out on the oils and source rocks of the Niger Delta and these include those by Eneogwe & Ekundayo, (2003); Sonibare *et al*., (2008); Akinlua & Ajayi, (2009); Samuel *et al*., (2009) and Lehne & Dieckmann (2010). However, there are numerous examples of oil to oil correlation (e.g. Hughes *et al*., 1985; Clayton *et al*., 1987; Curiale *et al*., 2000; Kruge, 2000; Peters *et al*., 2000; Smith & Bend 2004; Zhang & Huang 2005; Hill *et al*., 2007; He *et al*., 2011) and oil to source rock correlation (e.g. Chung *et al*., 1992; Peters *et al*., 2005; Waples & Curiale 1999; Curiale & Sperry, 2000; Gratzer *et al*., 2011) studies on many basins from around the world.

The possibility of a complex relationship always exists in any regional correlation study, where the most obvious challenge will be to decipher genetic relationship in a large data set and how to eliminate parameters that does not show any obvious relationships (Peters *et al*., 2005). In order to help overcome this, geochemists now routinely use chemometric analysis (e.g. Telnaes & Dahl 1985; Peters *et al*., 1986; Zumberge 1987, Zumberge & Ramos 1996; Peters *et al*., 2000; Eneogwe & Ekundayo 2003; Gurgey 2003; He *et al*., 2011) which can be defined as the use of multivariate statistics to extract useful information and draw out patterns from a group of measured data (e.g. Kramer, 1998). The usefulness of chemometrics cannot be overemphasized, especially when dealing with large geochemical data set (Christie *et al*., 1984; Christie, 1992).

Oil to oil correlations are generally only of use if they are based on parameters that can separate oils into their relevant source deposition environments and those parameters should not be significantly affected by secondary alteration processes (e.g. biodegradation, water washing, migration fractionation) that can change the original composition of an oil (Peters *et al*., 2005) or thermal maturation process that can lead to formation of oils with different compositions from their source rock facies at different stages of maturity (Curiale, 2008).

Principal component analysis (PCA) which is tool used in chemometric analysis, helps to simplify complex data with large numbers of variables, into a new compressed variable while filtering out noise and data that show no relationships (e.g. Parfitt & Farrimond, 1998; He *et al*., 2012); variables that plot in the same cluster hold similar interpretations and those that plots away from each other are either not related or negatively related (Gurgey, 2003).

In addition to conventional molecular marker distribution measurements and parameters use in correlation, the compound specific isotope analysis of *n*-alkanes is also a very useful tool for correlation of either oils to oils or oil to source rocks (e.g. Murray *et al*., 1993) and has proved extremely useful when dealing with comingled oil (Rooney *et al*., 1998; Peters *et al*., 2005). Carbon isotope ($^{13}C/^{12}C$) and hydrogen isotope (D/H) ratios have been used as a diagnostic tools in several geochemical studies (e.g. Murray *et al*., 1993; Rooney *et al*., 1998; Santos Neto & Hayes, 1999; Li *et al*., 2001; Schimmelmann *et al*., 2004; Pedentchouk *et al*., 2004; 2006; Sun *et al*., 2005) for either finding a positive or negative correlations among oil and their probable source rocks, while anomalies seen in isotopic signatures can help unravel new petroleum systems and exploration targets (Summons *et al*., 1998).

An oil-source rock correlation can be seen as a study that tries to establish a genetic relationship between an oil which was derived in whole or part from an oil prone source

rock that must have a comparable chemical/geochemical (elemental, molecular and isotopic) and geological (basin formation, sediments transportation, deposition, compaction, fluid flow, heat flow) relationship with the said oil (Curiale, 2008). Although there appear appreciable improvement in geochemical oil source correlation techniques since some of the first work by Hunt *et al*. (1954), there still remain a lot of uncertainties in defining the geological influences in a successful oil-source correlation study and these uncertainties can be as a result of our limited knowledge of fine scale vertical and lateral variability in the depositional system of source and reservoir rocks (Keller & Macquaker, 2001; Barker *et al*., 2001).

Other problems in oil-source rock correlation include:

1. In addition to the geochemical knowledge, a successful oil source correlation will depend on our interpretation of organic matter facies variability within same depositional settings (Curiale, 2008).
2. Most geochemist use solvent to extract bitumen out of source rock and this is different from the expulsion of hydrocarbons within the subsurface with a different time scale (Curiale, 2008).
3. Correlation of multiply sourced oil and mixed hydrocarbons with multiple thermal maturity levels can introduce significant compositional variability within the trapped hydrocarbons (Seifert *et al*., 1979; Peters *et al*., 1989; Chen *et al*., 2003a, b).
4. Apart from organic matter variability in source and reservoir rocks, there is also the possibility of significant organic matter variability in carrier beds during secondary migration that might have partitioning effects on some chemical compounds (e.g. carbazoles and phenols) and migration contamination of the oil (Hughes & Dzou, 1995; Pang *et al*., 2003; Larter *et al*., 2006).

5. The effect of migration fractionation, gas washing and phase changes can altogether be missed during routine geochemical oil source rock correlation and this will render correlation unachievable (Curiale & Bromley, 1996; Curiale, 2002).

Despite all these potential problems associated with oil-source rock correlation, the importance of any oil-source rock correlation cannot be overemphasized as a possible oil-source rock correlation study is better than one without any possible correlation established (Peters *et al*., 2005).

1.7 Aims and objectives of this study

The Niger Delta Basin is generally defined as a 'Giant Basin' in terms of its reserve and current daily production rate, but despite more than 50 years of oil exploration in the basin, the main source rocks have been poorly defined. The non-availability of mature source rock samples and variability in fluid types (oil/gas/condensates) from the various sub-basins in the Niger Delta even at very close proximity to each other have been an issue when trying to ascertain the source of the hydrocarbons in the basin.

The overall aim of this project is to gain a better understanding of the Niger Delta petroleum system with a view to predicting the source rocks of the oil from the basin and ultimately be able to predict the likely mixing percentages of high maturity sourced oils with those of lower thermal maturity and how this mixing may change across the regions of the delta. The specific objectives include:

1. To infer the organic facie and depositional environment of source rocks of the Niger Delta Basin oil based on the geochemistry of a large data set of oil.
2. To determine the possible migration distances and alteration processes that has affected the produced oil samples.
3. To access the information from diamondoid parameters and concentration as to the potential mixing of hydrocarbon from a deep source.

4. To access source potential of transgressive shales of Niger Delta Basin based on limited well cutting samples.

1.8 Scope and limitations

This project measures bulk geochemical parameters on oils and potential source rock samples and uses gas chromatography (GC) and gas chromatography – mass spectrometry (GC-MS) of selected saturated and aromatic hydrocarbon fractions to provide detailed compositional information on them. In particular, the diamondoid hydrocarbons in the oils are quantitatively analysed by GC-MS in order to better classify the oils and their sources, while compound specific stable carbon isotope ratio analysis (CSIA) of individual *n*-alkanes is also undertaken for this purpose.

The research would have been able to place a tighter constraints on the petroleum systems of the Niger Delta if more data on the samples had been available and particularly:

1. Information on geological background of the potential source rock samples, oil sample potential migration routes, reservoir conditions, fluid properties and burial histories of the basin.
2. Fluid information such as API gravity, pour point, viscosity, GOR etc.
3. Compound specific isotope measurements of isolated diamondoids from crude oil.
4. Core samples of mature source rocks.
5. Stratigraphic information and geographic location of well cutting samples.

CHAPTER TWO

MATERIALS AND EXPERIMENTAL METHODS

2.0 Introduction.

Several geochemical methods were used in this work and care was taken to follow standard laboratory procedures, which included quality controls by repeatedly analysing one particular sample with each batch of analyses to check for the reproducibility and reliability of the results generated. The standard geochemical procedure used for this research included: determination of total organic carbon content, source rock pyrolysis, Soxtec™ extraction (for cutting samples) and Iatroscan thin layer chromatography with flame ionisation detection (TLC-FID), deasphaltening, solid phase extraction (SPE) separation, gas chromatography (GC), gas chromatography-mass spectrometry (GC-MS), gas chromatography-mass spectrometry-mass spectrometry (GC-MS/MS) and gas chromatography-isotope ratio-mass spectrometry (GC-IRMS) for both cuttings and oil samples. Attempts were made to separate the diamondoid hydrocarbons from the aliphatic fraction for compound specific isotope analyses (CSIA) but this was not achievable as only the branched/cyclic fractions were separated and the isolation of diamondoids from these fractions was not possible with the techniques used.

2.1 Sample selection

A total of 180 oil samples from 40 oil fields in the Niger Delta were used for the current study. In addition to this, 50 cuttings samples from six oil wells from different parts of the delta were subjected to initial geochemical screening, after which 30 cutting samples were selected for further geochemical analysis. The cutting samples were selected from different depths depending on the depth of the exploratory well.

The initial selection of the well cuttings samples was based on colour (preference was given to dark coloured samples over light coloured ones), grain size (very fine and fine sized

cuttings samples were preferentially selected to the coarse ones), sorting (well sorted samples were preferentially selected to samples with uneven grain size) and texture (samples with pliable texture were selected ahead of those with coarse texture). Selection of the oil samples was based mainly on the geographic regions and wells available with oil samples selected from at least two points in a well i.e. a deep reservoir and a shallow reservoir.

The oil samples were subdivided into Western Delta, Central Delta, Eastern Delta and Southern Delta to enable ease of interpretation and to show variation in interpretation based on the part of the Delta where the oil sample were collected (Figure 2.1).

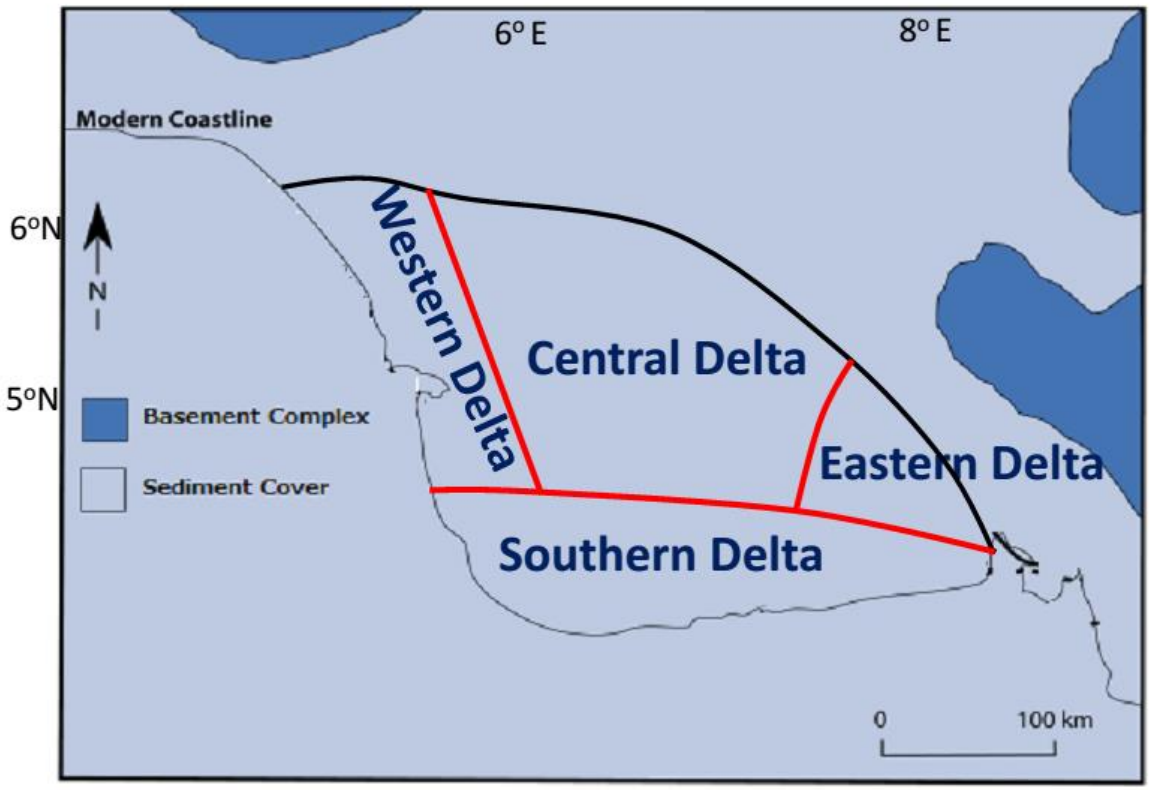

Figure 2.1: Map of Niger Delta Basin showing the division of the delta into Western Delta, Central Delta, Eastern Delta and Southern Delta.

2.2 Total Organic Carbon (TOC) content.

An aliquot (~0.1g) of each of the pulverised well cuttings samples was weighed and placed inside a porous crucible. A reference sample of known TOC was equally weighed and replicated after 10 sample runs to check for reproducibility of the results. Aliquots of

approximately 1 ml of 4 mol/l hydrochloric acid were added to the grounded rock samples in the crucibles to remove inorganic carbonate ($CaCO_3$) carbon leaving only the residual organic carbon in the sample. The acid was then allowed to drain from the samples in a fume cupboard for about 8 hours. Thereafter, the crucibles were placed in the oven at 65 °C and left for 24 hours. Prior to sample analysis the LECO CS-244 carbon-sulphur analyser instrument was calibrated using a LECO steel standard of known carbon content. Iron chips (~5g) as metal accelerator for the induction furnace were added to the sample to help facilitate combustion at 1500 °C. The carbon present in the sample was then oxidized to CO_2 in the presence of O_2 and the CO_2 measured by a thermal conductivity detector. The results were reported as sample weight percent carbon.

2.3 Source rock pyrolysis.

Pyrolysis was performed on aliquots of approximately 100 mg of powdered well cuttings samples, with each sample analysed in duplicate and a standard sample analysed before, during and after each run for equipment calibration. A Delsi oil show analyser (OSA) running on Delsi Rockplus software was used. The sample was heated at 100 °C for a period of three minutes, during which free volatile hydrocarbons (gas) are released (S_0). The temperature was then increased from 100 °C to 300 °C and held for three minutes to allow the expulsion of free hydrocarbons (oil) from the sample (S1). The furnace temperature was then ramped from 300 °C to 550 °C at a rate of 25 °C /min and held at 550 °C for 2 minutes, during which any heavy hydrocarbons are volatilised and the kerogen is thermally cracked. The hydrocarbon products of this thermal cracking are detected by the flame ionisation detector (FID). This gives the S2 peak and the temperature at which maximum petroleum generation occurred, Tmax (°C) was also recorded.

2.4 Soxtec extraction of source rocks.

Aliquots (Ca. 15g) of grinded well cutting samples were placed in pre-extracted cellulose thimbles. The thimbles containing samples were plugged with pre-extracted cotton wool and placed in the Soxtec apparatus and extracted using 125 ml of an azeotropic mixture of distilled DCM/Methanol (93:7, v/v). The thimble and sample was immersed in boiling solvent for 2 hours 10 minutes and rinsed for 2 hours at a heater temperature of 125 °C, the solvents were then allowed to drain from the samples and the thimbles for 20 minutes at a temperature of 20 °C with the total run time of total 4 hours 30 minutes. Activated copper turnings were added to the solvent mixture to absorb elemental sulphur and also anti-bumping granules. After extraction of the solvent soluble organic matter from the samples, the extracts were further analysed by Iatroscan (TLC-FID), then further fractionated into aliphatic and aromatic hydrocarbon and polar fractions using the C-18 and silica SPE separation method prior to GC, GC-MS, GC-MS-MS and GC-IR-MS analyses.

2.5 Iatroscan (TLC-FID).

The percentages of the saturated hydrocarbons, aromatic hydrocarbons, resins and asphaltenes (SARA) of the extracts and oils were determined using Iatroscan TLC-FID analyser *(c.f.* Karlsen & Larter, 1991*)*. A 3µl aliquot of each diluted extract or oil sample (Ca. 10mg extract in 1 ml DCM) was used. Each sample was analysed in duplicate to assess the repeatability of the method. Blanks were also analysed on all the racks to assess any contamination. The bottom of the rack of rods was immersed in a tank containing 150 ml of n-hexane as a mobile phase until the solvent reached a mark of ~95%. The rods were then left to dry for 3 minutes, after which, the rods were immersed in a tank containing 150 ml of toluene, which was allowed to pass up the rods until it reached the 60% mark; they were then removed and left to dry for 6 minutes, before being immersed in a final tank containing 150 ml of a mixture of DCM/Methanol (93:7, v/v), and the solvent front allowed

to get to the 30% mark before removing the rods. The rods were then left for 90 seconds in a 30 °C oven before being analysed on an Iatroscan MK-5 TLC-FID analyzer and the chromatograms stored on a Thermo Lab Systems Atlas laboratory system. A Norwegian Petroleum Directorate geochemical standard North Sea Oil (NSO-1) aliquot #11.27 from the Oseberg field, was always run on the first two rods of every rack. The NSO-1 analyses were used to assess the reliability of the results obtained.

2.6 Deasphaltening of extracts.

The cutting extracts were deasphaltened before solid phase extraction (SPE) fractionation to avoid the precipitation of asphaltenes which can lead to blocking of the column when hexane is used to elute the hydrocarbon fraction from the C-18 SPE column. Approximately 50mg of extract was weighed into an Iatroscan vial and 9 ml of cold hexane was added to the vial, which was then sealed with a crimping tool and shaken before sonicating in a sonic-bath for about 4 minutes. It was then left in a refrigerator at 4 °C for at least 15 hours to allow asphaltenes to precipitate and was later centrifuged at ca. 3000rpm for 5 minutes before the seal was removed using decrimping tool. The clear supernatant was carefully removed with pipette pasture and added to a 100 ml round bottomed (RB) flask. The asphaltenes were washed 5-6 times with 9 ml cold hexane until the supernatant appeared colourless. The hexane fractions were evaporated to ca. 1 ml using a rotary evaporator, transferred to a vial and evaporated using nitrogen gas to ca. 0.3 ml ready for the C-18 SPE separation.

2.7 Solid Phase Extraction (SPE) Separation.

The chromatographic sorbent used was non-endcapped 500 mg silica in a 3 ml octadecyl C-18 SPE tube. The columns were filled with DCM (ca. 3 ml) and allowed to drain completely before another 3 ml of DCM was added again and allowed to drain before

excess solvent was flushed out with gentle air using 10 ml syringe. The columns were arranged on to aluminium foil in a batch of 10 and placed on top of the oven set at 80 °C overnight to dry. Following the pre-extraction of the columns about 5 ml of hexane was used to precondition the column. The excess hexane in the column was removed using a 10 ml plastic syringe with PTFE adapter by applying a gentle air flush to displace the residual solvent and the tip of the column was washed with ca. 0.5 ml DCM. Approximately 40-50 mg of whole oil was weighed onto the frit of the column and kept away from the sides of the cartridge but allowed to absorb onto the sorbent before *n*-heptadecylcyclohexane (HDCH) approximately 800 μg and 1,1'-binaphthyl (1,1-BN) approximately 50 μg, were added as internal standards . The sample was eluted using 5 ml hexane in two aliquots into a 10 ml glass vial and excess hexane was removed from the column by applying a gentle air flush where necessary. The tip of the column was then rinsed using ca. 0.5 ml hexane, collecting the washings together with the hexane elute. The hexane elute containing the aliphatic and aromatic hydrocarbons were then capped and stored. A new 10 ml vial was placed beneath the column and 6 ml DCM was used to elute the polar fractions in 3 aliquots, the tip of the column was rinsed with 0.5 ml of DCM and the washing was collected together with the DCM elute which contains the carbazoles and phenols. The polar fraction was reduced to 500 μl under gentle flow of nitrogen gas and transferred into an autosampler vial before approximately 8 μg of D-8 carbazole was added as the internal standard.

The stored hexane fraction was evaporated under a gentle flow of nitrogen gas to 1 ml and a 100 μl (10%) aliquot taken for further separation using a silver (Ag^+) impregnated silica gel (Kieselgel 60G) packed 3 ml SPE column. The Ag^+ impregnated silica was prepared using a stock made of 30g of Kieselgel 60G weighed carefully into a 250 ml conical flask covered with aluminium foil followed by the addition of 60 ml distilled water then 3 g silver nitrate (analar) was dissolved in a 100 ml measuring cylinder. The slurry was

vigorously shaken until thoroughly mixed to form a homogenous creamy liquid with no silica lumps visible, the flask was completely wrapped with aluminium foil and left to dry in an oven at ca.80 °C. A mortar and pestle was used to crush the dry lumps into fine powder which was later kept in the flask and stored in the oven for further use, care was taken not to store it for more than 3 weeks as the separating power tended to reduce with increase in storage time.

A clean PTFE frit was placed into the base of an empty 3 ml cartridge barrel using tweezers and steel rod before adding ~550 mg of the silver nitrate impregnated silica using a narrow spatula and compacted with a steel road, then covered with another frit on top of the column. The column was then further carefully compacted to a depth of about 13-15 mm using a glass rod. The prepared column was pre-cleaned with 5 ml hexane and excess solvent was flushed through the column using a gentle flow of air with syringe and adapter. The 100 µl aliquot of hexane solution containing the aliphatic and aromatic hydrocarbon fractions was carefully added to the frit of the packed Ag^+ after which 2 ml of hexane was used to elute the aliphatic hydrocarbon fraction with gentle air flush onto a 10 ml vial. The aromatic hydrocarbon fraction was collected in a 10 ml vial after eluting with 4 ml DCM.

The aliphatic and aromatic hydrocarbon fractions were reduced to 500 µl and 200 µl, respectively, under gentle flow of nitrogen gas and transferred into autosampler (aliphatics) or autosampler with insert (aromatics) vials prior to GC, GC-MS, GC-MS-MS and GC-IR-MS analyses.

2.8 Branched/cyclic alkane separation.

Silicalite (a Union Carbide zeolite) pellets (~10 g) were placed in a mortar and pestle and crushed into fine powder and placed in a ceramic crucible before placing on a Bunsen burner for 20 minutes and stirred occasionally to heat thoroughly at a temperature of about 600 °C. The activated silicate powder was allowed to cool before use, then a pasteur pipette

was cleaned with iso-octane solvent and plugged with pre-extracted cotton wool before adding about 2 cm of alumina and about 3 cm of activated (cooled) silicalite powder and finally about 0.5 cm alumina on the silicalite giving a pipette column adsorbent bed depth of about 5.5 cm. The aliphatic hydrocarbon fraction aliquot was dried under gentle flow of nitrogen gas and then re-dissolved in 2 ml of 2,2,4-trimethylpentane (iso-octane) in a 10 ml vial. The solution was then pipetted into the column and allowed to slowly drip through into a clean vial. The vial containing the resolved aliphatic fraction was washed three times with 1 ml iso-octane each time and added unto the column and allowed to pass through using gentle flow of nitrogen gas. The 5 ml elute of iso-octane was then evaporated down to 200 µl under gentle flow of nitrogen gas and transferred onto auto sampler with insert prior to GC and GC-MS analyses. This fraction contained only the branched/cyclic alkanes.

2.9 Gas Chromatography (GC).

Gas chromatography (GC) was used to analyse the aliphatic and aromatic fractions in order to obtain *n*-alkane and acyclic isoprenoid alkane data and also to determine the concentration of sample to be used for gas chromatography-mass spectrometry (GC-MS) and gas chromatography-isotope ratio mass spectrometry (GC-IRMS). The GC-FID (Flame Ionisation Detector) analysis was performed on a Hewlett-Packard 5890 Series II GC with injector at 280 °C and FID at 310 °C. The sample (1 µl) was injected by an HP6890 autosampler in splitless mode. The oven temperature ramp program used was from 50 °C (held for 2 minutes) to 300 °C at 5 °C per min. and held at the final temperature (300 °C) for 20 minutes, with a total run time of 74 minutes. Hydrogen was used as the carrier gas, with flow rate of 1 ml/min, inlet pressure of 50kPa and split set at 30 mls/min. Separation was performed on a fused silica capillary column (30m x 0.25mm i.d) coated with 0.25µm 5% phenylmethylpolysiloxane (HP-5 phase).

A Nigerian oil sample was run with each batch of the analysis to check for variations in instrument sensitivity with time and also to check for reproducibility of the data by comparing several calculated ratios between batch results.

2.10 Gas Chromatography-Mass Spectrometry (GC-MS).

GC-MS analysis of the aliphatic and aromatic hydrocarbon fractions was performed on a Agilent 7890A GC fitted with a split/split less injector (at 280 °C) linked to an Agilent 5975C MSD (electron voltage 70eV, source temperature 230 °C, quadrupole temperature 150 °C multiplier voltage 1800V, interface temperature 310 °C); data acquisition and processing was by Agilent Chemstation software. Selected samples were analysed in full scan mode (50-600 amu/sec) but all samples were analysed in selected ion monitoring (SIM) mode (30 ions, 0.7cps, 35 ms dwell) for greater sensitivity. The sample (1 µl) in diluted in hexane/DCM was injected using an Agilent 7683B autosampler and the split opened 1 minute after the solvent peak had passed and the GC temperature programme and data acquisition commenced. Separation was performed on an Agilent fused silica capillary column (30 m x 0.25 mm i.d) coated with 0.25 µm 5% phenylmethylpolysiloxane (HP-5) phase. The GC was temperature programmed from 50-310 °C at 5 °C min and held at final temperature for 10 minutes with helium as the carrier gas (flow rate of 1 ml/min, initial inlet pressure of 50kPa, split at 30 ml/min).

The ions monitored in SIM mode for the aliphatic fractions included: *m/z* 85 (*n*-alkanes and isoprenoids), *m/z* 109 (diterpanes), *m/z* 123 (diterpanes and tricyclic terpanes), *m/z* 135 (methyladamantane, ethyladamantane), *m/z* 136 (adamantane), *m/z* 149 (dimethyladamantane, ethylmethyladamantane and trisnorhopanes), *m/z* 163 (trimethyladamantane and ethyldimethyladamantane), *m/z* 177 (tetramethyladamantane), *m/z* 183 (acylic isoprenoids and HDCH internal standard), *m/z* 187 *(*methyldiamantane*),* *m/z* 188 (diamantane), *m/z* 191 (triterpane), *m/z* 201 (dimethyldiamantane), *m/z* 205

(methyhopanes), *m/z* 215 (trimethyldiamantane), *m/z* 217 (regular steranes), *m/z* 218 (iso-steranes), *m/z* 231 (methyl steranes), *m/z* 238 (botryococcanes), *m/z* 257 (17α-steranes), *m/z* 259 (diasteranes), *m/z* 318 (C_{23} tricyclic terpanes), *m/z* 330 (C_{24} tetracyclic terpanes), *m/z* 358 (steranes), *m/z* 369 (triterpanes), *m/z* 370 (C_{27} triterpanes), *m/z* 372 (C_{27} steranes), *m/z* 384 (C_{27} triterpanes), *m/z* 386 (C_{28} steranes), *m/z* 398 (C_{27} triterpanes), *m/z* 400 (C_{29} steranes), *m/z* 410 (hopanes), *m/z* 412(C_{30} triterpanes), *m/z* 414 (triterpanes), *m/z* 426 (homohopanes).

The ions monitored in SIM mode for the aromatic fraction included: *m/z* 128 (naphthalene), *m/z* 142 (methylnaphthalenes), *m/z* 156 (dimethylnaphthalenes), *m/z* 170 (trimethylnaphthalenes), *m/z* 178 (phenanthrene), *m/z* 192 (methylphenanthrenes), *m/z* 184 (dibenzothiophene and tetramethylnaphthalenes), *m/z* 198 (methyldibenzothiophenes and pentamethylnaphthalenes), *m/z* 206 (dimethylphenanthrenes), *m/z* 212 (methyldibenzothiophenes), *m/z* 220 (trimethylphenanthrenes), *m/z* 226 (dimethyldibenzothiophenes), *m/z* 231 (triaromatic steroids), *m/z* 245 (methyltriaromatic steroids) and *m/z* 253 (monoaromatic steroids and 1,1-BN standard).

GC-MS analysis of the carbazole fraction was performed on a Agilent 7890A GC with a split/splitless injector (at 310 °C) linked to a Agilent 5975C MSD (electron voltage 70eV, source temperature 230 °C, quadrupole temperature 150 °C, multiplier voltage 1800V, interface temperature 310 °C) in SIM mode (23 ions 0.7cps 50ms dwell) for greater sensitivity. Data acquisition and processing was done using Agilent Chemstation software. The sample (1µl) in DCM was injected using an Agilent 7683B autosampler and the split opened after 1 minute. After the solvent peak had passed the GC temperature programme and data acquisition commenced. Separation was performed on an Agilent fused silica capillary column (30 m x 0.25 mm i.d) coated with 0.25µm 5% phenylmethylpolysiloxane (HP-5) phase. The GC oven was temperature programmed from 40-200 °C at 10 °C then

to 310 °C at 4 °C min and held at final temperature for 15 minutes with helium as the carrier gas (flow rate of 1 ml/min, initial pressure of 50kPa, split at 30 mls/min).

The ions monitored in the in SIM mode for the carbazole fraction included: *m/z* 167 (carbazole), *m/z* 175 (D_8-carbazole standard), *m/z* 181 (C_1 carbazole), *m/z* 195 (C_2 carbazole), *m/z* 209 (C_3 carbazole), *m/z* 223 (C_4 carbazole), *m/z* 237 (C_5 carbazole), *m/z* 217 (C_0 benzocarbazole), *m/z* 231 (C_1 benzocarbazole), *m/z* 245 (C_2 benzocarbazole) and *m/z* 259 (C_3 benzocarbazole).

GC-MS analysis of the light hydrocarbon (whole oil) compounds was performed on an Agilent 7890A GC split/split less injector (280 °C) linked to a Agilent 5975C MSD as above. All of the samples were analysed in full scan mode (10-235 amu/sec). The sample (ca. 0.2 µl of whole oil) was injected manually into the GC in split mode and separation was performed on an Agilent fused silica capillary column (60 m x 0.25 mm i.d) coated with 0.25 um 5% phenylmethyl polysiloxane (HP-5) phase. Helium was used as the carrier gas with flow rate of 1 ml/min and initial inlet pressure of 50 kPa and split at 30 mls/min. The GC was temperature programmed from 32 °C (where it was held for 5 mins) to 320 °C at a rate of 5 °C/min and then held for 12.4 mins, with total run time of 72 minutes. The injection/needle used for injecting the sample was always cleaned with methanol and DCM several times before allowing it to dry for about 60 minutes and then ready for use on the next sample.

Determination of concentration of individual compounds was based on comparing the peak area of a known concentration of an internal standard with those of the compounds to be measured. The analytes compound concentrations were measured using heptadecylcyclohexane as internal standard, which was later standardised using a condensate sample of known diamondoid and 5α cholestane concentrations.

The concentration of individual compounds was based on the equation below:

$X_A = (A_A/A_{IS})$ **x** C_{IS} **x** (1000/Oil wt).

Where:

X_A = Concentration of compound A.

Oil wt = Weight of oil.

C_{IS} = Concentration of internal standard added to sample.

A_A = Peak area of analyte.

A_{IS} = Peak area of internal standard.

Relative response factors (RRF) were calculated using the equation below:

$RRF = (A_X \mathbf{x} C_{IS}) / (A_{IS} \mathbf{x} C_X)$

Where:

RRF = Relative response factor

A_X = Area of compound

C_{IS} = Concentration of compounds

A_{IS} = Area of internal standard

C_X = Concentration of internal standard

2.11 Gas Chromatography-Mass Spectrometry/Mass Spectrometry (GC-MS-MS).

In order to confirm the peak identities, selected sample were analysed on a GC-MSMS instrument in multiple reaction monitoring (MRM) ms-ms mode to give parent-daughter transition chromatograms. GC-MSMS analysis of aliphatic compounds was performed on a Varian CP3800 GC split/splitless injector (280 °C) linked to a Varian 1200 triple quadrupole mass spectrometer (electron voltage 70eV, filament current 175uA, source temperature 230 °C, quadrupole temperature 40 °C multiplier voltage 1300V, interface temperature 300 °C). The acquisition was controlled by a Varian Software. Data were acquired in MS/MS (MRM) mode where up to 10 parent/daughter transitions could be monitored using argon as collision gas at a pressure of 2 mTorr in Q2, with collision energy of -10ev.

The sample (1µl) in DCM was injected using a Varian CP8400 autosampler and the split opened after 1 minute. After the solvent peak had passed, the GC temperature programme and data acquisition commenced and separation was performed on a fused silica capillary column (30m x 0.25mm i.d) coated with 0.25um 5% phenylmethylsilicone (HP-5), with helium as the carrier gas (flow 1 ml/min initial pressure of 50kPa, split at 30 ml/min). The

GC was temperature programmed from 50 °C -310 °C at 5 °C min and held at final temperature for 10 minutes.

The following parent-to-daughter ions transitions were monitored: for the steranes; 358→217 (C_{26} steranes), 372→217 (C_{27} steranes), 386→217 (C_{28} steranes), 400→217 (C_{29} steranes), 414→217 (C_{30} steranes), 412→369 (C_{30} bicadinanes), 426→383 (methylbicadinanes), 414→231 (dinosteranes) for the pentacyclic and tricyclic terpanes; 370→191 (C_{27} pentacyclic terpanes), 384→191 (C_{28} pentacyclic terpanes), 398→191 (C_{29} pentacyclic terpanes), 412→191 (C_{30} pentacyclic terpanes), 426→191 (C_{31} pentacyclic terpanes), 440→191 (C_{32} pentacyclic terpanes), 454→191 (C_{33} pentacyclic terpanes), 468→191 (C_{34} pentacyclic terpanes), 496→191 (C_{34} pentacyclic terpanes), 346→191 (C_{25} tricyclic terpanes), 360→191 (C_{26} tricyclic terpanes), 374→191 (C_{27} tricyclic terpanes), 388→191 (C_{28} tricyclic terpanes), 402→191 (C_{29} tricyclic terpanes), 346→177 (C_{25} demethylated tricyclic terpanes), 360→177 (C_{26} demethylated tricyclic terpanes), 374→177 (C_{27} demethylated tricyclic terpanes), 388→177 (C_{28} demethylated tricyclic terpanes), for the diamondoids; 136→93 (adamantane), 150→135 (methyladamantane), 164→149 (dimethyladamantane), 178→163 (trimethyladamantane), 164→135 (ethyladamantane), 178→149 (ethylmethyladamantane), 188→131 (diamantane), 201→187 (methyldiamantane), 216→201 (dimethyldiamantane) and 203→215 (trimethyldiamantane).

2.12 Gas Chromatography Isotope Ratio Mass Spectrometry (GC-irMS).

Compound specific isotope ratio analysis (CSIA) measurements were performed on individual *n*-alkanes in the aliphatic hydrocarbon fractions using a ThermoFinnigan Delta V+ system. The *n*-alkanes sample diluted in hexane solvent (1 µl) was injected, using a CTC GC-PAL autosampler, via a heated split/splitless injector into a Thermo Trace GC fitted with an Agilent fused silica capillary column (30 m x 0.25 mm i.d) coated with 0.25

μm 5% phenylmethylpolysiloxane (HP-5) phase with helium as carrier gas. Each component eluting from the column passed into a cross piece union where 10% flowed to the GC-FID and an external split and 90% was diverted to a furnace tube where the compounds were oxidized in the GC Combustion III interface and converted to either carbondioxide (CO_2) or reduced to hydrogen depending on which mode the machine was set to.

In carbon mode, after passing through the heated (940 °C) oxidation furnace tube the compounds were oxidized and the gases generated passed through to a reduction furnace (640 °C) where any nitrous oxides were reduced to N_2 and surplus oxygen is removed from the analyte stream. The resulting CO_2 gas then passed into a capillary interface where water was removed in a Nafion tube and then to an open split narrow bore capillary interface. The analyte gas was then transferred to the IRMS through a micro capillary isolation valve, where the gas was ionized and the resulting ions separated in a magnetic field to give an isotopic ratio value determined from a pulsed reference gas calibrated from a reference alkane prepared by Dr. A. Schimmelmann of Indiana University, USA.

In hydrogen mode, after passing through the heated furnace tube (1400 °C) the analyte compound gases generated passed into a capillary interface where water was removed via a Nafion tube and then to an open split narrow bore capillary interface. The analyte gas stream was then transferred to the IRMS, through a micro capillary isolation valve, where the gas was ionized and the resulting H^+, H_2^+, H_3^+ ions separated in a magnetic field to give an isotopic ratio value determined from a reference alkane.

Several replicates were run with batches to check the reproducibility of the results; compound peaks with intensities outside the range of 1-5 volts were rejected since very low or high values have low reproducibility.

CHAPTER THREE
POTENTIAL SOURCE ROCK RESULTS AND CHARACTERISATION

3.0 Introduction

Fifty cuttings samples were selected from 6 wells across the Niger Delta Basin based mainly on their grain size (fine) and colour (dark), some wells had a higher number of samples taken than others because of the number of samples available in those wells and the depths sampled. It should be noted that no background information was provided on these wells and the basis of their selection was not disclosed.

The second part investigates the cuttings samples of potential source rocks from the wells. Since the basin is highly petroliferous then the source for the vast amount of hydrocarbons in the basin must be very rich, with good generative potential, thermally mature and the trapping system must have been in place before or during expulsion and migration of the hydrocarbon from the source. It has been noted that well cuttings samples are easily contaminated and should only be used where there is no core sample available for geochemical analyses (Peters *et al*., 2005), but this study takes care to identify potential sample contamination.

3.1 POTENTIAL SOURCE ROCK SAMPLES RESULTS

In an attempt to present a detailed geochemical study of the cuttings samples from the 6 Niger Delta wells, several parameters (mainly ratios and some concentrations) were calculated from the TOC (50 samples), Rock-Eval pyrolysis (33 samples), TLC-FID (30 samples) and the numerous peaks measured in the GC and GC-MS (30 samples) and GCIRMS (15 samples in carbon mode and 6 samples in hydrogen mode) analyses.

Three cuttings samples were selected from well BA-1 (10,100 – 11,145 ft., offshore), 4 cuttings samples were selected from well BA-SW (12,815 – 13,400 ft., offshore), 10 cuttings samples were selected from well EA (3,950 – 7,423 ft., shallow offshore), 5

cuttings samples were selected from well KA (6,961 – 9,780 ft., shallow offshore), 3 cuttings samples were selected from well KI (8,437 – 8,569 ft., Eastern Delta) and 25 cuttings samples were selected from well JK (3,670 – 12,980 ft., Western Delta).

3.1.1 Total Organic Carbon (TOC) content / Source rock pyrolysis

The total organic carbon (TOC) content of the source rocks varies widely but is generally very low in cuttings samples from well EA and high in cuttings samples from well JK (Figure 3.1). The TOC of cuttings samples from well BA-1 range from 0.97% to 1.34% with an average of 1.16% and that of cuttings samples from well BA-SW, ranges from 0.56% to 0.68% with an average of 0.62%. The TOC of cuttings samples from well EA range from 0.08% to 2.87% with an average of 0.56% and that of cuttings samples from well JK ranges from 0.57% to 5.26% with an average of 1.92%. The TOC of cuttings samples from well KA range from 0.02% to 4.12% with an average of 1.51%, that of cuttings samples from well KI ranges from 0.5% to 1.7% with an average of 1.14% (Figure 3.1). The TOC of the cuttings samples from the six wells does not show any relationship with change in depth (Table 3.1).

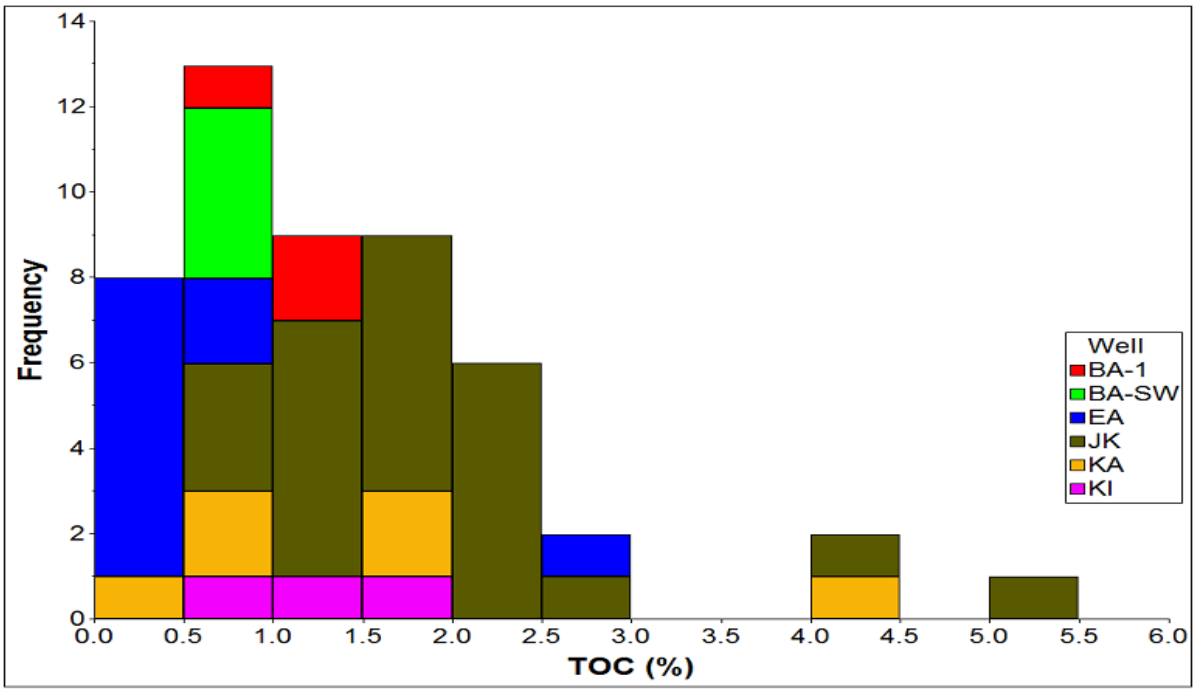

Figure 3.1: Variation in TOC contents in the cuttings samples from the 6 Niger Delta wells, showing low TOC values in most intervals of well EA and high TOC values in most intervals of well JK. The other wells have marginal concentrations of organic matter in most of the sampled intervals.

There is a wide variation in S2 values in the sampled wells with several units within a well having widely different values and also wide differences from well to well (Figure 3.2). Well KA cuttings samples have S2 contents averaging around 4 mg HC/g rock, with the exception of one interval with high S2 values (16 mg HC/g rock); well JK cuttings samples have an average of 4.6 mg HC/g rock. The cuttings samples of well BA-1 have values between 4.18 to 7.22 mg HC/g rock, whereas the values for the cuttings samples from wells BA-SW, EA and KI are generally below 2 mg HC/g rock (Figure 3.2).

The Tmax values of the cuttings samples from well EA are generally lower than 425 °C whereas those of well BA-SW are generally higher than 475 °C and the other cuttings samples from the other wells (BA-1, JK, KA and KI) are generally within the 425 to 475 °C range (Figure 3.3). The average hydrogen index (HI) of the cuttings samples from the different wells varies considerably, with the average HI of cuttings samples from well KI being 73.8 mg/gTOC, well KA is 144 mg/gTOC, well EA is 146 mg/gTOC, well JK is 217 mg/gTOC, well BA-SW is 307 mg/gTOC and BA-1 is 456 mg/gTOC (Table 3.1).

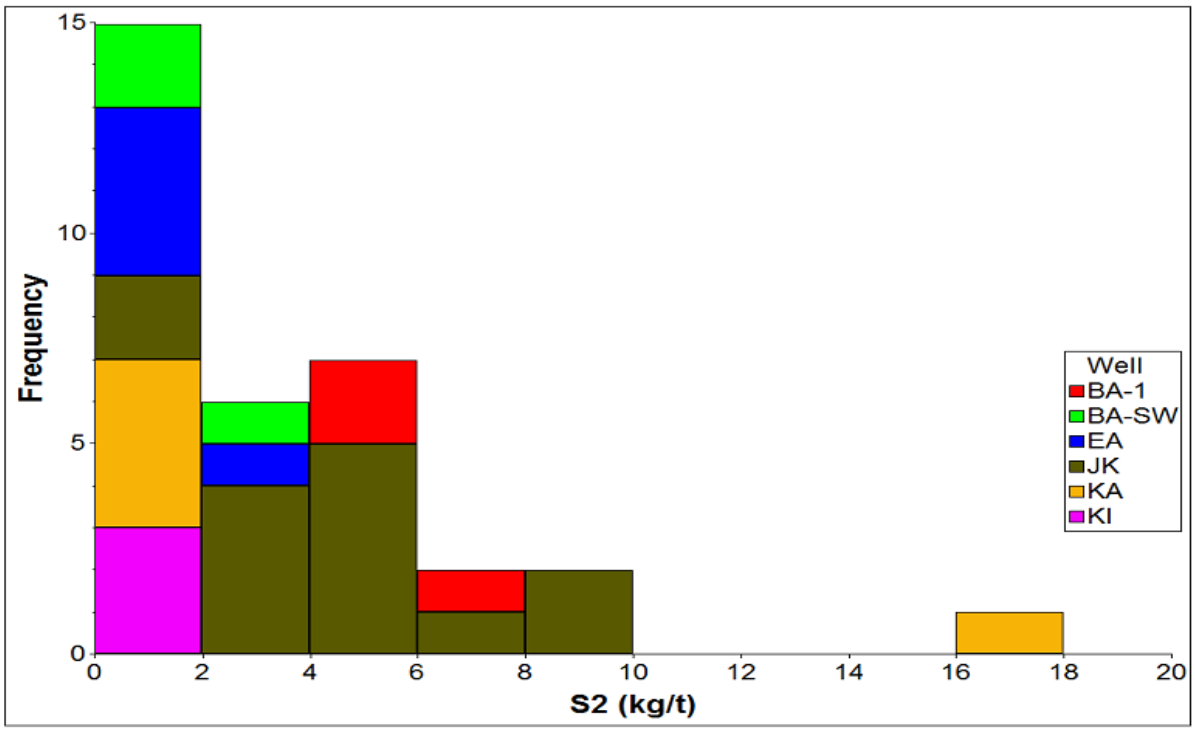

Figure 3.2: Variation in Rock-Eval S2 values across the 6 Niger Delta wells showing low values in most wells whereas well JK and BA-1 have high values in most sampled intervals.

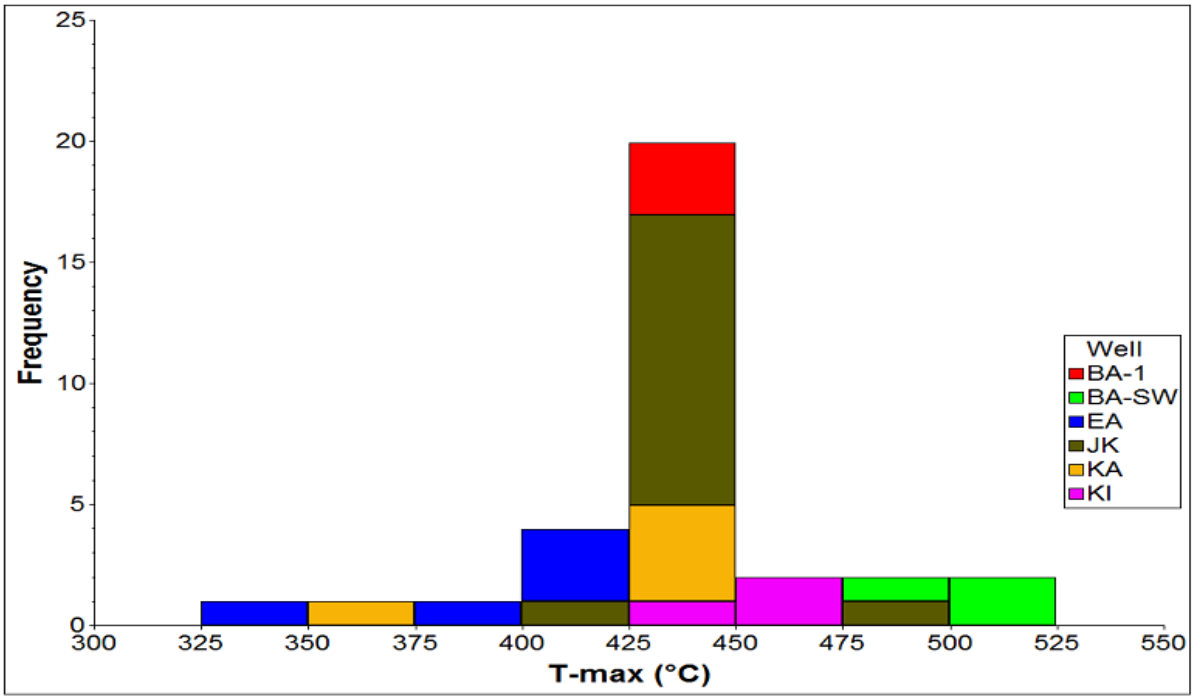

Figure 3.3: Variation in Rock-Eval Tmax values across 6 Niger Delta wells showing the low values in well EA and high values in well BA-SW.

Table 3.1: Summary of TOC and Rock-Eval pyrolysis data from the well cuttings samples.

	Well	Top-Depth (ft)	Base-Depth (ft)	TOC (wt%)	S0 (mg/g)	S1 (mg/g)	S2 (mg/g)	T-max (°C)	HI (mg/gTOC)	PI
OEE 1	BA-1	10100	10105	0.97	0.02	1.42	4.18	425	431	0.25
OEE 21	BA-1	10580	10585	1.34	0.09	4.56	7.22	436	539	0.39
OEE 2	BA-1	11145	11150	1.17	0	1.77	4.66	427	398	0.28
OEE 3	BA-SW	12815	12820	0.61	0	0.15	1.95	490	320	0.07
OEE 22	BA-SW	12905	12910	0.56	nm	nm	nm	nm	nm	nm
OEE 4	BA-SW	13115	13120	0.65	0	0.11	2.25	502	346	0.05
OEE 5	BA-SW	13400	13405	0.68	0	0.33	1.74	504	256	0.16
OEE 23	EA	3950	3955	0.55	0	6.93	2.3	334	418	0.75
OEE 24	EA	4784	4789	0.08	nm	nm	nm	nm	nm	nm
OEE 7	EA	4955	4960	0.29	0.21	0.35	0.5	394	172	0.41
OEE 8	EA	4966	4971	0.24	0	0.18	0.22	405	92	0.45
OEE 6	EA	6022	6027	2.87	0	0.54	0.98	410	34	0.36
OEE 25	EA	6157	6162	0.28	nm	nm	nm	nm	nm	nm
OEE 26	EA	6386	6391	0.13	nm	nm	nm	nm	nm	nm
OEE 27	EA	7050	7060	0.26	nm	nm	nm	nm	nm	nm
OEE 9	EA	7080	7085	0.81	0	0.52	0.12	411	15	0.81
OEE 28	EA	7423	7428	0.09	nm	nm	nm	nm	nm	nm
OEE 16	KA	6961	6966	1.51	0.03	0.59	0.58	427	38	0.5
OEE 47	KA	7021	7026	4.12	0	12.87	16.01	368	389	0.45
OEE 17	KA	9710	9715	1.83	0.02	2.43	1.97	427	108	0.55
OEE 48	KA	9716	9721	0.72	0	0.25	0.66	430	92	0.27
OEE 49	KA	9768	9773	0.02	nm	nm	nm	nm	nm	nm
OEE 18	KA	9780	9785	0.86	0	0.09	0.82	438	95	0.1
OEE 19	KI	8437	8442	1.2	0	0.05	0.41	450	34	0.11
OEE 50	KI	8448	8453	1.72	0.07	0.16	1.71	449	99	0.09
OEE 20	KI	8569	8564	0.51	0	0.02	0.45	451	88	0.04
OEE 10	JK	3670	3675	2.65	0	5.5	1.13	403	43	0.83
OEE 29	JK	4070	4075	1.03	0.12	7.05	1.38	484	134	0.84
OEE 30	JK	4550	4555	0.57	nm	nm	nm	nm	nm	nm
OEE 31	JK	4580	4585	0.93	nm	nm	nm	nm	nm	nm
OEE 32	JK	4670	4675	1.94	nm	nm	nm	nm	nm	nm
OEE 33	JK	4910	4915	2.45	0.08	22.97	3.46	429	141	0.87

Contd.

Table 3.1 (Contd.): Summary of TOC and Rock-Eval pyrolysis data from the well cuttings samples.

	Well	Top-Depth (ft)	Base-Depth (ft)	TOC (wt%)	S0 (mg/g)	S1 (mg/g)	S2 (mg/g)	T-max (°C)	HI (mg/gTOC)	PI
OEE 34	JK	5330	5335	2.29	0.01	24.88	4.4	431	192	0.85
OEE 11	JK	5600	5605	1.54	0	19.77	3.6	432	234	0.85
OEE 35	JK	5990	5995	1.81	nm	nm	nm	nm	nm	nm
OEE 36	JK	6200	6205	1.3	0	11.04	3.54	436	272	0.76
OEE 37	JK	6590	6595	1.53	nm	nm	nm	nm	nm	nm
OEE 38	JK	6920	6925	5.26	0.01	26.82	8.26	427	157	0.76
OEE 39	JK	7340	7345	2.02	0.01	24	4.17	430	206	0.85
OEE 12	JK	7610	7615	1.29	0	14.65	3.08	427	239	0.83
OEE 40	JK	8390	8395	2.42	nm	nm	nm	nm	nm	nm
OEE 41	JK	8900	8905	0.96	nm	nm	nm	nm	nm	nm
OEE 13	JK	9620	9625	1.44	0.01	22.16	4.8	428	333	0.82
OEE 42	JK	9980	9985	1.71	nm	nm	nm	nm	nm	nm
OEE 43	JK	10490	10495	1.45	nm	nm	nm	nm	nm	nm
OEE 44	JK	10910	10910	1.12	nm	nm	nm	nm	nm	nm
OEE 14	JK	11600	11605	1.6	0.05	38.84	5.47	433	342	0.88
OEE 45	JK	12020	12025	2.28	0	38.58	4.92	427	216	0.89
OEE 46	JK	12560	12565	4.11	0.06	38.21	8.75	430	213	0.81
OEE 15	JK	12980	12985	2.36	0.04	46.18	7.65	435	324	0.86
Replicate (avg.)				2.91	0.00	0.53	0.96	410	32.9	0.36
Replicate (std. error)				1.19		1.79	2.32	0.32	2.14	1.86

TOC: Total Organic Carbon content (%) in rock, S0: Pyrolysis peak S0, free gas hydrocarbons, S1: Pyrolysis peak S1, free liquid hydrocarbons, S2: Pyrolysis peak S2, pyrolysate hydrocarbons, T-max: Temperature of maximum pyrolysate yield, HI: S2 normalised to the organic carbon content (S2/TOC) x 100, PI: S1/(S1+S2), nm: not measured.

3.1.2 Extractable Organic Matter (EOM) and Iatroscan (TLC-FID)

The extractable organic matter (EOM) yields of the cuttings sample from five of the six wells are similar, i.e. generally lower than 10 mg/g in all the wells with the exception of one interval which is above 10 mg/g in well EA and almost all the intervals in well JK are also above 10 mg/g (Figure 3.4). The cuttings samples from well JK had a distinct smell of hydrocarbons and looked very dark, which might indicate that they are either rich in organic matter or contaminated with drilling mud.

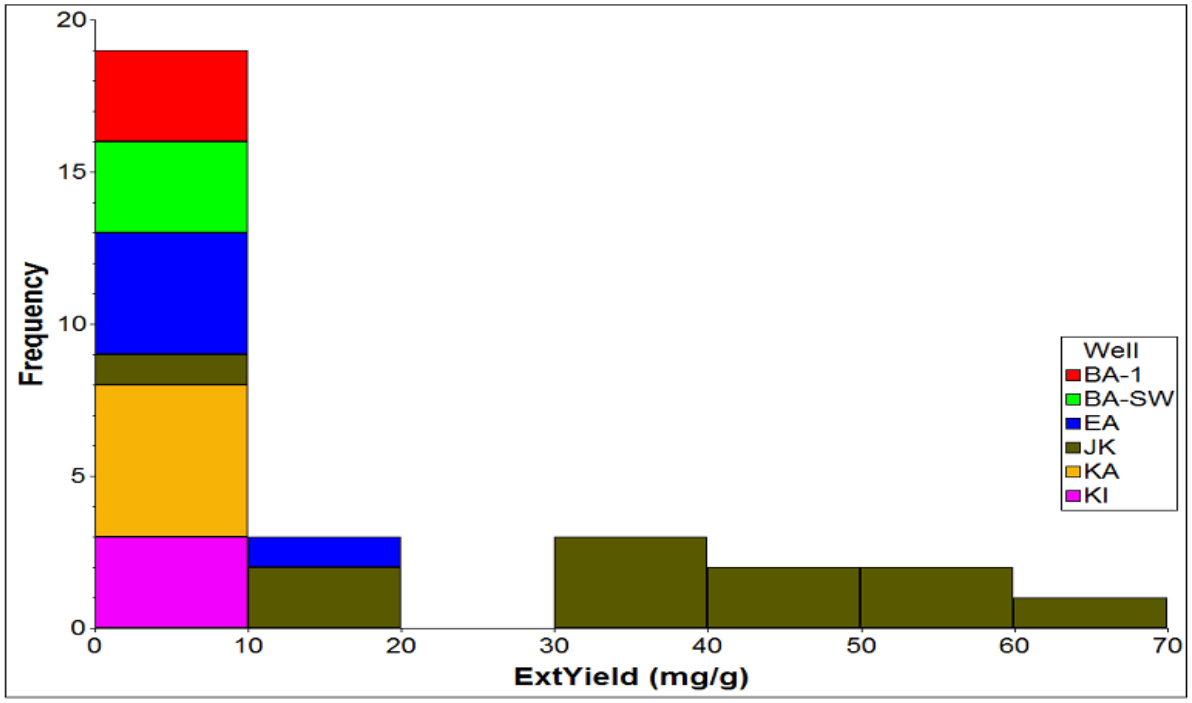

Figure 3.4: Variation in Extractable Organic Matter yield (EOM) across 6 Niger Delta wells showing the high yields in well JK and low yields in most intervals of the other wells.

Iatroscan TLC-FID SARA analysis (Figure 3.5) of the well cuttings extracts shows variations in the bulk composition and a ternary plot (Figure 3.6) indicates that the cuttings samples of well JK have relatively high saturated and aromatic hydrocarbon contents and are different from the other cuttings sample of the other wells with the exception of two intervals in well EA. The cuttings samples from wells BA-SW, BA-1 and KI have relatively lower saturated

and aromatic hydrocarbon contents but with high polar contents. The cuttings samples from well KA has a wide variation as in all the sampled intervals, as shown in figure 3.6.

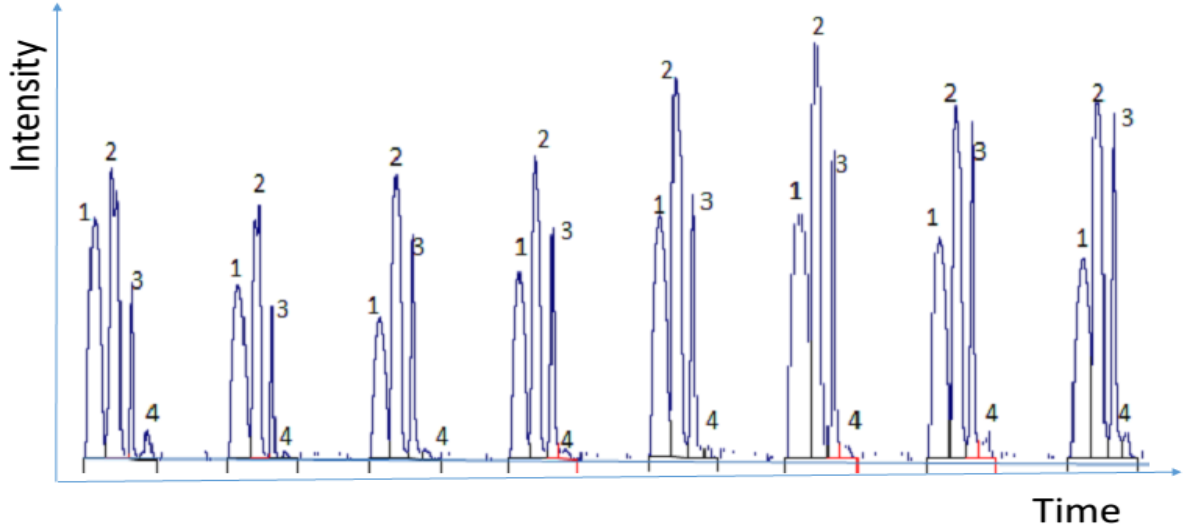

Figure 3.5: Representative TLC-FID chromatograms of cuttings extract samples showing SARA contents.
1= Saturated hydrocarbon fraction. **2=** Aromatic hydrocarbon fraction. **3=** Polar (NSO) fraction. **4=** Asphaltenes fraction.

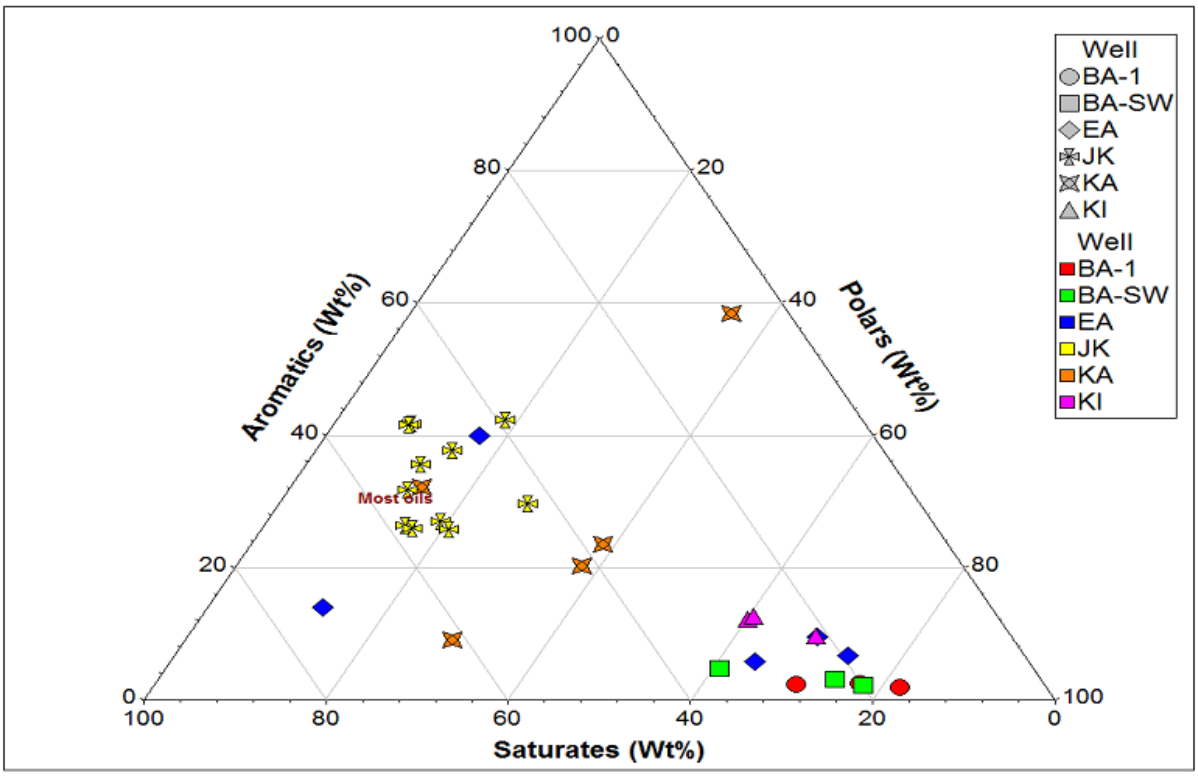

Figure 3.6: Ternary plot of saturates, aromatics and polars content in Niger Delta well cuttings samples as determined by Iatroscan TLC-FID. Note the wide range of bulk geochemical compositions across the Niger Delta.

Table 3.2: Summary of extract yields and Iatroscan (TLC-FID) data from well cuttings samples.

	ExtYield (mg/g)	Sats (Wt%)	Arom (Wt%)	NSO (Wt%)	Asph (Wt%)	CNE (mgExtr/gTOC)	CNH (mgHC/gTOC)	Sats/Arom
OEE 1	4.80	15.0	2.2	76.8	6.0	498	86	6.87
OEE 2	6.40	10.4	2.1	79.6	7.9	549	69	5.02
OEE 3	2.20	9.7	2.1	63.6	24.6	363	43	4.58
OEE 4	0.90	8.3	1.5	63.9	26.4	144	14	5.69
OEE 5	1.50	16.8	3.8	59.0	20.4	221	45	4.41
OEE 6	3.10	10.8	7.8	69.2	12.2	108	20	1.37
OEE 7	0.60	8.8	4.9	66.5	19.8	191	26	1.79
OEE 8	0.60	14.2	4.4	60.3	21.1	241	45	3.20
OEE 9	0.60	56.6	17.4	19.5	6.5	77	57	3.25
OEE 10	8.90	37.1	30.1	26.1	6.7	334	225	1.24
OEE 11	30.50	33.8	37.6	16.4	12.2	1977	1412	0.90
OEE 12	15.40	29.4	22.9	22.4	25.3	1192	624	1.28
OEE 13	32.90	29.6	38.2	18.7	13.4	2284	1550	0.78
OEE 14	55.30	33.3	45.3	11.3	10.2	3453	2711	0.74
OEE 15	49.10	31.5	42.3	10.3	15.9	2079	1532	0.74
OEE 16	2.80	22.8	23.1	46.5	7.6	182	84	0.99
OEE 17	3.30	38.1	37.2	20.4	4.3	178	134	1.02
OEE 18	0.90	25.1	19.8	45.3	9.8	100	44	1.27
OEE 19	2.70	14.3	10.2	62.0	13.5	227	55	1.39
OEE 20	0.60	10.2	7.5	65.5	16.9	116	20	1.37
OEE 21	7.50	8.1	1.6	82.1	8.2	558	54	5.21
OEE 23	12.30	29.3	44.0	22.6	4.0	2227	1634	0.67
OEE 36	16.10	18.0	20.2	22.7	39.1	1239	473	0.89
OEE 38	41.90	39.7	29.3	21.0	10.0	796	549	1.36
OEE 40	38.90	37.0	27.0	21.1	14.9	1609	1030	1.37
OEE 45	56.70	36.1	33.7	16.9	13.3	2484	1734	1.07
OEE 46	60.10	24.6	43.2	23.1	9.2	1463	991	0.57
OEE 47	10.00	3.3	48.4	35.8	12.5	242	125	0.07
OEE 48	2.70	43.6	10.4	41.3	4.7	377	203	4.19
OEE 50	2.20	14.1	10.9	63.7	11.3	128	32	1.29
Replicate (avg.)		55.66	35.53	5.30	3.51			1.57
Replicate (std. error)		0.72	0.45	0.27	1.57			0.03

ExtYield: weight of extract normalised to the amount of rock sample extracted (Weight Extract /Weight Rock), Sat%: % of saturated hydrocarbon fraction, Aro%: % of aromatic hydrocarbon fraction. NSO%: % of polar hydrocarbon fraction. Asph%: % of Asphaltene hydrocarbon fraction, CNE: amount of extracted organic matter (EOM) relative to TOC (Extract yield) / (TOC content), CNH: Carbon Normalised Hydrocarbons (% Saturated and Aromatic hydrocarbons) x CNE.

3.1.3 *n*-alkanes and Isoprenoids

The *n*-alkane/isoprenoid alkane variations are based on ratios calculated from the gas chromatograms of the aliphatic hydrocarbon fractions (Figure 3.7 & 3.8). Although calculations which involved high molecular weight *n*-alkanes were not possible for samples from well JK because peaks higher than nC_{26} were not present in their chromatograms (Figure 3.8), the following ratios were calculated: Pr/Ph (c.f. Peters & Moldowan, 1993); norPr/Pr (c.f. Peters & Moldowan, 1993); Pr/nC_{17} (c.f. Peters & Moldowan, 1993); Ph/nC_{18} (c.f. Peters & Moldowan, 1993); nC_{17}/nC_{27} (c.f. Peters & Moldowan, 1993); CPI-1 (c.f. Philippi, 1965); CPI-2 (c.f. Bray & Evans, 1961); CPI-3 (c.f. Scalan & Smith, 1970).

The Pr/Ph ratios of the well cuttings samples (Figure 3.9) show that samples from well JK have low values (< 1.5) whereas cuttings samples from well KA are between 2 and 2.5. Cuttings samples from wells BA-1 and BA-SW have values between 1 and 2.5, whereas cuttings samples from well EA and KI varies with sampled interval and a wide range is possible (1 to 3.5) for these wells (Figure 3.9). The Pr/nC_{17} and Ph/nC_{18} results (Figures 3.10 & 3.11) shows that the cuttings samples from well JK generally have values less than 0.5 but those for well EA have elevated values which are far higher than the other wells and the values are in the range of 1 to 4 (Pr/nC_{17}) and 0.5 to 2.5 (Ph/nC_{18}). Cuttings from wells BA-SW, BA-1, KA and KI have values in the range of 0.5 to 2 (Pr/nC_{17}) and 0.5 to 1.5 (Ph/nC_{18}) as shown on figures 3.10 & 3.11.

The nC_{17}/nC_{27} ratios of the cuttings samples show no results for well JK because of the apparent absence of nC_{27} in the extracts from the samples, whereas wells BA-1 and BA-SW generally have values below 8 and samples from well KA have values less than 4. Well EA cuttings samples have values less than 4 with the exception of an interval with a value greater than 20 and well KI samples generally show elevated values generally higher than 16 but less than 36 (Figure 3.12 and Table 3.3).

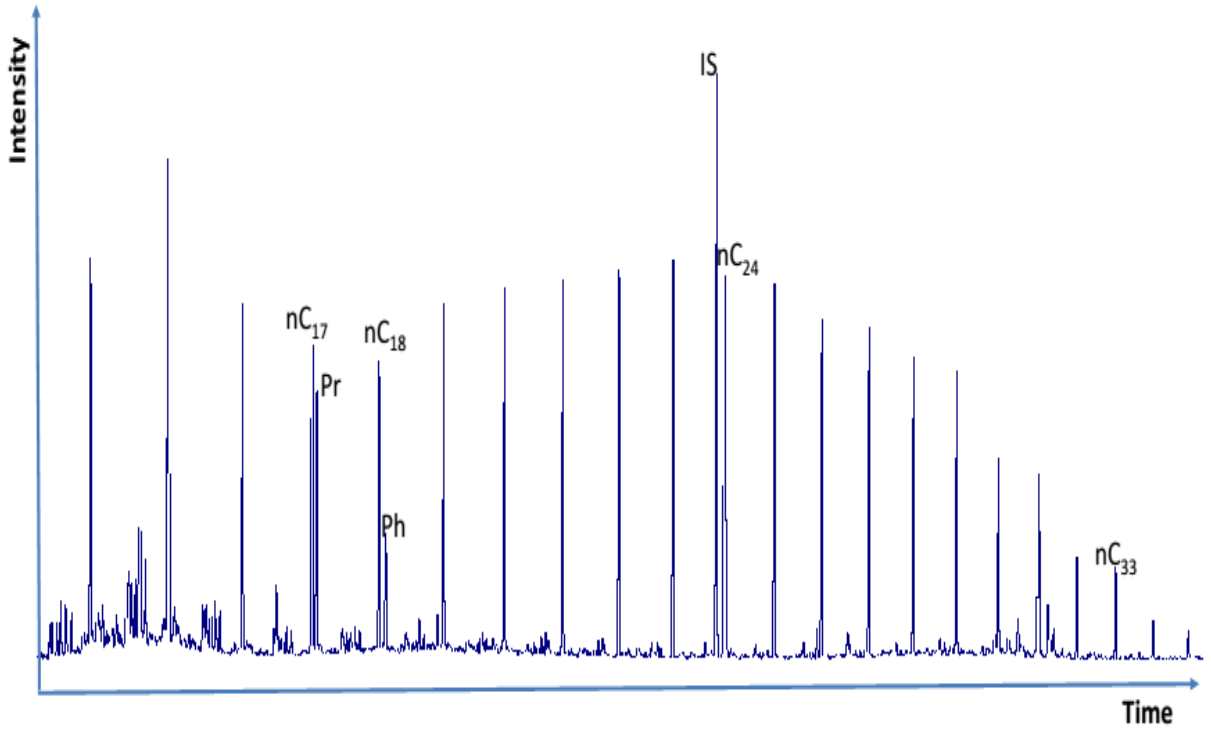

Figure 3.7: Representative gas chromatogram of the aliphatic hydrocarbon fraction of cuttings sample OEE016 (Well KA, Depth 6,966 ft).

nC_{13}: n-Tridecane, nC_{17}: n-Heptadecane, pr: pristane, nC_{18}: n-Octadecane, ph: phytane, I.S (internal standard): n-heptadecylcyclohexane (HCDH), nC_{30}: n-Tricontane.

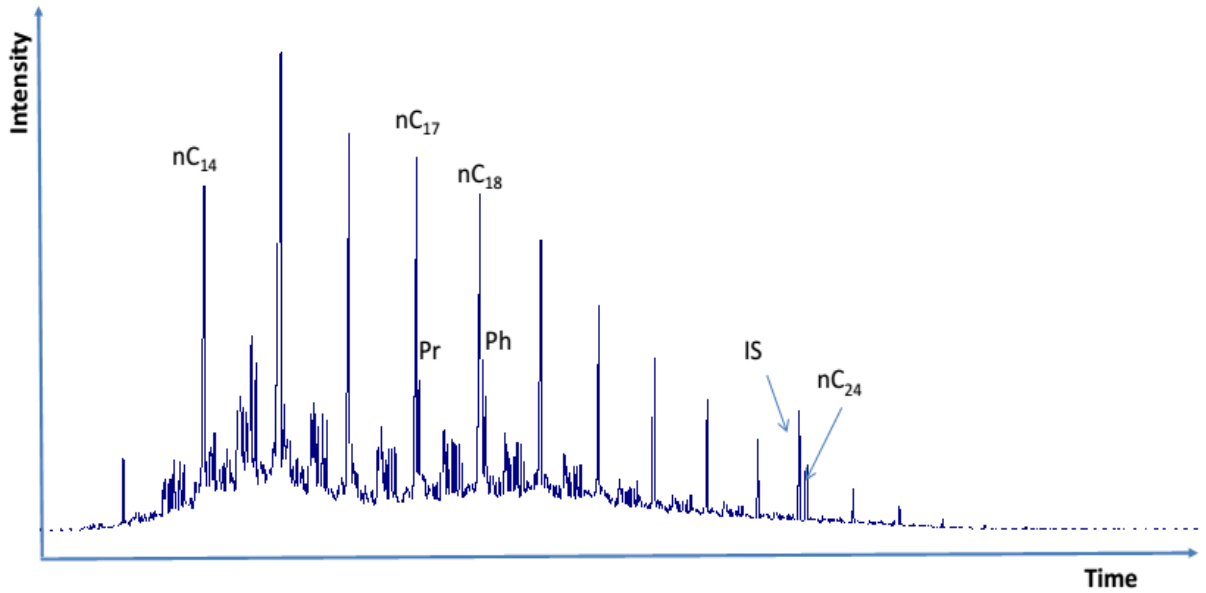

Figure 3.8: Representative GC chromatogram of aliphatic hydrocarbon fraction from well JK cuttings with some possibility of contamination with drilling mud (OEE015, Depth 12,985 ft).

nC_{13}: n-Tridecane, nC_{17}: n-Heptadecane, pr: pristane, nC_{18}: n-Octadecane, ph: phytane, I.S (internal standard): n-heptadecylcyclohexane (HCDH)). Note the range of *n*-alkane present (nC_{13} to nC_{26}).

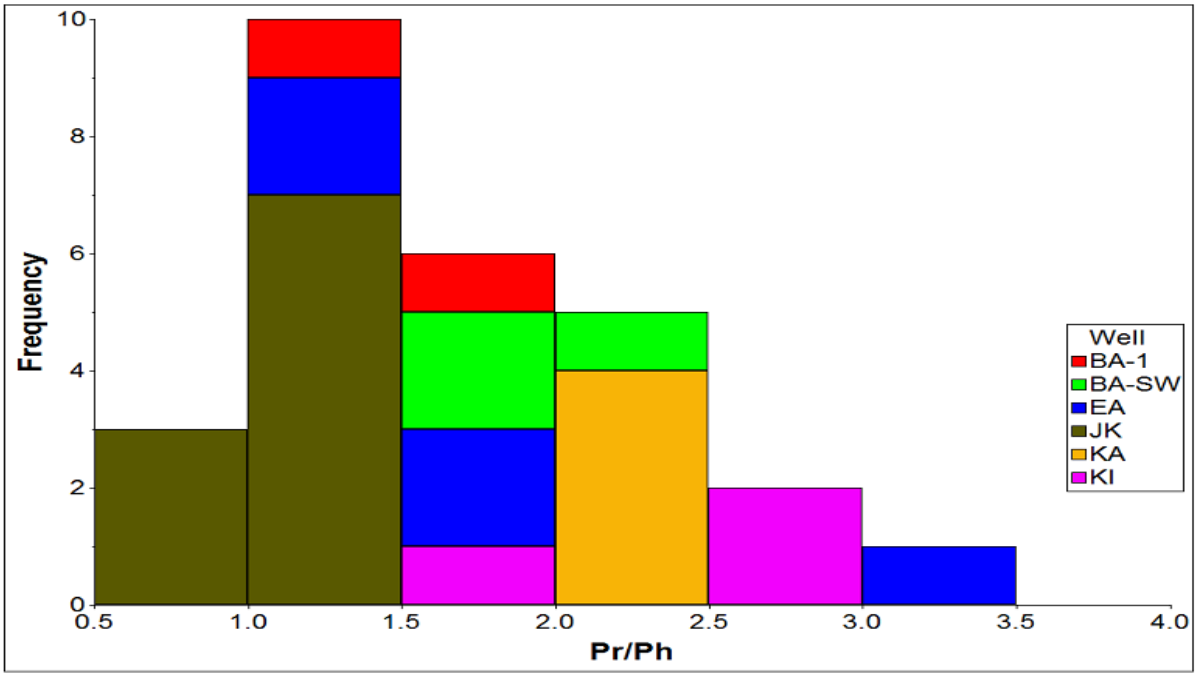

Figure 3.9: Variation in Pr/Ph ratios of the cuttings samples from the 6 Niger Delta wells showing low Pr/Ph in well JK samples when compared to other well cuttings extracts.

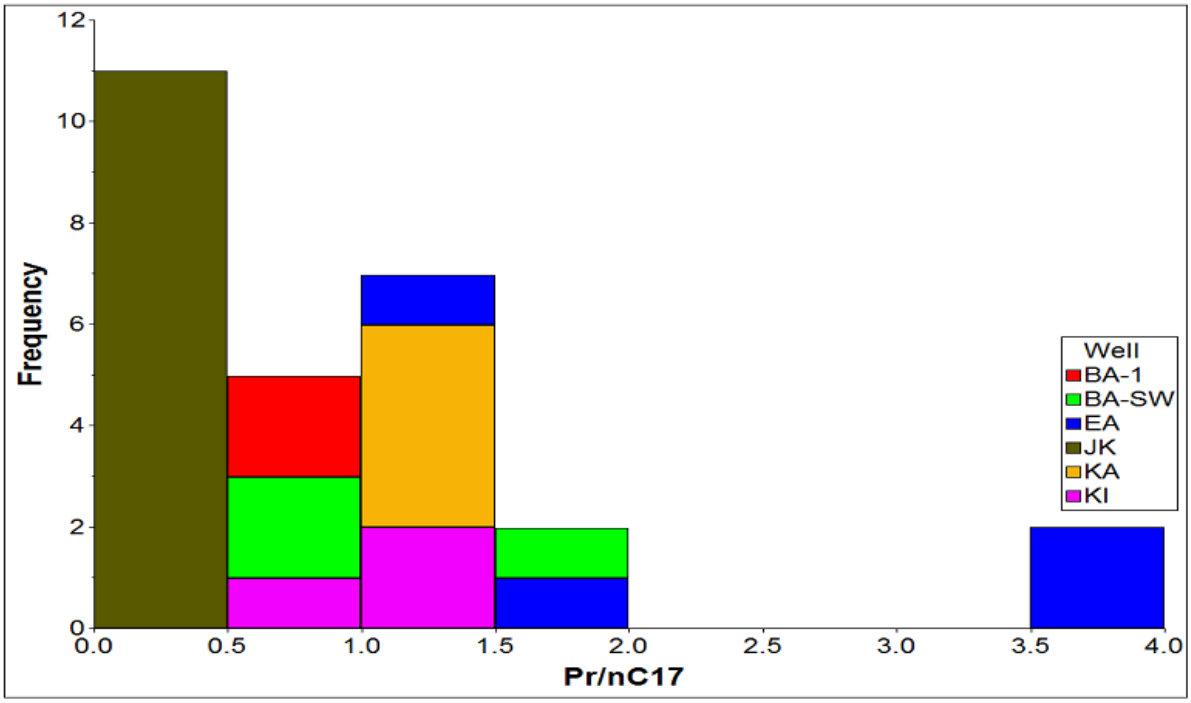

Figure 3.10: Variation in Pr/nC_{17} ratios of the cuttings samples from the 6 Niger Delta wells showing low Pr/nC_{17} in well JK samples and high Pr/nC_{17} in well EA samples when compared to other well cuttings extracts.

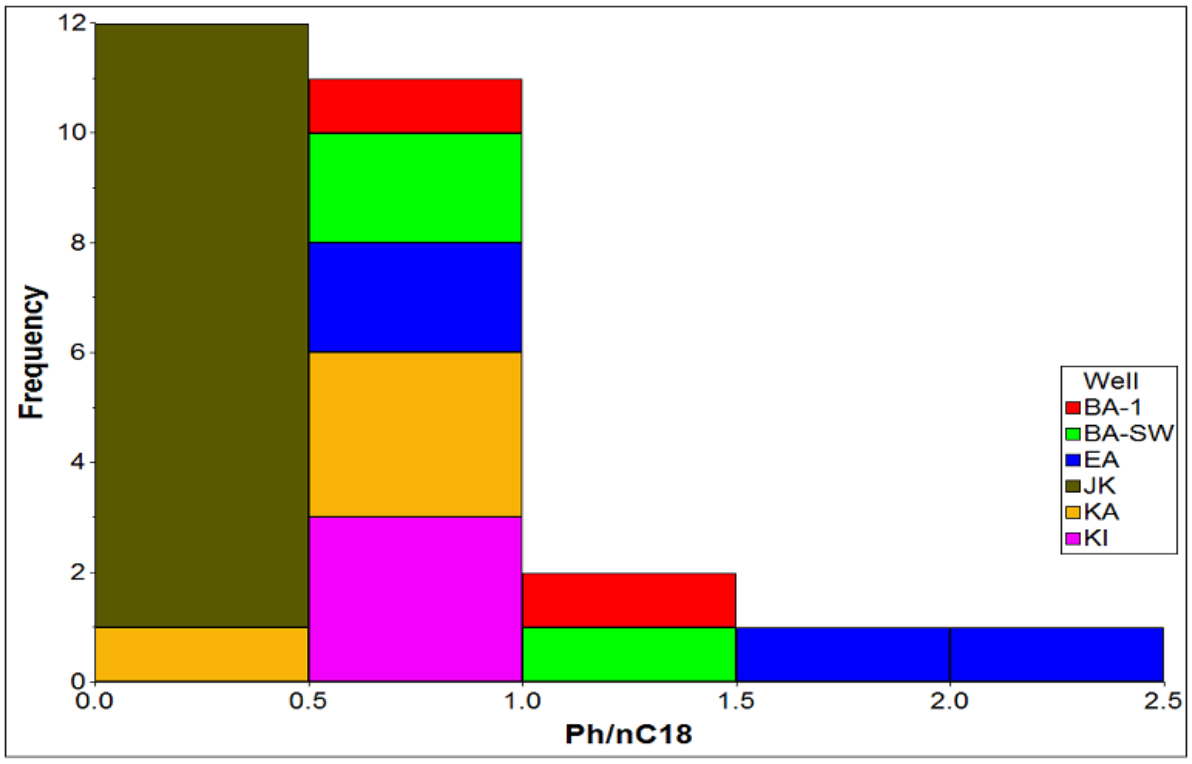

Figure 3.11: Variation in Ph/nC_{18} ratios of the cuttings samples from the 6 Niger Delta wells showing low Ph/nC_{18} in well JK samples and high Ph/nC_{18} in well EA samples when compared to other well cuttings extracts.

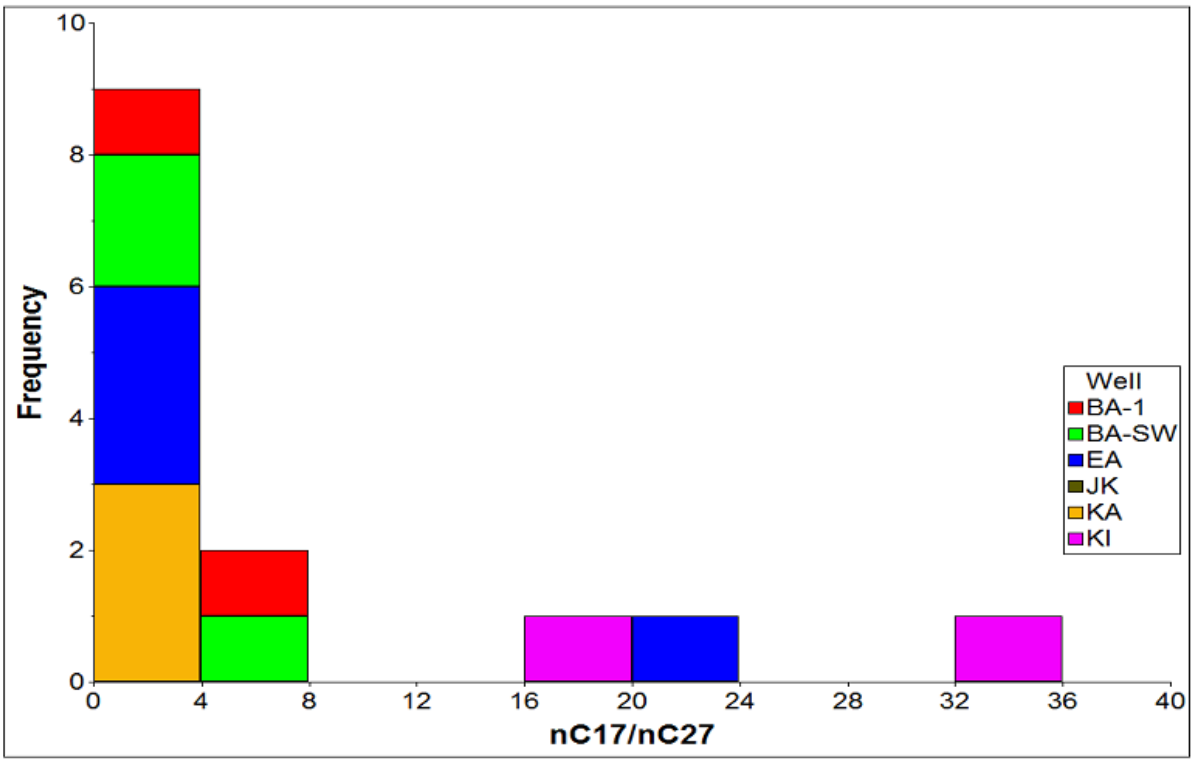

Figure 3.12: Variation in *n*C_{17}/*n*C_{27} ratio of the cuttings samples from the 6 Niger Delta wells showing high nC_{17}/nC_{27} in well KI samples and one interval in well EA when compared to other well cuttings extracts.

Table 3.3: Summary of *n*-alkane and isoprenoid results from the well cuttings samples.

	Pr/Ph	norpr/pr	Pr/nC_{17}	Ph/nC_{18}	nC_{17}/nC_{27}	CPI-1	CPI-2	CPI-3
OEE 1	1.63	0.19	0.77	1.07	2.91	1.46	nm	1.48
OEE 2	1.35	0.12	0.63	0.79	4.37	2.70	nm	2.77
OEE 3	1.96	0.14	0.81	0.64	3.27	2.20	nm	2.24
OEE 4	1.84	0.07	1.59	1.30	1.19	2.34	nm	2.40
OEE 5	2.06	0.16	0.84	0.83	5.15	2.33	nm	2.36
OEE 6	3.20	0.36	1.42	0.56	21.78	1.07	nm	0.97
OEE 7	1.66	0.03	3.67	2.03	3.62	1.37	nm	1.33
OEE 8	1.28	0.14	6.41	4.61	2.93	1.45	nm	1.41
OEE 9	1.74	0.20	1.86	0.69	0.22	1.12	1.13	1.12
OEE 10	1.26	0.33	0.25	0.27	nm	nm	nm	nm
OEE 11	1.22	0.36	0.25	0.25	nm	nm	nm	nm
OEE 12	1.15	0.82	0.25	0.26	nm	nm	nm	nm
OEE 13	1.01	0.35	0.23	0.23	nm	nm	nm	nm
OEE 14	1.29	0.19	0.22	0.22	nm	nm	nm	nm
OEE 15	1.04	0.82	0.23	0.25	nm	nm	nm	nm
OEE 16	2.29	0.22	1.18	0.52	0.83	1.20	1.15	1.17
OEE 17	2.13	nm	1.07	0.44	0.35	1.18	nm	1.16
OEE 18	2.15	0.21	1.09	0.64	2.44	2.27	nm	2.29
OEE 19	2.74	0.20	1.13	0.70	nm	nm	nm	nm
OEE 20	1.98	0.22	1.37	0.65	35.40	nm	nm	nm
OEE 23	1.44	nm	3.66	1.72	nm	nm	nm	nm
OEE 36	7.24	0.80	0.28	0.05	nm	nm	nm	nm
OEE 38	1.08	0.64	0.33	0.36	nm	nm	nm	nm
OEE 40	0.88	0.33	0.26	0.34	nm	nm	nm	nm
OEE 45	0.92	0.30	0.25	0.32	nm	nm	nm	nm
OEE 46	0.91	0.26	0.23	0.31	nm	nm	nm	nm
OEE 48	2.08	0.23	1.46	0.80	nm	nm	nm	nm
OEE 50	2.61	0.46	0.80	0.74	19.64	0.24	nm	0.23
Replicate (avg.)	2.81	0.34	3.08	1.34	2.20	1.26	1.24	1.25
Replicate (std dev.)	0.04	0.01	0.07	0.01	0.01	0.03	0.01	0.03

Pr/Ph: The ratio of pristane to phytane, norPr/Pr: The ratio of norpristane to pristine, Pr/nC_{17}: The ratios of pristane to n-heptadecane (nC_{17}), Ph/nC_{18}: The ratios of phytane to n-octadecane (nC_{18}), nC_{17}/nC_{27} = The ratio of *n*-Pentadecane/*n*-Pentacosane, CPI-1= Carbon-Preference Indices (Philippi, 1965), CPI-2 = Carbon-Preference Indices (Evans, 1961), CPI-3 = Carbon-Preference Indices (Scanlan and Smith, 1970) nm: Data could not be measured due to non-availability of peaks of *n*-alkane.

3.1.4 Diamondoids

GC-MS of the aliphatic hydrocarbon fractions from the well cuttings samples was used to analyse the diamondoid hydrocarbons and the ions monitored included *m/z* 136, 135, 149, 163,177 for the adamantanes and *m/z* 188, 187, 201, 215 for the diamantanes (e.g. Figure 3.13). The peak areas were used for the calculation of several ratios as presented in Table 3.4.

The calculated/measured parameters includes; 3+4- MD (ppm) (c.f. Dahl et al., 1999); MAI (c.f. Chen *et al*., 1996); MDI (c.f. Chen *et al*., 1996); DMDI (c.f. Schulz *et al*., 2001); EAI (c.f. Schulz *et al*., 2001); TMAI (c.f. Zhang *et al*., 2005); MA/AD (c.f. Grice *et al* 2000); MD/D (c.f. Grice *et al* 2000); MA/EA (c.f. Wang *et al*., 2006; Yang *et al*., 2006); MA/DMA; (c.f. de Araujo *et al.*, 2012); MA/TMA (c.f. de Araujo *et al*., 2012); MA/TeMA (c.f. de Araujo *et al*., 2012); DMA/TMA (c.f. de Araujo *et al*., 2012); TA/TMA (c.f. de Araujo *et al*., 2012); TMA/TMA (c.f. Wang *et al* 2006; de Araujo *et al*., 2012); TeMA/TeMA (c.f. de Araujo *et al*., 2012).

There is no marked variation in most of the calculated ratios based on the wells (Table 3.4) however, the concentration of 3+4- MD (ppm) shows some marked variation especially in the well cuttings from JK where the 3+4- MD concentration is elevated between 20 – 65 ppm whereas well cuttings samples from the other wells generally have below 6 ppm 3+4- MD concentration (Figure 3.14).

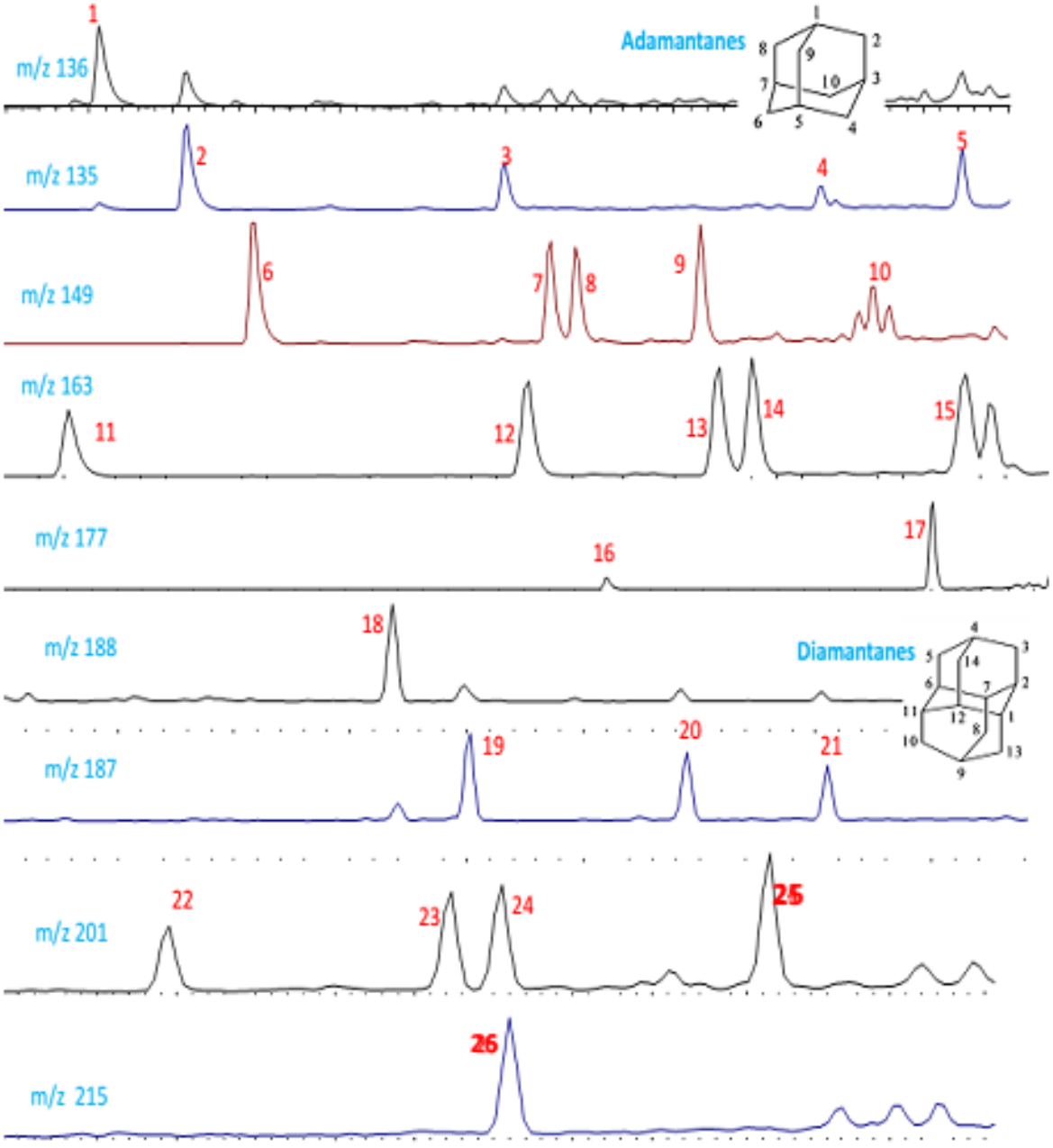

Figure 3.13: Representative mass chromatograms of adamantanes (*m/z* 136, 135, 149, 163,177) and diamantanes (*m/z* 188, 187, 201, 215) showing their distributions in a well cuttings sample (well JK, Depth 4675 ft OEE032).

1= Adamantane (AD). **2=** 1-Methyladamantane (1-MA). **3=** 2-Methyladamantane (2-MA). **4=** 1-Ethyladamantane (1-EA). **5=** 2-Ethyladamantane (2-EA). **6=** 1,3-Dimethyladamantane (1,3-DMA). **7=** 1,4-Dimethyladamantane,cis (1,4-DMA cis). **8=** 1,4-Dimethyladamantane,trans (1,4-DMA trans). **9=** 1,2-Dimethyladamantane (1,2-DEA). **10=** 1-Ethyl-3-methyladamantane (1E,3,-MA). **11**= 1,3,5 Trimethyladamantane (1,3,5-TMA). **12**= 1,3,6-Trimethyladamantane (1,3,6-TEA). **13=** 1,3,4-Trimethyladamantane,cis (1,3,4-TEA cis). **14**= 1,3,4-Trimethyladamantane,trans (1,3,4-TEA trans). **15=** 1-Ethyl-3,5-dimethyladamantane (1E,3,5-DMA). **16:** 1,3,5,7-Tetramethyladamantane (1,3,5,7-TtMA). **17=** 1,2,5,7-Tetramethyladamantane (1,2,5,7-TtMA). **18=** Diamantane (D). **19=** 4-Methyldiamantane (4-MD). **20=** 1-Methyldiamantane (1-MD). **21=** 3-Methyldiamantane (3-MD). **22=** 4,9-Dimethyldiamantane (4,9-DMD). **23=** 1,4 and 2,4-Dimethyldiamantane (1,4 and 2,4-DMD). **24=** 4,8-Dimethyldiamantane (4,8-DMD), **25=** 3,4-Dimethyldiamantane (3,4-DMD). **26=** Trimethyldiamantane (TED).

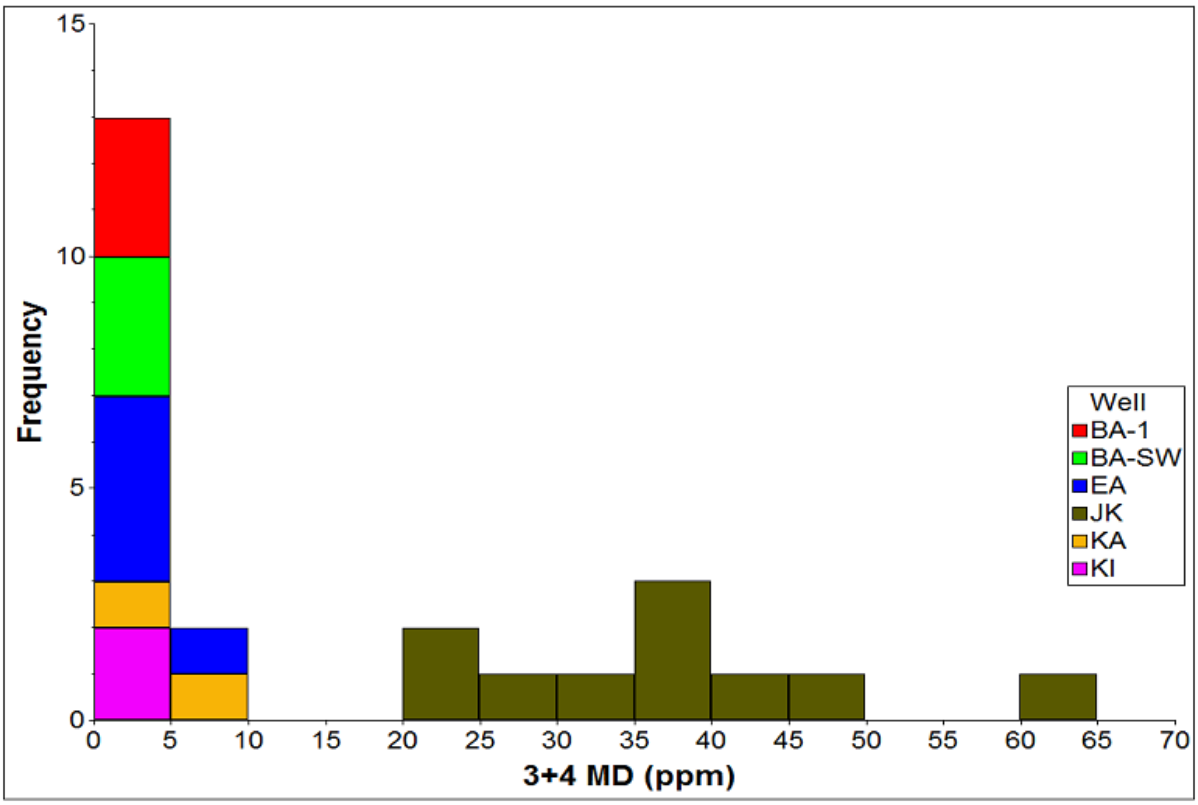

Figure 3.14: Variation in 3+4- methyldiamantane (MD) concentrations in the well cuttings extract from the 6 Niger Delta wells, showing high concentration in well JK cuttings extracts when compared to other well cuttings extracts.

Table 3.4: Summary of diamondoid hydrocarbon source, cracking and maturity parameters from the well cuttings samples

	C_{29} (ppm)	3+4-MD	EAI	DMDI	MA/AD	MD/D	MA/EA	MA/TMA	DMA/TMA	TMA/TMA	TeMA/TeMA
OEE 1	30.20	1.60	0.67	0.43	5.94	2.51	1.26	1.10	1.54	0.85	0.51
OEE 2	21.98	1.25	0.74	0.39	8.23	2.45	0.90	1.07	1.70	0.92	0.41
OEE 3	33.65	2.13	0.70	0.39	3.81	2.63	1.23	1.15	1.27	1.26	1.14
OEE 4	39.57	1.57	0.72	0.38	8.13	2.34	0.46	0.55	1.25	0.60	0.26
OEE 5	44.00	4.23	0.75	0.42	14.87	2.46	0.33	0.38	1.01	0.39	0.18
OEE 6	26.01	5.98	0.75	0.27	14.43	2.91	0.46	0.56	1.02	0.61	0.15
OEE 7	4.22	0.35	0.70	0.31	8.00	3.03	0.76	0.71	2.16	0.93	0.37
OEE 8	6.40	0.30	0.69	0.36	7.24	3.04	1.02	0.80	1.47	0.80	0.49
OEE 9	35.27	0.21	0.59	0.32	6.83	2.13	1.79	1.24	1.75	1.35	0.58
OEE 10	2.93	20.47	0.71	0.40	7.88	2.69	1.06	0.93	0.90	1.55	0.80
OEE 11	7.70	37.50	0.76	0.40	5.81	2.78	0.65	0.77	0.99	0.80	0.83
OEE 12	8.12	27.02	0.70	0.39	5.29	2.81	0.56	0.66	0.96	0.74	0.43
OEE 13	8.93	31.12	0.78	0.40	5.92	2.75	0.27	0.33	0.74	0.80	0.49
OEE 14	6.09	48.57	0.76	0.40	4.14	2.81	0.86	1.24	0.68	1.02	0.21
OEE 15	15.72	63.82	0.82	0.40	5.86	2.74	0.27	0.48	0.62	0.92	0.19
OEE 16	59.96	5.32	0.79	0.41	4.97	2.74	0.81	1.08	1.17	0.74	0.39
OEE 18	45.37	1.03	0.82	0.31	11.04	2.62	0.24	0.62	2.17	0.41	0.20
OEE 19	4.88	0.62	0.82	0.33	6.09	2.75	0.22	0.54	1.13	0.43	0.17
OEE 20	7.12	0.31	0.72	0.44	7.45	2.72	0.71	1.09	1.17	0.80	1.29
OEE 21	3.00	0.11	0.78	0.36	8.79	2.81	0.76	0.88	1.34	1.67	1.85
OEE 23	139.69	1.31	nm	0.38	nm	2.02	nm	nm	nm	nm	nm
OEE 36	4.16	23.34	nm	0.41	nm	2.64	nm	nm	nm	0.47	0.44
OEE 38	7.67	40.55	0.70	0.37	9.37	2.57	0.93	1.34	1.10	1.35	0.65
OEE 40	0.09	35.02	nm	0.40	nm	2.5	nm	nm	nm	nm	nm
OEE 45	4.13	36.23	nm	0.35	nm	2.97	nm	nm	nm	0.68	nm
Replicate (avg.)	22.55	54.04	72.05	67.38	6.06	2.83	1.55	1.47	1.47	0.77	0.18
Replicate (std. dev.)	0.57	0.25	0.09	0.26	0.11	0.05	0.02	0.00	0.04	0.02	0.00

C_{29}ααα20R = C_{29} 5α(H), 14α(H), 17α(H)-20R stigmastane (ppm). **3+4 MD**= 3-methyldiamnatane + 4-methyldiamantane (ppm). **DMDI**= 100*3,4-dimethyldiamantane/3,4- + 4,9-dimethyldiamantane. **EAI**= 100*2-ethyladamantane/ 2- +1-ethyladamnatane. **MA/AD**= 1-+2-methyladamntane/adamantane. **MD/D**= 1-+3-+4-methyldiamantane/diamantane. **MA/EA**= 1-methyldiamantane/2-ethyldiamantane. **MA/TMA**= 1-methyladamantane/1,3,4-trimethyladamantane. **DMA/TMA**=1,4-dimethyladamantane/1,3,4-trimethyladamantane. **TA/TMA=** 1,3,5-trimethyladamantane/1,2,5,7-trimethyladamnatane. **TMA/TMA=** 1,3,5-trimethyladamantane/1,3,6-trimethyladamantane. **TeMA/TeMA=** 1,3,5,7-tetramethyladamantane/1,2,5,7-tetramethyladamantane, nm: ratio could not be calculated due to either low level of one or more of the compounds in the calculated ratio.

3.1.5 Steranes

Peak areas from *m/z* 217 & 218 mass chromatograms (e.g. Figures 3.15 & 3.16) were used for the calculation of several sterane biomarker ratios and their results are presented in Table 3.5. The calculated parameters includes; Preg (c.f. Mackenzie, 1984); %DiaSt (c.f. Mackenzie, 1984); St29S/R (c.f. Seifert & Moldowan, 1981); St29I/R (c.f. Seifert & Moldowan, 1981); 27St217 (c.f. Huang & Meinschein, 1979; Peters & Moldowan, 1993); 28St217 (c.f. Huang & Meinschein, 1979; Peters & Moldowan, 1993); 29St217 (c.f. Huang & Meinschein, 1979; Peters & Moldowan, 1993); St27Iso (c.f. Huang & Meinschein, 1979; Peters & Moldowan, 1993); St28Iso (c.f. Huang & Meinschein, 1979; Peters & Moldowan, 1993); St29Iso (c.f. Huang & Meinschein, 1979; Peters & Moldowan, 1993); St30Iso (c.f. Moldowan et al., 1990).

There is no strong variation in the calculated sterane parameters in most well cuttings extracts with the exception of those from well JK. The St29Iso [$C_{29}\alpha\beta\beta$ 20(R+S)/$C_{27\text{-}29}\alpha\beta\beta$ 20(R+S)] parameter shows that cuttings samples from well JK has lower values when compared to other wells, with a range of 0.1 to 0.4, while cuttings samples from well KA has elevated values with a range of 0.5 to 0.75 and cuttings samples from the other wells (EA, KI, BA-1, BA-SW) fall in a short range of 0.4 to 0.5 (Figure 3.17) although a sample from well EA has a value of 0.75. The St27Iso [$C_{27}\alpha\beta\beta$ 20(R+S)/$C_{27\text{-}29}\alpha\beta\beta$ 20(R+S)] parameter shows that cuttings samples from well JK have a range of 0.3 to 0.5, while those from well KA have lower values and they are generally lower than 0.23, cuttings samples from wells BA-1, BA-SW and EA have a range of 0.2 to 0.3 (Figure 3.17). The plot of The St29Iso against St27Iso shows a strong negative correlation, although this correlation is not so pronounced for samples from well KI (Figure 3.17).

The cross plot between pregnane and diasterane ratios (Figure 3.19) shows a strong positive correlation between these two ratios, with the cuttings samples from well JK having values generally greater than 0.4 for both ratios whereas those from the other wells have values less

than 0.4 for both wells and of special interest are the samples from well BA-1, BA-SW and KA which have pregnane and diasterane ratio values lower than 0.1 and 0.2, respectively (Figure 3.19).

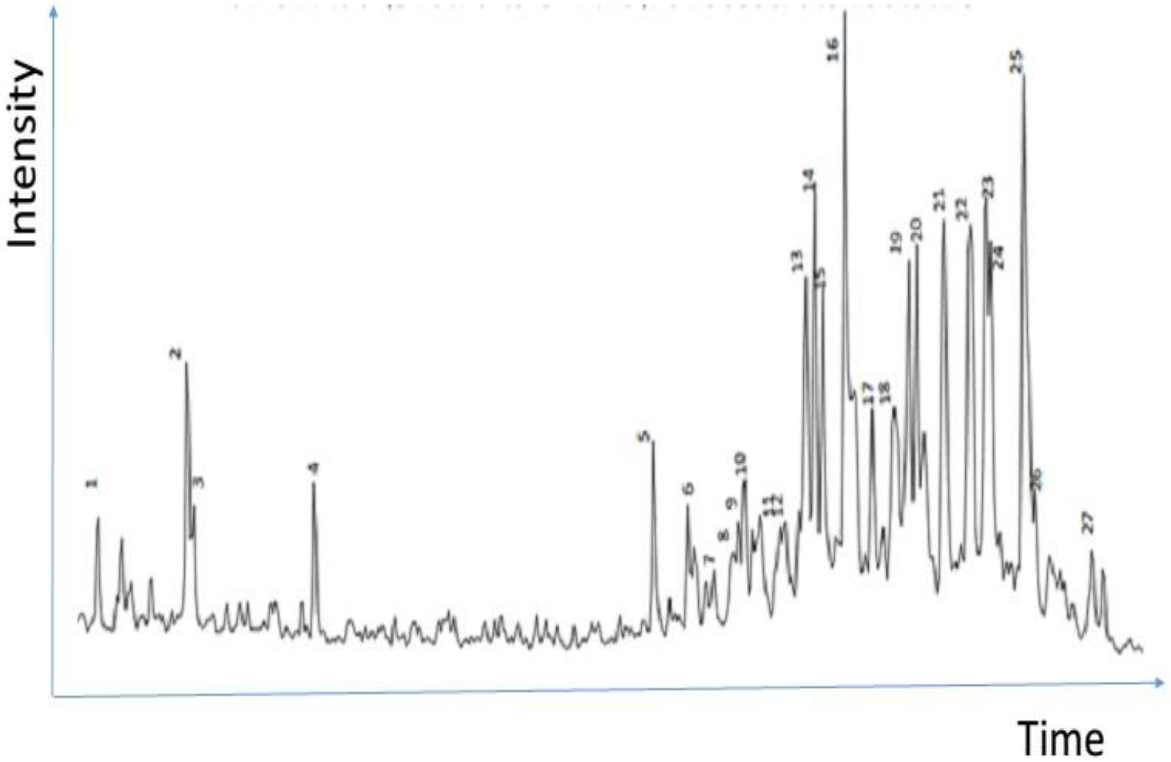

Figure 3.15: Representative *m/z* 217 mass chromatogram of aliphatic hydrocarbon fraction of well BA-1, depth 11,150 ft cuttings sample OEE002 showing the distribution of steranes.
1= Diapregnane. **2=** Pregnane. **3=** Homodiapregnane. **4=** Methyl Pregnane. **5=** 13β, 17α (20S) Diacholestane. **6=** 13β, 17α (20R) Diacholestane. **7=** C_{27} 13α (20S) diasterane. **8=** C_{27} 13α (20R) diasterane. **9=** C_{28} 13β (20S) diasterane. **10=** C_{28} 13β (20S) diasterane. **11=** C_{28} 13β (20R) diasterane. **12=** C_{28} 13β (20R) diasterane. **13=** C_{27} 5α,14α,17α (20S). **14=** C_{27} 5α,14β,17β (20R) + C_{29} (20S) diasterane. **15=** C_{27} 5α,14β,17β (20S). **16=** C_{27} 5α,14α,17α (20R). **17=** C_{29} (20R) diasterane. **18=** C_{28} 5α, 14α, 17α (20S). **19=** C_{28} 5α,14β,17β (20R). **20=** C_{28} 5α,14β,17β (20S). **21=** C_{28} 5α,14α,17α (20R). **22=** C_{29} 5α,14α,17α (20S). **23=** C_{29} 5α,14β,17β (20R). **24=** C_{29} 5α,14β,17β (20S). **25=** C_{29} 5α,14α,17α (20R). **26=** C_{30} 5α,14α,17α (20S). **27=** C_{30} 5α,14α,17α (20R).

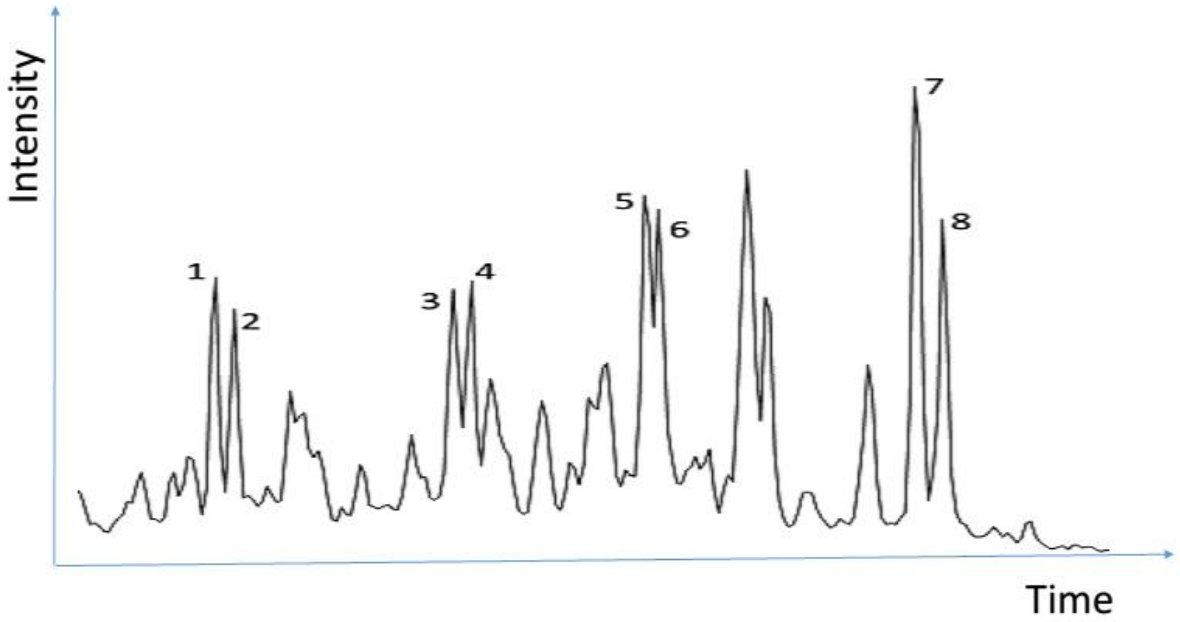

Figure 3.16: Representative *m/z* 218 mass chromatogram of aliphatic hydrocarbon fraction of well EA depth 4960 ft cuttings sample OEE007 showing the distribution of steranes.
1= C_{27} 5α,14β,17β (20R). **2=** C_{27} 5α,14β,17β (20S**). 3=** C_{28} 5α,14β,17β (20R). **4=** C_{28} 5α,14β,17β (20S). **5=** C_{29} 5α,14β,17β (20R). **6=** C_{29} 5α,14β,17β (20S). **7=** C_{30} 5α,14β,17β (20R). **8=** C_{30} 5α,14β,17β (20S).

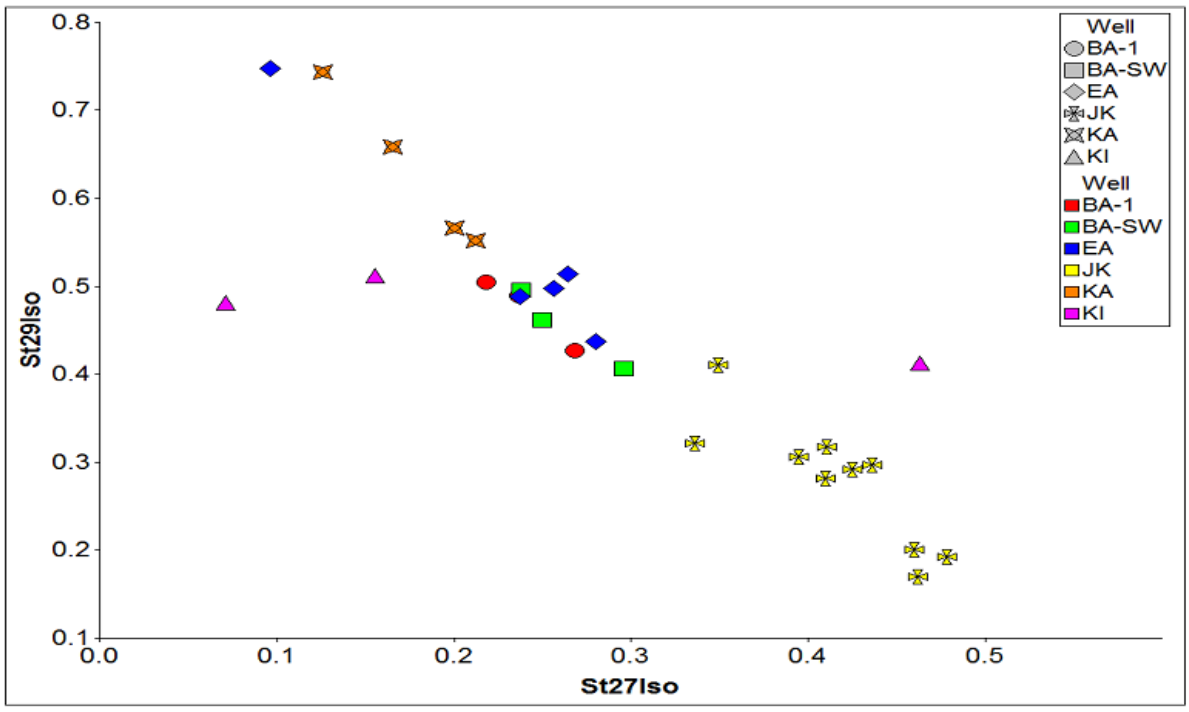

Figure 3.17: Plot of C_{29}αββ 20(R+S)/$C_{27\text{-}29}$αββ 20(R+S) against C_{27}αββ 20(R+S)/$C_{27\text{-}29}$αββ 20(R+S) (measured from *m/z* 218). Note Well JK cuttings samples has relatively lower St29Iso and relatively higher St27Iso, whereas well KA has the opposite.

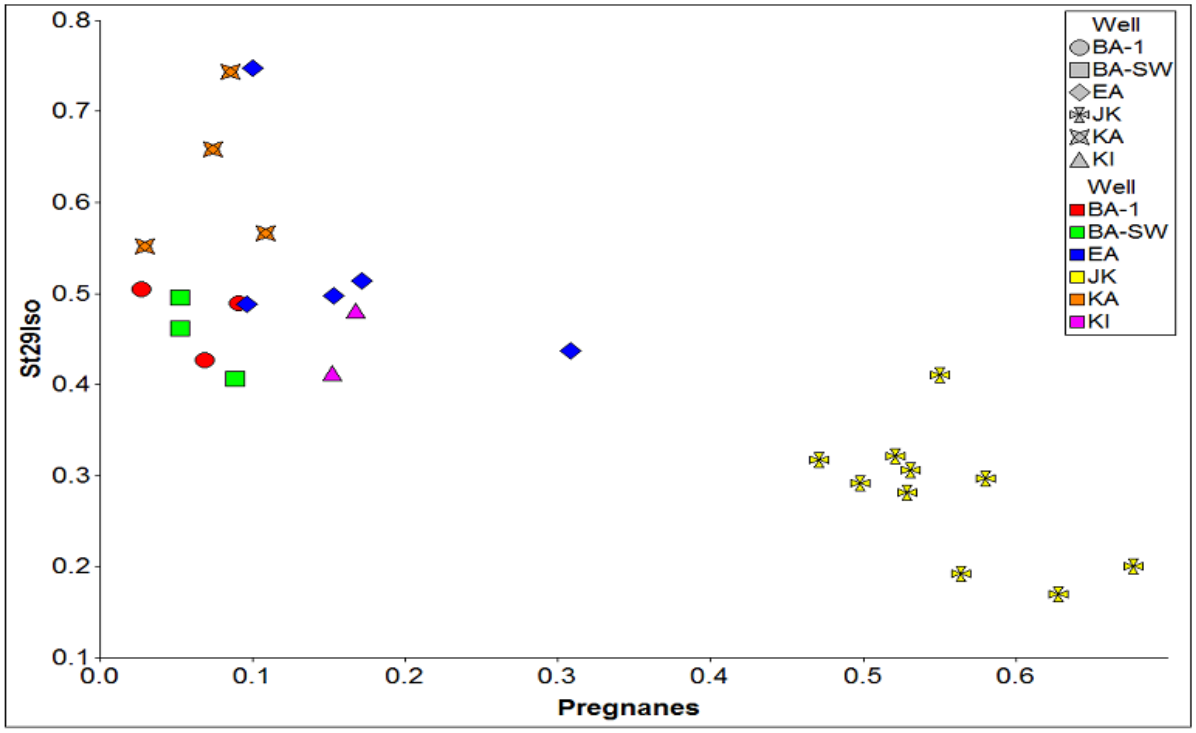

Figure 3.18: Plot of C_{29}αββ 20(R+S)/$C_{27\text{-}29}$αββ 20(R+S) against pregnanes ratio [(C_{21}5α(H)-pregnane + C_{22}5α(H)-20-methylpregnane)/(C_{21}5α(H)-pregnane+C_{22}5α(H)-20-methylpregnane + C_{29} ααα 20(S) + C_{29} αββ 20(R) + C_{29} αββ 20(S) + C_{29} ααα 20(R))]. Note Well JK cuttings samples has relatively higher pregnanes ratio whereas the other samples have relatively lower pregnanes ratios.

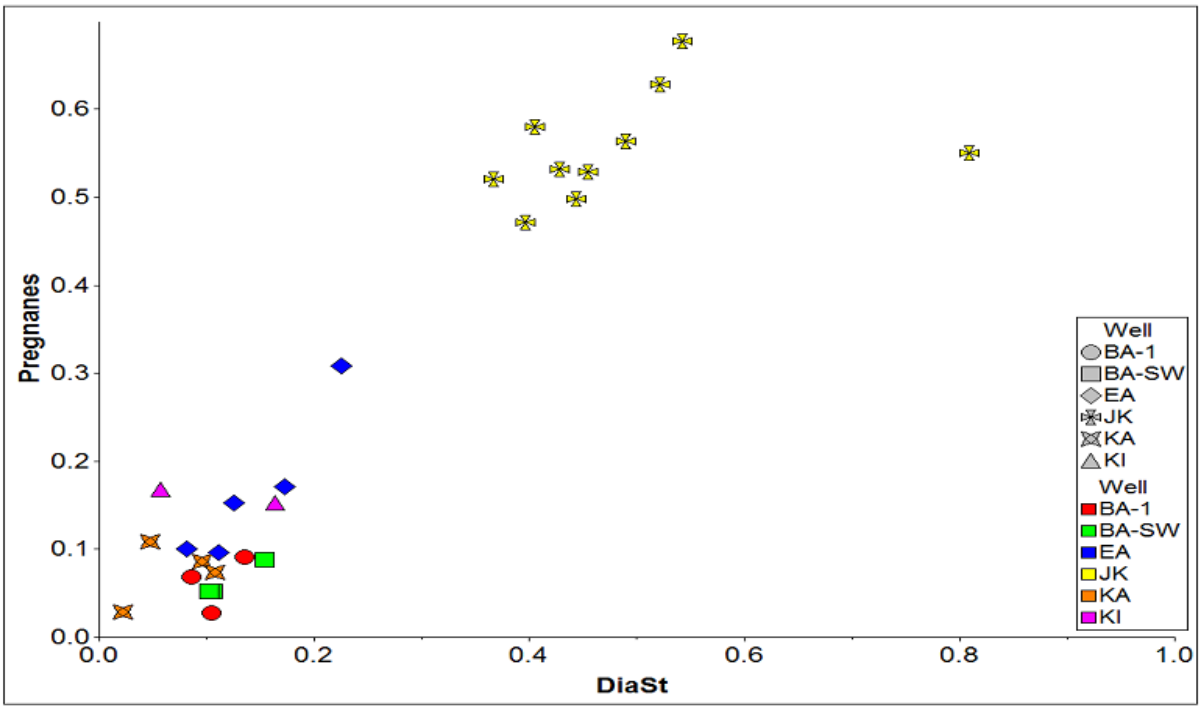

Figure 3.19: Plot of pregnanes ratio against diasteranes ratio [(C27αβ(20S+20R) diasteranes) /(C27αβ(20S+20R) diasterane + C_{29} ααα 20(S) + C_{29} αββ 20(R) + C_{29} αββ 20(S) + C_{29} ααα 20(R))]. Note cuttings samples from well JK has relatively higher diasteranes ratio whereas cuttings samples from wells KA, BA-1 and BA-SW having relatively lower diasteranes ratios.

Table 3.5**:** Summary of source and maturity sterane biomarker parameters of well cuttings samples

	Pregnanes	DiaSt	St29S/R	St29I/R	St27 ααα	St28 ααα	St29 ααα	St27Iso	St28Iso	St29Iso	St30Iso
OEE 1	0.07	8.61	0.28	0.31	26.80	30.53	42.67	26.57	31.90	41.53	0.22
OEE 2	0.09	13.54	0.18	0.31	23.62	27.41	48.97	24.34	32.27	43.39	0.25
OEE 3	0.05	10.58	0.19	0.25	23.79	26.62	49.59	24.07	29.68	46.25	0.35
OEE 4	0.05	10.25	0.15	0.27	24.97	28.89	46.14	18.42	34.96	46.62	0.31
OEE 5	0.09	15.42	0.24	0.28	29.56	29.79	40.65	25.08	35.69	39.24	0.33
OEE 6	0.10	8.12	0.30	0.35	9.64	15.56	74.80	28.02	28.28	43.70	nm
OEE 7	0.17	17.23	0.40	0.33	26.41	22.19	51.40	29.03	33.30	37.68	0.62
OEE 8	0.31	22.52	0.42	0.32	28.02	28.28	43.70	27.44	38.03	34.53	0.53
OEE 9	0.15	12.54	0.40	0.28	25.64	24.64	49.72	28.34	37.94	33.72	0.97
OEE 10	0.55	80.91	0.33	0.38	34.89	24.11	41.00	46.84	22.78	30.38	0.13
OEE 11	0.52	45.45	0.40	0.40	41.00	30.86	28.14	33.01	26.55	40.44	0.12
OEE 12	0.56	48.93	0.51	0.43	47.84	32.94	19.22	34.47	36.95	28.57	0.13
OEE 13	0.58	40.47	0.35	0.37	43.59	26.77	29.64	34.35	34.66	30.99	0.18
OEE 14	0.67	54.27	0.42	0.46	45.95	33.98	20.06	37.96	24.33	37.71	0.11
OEE 15	0.62	52.15	0.52	0.43	46.19	36.84	16.97	40.29	33.49	26.22	0.13
OEE 16	0.08	9.57	0.29	0.27	12.57	13.11	74.32	16.24	18.28	65.48	0.08
OEE 17	0.07	10.81	0.37	0.29	16.56	17.58	65.86	23.50	27.66	48.85	0.82
OEE 18	0.03	2.24	0.04	0.27	21.23	23.58	55.19	46.28	12.46	41.26	nm
OEE 19	0.17	5.69	0.33	0.43	7.11	44.83	48.07	21.80	27.76	50.44	nm
OEE 20	0.15	16.32	0.10	0.44	46.28	12.46	41.26	20.89	22.84	56.27	0.04
OEE 21	0.03	10.44	0.19	0.28	21.80	27.76	50.44	19.72	32.56	47.72	0.30
OEE 23	0.09	11.10	0.45	0.26	23.70	27.49	48.81	22.36	39.97	37.68	0.76
OEE 36	0.49	44.35	0.40	0.36	42.47	28.35	29.18	28.20	25.09	46.71	0.11
OEE 40	0.47	39.67	0.38	0.36	41.07	27.22	31.71	31.74	31.35	36.92	0.13
OEE 45	0.53	42.78	0.46	0.35	39.48	29.94	30.57	34.10	32.18	33.73	0.15
OEE 46	0.52	36.68	0.34	0.37	33.62	34.21	32.17	27.85	22.50	49.65	0.15
OEE 48	0.11	4.75	0.06	0.32	20.03	23.32	56.65	17.34	31.62	51.04	0.48
Replicate (avg.)	14.48	18.46	0.42	0.36	27.86	29.13	43.01	28.74	32.83	38.44	0.18
Replicate (std. dev.)	0.72	0.91	0.01	0.04	0.72	0.45	0.27	0.99	0.60	0.84	0.00

Pregnanes: The abundance of pregnanes relative to regular steranes, %DiaSt: The abundance of diasteranes relative to steranes, St29S/R: C_{29} Regular steranes 20S to 20R Isomerisation, St29I/R: 29 Iso to Regular steranes ratio, %St27: C_{27} ααα 20R abundance relative to sum C_{27} to C_{29} ααα 20R, %St28: C_{28} ααα 20R abundance relative to sum C_{27} to C_{29} ααα 20R, %St29: C_{29} ααα 20R abundance relative to sum C_{27} to C_{29} ααα 20R, St27Iso: C_{27} αβ(S+R)/$C_{27\text{-}29}$ αβ(S+R) from *m/z* 218, St27Iso: C_{27} αβ(S+R)/$C_{27\text{-}29}$ αβ(S+R) from *m/z* 218, St28Iso: C_{28} αβ(S+R)/$C_{27\text{-}29}$ αβ(S+R) from *m/z* 218, St29Iso: C_{29} αβ(S+R)/$C_{27\text{-}29}$ αβ(S+R) from *m/z* 218, St30Iso: C_{30} αβ(S+R)/$C_{27\text{-}30}$ αβ(S+R) from *m/z* 218. nm: ratio could not be calculated due to either low level of one or more of the compounds in the calculated ratio.

3.1.6 Hopanes

The terpane and hopane hydrocarbon biomarkers in the aliphatic hydrocarbon fractions of the well cuttings samples were measured by GC-MS using mainly the *m/z* 191, 193 and 414 mass chromatograms (e.g. Figure 3.20, 3.21, 3.22 & 3.23). Peak areas were used for the calculation of several ratios and the results are presented in Table 3.6. The calculated parameter includes; t_{19}/t_{23} (c.f. Zumberge, 1987; Rooney *et al*., 1998; Peters *et al*., 2005; He *et al*., 2012); Ts/Tm (c.f. Seifert & Moldowan 1978; Moldowan *et al.*, 1986); 29Hops (c.f. Ourisson *et al.*, 1987; Killops *et al*., 1998); 30Hops (c.f. Ourisson *et al*., 1987; Killops *et al*., 1998); 31Hops (c.f. Ourisson *et al*., 1987; Killops *et al*., 1998); Hop/Mor (c.f. Seifert & Moldowan 1980; Rullkotter &Marzi 1988); 29Ts/29Tm (c.f. Seifert & Moldowan 1978; Moldowan *et al*., 1986); Hop32(S/R) (c.f. Seifert & Moldowan 1986); Hop(30/29) (c.f. p:IGI geochemical manual 2004); HomoHop (c.f. Peters & Moldowan 1991; 1993); OleanIndex (c.f. Ekweozor & Telnaes, 1990).

The cuttings extracts from wells BA-SW and BA-1 have oleanane index values lower than 0.3, while those from well JK extracts have values between 0.2 to 0.5 and those from the other wells have values between 0.3 to 0.9, with one interval from well EA having above 0.8 (Figure 3.24). The %A+B i.e. [%A+B= (A+B/A+B+C+D)*100], where A+B, C, and D are novel C_{15} sesquiterpanes (c.f Nytoft *et al*., 2009) from *m/z* 193 shows that cuttings samples from well JK generally have values below 15% while those from well BA-1 have values less than 20%, the other wells are between 15 to 50% (Figure 3.25); most of the elevated values are from well KA extracts which range from 35 to 50% (Figure 3.5).

Figure 3.26 shows the cross plot of $Y/(Y+TC_{24})$ against $X/(X+TC_{20})$ (c.f Samuel et al., 2010; where X and Y are novel tricyclic compounds, TC_{20}= C_{20} tricyclic terpane and TC_{24}= C_{24} tricyclic terpane) and the values indicate that cuttings samples from wells BA-1, BA-SW and JK generally have values below 0.5 for both parameters, while those from well EA, KA and KI usually have values above 0.5 for both parameters. The A+B/A+B+C+D and

the K index (Samuel, 2008; where A1, A2, B1, B2 are tentatively identified as seco-oleananes and C tentatively identified as seco-hopane) cross plot (Figure 3.27) shows that wells BA-1, BA-SW and JK samples usually have values below 0.2 for their A+B/A+B+C+D ratios and below 4 for their K index values, although one interval in well BA-SW has value of 0.28 A+B/A+B+C+D and another interval in well JK has a K index value of 4.3. Cuttings samples from well EA, KA and KI generally have A+B/A+B+C+D ratio values greater than 0.25 and K index values greater than 4 (Figure 3.27).

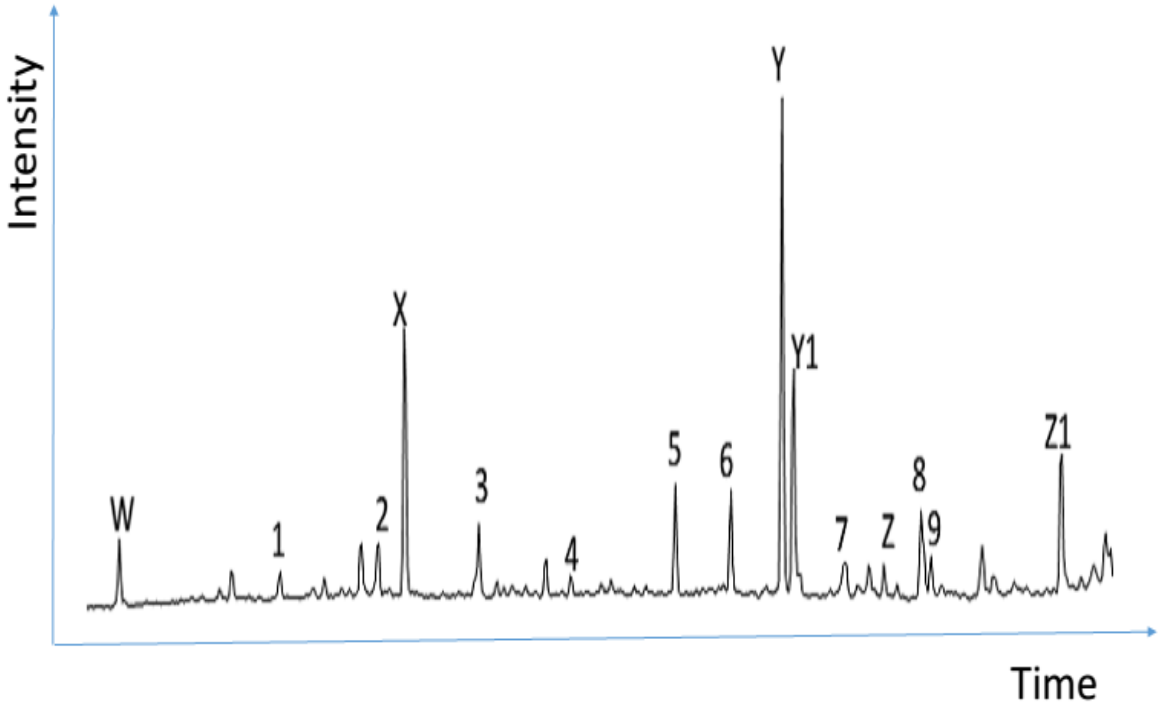

Figure 3.20: Representative partial *m/z* 191 mass chromatogram from cuttings sample OEE009 from well EA, depth 7085 ft showing the distributions of tricyclic and tetracyclic terpane compounds.

W= Unknown Tricyclic terpane. 1= C_{19} Tricyclic terpane. 2= C_{20} Tricyclic terpane. X= Unknown C_{21} Tricyclic terpane. 3= C_{21} Tricyclic terpane. 4= C_{22} Tricyclic terpane. 5= C_{23} Tricyclic terpane. 6= C_{24} Tricyclic terpane. Y= Unknown C_{25} Tricyclic terpane. Y1= 10β-des-A-oleanane (C_{24} Tetracyclic terpane). 7= C_{25} Tricyclic terpane (22S & 22R isomers). Z= 10β-des-A-ursane (C_{24} Tetracyclic terpane). 8= C_{24} Tetracyclic terpane. 9= C_{26} (22S+22R) Tricyclic terpane. Z1= Unknown C_{27} terpane).

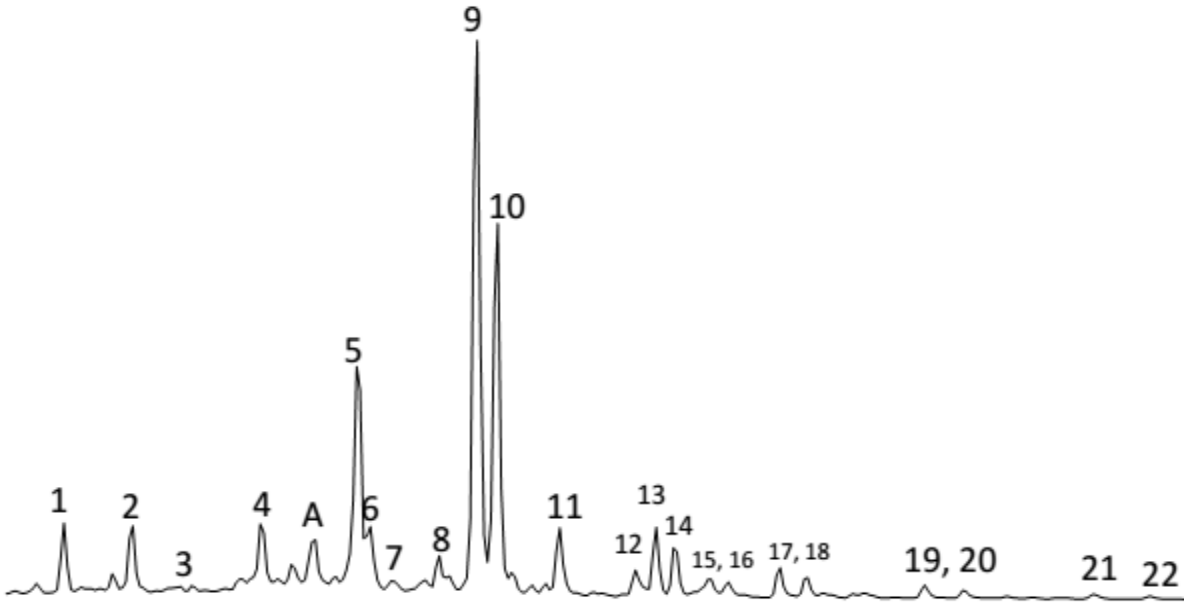

Figure 3.21: Representative partial *m/z* 191 mass chromatogram from cuttings sample OEE009 from well EA, depth 7085 ft showing the distributions of pentacyclic terpanes compounds.

1= 18α 22,29,30-trisnorneohopane (Ts). **2=** 17α 22,29,30-trisnorhopane (Tm). **3=** C_{30} (22S+22R) tricyclic terpane. **4=** C_{28} 17α, 21β norhopane. **A**= unknown C_{29} hopane. **5=** C_{29} 17αH,21βH 30-norhopane, **6=** 18α 30-norneohopane (C_{29}Ts), **7=** 17α diahopane (Hopane-X). **8=** 17β,21α 30-normoretane. **9=** 18α oleanane. **10=** C_{30} 17α,21β hopane. **11=** 17β,21α moretane. **12=** 19α-taraxastane. **13=** C_{31} 17α,21β 22S homohopane. **14=** C_{31} 17α,21β 22R homohopane. **15=** 17β,21α 22S homomoretane. **16=** 17β,21α 22R homomoretane. **17=** C_{32} 17α,21β 22S bishomohopane. **18=** C_{32} 17α,21β 22R bishomohopane. **19:** C_{33} 17α,21β 22S trishomohopane. **20**: C_{33} 17α,21β 22R trishomohopane. **21=** C_{34} 17α,21β 22S tetrakishomohopane. **22=** C_{34} 17α,21β 22R tetrakishomohopane.

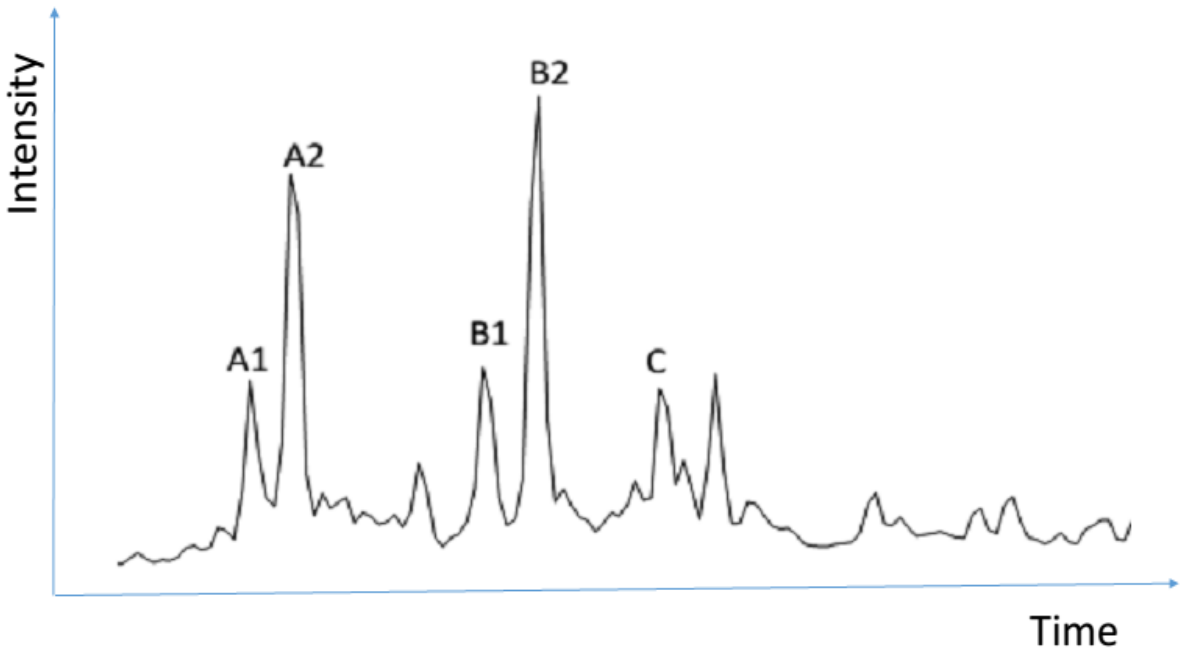

Figure 3.22: Representative partial *m/z* 414 mass chromatogram from cuttings sample OEE009 from well EA, depth 7085 ft showing the distributions of the seco-oleananes (A1, A2, B1, B2) and seco-hopane (C).

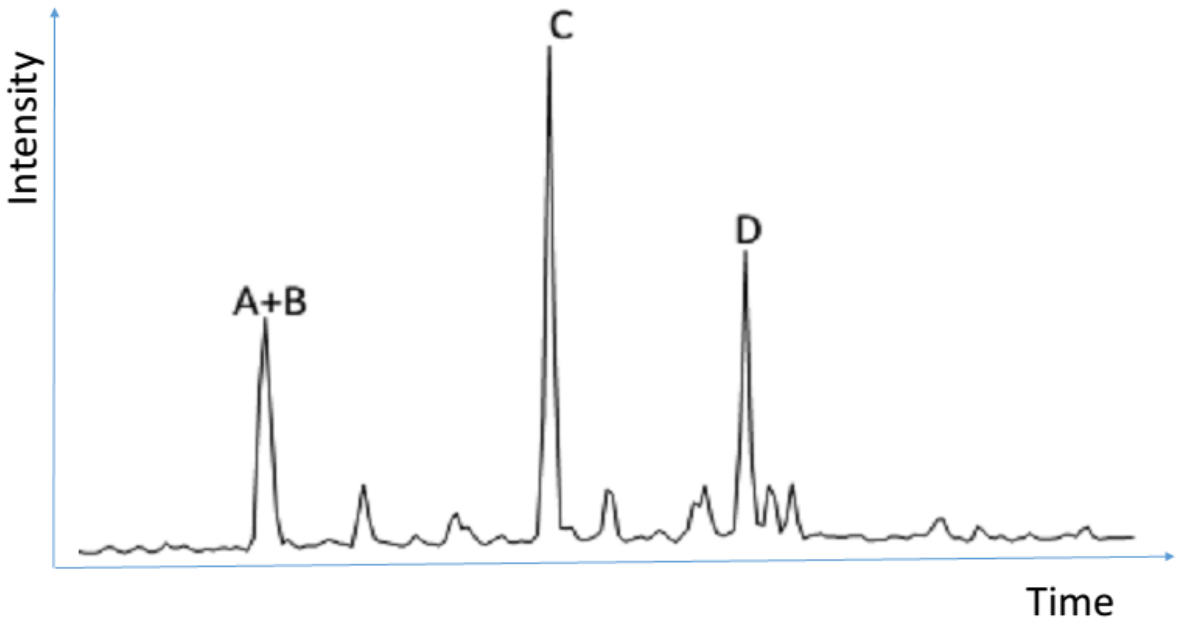

Figure 3.23: Representative partial *m/z* 193 mass chromatogram from cuttings sample OEE009 from well EA, depth 7085 ft of well cuttings showing the distributions of the C_{15} sesquiterpanes.

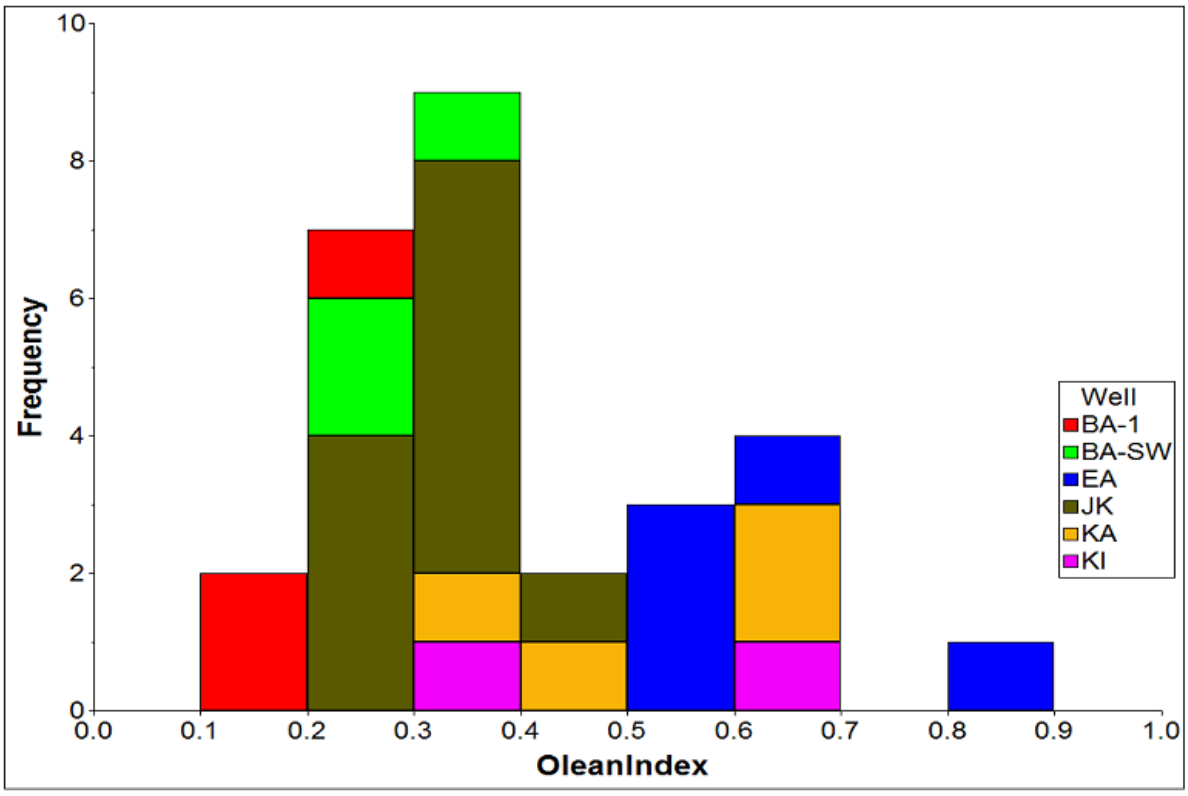

Figure 3.24: Variation of oleanane index values in the cuttings samples from the 6 Niger Delta wells, showing relatively high values in well EA extracts and relatively lower values in samples from wells BA-1, BA-SW and in most intervals of well JK extracts.

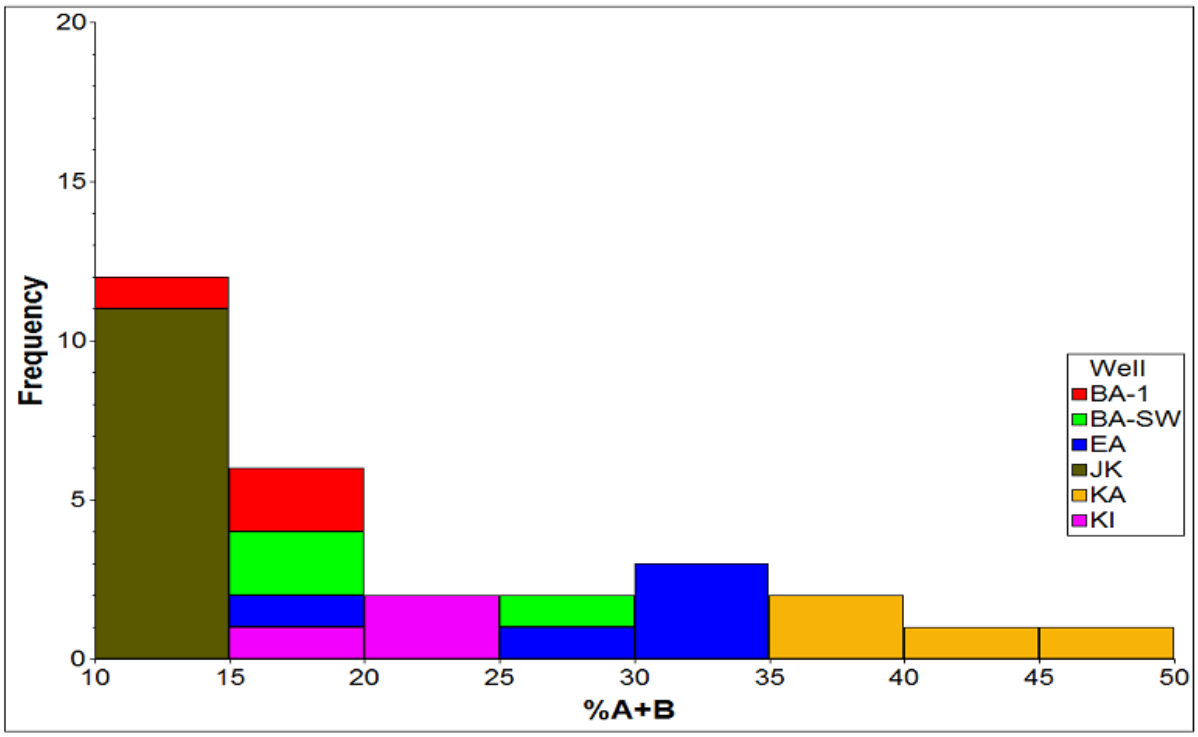

Figure 3.25: Variation in %A+B values from the cuttings samples from the 6 Niger Delta wells, showing relatively high %A+B values in samples from well KA and relatively low values in those from wells JK and BA-1.

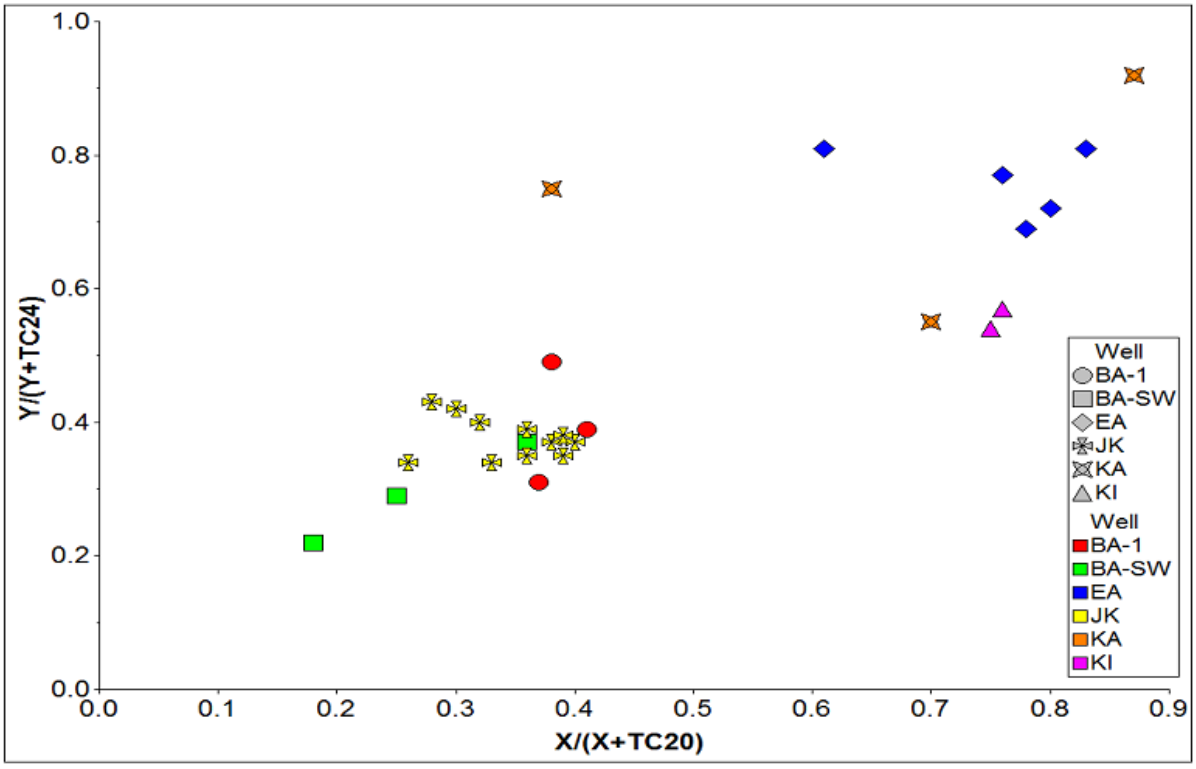

Figure 3.26: Plot of $Y/(Y+TC_{24})$ against $X/(X+TC_{20})$ showing cuttings samples from well EA having high values for both parameters whereas those from Wells BA-1, BA-SW and JK have lower values.

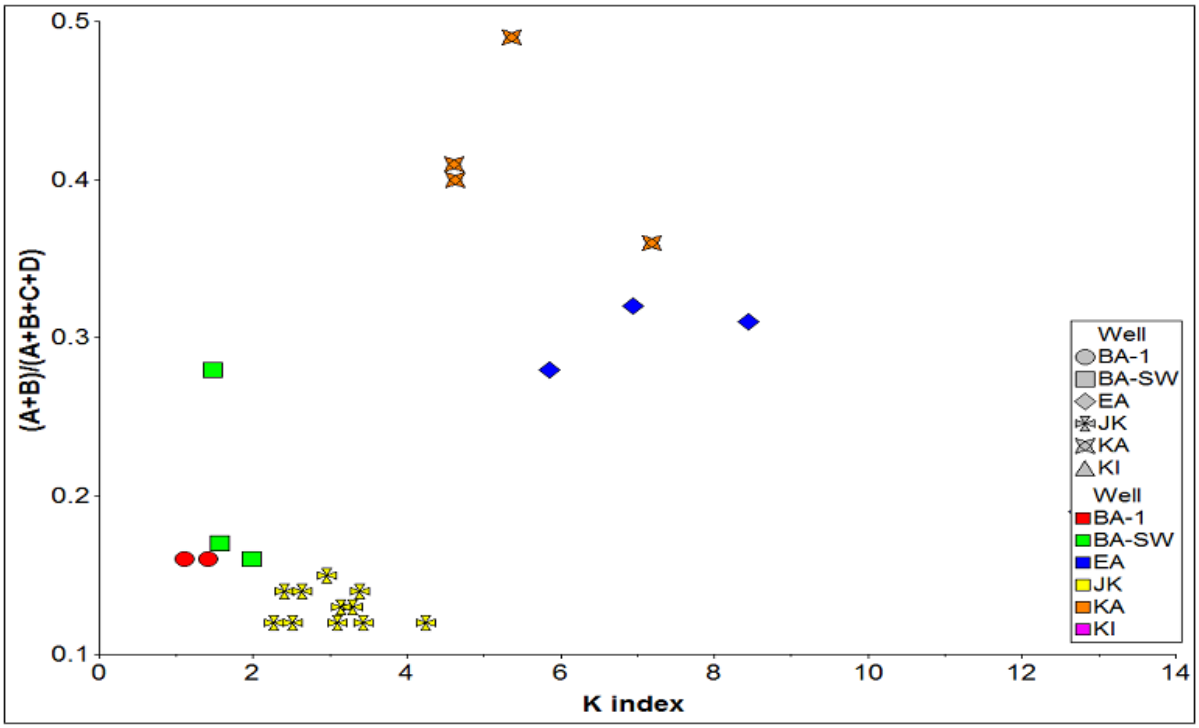

Figure 3.27: Cross plot of K index against (A+B)/(A+B+C+D) in the Niger Delta cuttings samples showing the variations in the study wells.

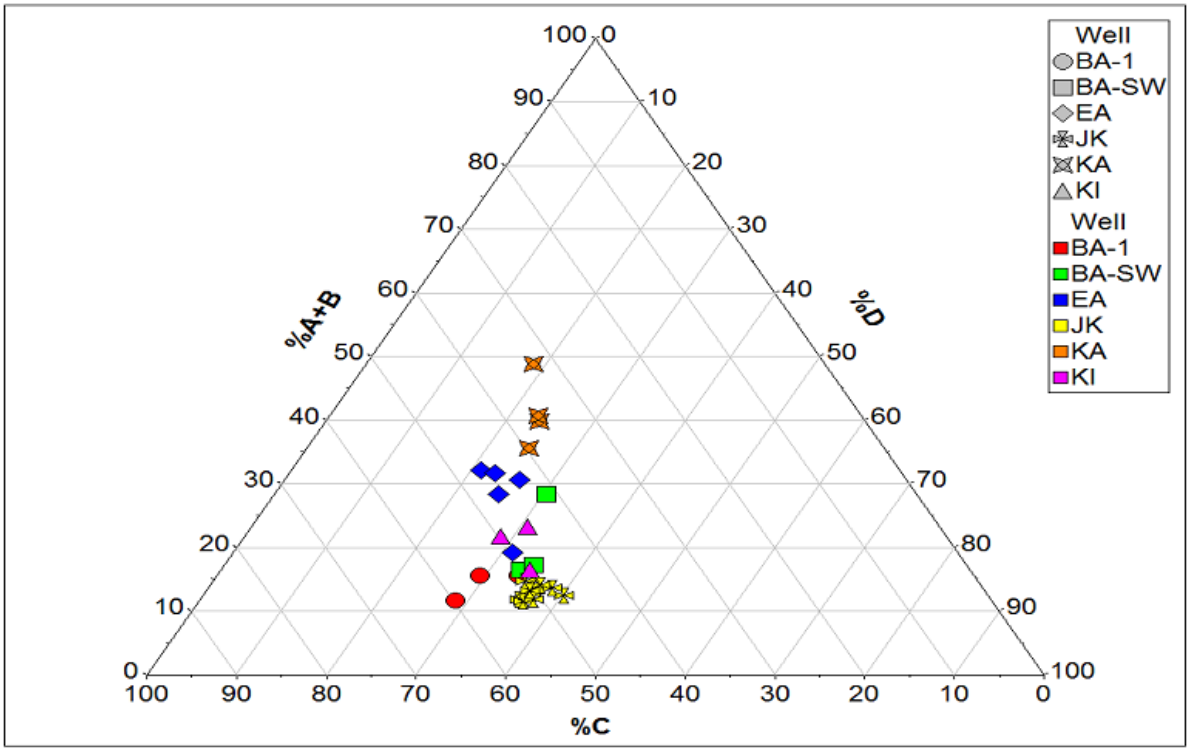

Figure 3.28: Ternary plot of %A+B, %C and %D from *m/z* 193. Note the separation of the samples from well KA and EA from the other well cuttings samples.

Table 3.6: Summary of terpane biomarker source and maturity parameters from the well cuttings samples

	t_{19}/t_{23}	Ts/Tm	29Hops	30Hops	31Hops	NorH/NorM	Hop/Mor	29Ts/29Tm	Hop32(S/R)	Hop(30/29)	HomoHop	OleanIndex
OEE 1	0.25	0.47	0.47	1.07	0.19	6.31	7.77	0.21	0.57	1.62	0.40	0.37
OEE 2	0.41	0.35	0.42	0.98	0.26	3.20	4.79	0.24	0.69	1.67	0.39	0.20
OEE 3	0.42	0.34	0.44	0.99	0.25	4.36	4.35	0.26	0.53	1.63	0.38	0.41
OEE 4	0.46	0.38	0.45	0.92	0.26	3.79	4.16	0.24	0.44	1.55	0.39	0.40
OEE 5	0.58	0.40	0.45	1.03	0.23	4.98	4.60	0.22	0.70	1.64	0.33	0.43
OEE 6	1.84	0.48	0.00	2.63	0.37	0.01	0.15	0.50	0.62	1.64	nm	5.46
OEE 7	0.43	0.51	0.48	1.09	0.18	6.42	6.75	0.20	0.60	1.60	0.35	1.28
OEE 8	0.24	0.45	0.56	1.05	0.15	7.35	7.30	0.18	0.57	1.43	0.23	1.40
OEE 9	0.39	0.45	0.47	1.13	0.18	5.58	5.91	0.22	0.62	1.66	0.29	1.51
OEE 10	0.67	0.44	0.71	0.80	0.16	6.42	4.87	0.20	0.60	1.07	nm	0.80
OEE 11	0.51	0.41	0.80	0.75	0.15	8.12	4.23	0.19	0.59	0.97	nm	0.42
OEE 12	0.46	0.36	0.67	0.89	0.15	6.99	4.89	0.28	0.67	1.17	nm	0.44
OEE 13	0.46	0.39	0.63	0.99	0.13	7.10	5.11	0.19	0.56	1.29	nm	0.36
OEE 14	0.61	0.38	0.56	1.00	0.16	8.65	4.58	0.33	0.71	1.39	nm	0.34
OEE 15	0.43	0.37	0.76	0.87	0.11	6.80	4.94	0.30	0.63	1.08	nm	0.42
OEE 16	1.33	0.35	0.57	1.20	0.10	5.61	4.47	0.19	0.65	1.50	0.18	1.88
OEE 17	0.71	0.41	0.56	1.01	0.16	7.47	4.94	0.20	0.58	1.40	0.27	2.05
OEE 18	1.21	0.32	0.51	1.16	0.14	1.23	4.56	0.22	0.62	1.60	0.21	0.46
OEE 19	5.60	nm	nm	nm	nm	nm	2.66	nm	0.68	nm	nm	1.69
OEE 20	1.65	0.41	nm	nm	nm	nm	1.28	nm	0.63	nm	nm	0.60
OEE 21	0.61	0.38	0.40	0.93	0.30	2.73	4.91	0.14	0.54	1.68	0.60	0.22
OEE 23	0.34	0.49	0.55	0.96	0.18	5.44	4.75	0.19	0.57	1.37	0.37	1.42
OEE 36	0.59	0.47	0.66	0.86	0.16	6.04	4.34	0.18	0.65	1.16	nm	0.44
OEE 38	0.50	0.41	0.74	0.77	0.17	6.83	3.58	0.16	0.61	1.03	nm	0.50
OEE 40	0.47	0.40	0.66	0.75	0.21	5.79	3.65	0.20	0.54	1.08	nm	0.51
OEE 45	0.51	0.40	0.72	0.85	0.14	7.81	5.16	0.11	0.47	1.10	nm	0.43
OEE 46	0.49	0.33	0.69	0.88	0.14	6.44	3.36	0.17	0.49	1.14	nm	0.44
OEE 48	0.52	0.38	0.50	1.03	0.19	2.79	4.85	0.22	0.38	1.53	nm	0.91
Replicate (avg.)	0.61	0.41	0.49	0.88	0.24		6.10	0.23	0.56	1.40	0.50	0.45
Replicate (std. dev.)	0.01	0.00	0.01	0.02	0.03		0.00	0.06	0.00	0.02	0.06	0.01

t_{19}/t_{23}: C_{19} Tricyclic/C_{23} Tricyclic terpane, Ts/Ts+Tm: Trisnor-neohopane relative to Trisnor-hopane, 29Hops: C_{29} regular hopane relative to the C_{29} to C_{31} regular hopanes, 30Hops: C_{30} regular hopane relative to the C_{29} to C_{31} regular hopanes, 31Hops: C_{31} regular hopane relative to the C_{29} to C_{31} regular hopanes, NorH/NorM: C_{29} nor-Hopane relative to C_{29} nor-Moretane, 29Ts/29Ts+29Tm: C_{29} neohopane (C_{29}Ts) relative to the C_{29} hopane, Hop32(S/S+R): C_{32} 22S homo-Hopane relative to C_{32} 22R homo-Hopane, Hop(30/29): C_{30} Hopane relative to C_{29} nor-Hopane, HomoHop: C_{31} to C_{35} homo-Hopanes (22S+22R) relative to C_{27} to C_{30} Hopanes, Olean Index: Oleanane relative to C_{30} Hopane, nm: ratio could not be calculated due to either low level of one or more of the compounds in the calculated ratio.

3.1.7 Compound Specific Isotope Analysis (CSIA)

The compound specific isotope analysis (CSIA) of individual *n*-alkanes from the well cuttings samples was carried out for selected samples both in carbon and hydrogen mode. The replicate results of three runs done over a period of time (i.e. with different batch of analysis) indicate that the results have low percentage errors (e.g. Figures 3.29 and 3.30), although an increase in the standard error value around the nC_{30} to nC_{33} region (Table 3.7) was noticed in the carbon mode but since the concentration in this range was very low for the well cuttings extracts, those reading were not used.

The percentage error in hydrogen mode (e.g. Figure 3.30), shows a greater variation than the carbon mode measurement and this can be attributed to the wider range of values in the hydrogen mode (-54 to -178), but overall the values are well within an acceptable standard range with high reproducibility although the CV is higher in the hydrogen mode with range of 3 to 19 than in the carbon mode with range of 3 to 9.

Some *n*-alkanes were excluded from the plots because they were not well separated (i.e. co-elutions) and integration of these compounds thus introduced errors into the data. These compounds included: nC_{17} and pristane; nC_{18} and phytane; nC_{24} and HCDH (internal standard).

3.1.7.1 Carbon mode CSIA

A total of 15 samples were analysed in CSIA carbon mode, with 1 cuttings sample from well BA-1, 2 samples from well BA-SW and 3 samples from each of wells EA, JK, KA and KI (Table 3.7). The well JK *n*-alkanes were isotopically relatively light while those from well KI were isotopically heavier, the other wells showed a range of values (Figure 3.29).

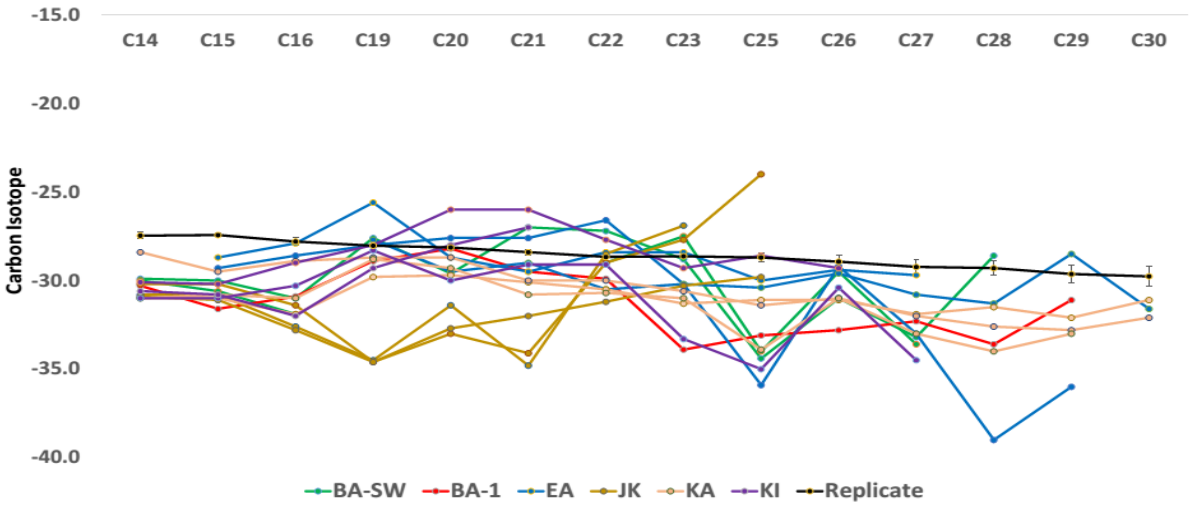

Figure 3.29: The *n*-alkane stable carbon isotope value plot from cuttings samples from 6 wells in the delta

3.1.7.2 Hydrogen mode CSIA

A total of 6 samples was analysed in hydrogen mode, with 1 cuttings sample from wells BA-1, BA-SW, EA, JK and 2 samples from well KA (Table 3.8). Cuttings samples from well BA-SW are isotopically lighter whereas those from wells BA-1 and JK change from being isotopically lighter at the lower *n*-alkanes to isotopically heavier around C_{20} and upwards. Cuttings samples from wells EA and KA are isotopically heavier than those from the other wells (Figure 3.30).

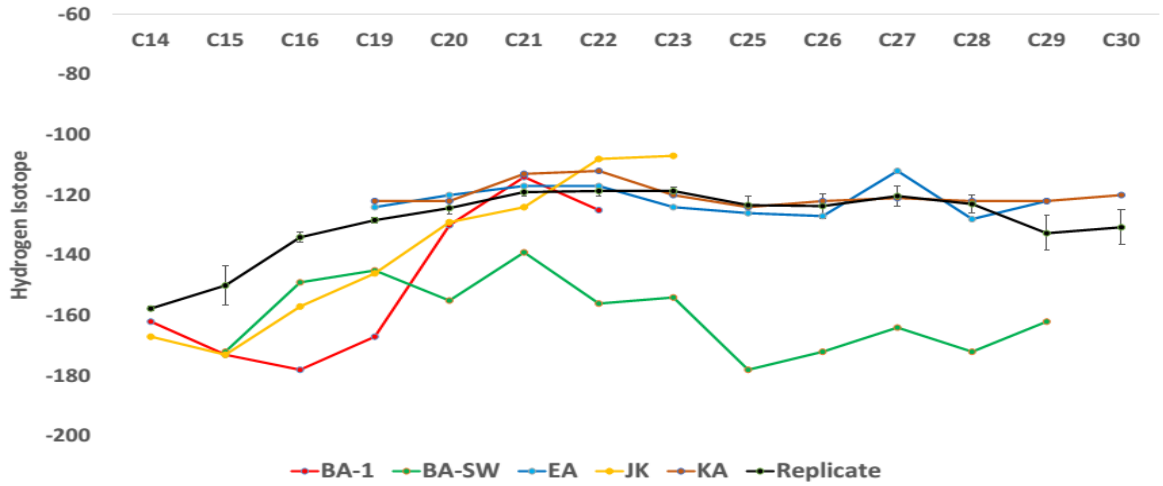

Figure 3.30: The *n*-alkane stable hydrogen isotope plot of cuttings samples from 5 wells in the delta.

Table 3.7: Summary of *n*-alkane stable carbon isotope $\delta^{13}C$ (‰) measurements from well cuttings samples

	Well	C_{14}	C_{15}	C_{16}	C_{19}	C_{20}	C_{21}	C_{22}	C_{23}	C_{25}	C_{26}	C_{27}	C_{28}	C_{29}	C_{30}
OEE2	BA-1	-30.3	-31.6	-30.9	-28.9	-28.2	-29.5	-29.9	-33.9	-33.1	-32.8	-32.3	-33.6	-31.1	nm
OEE3	BA-SW	-29.9	-30.0	-31.0	-27.6	-29.6	-27.0	-27.2	-28.8	-34.4	-31.0	-33.2	-28.6	nm	nm
OEE5	BA-SW	-30.0	-30.6	-31.9	nm	nm	nm	-29.0	-27.5	-34.0	-29.5	-33.6	nm	nm	nm
OEE6	EA	nm	-28.7	-27.9	-25.6	-28.7	-29.5	-28.4	-28.4	-30.0	-29.4	-29.7	nm	nm	nm
OEE7	EA	nm	-29.3	-28.6	-28.0	-27.6	-27.6	-26.6	-30.2	-35.9	-29.2	-33.0	-39.0	-36.0	nm
OEE9	EA	nm	nm	nm	-27.7	-29.5	-29.0	-30.5	-30.2	-30.4	-29.6	-30.8	-31.3	-28.5	-31.6
OEE11	JK	-30.8	-30.8	-32.6	-34.5	-31.4	-34.8	-28.5	-26.9	nm	nm	nm	nm	nm	nm
OEE12	JK	-30.2	-30.2	-31.4	-34.6	-33.0	-34.1	-29.0	-27.7	-24.0	nm	nm	nm	nm	nm
OEE15	JK	-30.9	-31.1	-32.8	-34.6	-32.7	-32.0	-31.2	-30.3	-29.8	nm	nm	nm	nm	nm
OEE16	KA	-31.0	-31.0	-31.9	-29.8	-29.7	-30.1	-30.5	-31.3	-31.1	-31.1	-31.9	-31.5	-32.1	-31.1
OEE17	KA	-28.4	-29.5	-28.9	-28.7	-28.7	-30.0	-30.0	-30.6	-31.4	-31.0	-32.0	-32.6	-32.8	-32.1
OEE48	KA	-31.0	-30.8	-31.0	-28.8	-29.3	-30.8	-30.7	-31.0	-33.9	-31.0	-33.0	-34.0	-33.0	nm
OEE19	KI	-31.0	-31.0	-30.3	-28.3	-30.0	-29.1	-29.1	-33.3	-35.0	-30.4	-34.5	nm	nm	nm
OEE20	KI	-30.1	-30.2	-29.0	-28.0	-26.0	-26.0	-27.7	-29.3	-28.6	-29.3	nm	nm	nm	nm
OEE50	KI	-30.6	-30.8	-32.0	-29.3	-28.0	-27.0	nm	nm	nm	nm	nm	nm	nm	nm
Replicate (Average)		-27.5	-27.4	-27.8	-28.0	-28.1	-28.4	-28.7	-28.6	-28.7	-28.9	-29.2	-29.3	-29.6	-29.8
Replicate (std error)		0.18	0.09	0.21	0.09	0.18	0.15	0.24	0.18	0.25	0.34	0.38	0.42	0.49	0.57

nm: result was rejected due to very low concentration level of the targeted compound, std error: standard error.

Table 3.8: Summary of *n*-alkane stable hydrogen isotope δD (‰) measurements from well cuttings samples

	Well	C_{14}	C_{15}	C_{16}	C_{19}	C_{20}	C_{21}	C_{22}	C_{23}	C_{25}	C_{26}	C_{27}	C_{28}	C_{29}	C_{30}
OEE02	BA-1	-162	-173	-178	-167	-130	-114	-125	nm	nm	nm	nm	nm	nm	nm
OEE03	BA-SW	nm	-172	-149	-145	-155	-139	-156	-154	-178	-172	-164	-172	-162	nm
OEE09	EA	nm	nm	nm	-124	-120	-117	-117	-124	-126	-127	-112	-128	-122	nm
OEE15	JK	-167	-173	-157	-146	-129	-124	-108	-107	nm	nm	nm	nm	nm	nm
OEE16	KA	nm	nm	nm	-122	-122	-113	-112	-120	-124	-122	-121	-122	-122	-120
OEE17	KA	nm	nm	nm	-124	-108	-122	-118	-129	-126	-124	-122	-124	-126	-117
Replicate (Average)		-158	-150	-134	-128	-124	-119	-119	-119	-123	-124	-120	-123	-133	-131
std error (Replicate)		0.9	6.6	1.5	0.9	1.9	1.5	1.9	1.3	2.8	4.2	3.3	2.9	5.8	5.8

nm: result was rejected due to very low concentration level of the targeted compound, std error: standard error.

3.2 POTENTIAL SOURCE ROCK SAMPLES CHARACTERISATION

The accurate assessment of the petroleum source potential of a sedimentary facies helps geochemists define how effective a source rock is, or might be, in a petroleum system if other conditions remain favourable with productivity, preservation and dilution generally the major controlling factors in the formation of organic rich source rocks.

To have high TOC source rocks, the environment of deposition must have been mainly anoxic with sediments deposited in layers and preservation at his peak, and with right depth of burial and formation temperature hydrocarbon will be expelled (primary migration) from such source rock with several mechanism which includes diffusion; oil phase expulsion; solution in gas and micro-fracturing.

The quantity and type of hydrocarbon produced by a source rock depend to a large extent on the organic facie type, depth of burial (temperature/time) and the hydrocarbon generative potential of any source rocks depends on their TOC; HI; PI; and Tmax.

3.2.1 Well cuttings sample descriptions

The general criteria of well cuttings sample selection for analysis was based on grain size: fine grain samples were selected and those with coarse grain were rejected, and also colour with darker samples being selected ahead of the lighter coloured samples, although some lighter coloured samples were selected for analyses because there were no suitable dark cuttings samples in the well.

The selected cuttings samples from well BA-SW were generally grey in colour and were muddy with some ductile properties; there were no dark/black intervals in this well, unlike well BA-SW, well BA-1 which showed gradation in colour from dark grey to grey and from mud to shales. Cuttings samples from well EA were generally light grey to dark grey and ranged from clay to silty mud and fissile shales. Cuttings sample colours from well JK ranged from black to dark brown, muddy and left an oily stain on any material it came in

contact with; there is therefore a high probability that the samples from this well might have been contaminated with drilling mud or migrated hydrocarbon. The selected cuttings from well KA were light to dark grey shales with some muddy shales and this also applied to cuttings samples from well KI.

3.2.2 Source rock generative potential

The Total Organic Carbon (TOC) content of the rock provides a guide to the possible petroleum generative potential of a sample (Espitalie *et al*., 1977; Peters *et al*., 2005) and geochemists generally do not select sample with less than 0.5 mg/g TOC for further analysis (Hunt, 1996) because they do not have the quantity of TOC to saturate the source rock for effective oil expulsion to take place (Pepper & Corvi, 1995).

The cuttings samples from Well BA-SW were selected from depths around 3.9 to 4.1 km and they showed only fair potential to generate hydrocarbons (Figure 3.31). However, these samples might have produced hydrocarbons in the past because they are over-mature at the current burial depth and when TOC correction was done based on the formula proposed by Cornford *et al*., (2001), it can be concluded that they may have had good potential to generate hydrocarbons (TOC 1.72 to 2.2%) but it should be noted that the Tmax of these samples are far above the maximum recommended Tmax value of 470 ºC which Cornford *et al*., (2001) based their interpretations on. The cuttings samples from Well BA-1 were selected from depth intervals between 3.1 to 3.4 km and show that they had good potential to generate hydrocarbon at the right maturity (Figure 3.31). The cuttings samples from well JK were selected from depths of around 1- 4 km and show fair to excellent source potential based on their TOC and S2 values. The TOC, S1 and S2 values from this well (JK) does not show any variation with depth, however it is possible that samples from different intervals were deposited under different depositional settings as the delta progrades. The cuttings samples from Well EA were selected from depths around 1.2 to 2.3 km and they

generally show that they have poor to fair potential to generate hydrocarbons (Figure 3.31), although the sample from 1.8 km depth has very good potential to generate hydrocarbons based on its TOC, its present day free hydrocarbons (S1) and the remaining hydrocarbon potential of the kerogen (S2) values does not support this. The cuttings samples from Well KA were selected from depths of around 2.1 to 3 km and showed that they had poor to excellent potential to generate hydrocarbons (Figure 3.31). The cuttings samples from Well KI were selected from depths around 2.5 to 2.7 km and generally show that they have fair to good potential to generate hydrocarbons under the right maturity condition (Figure 3.31). The present day free hydrocarbons (S1) and the remaining hydrocarbon potential of the kerogen (S2) make up the total hydrocarbon potential and is best used when a samples has not produced/expelled hydrocarbon (i.e. Tmax not in the oil window) (Espitalie *et al*., 1977; Peters *et al*., 2005).

The Niger Delta is a prograding delta and samples from different depths must have been deposited at different times under different oxygenation conditions therefore their depositional settings will be different.

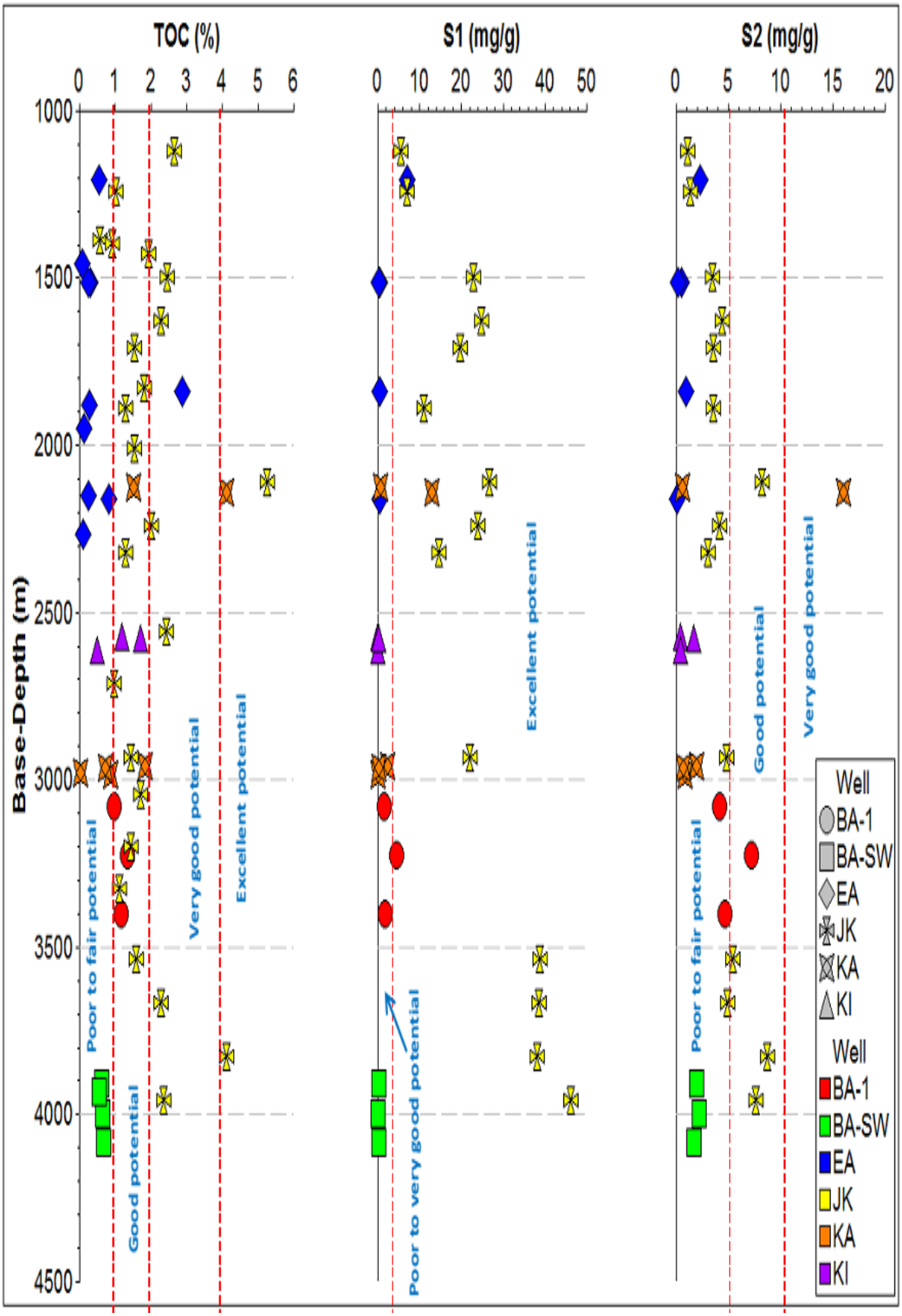

Figure 3.31: Total organic carbon content and Rock-Eval derived generative potential parameters of cuttings samples from the six Niger Delta wells.

3.2.3 Kerogen quality/Type of organic matter

The volume and type of fluid generated and expelled from a source rock does not only depend on thermal maturity but also on the quality/type of the organic matter which makes up the source rock and its chemical composition determines if a source rock will be oil or gas prone (Espitalie *et al*., 1977; Peters *et al*., 2005).

The cuttings samples from wells EA, KA and KI contained mainly Type III kerogen and based on this we can infer that given the right burial and at the right maturity they will mainly generate gas and maybe some oil (Peters *et al*., 2005), whereas well cuttings sample from wells BA-1 and JK were of mainly Type II organic matter (Figure 3.32) and given the right maturity/burial depth they will generate oil and some gas (Peters *et al*., 2005) and those from well BA-SW are over mature and might have produced and expelled hydrocarbon.

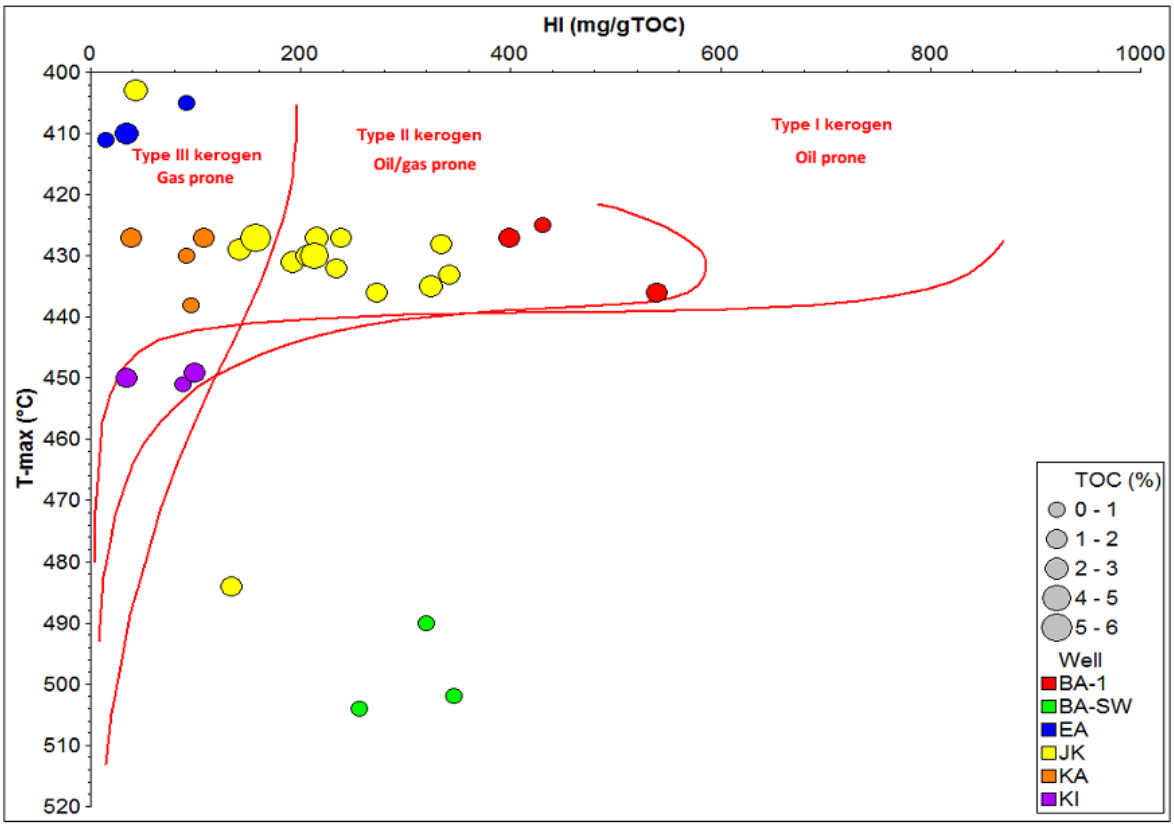

Figure 3.32: Plot of T-max against Hydrogen Index of cuttings samples from the six Niger Delta wells indicating the kerogen types of the samples.

The type of organic matter (OM) in the well cuttings samples is very useful when inferring the paleo-environmental depositional conditions of the samples. The cuttings samples contained mixed planktonic/bacterial/land plant derived organic matter (Figure 3.33) with samples from well KA mainly land plant organic matter, while the OM in cuttings samples from wells BA-1, BA-SW, EA and KI was mainly sourced from mixed planktonic/bacterial/land plants; cuttings samples from well JK mainly had OM input from mixed planktonic/bacterial with minimal land plant input (Figure 3.33).

There have been several instance of transgression and regression of the sea in the delta and this is reflected in the depositional environment indicators of the cuttings samples, with those of well JK mainly deposited in an open marine environment (Figure 3.34), samples from well BA-1, BA-SW and EA deposited in shallow marine/ coastal environments and samples from wells KA and KI were deposited in mainly deltaic environments (Figure 3.34).

The oxygenation regime in the depositional environment to a large extent decides the level of preservation of an organic matter and this is also reflected in the molecular markers. Cuttings samples from wells JK and BA-1 were deposited in a reducing environment, while the other well cutting samples were deposited in mixed regimes (partly oxidizing and partly reducing) but those of the samples from wells EA and KA tends to be more oxidizing than reducing (Figure 3.35).

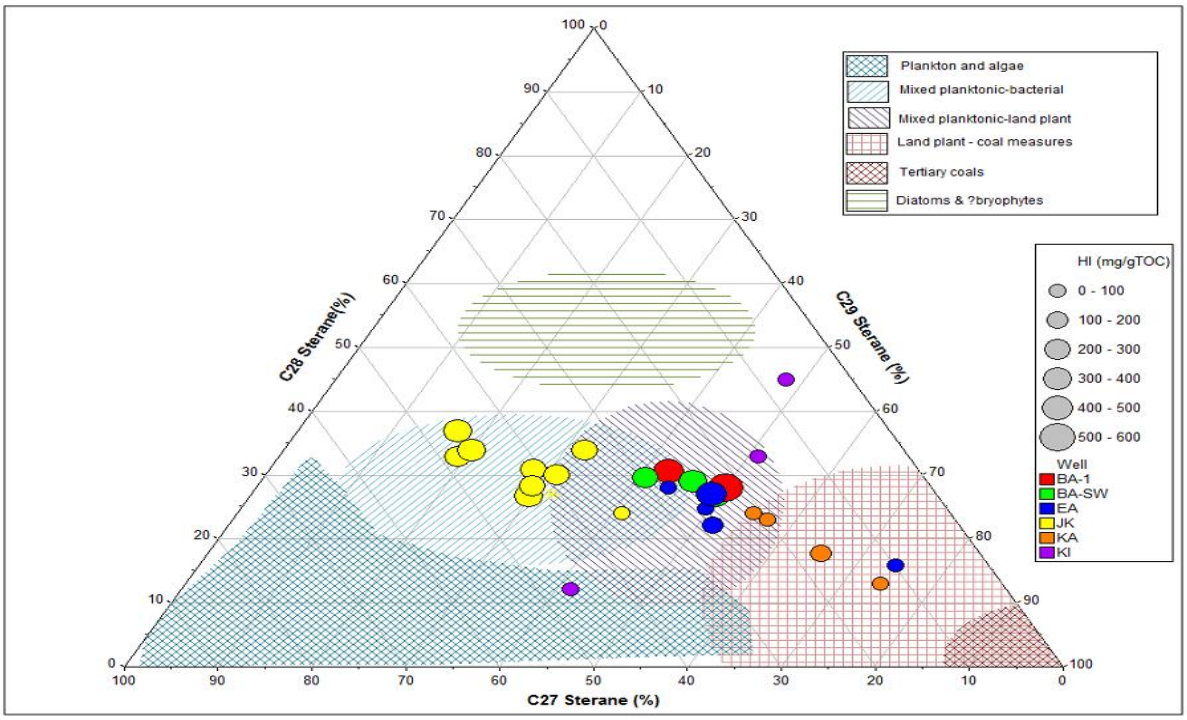

Figure 3.33: Ternary diagram showing the distribution of percentage C_{27}, C_{28} and C_{29} regular sterane 5α(H),14α(H),17α(H) 20R configuration of the Niger Delta well cutting samples showing the organic matter type. Interpretation overlay from p:IGI 3.5 (modified after Huang and Meinschein 1979).

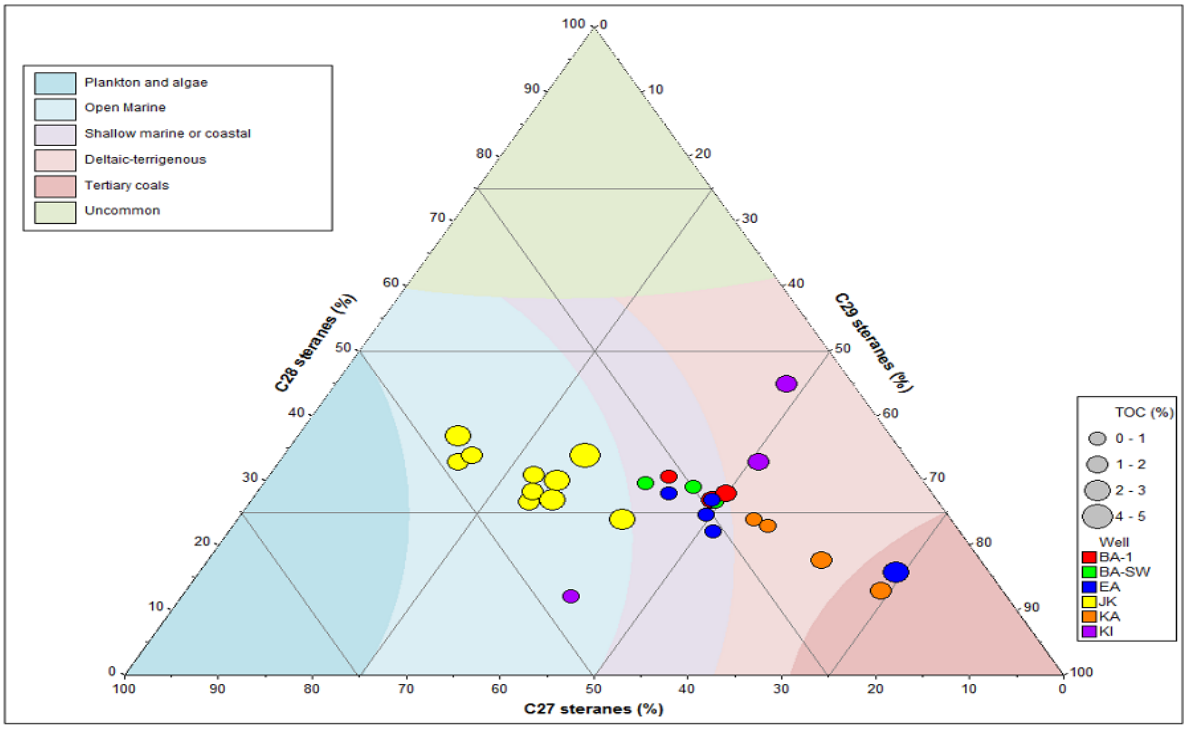

Figure 3.34: Ternary diagram showing the distribution of percentage C_{27}, C_{28} and C_{29} regular sterane 5α(H),14α(H),17α(H) 20R configuration showing the source environment of deposition of the Niger Delta well cutting samples. Interpretation overlay from p:IGI 3.5 (modified after Huang and Meinschein 1979).

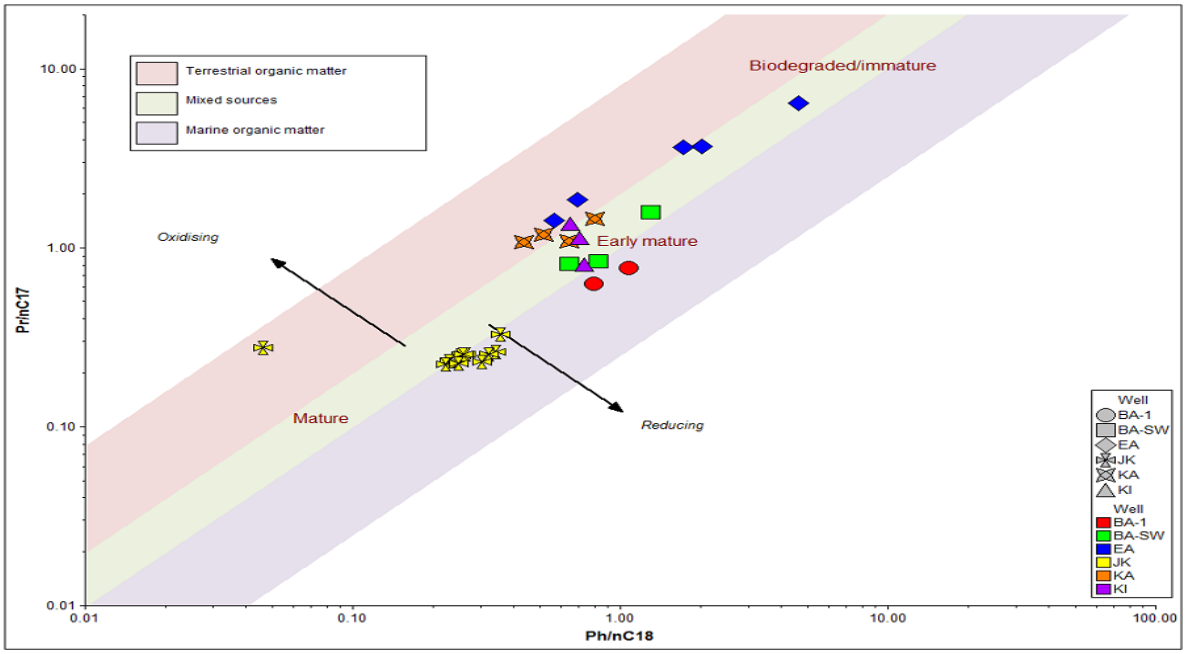

Figure 3.35: Cross plot of Pr/nC$_{17}$ against Ph/nC$_{18}$ showing the kerogen type, maturity and depositional environment of the Niger Delta well cutting samples. Interpretation overlay from p:IGI 3.5 (modified after Shanmugam 1985).

3.2.4 Thermal Maturity

Thermal maturity has been estimated over the years with the use of Rock-Eval Tmax and Production Index (PI) (Espitalie *et al*., 1977; Peters *et al*., 2005). Tmax is related to the depth of burial/temperature and PI is related to the petroleum that has been generated from the organic matter, which is usually a function of both the temperature and kerogen type. Based on Tmax values most of the well cuttings samples in this study appear immature (BA-1, EA, JK, KA) with the samples from well KI in the oil window and those from well BA-SW in the over-mature range (Figure 3.36). However, there seems to be little or no correlation between the Tmax values and the PI values (Figure 3.36), based on PI values of the cutting samples in this study, those from well BA-SW appear immature to oil window mature rather than over-mature from the Tmax values, and wells EA, KA and JK cutting samples are mainly over-mature from the PI values (Figure 3.36), but maturity indications from PI values are known to be very dependent on the kerogen type and expulsion efficiency of the source rocks (Peters *et al*., 2005). The production index of cuttings

samples from well JK can be interpreted as exhausted, with values generally more than 2 but Tmax suggests otherwise.

Isomerisation of some sterane biomarkers can help to indicate thermal maturity, and based on these, the cuttings samples from well JK appear to be of early maturity, whereas those from wells EA, KA, KI, BA-1 and BA-SW are all immature (Figure 3.37). The cutting samples from well BA-SW are post mature based on Tmax measurement, however these samples are of low thermal maturity based on sterane isomerisation, which give contradictory measurement between those two parameters.

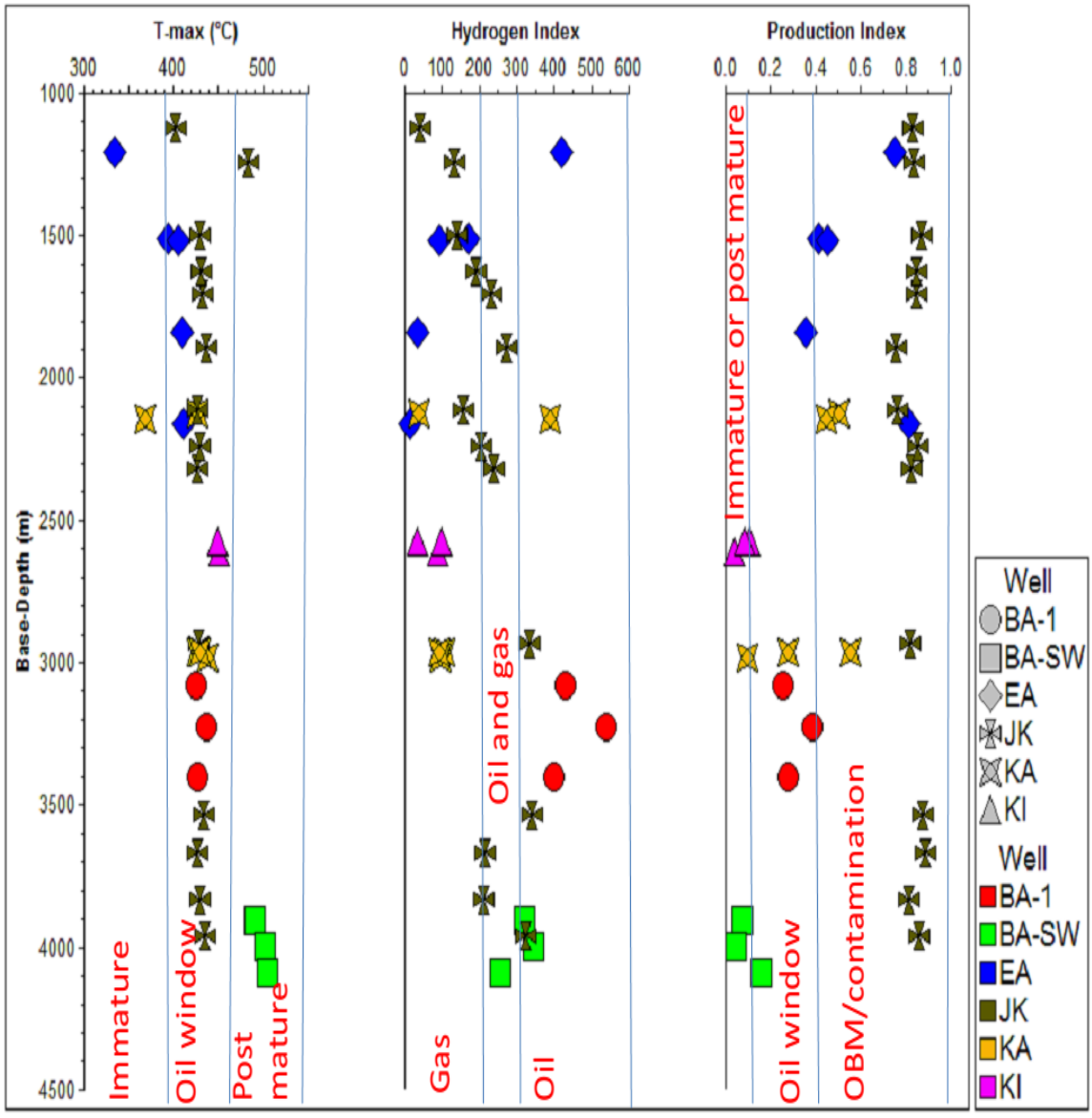

Figure 3.36: Plot of Rock-Eval Tmax and Production Index values against depth for the cuttings samples from the six Niger Delta wells. Possible contamination of well JK cutting samples by oil base mud (OBM).

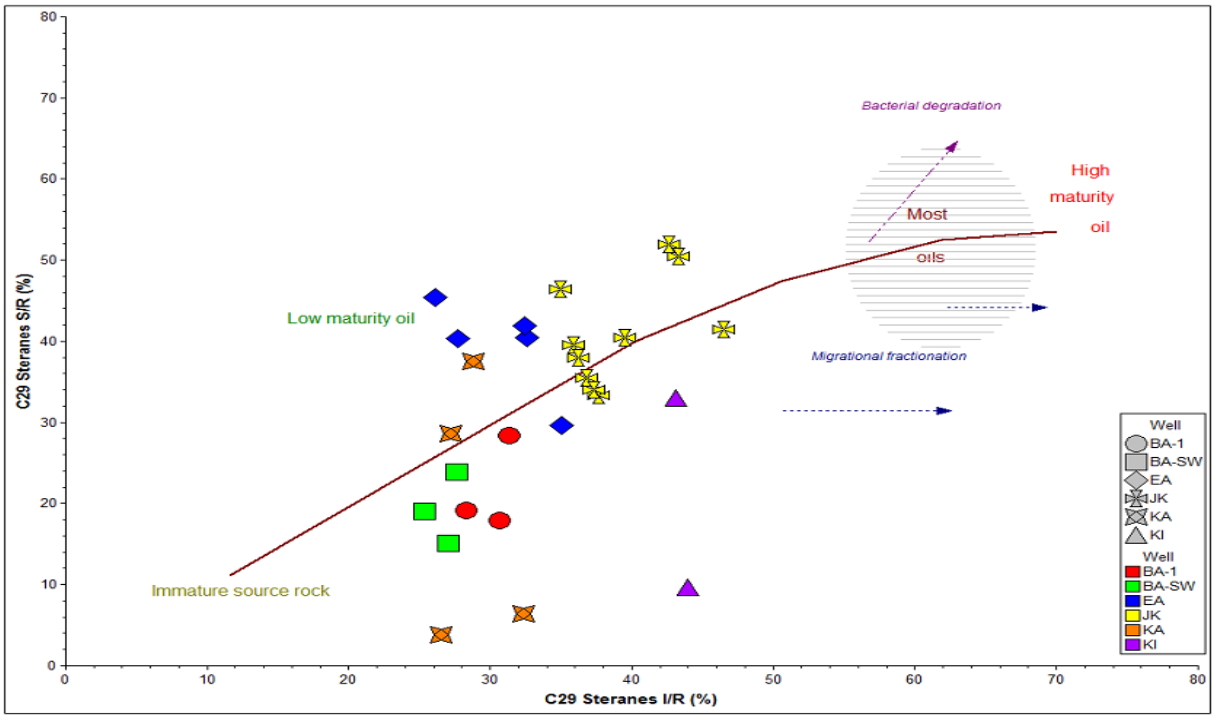

Figure 3.37: Plot of %C_{29} 20S/20S+20R (5α(H),14α(H),17α(H)) against %C_{29} I/I+R [(5α(H),14β(H),17β(H)-20S+20R)/(5α(H),14β(H),17β(H)-20S + 20R+5α(H),14α(H),17α(H)-20S+20R)] sterane isomerisation maturity parameters showing that most of the Niger Delta well cutting samples are of low maturity (modified after Seifert & Moldowan, 1986). Interpretation overlay from p:IGI 3.5.

3.2.5 Contamination

The use of well cutting samples for geochemical analysis has always been prone to contamination and where possible, the results generated should always be compared with those from side wall core to validate/corroborate them. However, in this study, no core material was available and well cuttings were the only available source rock samples, and thus analytical results based on them are susceptible to contamination from drilling mud, cavings and artefacts of drilling activities. Cuttings samples from well JK are believed to be highly contaminated with drilling mud based on the following observations:

1. Tmax remains constant over a very large depth range (1to 4 km)
2. S1 values are generally very high (mostly between 10 to 50 mg/g)
3. Unusually high PI values of between 0.76 to 0.89
4. GC peaks of *n*-alkanes are dominated by diesel range peaks (*n*C_{12} to *n*C_{24}).

5. Very high 3+4 methyldiamantane concentration (20 to 63 ppm) which indicates highly cracked extract. This is seen even at shallow depth.

3.2.6 Conclusions

The studied well cuttings samples were collected from a depth interval of about 1 to 4.1 km from 6 wells from different parts of the Niger Delta. They were mainly silty to fissile mud or shales with a wide range of colours generally from grey to dark grey through dark brown to black.

Based on TOC, they have poor to excellent petroleum generative potential and S2 measurement shows that they have poor to very good potential to generate hydrocarbon given the right condition.

The kerogen type were mainly Type III with some Type II, from the plot of Tmax against HI and are composed of mixed planktonic/bacterial/land-plant organic matter, deposited in open marine/shallow marine/deltaic environment based on sterane biomarker which was partly oxidizing and partly reducing during deposition period from the *n*-alkane/isoprenoid plot.

Some of the samples have contradictory maturity parameters as Rock-Eval shows that the samples are immature to post mature, however *n*-alkane/isoprenoid plot and sterane biomarkers indicates that our well cutting samples are mainly immature.

Cuttings samples from well JK recovered from depths of 1 to 4 km contained Type II kerogen deposited under open marine environments and had fair to excellent potential to generate hydrocarbons and were in the oil window maturity range. However, the cuttings samples from this well had been heavily contaminated with what appeared to be an oil based drilling fluid and so the cuttings geochemical results from this well could be misleading. Overall the analysed transgressive shales of the Agbada formation are not the source of the hydrocarbons in the Niger Delta Basin.

CHAPTER FOUR
OIL GEOCHEMICAL RESULTS

4.0 Introduction

In order to undertake a detailed geochemical study of the 180 Niger Delta oil samples, about 130 parameters were calculated, mainly as ratios and concentrations from the numerous measured peaks from the TLC-FID, GC and GC-MS and GCIRMS and presented and interpreted.

The Niger Delta was subdivided into four sub-divisions (Western, Eastern, Central and Southern) and these areas have different size, therefore the number of samples selected from each area varies. The mean (arithmetic average), standard deviation and coefficient of variation was used to check for variations in the results between the different regions and the data was presented in a tabular form. Below is a brief explanation of the statistical parameters used to summarise the data in the tables.

Number of samples (no): This is the total number of samples used to compute the mean of a calculated geochemical parameter (i.e. the total number of samples from a particular region).

Mean (M): This is the same as the average or the arithmetic mean and can be calculated by summing up the values of a parameter (for any region) and dividing by the number of samples (in that particular region). The mean can be influenced to a large extent by outliers.

Standard Deviation (SD): This is generally a measure of the dispersion/variation from the average, therefore a data with a close range will have a low standard deviation and one with a high range will have a high standard deviation.

Coefficient of Variation (CV): The CV helps to describe the difference in a variable while comparing different sample/parameter/areas. The lower the difference in a data the lower the CV value and verse versa. It is usually calculated by SD/M in percentage, therefore it

can be used as a comparison base within a data set (it fuses SD and M into just one result). The CV helps to compare a parameter between the different regions because it reduces dimensionality and place values on the same scale for comparison.

The presented data was checked for outliers that might affect the outcome of the results generated, which could lead to misinterpretation and histogram plots are only shown for parameters with variations across the delta. XY and ternary plots are used to show variations in some parameters and how they correlate with other parameters.

4.1 Gasoline Range/ Light Hydrocarbons

Gas chromatography of whole oils was used to study the light hydrocarbon fractions, and more emphasis was placed on the C_7 range because of evaporative losses experienced by lighter ends during storage. The peaks measured (where possible) are shown in Figure 4.1 and the results are presented in Table 4.1. The onset of biodegradation where the light ends of the *n*-alkane is attacked renders some parameters unable to be measured: the parameters calculated includes: HeptRat (c.f. Thompson 1979; 1983); P1/hept (c.f. Thompson 1979; ten Haven 1996; Mango 1997); P3/N2 (c.f. ten Haven 1996; Mango 1997); IsohepRat (c.f. Thompson 1979; 1983); P2/Hept (c.f. Philippi 1975; Thompson 1979; ten Haven 1996; Mango 1997); N15/N16 (c.f. ten Haven 1996; Mango 1997); cH/bcC_7 (c.f. ten Haven 1996; Mango 1997); cP/bcC_7 (c.f. ten Haven 1996; Mango 1997); b/bcC_7 (c.f. ten Haven 1996; Mango 1997); 22/24dmP (c.f. p:IGI geochemical manual 2004); 11/1c3dmcP (c.f. p:IGI geochemical manual 2004); 2/3mH(c.f. p:IGI geochemical manual 2004); e/11dmcP (c.f. p:IGI geochemical manual 2004); dmc/dmP (c.f. p:IGI geochemical manual 2004); Bz/cH (c.f. p:IGI geochemical manual 2004); mcP/*n*C_6 (c.f. Mango 1997); mcH/mcP (c.f. Mango 1997); mcH/*n*C_7 (c.f. Mango 1997); dmcP/mH (c.f. Mango 1997); Tol/mcH (c.f. Mango 1997); mcH/cH (c.f. p:IGI geochemical manual 2004); *n*C_7/*n*C_6 (c.f. p:IGI geochemical manual 2004); Tol/Bz (c.f. p:IGI geochemical manual 2004); C_7Paraf (c.f. p:IGI

geochemical manual 2004); C_7Naph (c.f. p:IGI geochemical manual 2004); C_7 Arom (c.f. p:IGI geochemical manual 2004).

There is no significant variation in these parameters/ratios in samples from the same part of delta (Table 4.1). However, the HeptRat and the C_7paraf show marked differences, with the Central Delta oils having low values whereas most of the Southern Delta oils have higher values for both parameters (Figure 4.2 & 4.3).

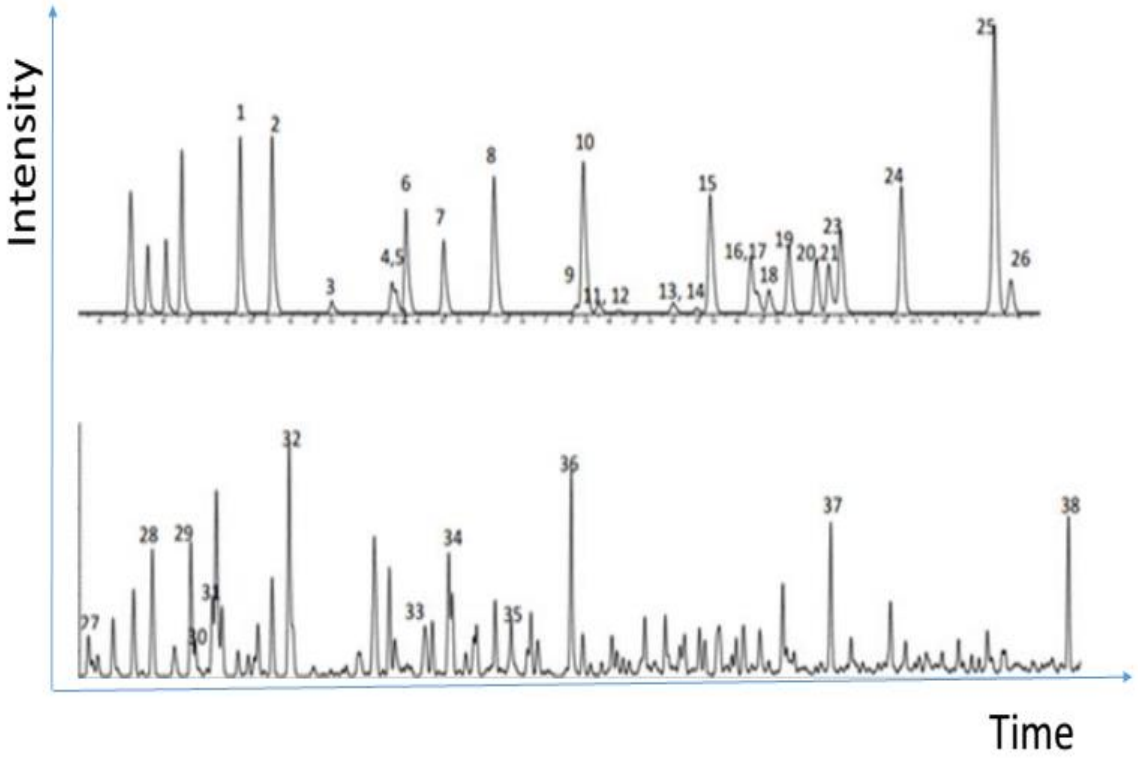

Figure 4.1: Representative partial GCMS total ion current (TIC) chromatogram of a whole oil (OE044).

1= iso-Pentane (C_5 mono-branched). 2= normal-Pentane (C_5 straight). 3= 2,2-dimethyl-Butane (C_6 di-branched). 4= cyclo-Pentane (C_5 cyclo). 5= 2,3-dimethyl-Butane (C_6 di-branched). 6= 2-methylpentane (C_6 mono-branched). 7= 3-methylpentane (C_6 mono-branched). 8= normal hexane (C_6 straight). 9= 2,2-dimethylpentane (C_7 di-branched). 10= methylcyclopentane (C_6 cyclo). 11= 2,4-dimethylpentane (C_7 di-branched). 12= 2,2,3-trimethylbutane(C_7 tri-branched). 13= Benzene (C_6 aromatic). 14= 3,3-dimethylpentane (C_7 di-branched). 15= cyclohexane (C_6 cyclo). 16= 2-methylhexane (C_7 mono-branched). 17= 2,3-dimethylpentane (C_7 di-branched). 18= 1,1-dimethylcyclopentane (C_7 cyclo). 19= 3-methylhexane (C_7 di-branched). 20= 1-cis-3-dimethylcyclopentane (C_7 cyclo). 21= 1-trans-3-dimethylcyclopentane (C_7 cyclo). 22= 3-ethylpentane (C_7 mono-branched). 23= trans-1,2-dimethylcyclopentane. 24= normal heptane (C_7 straight). 25= methylcyclohexane (C_7 cyclo). 26= 1-cis-2-dimethylcyclopentane (C_7 cyclo). 27= ethylcyclopentane. 28= Toluene. 29= 2-methylheptane. 30= 4-methylheptane. 31= 3-methylheptane. 32= nOctane. 33= ethylbenzene, 34= meta & para xylene. 35= ortho xylene. 36= nNonane. 37= nDecane, 38= nUndecane.

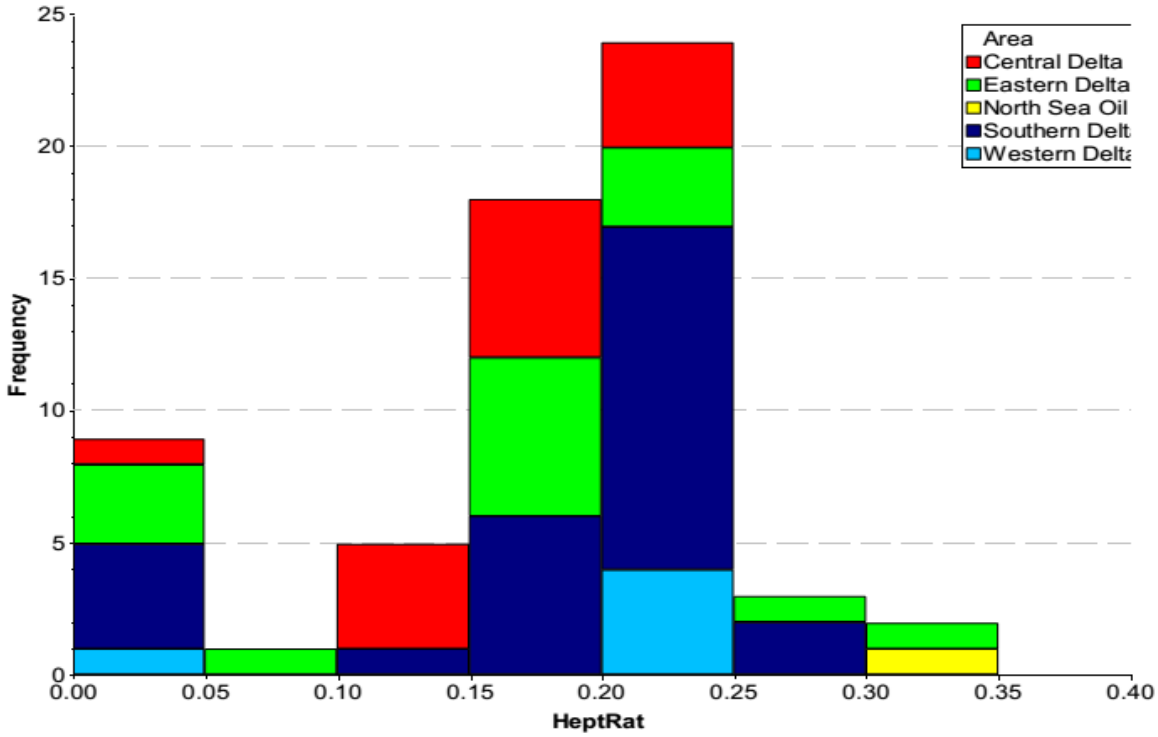

Figure 4.2: Variation of HeptRat in Niger Delta oil. Note the wide range of the ratio, with most of the Central Delta oils having a low value whereas most of the Southern Delta oils have a high value.

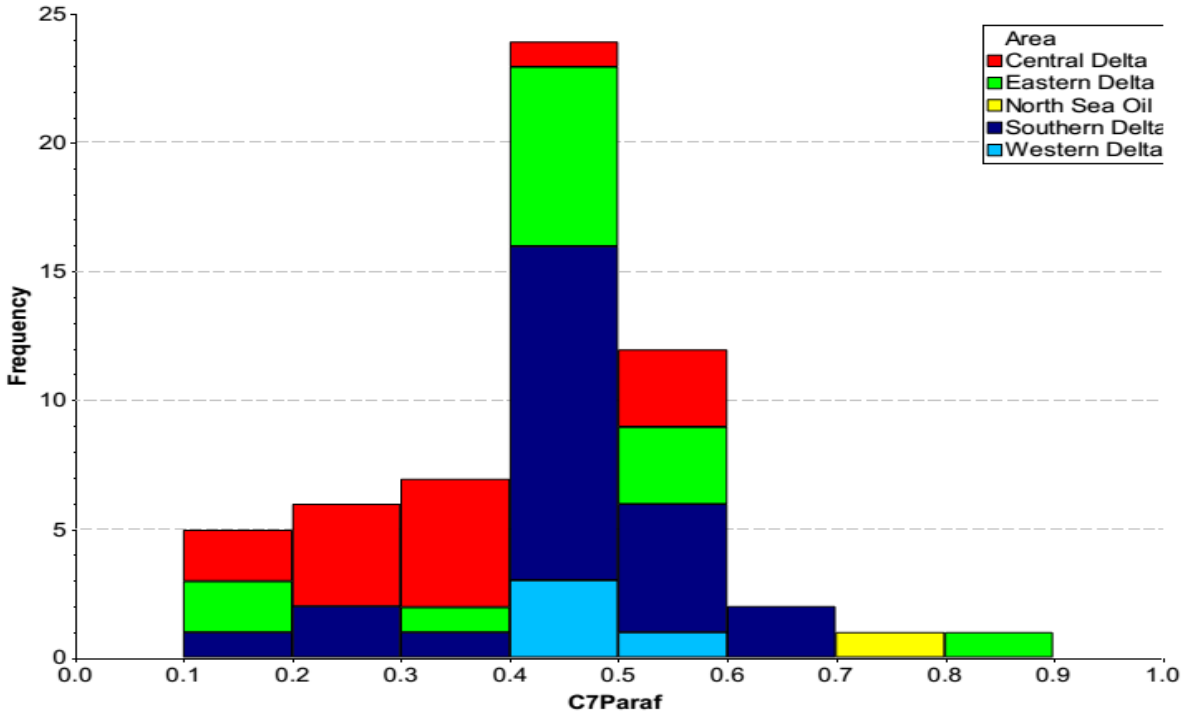

Figure 4.3: Variation of C_7paraf in Niger Delta oil. Note the wide range of the ratio with most of the Central Delta oils having a low value whereas most of the Southern Delta oils have a high value.

The average HeptRat for the Central Delta is 13.97%, for Eastern Delta is 13.51%, while Western Delta is 14.93% and Southern Delta is 14.86%. A cross plot of the HeptRat and the C_7Paraf shows a strong positive correlation and this indicates that with increasing HeptRat there is a corresponding increase in the C_7Paraf, with the Central Delta samples having relatively lower C_7Paraf values (Figure 4.4)

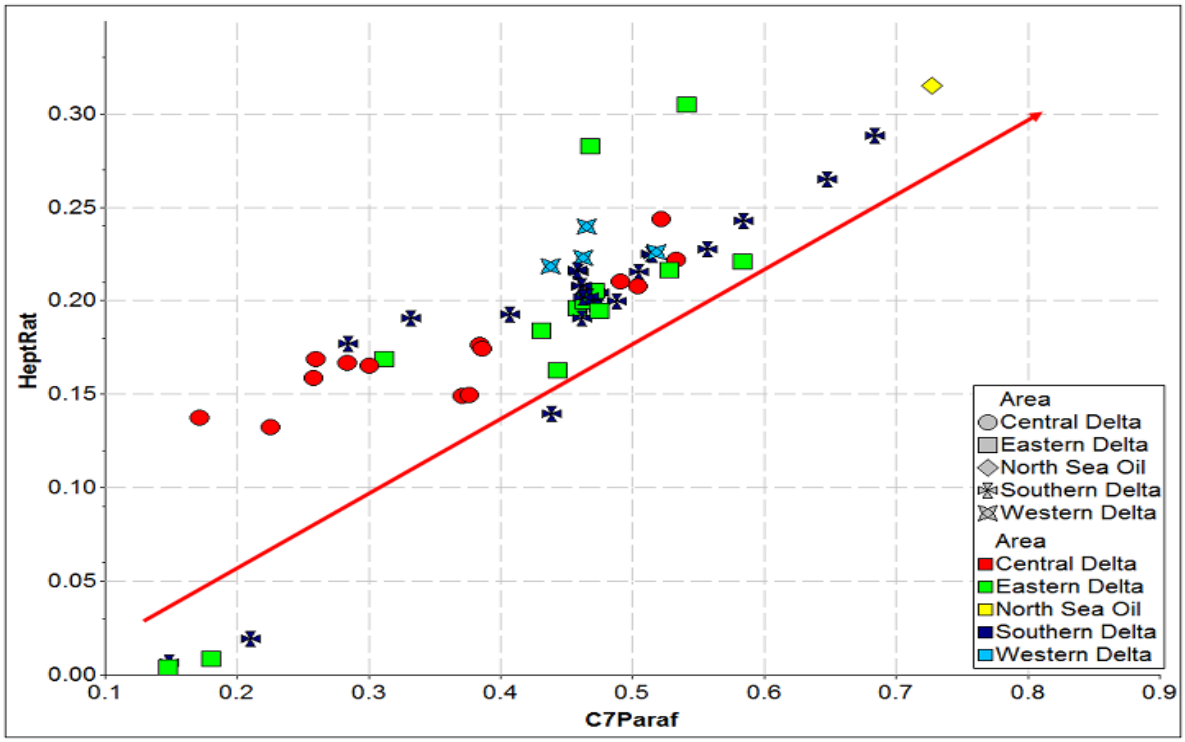

Figure 4.4: Plot of HeptRat vs C_7Paraf showing a positive correlation between the paraffin content and HeptRat.

The C_7Paraf; C_7Naph and C_7Arom values of the oil samples shows a clear relationship but there exist two groups of outliers (Figure 4.5). Most of the samples have between 35-45% C_7Paraf; 40-65% C_7Naph and 5-25% C_7Arom, whereas a group of mainly Central Delta oils (OE39, OE55, OE 98, OE117, OE149 and OE150) plot away from the main group and have 10-25% C_7Paraf; 40-50% C_7Naph and 25-50% C_7 Arom. Four other samples which include two samples from the Southern Delta (OE21 and OE22) and two samples from Eastern Delta (OE135 and OE158) plot away from the general trend towards the C_7Naph end (Fig 4.5).

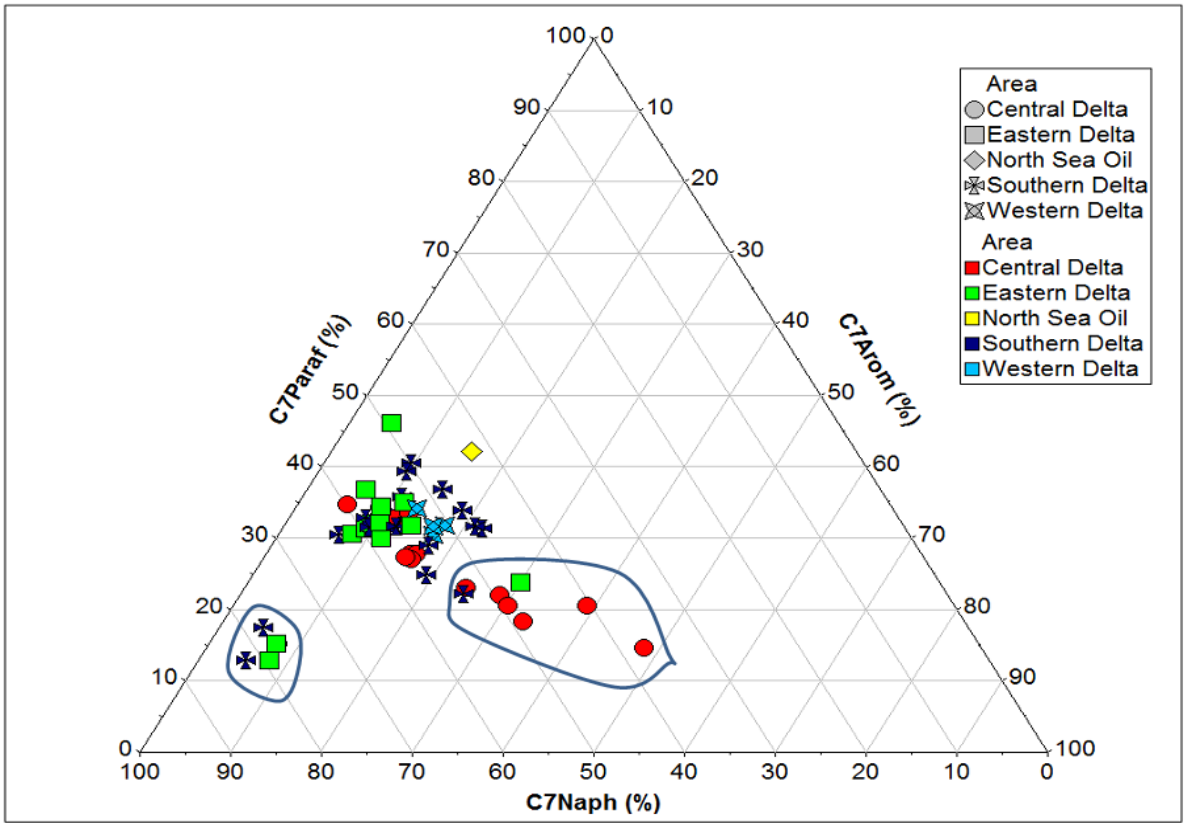

Figure 4.5: Variation of C_7 paraffin; C_7aromatic & C_7naphthenes content in the Niger Delta oils, showing two outlier groups.

The calculated temperature of expulsion from Mango (1997) ($^oC_{temp}$ = 140 + 15(ln[2,4-DMP/2,3-DMP]) is between 118 to 140 ^{o}C and these temperature does not show any trend with most of the other calculated gasoline parameters (e.g HeptRat, P1/hept, P3/N2, IsohepRat, P2/Hept, N15/N16, cH/bcC_7, cP/bcC_7, b/bcC_7, 22/24dmP, 11/1c3dmcP, 2/3mH, e/11dmcP, , Bz/cH, mcP/*n*C6, mcH/mcP, mcH/*n*C_7, dmcP/mH, Tol/mcH, mcH/cH, *n*C_7/*n*C_6, Tol/Bz, C_7Paraf, C_7Naph, C_7 Arom).

Table 4.1: Summary of source, alteration and maturity from light hydrocarbon parameters of oil samples

		Central Delta			Eastern Delta			Western Delta			Southern Delta			Replicate			NSO-1
Parameter	unit	no Mean	SD	CV	no Mean	SD	CV	no Mean	SD	CV	no Mean	SD	CV	no Mean	SD	CV	
HeptRat	%	15 13.97	4.27	31	15 13.51	7.39	55	5 14.93	7.99	54	26 14.86	6.25	42	3 22.9	0.66	3	23.95
P1/hept	a/b	15 0.13	0.05	39	14 0.15	0.07	51	4 0.20	0.01	7	24 0.16	0.05	32	3 0.26	0.01	4	0.27
P3/N2	a/b	15 0.53	0.11	21	15 0.60	0.48	81	5 0.49	0.07	15	26 0.59	0.19	32	3 0.93	0.12	13	0.94
IsohepRat	a/b	15 0.76	0.18	24	15 0.73	0.32	44	5 0.73	0.35	47	26 0.84	0.41	48	3 1.36	0.09	7	1.38
P2/Hept	a/b	15 0.10	0.03	31	14 0.12	0.03	27	4 0.13	0.01	8	24 0.13	0.03	26	3 0.18	0.00	0	0.17
N15/N16	a/b	15 0.19	0.10	52	14 0.28	0.09	31	4 0.21	0.02	12	25 0.24	0.08	33	3 0.21	0.04	19	0.21
cH/bcC7	a/b	15 1.96	0.98	50	14 1.16	0.40	35	4 1.41	0.07	5	24 1.27	0.30	23	3 1.16	0.02	2	1.16
cP/bcC7	a/b	15 0.28	0.12	42	14 0.38	0.11	29	4 0.30	0.03	11	24 0.34	0.10	30	3 0.23	0.00	0	0.25
b/bcC7	a/b	15 0.19	0.06	30	14 0.27	0.15	56	4 0.23	0.01	6	24 0.25	0.05	22	3 0.37	0.01	3	0.36
22/24dmP	a/b	15 1.01	1.25	124	15 1.67	3.66	222	5 0.84	0.43	51	26 0.80	0.22	27	3 0.78	0.06	8	0.78
11/1c3dmcP	a/b	15 0.56	0.12	21	15 0.53	0.16	31	5 0.52	0.09	17	26 0.59	0.09	16	3 0.71	0.03	4	0.70
2/3mH	a/b	15 0.81	0.11	13	15 0.70	0.23	33	5 0.76	0.21	27	26 0.90	0.40	45	3 0.93	0.09	10	0.93
e/11dmcP	a/b	15 1.06	0.39	36	15 1.11	0.87	78	5 1.04	0.19	18	26 0.93	0.30	32	3 1.11	0.21	19	1.07
dmc/dmP	a/b	15 2.17	0.90	41	15 2.45	0.73	30	5 1.94	0.19	10	26 2.02	0.72	36	3 1.05	0.13	12	1.10
Bz/cH	a/b	15 0.37	0.33	89	14 0.23	0.24	105	4 0.21	0.08	40	26 0.22	0.14	65	3 0.44	0.04	9	0.44
mcP/nC_6	a/b	15 1.37	0.89	65	15 1.92	2.47	129	5 2.21	2.87	130	27 1.95	3.04	156	3 0.52	0.11	21	0.50
mcH/mcP	a/b	15 3.74	1.31	35	15 7.19	11.58	161	5 2.68	0.27	10	27 4.18	3.30	79	3 2.99	0.03	1	3.01
mcH/nC_7	a/b	15 6.63	14.32	216	15 14.34	31.16	217	5 15.06	29.21	194	27 7.29	16.16	222	3 1.27	0.04	3	1.26
dmcP/mH	a/b	15 1.09	0.28	26	15 1.08	0.70	65	5 1.59	1.40	88	26 1.27	0.95	74	3 0.73	0.00	0	0.70
Tol/mcH	a/b	15 0.63	0.45	71	14 0.32	0.20	64	4 0.51	0.09	17	25 0.41	0.22	54	3 0.54	0.05	9	0.58
mcH/cH	a/b	15 2.91	0.73	25	15 8.13	17.84	219	5 2.43	0.32	13	27 3.36	1.39	41	3 1.84	0.10	5	1.84
nC_7/nC_6	a/b	15 1.35	0.53	39	15 1.58	1.63	103	5 1.08	0.48	45	27 1.71	1.65	96	3 1.23	0.11	9	1.20
Tol/Bz	a/b	15 7.23	6.79	94	14 10.22	8.39	82	4 6.60	1.64	25	25 8.38	7.50	90	3 2.39	0.07	3	2.42
C_7Paraf	%	15 25.34	6.75	27	14 30.33	8.41	28	4 3.99	1.54	5	24 30.88	6.20	20	3 42.06	0.21	0	42.11
C_7Naph	%	15 53.68	9.05	17	14 58.97	9.15	16	4 51.76	0.90	2	24 56.24	8.35	15	3 42.19	0.37	1	42.44
C_7Arom	%	15 20.98	12.46	59	14 10.69	6.05	57	4 16.25	1.88	12	24 12.88	5.18	40	3 15.81	0.51	3	15.44

HeptRat= *n*-heptane/ most naphthenic heptanes. **P1/hept**= *n*-heptane/ total C_7 hydrocarbons. **P3/N2**= ratio of P2 daughters. **IsohepRat**= (2mH+3mH)/(1c3dmcP+1t3dmcP+1t2dmcP). **P2/Hept**= Methyl hexanes/ total C_7 hydrocarbons. **N15/N16**= (ecP+1c2dmcP+1t2dmcP)/ (mcH + Toluene). **cH/bcC_7**= Cyclohexane/ branched + cyclic C_7 hydrocarbons. **cP/bcC_7**= Cyclopentane/ branched + cyclic C_7 hydrocarbons. **b/bcC_7**= C_7 branched hydrocarbons/ branched + cyclic C_7 hydrocarbons. **22/24dmP**= 2,2- dimethylpentane/ 2,4- dimethylpentane. **11/1c3dmcP**= 1,1- dimethylcyclopentane/ 1cis3-dimethylcyclopentane. **2/3mH**= 2- methylhexane/ 3-methylhexane. **e/11dmcP**= ethyl cyclopentane/ 1,1-dimethylcyclopentane. **dmc/dmP**= 1cis3-dimethylcyclopentane/2,3-dimethylpentane. **Bz/cH**= benzene/cyclohexane. **mcP/*n*C6**= methylcyclopentane/ *n*-hexane. **mcH/mcP**= methylcyclohexane/ methylcyclopentane. **mcH/*n*C_7**= methylcyclohexane/ *n*-heptane. **dmcP/mH**= 1trans3-dimethylcyclopentane/ 3-methylhexane. **Tol/mcH**= toluene/ methylcyclohexane. **mcH/cH**= methylcyclohexane/ cyclohexane. ***n*C_7/*n*C_6**= *n*-heptane/ *n*-hexane. **Tol/Bz**= toluene/ benzene. **C_7Paraf**= C_7 paraffins/ total C_7 hydrocarbons. **C_7Naph**= C_7 naphthenes/ total C_7 hydrocarbons. **C_7 Arom**= C_7 aromatics/ total C_7 hydrocarbons.

4.2 Bulk geochemistry/ *n*-alkanes and Isoprenoids

The SARA composition of the oil samples from Niger Delta basin was investigated using the Iatroscan (TLC-FID) technique, which yields the proportions of the four major fractions, i.e. the Saturated hydrocarbon fraction; Aromatic hydrocarbon fraction; Resins or polar (NSO - containing) fraction; and Asphaltenes fraction (Figure 4.6). The SARA compositions of the oil samples have high variations but without any particular trend across the Delta (Figure 4.7). The Central Delta samples have the lowest average saturates proportion (44 %), whereas the other regions have values around 50 %; on the other hand the Central Delta oils have a higher average value of aromatics (44 %) whereas those of the other regions have value of about 40 %. The NSO and asphaltene composition of the oils is fairly similar across the delta.

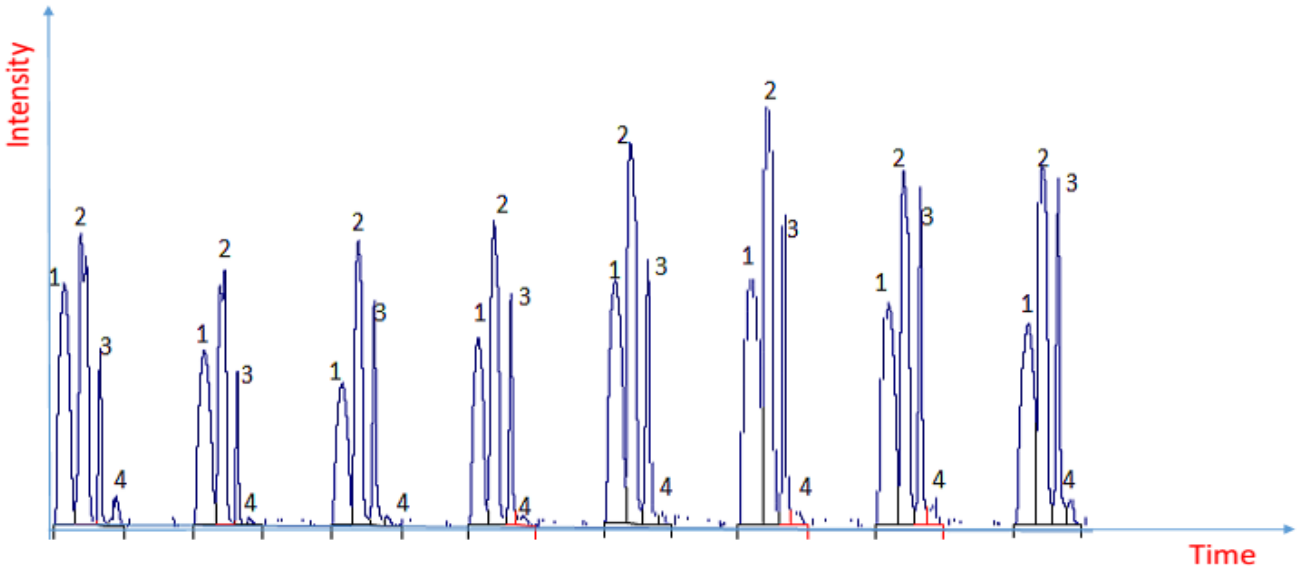

Figure 4.6: Representative TLC-FID chromatograms of oil samples showing SARA contents. **1=** Saturated hydrocarbon fraction. **2=** Aromatics hydrocarbon fraction. **3=** Polar (NSO) hydrocarbon fraction. **4=** Asphaltenes hydrocarbon fraction.

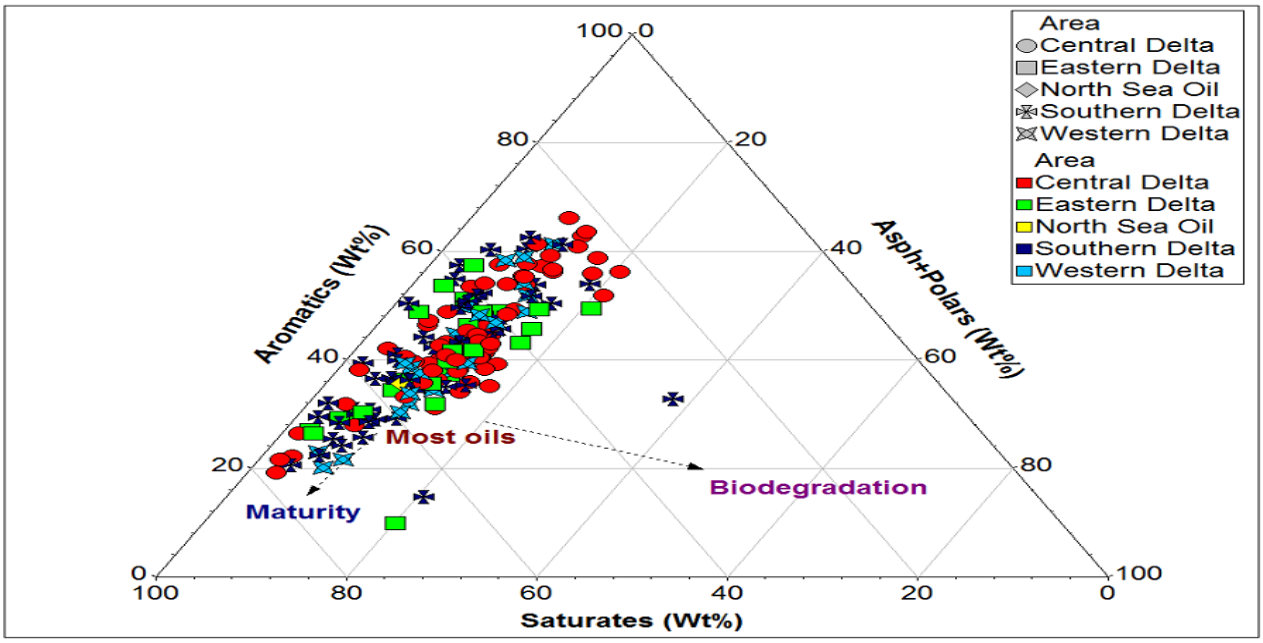

Figure 4.7: Ternary plot of SARA contents of the Niger Delta oil samples as determined by Iatroscan -FID method. Note the wide range of bulk geochemical compositions across the Delta. Overlay field after p:IGI-3.5 geochemical interpretation software.

Calculated ratios from *n*-alkane and isoprenoid hydrocarbon (Table 4.2) (e.g. Pr/Ph; norPr/Pr; Pr/nC$_{17}$; Ph/nC$_{18}$; nC$_{17}$/nC$_{27}$; CPI) from the gas chromatograms of the aliphatic hydrocarbon fractions (e.g. Figure 4.8). Although measurements were not possible for all the samples because of biodegradation (loss of *n*-alkanes), the samples with *n*-alkane peaks and/or isoprenoids present had the following ratios calculated: Pr/Ph (c.f. Peters & Moldowan, 1993); norPr/Pr (c.f. Peters & Moldowan, 1993); Pr/nC$_{17}$ (c.f. Peters & Moldowan, 1993); Ph/nC$_{18}$ (c.f. Peters & Moldowan, 1993); nC$_{17}$/nC$_{27}$ (c.f. Peters & Moldowan, 1993); CPI-1 (c.f. Philippi, 1965); CPI-2 (c.f. Bray & Evans, 1961); CPI-3 (c.f. Scalan & Smith, 1970). There was no marked variation in those ratios (Table 4.1) with the exception of nC$_{17}$/nC$_{27}$ where the Central Delta and Western Delta generally have lower values than the Southern Delta, whereas the Eastern Delta shows a wide range of values (Figure 4.9).

The average nC$_{17}$/nC$_{27}$ ratio for the Central Delta is 1.86, for Eastern Delta is 2.40, while Western Delta is 2.05 and Southern Delta is 3.32 (Table 4.2).

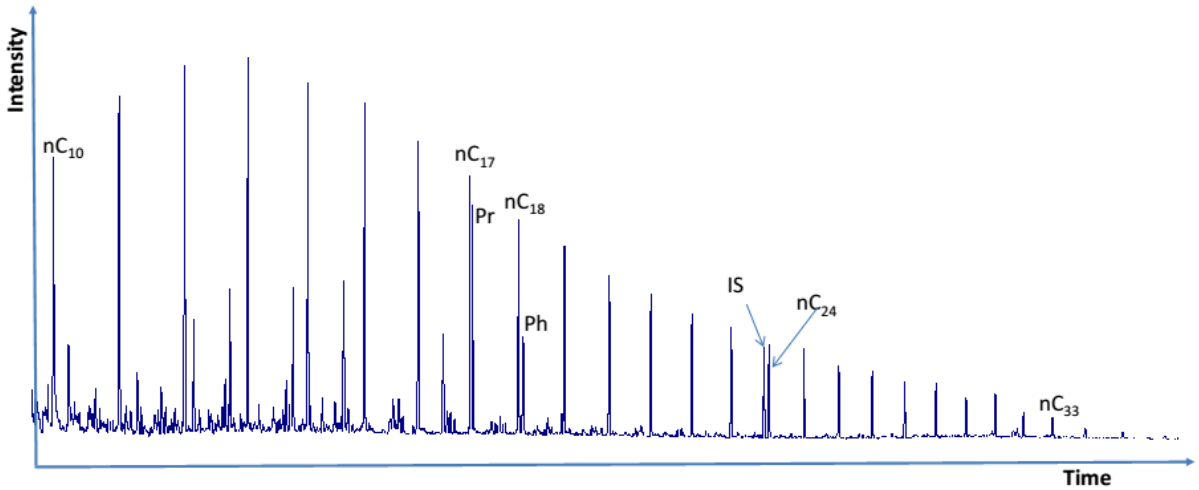

Figure 4.8: Representative gas chromatogram of an aliphatic hydrocarbon fraction (from oil OE169).

***n*C$_{10}$= *n*-Decane. *n*C$_{17}$= *n*-Heptadecane. Pr= Pristane. *n*C$_{18}$= *n*-Octadecane. Ph= Phytane. I.S (internal standard) = *n*-heptadecylcyclohexane (HDCH). *n*C$_{30}$= n-Tritriacontane.**

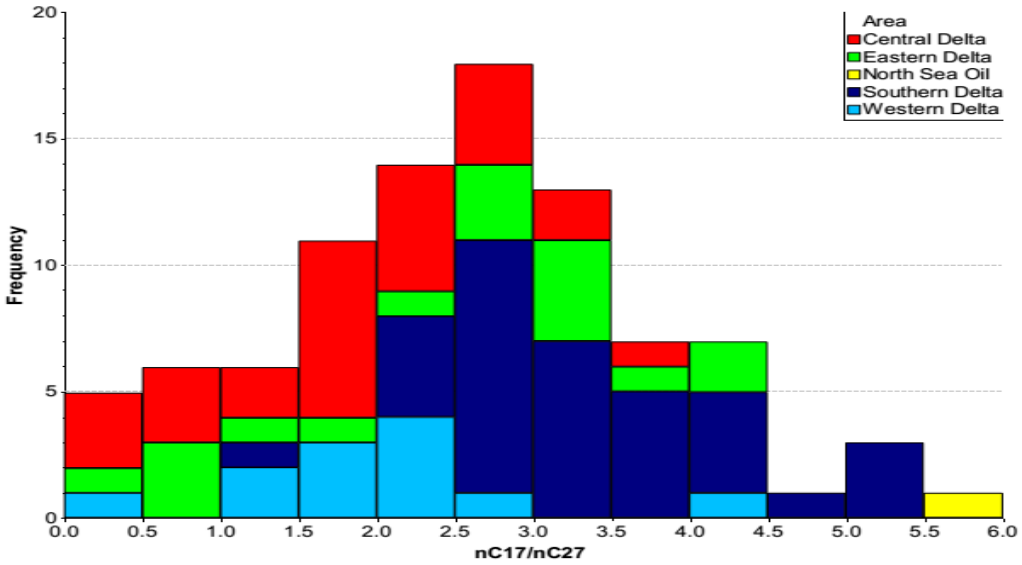

Figure 4.9: Variation of *n*C$_{17}$/*n*C$_{27}$ ratios in the Niger Delta oils showing the wide range of across the Delta, especially in the Eastern Delta oils. Note also the difference between the Central and the Southern Delta oil samples.

Table 4.2: Summary of Iatroscan, *n*-alkane and isoprenoid alkane ratio data from the oil samples

Parameter	Unit	Central Delta			Eastern Delta			Western Delta			Southern Delta			Replicate			NSO-1
		no Mean	SD	CV	no Mean	SD	CV	no Mean	SD	CV	no Mean	SD	CV	no Mean	SD	CV	
Sats	(wt%)	75 44.75	12.27	27	29 49.95	11.02	22	23 48.84	12.64	26	53 50.51	13.05	26	3 55.66	0.72	1	56.44
Arom	(wt%)	75 44.39	10.20	23	29 39.92	10.08	25	23 41.11	11.78	29	53 40.47	11.69	29	3 35.53	0.45	1	35.64
NSO	(wt%)	75 9.85	3.72	38	29 9.37	4.64	49	23 9.20	2.03	22	53 8.19	5.66	69	3 5.30	0.27	5	5.94
Asph	(wt%)	75 1.01	0.89	88	29 0.75	0.74	98	23 0.85	0.68	80	53 0.83	0.71	85	3 3.51	0.22	6	1.98
Sats/Arom	(a/b)	75 1.15	0.68	59	29 1.15	1.21	80	23 1.41	0.87	61	53 1.47	0.86	58	3 1.57	0.03	2	1.58
pr/ph	(a/b)	37 3.07	0.63	21	19 2.69	0.47	17	12 2.44	0.65	27	43 2.99	0.56	19	3 2.81	0.04	1	1.55
norpr/pr	(a/b)	35 0.30	0.10	34	19 0.40	0.05	14	12 0.44	0.07	16	43 0.40	0.08	19	3 0.34	0.01	2	0.49
pr/nC_{17}	(a/b)	29 3.79	7.15	189	17 3.03	4.68	154	10 4.20	3.50	86	40 2.88	5.62	195	3 3.08	0.07	2	0.66
ph/nC_{18}	(a/b)	29 1.15	2.20	191	17 1.04	1.30	125	10 2.82	2.81	100	40 1.42	2.89	203	3 1.34	0.01	0	0.54
nC_{17}/nC_{27}	(a/b)	28 1.86	0.91	49	17 2.40	1.29	54	10 2.05	0.93	46	39 3.32	0.90	27	3 2.20	0.01	0	5.81
CPI-1	(a/b)	27 1.06	0.06	6	17 1.10	0.06	6	10 1.08	0.17	15	33 1.13	0.12	10	3 1.26	0.03	2	1.02
CPI-2	(a/b)	12 1.19	0.19	16	12 1.13	0.03	3	3 1.11	0.05	5	17 1.12	0.02	2	3 1.24	0.01	1	1.05
CPI-3	(a/b)	27 1.07	0.05	5	17 1.10	0.05	5	10 1.14	0.18	16	33 1.14	0.15	13	3 1.25	0.03	2	1.04

Sats= 100* weight of saturated hydrocarbon/weight of (saturate+aromatics+NSO+asphaltene). **Arom=** 100* weight of aromatics hydrocarbon/ weight of (saturate+aromatics+NSO+asphaltene). **NSO=** 100* weight of polars/weight of (saturate+aromatics+NSO+asphaltene). **Asph=** 100* weight of asphaltene/ weight of (saturate+aromatics+NSO+asphaltene). **Sats/Arom=** weight of saturated hydrocarbons/ weight of aromatics hydrocarbon. **Pr/Ph=** pristine/phytane. **norPr/Pr=** norpristane (C_{18}) isoprenoid/pristine. **Pr/*n*C_{17}=** pristine/*n*-alkane with 17 carbon chain length. **Ph/*n*C_{18}=** phytane/*n*-alkane with 18 carbon chain length, ***n*C_{17}/*n*C_{27}=** *n*-alkane with 17 carbon chain length/*n*-alkane with 27 carbon chain length. **CPI-1=** odd/even predominance in C_{28} to C_{30} *n*-alkane (Philippi, 1965). **CPI-2=** odd/even predominance in C_{25} to C_{33} *n*-alkane (Bray & Evans, 1961). **CPI-3=** odd/even predominance in C_{27} to C_{31} *n*-alkane (Scalan & Smith, 1970).

4.3 Diamondoid hydrocarbons

The GC-MS of the aliphatic hydrocarbon fraction was used to monitor the diamondoids and several *m/z* values were used for this including *m/z* 136, 135, 149, 163,177 for adamantanes and the alkylated adamantanes and *m/z* 188, 187, 201, 215 for the diamantanes (Fig 4.10). Peak areas from these ion chromatograms were used for the calculation of several ratios as presented in Table 4.3.

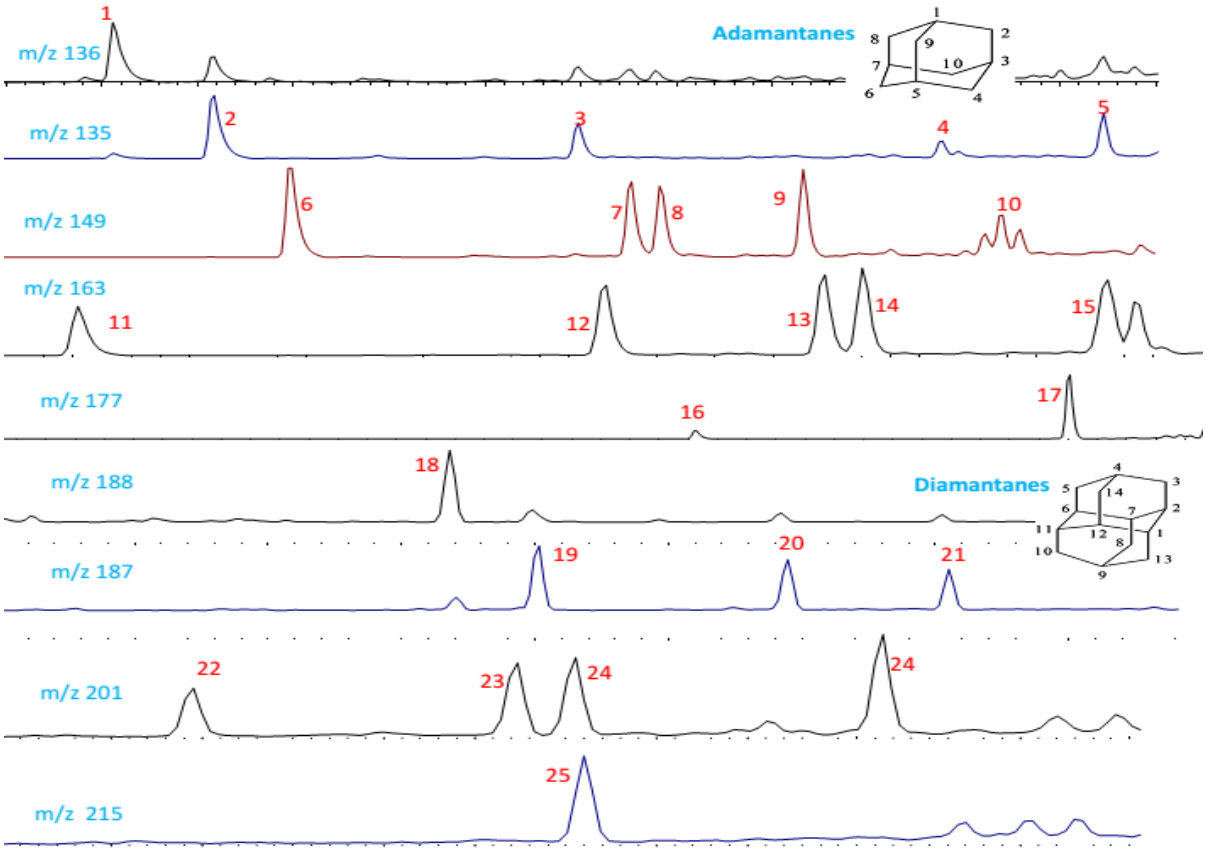

Figure 4.10: Representative mass chromatograms of adamantanes (*m/z* 136, 135, 149, 163,177) and diamantanes (*m/z* 188, 187, 201, 215) from sample OE149 showing their distribution and elution order.

1= Adamantane (AD). **2=** 1-Methyladamantane (1-MA). **3=** 2-Methyladamantane (2-MA). **4=** 1-Ethyladamantane (1-EA). **5=** 2-Ethyladamantane (2-EA). **6=** 1,3-Dimethyladamantane (1,3-DMA). **7=** 1,4-Dimethyladamantane,cis (1,4-DMA cis). **8=** 1,4-Dimethyladamantane,trans (1,4-DMA trans). **9=** 1,2-Dimethyladamantane (1,2-DEA). **10=** 1-Ethyl-3-methyladamantane (1E,3,-MA). **11**= 1,3,5 Trimethyladamantan (1,3,5-TMA). **12**= 1,3,6-Trimethyladamantane (1,3,6-TEA). **13=** 1,3,4-Trimethyladamantane,cis (1,3,4-TEA cis). **14**= 1,3,4-Trimethyladamantane,trans (1,3,4-TEA trans). **15=** 1-Ethyl-3,5-dimethyladamantane (1E,3,5-DMA). **16:** 1,3,5,7-Tetramethyladamantane (1,3,5,7-TtMA). **17=** 1,2,5,7-Tetramethyladamantane (1,2,5,7-TtMA). **18=** Diamantane (D). **19=** 4-Methyldiamantane (4-MD). **20=** 1-Methyldiamantane (1-MD). **21=** 3-Methyldiamantane (3-MD). **22=** 4,9-Dimethyldiamantane (4,9-DMD). **23=** 1,4 and 2,4-Dimethyldiamantane (1,4 and 2,4-DMD). **24=** 4,8-Dimethyldiamantane (4,8-DMD), **25=** 3,4-Dimethyldiamantane (3,4-DMD). **26=** Trimethyldiamantane (TED).

The calculated/measured parameters includes; 3+4 MD (ppm) (c.f. Dahl et al., 1999); MAI (c.f. Chen *et al*., 1996); MDI (c.f. Chen *et al*., 1996); DMDI (c.f. Schulz *et al*., 2001); EAI (c.f. Schulz *et al*., 2001); TMAI (c.f. Zhang *et al*., 2005); MA/AD (c.f. Grice *et al* 2000); MD/D (c.f. Grice *et al* 2000); MA/EA (c.f. Wang *et al*., 2006; Yang *et al*., 2006); MA/DMA; (c.f. de Araujo *et al.*, 2012); MA/TMA (c.f. de Araujo *et al*., 2012); MA/TeMA (c.f. de Araujo *et al*., 2012); DMA/TMA (c.f. de Araujo *et al*., 2012); TA/TMA (c.f. de Araujo *et al*., 2012); TMA/TMA (c.f. Wang *et al* 2006; de Araujo *et al*., 2012); TeMA/TeMA (c.f. de Araujo *et al*., 2012).

There is no marked variation in most of the calculated ratios when comparing the samples based on the part of Delta where they were sourced from (Table 4.3) however, the 3+4 MD and the MA/EA parameters shows some marked variations especially in the Western Delta oils. There is a general variation in the 3+4 MD concentrations in samples from across the region with the exception of the Western Delta, where most of the samples have concentrations of about 40 ppm, while the Eastern Delta oils seems to be depleted in the 3+4 MDs as most of their samples contain about 21 ppm (Fig 4.11). The MA/EA ratios of the samples generally have a wide range in most area of the delta, with the exception of Southern Delta which is skewed towards the high end and with the lowest value been 1.2, the Eastern and Southern Delta has average values of 1.28 and 1.29, whereas the Central and Western Delta has average values of 1.46 and 1.61 (Figure 4.12 and Table 4.3).

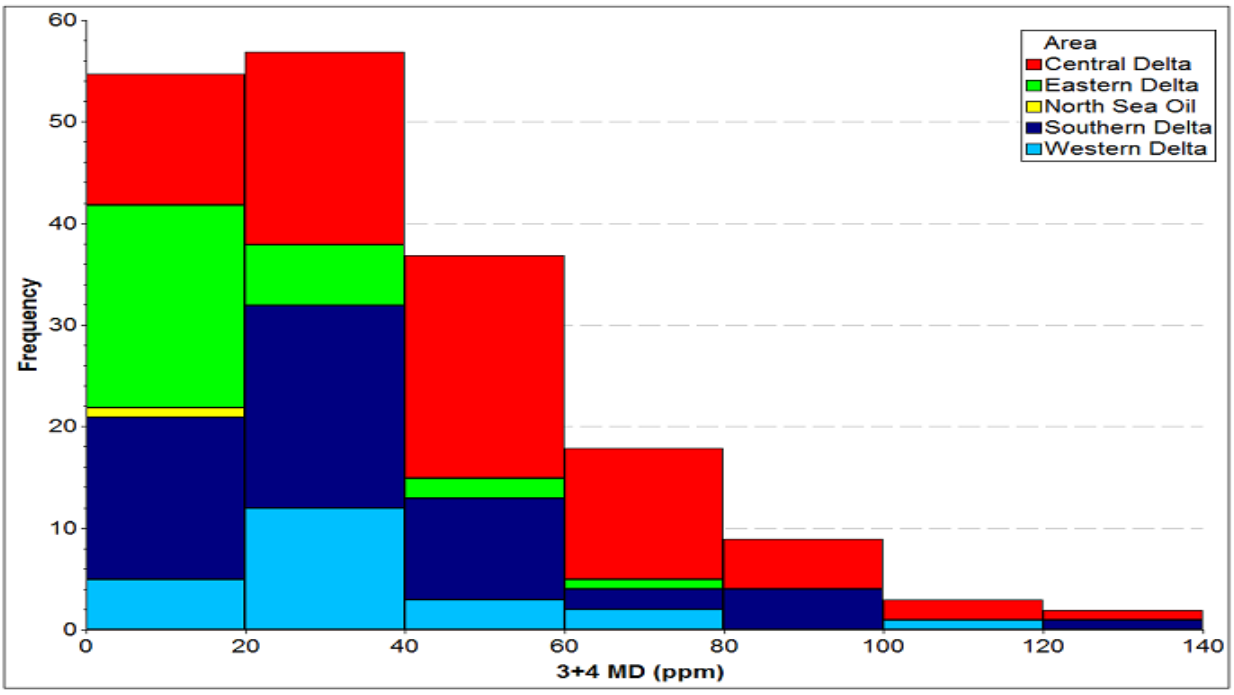

Figure 4.11: Variation of 3- + 4-methydiamantane (MD) concentrations in oils across the delta. Note the Eastern Delta oils have lower concentrations than those from the other parts of the delta.

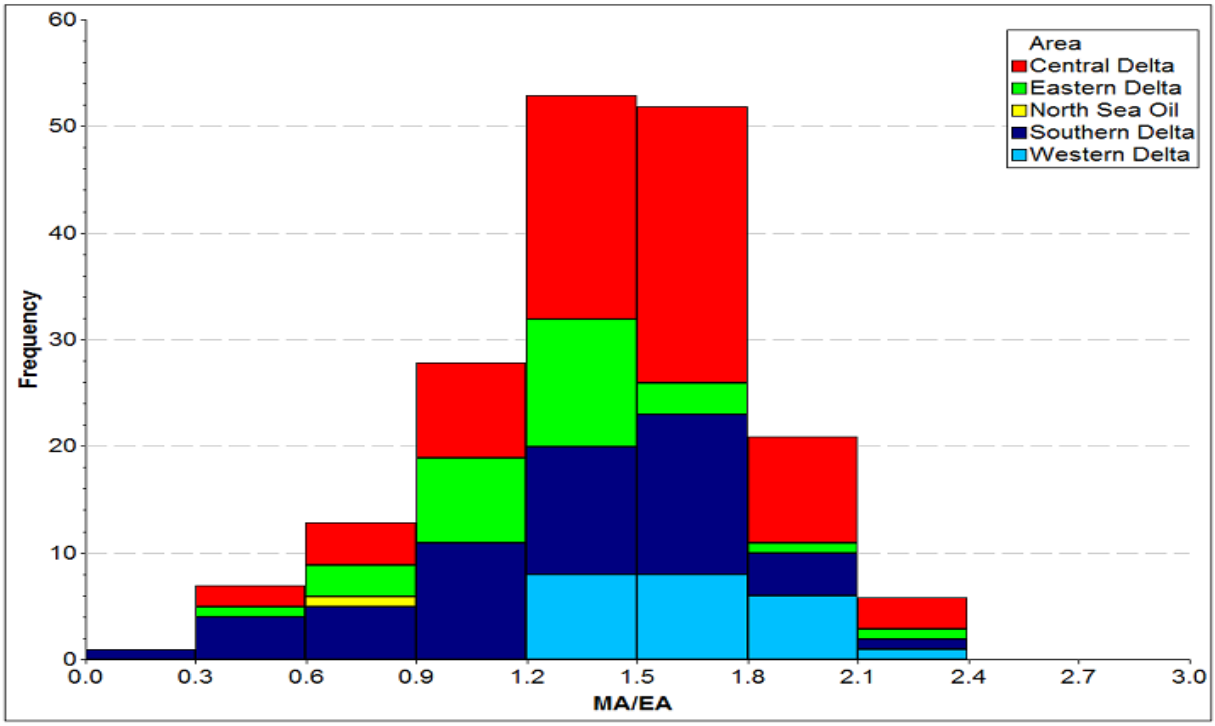

Figure 4.12: Variation of MA/EA ratios in oils across the delta. Note the Western Delta oils have only high values.

Table 4.3: Summary of source, cracking and maturity diamondoid hydrocarbon parameters of oil samples

Parameter	unit	Central Delta			Eastern Delta			Western Delta			Southern Delta			Replicate			NSO-1
		no Mean	SD	CV	no Mean	SD	CV	no Mean	SD	CV	no Mean	SD	CV	no Mean	SD	CV	
3+4 MD	ppm	75 46.36	27.34	59	29 20.58	16.92	82	23 35.06	23.93	68	53 37.22	25.93	70	2 54.04	0.25	0	2.04
MAI	%	75 65.37	4.83	7	29 65.80	3.41	5	23 68.20	1.80	3	53 64.96	6.82	10	2 68.92	0.23	0	45.12
MDI	%	75 40.81	2.08	5	29 39.72	2.03	5	23 42.27	1.82	4	53 40.49	2.46	6	2 41.43	0.44	1	26.21
DMDI	%	75 65.85	3.83	6	29 67.13	2.53	4	23 63.64	2.63	4	53 66.34	2.98	4	2 67.38	0.26	0	70.55
EAI	%	75 72.25	3.21	4	29 73.87	2.97	4	23 72.61	2.37	3	53 72.78	2.86	4	2 72.05	0.09	0	73.55
TMAI-1	a/b	75 0.42	0.03	6	29 0.42	0.02	5	23 0.44	0.02	4	53 0.42	0.03	8	2 0.43	0.01	1	0.34
TMAI-2	a/b	75 0.25	0.03	10	29 0.25	0.02	9	23 0.27	0.02	7	53 0.25	0.03	13	2 02.27	0.00	0	0.19
MA/AD	a/b	75 6.81	2.05	30	29 7.11	1.04	15	23 6.23	0.46	7	53 8.09	4.03	50	2 6.06	0.11	2	5.27
MD/D	a/b	75 3.06	0.40	13	29 3.40	0.24	7	23 3.18	0.31	10	53 3.28	0.41	13	2 2.83	0.05	2	3.19
MA/EA	a/b	75 1.46	0.39	27	29 1.28	0.37	29	23 1.61	0.26	16	53 1.29	0.47	37	2 1.55	0.02	1	0.65
MA/DMA	a/b	75 1.76	0.34	19	29 1.70	0.28	16	23 1.93	0.18	10	53 1.65	0.45	27	2 1.91	0.01	1	1.41
MA/TMA	a/b	75 1.42	0.31	22	29 1.30	0.24	19	23 1.54	0.15	10	53 1.23	0.35	29	2 1.47	0.00	0	1.51
MA/TeMA	a/b	75 4.70	1.02	22	29 4.23	0.89	21	23 4.99	0.61	12	53 3.83	1.25	33	2 4.86	0.04	1	5.70
DMA/TMA	a/b	75 1.46	0.14	9	29 1.42	0.11	7	23 1.47	0.09	6	53 1.39	0.16	11	2 1.47	0.04	2	1.89
TA/TeMA	a/b	75 1.12	0.12	11	29 1.10	0.13	11	23 1.20	0.09	7	53 1.04	0.21	20	2 1.14	0.02	2	0.91
TMA/TMA	a/b	75 0.72	0.07	10	29 0.73	0.06	9	23 0.80	0.06	7	53 0.72	0.09	13	2 0.77	0.02	2	0.50
TeMA/TeMA	a/b	75 0.20	0.20	100	29 0.17	0.02	14	23 0.18	0.02	10	53 0.17	0.02	13	2 0.18	0.00	2	0.20

C_{29}ααα20R = C_{29} 5α(H), 14α(H), 17α(H)-20R stigmastane (ppm). **3+4 MD**= 3-methyldiamnatane + 4-methyldiamantane (ppm). **MAI**= 100*1-methyadamantane/1- +2-methyladamantane. **MDI**= 100*4-methyldiamantane/4- + 1- +3-methyldiamantane. **DMDI**= 100*3,4-dimethyldiamantane/3,4- + 4,9-dimethyldiamantane. **EAI**= 100*2-ethyladamantane/ 2- +1-ethyladamnatane. **TMAI**= 1,3,5-trimethyladamamntane/ 1,3,5- + 1,3,6-trimethyladamantane. **MA/AD**= 1-+2-methyladamntane/adamantane. **MD/D**= 1-+3-+4-methyldiamantane/diamantane. **MA/EA**= 1-methyldiamantane/2-ethyldiamantane. **MA/DMA**= 1-methyladamantane/2-ethyladamantane. **MA/TMA**= 1-methyladamantane/1,3,4-trimethyladamantane. **MA/TeMA**= 1-methyladamantane/1,2,5,7-tetramethyladamantane. **DMA/TMA**=1,4-dimethyladamantane/1,3,4-trimethyladamantane. **TA/TMA=** 1,3,5-trimethyladamantane/1,2,5,7-trimethyladamnatane. **TMA/TMA=** 1,3,5-trimethyladamantane/1,3,6-trimethyladamantane. **TeMA/TeMA=** 1,3,5,7-tetramethyladamantane/1,2,5,7-tetramethyladamantane.

4.4 Aromatics

The oil aromatic hydrocarbon fractions were analysed by GC-MS in scan and SIM mode using several *m/z* values including *m/z* 128, 142, 178, 192, 156, 170, 184, 198, 231 and 253 (Fig 4.13; 4.14 and 4.15). The peak area of selected peaks were used for the calculation of several ratios as presented in Table 4.4. The calculated parameter includes; MNR (c.f. Radke *et al*., 1982; 1986); DMNR; MP(3+2/9+1); MPI-1 (c.f. Radke & Welte 1983; Radke *et al.*; 1986); MPI-2 (c.f. Radke *et al.*; 1986); Rc(Ro<1.35) (c.f. Radke & Welte 1983); MPR (c.f. Radke *et al*., 1982; 1986); MAS21+22/tot; C_{21}+C_{22}; MAS/total MAS; MAS29S/R; TAS20+21/tot (c.f. Mackenzie 1984; Beach *et al*., 1989); TAS28S/R; TAS26 (c.f. Peters & Moldowan 1993); TAS27 (c.f. Peters & Moldowan 1993); TAS28 (c.f. Peters & Moldowan 1993); TMNr (c.f. van Aarssen *et al*., 1999); TeMNr (c.f. van Aarssen *et al*., 1999) and PMNr (c.f. van Aarssen *et al*., 1999).

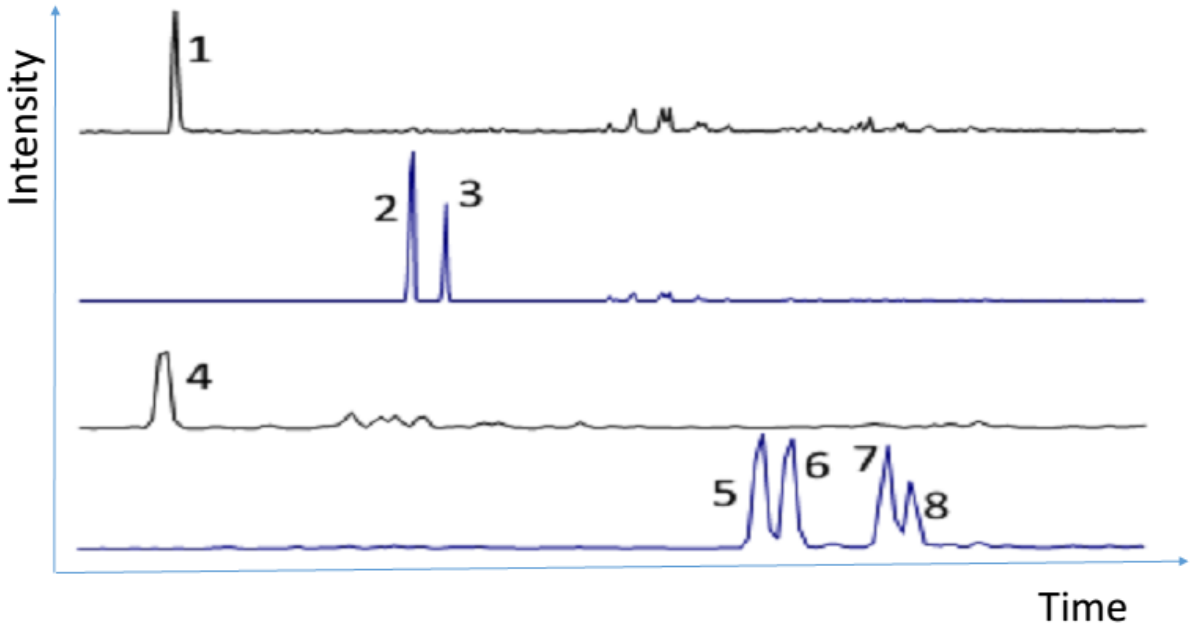

Figure 4.13: Representative partial *m/z* 128,142, 178 and 192 mass chromatograms showing the distributions of naphthalene, methylnaphthalenes, phenanthrene and methylphenanthrenes, respectively (OE016).

1= Naphthalene. 2= 2-methylnaphthalene. 3= 1-methylnaphthalene. 4= Phenanthrene. 5= 3-methylphenanthrene. 6= 2-methylphenanthrene. 7= 9-methylphenanthrene. 8= 1-methylphenanthrene.

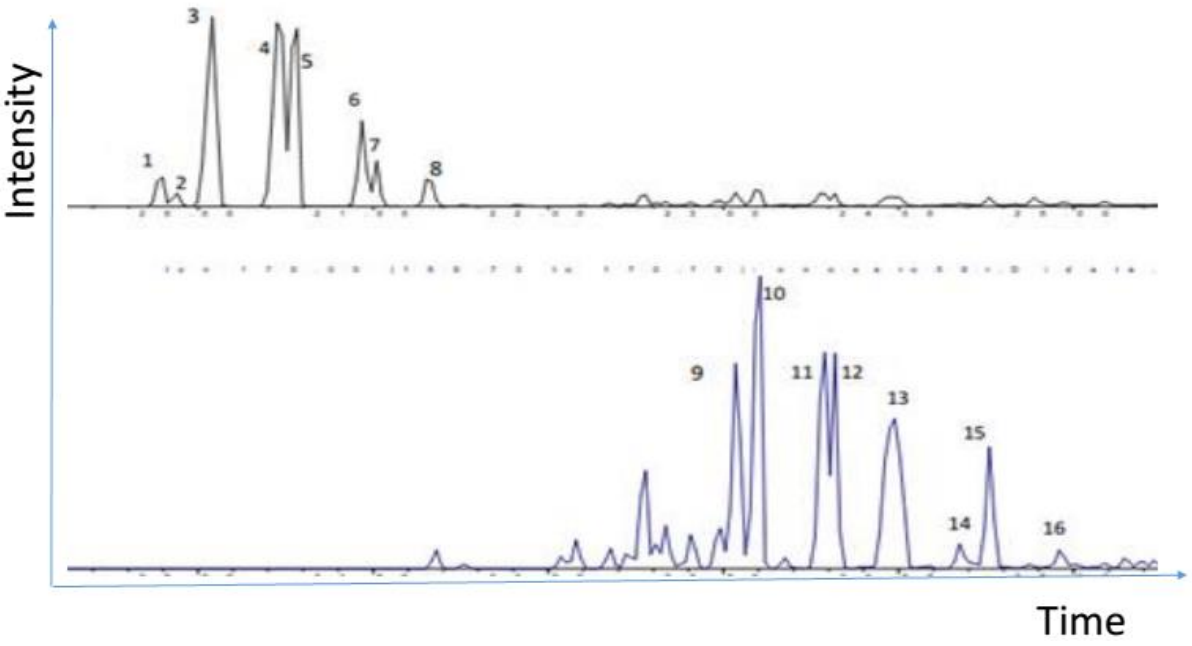

Figure 4.14: Representative partial *m/z* 156 and 170 mass chromatograms showing the distribution of dimethylnaphthalenes and trimethylnaphthalenes, respectively (OE016).
1= 2-Dimethylnaphthalenes. **2=** 1-Dimethylnaphthalenes. **3=** 2,6+2,7-Dimethylnaphthalenes. **4=** 1,3+1,7-Dimethylnaphthalenes. **5=** 1,6-Dimethylnaphthalenes. **6=** 1,4+2,3-Dimethylnaphthalenes. **7=** 1,5-Dimethylnaphthalenes. **8=** 1,2-Dimethylnaphthalenes. **9=** 1,3,7-Trimethylnaphthalenes. **10=** 1,3,6-Trimethylnaphthalenes. **11=** 1,3,5-Trimethylnaphthalenes. **12=** 1,4,6-Trimethylnaphthalenes. 13= 1,4,7+1,2,6+1,6,9-Trimethylnaphthalenes. **14=** 1,2,4-Trimethylnaphthalenes. **15=** 1,2,5-Trimethylnaphthalenes. **16=** 1,2,3-Trimethylnaphthalenes.

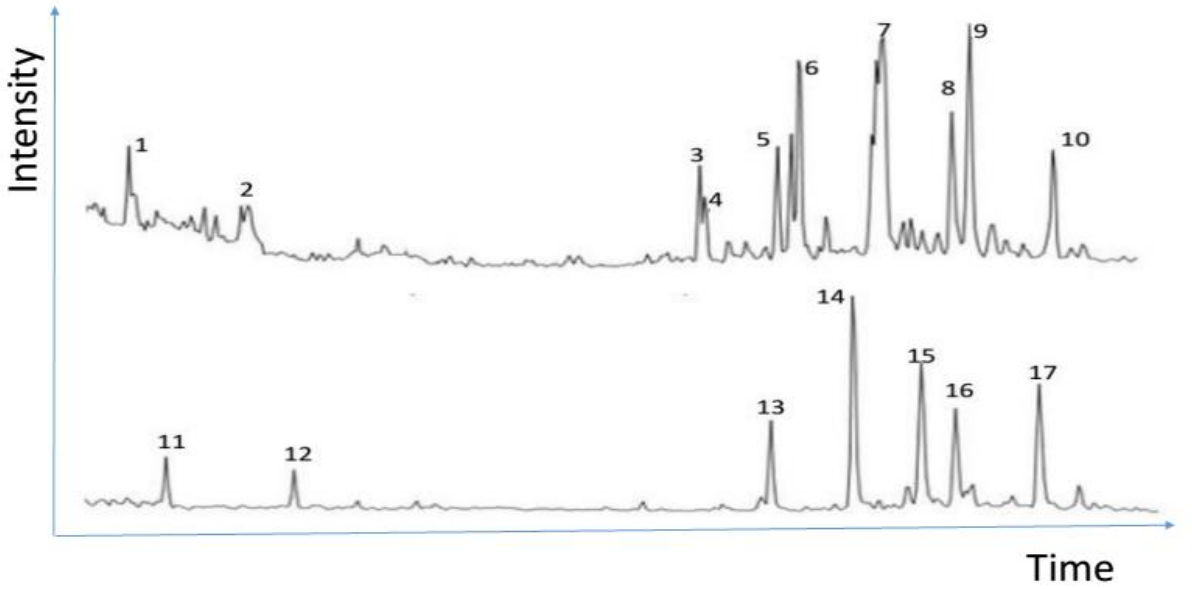

Figure 4.15: Representative partial *m/z* 253 and 231 mass chromatograms showing the distribution of monoaromatics and triaromatics, respectively (OE016).
1= C_{21} monoaromatic. **2=** C_{22} monoaromatic. **3=** C_{27} 5β 20S monoaromatic. **4=** C_{27}Dia 5β 20S monoaromatic. **5=** C_{27} 5β 20R monoaromatic. **6=** C_{28} 5β 20S monoaromatic. **7=** C_{28} 5β 20R monoaromatic. **8=** C_{29} 5α 20S monoaromatic. **9=** C_{29} 5β 20R monoaromatic. **10=** C_{29} 5α 20R monoaromatic. **11=** C_{20} triaromatic. **12=** C_{21} triaromatic. **13=** C_{26} 20S triaromatic. **14=** C_{26} 20R + C_{27} 20S triaromatic. **15=** C_{28} 20S triaromatic. **16=** C_{27} 20R triaromatic. **17=** C_{28} 20R triaromatic.

There was no significant variation in the calculated ratios when comparing the samples based on the part of Delta where they were sourced from (Table 4.4). However, Figure 4.16 and Table 4.4 show that for most samples from the Central Delta the % TAS26 parameter values are lower than 24%, with an average value of 19.88%, whereas the oils from the other parts of the Delta have values higher than 20%.

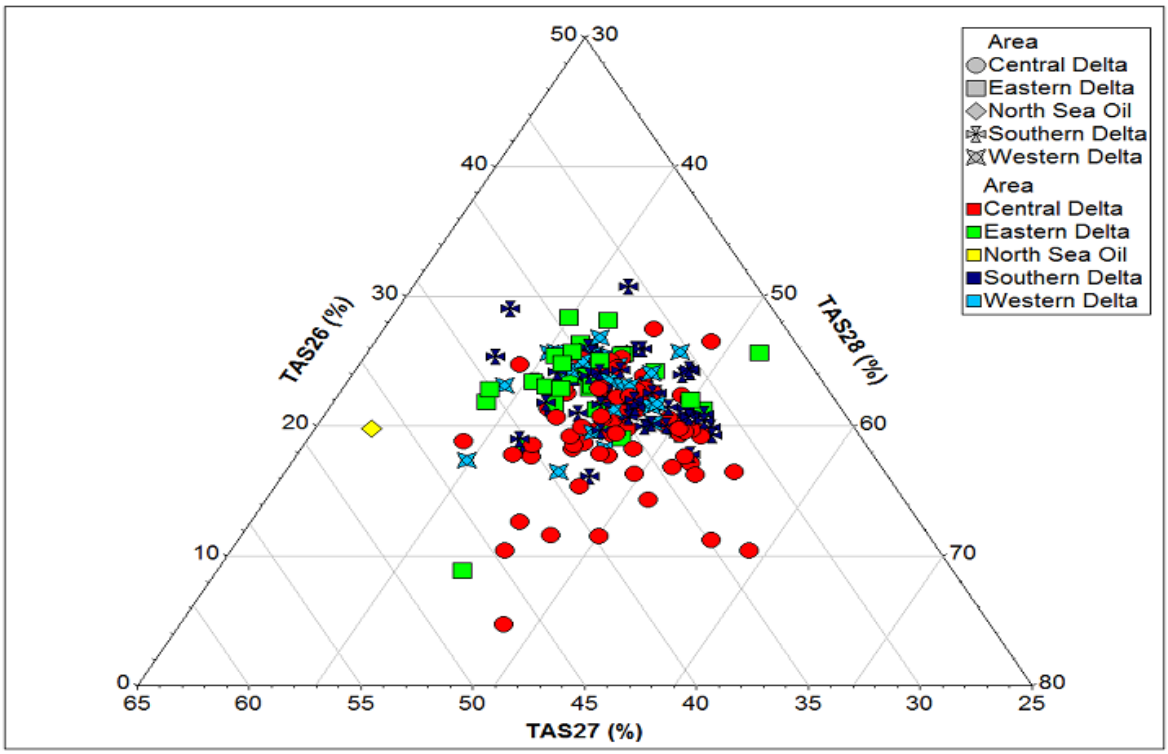

Figure 4.16: Ternary plot of triaromatic steroid %C_{26}, C_{27} and C_{28} compositions, showing that most of the Central Delta oils are depleted in C_{26}.

Table 4.4: Summary of source and maturity molecular indicators from the aromatic hydrocarbon fractions of the oil samples

		Central Delta			Eastern Delta			Western Delta			Southern Delta			Replicate			NSO-1
parameter	unit	no Mean	SD	CV	no Mean	SD	CV	no Mean	SD	CV	no Mean	SD	CV	no Mean	SD	CV	
MNR	a/b	56 1.50	0.64	43	25 1.38	0.58	42	22 1.23	0.41	33	49 1.35	0.30	22	3 1.27	0.01	1	1.21
DMNR	a/b	43 6.20	2.96	48	28 7.02	4.43	63	21 5.85	2.84	48	49 7.77	3.94	51	3 6.34	0.01	0	4.05
MP(3+2/9+1)	a/b	60 1.22	0.31	26	28 1.05	0.34	33	20 1.04	0.30	29	52 0.97	0.26	27	3 1.08	0.04	4	0.80
MPI(1)	a/b	60 0.86	0.24	28	28 0.81	0.27	34	20 0.77	0.19	24	51 0.76	0.23	31	3 0.96	0.01	1	0.70
MPI(2)	a/b	60 0.83	0.22	27	28 0.80	0.32	40	20 0.75	0.17	23	51 0.75	0.24	32	3 0.92	0.03	3	0.77
Rc(Ro<1.35)	a/b	60 0.91	0.14	15	28 0.88	0.16	18	20 0.86	0.11	13	51 0.86	0.14	16	3 0.98	0.01	1	0.80
MPR	a/b	60 1.54	0.72	47	28 1.31	0.48	36	20 1.03	0.46	44	52 1.29	0.83	64	3 1.24	0.00	0	2.06
MAS21+22/tot	a/b	60 0.11	0.06	51	26 0.11	0.02	20	18 0.10	0.04	36	40 0.16	0.13	82	3 0.12	0.00	0	0.40
MAS29S/R	a/b	60 1.20	0.21	18	26 1.32	0.31	23	18 1.19	0.22	19	40 1.30	0.13	10	3 1.24	0.00	0	1.25
TAS20+21/tot	a/b	75 0.18	0.13	75	29 0.21	0.24	116	23 0.18	0.16	91	52 0.19	0.11	58	3 0.18	0.01	5	0.26
TAS28S/R	a/b	75 1.17	0.14	12	29 1.12	0.13	12	23 1.16	0.15	13	52 1.17	0.21	18	3 1.15	0.01	1	1.25
TAS26	%	75 19.88	4.49	23	29 23.55	4.10	17	23 23.07	3.39	15	52 22.89	2.94	13	3 19.98	0.30	1	20.06
TAS27	%	75 35.64	2.34	7	29 36.18	3.07	8	23 35.61	2.86	8	52 35.07	2.48	7	3 37.62	0.68	2	47.20
TAS28	%	75 44.78	3.41	8	29 41.81	3.07	7	23 42.55	2.92	7	52 44.41	3.60	8	3 42.41	0.38	1	33.99
TMNr	a/a+b	50 0.56	0.15	27	24 0.59	0.09	16	18 0.51	0.21	40	44 0.55	0.13	25	3 0.57	0.01	2	0.71
TeMNr	a/a+b	51 0.56	0.09	16	24 0.54	0.13	24	18 0.55	0.17	31	44 0.51	0.12	25	3 0.53	0.02	4	0.57
PMNr	a/a+b	51 0.54	0.15	28	25 0.45	0.15	33	18 0.48	0.18	38	45 0.39	0.13	34	3 0.52	0.01	2	0.73

MNR= 2- Methylnaphthalene/ 1-Methylnaphthalene. **DMNR**= 2-6 + 2-7 Dimethylnaphthalene/1-5 Dimethylnaphthalene. **MP(3+2/9+1)**= 2- + 3-methyl phenanthrene/ 1- + 9-methylphenanthrene. **MPI-1**= [1.5 x (2- + 3-methylphenanthrenes)] / [phenanthrene + 1- + 9- methylphenanthrenes]. **MPI-2**= (3 x 2-methylphenanthrenes) / [phenanthrene + 1- + 9- methylphenanthrenes]. **Rc(Ro<1.35)**= 0.6(MPI-1)+ 0.4. **MPR**= 2-methylphenanthrene/1-methyl phenanthrene. **MAS21+22/tot**= C_{21}+C_{22} MAS / Total MAS. **MAS29S/R**= C_{29} 5α(H) 20S monoaromatic/ C_{29} 5α(H) 20R monoaromatic ethyl. **TAS20+21/tot**= C_{20}+C_{21} Triaromatic / Total Triaromatic. **TAS28S/R**= long chain triaromatic/ long chain monoaromatic. **TAS26**= 100*TAS26/(TAS26+TAS27+TAS28). **TAS27**= 100* TAS27/(TAS26+TAS27+TAS28). **TAS28**= 100* TAS28/(TAS26+TAS27+TAS28). **TMNr**= 1,3,7-Trimethynepthalene/ 1,3,7- + 1,2,5,7-Trimethynepthalene. **TeMNr**= 1,3,6,7-Tetramethynapthalene/ 1,3,6,7- + 1,2,5,6- +1,2,3,6-Tetramethylnaphthalanes. **PMNr**= 1,2,4,6,7-Pentamethylnaphthalane/ 1,2,4,6,7- + 1,2,3,5-6-pentamethylnaphthalane.

4.5 Steranes

The sterane hydrocarbon distributions in the oil aliphatic hydrocarbon fractions were monitored by GC-MS mainly using *m/z* 217 and 218 (e.g. Fig 4.17 & 4.18). Peak areas were used for the calculation of several ratios and their results are presented in Table 4.5. Some samples which are heavily biodegraded show depleted sterane concentration and the peaks were not easily resolved. The calculated parameters includes; Preg (c.f. Mackenzie 1984); %C_{27}ααα (c.f. Peters *et al*., 2005); %C_{28}ααα (c.f. Peters *et al*., 2005); %C_{29}ααα (c.f. Peters *et al*., 2005); %DiaSt (c.f. Mackenzie 1984); St29S/R (c.f. Seifert & Moldowan 1981); St29I/R (c.f. Seifert & Moldowan 1981); 27St217 (c.f. Huang & Meinschein 1979; Peters & Moldowan 1993); 28St217 (c.f. Huang & Meinschein 1979; Peters & Moldowan 1993); 29St217 (c.f. Huang & Meinschein 1979; Peters & Moldowan 1993); 30St217 (c.f. Moldowan *et al*., 1990); St27Iso (c.f. Huang & Meinschein 1979; Peters & Moldowan 1993); St28Iso (c.f. Huang & Meinschein 1979; Peters & Moldowan 1993); St29Iso (c.f. Huang & Meinschein 1979; Peters & Moldowan 1993); St30Iso (c.f. Moldowan *et al*., 1990).

There are no marked variations in the calculated sterane parameters with the exception of the %C_{29} steranes, which show an increase in the Central Delta oils compared to those of the other part of the delta. The central Delta oil samples have an average of 42% for the St29iso whereas those of the Eastern Delta and Southern Delta have an average value of 37% and the Southern Delta have a value of 36%. A cross plot of St29iso with St27iso (Fig. 4.19) show a negative correlation between those two parameters, i.e. with a corresponding increase in the St29iso value there is always a corresponding decrease in the St27iso value and verse versa.

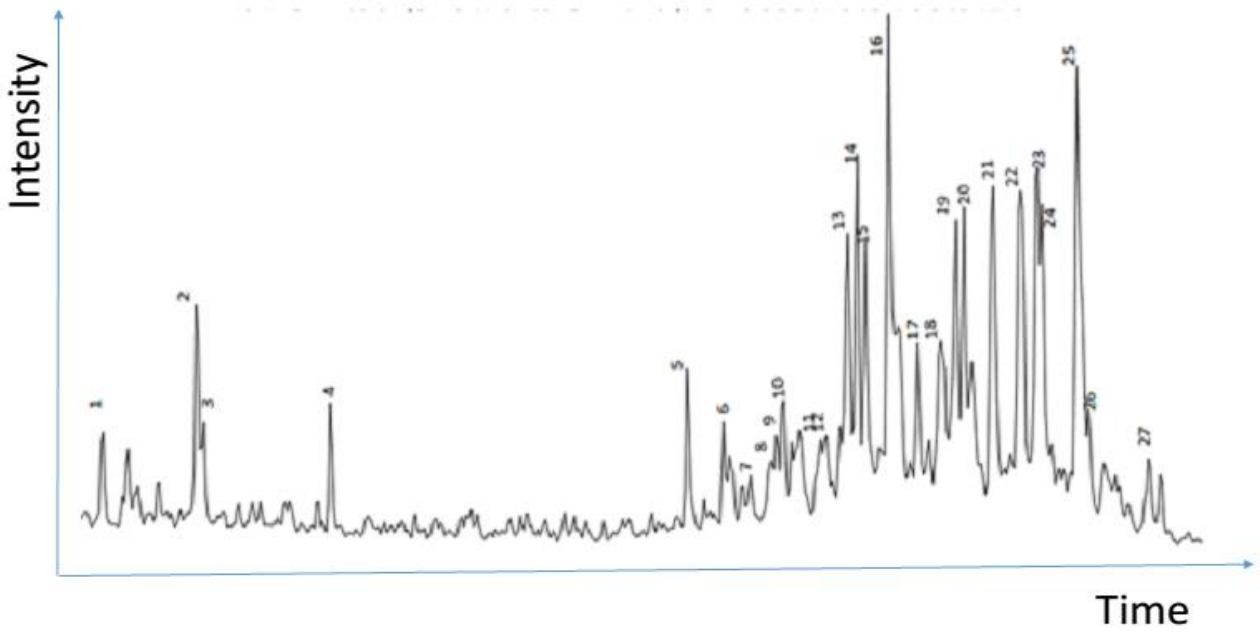

Figure 4.17: Representative partial *m/z* 217 mass chromatogram of the aliphatic hydrocarbon fraction showing the distribution of steranes in oil sample OE016.
1= Diapregnane. **2=** Pregnane. **3=** Homodiapregnane. **4=** Methyl Pregnane. **5=** 13β, 17α (20S) Diacholestane. **6=** 13β,17α (20R) Diacholestane. **7=** C_{27} 13α (20S) diasterane. **8=** C_{27} 13α (20R) diasterane. **9=** C_{28} 13β (20S) diasterane. **10=** C_{28} 13β (20S) diasterane. **11=** C_{28} 13β (20R) diasterane. **12=** C_{28} 13β (20R) diasterane. **13=** C_{27} 5α,14α,17α (20S). **14=** C_{27} 5α,14β,17β (20R) + C_{29} (20S) diasterane. **15=** C_{27} 5α,14β,17β (20S). **16=** C_{27} 5α,14α,17α (20R). **17=** C_{29} (20R) diasterane. **18=** C_{28} 5α,14α,17α (20S). **19=** C_{28} 5α,14β,17β (20R). **20=** C_{28} 5α,14β,17β (20S). **21=** C_{28} 5α,14α,17α (20R). **22=** C_{29} 5α,14α,17α (20S). **23=** C_{29} 5α,14β,17β (20R). **24=** C_{29} 5α,14β,17β (20S). **25=** C_{29} 5α,14α,17α (20R). **26=** C_{30} 5α,14α,17α (20S). **27=** C_{30} 5α,14α,17α (20R).

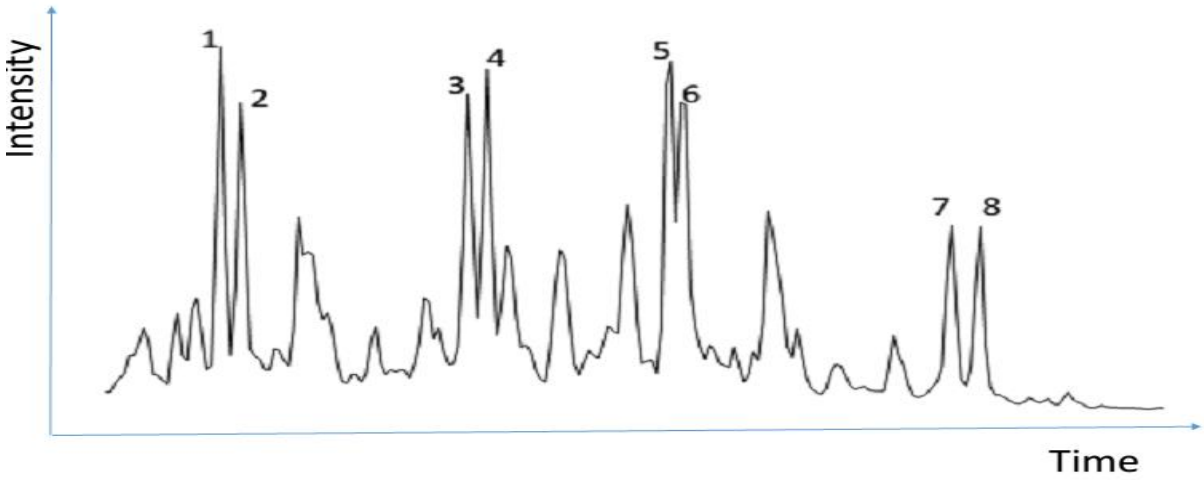

Figure 4.18: Representative partial *m/z* 218 mass chromatogram of the aliphatic hydrocarbon fraction showing the distribution of steranes in oil sample OE016.
1= C_{27} 5α,14β,17β (20R). **2=** C_{27} 5α,14β,17β (20S**).** **3=** C_{28} 5α,14β,17β (20R). **4=** C_{28} 5α,14β,17β (20S). **5=** C_{29} 5α,14β,17β (20R). **6=** C_{29} 5α,14β,17β (20S). **7=** C_{30} 5α,14β,17β (20R). **8=** C_{30} 5α,14β,17β (20S).

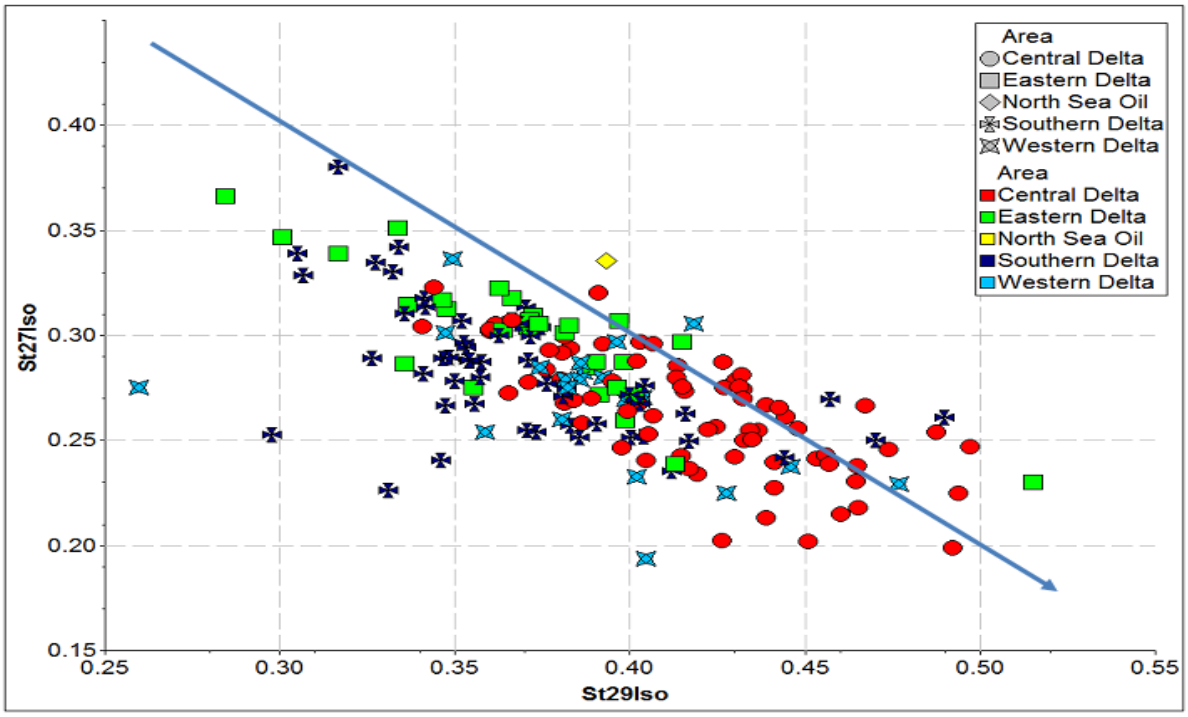

Figure 4.19: Plot of $C_{29}\alpha\beta\beta$ 20(R+S)/$C_{27\text{-}29}\alpha\beta\beta$ 20(R+S) with $C_{27}\alpha\beta\beta$ 20(R+S)/$_{C27\text{-}29}\alpha\beta\beta$ 20(R+S) from *m/z* 218. Note the Central Delta oils has relatively higher C_{29} steranes.

The C_{29} abundance ratio shows a general correlation with some terpane parameters as shown in Figure 4.20 and 4.21. It should be noted that a positive correlation exists with the t_{19}/t_{23} parameter but a negative correlation with the Tri/Tetra parameter. The C_{29} ratio also shows variation with the TAS26 and TAS28 triaromatics parameter. There is no notable variation with other parameters with the exception of a minor negative correlation with the C_7Paraf ratio and this shows that with an increase in C_{29} ratio there is always a corresponding decrease in the C_7Paraf ratio and verse versa (Figure 4.22).

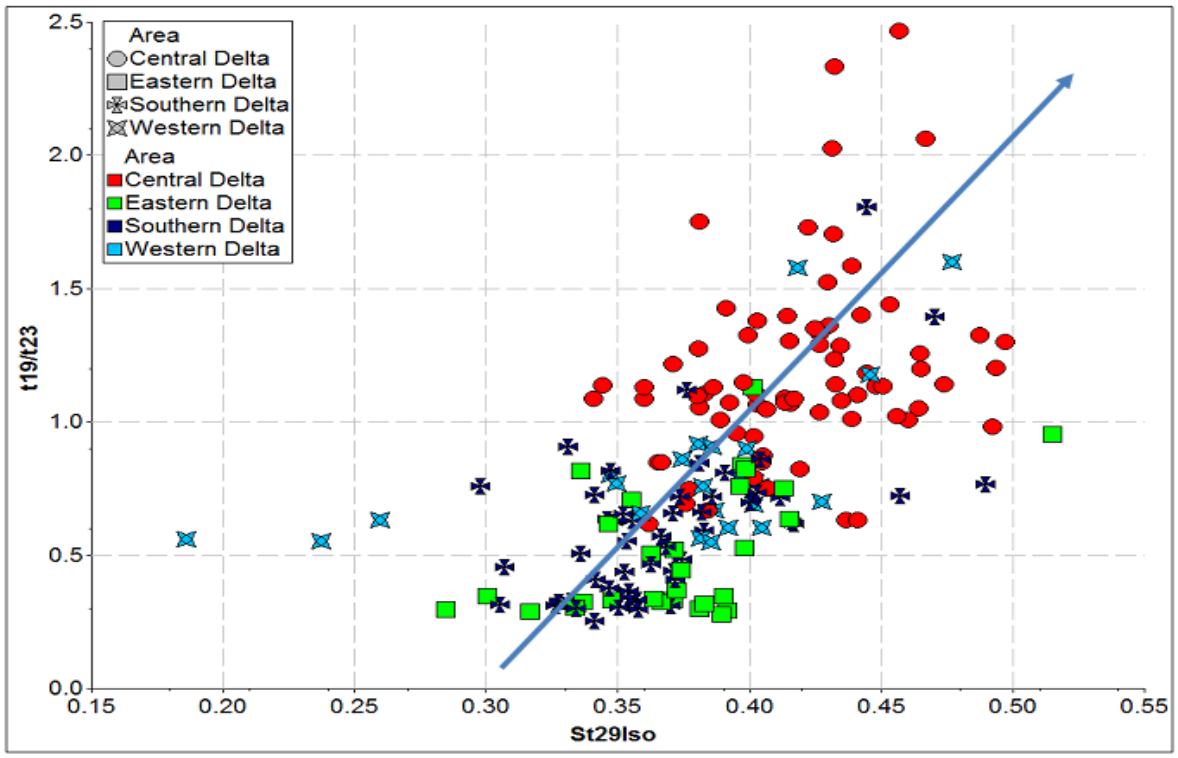

Figure 4.20: Plot of oil $C_{29}\alpha\beta\beta$ 20(R+S)/$C_{27\text{-}29}\alpha\beta\beta$ 20(R+S) against C_{19} tricyclic/ C_{23} tricyclic terpane showing a positive correlation.

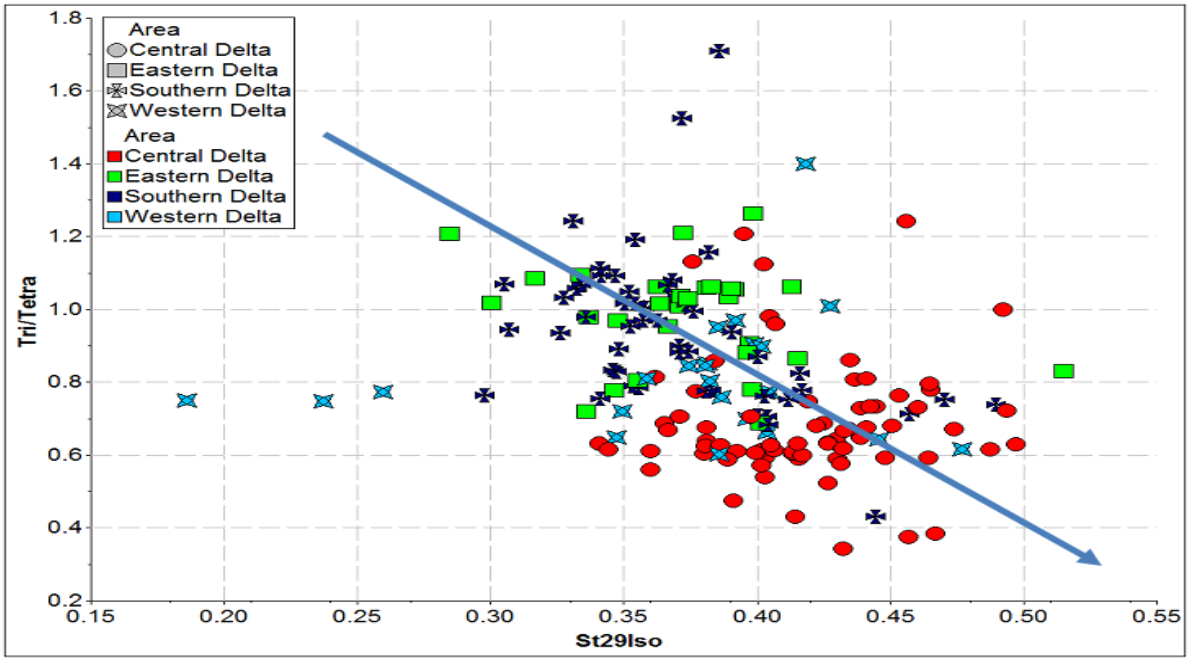

Figure 4.21: Plot of oil $C_{29}\alpha\beta\beta$ 20(R+S)/$C_{27\text{-}29}\alpha\beta\beta$ 20(R+S) with C_{23} tricyclic terpane/ C_{24} tetracyclic terpane showing a negative correlation.

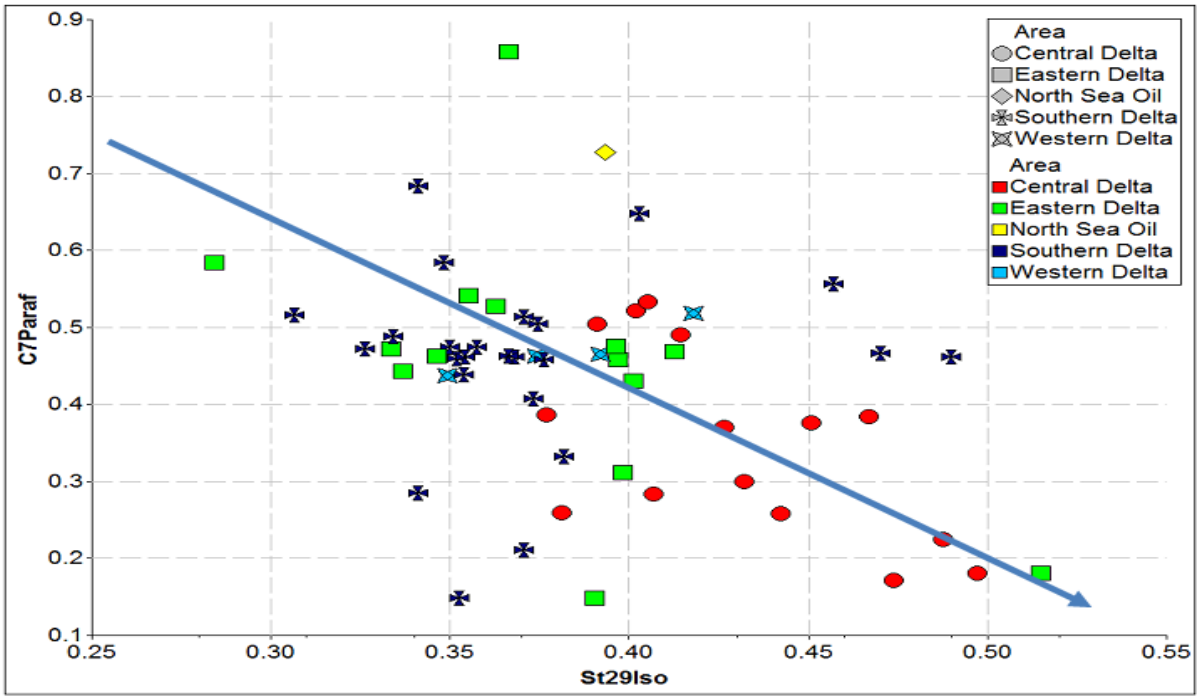

Figure 4.22: Plot of oil $C_{29}\alpha\beta\beta$ 20(R+S)/$C_{27\text{-}29}\alpha\beta\beta$ 20(R+S) with C_7Paraf ratios showing a negative correlation.

Table 4.5: Summary of source and maturity sterane biomarker parameters of oil samples

Parameter	Unit	Central Delta			Eastern Delta			Western Delta			Southern Delta			Replicate			NSO-1
		no Mean	SD	CV	no Mean	SD	CV	no Mean	SD	CV	no Mean	SD	CV	no Mean	SD	CV	
27ααα	(%)	75 27.63	6.00	22	29 31.39	3.38	11	23 31.79	5.04	16	52 29.74	3.19	11	3 27.86	0.72	1	49.31
28ααα	(%)	75 27.29	2.59	10	29 28.01	1.81	6	23 28.17	3.39	12	52 27.60	2.36	9	3 29.13	0.45	1	16.23
29ααα	(%)	75 45.08	5.12	11	29 40.59	4.24	10	23 40.03	7.67	19	52 42.66	4.78	11	3 43.01	0.27	5	34.45
Pregnanes	(%)	75 12.92	2.62	20	29 14.15	2.38	17	23 15.72	6.22	40	52 16.85	6.98	41	3 14.48	0.72	5	24.89
DiaSt	(%)	75 14.99	2.37	16	29 18.00	3.30	18	23 14.87	5.54	37	52 15.37	4.21	27	3 18.46	0.91	5	33.85
St29S/R	(a/a+b)	75 0.48	0.08	16	29 0.43	0.04	10	23 0.46	0.06	14	52 0.42	0.04	10	3 0.42	0.01	2	0.77
St29I/R	(a/a+b)	75 0.38	0.06	15	29 0.37	0.05	14	23 0.35	0.04	13	52 0.34	0.04	11	3 0.36	0.04	11	0.65
St27Iso	(%)	75 26.38	2.77	11	29 29.98	3.06	10	23 28.37	5.68	20	52 28.34	3.11	11	3 28.74	0.99	3	33.53
St28Iso	(%)	75 31.85	2.49	8	29 32.75	2.40	7	23 34.33	3.85	11	52 34.76	3.44	10	3 32.83	0.60	2	27.15
St29Iso	(%)	75 41.77	3.58	9	29 37.26	4.24	11	23 37.30	6.53	18	52 36.89	3.98	11	3 38.44	0.84	2	39.32
St30Iso	a/b	75 0.25	0.06	25	29 0.21	0.14	68	23 0.28	0.15	53	52 0.36	0.19	54	3 0.18	0.00	3	0.19
C29ααα20R	ppm	75 45.88	22.81	50	29 42.55	23.51	55	23 48.40	18.54	38	53 41.29	25.15	61	2 22.55	0.57	3	10.56

C_{27}ααα= 100*C_{27} 5α(H),14α(H),17α(H)-20R/$C_{27\text{-}29}$ 5α(H),14α(H),17α(H)-20R (*m/z* 217). **C_{28}ααα**= 100*C_{28} 5α(H),14α(H),17α(H)-20R/$C_{27\text{-}29}$ 5α(H),14α(H),17α(H)-20R (m/z 217). **C_{29}ααα**= 100*C_{29} 5α(H),14α(H),17α(H)-20R/$C_{27\text{-}29}$ 5α(H),14α(H),17α(H)-20R (*m/z* 217). **Preg**= diginane + 5α(H)-pregnane + 20-methyldiginane + 5α(H)-20-methylpregnane/ same + C_{29} 5α(H),14α(H),17α(H)-20R + C_{29} 5α(H),14α(H),17α(H)-20S + C_{29} 5α(H),14β(H),17β(H)-20R + C_{29} 5α(H),14β(H),17β(H)-20S. **DiaSt**= C_{27} 13β(H),17α(H)-20S + C_{27} 13β(H),17α(H)-20R/ same + C_{29} 5α(H),14α(H),17α(H)-20R + C_{29} 5α(H),14α(H),17α(H)-20S + C_{29} 5α(H),14β(H),17β(H)-20R + C_{29} 5α(H),14β(H),17β(H)-20S. **St29S/R**= C_{29} 5α(H),14α(H),17α(H)-20S / C_{29} 5α(H),14α(H),17α(H)-20 (S+R). **St29I/R**= C_{29} 5α(H),14β(H),17β(H)-20 (S+R)/ C_{29} 5α(H),14β(H), 17β(H)-20 (S+R) + C_{29} 5α(H),14α(H),17α(H)-20 (S+R). **St27Iso**= 100*C_{27} 5α(H),14β(H),17β(H)-20R + C_{27} 5α(H),14β(H),17β(H)-20S/ $C_{27\text{-}29}$ 5α(H),14β(H),17β(H)-20R + $C_{27\text{-}29}$ 5α(H),14β(H),17β(H)-20S (*m/z* 218). **St28Iso**= 100*C_{28}5α(H),14β(H),17β(H)-20R + C_{28} 5α(H),14β(H),17β(H)-20S/ $C_{27\text{-}29}$ 5α(H),14β(H),17β(H)-20R + $C_{27\text{-}29}$ 5α(H),14β(H),17β(H)-20S (*m/z* 218). **St29Iso**= 100*C_{29} 5α(H),14β(H),17β(H)-20R + C_{29} 5α(H),14β(H),17β(H)-20S/ $C_{27\text{-}29}$ 5α(H),14β(H),17β(H)-20R + $C_{27\text{-}29}$ 5α(H),14β(H),17β(H)-20S (*m/z* 218). **St30Iso**= 100*C_{30} 5α(H),14β(H),17β(H)-20R + C_{30} 5α(H),14β(H),17β(H)-20S/ $C_{27\text{-}29}$ 5α(H),14β(H),17β(H)-20R + $C_{27\text{-}30}$ 5α(H),14β(H),17β(H)-20S (*m/z* 218).

4.6 Hopanes

The hopane hydrocarbon biomarkers in the oils were monitored by GC-MS of the aliphatic hydrocarbon fractions using mainly *m/z* 191, 193 and 414 (e.g. Figures 4.23, 4.24, 4.25 & 4.26). Peak areas were used for the calculation of several ratios and their results are presented in Table 4.6. Some samples which are heavily biodegraded show depleted hopane concentrations and the peaks were not easily resolved. The calculated parameter includes; t_{19}/t_{23} (c.f. Zumberge, 1987; Rooney *et al*., 1998; Peters *et al*., 2005; He *et al*., 2012); t_{20}/t_{21} (c.f. p:IGI geochemical manual 2004); t_{22}/t_{21} (c.f. Peters *et al*., 2005; He *et al*., 2012); t_{24}/t_{23} (c.f. Peters *et al*., 2005; He *et al*., 2012); t_{23}/T30H (c.f. Seifert & Moldowan 1978; AquinoNeto *et al*., 1983; De Grande *et al*., 1983); Tri/Tetra (c.f. Seifert & Moldowan 1978; AquinoNeto et al., 1983; De Grande *et al*., 1983); Tetra/Hop (c.f. Peters & Moldowan 1983); Ts/Tm (c.f. Seifert & Moldowan 1978; Moldowan *et al.*, 1986); 29Hops (c.f. Ourisson et al., 1987; Killops *et al*., 1998); 30Hops (c.f. Ourisson *et al*., 1987; Killops *et al*., 1998); 31Hops (c.f. Ourisson *et al*., 1987; Killops *et al*., 1998); Hop/Mor (c.f. Seifert & Moldowan 1980; Rullkotter &Marzi 1988); Dia/NorM (c.f. Conford *et al*., 1986); 29Ts/29Tm (c.f. Seifert & Moldowan 1978; Moldowan *et al*., 1986); Hop32(S/R) (c.f. Seifert & Moldowan 1986); Hop(30/29) (c.f. p:IGI geochemical manual 2004); HomoHop (c.f. Peters & Moldowan 1991; 1993); OleanIndex (c.f. Ekweozor & Telnaes, 1990).

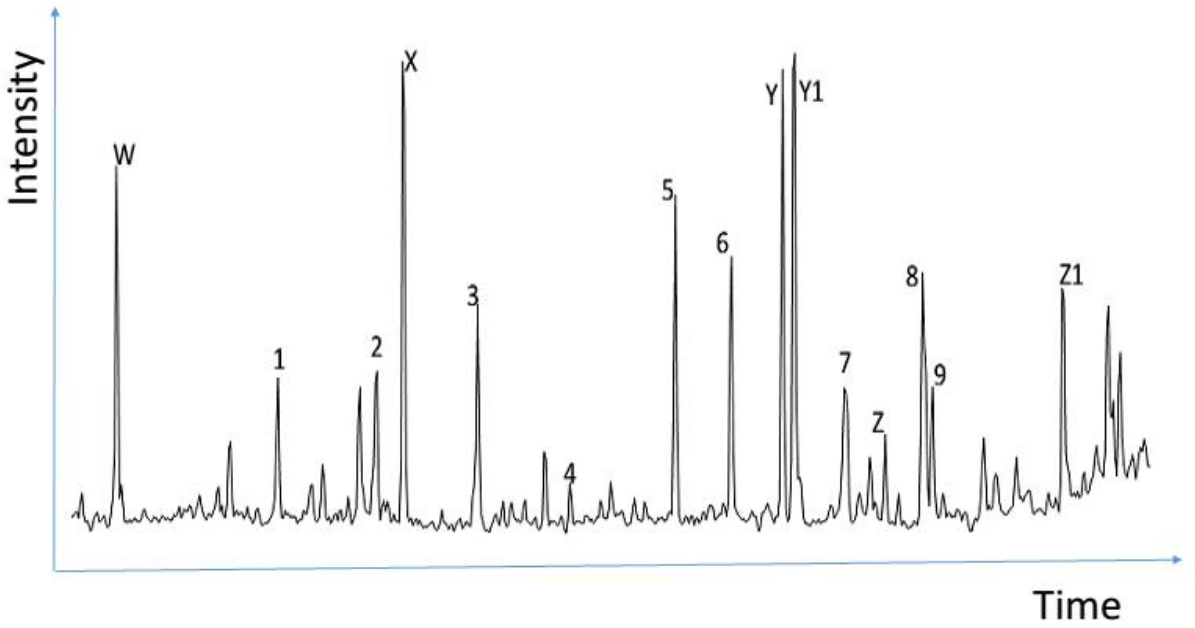

Figure 4.23: Representative partial *m/z* 191 mass chromatogram of the aliphatic hydrocarbon fraction showing the distributions of tricyclic and tetracyclic terpanes in oil sample OE016.

W= Unknown Tricyclic terpane. **1=** C_{19} Tricyclic terpane. **2=** C_{20} Tricyclic terpane. **X=** Unknown C_{21} Tricyclic terpane. **3=** C_{21} Tricyclic terpane. **4=** C_{22} Tricyclic terpane. **5=** C_{23} Tricyclic terpane. **6=** C_{24} Tricyclic terpane. **Y=** Unknown C_{25} Tricyclic terpane. **Y1**= 10β-des-A-oleanane (C_{24} Tetracyclic terpane). **7**= C_{25} Tricyclic erpane (22S & 22R isomers). **Z**= 10β-des-A-ursane (C_{24} Tetracyclic terpane). **8=** C_{24} Tetracyclic terpane. **9=** C_{26} (22S+22R) Tricyclic terpane. **Z1=** Unknown C_{27} terpane).

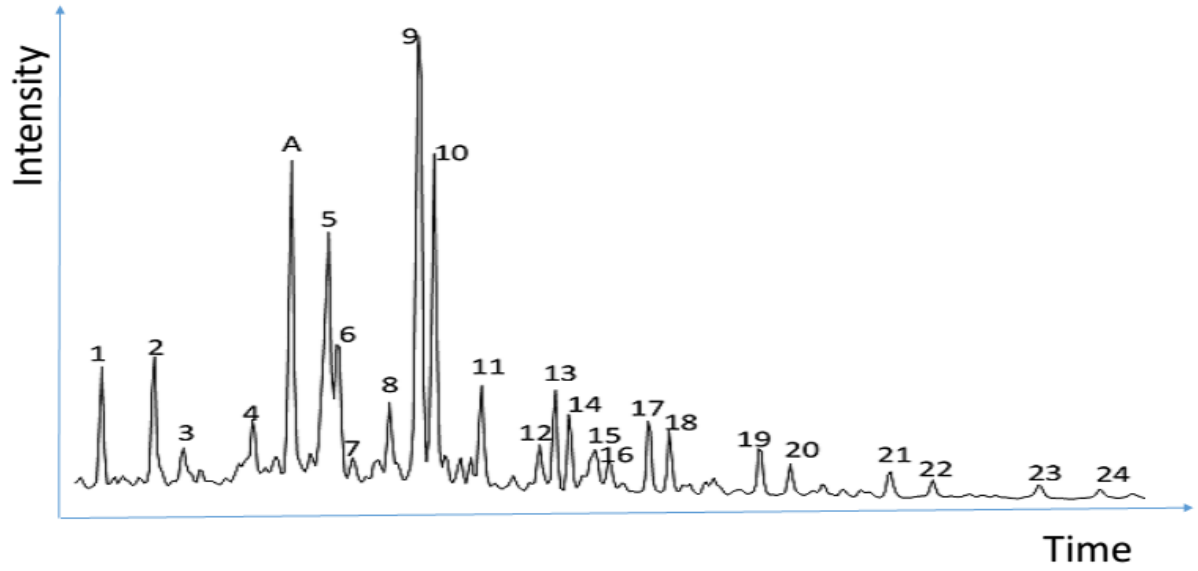

Figure 4.24: Representative partial *m/z* 191 mass chromatogram of the aliphatic hydrocarbon fraction showing the distributions of pentacyclic terpanes in oil sample OE081.

1= 18α 22,29,30-trisnorneohopane (Ts). **2=** 17α 22,29,30-trisnorhopane (Tm). **3=** C_{30} (22S+22R) Tricyclic terpane. A= Unknown C_{29} Hopane. **4=** C_{28} 17α, 21β norhopane. **5=** C_{29} 17αH,21βH 30-nor-Hopane, **6=** 18α 30-nor-Neohopane (C_{29}Ts), **7=** 17α Diahopane (Hopane-X). **8=** 17β,21α 30-nor-Moretane. **9=** 18α Oleanane. **10=** C_{30} 17α,21β Hopane. **11=** 17β,21α Moretane. **12=** 19α-taraxastane. **13=** C_{31} 17α,21β 22S Hopane. **14=** C_{31} 17α,21β 22R Hopane. **15=** 17β,21α 22S Moretane. **16=** 17β,21α 22R Moretane. **17=** C_{32} 17α,21β 22S bishomo-Hopane. **18=** C_{32} 17α,21β 22R bishomo-Hopane. **19:** C_{33} 17α,21β 22S trishomo-Hopane. **20**: C_{33} 17α,21β 22R trishomo-Hopane. **21=** C_{34} 17α,21β 22S tetrakishomo-Hopane. **22=** C_{34} 17α,21β 22R tetrakishomo-Hopane. **23=** C_{35} 17α,21β 22S pentakishomo-Hopane. **24=** C_{35} 17α,21β 22R pentakishomo-Hopane.

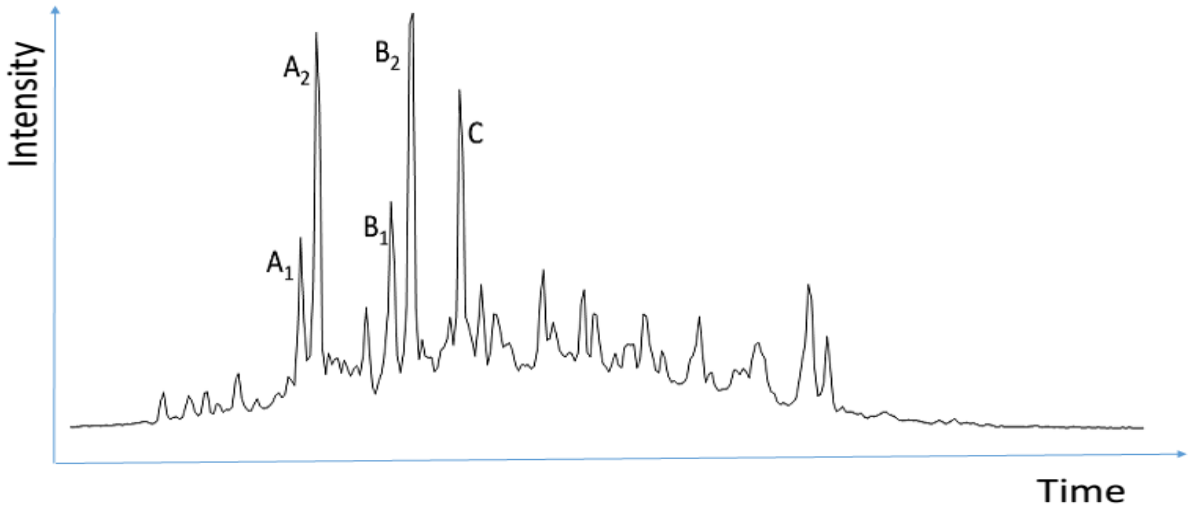

Figure 4.25: Representative partial *m/z* 414 mass chromatogram showing the distributions of compounds A1, A2, B1, B2 and C (C_{30} tetracyclic) in oil sample OE016.

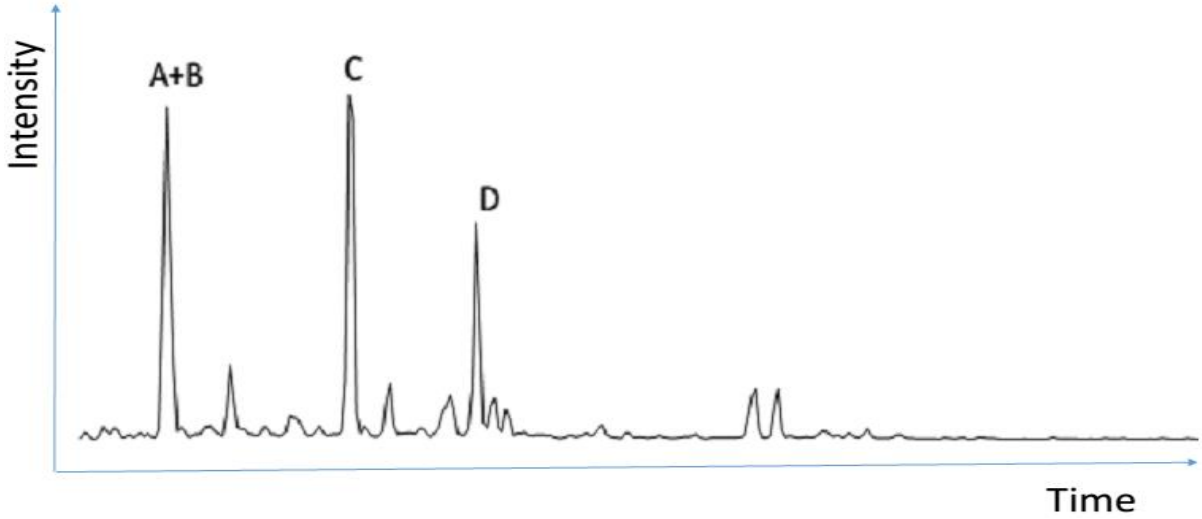

Figure 4.26: Representative partial *m/z* 193 mass chromatogram showing the distributions of the C_{15} sesquiterpanes (A-D) in oil sample OE016.

Most of the calculated parameters does not show any significant variation across the Delta, however some parameters show marked variations. The parameters that show significant variation includes the t_{19}/t_{23} tricyclic terpane ratio, which shows very high average value in samples from the Central Delta oil samples (1.19) and low values for samples from the Eastern (0.51) and Southern Delta (0.61) (Figure 4.27). The tri/tetra ratio shows the opposite variation pattern to what is observed with the t_{19}/t_{23} (Figure 4.28), with the Central Delta having an average value of 0.69, the Eastern Delta has an average value of 0.98 and the Western and Southern Delta has average values of 0.81 and 0.94, respectively.

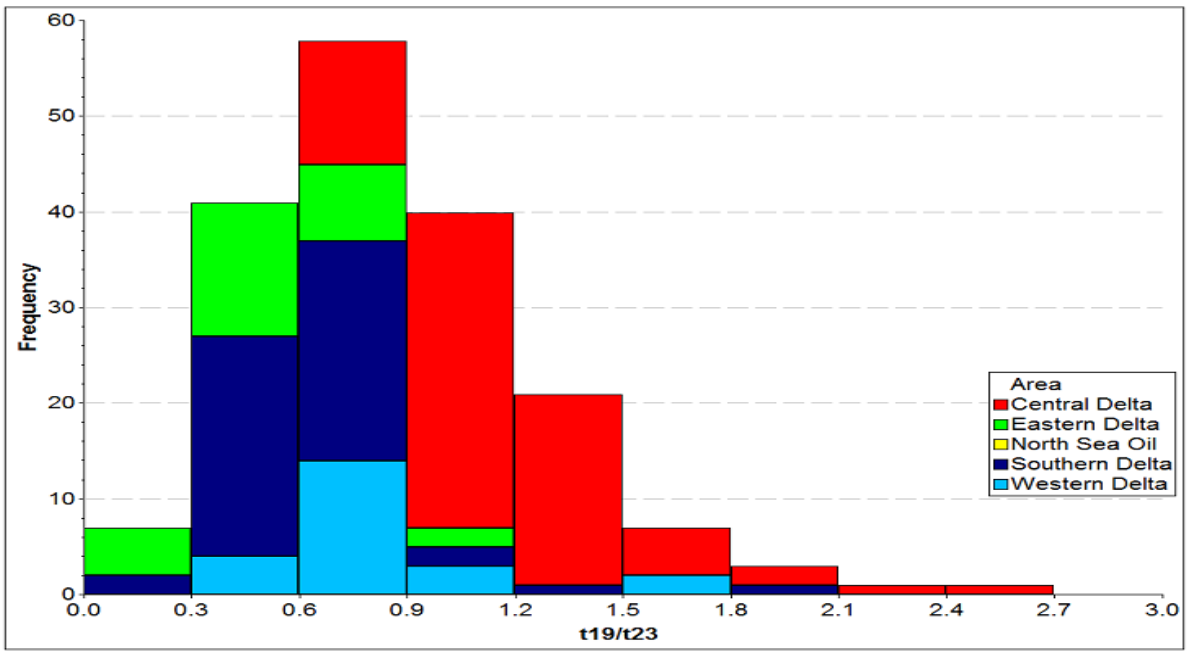

Figure 4.27: Variation of t_{19}/t_{23} ratios in Niger Delta oils. Note the wide range of t_{19}/t_{23} ratio across the Delta, with the Centra Delta having very high values when compared to the other parts.

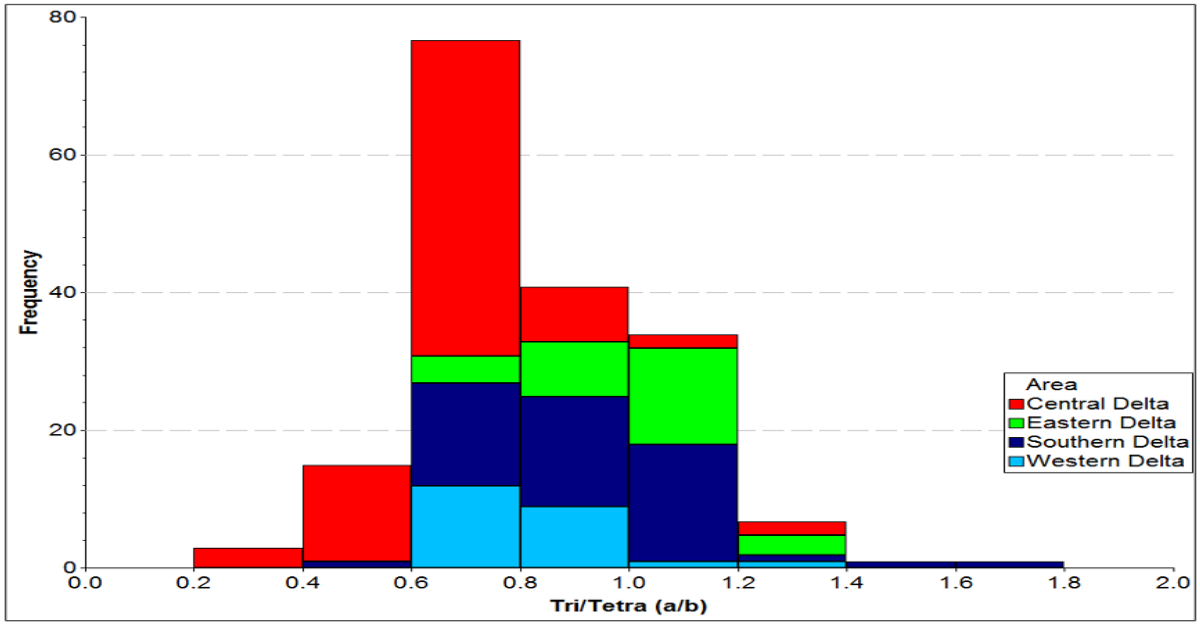

Figure 4.28: Variation of Tri/Tetra ratios in Niger Delta oils. Note the wide range of Tri/Tetra ratios across the Delta with the Centra Delta having low values when compared to other parts.

The K index (Samuel, 2008) shows that the Central Delta oil samples have lower values (2.37) than the other part of the delta, especially the Southern Delta oil samples which have an average of 4.22 (Figure 4.29). The $Y/(Y+TC_{24})$ and $X/(X+TC_{20})$ parameters separate the Delta oil samples into groups (Figure 4.31) with most of the Eastern Delta oil samples

having low values for both parameters and the Southern Delta oil samples have a higher value for both parameters and both area shows a positive correlation for the two parameters, whereas the Central and Western Delta oils do not show any particular trend (Figure 4.30).

A plot of oleanane index against A/(A+H29) where A is the unknown peak in the *m/z* 191 (Figure 4.26) shows a very positive relationship with the samples and the possibility of two trends. Samples from Central Delta, Eastern Delta and Western Delta all has same trend but samples from the Southern Delta have a higher gradient when compared to the other regions (Figure 4.31). The Central Delta oil samples has an average A/(A+H29) value of 0.28, the Western Delta oil samples has an average value 0.24 whereas the Eastern and Southern Delta has average values of 0.18 and 0.15 respectively (Table 4.6).

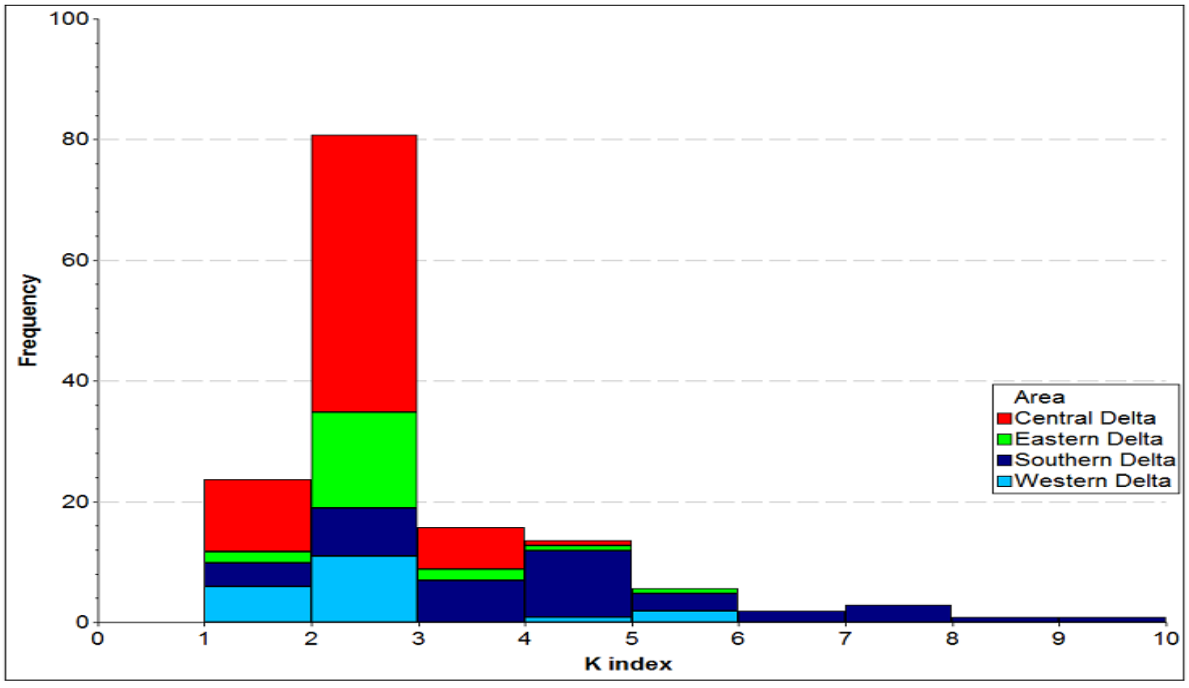

Figure 4.29: Variation of K index in Niger Delta oil. Note the wide range of K index across the Delta, with the Central and Western delta having lower values than the Southern Delta.

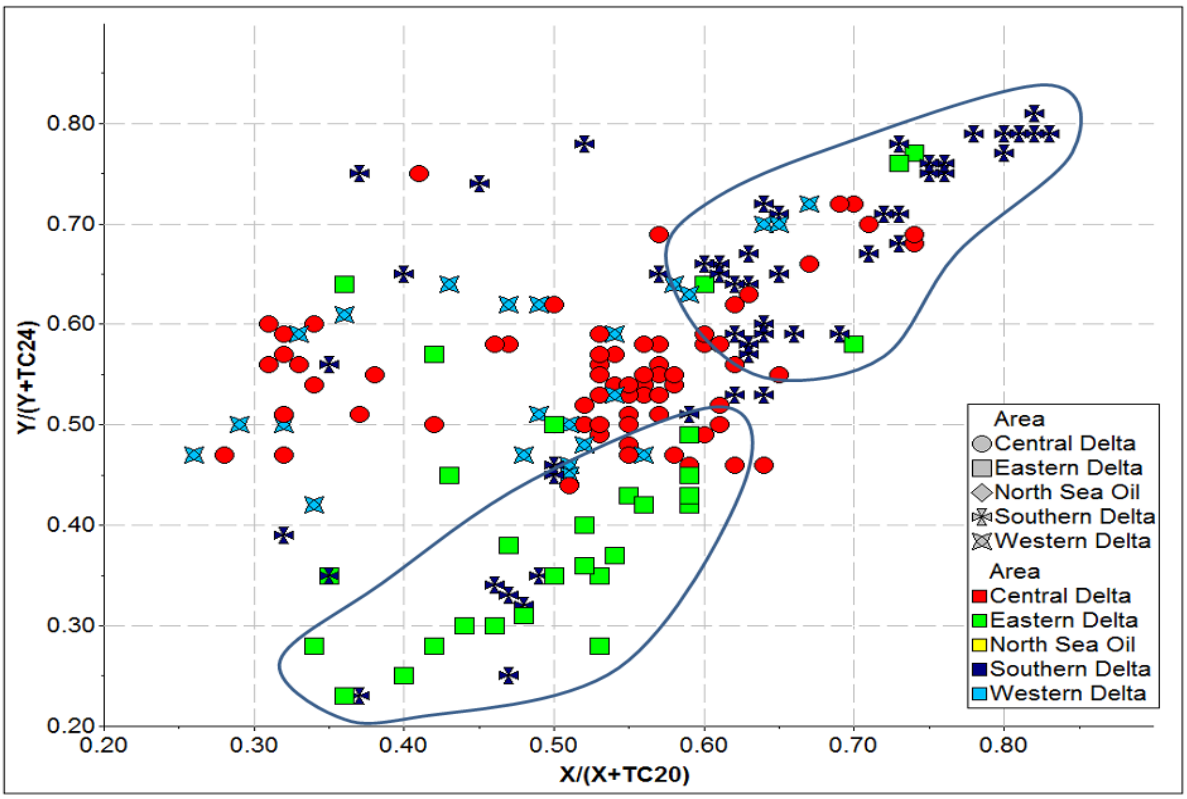

Figure 4.30: Plot of Y/(Y+TC_{24}) against X/(X+TC_{20}) showing the possibility of separating the oil samples into several groups, with the Southern Delta having a high values for both parameters and the Eastern Delta having a low values for both parameters.

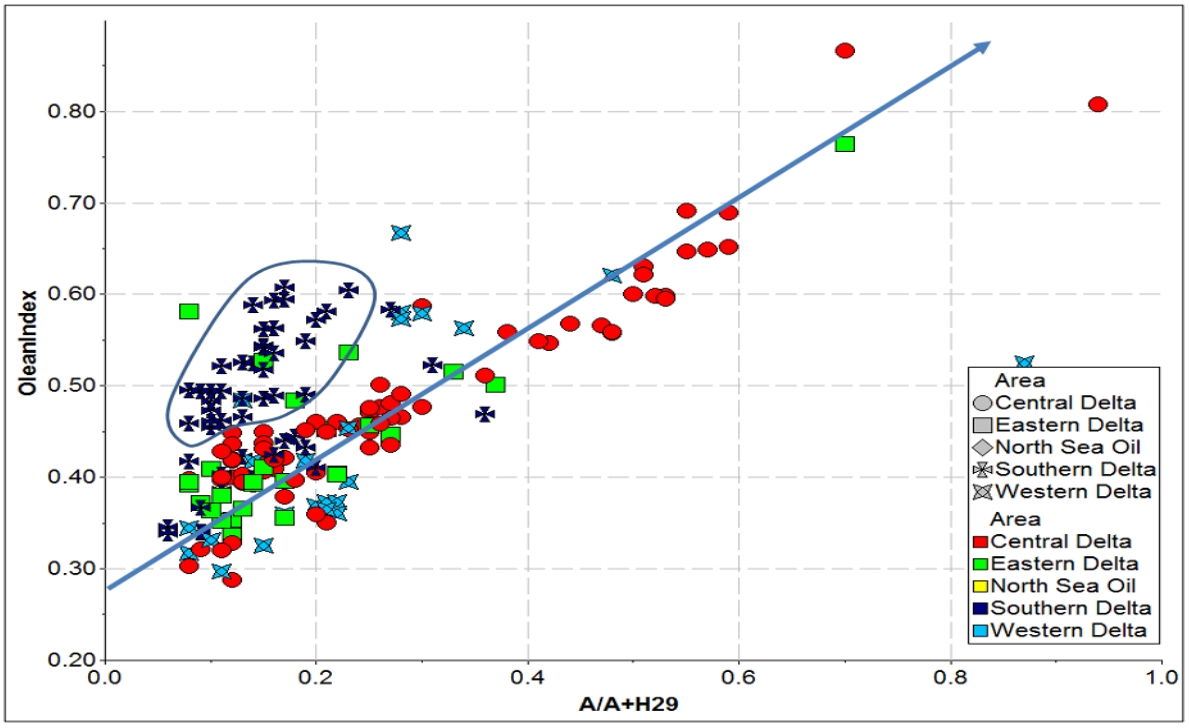

Figure 4.31: Plot of oleanane index against A/(A+C_{29}αβ hopane) showing positive trend for the samples. Note the possibility of another trend in the samples from the Southern Delta.

A Ternary plot of %A+B, %C and %D from *m/z* 193 mass chromatograms shows the separation of Southern Delta oil samples from Central Delta oil samples; the Eastern and Western Delta oil samples do not show any particular trend (Figure 4.32). Some oil samples from Central and Western Delta plots away from other samples as they have elevated %A+B, which is usually greater than 70%. The Central and Western Delta oils have average values of 46 and 47 for the %A+B parameter, whereas, the Eastern and Southern Delta have average values of 36 and 37, respectively. The peak A+B is not present in the North Sea NSO-1 sample.

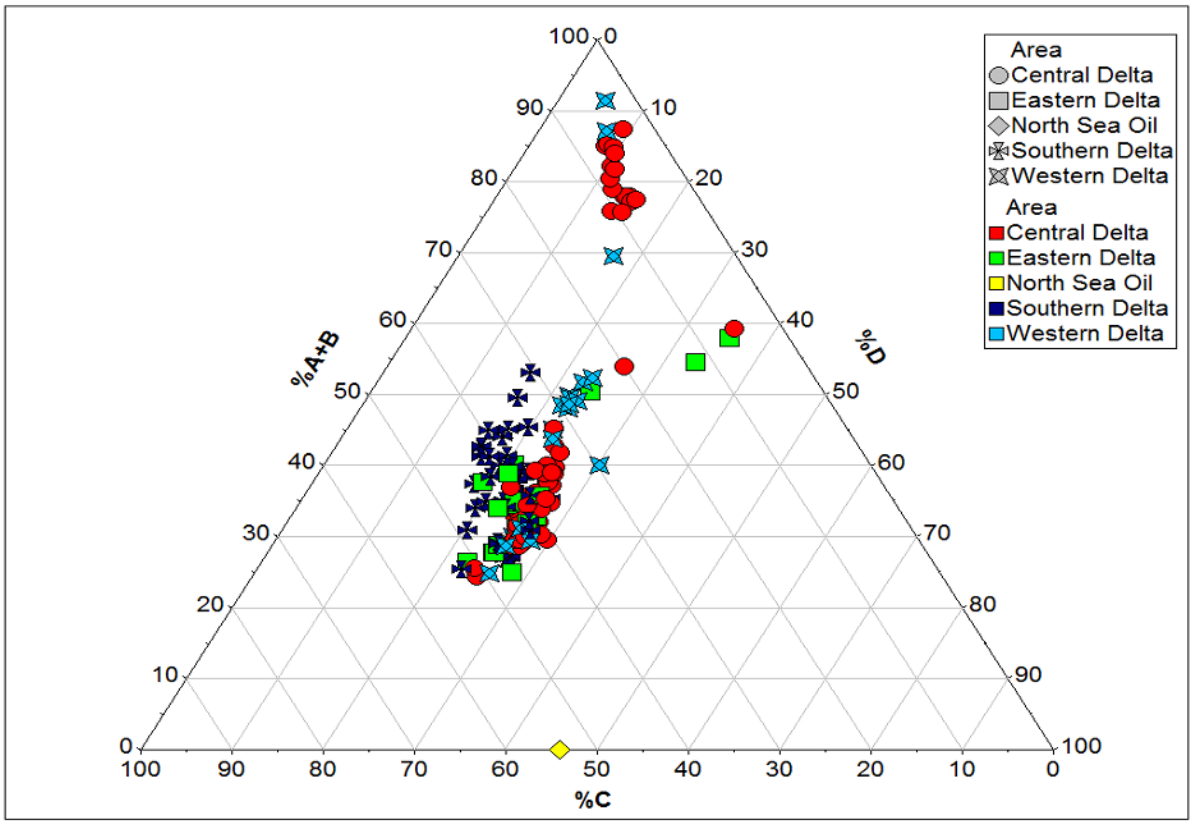

Figure 4.32: Ternary plot of %A+B, %C and %D from the *m/z* 193 mass chromatograms. Note the separation of most of the Southern Delta oil samples from Central Delta oil samples; the peak A+B is not present in the North Sea oil (NSO-1) sample.

Table 4.6: Summary of source and maturity terpane biomarker parameters of the oil samples

		Central Delta			Eastern Delta			Western Delta			Southern Delta			Replicate			NSO-1
parameter	unit	no Mean	SD	CV	no Mean	SD	CV	no Mean	SD	CV	no Mean	SD	CV	no Mean	SD	CV	
t_{19}/t_{23}	a/b	75 1.19	0.35	30	29 0.51	0.24	47	23 0.81	0.29	36	52 0.61	0.28	47	3 0.61	0.01	2	nd
t_{20}/t_{21}	a/b	75 2.02	1.97	97	29 1.52	1.91	125	23 2.39	2.20	92	52 1.32	1.11	84	3 0.91	0.02	2	nd
t_{22}/t_{21}	a/b	75 0.25	0.1	40	29 0.30	0.19	63	23 0.29	0.09	31	52 0.24	0.06	25	3 0.23	0.04	17	nd
t_{24}/t_{23}	a/b	75 0.94	0.11	12	29 0.86	0.09	10	23 0.91	0.11	12	52 0.89	0.1	11	3 0.86	0.05	6	nd
t_{23}/T30H	%	75 5.26	3.72	71	29 6.59	4.21	64	23 5.99	1.78	30	52 5.36	1.60	30	3 5.89	0.16	3	nd
Tri/Tetra	a/b	75 0.69	0.17	24	29 0.98	0.14	15	23 0.81	0.17	21	52 0.94	0.21	22	3 0.90	0.03	3	nd
Tetra/Hop	a/b	75 0.09	0.09	97	29 0.07	0.06	75	23 0.08	0.03	36	52 0.06	0.02	26	3 0.08	0.00	0	nd
Ts/Tm	a/(a+b)	75 0.45	0.03	6	29 0.43	0.04	8	23 0.47	0.05	10	52 0.43	0.04	9	3 0.41	0.00	0	0.47
29Hops	a/b	75 0.51	0.12	24	29 0.47	0.10	21	23 0.49	0.14	28	52 0.51	0.05	10	3 0.49	0.01	2	0.24
30Hops	a/b	75 0.98	0.23	24	29 1.01	0.23	22	23 0.96	0.28	29	52 0.98	0.09	10	3 0.88	0.02	2	1.02
31Hops	a/b	75 0.22	0.03	12	29 0.23	0.03	14	23 0.24	0.05	19	52 0.21	0.04	17	3 0.24	0.03	13	0.43
Hop/Mor	a/b	75 5.63	1.40	25	29 6.04	1.35	22	23 5.83	1.30	22	52 5.87	1.00	17	3 6.10	0.00	0	10.58
Dia/NorM	a/b	75 0.69	1.41	206	29 0.54	0.34	63	23 0.52	0.34	66	52 0.44	0.17	39	3 0.34	0.03	9	1.17
29Ts/29Tm	a/(a+b)	75 0.23	0.11	45	29 0.20	0.07	34	23 0.24	0.15	65	52 0.19	0.05	25	3 0.23	0.06	26	0.27
Hop32(S/R)	a/(a+b)	75 0.58	0.03	5	29 0-.58	0.03	6	23 0.58	0.03	5	52 0.58	0.03	5	3 0.56	0.00	0	0.55
Hop(30/29)	a/b	75 1.53	0.55	36	29 1.69	0.80	47	23 2.09	3.11	149	52 1.48	0.15	10	3 1.40	0.02	1	2.61
HomoHop	a/b	73 0.49	0.11	22	27 0.52	0.17	32	23 0.52	0.10	19	45 0.39	0.12	29	3 0.50	0.06	12	1.41
Hop(35/34)	a/b	73 0.58	0.17	29	27 0.57	0.22	39	23 0.58	0.24	40	45 0.49	0.21	44	3 0.60	0.03	5	0.74
OleanIndex	a/(a+b)	75 0.49	0.12	25	29 0.41	0.11	26	23 0.43	0.12	28	53 0.46	0.10	22	3 0.45	0.01	2	nd
$A/(A+C_{29}\alpha\beta H)$	a/(a+b)	75 0.28	0.18	63	29 0.18	0.12	68	23 0.24	0.17	69	52 0.15	0.06	41	3 0.21	0.01	6	nd
$x/(x+t_{20})$	a/(a+b)	66 0.53	0.11	21	22 0.49	0.11	22	20 0.47	0.11	24.4	40 0.61	0.15	25	3 0.59	0.01	2	nd
$Y/(Y+t_{23})$	a/(a+b)	66 0.53	0.07	13	22 0.39	0.15	39	20 0.52	0.10	18.7	40 0.59	0.18	31	3 0.46	0.01	2	nd
K index	a/b	66 2.37	0.55	23	22 2.67	0.91	34	20 2.68	1.16	43.1	40 4.22	1.95	46	3 2.45	0.12	5	nd
A+B	%	66 46.16	20.49	44	22 36.02	8.58	24	20 47.427	18.09	38.1	40 37.16	6.42	17	3 42.14	0.40	1	0.00
C	%	66 31.37	14.96	48	22 38.84	10.87	28	20 30.37	12.62	41.5	40 41.53	4.15	10	3 34.88	0.52	1	54.10
D	%	66 22.48	6.33	28	22 25.14	3.77	15	20 22.20	6.08	27.4	40 21.30	3.57	17	3 22.98	0.30	1	45.90
(A+B)/(A+B+C+D)	a/a+b	66 0.46	0.21	44	22 0.36	0.09	24	20 0.47	0.18	38	40 0.37	0.06	17	3 0.42	0.00	1	nd

t_{19}/t_{23}= C_{19} Tricyclic/ C_{23} Tricyclic terpane. **t_{20}/t_{21}**= C_{20} Tricyclic/C_{21} Tricyclic terpane**.** **t_{22}/t_{21}**= C_{22} Tricyclic/C_{23} Tricyclic terpane. **t_{24}/t_{23}**= C_{24} Tetracyclic/C_{23} Tricyclic terpane. **t_{23}/T30H**= C_{23} Tricyclic terpane/ C_{30} 17(α), 21(β) hopane. **Tri/Tetra**= C_{23} Tricyclic terpane/ C_{24} Tetracyclic terpane. **Tetra/Hop**= C_{24} Tetracyclic terpane/ C_{30} Hopane. **Ts/Tm**= 18α(H)-trinorneohopane/18α(H)-trinorneohopane+ 17(α)H-trinorhopane. **29Hops**= C_{29} 17(α) regular hopane/ $C_{29\text{-}31}$ regular hopanes. **30Hops**= C_{30} 17(α) regular hopane/ $C_{29\text{-}31}$ regular hopanes. **31Hops**= C_{31} 17(α) regular hopane/ $C_{29\text{-}31}$ regular hopanes. **Hop/Mor**= C_{29} 17α(H)-norhopane/C_{29} 17β(H)-normoretane. **Dia/NorM**= C_{30} 17α(H)diahopane/ C_{29} 17β(H)-normoretane. **29Ts/29Tm**= C_{29} 18α(H)-norneohopane/ C_{29} 18α(H)-norneohopane + C_{29} 17α(H)-norhopane. **Hop32(S/R)**= 17α(H), 21β(H)-bishomohopane 22S/22S+22R. **Hop(30/29)**= C_{30} 17α(H)-hopane/ C_{29} 17α(H)-norhopane. **HomoHop**= $C_{31\text{-}35}$ 17α(H)-homohopanes (22S+22R)/ $C_{27+29+30}$ 17α(H)-hopanes. **OleanIndex**= 18α(H)-oleanane/ 18α(H)-oleanane + C_{30} 17α(H)-hopane. **nd**= not determined.

4.7 Carbazoles

The pyrrolic nitrogen carbazole compounds in the carbazole fraction were monitored by GC-MS using *m/z* 167, 181 and 217 (Fig 4.33). Although the Niger Delta oil samples have been noted to have very low carbazole concentrations (Bennett *et al*., 2002), carbazole peaks are still prominent in some samples of the current study. Of special importance are oil samples from the Western Delta, where 8 samples was selected for analysis from this region but only 2 of them have carbazoles detectable in them and the other 6 samples (OE048, OE073, OE099, OE131, OE132 and OE159) do not contain quantifiable carbazoles.

Peak areas were used for the calculation of several ratios and concentrations, and the results are presented in Table 4.7. The calculated parameters/concentrations include; C (ppm) (c.f. Li *et al*., 1997), 1-mC (ppm) (c.f. Li *et al*., 1997), 3-mC (ppm) (c.f. Li *et al*., 1997), 2-mC (ppm) (c.f. Li *et al*., 1997), 4-mC (ppm) (c.f. Li *et al*., 1997), (1+3+2+4)-mC (ppm) (c.f. Li *et al*., 1997), Benzo(a)carbazole (ppm) (c.f. Li *et al*., 1997), Benzo(c)carbazole (ppm) (c.f. Li *et al*., 1997), a/(a+c) (c.f. Li *et al*., 1997), b/a (c.f. Huang *et al*., 2002) 3/4mC (c.f. Li *et al*., 1997), 1/(1+4)mC (c.f. Li *et al*., 1997), (3+2)/4mC (c.f. Li *et al*., 1997), Benzocarbazole/methylcarbazole (c.f. Li *et al*., 1997).

Most of the calculated parameters do not show any significant variations across the Delta but some parameters show marked variations (Figures 4.36; 4.37; 4.38; 4.39). The two parameters that show significant variations are the 1-/4-mC and benzocarbazole/methylcarbazole ratios. The 1-/4-mC ratios show that the Central Delta oil samples have a higher average value (0.72) than samples from other part of the Delta (Figure 4.34), with those from the Eastern, Western and Southern Delta having average values of 0.66, 0.61 and 0.64, respectively. The total benzocarbazole/total methylcarbazole

ratios in the Niger Delta oil samples also show that the Southern Delta oil samples have lower values when compared to the other part of the Delta (Figure 4.35).

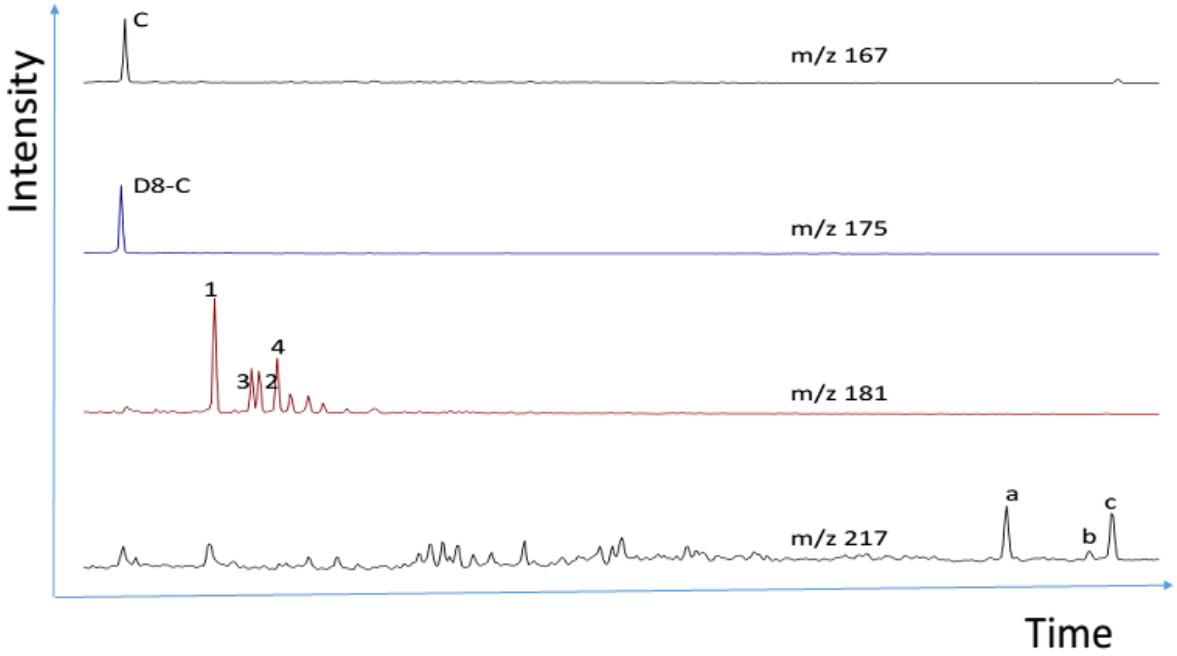

Figure 4.33: Representative partial *m/z* 167, 175, 181 and 217 mass chromatograms of the carbazoles from the polar fraction of oil OE016.
C= Carbazole, **D8-C**= D8-Carbazole (internal standard), **1**= 1-methylcarbazole, **3**= 3-methylcarbazole, **2**= 2-methylcarbazole, **4**= 4-methylcarbazole, **a**= Benzo(a)carbazole, **b**= Benzo(b)carbazole, **c**= Benzo(c)carbazole.

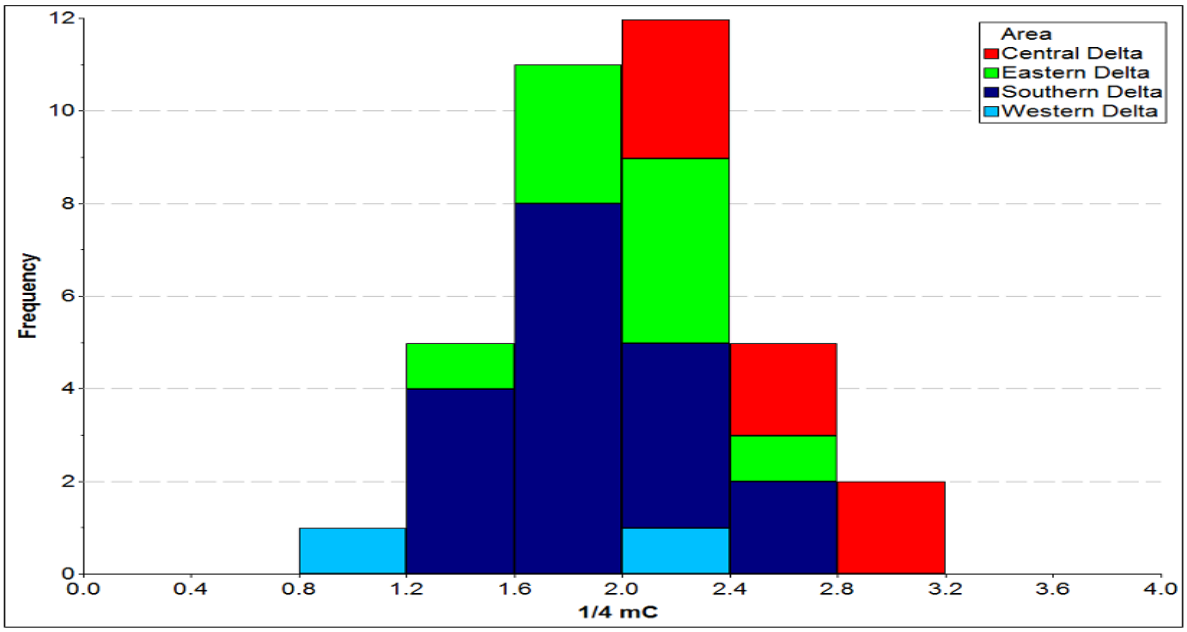

Figure 4.34: Variation of 1-methylcarbazole/4-methylcarbazole ratios in the Niger Delta oils, showing the wide range of values across the Delta (note the Southern Delta oil have relatively lower values when compared to the Central Delta oil samples).

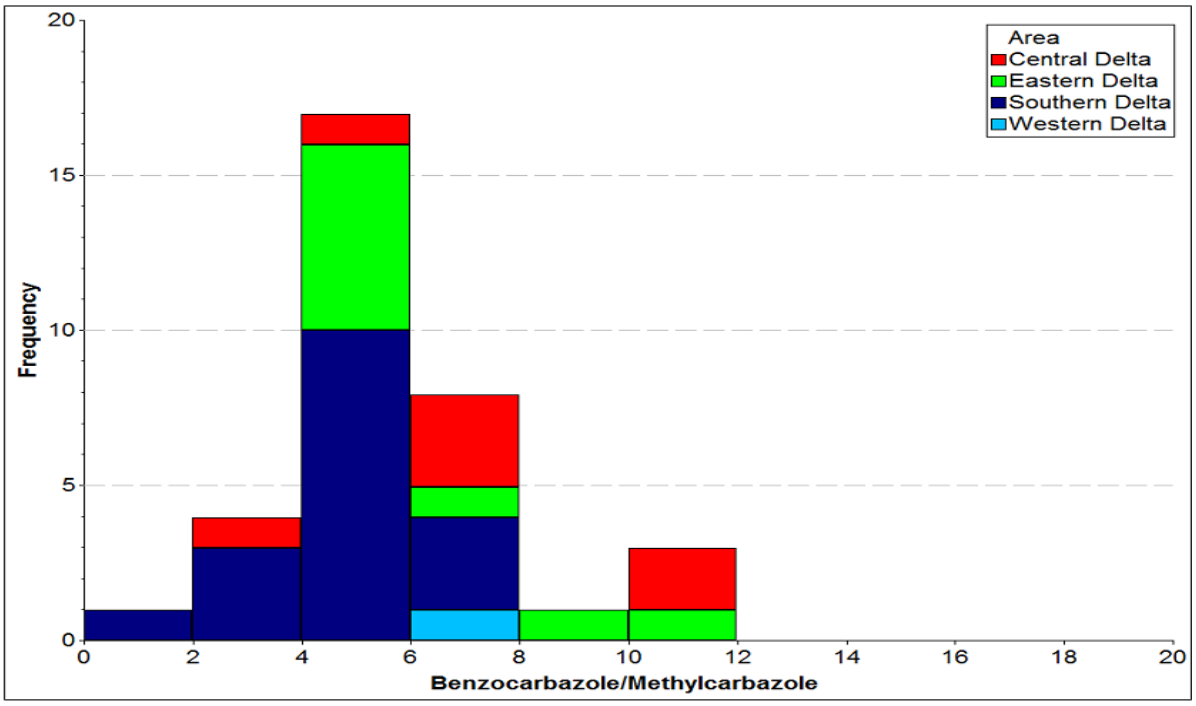

Figure 4.35: Variation of total benzocarbazole/total methylcarbazole ratios in the Niger Delta oils showing the wide range of values across the Delta (note the low values in the Southern Delta oils when compared to the other parts of the Delta).

Although not much variation was seen in the various calculated ratios, there were marked variations between some carbazole ratios and some other parameters which shows some interesting trends.

The plot of benzocarbazole (a/a+c) ratios against 3+4 methyldiamantane concentrations (Figure 4.36) shows that there is a negative correlation between those two parameter. The same negative trend was noticed when the benzocarbazole (a/a+c) ratio was plotted against the expulsion temperature (measured from the light hydrocarbons - see section 4.1), which shows that the lower the expulsion temperature, the higher the benzocarbazole ratio (Figure 4.37). There also exists a positive correlation between 1/1+4 mC and expulsion temperature (figure 4.38) and %(A+B)/(A+B+C+D) (Figure 4.39).

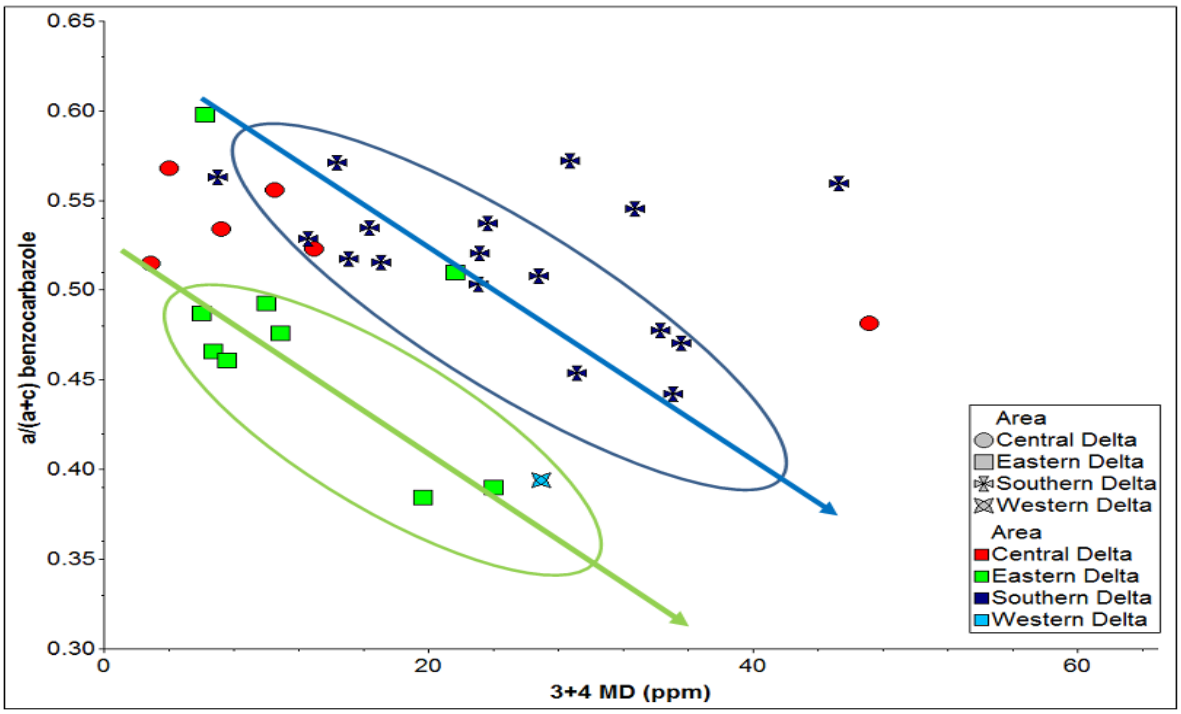

Figure 4.36: Plot of benzocarbazole (a/a+c) ratios against 3+4 methyldiamantane concentrations in the Niger Delta oil samples showing a nagative correlation between both parameters (note the two possible trends for the sets of oil samples from the Southern and Eastern Delta).

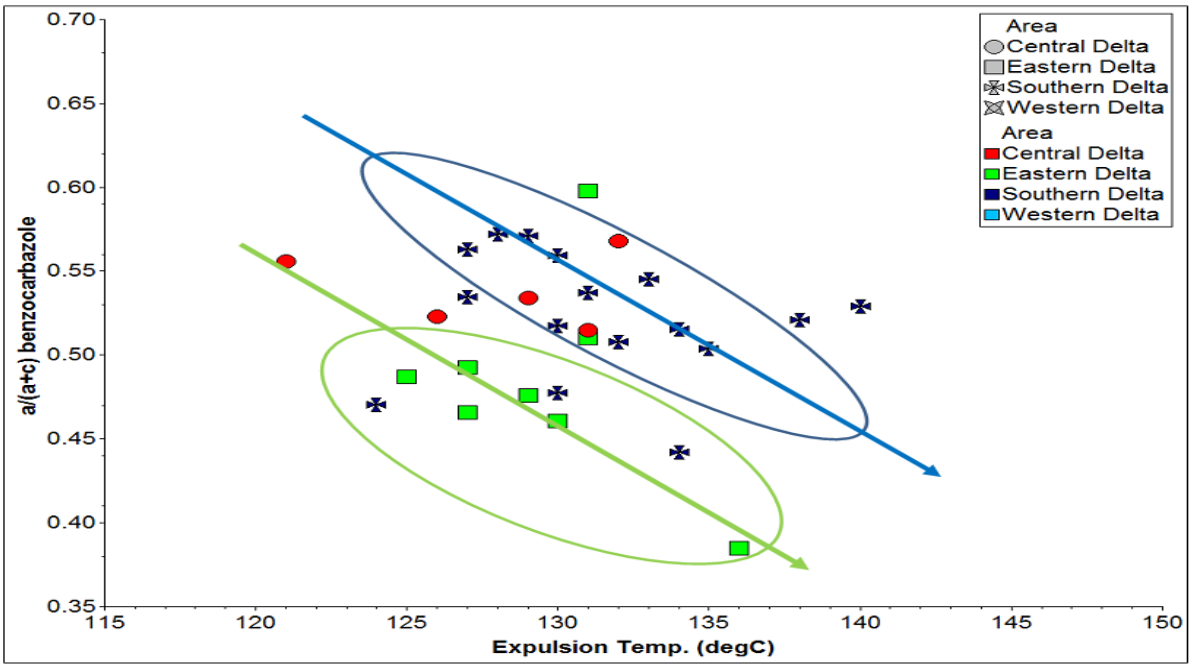

Figure 4.37: Plot of benzocarbazole (a/a+c) ratios against calculated temperatures of expulsion (°C) in the Niger Delta oil samples showing a negative correlation between both parameters (note the two possible trends for the sets of oil samples from the Southern and Eastern Delta).

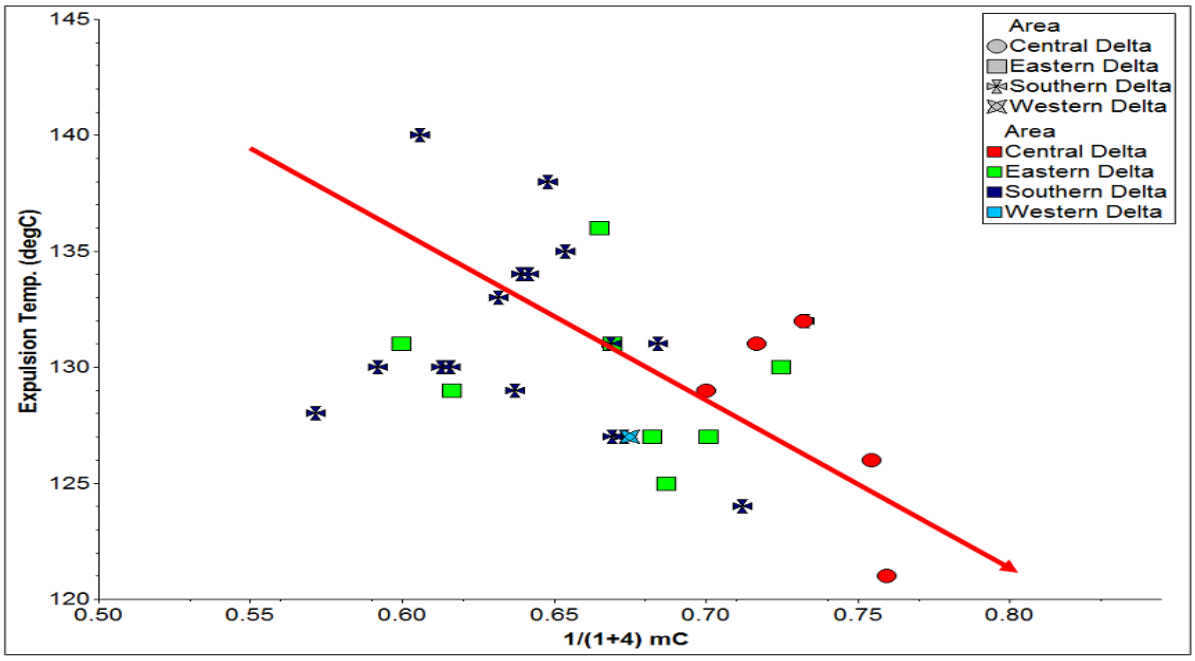

Figure 4.38: Plot of calculated temperature of expulsion (°C) against 1/(1+4) methylcarbazole ratios in the Niger Delta oil samples showing a negative correlation between both parameters.

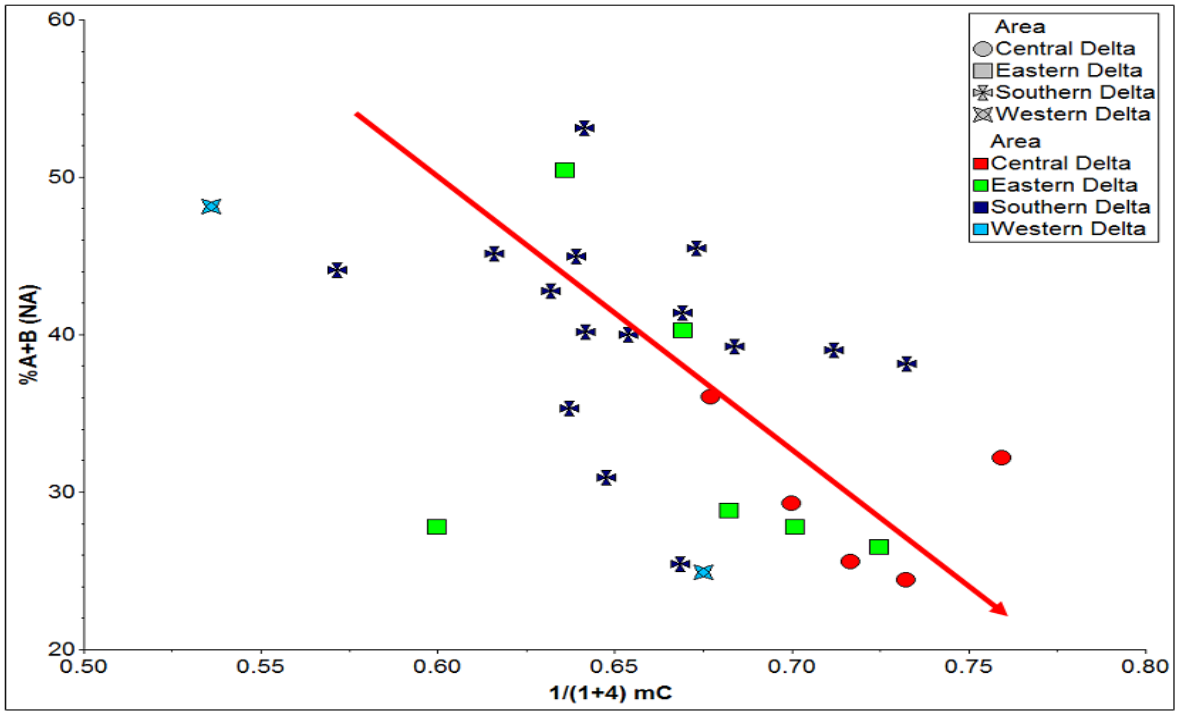

Figure 4.39: Plot of %(A+B)/(A+B+C+D) against 1/(1+4) methylcarbazole ratios in the Niger Delta oil samples showing a negative correlation between both parameters.

Table 4.7: Summary of carbazole parameters of oil samples

		Central Delta			Eastern Delta			Western Delta			Southern Delta			Replicate		
Parameter	unit	no Mean	SD	CV	no Mean	SD	CV	no Mean	SD	CV	no Mean	SD	CV	no Mean	SD	CV
C	ppm	7 1.54	1.24	80	9 1.48	2.27	153	2 0.31	0.01	4	17 1.36	2.23	165	2 1.41	0.01	1
1-mC	ppm	7 1.8	1.38	76	9 1.43	1.92	134	2 0.44	0.03	6	17 1.09	1.43	131	2 0.92	0.04	4
3-mC	ppm	7 1.05	0.82	78	9 0.63	0.65	103	2 0.33	0.07	21	17 0.51	0.51	100	2 0.49	0.01	2
2-mC	ppm	7 0.23	0.30	129	9 0.29	0.68	235	2 0.01	0.00	25	17 0.24	0.76	314	2 0.09	0.01	10
2+3-mC	ppm	7 1.28	1.11	87	9 0.92	1.31	143	2 0.35	0.07	21	17 0.75	1.26	167	2 0.58	0.00	0
4-mC	ppm	7 0.19	0.24	125	9 0.36	0.93	259	2 0.01	0.01	50	17 0.37	1.23	334	2 0.08	0.00	4
Benzo(a)	ppm	7 0.28	0.23	81	9 0.18	0.16	92	1 0.05			17 0.25	0.35	139	2 0.17	0.02	11
Benzo(b)	ppm	7 0.13	0.09	66	9 0.09	0.05	54	1 0.06			17 0.10	0.10	99	2 0.07	0.02	25
Benzo©	ppm	7 0.24	0.19	76	9 0.19	0.16	85	1 0.08			17 0.22	0.27	126	2 0.18	0.02	11
Benzo(a+c)	ppm	7 0.53	0.41	78	9 0.36	0.32	88	1 0.14			17 0.47	0.62	133	2 0.35	0.04	11
sum mC	ppm	7 3.30	2.72	82	9 2.71	4.15	153	2 0.8	0.11	13	17 2.21	3.89	176	2 1.58	0.04	2
1-/1- +2-mC	a/a+b	7 0.71	0.05	7	9 0.70	0.07	10	2 0.6	0.03	6	17 0.67	0.05	7	2 0.63	0.03	5
1-/1- +4-mC	a/a+b	7 0.72	0.03	4	9 0.66	0.04	6	2 0.61	0.10	16	17 0.64	0.04	6	2 0.67	0.02	3
2-/2- +3-mC	a/a+b	7 0.42	0.07	16	9 0.46	0.05	12	2 0.47	0.00	0	17 0.48	0.06	13	2 0.52	0.03	5
a/(a+c)	a/a+b	7 0.52	0.04	7	9 0.47	0.06	13	2 0.39			17 0.52	0.04	8	2 0.49	0.00	0

C= carbazole (ppm), **1-mC**= 1-methylcarbazole (ppm), **3-mC**= 3-methylcarbazole (ppm), **2-mC**= 2-methycarbazole (ppm), **2-+3-mC**= 2-methylcarbazole + 3-methylcarbazole (ppm), 4-**mC**= 4-methylcarbazole (ppm), **Benzo(a)**= Benzo(a)carbazole (ppm), **Benzo(b)**= Benzo(b)carbazole (ppm), **Benzo(c)**= Benzo(c)carbazole (ppm), **1/(1-+2-mC)**= 1-methycarbazole/ (1-methylcarbazole+2-methylcarbazole), **1/(1-+4-mC)**= 1-methycarbazole/(1-methylcarbazole+4-methylcarbazole), **2/(2-+3-mC)=** 2-methycarbazole/(2-methylcarbazole+3-methylcarbazole), **a/(a+c)**= Benzo(a)carbazole/(Benzo(a)carbazole+ Benzo(c)carbazole).

4.8 Compound Specific Isotope Analysis (CSIA)

The compound specific isotope analysis (CSIA) of individual *n*-alkanes for selected samples was carried out both in carbon and hydrogen mode. The replicate results of 3 runs done over a period of time (i.e. with different batches of analysis) indicate that the results are valid with very low standard deviation, although an increase in the standard deviation value around the nC$_{29}$ to nC$_{33}$ region was noticed in carbon mode.

The standard deviation values in hydrogen mode are higher than the carbon mode measurements and this can be attributed to the wider range of values in the hydrogen mode (-100 – -170‰), but overall the values are well within a standard range with high reproducibility. The standard deviation in Hydrogen mode range from 0.58 – 11.36‰ (per mil) and that of the Carbon mode range from 0.15 to 1.53 (per mil) (Table 4.8 and 4.9).

Some compounds were excluded from the measured data because their chromatographic peaks were not separated perfectly (Figure 4.40) and integration of those compounds will always then introduce errors into the data; those compounds include: nC$_{17}$ and pristane; nC$_{18}$ and phytane; nC$_{24}$ and HDCH (internal standard).

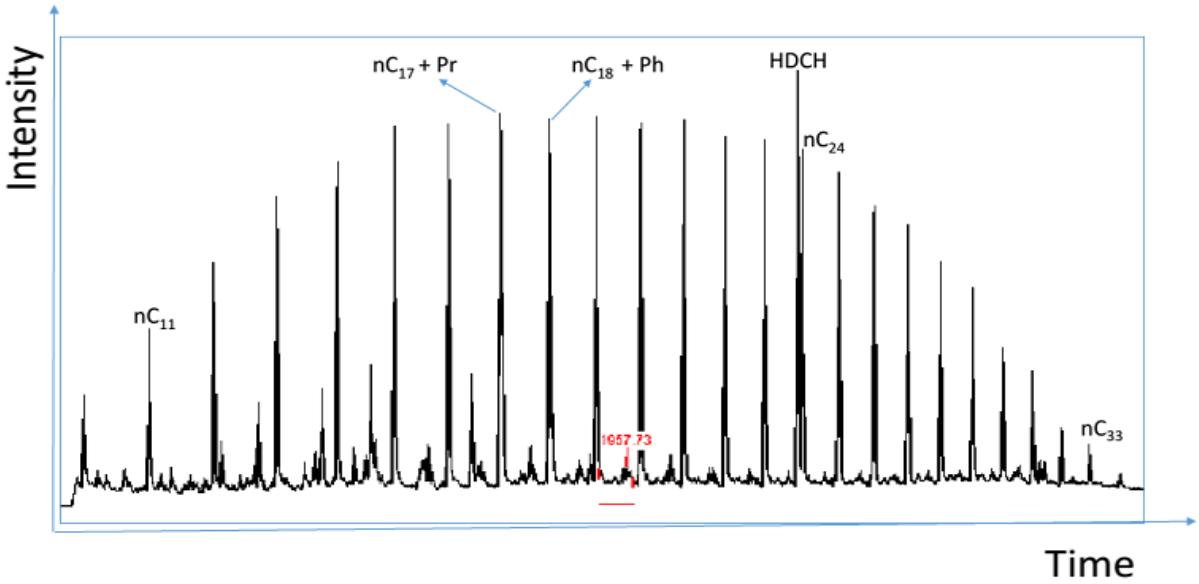

Figure 4.40: Representative GCIRMS chromatogram of an aliphatic hydrocarbon fraction (from oil OE16). Note co-elution of nC$_{17}$ and pristane; nC$_{18}$ and phytane; nC$_{24}$ and *n*-heptadecylcyclohexane (internal standard).

4.8.1 Carbon Isotopes

A total of 73 samples were analysed in carbon mode, with 21 samples selected from the Central Delta, 15 samples from the Eastern Delta, 33 samples from the Southern Delta and 4 samples from the Western Delta region. The mean $\partial^{13}C$ values of nC_{13} for the Western Delta is -26.60 (per mil), whereas the other region has values between -29.03 to -29.39 (per mil).

This trend is also seen in the other compounds with the Western Delta having a mean $\partial^{13}C$ values of -26.95 (per mil) for nC_{26}, whereas the other region has range of value between -28.80 to -29.41 (per mil) for the same compound. The Western Delta oil samples range is isotopically heavier than the other parts of the Delta (Table 4.8; Figure 4.41).

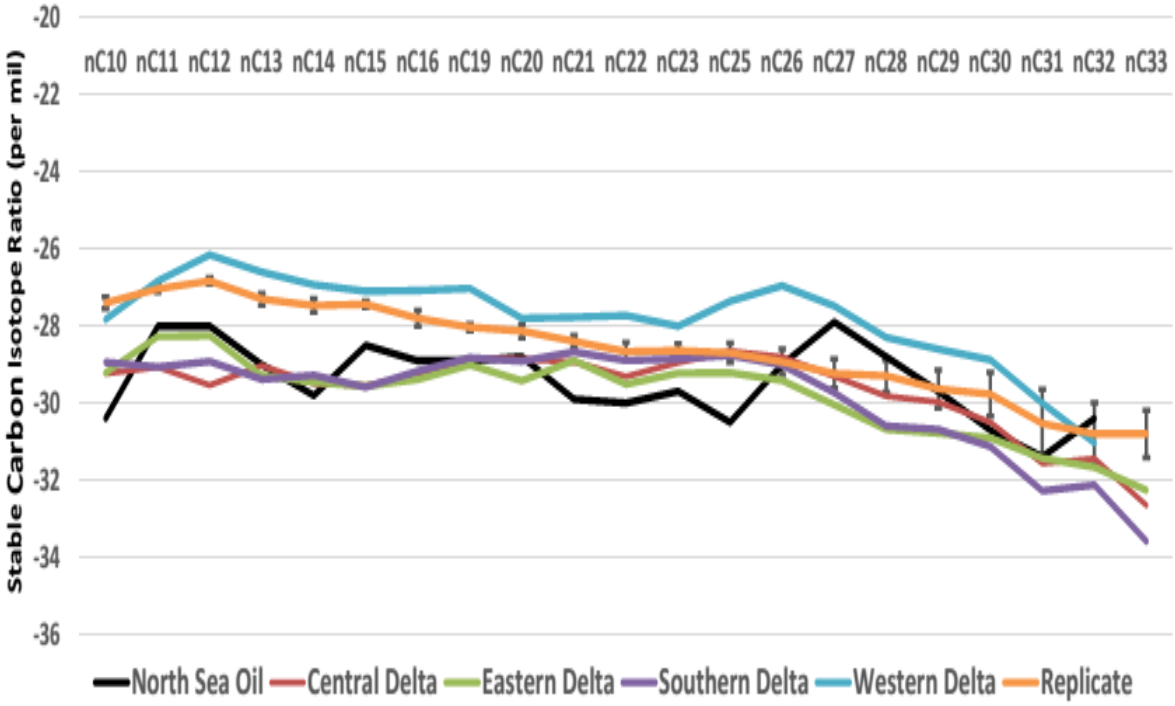

Figure 4.41: The *n*-alkane stable carbon isotope plot of mean of samples from different region in the delta

Table 4.8: Summary of *n*-alkane stable carbon isotope measurements on oil samples

	Central Delta			Eastern Delta			Western Delta			Southern Delta			Replicate			NSO-1
	Mean	SD	CV	Mean	SD	CV	Mean	SD	CV	Mean	SD	CV	Mean	SD	CV	
$_nC_{10}$	-29.24	1.51	-5.17	-29.22	1.89	-6.47	-27.83	1.34	-4.80	-28.94	2.03	-7.01	-27.40	0.26	-0.97	-30.40
$_nC_{11}$	-29.06	1.38	-4.74	-28.28	1.11	-3.94	-26.83	0.88	-3.28	-29.06	2.36	-8.13	-27.03	0.15	-0.57	-28.00
$_nC_{12}$	-29.53	1.86	-6.31	-28.25	1.12	-3.95	-26.15	1.46	-5.57	-28.92	2.18	-7.53	-26.83	0.15	-0.57	-28.00
$_nC_{13}$	-29.03	1.75	-6.03	-29.28	2.66	-9.07	-26.60	1.10	-4.14	-29.39	1.77	-6.02	-27.30	0.26	-0.97	-29.00
$_nC_{14}$	-29.49	1.59	-5.40	-29.45	2.11	-7.16	-26.93	1.65	-6.11	-29.28	1.84	-6.29	-27.47	0.31	-1.11	-29.80
$_nC_{15}$	-29.54	1.47	-4.99	-29.56	2.48	-8.40	-27.10	1.17	-4.31	-29.59	2.27	-7.66	-27.43	0.15	-0.56	-28.50
$_nC_{16}$	-29.28	1.02	-3.48	-29.38	1.83	-6.24	-27.08	1.67	-6.18	-29.18	1.86	-6.36	-27.80	0.36	-1.30	-28.90
$_nC_{19}$	-28.83	0.95	-3.30	-29.01	0.74	-2.53	-27.03	0.97	-3.61	-28.82	1.95	-6.75	-28.03	0.15	-0.54	-28.90
$_nC_{20}$	-28.86	1.25	-4.35	-29.42	1.48	-5.01	-27.80	2.53	-9.10	-28.91	1.74	-6.03	-28.13	0.31	-1.09	-28.80
$_nC_{21}$	-28.93	1.01	-3.48	-28.89	0.96	-3.31	-27.78	1.90	-6.83	-28.67	1.80	-6.27	-28.40	0.26	-0.93	-29.90
$_nC_{22}$	-29.31	1.19	-4.05	-29.51	0.98	-3.31	-27.73	1.64	-5.92	-28.89	1.71	-5.91	-28.67	0.42	-1.45	-30.00
$_nC_{23}$	-28.95	1.34	-4.62	-29.22	0.87	-2.96	-28.00	2.10	-7.50	-28.85	1.53	-5.30	-28.63	0.31	-1.07	-29.70
$_nC_{25}$	-28.66	1.25	-4.35	-29.21	1.32	-4.50	-27.35	1.22	-4.47	-28.76	1.64	-5.71	-28.70	0.44	-1.52	-30.50
$_nC_{26}$	-28.80	1.09	-3.78	-29.41	1.22	-4.15	-26.95	0.77	-2.85	-29.01	1.35	-4.64	-28.93	0.59	-2.03	-29.00
$_nC_{27}$	-29.30	1.41	-4.81	-30.04	1.50	-4.99	-27.48	0.98	-3.58	-29.73	1.38	-4.65	-29.23	0.67	-2.28	-27.90
$_nC_{28}$	-29.82	1.57	-5.28	-30.69	1.52	-4.96	-28.30	1.03	-3.64	-30.60	1.32	-4.31	-29.30	0.72	-2.46	-28.80
$_nC_{29}$	-29.97	1.27	-4.24	-30.78	1.55	-5.05	-28.60	1.06	-3.71	-30.69	1.28	-4.17	-29.63	0.85	-2.87	-29.70
$_nC_{30}$	-30.50	1.47	-4.83	-30.91	1.56	-5.05	-28.88	1.22	-4.22	-31.13	1.50	-4.81	-29.77	0.98	-3.30	-30.70
$_nC_{31}$	-31.57	2.02	-6.39	-31.44	1.64	-5.23	-30.00	2.13	-7.11	-32.28	1.62	-5.03	-30.53	1.53	-5.01	-31.40
$_nC_{32}$	-31.44	2.19	-6.96	-31.67	1.44	-4.55	-31.03	0.98	-3.16	-32.13	1.18	-3.66	-30.80	1.39	-4.50	-30.40
$_nC_{33}$	-32.66	2.01	-6.14	-32.26	1.43	-4.45				-33.59	1.52	-4.52	-30.80	1.06	-3.44	

4.8.2 Hydrogen Isotopes

A total of 20 samples was run in the carbon mode with 5 samples selected from the Central Delta; 7 samples selected from the Eastern Delta; 5 samples selected from the Southern Delta and 3 samples selected from the Western Delta region. The mean ∂D values of nC$_{13}$ for the Western Delta is -130 (per mil), whereas the other region has values between -141 to -142 (per mil).

This trend is also seen in most of the other nalkanes compounds with the Western Delta having a mean ∂D values of -124 (per mil) for nC$_{19}$, whereas the other region has range of value between -129 to -135 (per mil) for the same compound. The Western Delta oil samples range is isotopically heavier than the other parts of the Delta (Table 4.9; Figure 4.42).

It should also be pointed out that nC$_{14}$ has lighter values than all other carbon numbers (-135 to -160 per mil) and there is a sharp increase in the isotopic value of the Central and Western Delta oil around nC$_{26}$ from around -125 in nC$_{25}$ to -111 (Figure 4.42), this sharp increase in isotopic value around nC$_{26}$ is not seen in the other two regions (Figure 4.42). There is also a sharp reduction in value around the nC$_{32}$ in the Eastern (-144) and the Western (-152) Delta oil samples. The oil samples generally show same trend in their isotopic value around the different regions of the delta (Figure 4.42).

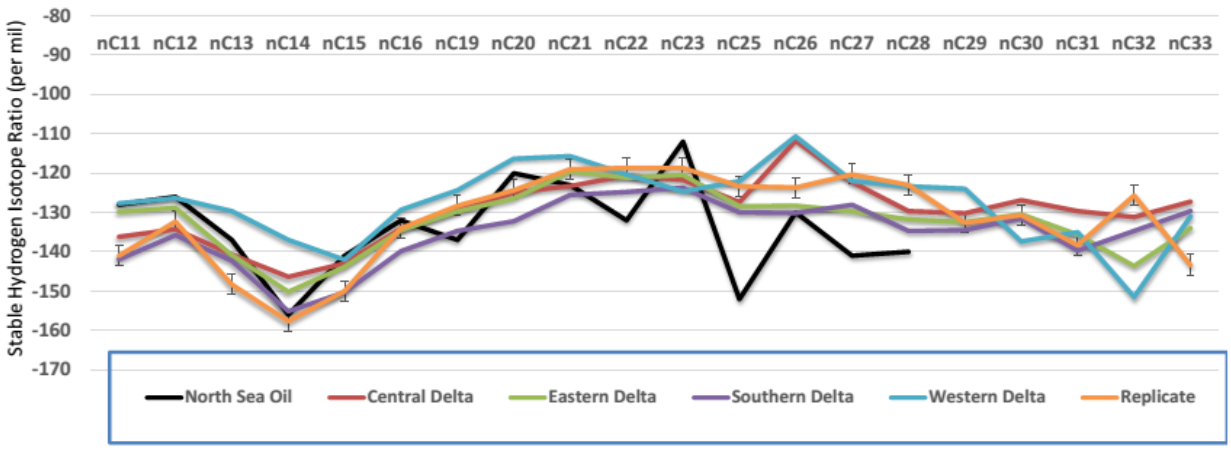

Figure 4.42: The *n*-alkane stable hydrogen isotope plot of mean of samples from different region in the delta

Table 4.9: Summary of *n*-alkane stable hydrogen isotope measurements on oil samples

	Central Delta			Eastern Delta			Western Delta			Southern Delta			Replicate			NSO-1
	Mean	SD	CV	Mean	SD	CV	Mean	SD	CV	Mean	SD	CV	Mean	SD	CV	
$^{n}C_{11}$	-136	8.96	-6.58	-130	15.58	-12.00	-128	11.85	-9.28	-142	9.47	-6.67	-141	2.00	-1.42	-128
$^{n}C_{12}$	-134	14.24	-10.61	-129	8.76	-6.80	-126	6.43	-5.09	-136	8.41	-6.20	-132	8.50	-6.43	-126
$^{n}C_{13}$	-141	15.40	-10.95	-141	13.76	-9.77	-130	8.74	-6.74	-142	13.92	-9.78	-148	3.79	-2.55	-137
$^{n}C_{14}$	-146	12.06	-8.24	-150	10.53	-7.01	-137	6.24	-4.56	-155	11.54	-7.44	-158	1.53	-0.97	-156
$^{n}C_{15}$	-143	22.93	-16.04	-144	12.06	-8.38	-142	12.49	-8.80	-150	10.03	-6.67	-150	11.36	-7.57	-141
$^{n}C_{16}$	-134	7.89	-5.88	-135	5.50	-4.09	-129	8.62	-6.67	-140	8.87	-6.35	-134	2.65	-1.97	-132
$^{n}C_{19}$	-129	5.84	-4.51	-130	6.68	-5.15	-124	5.51	-4.43	-135	10.28	-7.64	-128	1.53	-1.19	-137
$^{n}C_{20}$	-125	4.74	-3.79	-126	6.55	-5.18	-116	17.67	-15.19	-132	7.84	-5.93	-124	3.21	-2.59	-120
$^{n}C_{21}$	-123	7.14	-5.79	-120	9.98	-8.35	-116	6.66	-5.76	-126	7.23	-5.76	-119	2.65	-2.22	-123
$^{n}C_{22}$	-121	4.16	-3.45	-121	7.60	-6.28	-120	2.31	-1.92	-125	7.65	-6.13	-119	3.21	-2.71	-132
$^{n}C_{23}$	-122	5.92	-4.87	-120	9.78	-8.12	-125	5.69	-4.56	-124	3.24	-2.62	-119	2.31	-1.95	-112
$^{n}C_{25}$	-127	5.93	-4.66	-128	12.80	-9.97	-122	3.46	-2.84	-130	10.12	-7.78	-123	4.93	-4.00	-152
$^{n}C_{26}$	-112	26.44	-23.66	-128	12.93	-10.08	-111	21.39	-19.32	-130	7.48	-5.75	-124	7.23	-5.85	-130
$^{n}C_{27}$	-122	6.77	-5.54	-130	12.96	-9.99	-122	9.85	-8.07	-128	5.70	-4.45	-120	5.77	-4.80	-141
$^{n}C_{28}$	-130	4.46	-3.44	-132	11.09	-8.42	-123	0.58	-0.47	-135	11.76	-8.74	-123	5.00	-4.07	-140
$^{n}C_{29}$	-130	5.26	-4.04	-132	16.28	-12.29	-124	4.58	-3.70	-134	12.07	-8.98	-133	10.02	-7.55	
$^{n}C_{30}$	-127	6.60	-5.20	-130	12.34	-9.46	-137	9.87	-7.18	-131	15.28	-11.62	-131	10.12	-7.74	
$^{n}C_{31}$	-130	8.81	-6.79	-136	8.33	-6.14	-135	7.81	-5.79	-140	4.26	-3.05	-138	7.23	-5.23	
$^{n}C_{32}$	-131	25.33	-19.31	-144	11.44	-7.96	-152	6.36	-4.20	-135	7.38	-5.48	-126	2.08	-1.66	
$^{n}C_{33}$	-127	2.06	-1.62	-134	9.54	-7.12				-130	13.32	-10.27	-143	0.58	-0.40	

4.9 OIL STATISTICAL ANALYSIS RESULTS

Analysis of large data sets is usually challenging because of the large number of variables/parameters to be considered. In order to make meaningful deductions from any large data set, the data need to be compressed into a manageable form and statistical Principal Component Analysis (PCA) is one commonly used method for doing this (Kramer 1998; Peters *et al*., 2005). Processing of the data to be used for PCA is usually very important since, for example, some parameters need to be removed because they do not show any variability in the data set but only serve as background noise (Christie *et al*., 1984; Christie 1992; Gurgey, 2003; He *et al*., 2012).

The thesis generally investigates the compositional variations in several groups of biomarker and non-biomarker hydrocarbon compound classes in the oil samples, whose signatures reflect their histories which include, source, migration distance/route/contamination, maturity, biodegradation, fractionation, water washing, temperature of expulsion etc. effects. Recognising these effects is important to one of the main aims of the present research, which is unravelling the controlling factors of hydrocarbon mixing in the Niger Delta.

The geochemical parameters are divided into compound groups based mainly on thermal maturity indicators and biomarker types and the groups considered are; *n*-alkanes/isoprenoids, light hydrocarbons, diamondoid hydrocarbons, aromatic hydrocarbons, steranes and hopanes biomarkers.

4.9.1 Principal component analysis.

Principal component analysis (PCA) is a routine method used by statisticians to help transform complex data sets to aid easy visualisation of data similarities and differences and this method is of growing importance in many other fields including petroleum geochemistry (Telnaes & Dahl 1985; Peters *et al*., 1986; Zumberge 1987; Zumberge & Ramos 1996; Peters *et al*., 2000; Eneogwe & Ekundayo 2003; Gurgey 2003; He *et al*.,

2011). Groupings are usually based on scores plots and interpretation is possible from their loading plots, which describe their contribution and/or variability in the scores plot.

The statistical analysis was performed with the p:IGI-3.5 PCA software and several processing steps were taken to get a dataset that was not subject to analytical bias, including the following:

1. Zero validity was set to false since none of the calculated parameters are supposed to give a value of zero. Therefore, zero was rejected as a valid result.
2. The Cell Set command was avoided as it could bring errors into the data set. This command is used to set cells that were not calculated to: average, minimum or manually set the value. Some samples were removed before this stage to avoid setting values for parameters that were not calculated due to the absence of some peaks because of biodegradation.
3. The data were normalised to range from 0-100 to help give the parameters equal weight.
4. The data were auto scaled to help give each variable equal weight between parameters.
5. The mean was set to be the centre as median and range are not good measures of centre of tendency.

The loadings plot (PC1 vs PC2) of all the parameters was then considered and parameters that plotted close to the origin were rejected as they do not show any variation but serve as background noise in the data set and therefore reduces the percentage variance of each PC. The percentage variation of each PC was increased significantly after some parameters were rejected because the parameters left shows more variability in the data set. This work only considers PC1 and PC2 because they contain most of the variability in the data set

4.9.2 Principal component analyses of *n*-alkane/isoprenoid parameters.

A total of 86 samples and 7 parameters (Table 4.11) were used for the analysis and 5 parameters were rejected which includes: CPI-2, saturate %, aromatics %, NSO % and asphaltene %. A total of 94 samples were rejected because some of the peaks used in calculating some of the parameters were either absent or unresolvable, mainly due to biodegradation.

Table 4.10: Eigenvalues and percent variance of *n*-alkanes and isoprenoids for PC1-PC5

	PC1	**PC2**	**PC3**	**PC4**	**PC5**
Eigenvalue	5.08	0.82	0.73	0.25	0.11
Percent Variance	72.61	11.64	10.44	3.62	1.64

Table 4.11: Parameters used for the principal component analysis of *n*-alkanes and isoprenoids

Parameters	**Interpretation**	**Reference**
Pr/Ph	source, environment, maturity	Peters & Moldowan, 1993
norPr/Pr	source, environment	Peters & Moldowan, 1993
Pr/nC_{17}	source, maturity, biodegradation	Peters & Moldowan, 1993
Ph/nC_{18}	source, maturity, biodegradation	Peters & Moldowan, 1993
nC_{17}/nC_{27}	source, maturity	Peters & Moldowan, 1993
CPI-1	source, maturity	Philippi, 1965
CPI-3	source, maturity	Scanlan & Smith, 1970

Pr/Ph= pristane/phytane, norPr/Pr= norpristane/pristane, Pr/nC_{17}= pristane/*n*-heptadecane, Ph/nC_{18}= phytane/*n*-octadecane, nC_{17}/nC_{27}= *n*-heptadecane/*n*-heptacosane, CPI-1= C_{28}-C_{30} odd/even predominance, CPI-3= C_{27}-C_{31} odd/even predominance.

PC1 shows a percentage variance of 73 and an eigenvalue of 5.08, while PC2 shows a percentage variance of 12 and an eigenvalue of 0.82 (Table 4.10).

Some parameters were controlled by the same factors as shown on the loading plot (Fig 4.43). Those parameters that are related include; **Group 1**: Pr/nC_{17}, Ph/nC_{18} **Group 2:** CPI-1, CPI-3, nC_{17}/nC_{27}. Some parameters do not show any relationship with other parameters and those parameters include Pr/Ph and norpr/Pr. The scores plot (Figure 4.44) shows a

possibility of three broad groups and the North Sea oil (NSO-1) plots in the same area with group C while the replicates plots close to each other in group B.

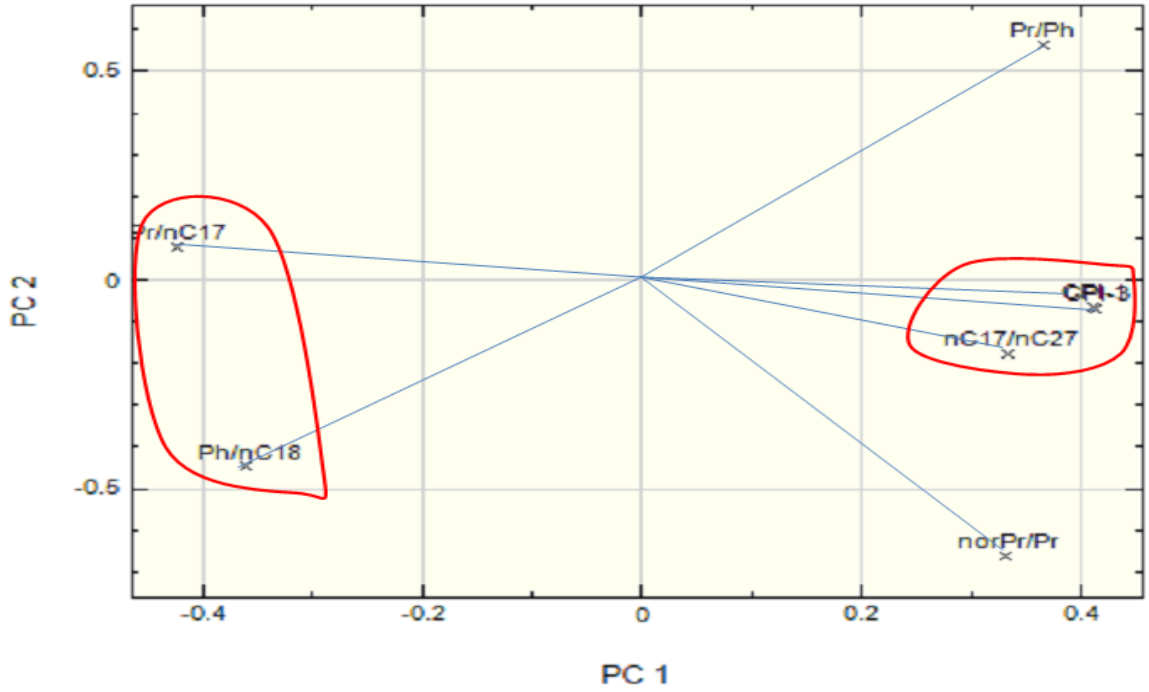

Figure 4.43: Loadings plot of first (73% of the variance) and second (12% of the variance) principal components of *n*-alkane/isoprenoid parameters showing relationships between parameters used for the analysis

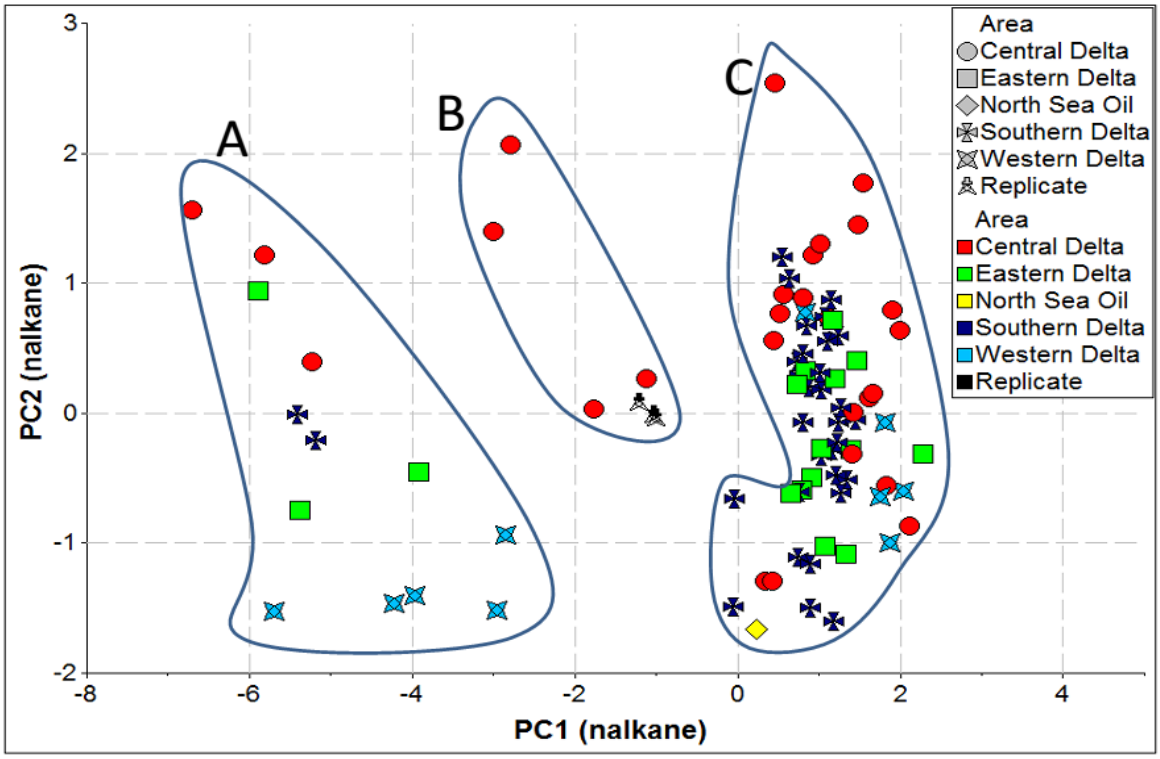

Figure 4.44: Scores plot of first (73% of the variance) and second (12% of the variance) principal components of *n*-alkane/isoprenoid parameters showing three possible grouping

4.9.3 Principal component analyses of light hydrocarbon parameters

A total of 58 samples and 15 parameters (Table 4.13) were used for the analysis and 10 parameters were rejected which includes: P3/N2, 22/24dmP, 11/1c3dmP, P2/3mH, e/11dmcP, dmc/dmP, Bz/cH, mcH/cH, nC$_7$/nC$_6$ and Tol/Bz. A total of 4 samples were rejected because some of the peaks used in calculating some of the parameters were either absent or unresolvable, mainly due to biodegradation and evaporation.

Table 4.12: Eigenvalues and percent variance of light hydrocarbon parameters for PC1-PC5

	PC1	**PC2**	**PC3**	**PC4**	**PC5**
Eigenvalue	6.43	5.14	1.55	0.72	0.50
Percent Variance	42.87	34.24	10.35	4.80	3.30

Table 4.13: Parameters used for the light hydrocarbon principal components analysis

Parameters	**Interpretation**	**References**
HeptRat	maturity	Thompson 1979; 1983
P1/hept	correlation, maturity, evaporative fractionation	Mango 1997; ten Haven 1996; Thompson 1979; Philippi 1975
IsohepRat	maturity	Thompson 1979; 1983
P2/Hept	correlation, maturity	Mango 1997; ten Haven 1996; Thompson 1979; Philippi 1975
N15/N16	correlation	Mango 1997; ten Haven 1996
cH/bcC$_7$	correlation	Mango 1997; ten Haven 1996
cP/bcC$_7$	correlation	Mango 1997; ten Haven 1996
b/bcC$_7$	correlation	Mango 1997; ten Haven 1996
mcP/nC$_6$	source, water washing, biodegradation, maturity	Mango 1997
mcH/nC$_7$	source, water washing, biodegradation, maturity	Mango 1997
dmcP/mH	water washing, correlation, maturity	Mango 1997
Tol/mcH	water washing, correlation, maturity	Mango 1997
C$_7$Paraf	correlation	P:igi geochemical manual
C$_7$Naph	correlation	P:igi geochemical manual
C$_7$Arom	correlation	P:igi geochemical manual

HeptRat= *n*-heptane/naphthenic heptanes, P1/hept= *n*-heptane/total C$_7$ hydrocarbon, IsohepRat= 2-+3-methylhexane/some dimethylcyclopentane, P2/Hept= isoheptane/total C$_7$ hydrocarbons, N15/N16= ratio of P1 daughters, cH/bcC$_7$= cyclohexyl contaning C$_7$/total branch+cyclic C7 hydrocarbons, cP/bcC$_7$= cyclopentyl contaning heptanes/total branch+cyclic C$_7$ hydrocarbons, b/bcC$_7$= branch C$_7$/ total branc + cyclic C$_7$ hydrocarbons, mcP/nC$_6$= methylcyclopentane/*n*-hexane, mcH/nC$_7$= methylcyclohexane/*n*-heptane, dmcP/mH= 1trans3-dimethylcyclopentane/methylhexane, Tol/mcH= toluene/methycyclohexane, C$_7$Paraf= C$_7$ paraffins/total C$_7$ hydrocarbons, C$_7$Naph= C$_7$ naphthenes/total C$_7$ hydrocarbons, C$_7$Arom= C$_7$ aromatics/total C$_7$ hydrocarbons.

PC1 shows a percentage variance of 43 and eigenvalue of 6.43 while, PC2 shows percentage variance of 34 and eigenvalue of 5.14 (Table 4.12).

Some parameters were controlled by the same factors shown on the loadings plot (Figure 4.45). Those parameters that are related include: **Group 1:** mcP/nC_6, mcH/*n*C_7, dmcP/mH, **Group 2**: C_7Naph, cP/bcC_7, N15/N16, **Group 3**:HeptRat, P1/hept, IsohepRat, C_7Paraf, P2/Hept, b/bcC_7, **Group 4:** cH/bcC_7, Tol/mcH, C_7Arom. The scores plot (Figure 4.46) shows a possibility of three broad groups and the North Sea oil (NSO-1) was also used as replicate.

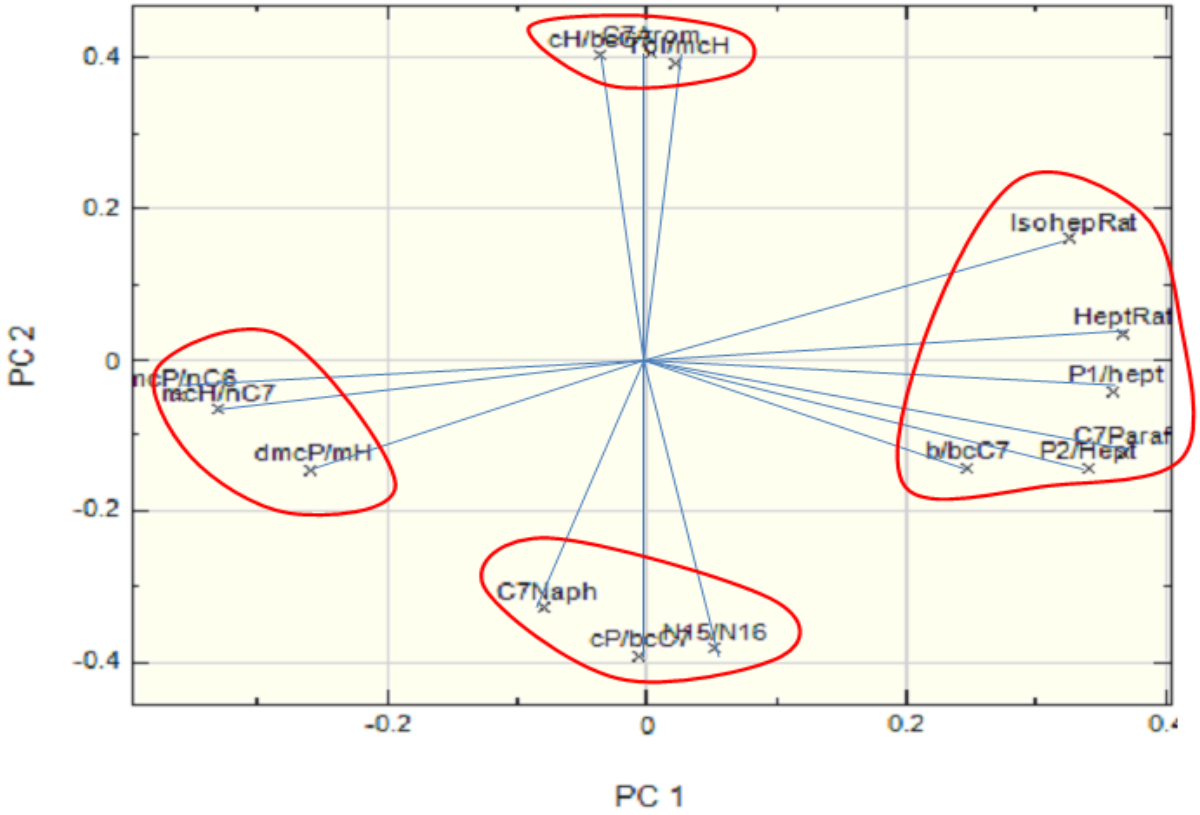

Figure 4.45: Loadings plot of first (43% variance) and second (34% variance) principal components of light hydrocarbon parameters showing relationships between parameters used for the analysis

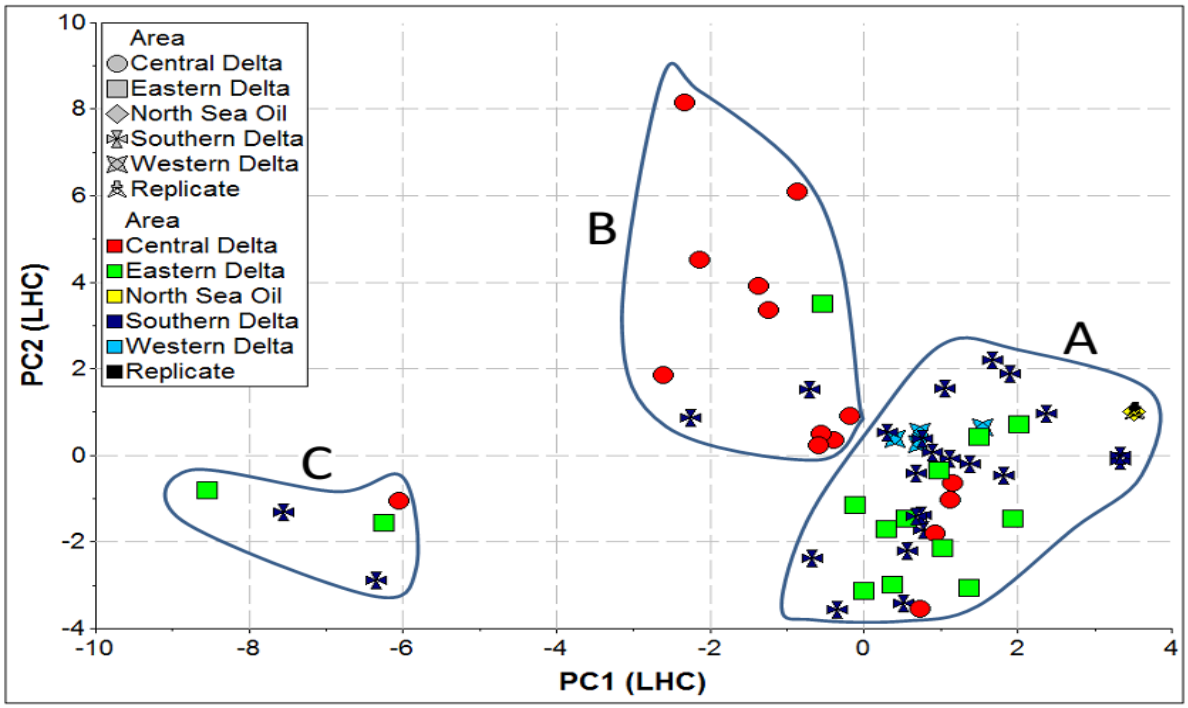

Figure 4.46: Scores plot of first (43% variance) and second (34% variance) principal components of light hydrocarbon parameters showing 3 possible grouping

4.9.4 Principal component analyses of diamondoid hydrocarbon parameters

A total of 180 samples and 10 parameters (Table 5.15) were used for the analysis and 8 parameters were rejected which includes: MAI, MDI, EAI-1, EAI-2, DMAI-1, DMAI-2, TMAI-1, and TMA1-2. Although the samples had been subjected to different range of biodegradation, none of them were rejected because the diamondoids were present in high concentrations and are also resistant to biodegradation.

Table 4.14: Eigenvalues and percent variance of diamondoid PC1-PC5

	PC 1	PC 2	PC 3	PC 4	PC 5
Eigenvalue	6.23	1.39	0.93	0.79	0.28
Percent Variance	62.31	13.85	9.27	7.93	2.82

Table 4.15: Parameters used for the principal components analysis of diamondoids

Parameters	Interpretation	References
MA/AD	biodegradation	Grice et al 2000
MD/D	biodegradation	Grice et al 2000
MA/EA	source, correlation	Wang et al., 2006; Yang et al 2006
MA/DMA	correlation	de Araujo et al., 2012
MA/TMA	correlation	de Araujo et al., 2012
MA/TeMA	correlation	de Araujo et al., 2012
DMA/TMA	correlation	de Araujo et al., 2012
TA/TeMA	correlation	de Araujo et al., 2012
TMA/TMA	correlation	Wang et al 2006; de Araujo et al., 2012
TeMA/TeMA	correlation	de Araujo et al., 2012

MA/AD= 1-+2-methyladamntane/adamantane, MD/D= 1-+3-+4-methyldiamantane/diamantane, MA/EA= 1-methyldiamantane/2-ethyldiamantane, MA/DMA= 1-methyladamantane/2-ethyladamantane, MA/DMA= 1-methyladamantane/2-ethyladamantane, MA/TMA= 1-methyladamantane/1,3,4-trimethyladamantane, MA/TeMA= 1-methyladamantane/1,3,4-tetramethyladamantane, DMA/TMA=1,4-dimethyladamantane/1,3,4-trimethyladamantane, DMA/TMA= 1,4-dimethyladamantane/1,3,4-trimethyladamantane, TA/TeMA= 1,3,5-trimethyladamantane/1,2,5,7-trimethyladamnatane, TMA/TMA= 1,3,5,7-trimethyladamantane/1,3,6-tetramethyladamantane, TeMA/TeMA= 1,3,5,7-tetramethyladamantane/1,2,5,7-tetramethyladamantane.

PC1 shows a percentage variance of 62 and eigenvalue of 6.23 while, PC2 shows a percentage variance of 14 and eigenvalue of 1.39 (Table 5.14).

Some parameters were controlled by the same factors as shown on the loadings plot (Figure 4.47). Those parameters that are related include; **Group 1:** MA/EA, MA/DMA, MA/DMA, MA/TMA, MA/TeMA, DMA/TMA, DMA/TMA, TA/TeMA, TMA/TMA . Some parameters did not show any relationship with other parameters and those parameters include: MD/D, MA/AD and TeMA/TeMA. The scores plot (Figure 4.48) shows the possibility of one major group and two sub groups; the North Sea oil (NSO-1) and the replicates plots in the same area with group A, which has about 173 samples in the family.

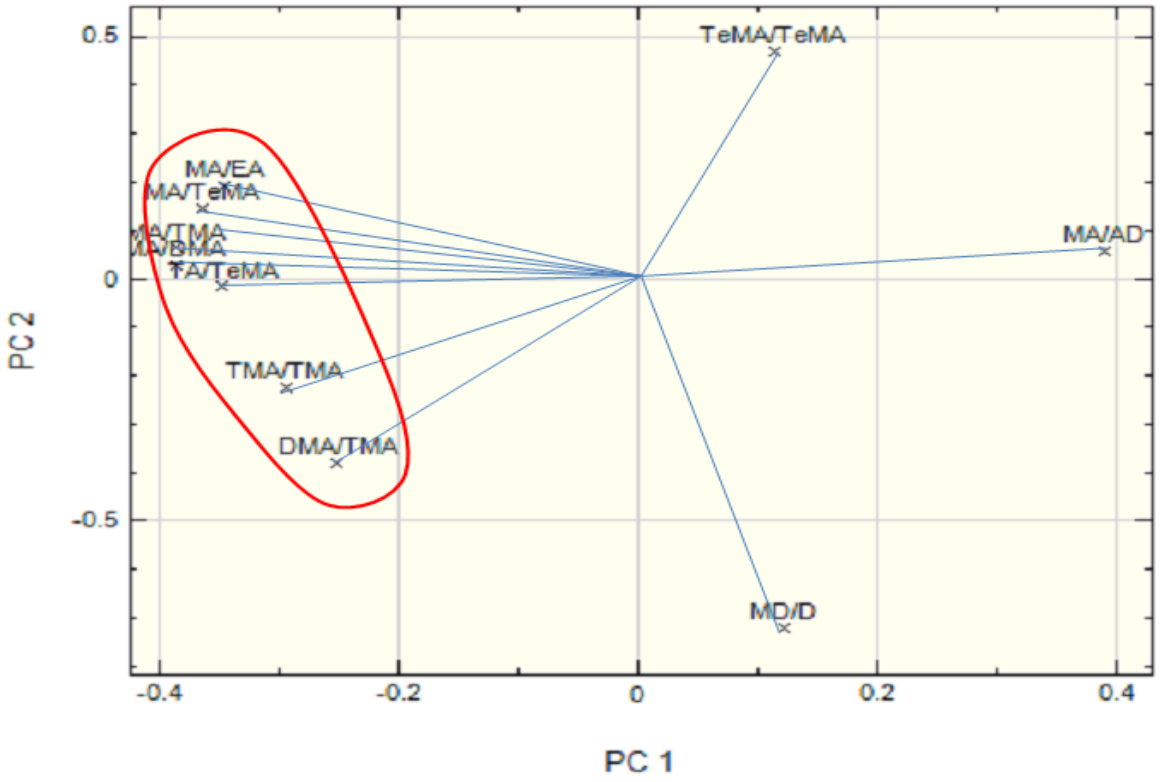

Figure 4.47: Loadings plot of first (62% of the variance) and second (14% of the variance) principal components of diamondoid parameters showing relationships between parameters used for the analysis.

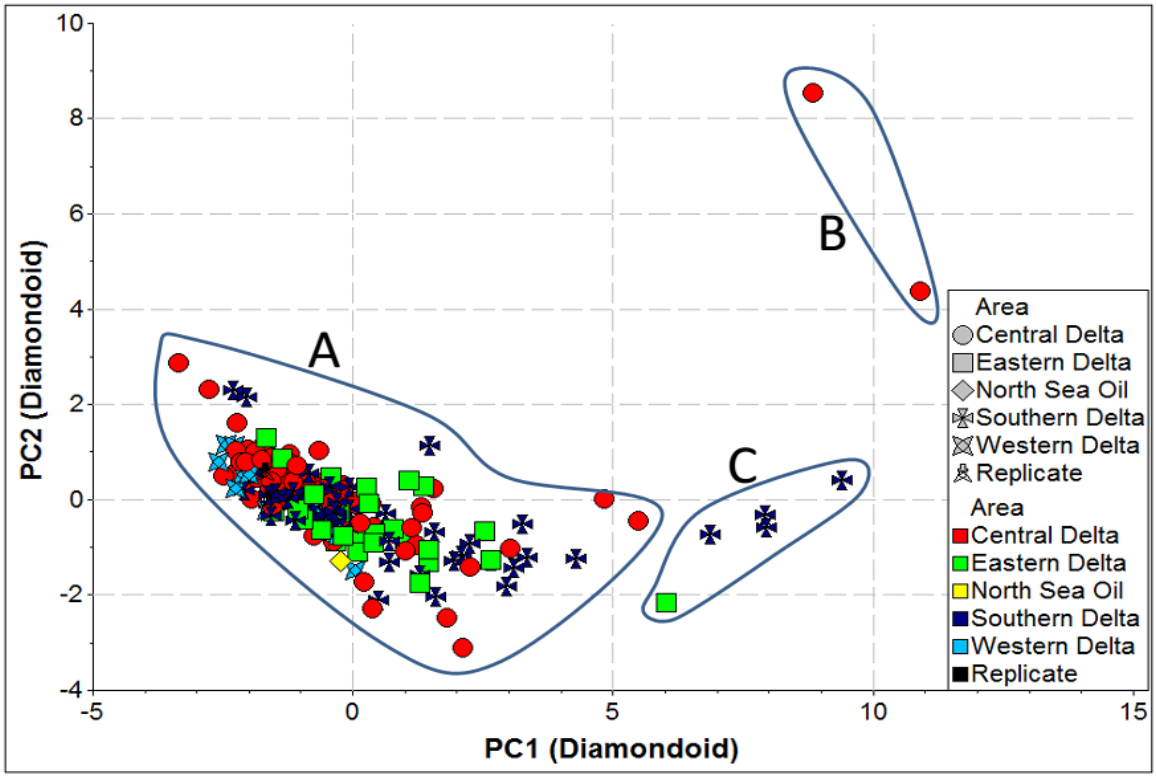

Figure 4.48: Scores plot of first (62% of the variance) and second (14% of the variance) principal components of diamondoid parameters showing three possible groupings.

4.9.5 Principal component analyses of aromatic hydrocarbon parameters

A total of 156 samples and 6 parameters (Table 4.17) were used for the analysis and 5 parameters were rejected which includes: MNR, DMN, MPR, MAS (21+22/total) and MAS29(S/S+R). A total of 24 samples were rejected because some of the peaks used in calculating some of the parameters were either absent or unresolvable, mainly due to biodegradation.

Table 4.16: Eigenvalues and percent variances of aromatic hydrocarbons for PC1-PC5

	PC1	PC2	PC3	PC4	PC5
Eigenvalue	3.77	1.92	0.28	0.04	0.00
Percent Variance	62.70	32.01	4.58	0.60	0.07

Table 4.17: Parameters used for the aromatic hydrocarbon principal components analysis

Parameters	Interpretation	References
MP(3+2/9+1)	maturity	p:IGI geochemical manual
MPI-1	maturity	Radke & Welte 1983; Radke et al; 1986
MPI-2	maturity	Radke et al; 1986
Rc(Ro<1.35)	maturity	Radke & Welte 1983
TAS 27	source	Peters & Moldowan 1993
TAS 28	source	Peters & Moldowan 1993

MP(3+2/9+1)= 3-+2-MP/9-+1-MP, MPI-1= 1.5(3-+2-MP)/P+9-+1-MP, MPI-2= 3*2-MP/P+9-+1-MP
Rc(Ro<1.35)= (0.6*MPI-1) + 0.4, TAS 27= C_{27} triaromatic/ C_{26-28} triaromatics, TAS 28= C_{28} triaromatic/ C_{26-28} triaromatics

PC1 shows a percentage variance of 63 and eigenvalue of 3.77, while PC2 shows a percentage variance of 32 and eigenvalue of 1.97 (Table 4.16).

Some parameters were controlled by the same factors as shown on the loadings plot (Figure 4.49). Those parameters that are related include; **Group 1:** MP(3+2/9+1), MPI-1, MPI-2 and Rc(Ro<1.35). The scores plot (Figure 4.50) shows a possibility of one main group with a possibility of a sub group inside the main group. The North Sea oil (NSO-1) plots outside the main group area but the replicates plot within the main group area.

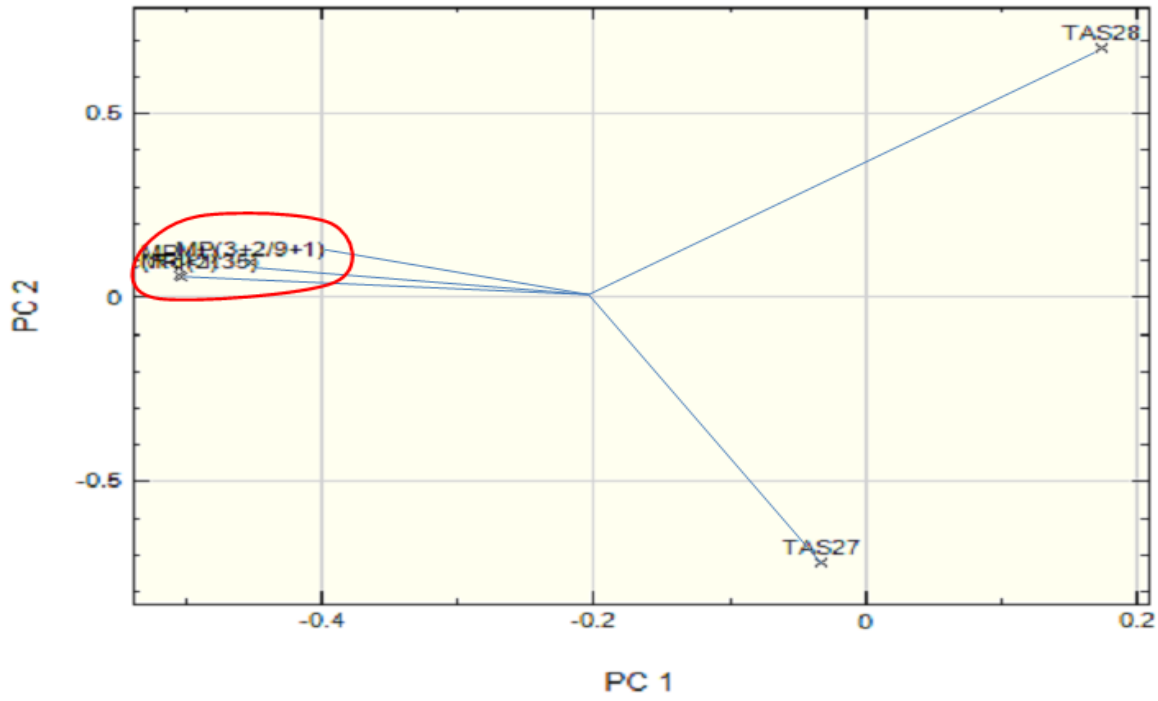

Figure 4.49: Loadings plot of first (63% variance) and second (32% variance) principal components of the aromatic hydrocarbon parameters showing the relationship between parameters used for the analysis

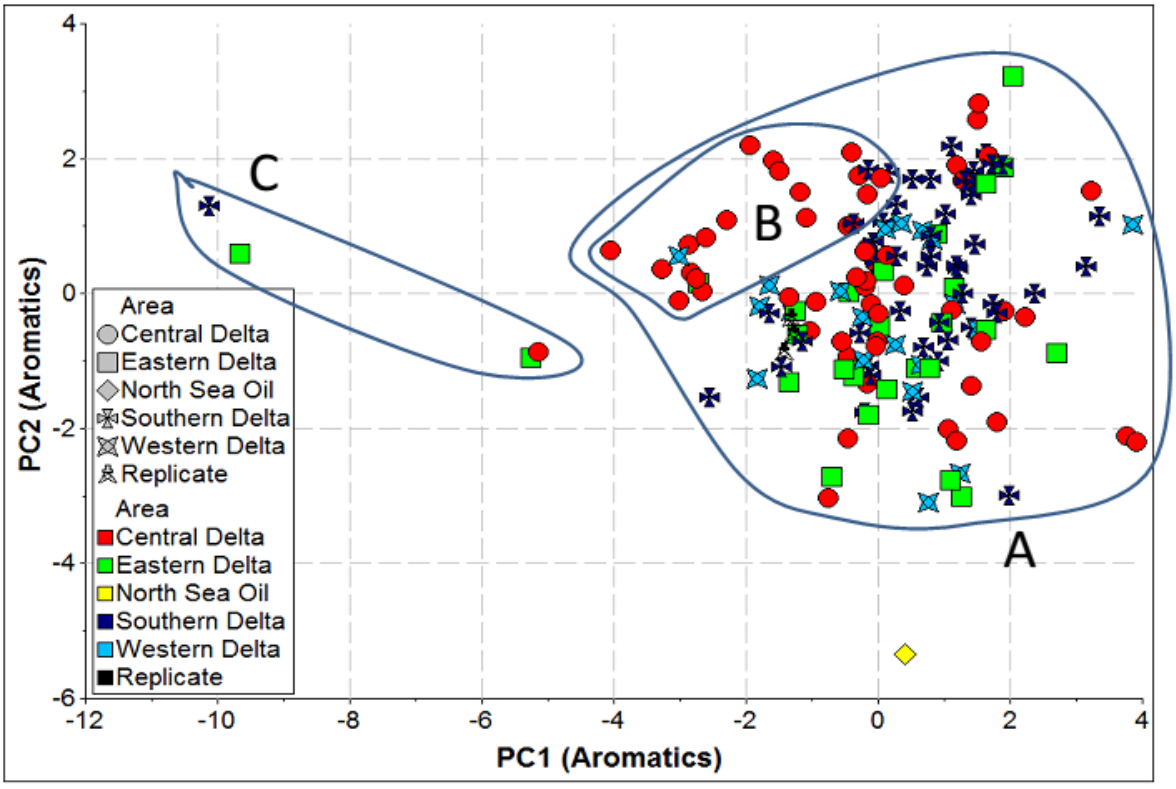

Figure 4.50: Scores plot of the first (63% of the variance) and second (32% of the variance) principal components of aromatic hydrocarbon parameters showing two possible grouping and two sub groups within group A.

4.9.6 Principal component analyses of sterane biomarker parameters

A total of 178 samples and 8 parameters (Table 4.19) were used for the analysis and 4 parameters were rejected which includes: pregnanes, DiaSt, St29(S/S+R), St29(I/I+R). A condensate sample (OE180) was not included in this analysis as it did not contain biomarkers.

Table 4.18: Eigenvalues and percent variance of sterane biomarker parameters for PC1-PC5

	PC1	PC2	PC3	PC4	PC5
Eigenvalue	4.05	1.49	1.41	0.54	0.43
Percent Variance	50.38	18.58	17.48	6.68	5.33

Table 4.19: Parameters used for the principal components analysis of sterane biomarkers

Parameters	Interpretation	References
27St217	Source, environment	Huang & Meinschein 1979; Peters & Moldowan 1993
28St217	Source, environment	Huang & Meinschein 1979; Peters & Moldowan 1993
29St217	Source, environment	Huang & Meinschein 1979; Peters & Moldowan 1993
30St217	Source, environment	Moldowan et al., 1990
St27Iso	Source, environment	Huang & Meinschein 1979; Peters & Moldowan 1993
St28Iso	Source, environment	Huang & Meinschein 1979; Peters & Moldowan 1993
St29Iso	Source, environment	Huang & Meinschein 1979; Peters & Moldowan 1993
St30Iso	Source, environment	Moldowan et al., 1990

27St217= C_{27}ααα 20R/C_{27}-C_{29}ααα 20R (*m/z* 217), 28St217= C_{28}ααα 20R/C_{27}-C_{29}ααα 20R (*m/z* 217), 29St217= C_{29}ααα 20R/C_{27}-C_{29}ααα 20R (*m/z* 217), 30St217= C_{30}ααα 20R/C_{27}-C_{30}ααα 20R (*m/z* 217), St27Iso= C_{27}αββ 20 (S+R)/C_{27}-C_{29}αββ 20(S+R) (*m/z* 218), St28Iso= C_{28}αββ 20(S+R)/C_{27}-C_{29}αββ 20(S+R) (*m/z* 218), St29Iso= C_{29}αββ 20(S+R)/C_{27}-C_{29} αββ 20(S+R) (*m/z* 218), St30Iso= C_{30}αββ 20S+R/C_{27}-C_{30}αββ 20 (S+R) (*m/z* 218).

PC1 shows a percentage variance of 50 and eigenvalue of 4.05 while, PC2 shows a percentage variance of 19 and eigenvalue of 1.49 (Table 4.18).

Some parameters were controlled by the same factors as shown on the loadings plot (Figure4.51). Those parameters that are related include; **Group 1**: 27St217, St27iso, **Group 2**: 28St217, St28iso, **Group 3**: 29St217, St29iso, **Group 4**: 30 St217, St30iso. The

scores plot (Figure 4.52) shows a possibility of one main group and three sub groups within the major group. The North Sea oil (NSO-1) plots away from the other samples but the replicates plot within the main group area.

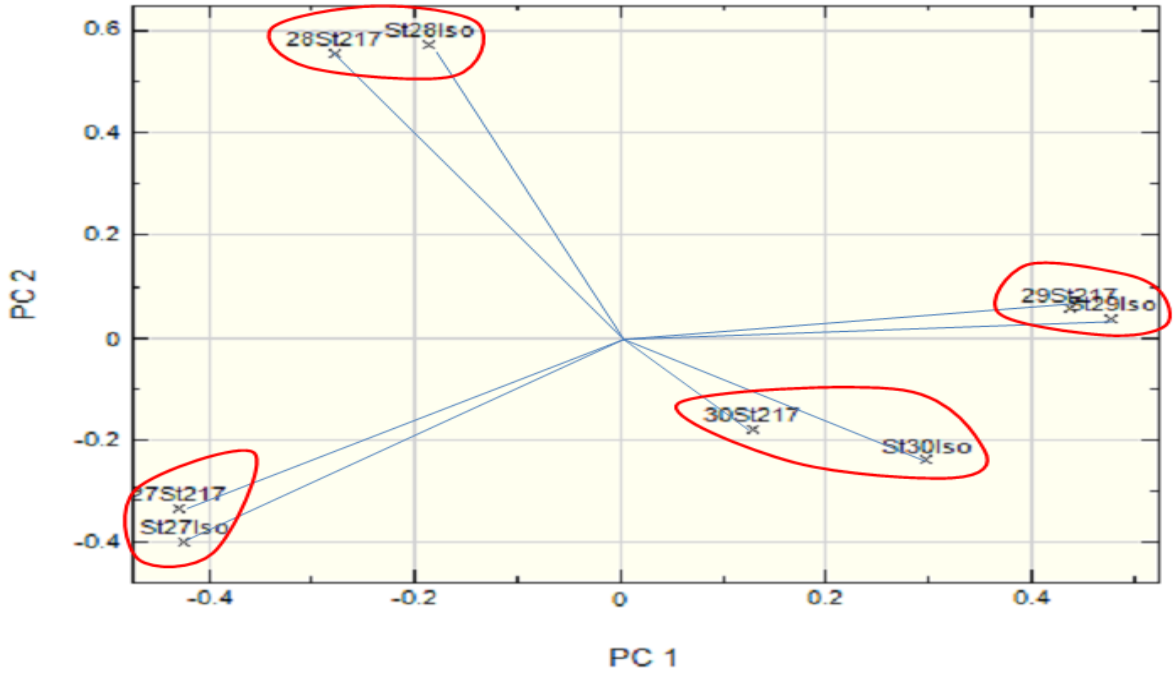

Figure 4.51: Loadings plot of first (50% of the variance) and second (19% of the variance) principal components of sterane hydrocarbon parameters showing relationships between parameters used for the analysis.

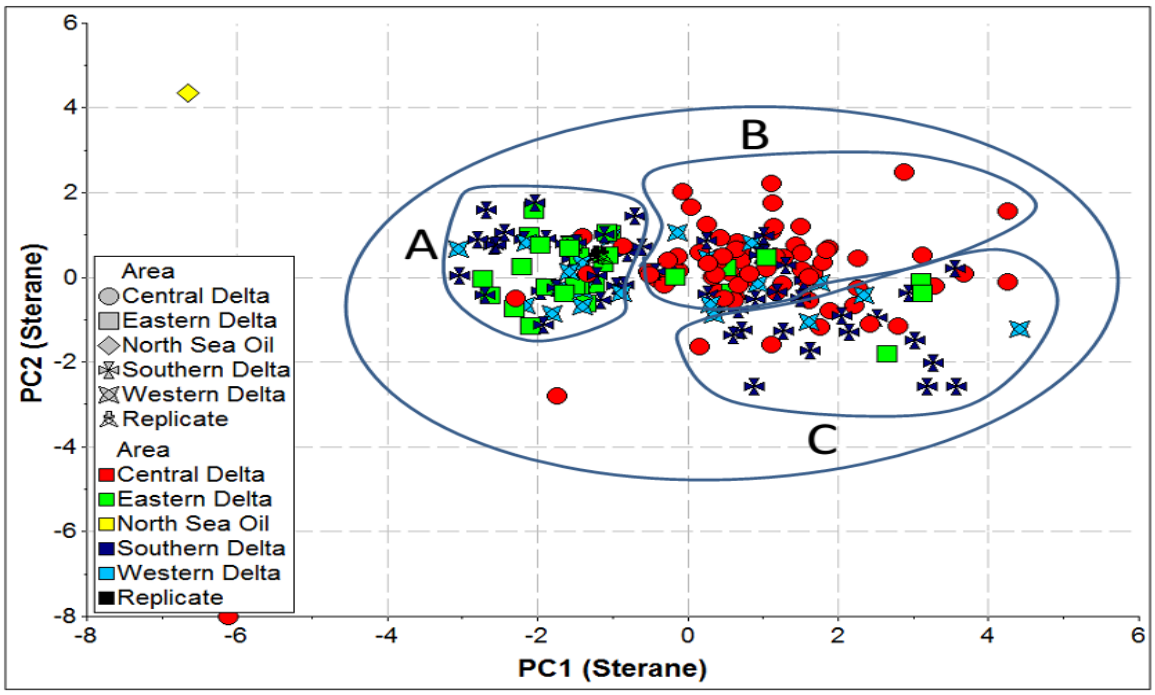

Figure 4.52: Scores plot of first (50% of the variance) and second (19% of the variance) principal components of sterane hydrocarbon parameters showing three sub groups within a large group.

4.9.7 Principal component analyses of hopane biomarker parameters

A total of 179 samples and 8 parameters (Table 4.21) were used for the analysis and 11 parameters were rejected which includes: t20/t21, t26/t25, t20-t26/T30H, Tri/Tetra, 31Hops, Hop/Mor, Dia/NorM, 29Ts/29Tm, Hop30/29, HomoHop, Hop34/35. A condensate sample (OE180) was not included in this analysis as it did not contain biomarkers.

Table 4.20: Eigenvalues and percent variance of hopane biomarkers for PC1-PC5

	PC1	PC2	PC3	PC4	PC5
Eigenvalue	5.85	0.96	0.58	0.38	0.14
Percent Variance	72.90	11.98	7.26	4.72	1.81

Table 4.21: Parameters used for the principal components analysis of hopane biomarkers

Parameters	Interpretation	References
t_{19}/t_{23}	source environment	Zumberge, 1987; Rooney et al., 1998; Peters et al., 2005; He et al., 2012
t_{23}/T30H	source, environment	Seifert & Moldowan 1978; AquinoNeto et al., 1983; De Grande et al., 1983
Tetra/Hop	source, environment	Peters & Moldowan 1983
Ts/Tm	source, environment, maturity	Seifert & Moldowan 1978; Moldowan et al 1986
29Hops	source, environment	Ourisson et al 1987; Killops et al 1998.
30Hops	source, environment	Ourisson et al 1987; Killops et al 1998.
Hop32(S/R)	maturity	Seifert & Moldowan 1986
OleanIndex	source, environment	Ekweozor & Telnaes, 1990

t_{19}/t_{23}= C_{19} cheilanthanes/ C_{23} cheilanthanes, t_{23}/T30H= C_{23} cheilanthanes/ C_{23} cheilanthanes +17α hopane, Tetra/Hop= de-E-Hopane/ de-E-Hopane +17α hopane, Ts/Tm= 18a trinorneohopane/18a trinorneohopane +17α trinorhopane, 29Hops= T29H/T29H+T30H+T31H (S+R), 30Hops= T30H/T29H+T30H+T31H (S+R), Hop32(S/R)= H32 22S/H32 22(S+R), OleanIndex= 100*H30 oleanane/ H30 oleanane+H30.

PC1 shows a percentage variance of 73 and eigenvalue of 5.85 while, PC2 shows a percentage variance of 11.96 and eigenvalue of 0.96 (Table 4.20).

Some parameters were controlled by the same factors as shown on the loadings plot (Figure 4.53). Those parameters that are related include; **Group 1**: t_{19}/t_{23}, OleanIndex, 29Hop, **Group 2**: Ts/Ts+Tm, Hop32 (S/S+R). Two parameters did not show any relationship with others and they plot far away from each other (Tetra/Hop, t_{23}/T30). The scores plot (Figure

4.54) shows a possibility of one main group and two minor groups within the major group. The North Sea oil (NSO-1) was not used for the PCA because the tricyclics peaks were generally very weak and were not well resolved.

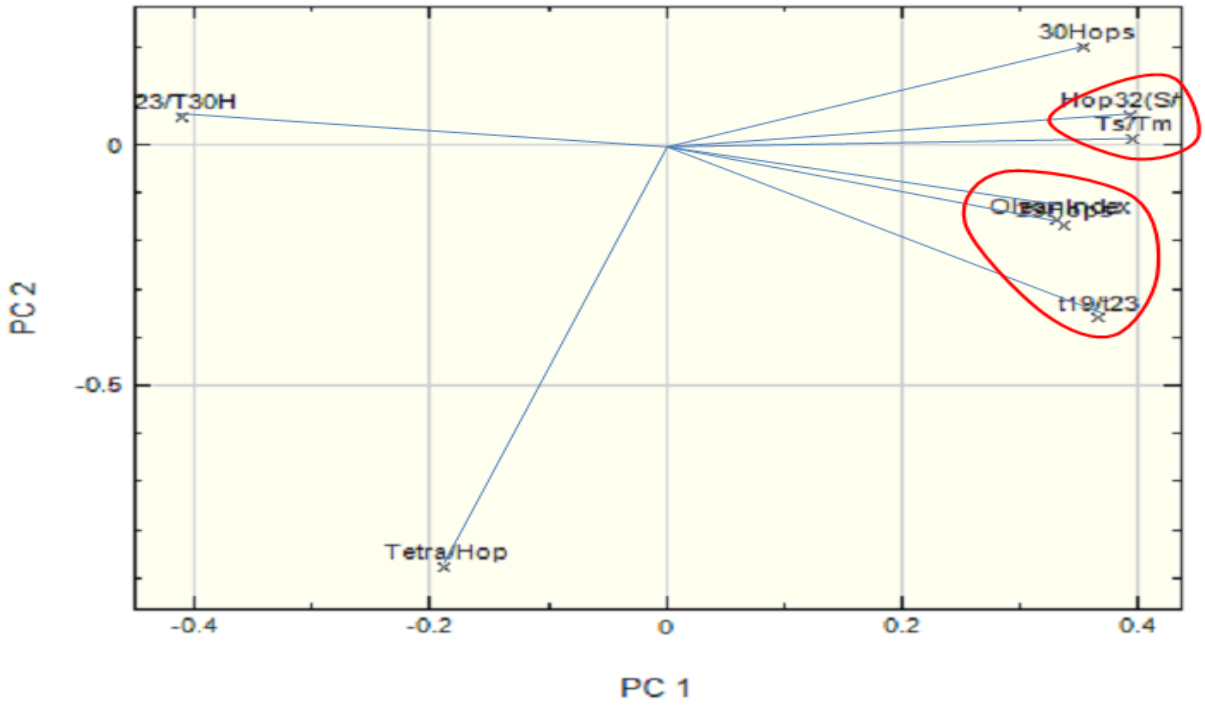

Figure 4.53: Loadings plot of first (73% variance) and second (12% of the variance) principal components of hopane hydrocarbon parameters showing relationship between parameters used for the analysis

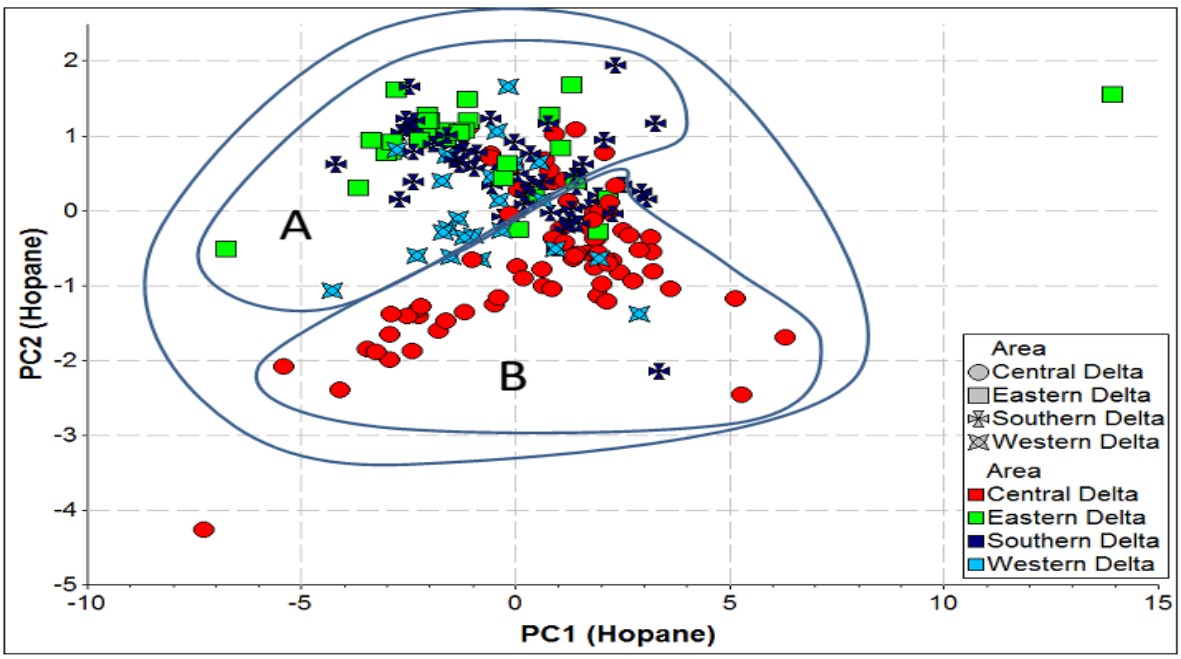

Figure 4.54: Scores plot of first (73% of the variance) and second (12% of the variance) principal components of hopane hydrocarbon parameters showing two possible sub-groupings within a group

4.9.8 Principal component analyses of unknown terpane biomarker parameters

A total of 148 samples and 8 parameters (Table 4.23) were used for the analysis of the novel/unknown terpane parameters. The PCA helps to show the relationships of the parameters to each other. The K index is related to the $x/(x+T_{20})$ and $Y/(Y+T_{23})$ whereas the $A/(A+C_{29}\alpha\beta H)$ is related to the (A+B)/(A+B+C+D) and (A+B)%. The C% and D% appears to be related (Figure 4.56).

Table 4.22: Eigenvalues and percent variance of unknown hopane biomarkers for PC1-PC5

	PC1	PC2	PC3	PC4	PC5
Eigenvalue	4.32	2.16	0.64	0.40	0.29
Percent Variance	53.95	26.98	7.95	5.04	3.59

Table 4.23: Parameters used for the principal components analysis of unknown hopane biomarkers

Parameters	Interpretation	Reference
$A/(A+C_{29}\alpha\beta H)$	Source, environment, biodegradation	This research
$x/(x+T_{20})$	Source, environment	Samuel *et al*., 2009; 2010
$Y/(Y+T_{24})$	Source, environment	Samuel *et al*., 2009; 2010
K index	Source, environment	Samuel unpublished PhD 2008
(A+B)%	Source, environment, biodegradation	This research
C%	Source, environment, biodegradation	This research
D%	Source, environment, biodegradation	This research
(A+B)/(A+B+C+D)	Source	Nytoft *et al*., 2009

$A/(A+C_{29}\alpha\beta H)$= unknown C_{29} hopane/(unknown C_{29} hopane + $C_{29}\alpha\beta$ Hopane); $x/(x+T_{20})$= unknown tricyclic terpane x/ (unknown tricyclic terpane x + C_{20} tricyclic terpane); $Y/(Y+T_{23})$= unknown tricyclic terpane Y/ (unknown tricyclic terpane Y + C_{23} tricyclic terpane); K index= $(A_1+A_2+B_1+B_2)/C$; (A+B)% = (A+B)*100/(A+B+C+D); C%= C*100/(A+B+C+D); D%= D*100/(A+B+C+D); (A+B)/(A+B+C+D)= (A+B)/(A+B+C+D).

PC1 shows a percentage variance of 54 and eigenvalue of 4.32 while, PC2 shows a percentage variance of 27 and eigenvalue of 2.16 (Table 4.22).

Some parameters were controlled by the same factors as shown on the loading plot (Figure 4.55). Those parameters that are related include; **Group 1**: K index, $x/(x+T_{20})$, $Y/(Y+T_{23})$, **Group 2**: $A/(A+C_{29}\alpha\beta H)$, (A+B)/(A+B+C+D), (A+B)%, **Group 3**: C% and D%. The scores plot (Figure 4.56) shows a possibility of two main groups and there is a possible of

two sub groups (A_1 and A_2) within the major group A. The North Sea oil (NSO-1) was not used for the PCA because the peak A from *m/z* 191, peak A+B from *m/z* 193 and peaks A1, A2, B1 and B2 from *m/z* 414 were absent.

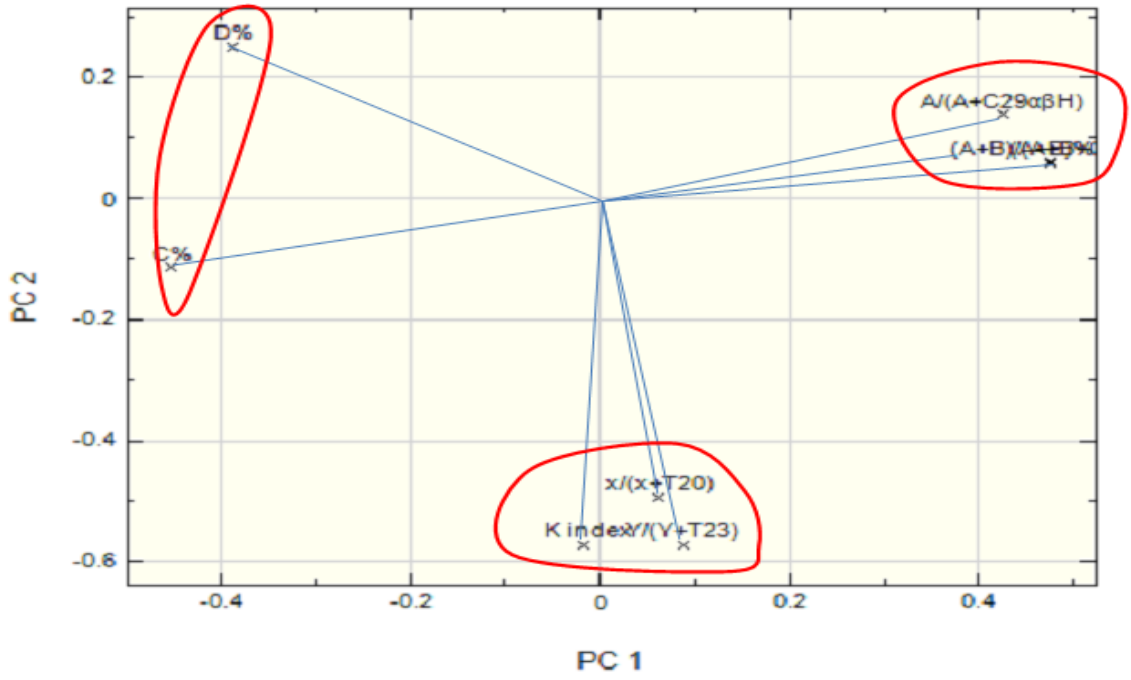

Figure 4.55: Loadings plot of the first (54% of the variance) and second (27% of the variance) principal components of unknown terpane hydrocarbon parameters showing relationships between parameters used for the analysis.

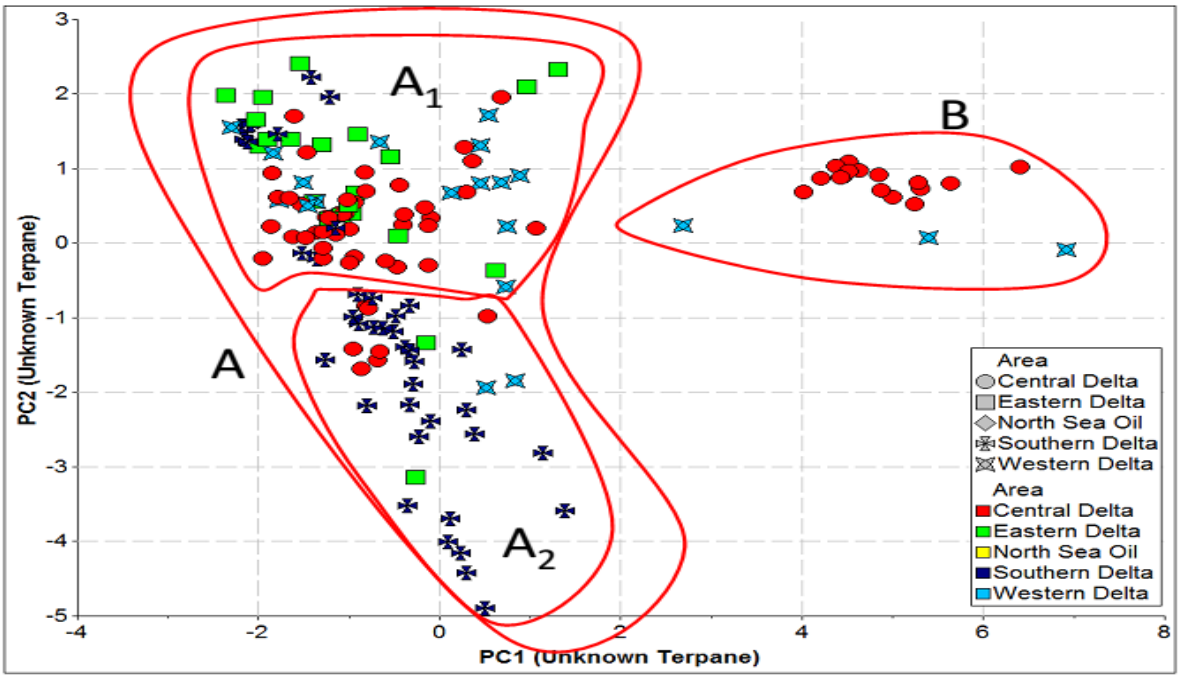

Figure 4.56: Scores plot of first (54% of the variance) and second (27% of the variance) principal components of unknown terpane hydrocarbon parameters showing three possible sub-groupings.

CHAPTER FIVE
OIL CHARACTERISATION

5.0 Introduction

Unravelling the history of the potentially mixed oil samples from the Niger Delta in this work is done using several approaches, but they are generally based on the different hydrocarbon components, i.e. gasoline range hydrocarbons, *n*-alkanes/isoprenoids, diamondoids, aromatics, and sterane and hopane biomarkers (Figure 5.1). The gasoline range parameters are important because they can make up about 30% of any hydrocarbon composition (Hunt *et al*., 1980) or over 50% of the carbon in any petroleum (Mango, 1997). The diamondoid hydrocarbons are also important because they occur naturally in low maturity oils in very low concentrations, usually about 5 ppm, but their concentrations generally increase with the onset of thermal cracking (Dahl *et al*., 1999) and can be used to assess maturity, mixing, cracking extent, source and biodegradation. Sterane, hopane and aromatic parameters are also used to unravel relationships in the potentially mixed oils from the Niger Delta basin.

Several authors have studied the thermal maturity of source rocks (Ekweozor & Okoye, 1980; Lambert-Aikhionbare & Ibe, 1984; Ekweozor & Daukoru, 1984; Ekweozor and Udo, 1987; Akinlau *et al*., 2005; Akinlua & Torto, 2011) and the Tertiary reservoired oils (Eneogwe & Ekundayo, 2003; Eneogwe *et al*., 2002; Sonibare *et al*., 2008; Samuel *et al*., 2009; Akinlau & Ajayi, 2009; Lehne & Dieckmann, 2010) of the Niger Delta. While some believe that the oils are of low maturity, others think that the oil is mature, the differences however might be due to differences in the thermal maturity parameters used for interpretation.

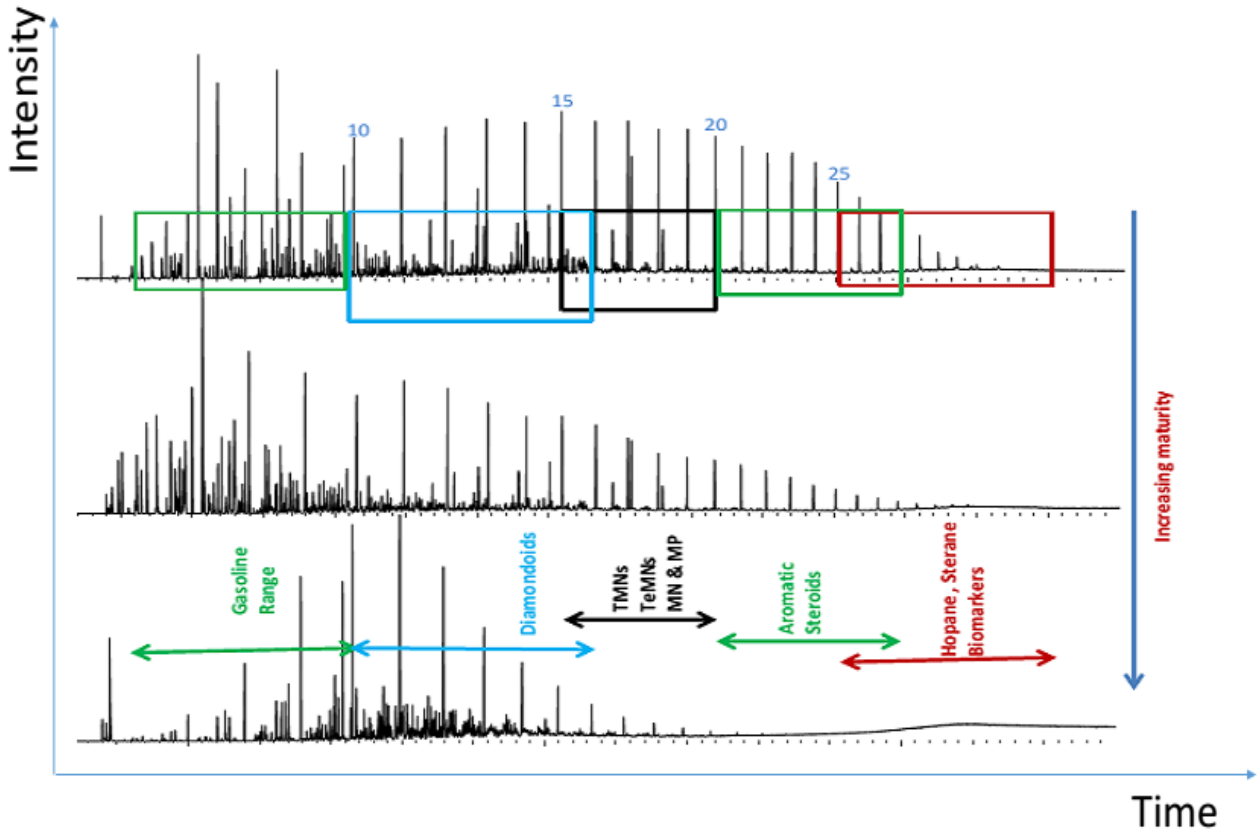

Figure 5.1a: Whole oil chromatograms of three representative oil samples (OE137 to, OE165 middle and a shell condensate bottom), showing the relative elution times of gasoline range hydrocarbons, diamondoids, phenanthrenes, naphthalenes, aromatic steroids and biomarkers. Note the depletions of the heavier end with increase in maturity.

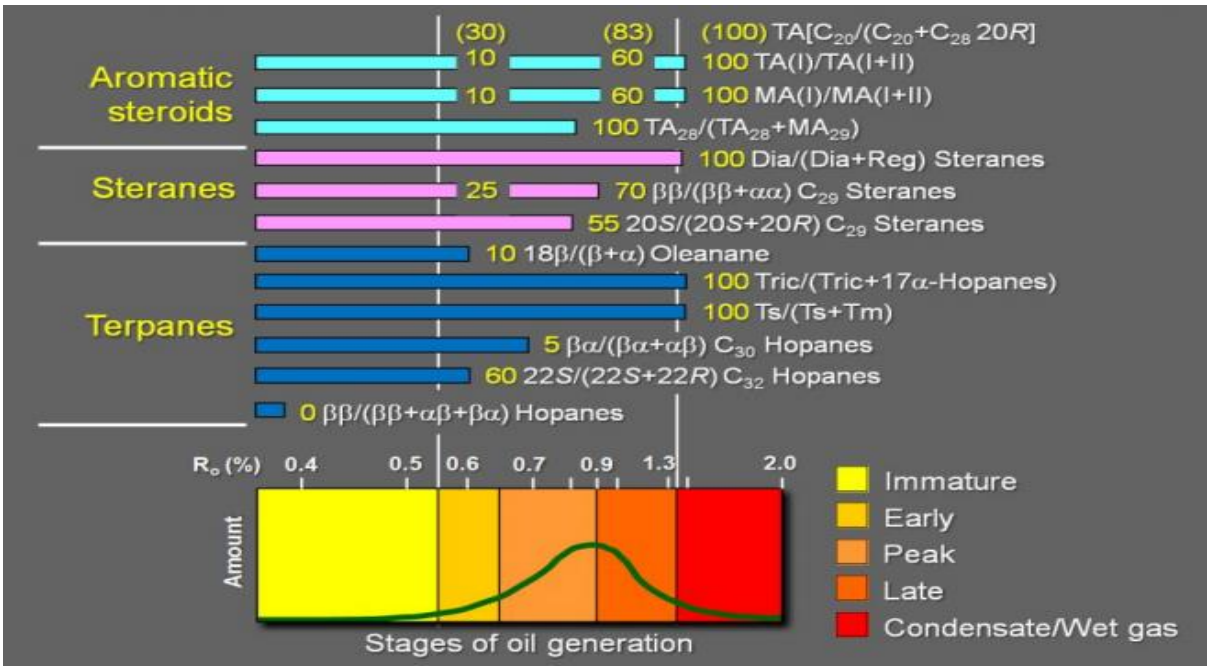

Figure 5.1b: Common maturity parameters and their response range compared to the stages of oil generation (Peters *et al.*, 2005).

5.1 Oil characterisation from gasoline range.

The terms light or gasoline range hydrocarbons generally refer to the C_4 to C_{10} range (Figure 5.1) and they account for approximately 30% of any oil sample (Hunt *et al*., 1980) although they have also been defined as the C_1 to C_9 hydrocarbon range and that they account for over 50% of carbon in petroleum (Mango, 1997). More representative information of the oil can be obtained from them than biomarkers which only make up a small fraction (about 1%) of the oil (Hunt *et al*., 1980). Oil characterisation based on the gasoline range hydrocarbons has been shown to be an extremely important tool (Mango 1990) especially in highly mature and mixed oils for their correlation and source rock deposition environment elucidation but they do have their own limitations (ten Haven, 1996).

5.1.1 Source kerogen type

The Thompson heptane and isoheptane ratios corresponds to various kerogen types depending on the trend line and area in which a sample plots (Thompson, 1983), the cross plot can also indicate maturity trends and biodegradation (Peters *et al*., 2005). The Thompson Type II kerogen plots on the aliphatic curve while the Thompson Type III kerogens plot on the aromatic curve (Thompson, 1983). Peters *et al*., (2005) believe that Type II/III oil sourced from pro-deltas plots midway between the Type II and Type III kerogen (Figure 5.2).

Highly aliphatic source rocks which are mainly sourced from lacustrine environments plot just above the Type II trend line (Thompson 1983; Peters *et al*., 2005), and since some Niger Delta oil samples plots above the trend line we can conclude that there exists the possibility that some of the Niger Delta oil samples have been sourced from lacustrine Type I source rock and those include 3 samples from the Central Delta and 3 samples also from the Southern Delta (Figure 5.2). The Eastern Delta and Western Delta oil samples are mainly sourced from a Type II kerogen; this is also true for the North Sea reference oil

(Figure 5.2). The Southern Delta and Central Delta oil samples plot in the region between the Thompson Type II kerogen and Type III kerogen and therefore can be said to be sourced from a Type II/III kerogen (Figure 5.2).

The interpretations based on the Thompson plot (Figure 5.2) are known to be very useful but there are exceptions to the normal trend, which include:

1. When dealing with Precambrian sourced oils; because they are depleted in cycloalkanes, they always have high isoheptane ratios (Peters *et al*., 2005)
2. Evaporative fractionation, phase separation and formation of retrograde condensates (Thompson 1987; 1988; Thompson & Kennicutt, 1990).

It can be concluded that the oil samples from the Niger Delta are mainly sourced from Type II/III kerogen with some Type II kerogen but there is no pure Type III kerogen sourced oil based on interpretation from the light hydrocarbons.

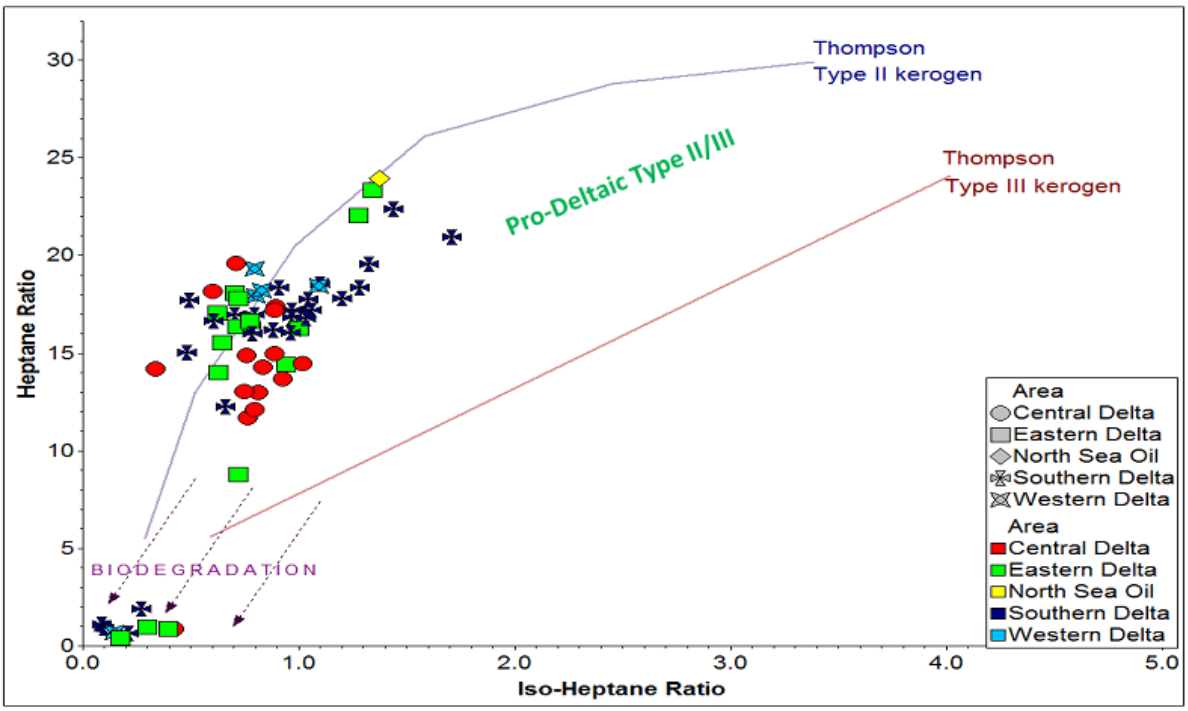

Figure 5.2: Plot of heptane versus isoheptane ratios of oil samples from the different regions of Niger Delta showing the source kerogen type. The oil samples are mainly Type II and mixture of Type II/III kerogen, note the absence of any pure Type III kerogen. Interpretation overlay from p:IGI 3.5 (modified after Thompson 1983 and Peters *et al*., 2005). Note the position of the North Sea oil which enables comparison with a marine sourced oil.

5.1.2 Source environment of deposition

The Niger Delta oil samples can be interpreted as being mainly sourced from terrigenous and marine environments (Figure 5.3) but there exists possibilities that some samples were sourced from lacustrine environments (Figure 5.3). This interpretation has some relationship with the kerogen type interpretation of the previous section (section 5.2.1 based on Figure 5.2) and it follows that those samples that plot in the kerogen Type II fields are deposited in marine environment whereas those that are of Type II/III kerogen are deposited mainly in the terrigenous environment or have contributions from this environment. Because of the wide overlaps of this plot, it has been generally agreed that for the plot to be useful it should be calibrated with relatively mature source rocks on a basin wise scale (e.g. ten Haven, 1996; Odden *et al*., 1998) which is not available in Niger Delta, and that, due to their wide ranges of values, there is a possibility of overlap even between the terrigenous and the lacustrine fields when dealing with Tertiary lacustrine organic matter (ten Haven, 1996).

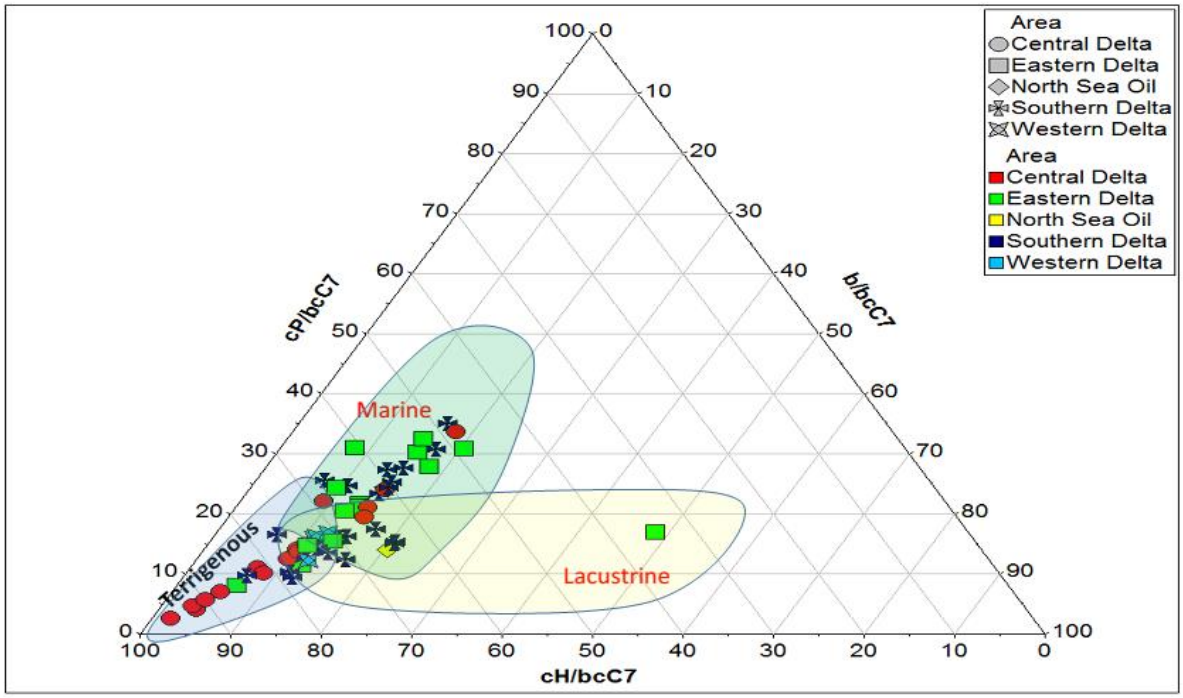

Figure 5.3: Ternary plot of Mango's ring-preference parameters (cP/bcC_7; b/bcC_7 and cH/bcC_7), showing the possible depositional environments of Niger Delta oils. Note the North Sea oil enables comparison with a marine sourced oil (c.f. ten Haven, 1996).

Zhang *et al*., (2005) used a cross plot of P_3 against (P_2 + N_2) to show the depositional environments of some oil samples from the Tarim basin and their results correspond with those based on isotope values to group the oils (Huang *et al.*, 1999) and the report based on statistical cluster analysis of molecular parameters of oils and source rock extracts (Hanson *et al*., 2000). Based on the cross plot of P_3 against (P_2 + N_2) it can be concluded that most of the samples in the present study were deposited in a marine environment and some samples (mainly Central Delta oil samples) were deposited in a terrigenous environment (Figure 5.4). The results shown on the ten Haven figure (Figure 5.3) bears some relationship to those from the Zhang *et al*., (2005) plot (Figure 5.4) if the overlap terrigenous field (Figure 5.3) is ignored in figure 5.3.

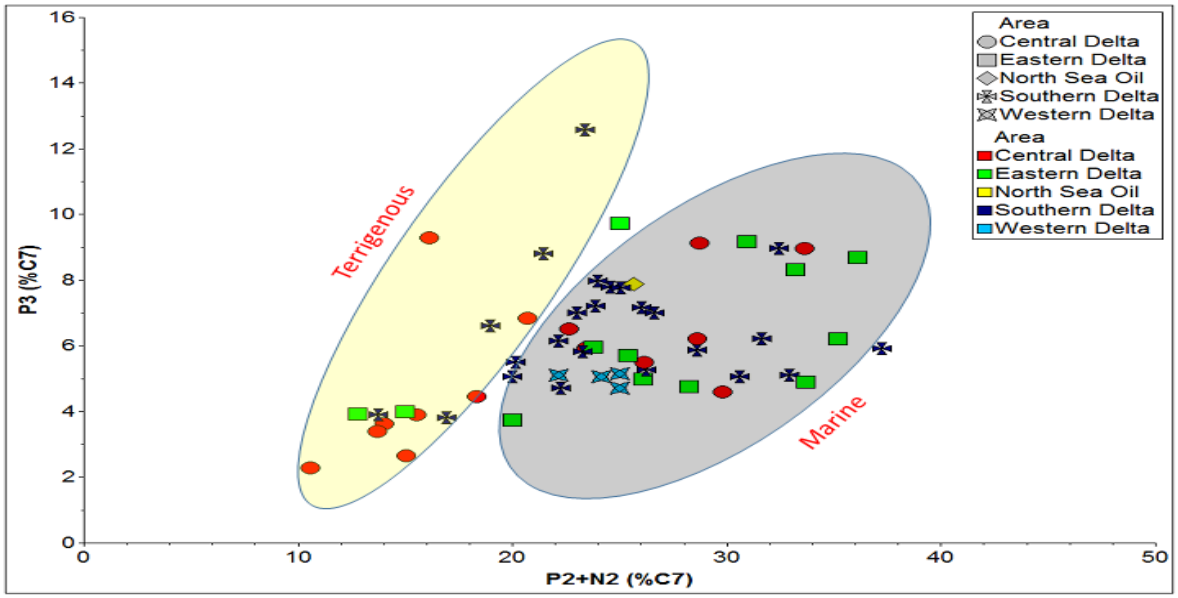

Figure 5.4: Cross plot of P_3 against (P_2 + N_2) showing the depositional environments of Niger Delta oil samples. Note the North Sea oil enables comparison with a marine sourced oil (Zhang *et al*., 2005).

5.1.3 Thermal maturity

The Niger Delta oil samples appear mainly as normal mature oils with most of the samples from all the regions plotting in this field (Figure 5.5); five samples from the Southern Delta (OEE29, OEE30, OEE87, OEE140, OEE174) and two samples from the Eastern Delta

(OEE91, OEE175) are in the mature field and those are of similar maturity to the North Sea oil (NSO-1). The biodegraded region has been placed to start from heptane value of 12 because it is possible to have low thermal maturity oil sample with heptane value of as low as 12 (Peters *et al.*, 2005). Based on the Thompson heptane and isoheptane values for thermal maturity it can be said that none of the Niger Delta oil samples are of very high thermal maturity and also none of them have been thermally cracked (Figure 5.5).

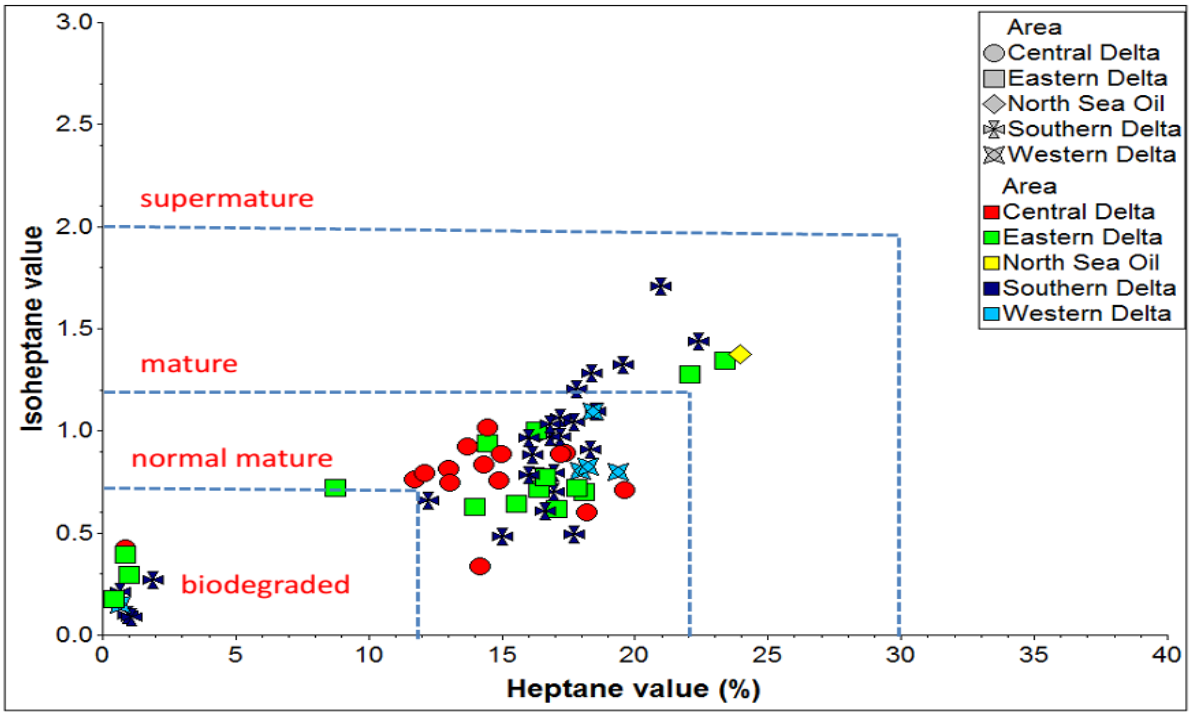

Figure 5.5: Variation in maturity of Niger Delta oil samples based on the isoheptane ratio and the heptane ratio. Interpretation overlay from p:IGI 3.5 (modified after Thompson 1983 and Peters et al., 2005). Note the North Sea oil enables comparison with a thermally matured marine sourced oil.

5.1.4 Summary of kerogen type, source and thermal maturity interpretations from light hydrocarbon data.

Based on the results from light hydrocarbons it can be summarised that:

1. The Niger Delta oil samples are sourced from a Type II and Type II/III kerogen
2. Most oil samples were sourced from a marine environment and some oil samples were sourced from a terrigenous deposition environment.

3. The Niger Delta oil samples are of "normal" maturities, with most of the oils lower in maturity than a typical North Sea oil.
4. Based on the samples analysed, we can conclude that there is no super mature oil sample in the Niger Delta therefore none of the oil sample has suffered cracking.

5.2 Oil characterisation from *n*-alkanes and isoprenoids

The *n*-alkanes and isoprenoids are usually monitored using GC and peak ratios from these results are always useful for preliminary geochemical screening (Peters *et al*., 2005) as they can be relatively cheap and fast, however *n*-alkane profiles can be very misleading as they can appear different for genetically related oil because of different thermal maturities and biodegradation (Hunt 1995; Peters *et al*., 2005) and can also lose all information at high biodegradation levels.

5.2.1 Source kerogen type

The Niger Delta oil samples tend to be sourced by Type III kerogen deposited in a terrigenous environments (Shanmugam 1985, Peters *et al*., 1999), with the bulk of the oil samples from the Central Delta region plotting in this field (Figure 5.7), however most samples from the Western Delta plot in the mixed Type II/III region.

Overall the samples in this study appear mainly sourced by Type III or some by Type II/III kerogens deposited in mainly oxidizing environments with possibility of some in reducing environments (Figure 5.7). However interpretation of this plot should be used in association with that of other data, as it can be affected by thermal maturity and biodegradation (Lijmbach, 1975; Alexander *et al*., 1981, Shanmugam, 1985).

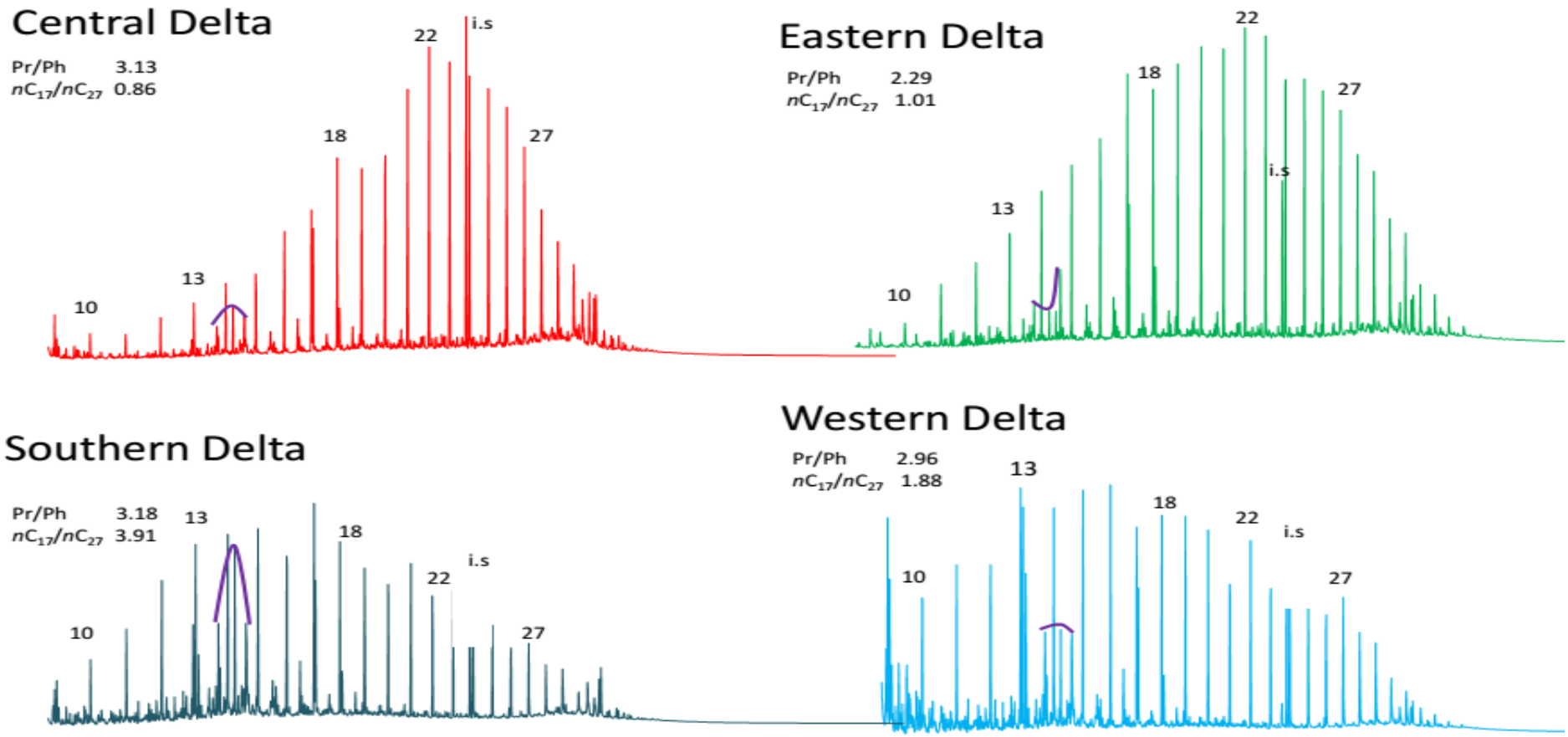

Figure 5.6: Representative *n*-alkane profiles of oils from the various regions of the Niger Delta. Note the different profiles, especially around the nC_{14}, and the presence of abundant C_{15} sesquiterpanes eluting around this *n*-alkane; i.s – internal standard (HDCH). (OE117 Central Delta, OE152 Eastern Delta, OE129 Southern Delta and OE143 Western Delta).

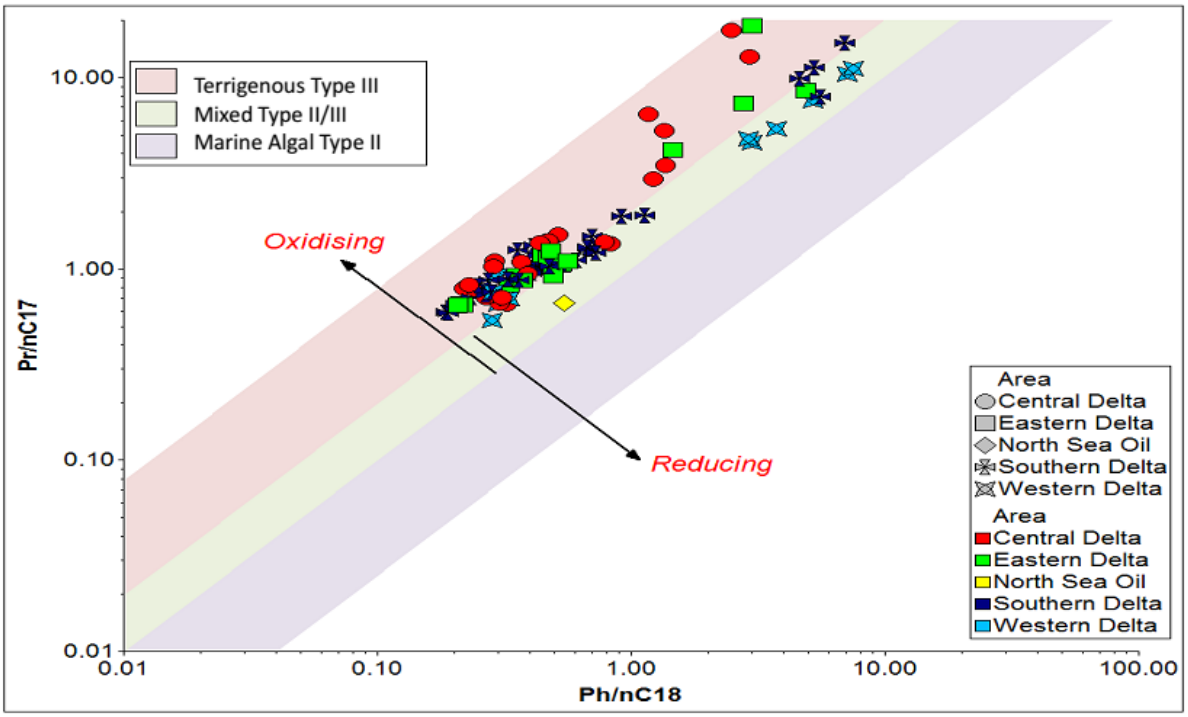

Figure 5.7: Cross plot of Pr/nC$_{17}$ against Ph/nC$_{18}$ ratios of oil samples from different Niger Delta regions showing the source kerogen type and depositional environment. Interpretation overlay from p:IGI 3.5 (modified after Shanmugam 1985). Note the North Sea oil enables comparison with a marine sourced oil.

5.2.2 Source environment of deposition

The Pr/Ph ratio helps indicate the source depositional environment of an oil (Didyk *et al.*, 1978) and based on this ratio we can infer that the oil samples in this study were sourced mainly from oxic environment with the possibility of dysoxic settings in some samples (Figure 5.8). The Western Delta oil samples were mainly deposited in a dysoxic environment (Figure 5.8) but this interpretation is based on the fact that the source organic matter was mainly from terrestrial plants as well as phytoplankton (Didyk *et al.*, 1978) without considering the fact that there are various other sources for pristane and phytane (e.g. ten Haven *et al.*, 1987; Volkman & Maxwell, 1986; Goossens *et al.*, 1984). However, even with the shortcomings of this ratio, it is believed that the ratio is still very useful in oil source depositional environment interpretation (Peters *et al.*, 2005).

The compound specific isotope analysis (CSIA) plot of individual *n*-alkanes indicates that our samples were sourced from different environments which included marine deltaic,

fluvio-deltaic and fresh water transitional environments (c.f. Murray *et al*., 1994), which are all possible sub-environments in a paralic delta. The slope of the fluvio-deltaic environment data trend is higher than that of the marine deltaic, as seen on the profiles shown in Figure 5.9.

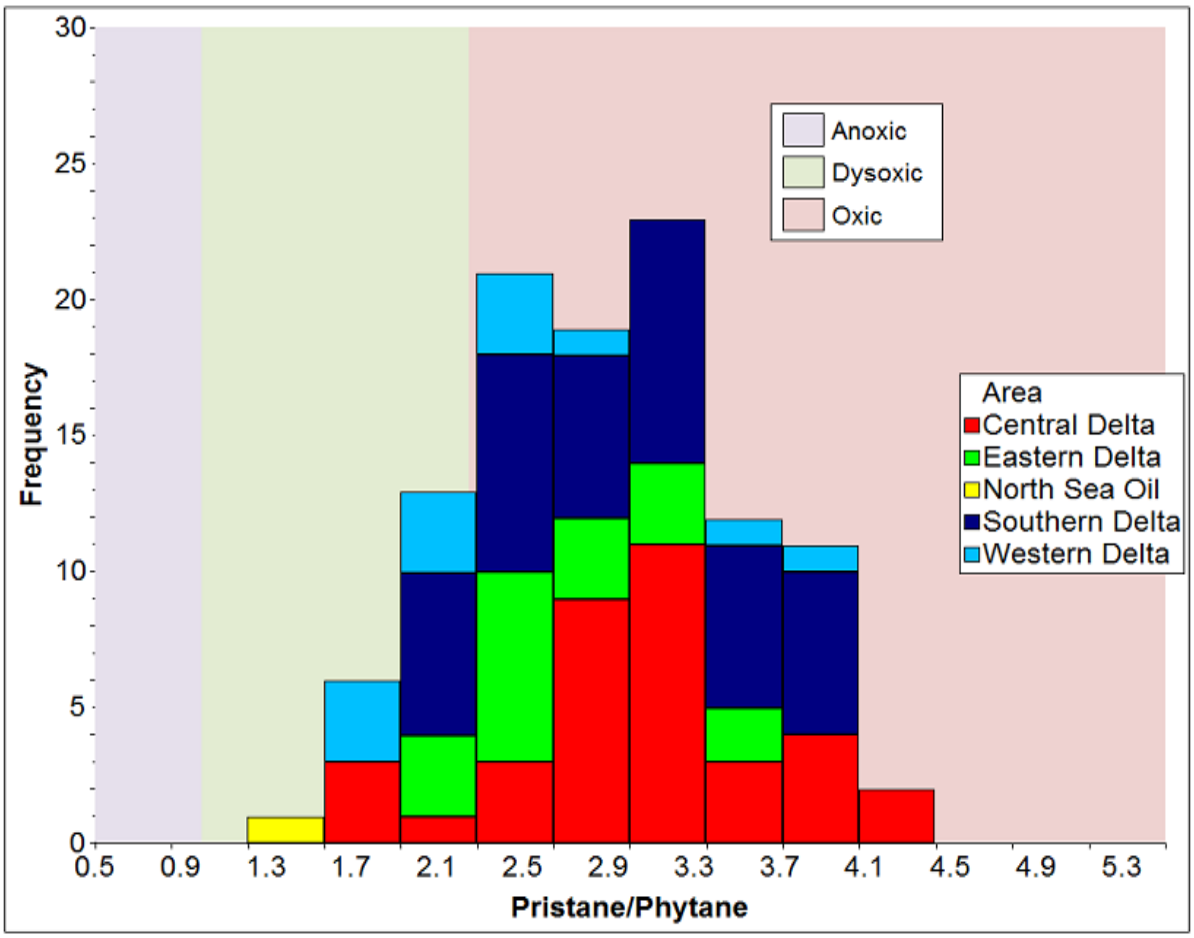

Figure 5.8: Source deposition environment inferred from Pr/Ph ratios for the Niger Delta oil samples. The wide range of Pr/Ph ratios (1.7 to 4.5) reflects variable source rock depositional environments. Interpretation overlay is from IGI's p:IGI-3.5 software. Note the North Sea oil enables comparison with a marine sourced oil.

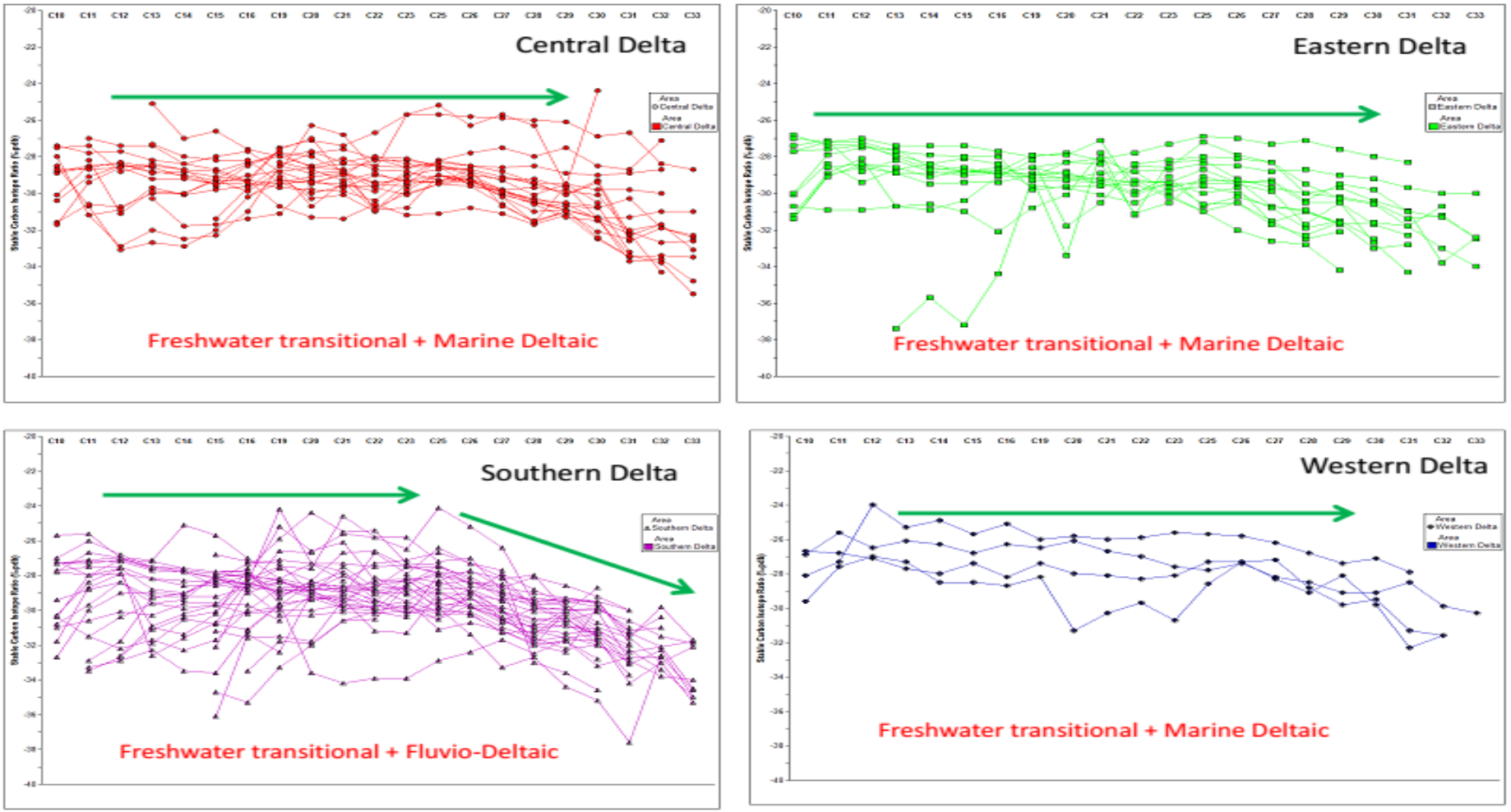

Figure 5.9: Compound specific carbon isotope profiles of *n*-alkanes from the different areas in the delta. The values of nC_{17}, pristane, nC_{18}, phytane and nC_{24} have been deleted due to partial co-elution effects. Note ^{13}C range from -24 to -38 $^{0}/_{00}$.

The average δD values of the oils in this study are very close to -150$^{0}/_{00}$ therefore it is possible to conclude that the Niger Delta oil samples were sourced from marine sediments (Figure 5.10) and none of the samples show the wide range of values which is present in terrigenous sediments, with reported results in the range of -245$^{0}/_{00}$ to -62 $^{0}/_{00}$ (Schimmelmann *et al*., 2004) and -250$^{0}/_{00}$ to -140$^{0}/_{00}$ (Xiong et al., 2005) but terrigenous input cannot be completely ruled out because the δD marine average of -150$^{0}/_{00}$ is still within the terrigenous range of -250$^{0}/_{00}$ to -62 $^{0}/_{00.}$

The δD values can also be used as indicators of palaeo-latitude/ palaeo-climatic conditions during sediment burial (Dawson *et al*., 2004) which can result from δD compositions of meteoric water in the depositional settings, with values greater than -140$^{0}/_{00}$ deposited in the tropical/warm/semiarid/ arid climates (Lloyds 1966; Sofer & Gat 1975) and values less than -160$^{0}/_{00}$ deposited in either glacier environments or when global glacier ice melting events were taking place (Shackelton, 1968). The source rocks that generated the oils in this study can thus be inferred to have been deposited in a tropical/ warm climate (Figure 5.10).

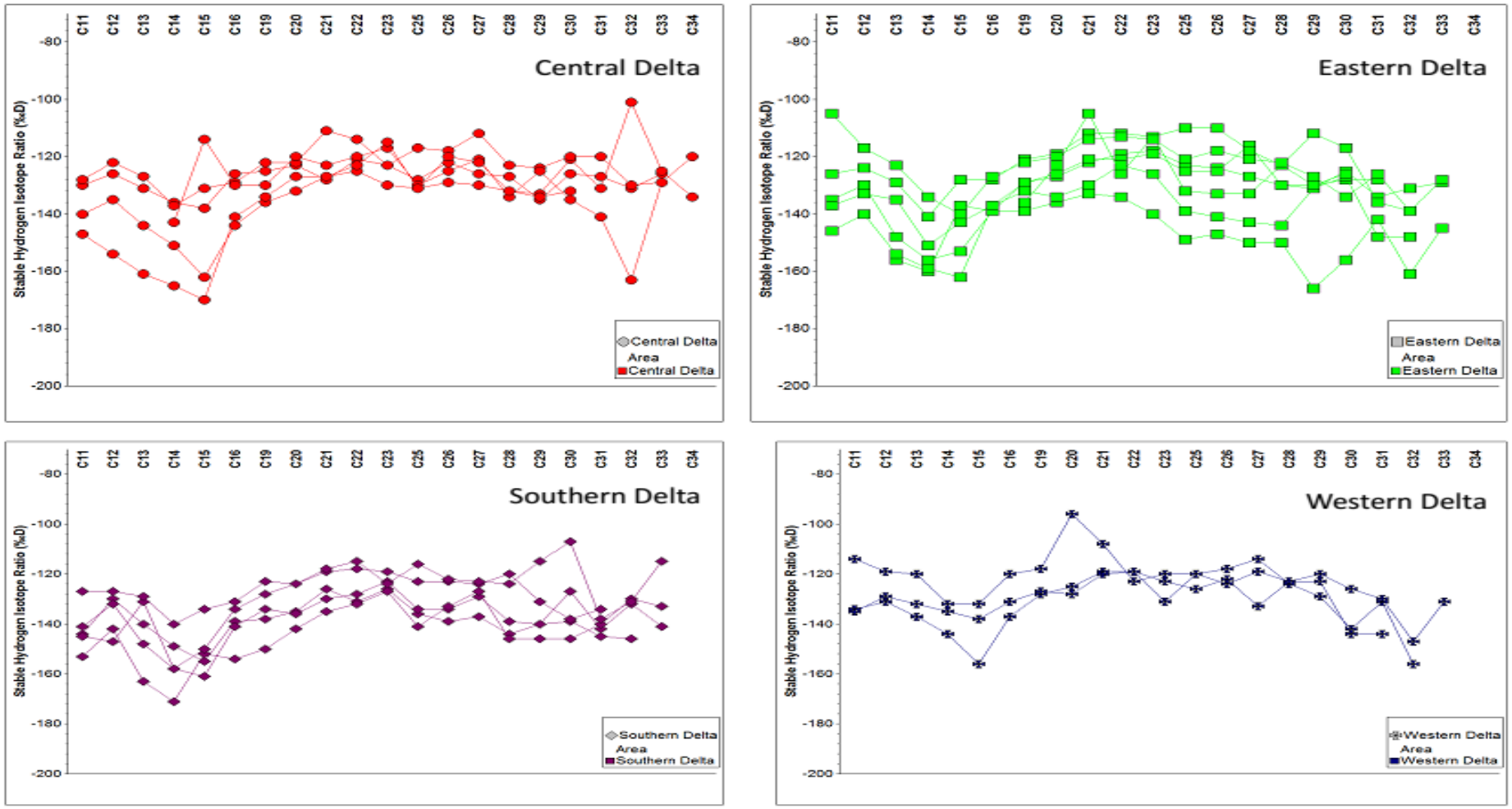

Figure 5.10: Compound specific hydrogen isotope profiles of *n*-alkanes for the different area in the delta. The values of nC_{17}, pristane, nC_{18}, phytane and nC_{24} have been deleted due to partial co-elution effects. Note the similarity in the profiles.

5.2.3 Thermal maturity, cracking and reservoir mixing

The *n*-alkane odd/even predominance has been shown to tend towards unity with increased thermal maturity, especially around nC_{25} to nC_{33} range (Bray & Evans, 1961; Philippi 1965; Scanlan & Smith 1970), Most of the Niger Delta oil samples appear to be of early maturity, with Carbon Preference Index (CPI) values (c.f. Bray & Evans, 1961) of between 1.05-1.2 and some are thermally mature with CPI values of 0.95-1.04. The western Delta samples have low CPI values (0.92) and plots in the field of oils probably sourced from carbonate source rocks, but this might be misleading as the profile appears to be very waxy (Figure 5.11).

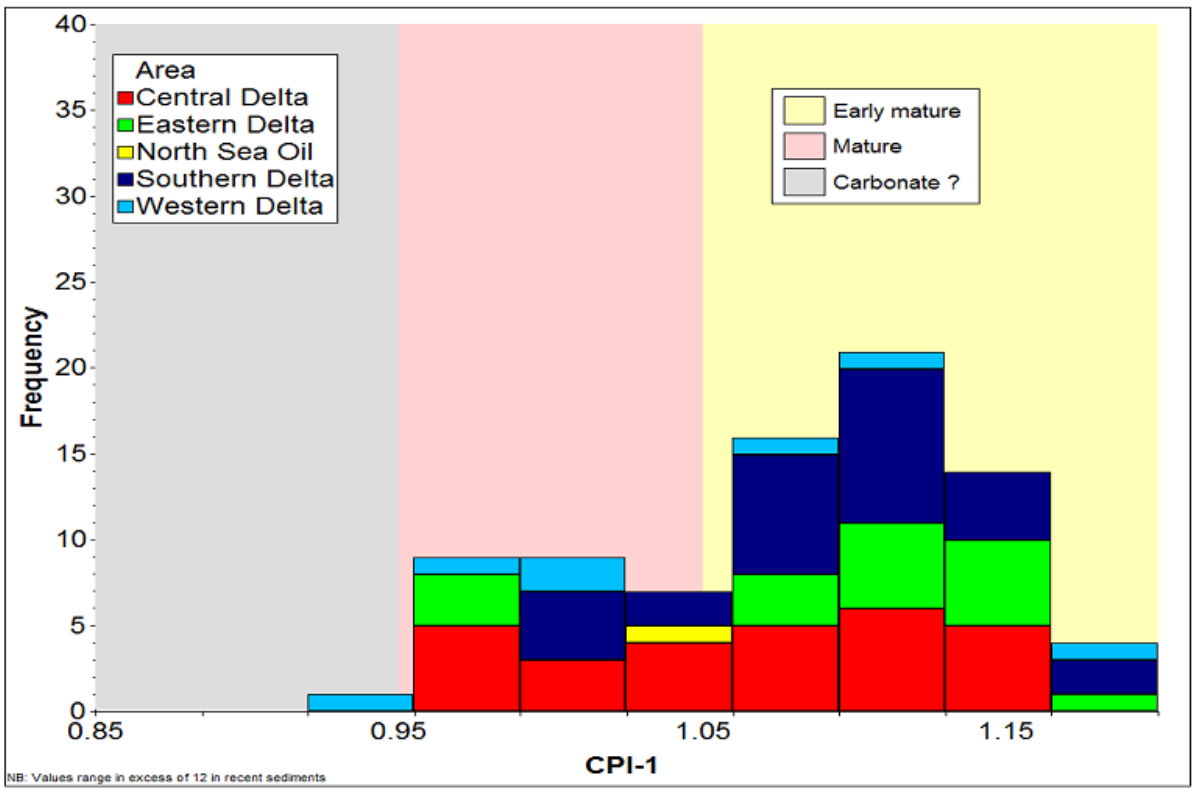

Figure 5.11: Thermal maturity of oil samples inferred from CPI-1 for the Niger Delta oil samples. Interpretation overlay from IGI's p:IGI-3.5 software. Note the North Sea oil enables comparison with a thermally mature marine sourced oil.

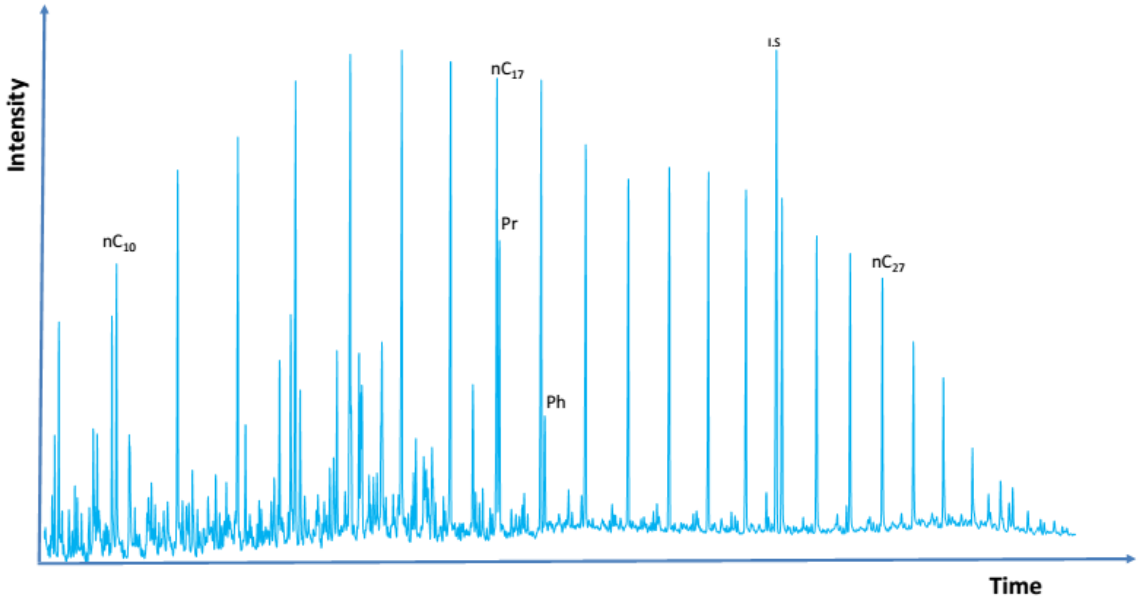

Figure 5.12: Gas chromatogram showing the distribution of *n*-alkanes and isoprenoids from sample oil OEE106 with a CPI-1 of 0.92

5.2.4 Summary of kerogen type, source and thermal maturity from *n*-alkane and isoprenoid hydrocarbon data interpretation.

Based on the results from *n*-alkanes and isoprenoid hydrocarbons it can be summarised that:

1. The Niger Delta oil samples are sourced mainly from a Type III kerogen with some mixed Type II/III
2. The depositional environments of the sources of the oil samples are mainly oxic but a few were deposited in dysoxic depositional settings.
3. The broad environment of deposition is a paralic delta (marine environment with some terrigenous input) that existed in tropical/warm climate conditions.
4. Most of the Niger Delta oil samples are thermally relatively immature but some others are thermally mature.

5.3 Oil characterisation from diamondoid hydrocarbons

Diamondoids are caged hydrocarbons with diamond-like structures which are present in crude oils and whose concentrations increase appreciably when subjected to very high thermal stress (Dahl *et al*., 1999). They are absent in recent organic matter and are not biomarkers, but are generated during progressive thermal maturation of organic matter (Peters *et al*., 2005; Wei *et al*., 2006, 2007) and are ubiquitous in nature (Peters *et al*., 2005). They are also conserved and concentrated over geological time because of their high structural stability during intense thermal stress (Dahl *et al.*, 1999, Fang *et al.*, 2012). Their concentrations and distributions are useful during interpretation of source, biodegradation, thermal maturity, correlation and quantitative mixing of oils they are present in (Dahl *et al*., 1999; Moldowan., *et al*., 2010; Araujo *et al.*, 2012). In most petroleums that have not been thermally cracked they are present only in minute amounts - generally less than 5 ppm (Wei *et al*., 2007; Dahl *et al*., 1999; Azevedo *et al*., 2008; Araujo *et al*., 2012; Fang *et al*., 2012).

5.3.1 Source kerogen type

The dimethydiamantanes (3,4-DMD; 4,8-DMD; 4,9-DMD) have been shown to be effective in determining the source kerogen type (Schulz et al., 2001) and a clear grouping of kerogen type fields has been achieved based on a ternary diagram of the dimethydiamantanes. The 180 Niger Delta oil samples plot in the Type II field (Figure 5.14) and only sample OE002 plots outside the field. In order to check the interpretation, a plot of DMDI-1% and EAI% (Figure 5.14, and see below for explanation of the parameters) also shows that these source kerogen type are overwhelmingly Type II. This interpretation does not agree with those from the light hydrocarbons and *n*-alkane and isoprenoid hydrocarbon parameters.

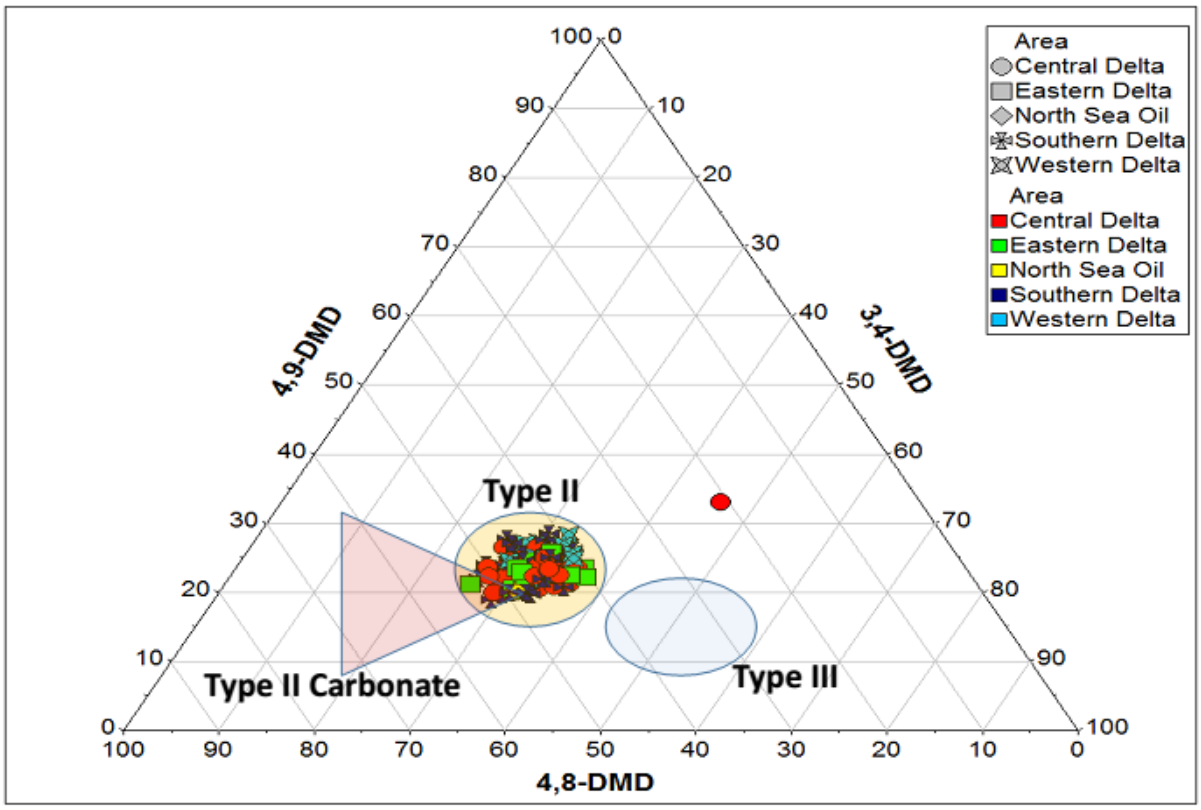

Figure 5.13: Ternary plot of the percentage distribution of 3,4-dimethydiamantanes, 4,8-dimethydiamantanes and 4,9-dimethydiamantanes showing that these Niger Delta oils were sourced from Type II organic matter (Modified after Schulz *et al*., 2001). Note the North Sea oil enables comparison with a marine sourced oil and this plots in amongst the Niger Delta oil samples.

5.3.2 Source environment of deposition

Several environments of deposition which included marine carbonate, terrigenous and marine silisiclastics facies were distinguished by Schulz *et al*. (2001) based on the use of dimethydiamantanes, and a plot of the dimethydiamantane index DMDI-I (3,4-DMD*100)/(3,4-DMD + 4,9-DMD) against ethyldiamantane index EAI (2-EA*100)/(2-EA + 1-EA) showed the source OM of some rock extracts analysed. This same type of plot indicates that the Niger Delta oils were from a Type II marine source (Figure 5.14), similar to the marine shale Spekk formation of the North Sea reported by Schulz *et al*. (2001). To confirm the source/organo-facies interpretation, a standard North Sea Oil from the Oseberg field also plots in the same field, indicating that their OM were deposited in similar environment (Figure 5.14) and this suggests that there has not been any major contribution

from a Type II/III or Type III formation, in contrast to that indicated by previous interpretations based on light hydrocarbons and *n*-alkane and isoprenoid hydrocarbons.

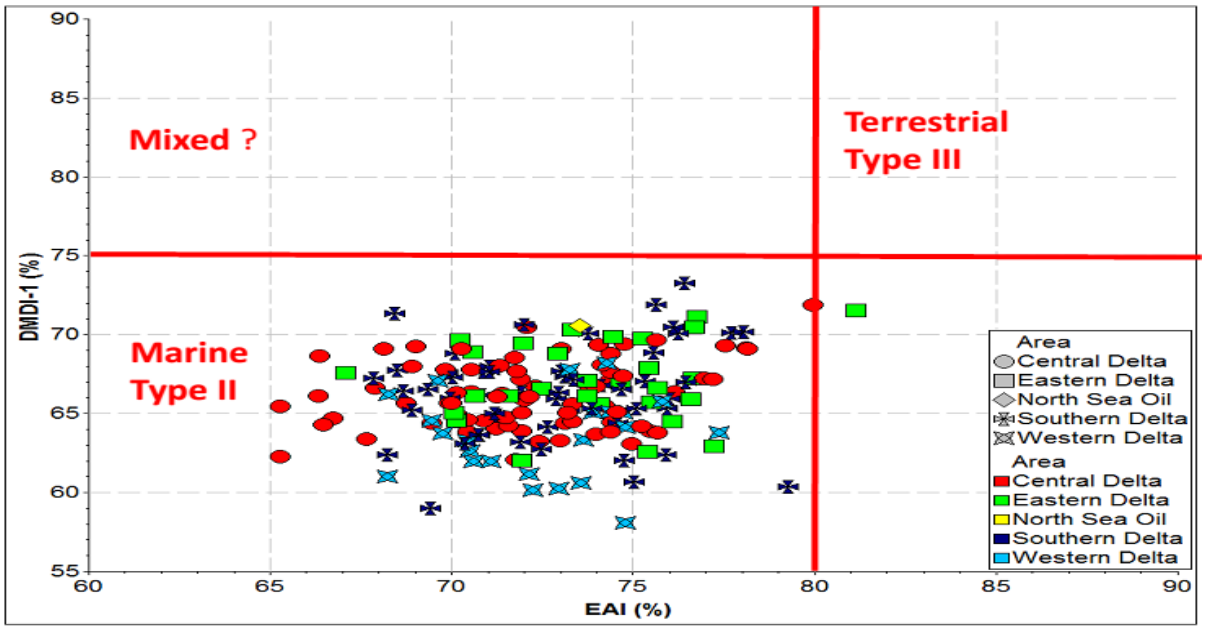

Figure 5.14: Diamondoid organic facies parameter plot of the Niger Delta oil samples indicating that the oil were from a Type II marine source facies similar to that of the North Sea oil (after Schulz *et al*., 2001).

5.3.3 Thermal maturity, cracking and reservoir mixing

The thermal maturity assessment of highly mature oils can be difficult because they are usually devoid of biomarkers. A cross plot of diamondoid maturity parameters 1-methyladamantane/(1-methyladamantane+2-methyladamantane)% (MAI) against 4-methyldiamantane/(1-methyldiamantane+3-methyldiamantane + 4-methyldiamantane) % (MDI) (Chen *et al*., 1996; Nasir & Fazeelat 2013) shows that the Niger Delta oil samples are in the late oil window and early gas window, with equivalent vitrinite reflectance values of 1.1-1.6 $\%VR_0$ (Figure 5.15), however it has been noted that there is a possible reversal in MDI value above 2.0 $\%VR_0$ (Li *et al*., 2000) these VR_0 values are much higher than the maturity of the North Sea oil (Figure 5.15). Thus, maturity calculations based on diamondoids is believed to reveal that there is a highly matured oil charge in the delta, with maturity far higher than those calculated from other parameters (e.g. light hydrocarbons, *n*-alkane and biomarker).

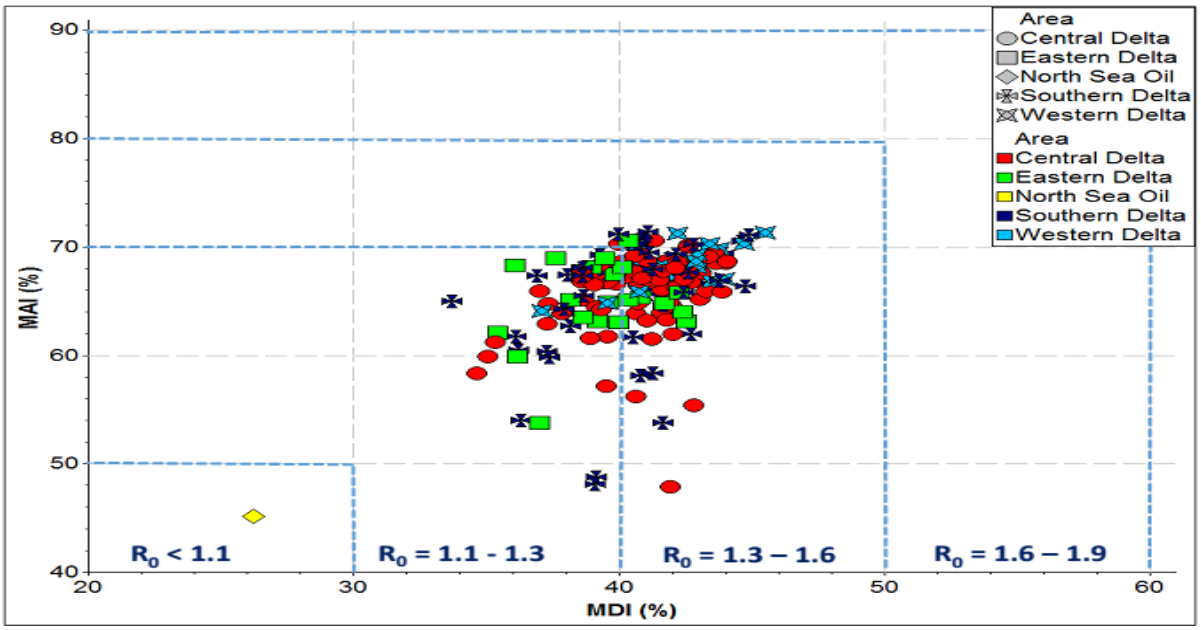

Figure 5.15: Diamondoid maturity parameters plot showing very high maturity in the Niger Delta oil (%VRo equivalent 1.1-1.6). Note the lower maturity of the North Sea oil when compared to the Niger Delta oils (Modified after Chen *et al*., 1996).

A thermal cracking map which was based on the concentrations of 3+4-methyldiamantanes (Figure 5.16) shows that the delta can be divided into two broad regions with the Western Delta region showing regional trend of highly cracked oil whereas the Eastern Delta region shows a lower cracking pattern. This regional cracking pattern bears a striking similarity to the combined gravity and magnetic variation basement structure map produced by Haack *et al*., (2000), which shows that most parts of the Western Delta have more than 11 km of sediment thickness, while that the Eastern Delta is less thick. The sediment thickness (burial depth) can be inferred as a major controlling factor on thermal maturity on the oil samples from the Niger Delta basin.

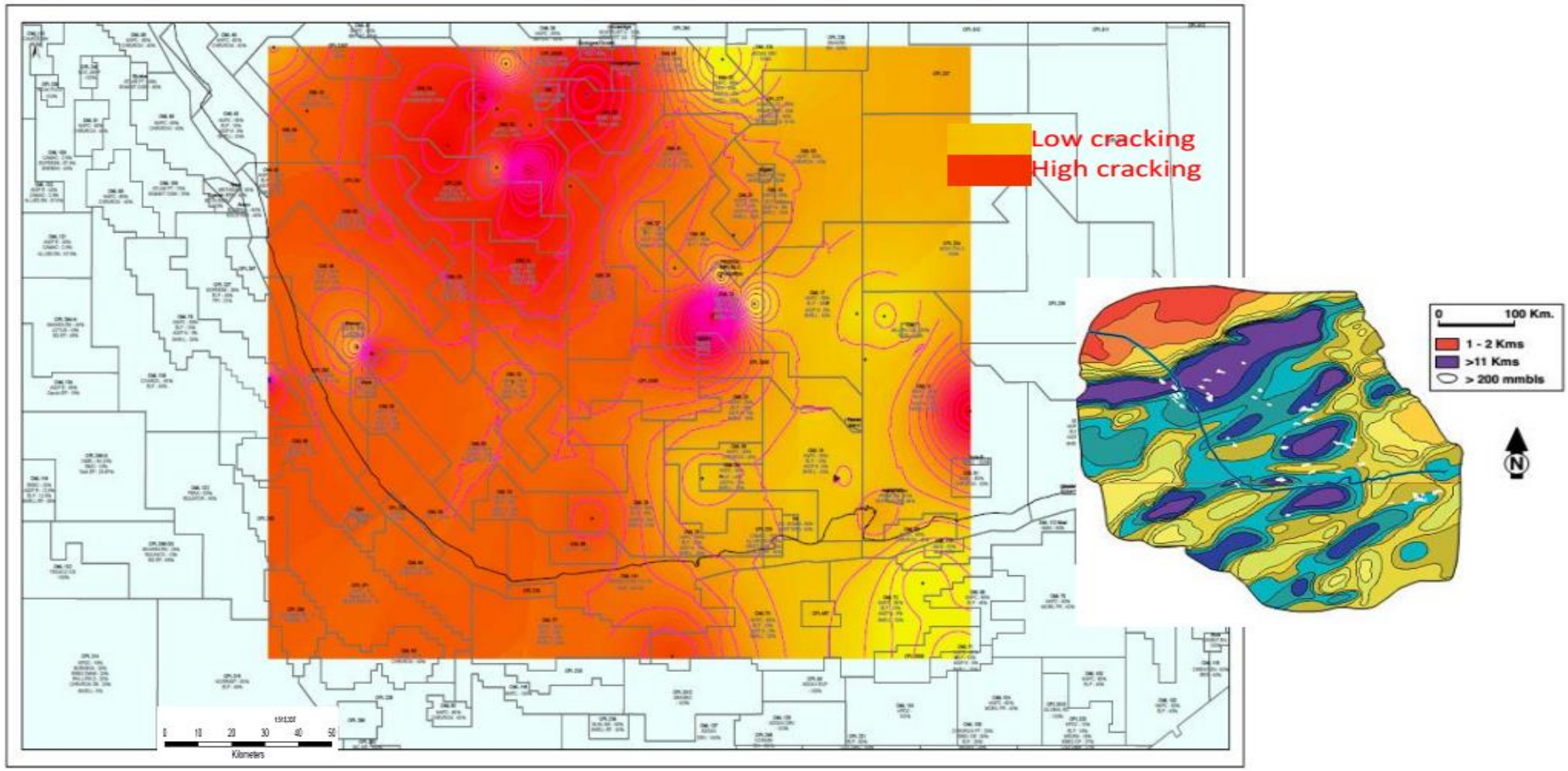

Figure 5.16: Regional diamondoid based cracking map showing high thermal cracking to the west and relatively low thermal cracking to the Eastern part of Niger Delta. Sediment thickness map of the Delta after Haack *et al* (2000) is inserted (Map was produced by Sadat Kolonic based on generated 3+4 MD results).

Diamondoid concentrations are known to increase appreciably with the onset of oil to gas cracking and are mainly generated through the condensate and wet gas generation stage (Fang *et al*., 2012) and are also of importance as they can be used in basins with mixed sourced oils consisting of low maturity oil and high maturity cracked oil (Dahl *et al*., 1999; Wei *et al*., 2007; Azevedo *et al*., 2008; Fang *et al*., 2012; Araujo *et al*., 2012).

The extent of thermal cracking (i.e. the percentage of original liquid converted to gas and pyrobitumen) was calculated based on the formula proposed by Dahl *et al*., 1999.

Extent of cracking = $[1-(C_0/C_C) * 100]$

C_0 = concentration of 3+4 methyldiamantane in the uncracked sample (diamondoid baseline)

C_C = concentration of 3+4 methyldiamantane in the cracked sample.

To know the extent of cracking and mixing in the Niger Delta oil samples, a plot of stigmastane (C_{29}ααα20R sterane) against 3+4-methyldiamantane (3+4MD) concentration (Figure 5.17) shows that the oil in the basin has been mixed to a variable extent with the cracked oils, in most cases up to about 50-90% mixed with oil of lower thermal maturity (Figure 5.17). The mixing percentage was calculated based on the following assumption:

1. Evaporative fractionation and biodegradation which will potentially concentrate the diamondoids was not put into account when calculating diamondoids concentration.
2. All oil samples irrespective of their source has same stigmastane (C_{29}ααα20R sterane) concentration at the same thermal maturity level.
3. There is no secondary contribution to stigmastane (C_{29}ααα20R sterane) concentration either during migration or in reservoir apart from expelled hydrocarbon source.
4. The stigmastane (C_{29}ααα20R sterane) concentration is only an indication of the thermal maturity of the hydrocarbon that has not been cracked.

The Central Delta oil samples appear to have been mixed with highly cracked oils, while Eastern oil samples have been mostly mixed with less cracked oil, which may be related to sediment thickness of >11 km in the Central Delta and far lower thickness in the Eastern Delta. The Southern and Western parts of the Delta have a wide range of mixing percentages.

The oil diamondoid baseline concentration was assumed to be 10 ppm, since no pure end member oil sample that was mature but not cracked/biodegraded/fractionated, and from the same highly mature source, was available. However, the maximum diamondoid (3+4-methyldiamantane) concentration of the studied source rock extracts was approximately 6 ppm, though those are thought to be the ones that generated lower maturity oil. Nevertheless, this gives an idea of the cut-off point for samples that have neither been cracked nor mixed with other highly matured oil. The 3+4-methyldiamantane used for calculating cracking extent, does not show any appreciable variation with biodegradation (Wei *et al*., 2007).

There is a possibility that the extent of oil cracking has been overestimated due to evaporative loss of light hydrocarbons during storage and laboratory separation (e.g. Wei *et al*., 2007), however, this approach is thought to be more accurate and yield more reliable results than the gas to oil ratio (GOR) approach due to difficulty in estimating the shrinkage factor (e.g. Welte *et al*., 1997)

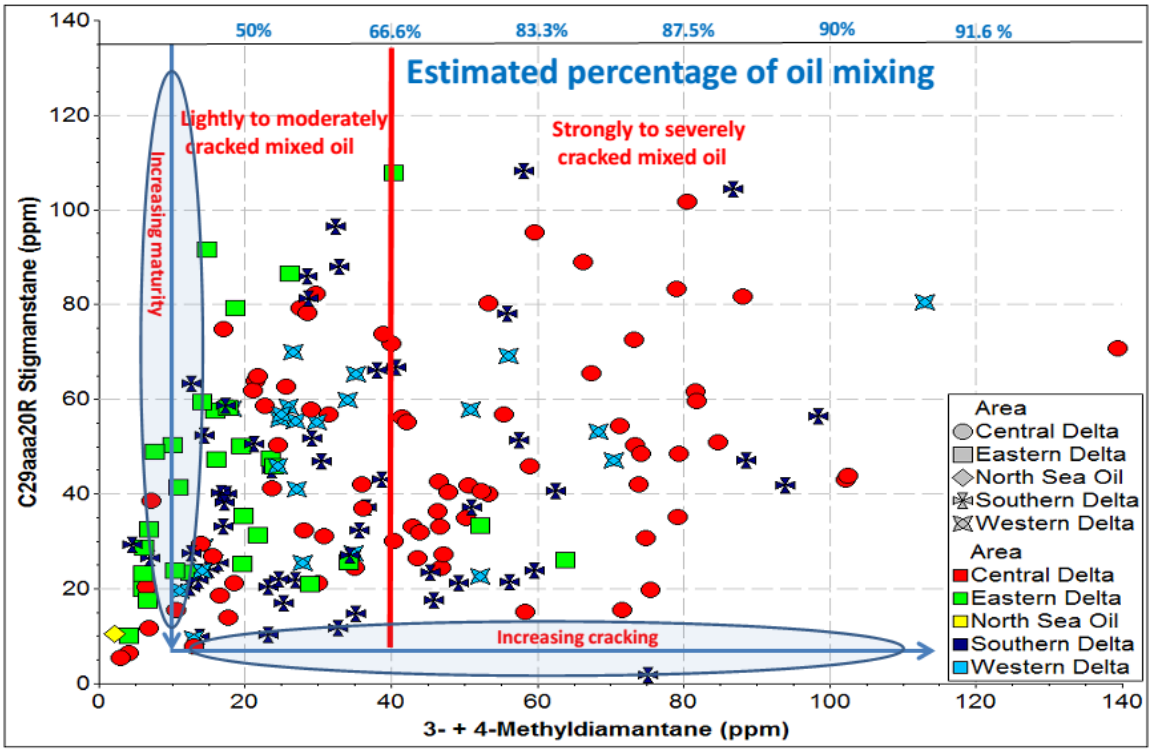

Figure 5.17: Plot of C_{29} ααα 20R stigmastane against 3- + 4-methyldiamantane concentrations, indicating cracking and mixing in Niger Delta oils (modified after He *et al.*, 2012). Note the large extent of cracking percentage and that sample OEE180 appears to be an end member for the highly mature oils (with 75 ppm of 3+4 MD with very low stigmastane concentrations). Note the position of the North Sea oil on the plot which enables comparison with an uncracked but thermally matured marine sourced oil.

5.3.4 Summary of kerogen type, source and thermal maturity information from the diamondoid hydrocarbons.

Based on the results from diamondoid hydrocarbon analyses, it can be summarised that:

1. The Niger Delta oil samples are sourced from a Type II kerogen
2. The oil were sourced from a source rock deposited in a marine environment
3. The oil samples are of very high maturity i.e. late oil window to early gas window (%R_0 = 1.1 to 1.6).
4. The oil samples contain thermally cracked oil, with most samples having more than 50% cracking index.
5. The Eastern Delta region contains the least cracked oils, whereas the Central Delta region is the most cracked.

6. The intensity of cracking appears to be controlled by the sediment pile thickness in the basin.
7. There has been intense mixing of the highly cracked mature oil with those of lower thermal maturity.
8. The mature oil has mostly contributed the greatest proportion in the mixing ratio.

5.4 Oil characterisation from aromatic hydrocarbons

Mono-, di- and triaromatic, including steroidal aromatic, hydrocarbons are present in sediments and crude oils and have found uses in source, deposition environment, correlation and maturity studies (Mackenzie *et al*., 1982; Moldowan *et al*., 1985; Moldowan & Fago, 1986; Radke & Welte 1983; Radke *et al*., 1982; 1988; 1986).

The aromatics are more resistant to biodegradation than many alkane molecular markers and therefore their results may be more accurate in samples that are either marginally biodegraded (Radke 1987) and also in samples of high thermal maturity when biomarkers have been destroyed (Peters *et al*., 2005).

5.4.1 Source environment of deposition

The Niger Delta oil samples analysed in this study appear to be mainly sourced from marine shales (e.g. Figure 5.18) because they generally have lower C_{29} monoaromatic steroids and few samples are terrigenous sourced as indicated by their high contents of C_{29} monoaromatic steroids (Figure 5.18). A few (14) samples, from different regions of the delta (Central, Eastern, Western and Southern regions), show indications that they were sourced from marine carbonates, but this might be misleading as oil samples sourced from algal dominated settings with little land plant input tend to plot in the marine carbonate region of such figures (Peters *et al*., 2005). Therefore, it is likely that those 14 oil samples were actually sourced from marine environments with little higher plant input and probably more algal influence (Figure 5.18).

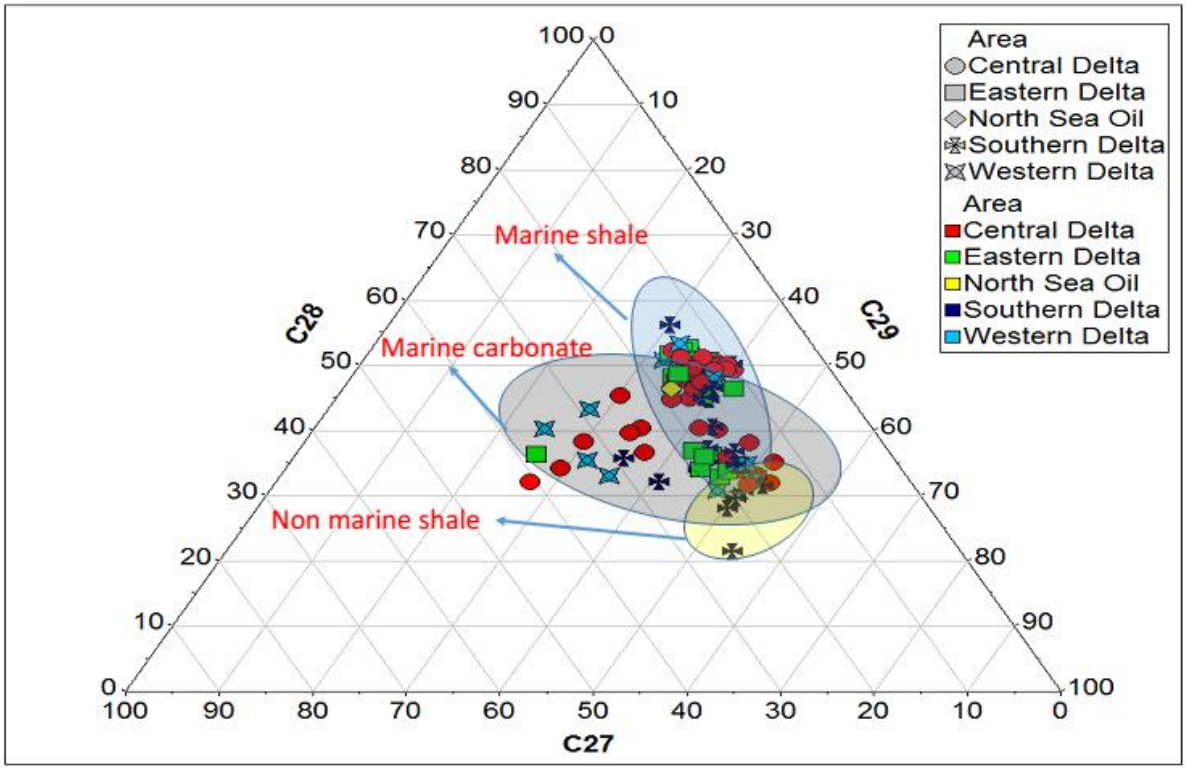

Figure 5.18: Source environment of deposition ternary plot of C_{27}-C_{28}-C_{29} C-ring monoaromatic steroids showing the Niger Delta oil samples (modified after Moldowan *et al*., 1985). Note the North Sea oil enables comparison with a known marine shale sourced oil.

5.4.2 Thermal maturity, cracking and reservoir mixing

There have been many conflicting reports on the thermal maturities of the Niger Delta oils mainly due to the different maturity parameters used for determining them. Although several authors have used different maturity parameters, Sonibare *et al*., (2008) and Akinlua & Ajayi (2009) pointed out that the Niger Delta oil are generally mature based on aromatic maturity parameters. They present results based on calculated vitrinite reflectance and MPI-2 showing that the Niger Delta oils are of peak to late oil window maturity (Figure 5.19). Unlike the results of the thermal maturity measurements based on the gasoline range hydrocarbons, which indicate that the North Sea oil is more mature than the Niger Delta oil samples, the aromatic parameter results shown in Figure 6.19 indicate otherwise.

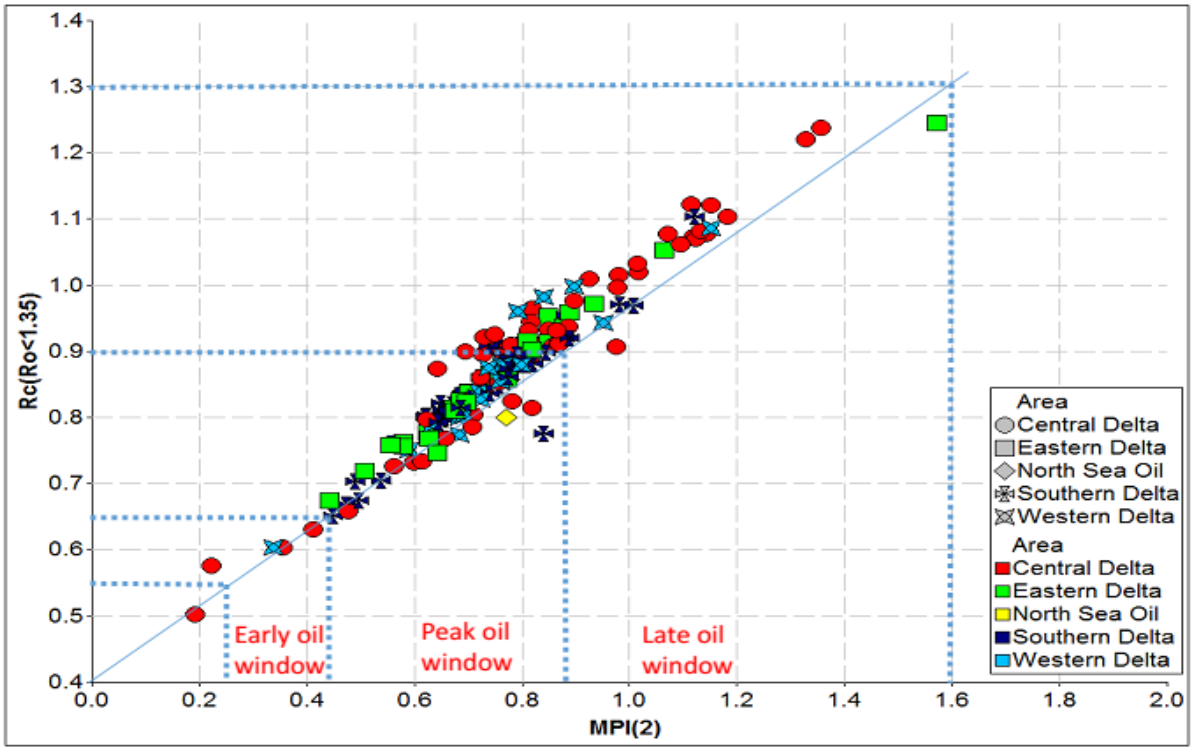

Figure 5.19: Plot of calculated vitrinite reflectance [0.6(MPI-1) + 0.4] against MPI-2 showing that the Niger Delta oil samples are in the peak to late oil window maturity range. Note the North Sea oil enables comparison with a mature marine sourced oil.

When two oil samples of different maturities are mixed together in a 50:50 ratio, the TMN distribution will be a reflection of the higher maturity oil and the PMN distribution will reflect that of the lower maturity oil (van Aarssen *et al*., 1999), the relationship of the TMNr, TeMNR and PMNr will therefore be distorted (van Aarssen *et al*., 1999).

A ternary plot of PMNr, TeMNr and TMNr is supposed to have all oil samples plotting inside the maturity centre if the oil has not been mixed or biodegraded (van Aarssen *et al*., 1999), but most of the Niger Delta samples plot outside the maturity centre (Figure 5.20) towards the TMNr axis, indicating that the Niger Delta oil samples are mixtures of different maturity oils. On the other hand, some samples, including the North Sea oil, plot inside the maturity centre, indicating that those oil samples have not been mixed, though it is not clear how a mixed oil sample will behave if the maturities of the contributing sources are similar.

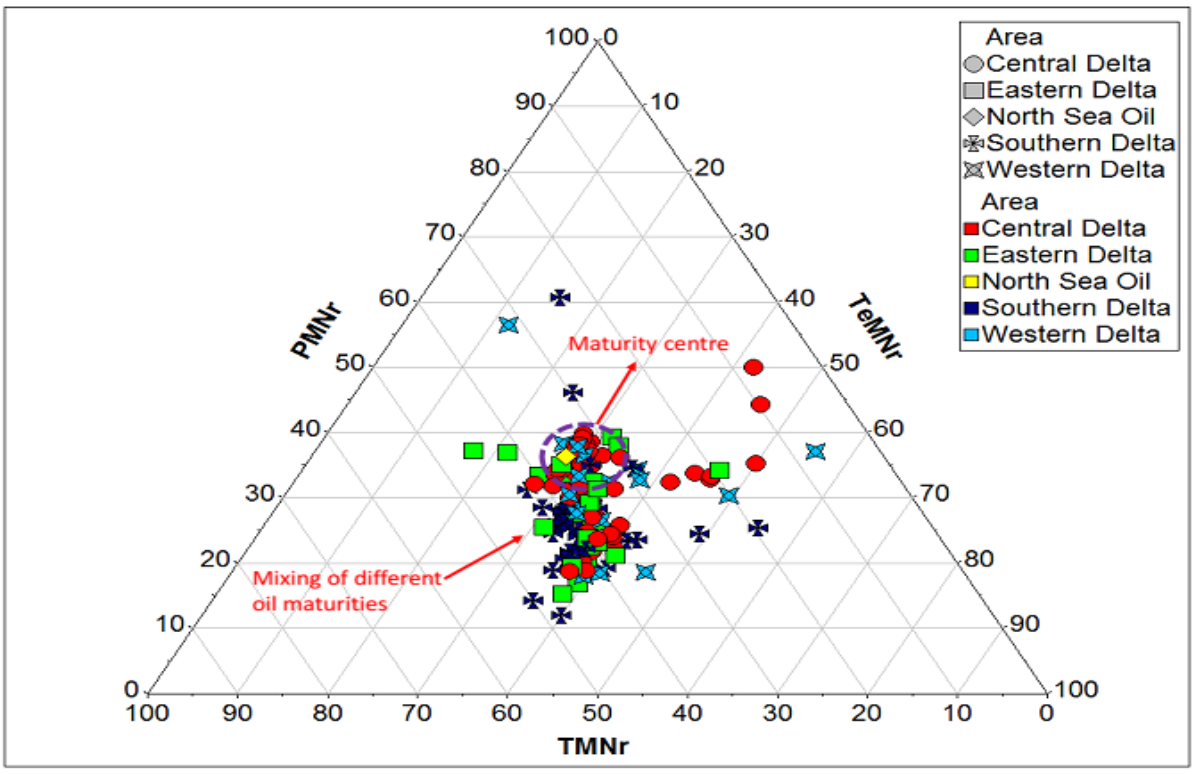

Figure 5.20: Ternary plot of TMNr, TeMNr and PMNr. Showing most Niger Delta oil samples plotting outside the maturity centre, which indicates mixing of oils with different maturities, or with indigenous organic matter, or biodegradation effects (modified after van Aarssen *et al*., 1999). Note the North Sea oil enables comparison with a mature marine sourced oil.

5.4.3 Summary of kerogen type, source and thermal maturity from aromatics hydrocarbon.

Based on the results from the aromatic hydrocarbons it can be summarised that:

1. The Niger Delta oils are mostly of marine origin with the possibility of some being sourced from non-marine depositional environments.
2. The source rocks are shales with variations in their higher plant inputs.
3. Most Niger Delta oils are thermally mature and are in the peak to late oil window (%VR_o equivalent 0.65 to 1.3).
4. The Niger Delta oil samples are potentially mixtures of oils of different thermal maturities.
5. The highly mature sources have contributed higher percentages to those mixed oils.

5.5 Oil characterisation from sterane biomarkers

Steranes are derived from steroids which are ubiquitous in plants and animals and they retain some of their characteristics even after diagenesis, but can lose or add new functional groups (Summons & Capons, 1988; 1991; Killops & Killops, 1993) and can also be affected by bacterial reworking of regular steroids (Moldowan *et al*., 1991).

The structural variations and carbon numbers of the steranes provide information about source, environment of deposition and thermal maturity (Huang & Meinschein 1979; Seifert & Moldowan 1981; MacKenzie 1984; Peters *et al*., 2005).

5.5.1 Source kerogen type

The Niger Delta oil samples can be said to be derived from mixed planktonic/bacterial/land plants (Figure 5.21), four samples (OEE37, OEE38, OEE82, OEE83) appears to have been sourced from mixed planktonic/bacterial without land plant inputs, but on close examination those samples have been biodegraded to PM level 6 which might explain the distortion in their peaks especially in their C_{29} 5α(H),14α(H),17α(H) 20R steranes . The Central Delta oils appears to have more land plant input and the Western Delta oil samples appear to have less land plant input.

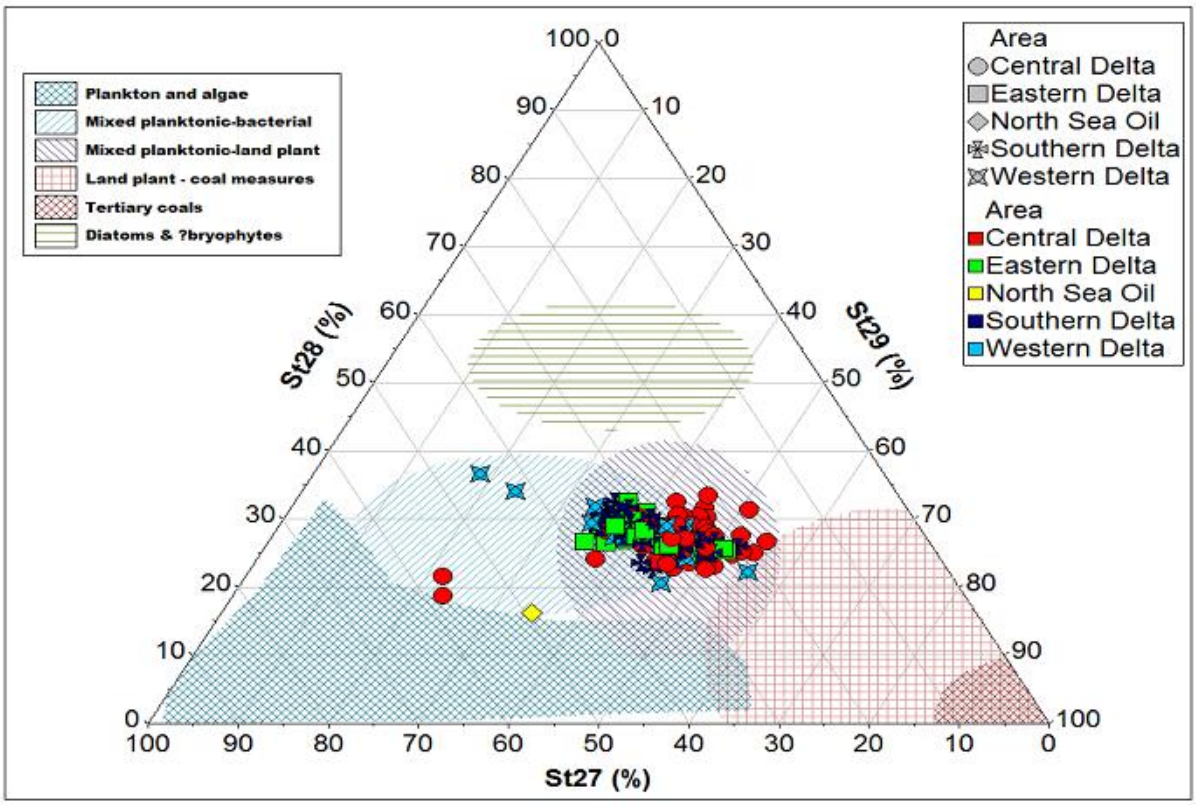

Figure 5.21: Ternary diagram showing the distribution of C_{27}, C_{28} and C_{29} regular steranes of 5α(H),14α(H),17α(H) 20R configuration in the Niger Delta oil samples. Organic matter interpretational overlay from p:IGI 3.5 (modified after Huang and Meinschein 1979). Note the North Sea oil enables comparison with a marine sourced oil.

5.5.2 Source environment of deposition

The ternary plot of C_{27}, C_{28} and C_{29} regular steranes with the 5α(H),14α(H),17α(H) 20R configuration has been a useful tool for source, depositional environment and correlation studies (Peters *et al*., 2005) but there is a possibility of overlaps in the interpretational fields. Moldowan *et al*. (1985) suggested that the plot should be used in association with the monoaromatics ternary plot (e.g. Figure 5.18) which show less overlap. Based on the sterane ternary plot, the Niger Delta oil samples were deposited in open marine/shallow marine/deltaic deposition settings (Figure 5.22), with most of the samples deposited in the shallow marine and fewer deposited in the deltaic depositional settings.

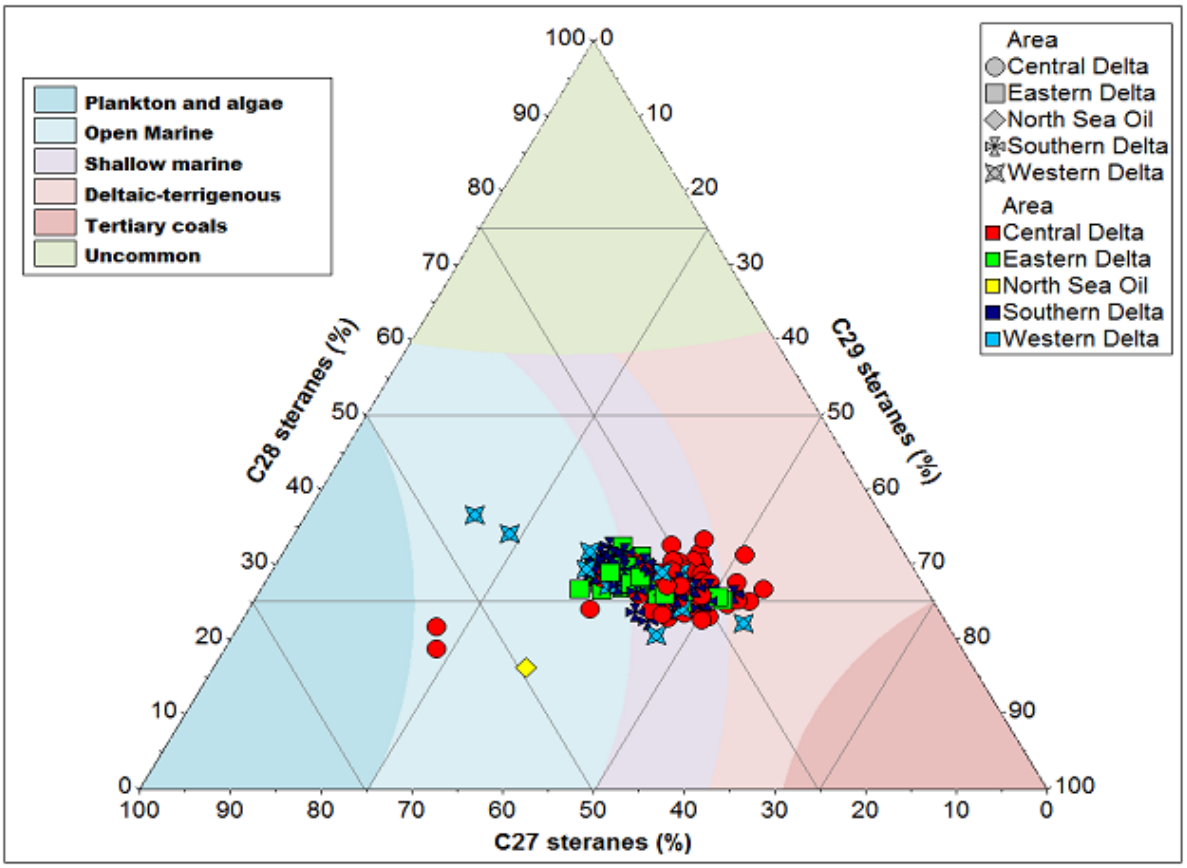

Figure 5.22: Ternary diagram showing the distribution of C_{27}, C_{28} and C_{29} regular steranes of 5α(H),14α(H),17α(H) 20R configuration of the Niger Delta oil samples. Depositional environment interpretational overlay from p:IGI 3.5 (modified after Huang and Meinschein 1979). Note the North Sea oil enables comparison with a marine sourced oil.

The sterane/hopane ratio reflects the level of influence of eukaryotic versus prokaryotic inputs in the source rock (Moldowan *et al*., 1985) and related oil samples are known to have similar values, but the ratio can be influenced by maturity (Seifert & Moldowan, 1978; Killops *et al*., 1988). A high sterane/hopane ratio indicates high contributions from marine organic matter (Moldowan *et al*., 1985) and a low sterane/hopane value indicates a terrigenous input or reworked organic matter (Tissot & Welte, 1984).

It can be concluded that the Niger Delta oil samples have terrigenous influence and do not show marine influence as much as the North Sea oil. The Eastern Niger Delta oil samples generally have more marine influence and the Central Delta samples generally have more terrigenous influence, the other two regions (Western and Southern Delta) show a wide range of influences (Figure 5.23). It should be noted that the 5 samples (OEE81, OEE82,

OEE37, OEE38 and OEE151) that plot away from the general trend have been biodegraded up to PM level 6 (Figure 5.23). It should also be pointed out that elevated C_{29} steranes can be derived from some marine cyanophytes (Moldowan *et al*., 1985) and not only from terrigenous sources.

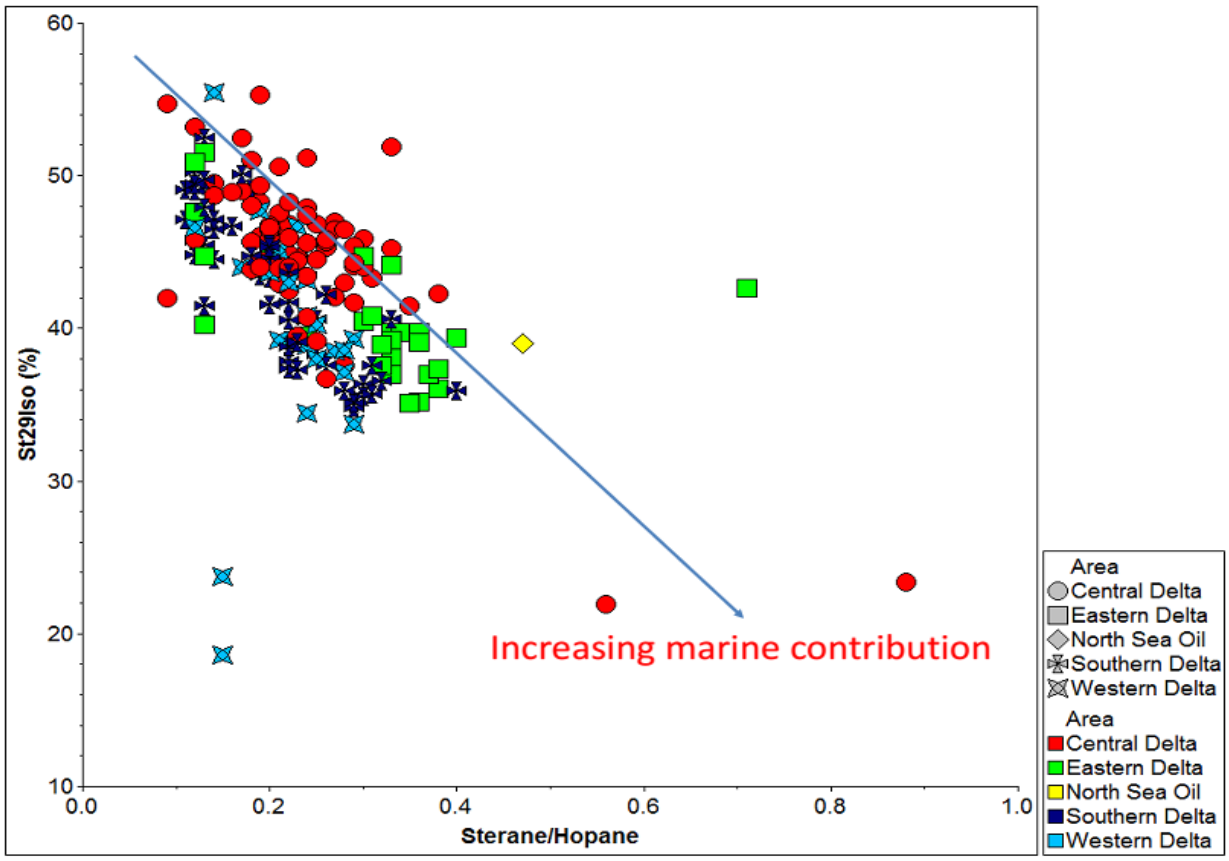

Figure 5.23: Plot of percentage C_{29} αββ (20S+20R) against sterane/17α(H)-hopane (($C_{27\text{-}29}$ ααα 20S+20R + $C_{27\text{-}29}$ αββ 20S+20R)/(C_{29}H +C_{30}H + $C_{31\text{-}33}$ 22S+22R)) ratios showing marine contributions to the Niger Delta oil samples. The five Niger Delta oil outliers have been biodegraded up to PM level 6. Note the North Sea oil enables comparison with a marine sourced oil.

5.5.3 Thermal maturity

Sterane isomerisation parameters have been used as thermal maturity indicators for Niger Delta oils and the result from this study indicates that the Niger Delta oil appear to be of low thermal maturity, whereas the North Sea oil is of peak oil window thermal maturity (Figure 5.24). This result is consistent with the work of Sonibare *et al*. (2008) and Akinlua & Ajayi (2009), but the sterane isomerisation ratio has been seen to be misleading in many Tertiary oils around the world because they are generally not at equilibrium due to rapid

sedimentation (e.g. Mackenzie & Mckenzie, 1983) and low heating rate (e.g. Grantham, 1986).

Facies overprint, weathering, biodegradation can influence sterane isomerisation (e.g. Peters *et al*., 1984; Moldowan *et al*., 1986; Huang *et al*., 1989; Peters *et al*., 2005) which can give high 20S/20S+20R results, especially because of the removal of the 20R epimer (Seifert *et al*., 1984). The sterane isomerisation plot (Figure 5.24) shows that there is a positive correlation between both parameters (Seifert & Moldowan, 1986) and the few samples that do not show this strong correlation can be as a result of differential source rock heating rate (Mackenzie & Mckenzie, 1983) and/or clay catalysis influence (Huang *et al*., 1990). Migration contamination has also been known to cause low sterane epimer maturity ratios because of the addition of immature hydrocarbons to mature oil and this has been seen in a wide range of samples around the world especially in Tertiary deltas (e.g. Hoffmann *et al*., 1984; Curiale & Bromley, 1996; Curiale *et al*., 2005).

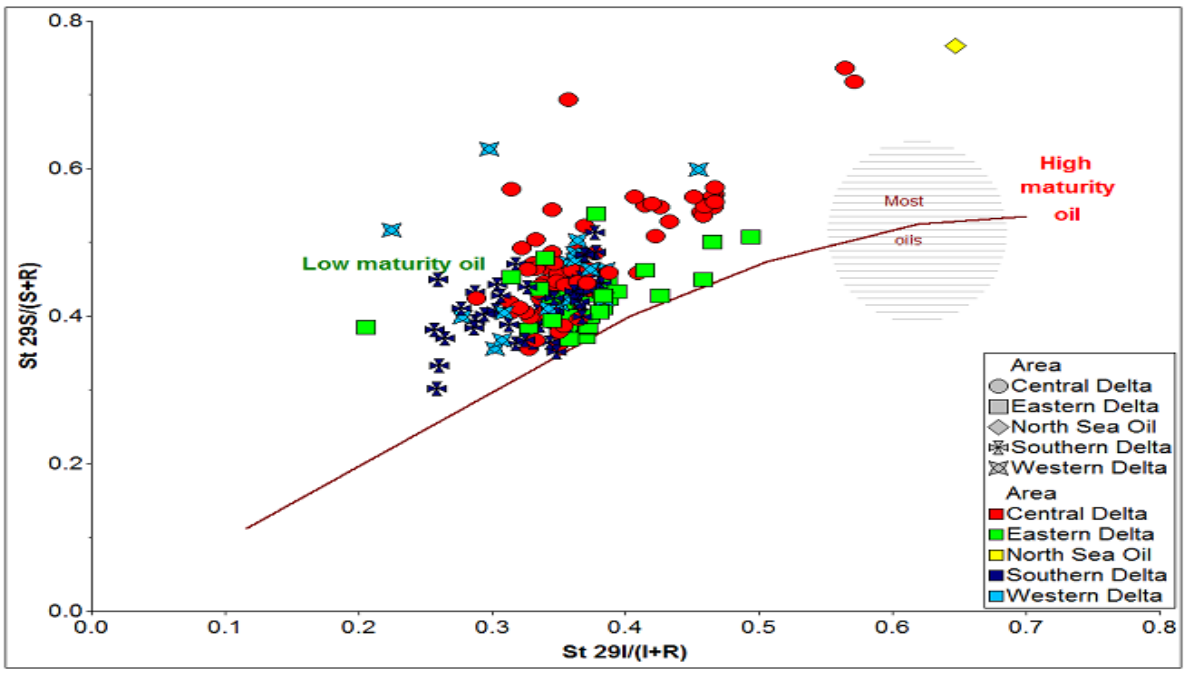

Figure 5.24: Plot of C_{29} 20S/20S+20R (5α(H),14α(H),17α(H)) against C_{29} I/I+R (5α(H),14β(H),17β(H)-20S +20R)/ (5α(H),14α(H),17α(H)- 20S+20R) sterane isomerisation maturity parameters showing that most of the Niger Delta oil samples appear of low maturity (modified after Seifert & Moldowan, 1986). Note the North Sea oil enables comparison with a thermally mature marine sourced oil. Interpretation overlay from p:IGI 3.5.

The 20S/(20S+20R) isomerisation in the C_{29} 5α,14α,17α(H)-sterane at the C-20 and the ββ/(ββ+αα) isomerisation at the C-14 and C-17 in the C_{29} 20S and 20R are known to be valid maturity indicators from the immature to mature range (Seifert & Moldowan, 1986), however a cross plot of the diasterane/sterane ratio (total C_{27-29} 13β,17α(H) 20S+20R diasteranes/ total C_{27-29} 5α,14β,17β(H) and 5α,14α,17α(H) 20S+20R) against the pregnane ratio (C_{21} +C_{22} regular sterane/ total C_{29} steranes) was used to further cross check this result to ascertain its validity in these samples as both these two ratios are regarded as valid even to early post mature (Peters *et al*., 2005).

The abundance of the pregnanes increases with increased thermal maturity relative to the regular steranes (p:IGI geochemical manual 2004) and the diasteranes are more stable than the regular steranes (Peters *et al*., 2005), however these ratios are affected by lithology and depositional environment (Moldowan *et al*., 1991; McKirdy *et al*., 1985). Results shows that the Niger Delta oil samples appear to be low thermal maturity and the North Sea oil is of a higher thermal maturity (Figure 5.25). The two outlier sample (OE037, OE038) are biodegraded up to PM level 6.

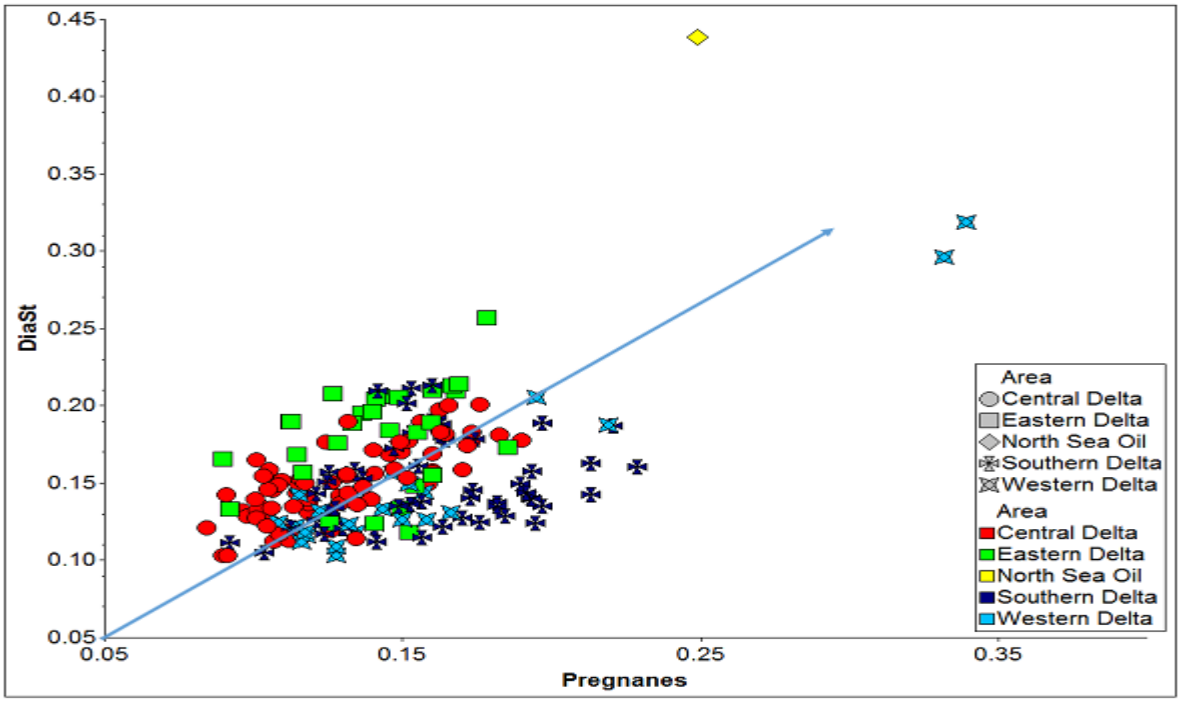

Figure 5.25: Plot of diasterane/sterane ratios against the pregnane ratios, showing that most of the Niger Delta oil samples appear of lower maturity than the thermally mature North Sea oil.

5.5.4 Sterane hydrocarbons summary

Based on the results from sterane and hopane hydrocarbons it can be summarised that:

1. The Niger Delta oil are mostly from marine depositional environment sources with some deltaic inputs
2. The oil is sourced from mixed planktonic/bacterial/land plant material.
3. The Niger Delta oils appear to be of low thermal maturity.

5.6 Oil characterisation from hopane biomarkers

The terpanes are made up of the sesquiterpanes, diterpanes, triterpanes and tetraterpanes, and are mostly used as organic matter source indicators (e.g. Seifert & Moldowan 1978; Aquino Neto *et al*., 1983; ten Haven 1988; Ekweozor & Telnaes 1990; Killops *et al*., 1998; Peters *et al*., 2005), depositional environment indicators (e.g. Seifert & Moldowan 1978; Aquino Neto *et al*., 1983; ten Haven 1988; Mello *et al*., 1988; Blanc & Connan 1992; Ekweozor & Telnaes 1990; Killops *et al*., 1998; Peters *et al*., 2005), and as thermal maturity indicators (e.g. Seifert & Moldowan 1978, 86; Cornford *et al*., 1983) because of their ubiquitous nature in oils and source rocks (Peters *et al*., 2005).

5.6.1 Source environment of deposition

The ratio of the C_{35} regular hopane/ C_{34} regular hopane can help to indicate redox conditions during deposition, with high values indicating anoxia while low values indicate oxic deposition condition (Peters & Moldowan 1991). Oil samples with exceptionally high values greater than 0.8 are thought to be sourced from carbonates rather than shale source rocks (Peters *et al*., 2005). Based on the C_{35} regular hopane/ C_{34} regular hopane ratio it can be concluded that the Niger Delta oil samples were sourced from mainly dysoxic/oxic depositional environments with minor anoxia (Figure 5.26). However this ratio cannot be used as a standalone parameter when discussing paleo-environment of deposition as it is known to be influenced by high hydrogen index of the source rock which can be as a result

of source organic matter type and excellent preservation conditions (Rangel *et al*., 2000) and also it decreases with increase in thermal maturity (Peters & Moldowan, 1991).

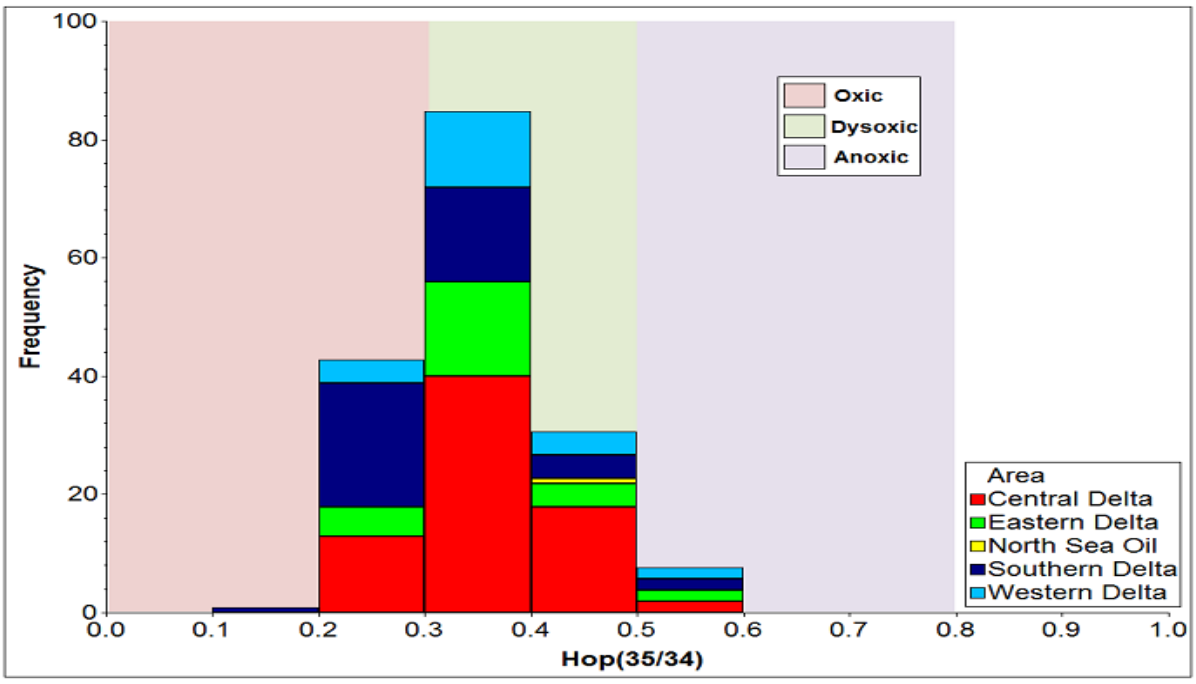

Figure 5.26: Source deposition environments inferred from C35/34 hopane ratios for the Niger Delta oil samples. The wide range of the ratio (0.1 to 0.6) reflects variable source rock depositional environments (e.g. ten Haven *et al*., 1988). Interpretational overlay is from IGI's p:IGI-3.5 software. Note the North Sea oil enables comparison with a marine sourced oil.

The ternary plot of percentage C_{29}, C_{30} and C_{31} 17α(H)-hopanes can be used to differentiate oils sourced from marine shales, lacustrine, coal and carbonate source origins. This ratio is useful for source/facies discrimination from the beginning of the oil window (Killops *et al*., 1998). It can be concluded that the Niger Delta oil samples were sourced from a marine shale (Figure 5.28) although there exists some likelihood that some samples might have either been sourced from coal beds or lacustrine environments (Figure 5.27).

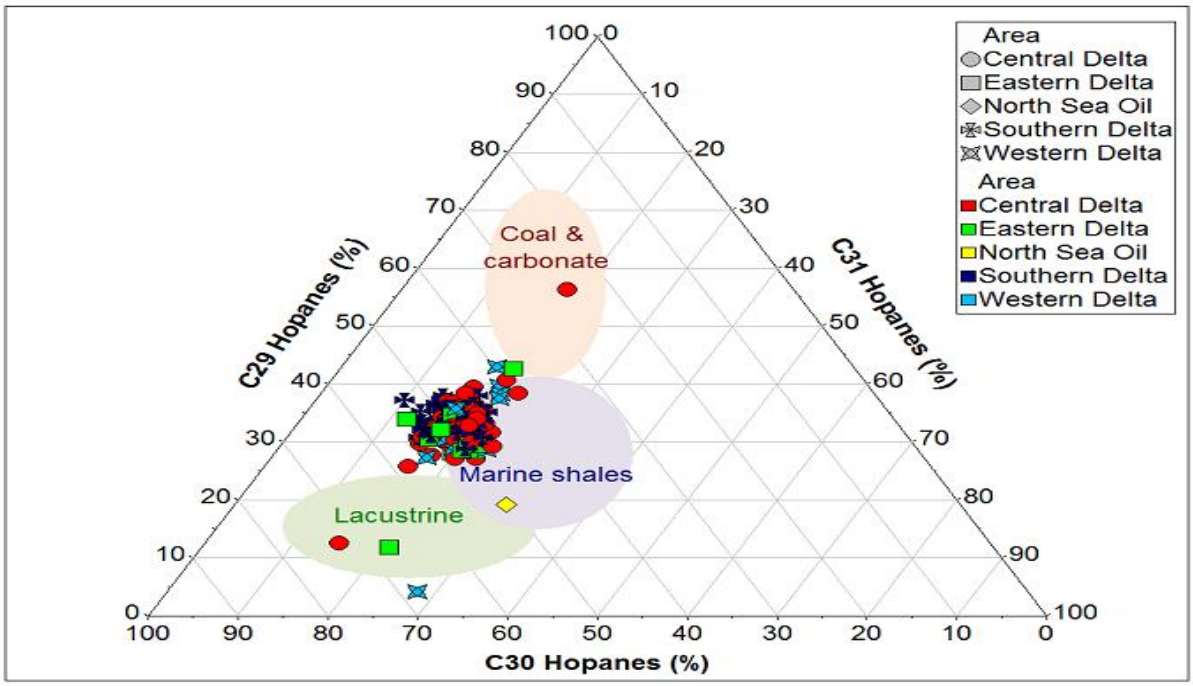

Figure 5.27: Ternary diagram showing the distribution of C_{28}, C_{29} and C_{30} hopanes in the Niger Delta oil samples indicating that they were sourced from marine shales (c.f. Killops *et al*., 1998). Interpretational overlay from p:IGI 3.5. Note the North Sea oil enables comparison with a marine shale sourced oil.

Samuel *et al*. (2010) identified novel tricyclic terpanes in Niger Delta oils and were able to use those terpanes to separate the Niger Delta oils into deep water (marine), shallow water (transitional) and onshore (terrigenous) source facies and they further show that parameters based on those compounds which he called the tricyclic terpane terrigenous indices (TTTI, $X/X+C_{20}$, and $Y/Y+C_{24}$) were not affected by thermal maturity, although this current project shows that oil maturity in the Niger Delta is dependent to a large extent on oil mixing ratios and how they affects the part/range of oil under investigation (i.e. gasoline range, diamondoids, aromatics, sterane and hopane biomarkers etc.) rather than just isomerisation of hopane and sterane biomarkers.

The plot of $X/X+C_{20}$ against $Y/Y+C_{24}$ tricyclic terpanes terrigenous indices (Figure 5.28) shows that most of the samples were sourced from a transitional environment, with the Eastern Delta oils showing relatively more marine contribution and the Southern Delta oil showing relatively more terrigenous contribution (Figure 5.26). The CSIA of individual *n*-alkanes (Figure 5.9) indicated that the Southern Delta oil has a substantial fluvio-deltaic

source influence, which is consistent with the interpretation from the novel tricyclic terpanes. In further support of this, a plot of Y/Y+C_{24} tricyclic terpanes against oleanane index (Figure 5.29) shows a positive correlation and almost a mirror image of the TTTI plot, while the only difference seen with this plot is that the oleanane index can increases with biodegradation, whereas the TTTI does not because oleanane is more resistant to biodegradation than the C_{30} αβ hopane used in calculating this ratio.

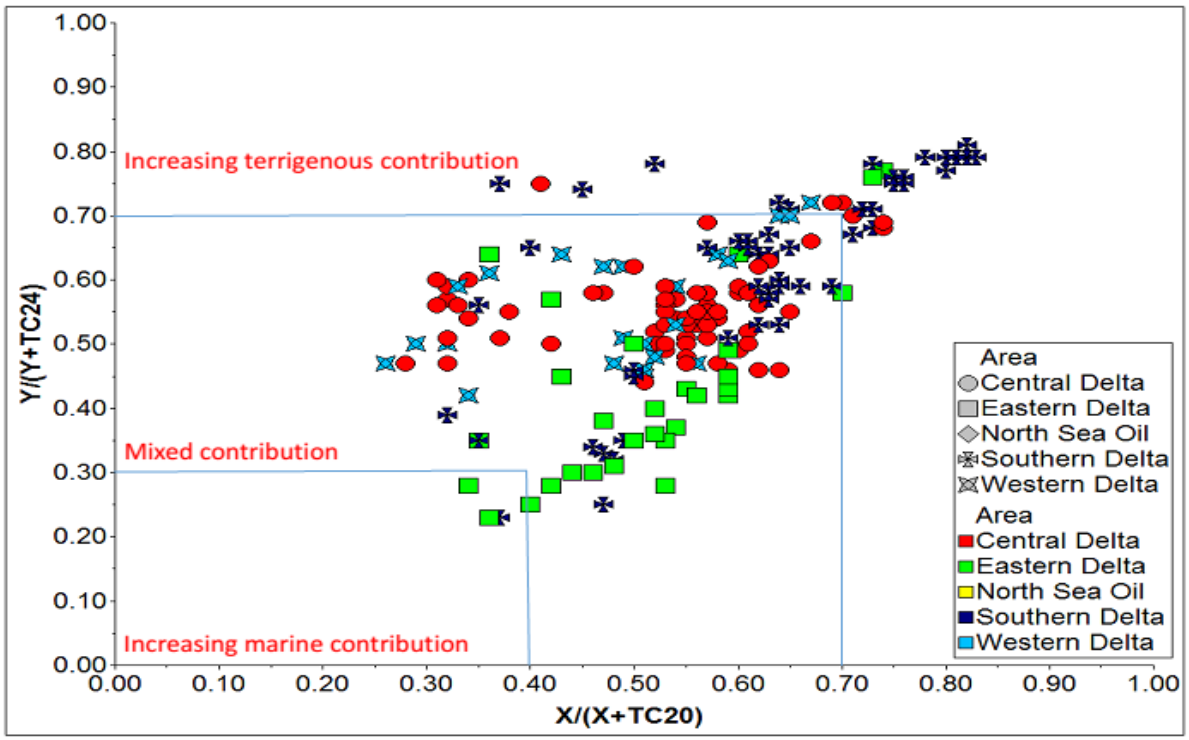

Figure 5.28: Plot of X/X+C_{20} against Y/Y+C_{24} tricyclic terpane terrigenous index (TTTI). X and Y are two unidentified tricyclic terpanes, while C_{20} and C_{24} are the well-known tricyclic terpanes containing 20 and 24 carbons (modified after Samuel *et al.*, 2009).

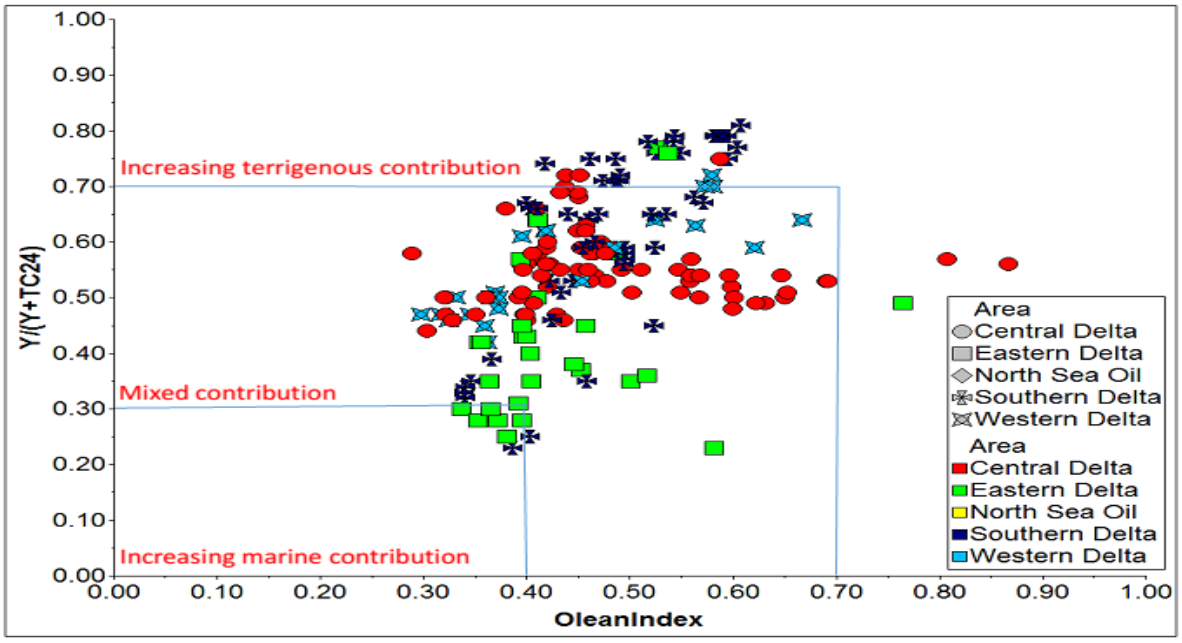

Figure 5.29: Plot of oleanane index against Y/Y+C_{24} tricyclic terpane terrigenous index (TTTI). Y is the unknown C_{25} tricyclic terpanes, while C_{24} is the well-known tricyclic terpane containing 24 carbons (modified after Samuel *et al*., 2009).

The presence of oleanane in crude oil has been attributed to higher plant input (Ekweozor & Udo 1988; Martin *et al.*, 1989) from Cretaceous or younger age and the Niger Delta oil has been shown to be abundant in them (Ekweozor *et al*., 1979). However, its absence in an oil sample does not necessarily mean that the oil was sourced from a source older than the Cretaceous age (Moldowan *et al*., 1994; Peters *et al*., 1999b), also oleanane preservation has been known to be enhanced if the precursors are deposited in deltaic environments and diagenesis takes place while the area is under some marine transgression (Murray *et al*., 1997). This ratio increases towards the offshore in some basins because of the influence of the marine environment (e.g. Beaufort Sea, reported by McCaffrey *et al*., 1994; Mahakam Delta, reported by Peters *et al*., 2000). The oleanane index has been known to vary with thermal maturity and comparison of this ratio in samples of different maturity has been discouraged (Ekweozor & Telnaes, 1990). Therefore, this ratio can be used to ascertain the relative contribution from higher plants, deposition environment and possible age.

Samuel (2008) used some unidentified terpanes to define a K index from five peaks visible in the *m/z* 414 mass chromatogram to calculate this ratio, i.e. (A_1+A_2+B_1+B_2)/C and this

ratio had a positive correlation with oleanane index. The same plot was used for the Niger Delta oils in this study and the result was similar to those from the tricyclic terpanes, except that the K index values for the Central Delta oils were generally lower than 4.The Southern Delta oil samples which have more terrigenous input are shown to have elevated oleanane and K index ratios (Figure 5.30) and those that generally have only elevated oleanane index are samples that have been highly biodegraded (Figure 5.30), therefore while the oleanane index can be influenced by biodegradation, the K index does not show any such influence.

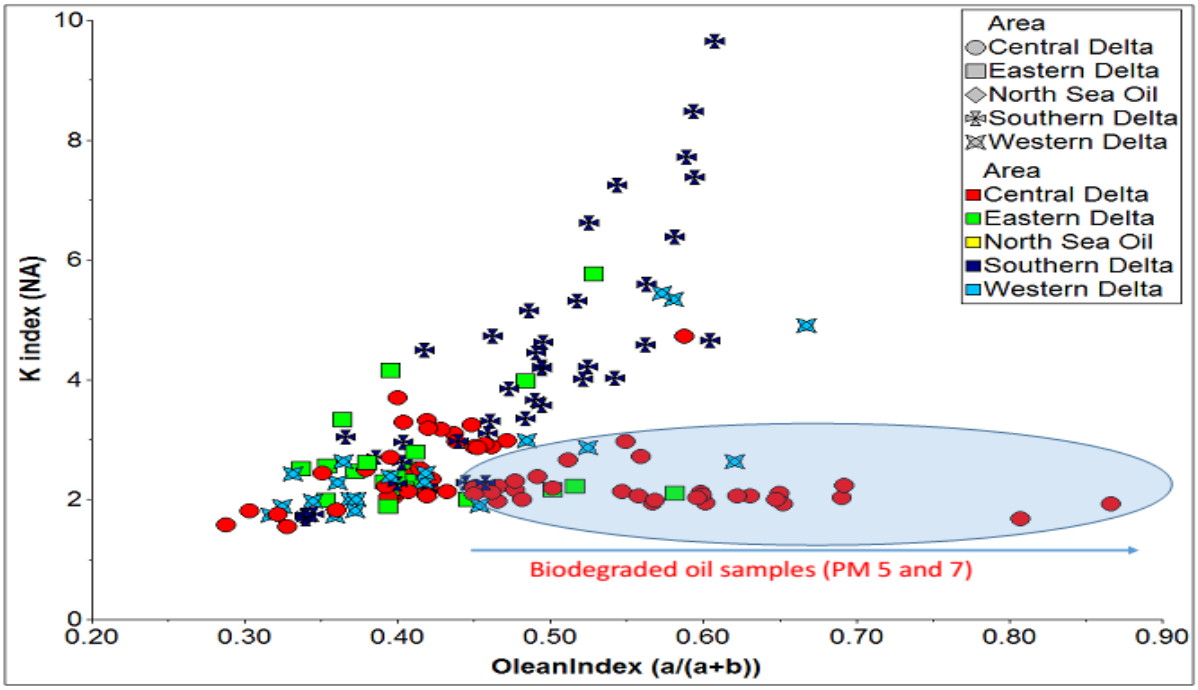

Figure 5.30: Cross plot of oleanane index against K index. Note the increase in biodegradation in the oil samples with elevated oleanane index whereas K index is not affected by biodegradation (Modified after Samuel 2008)

Some novel C_{15} sesquiterpanes were identified in *m/z* 193 mass chromatograms of Niger Delta oils by Nytoft *et al*. (2009) and their structures are similar to the D and E ring part of oleanane, and the ratio (A+B/A+B+C+D) has a strong correlation with the oleanane index, but peaks A+B are absent in marine oils that are older than Jurassic age although they are present in oil of very high thermal maturity, e.g. condensates (Nytoft *et al*., 2009). A plot of these ratios (oleanane index against sesquiterpanes (A+B)/(A+B+C+D)) shows a positive correlation with these oils samples and both are susceptible to biodegradation, with

the oleanane index having a wider range (Figure 5.31). It was noted that the C_{15} sesquiterpane distributions and show patterns and variations in the three peaks, i.e. A+B, C and D, therefore a ternary plot of these 3 peaks was made to help reveal how these C_{15} sesquiterpanes vary in these Niger Delta oils. The plot broadly classifies the samples into two major groups i.e. the Southern Delta oils and the Central Delta oils (Figure 5.32a & 5.32b) and a possibility that Western Delta oils forming a sub group (Figure 5.33b). These C_{15} sesquiterpanes are believed to indicate higher plant input, as peak A+B is absent in the North Sea oil (Figure 5.32a) but might also help correlate these samples into different families. However, peaks C and D are seen to be susceptible to biodegradation and with increase in biodegradation there is a corresponding increase in the relative percentage of the A+B peak. Oil samples that have less than 20% C and more than 55% A+B have been heavily biodegraded to at least PM level 5 (Figure 5.32a).

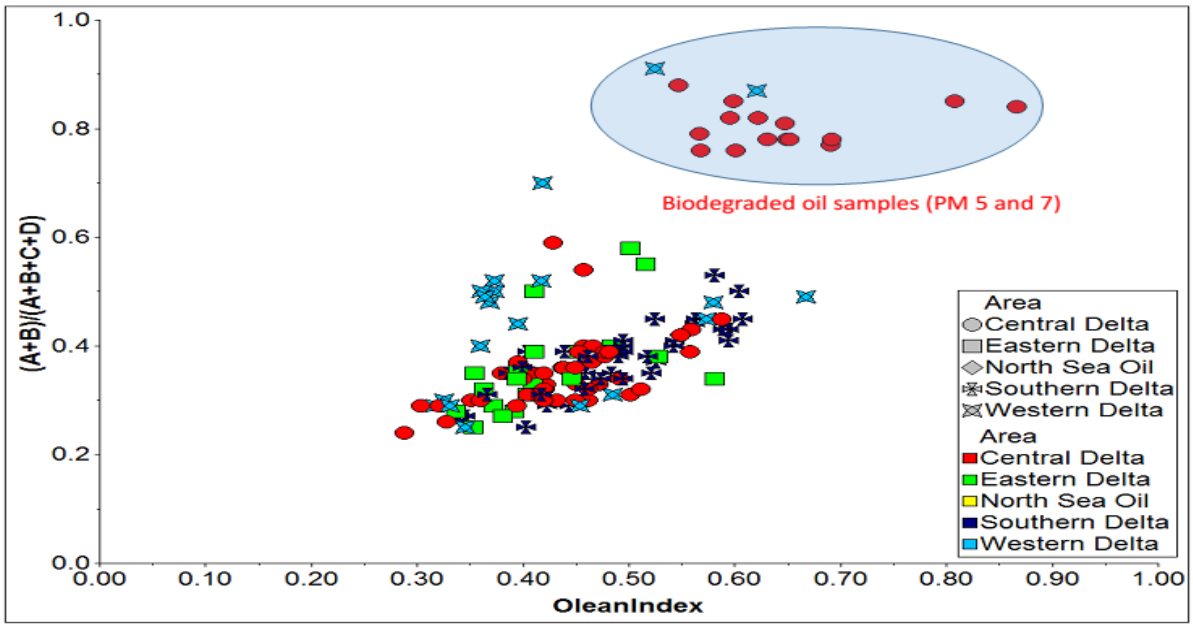

Figure 5.31: Cross plot of oleanane index against sesquiterpanes (A+B)/(A+B+C+D), showing elevated values in highly biodegraded oil samples because of the high resistance of peak (A+B) to biodegradation (modified after Nytoft *et al.*, 2009). Sesquiterpanes were measured from *m/z* 193 and oleanane from *m/z* 191 mass chromatograms.

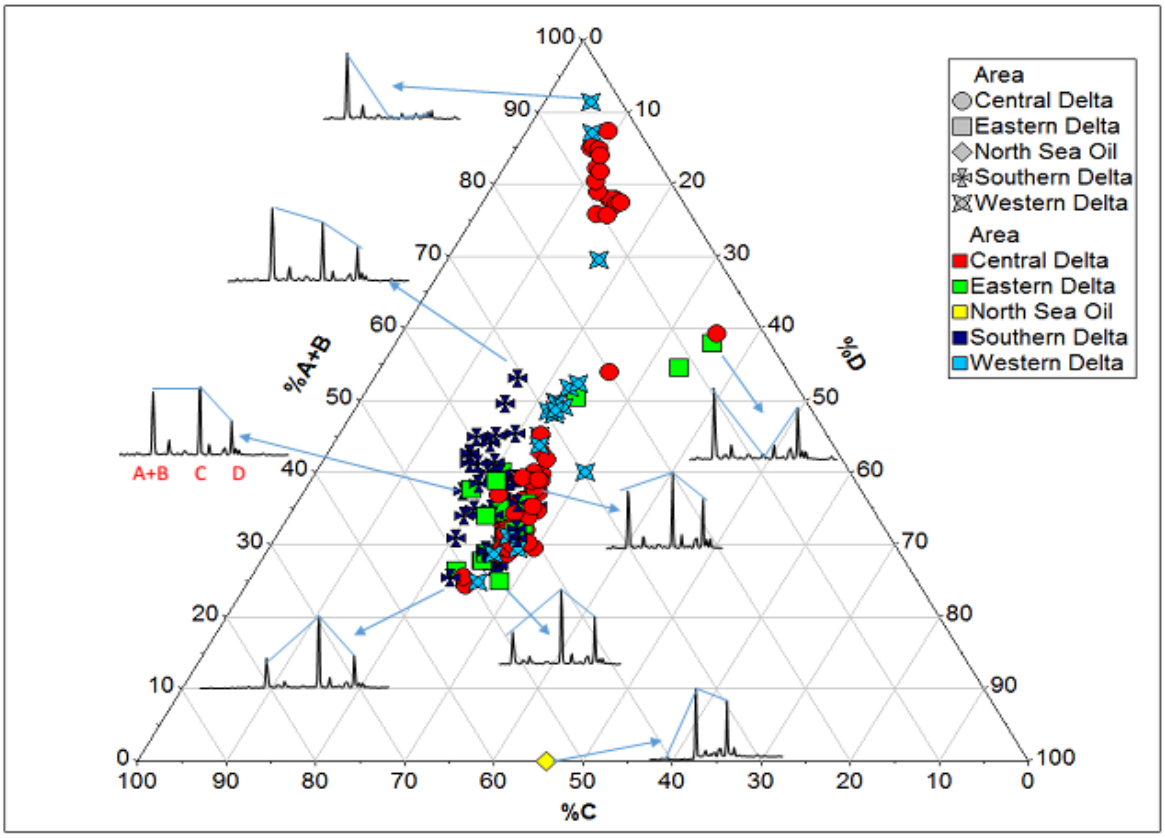

Figure 5.32a: Ternary plot of % A+B, C, D sesquiterpanes from *m/z* 193 mass chromatograms showing the separation of the Southern Delta oil samples from the Central Delta oil samples. Note the North Sea oil does not contain the peak A+B.

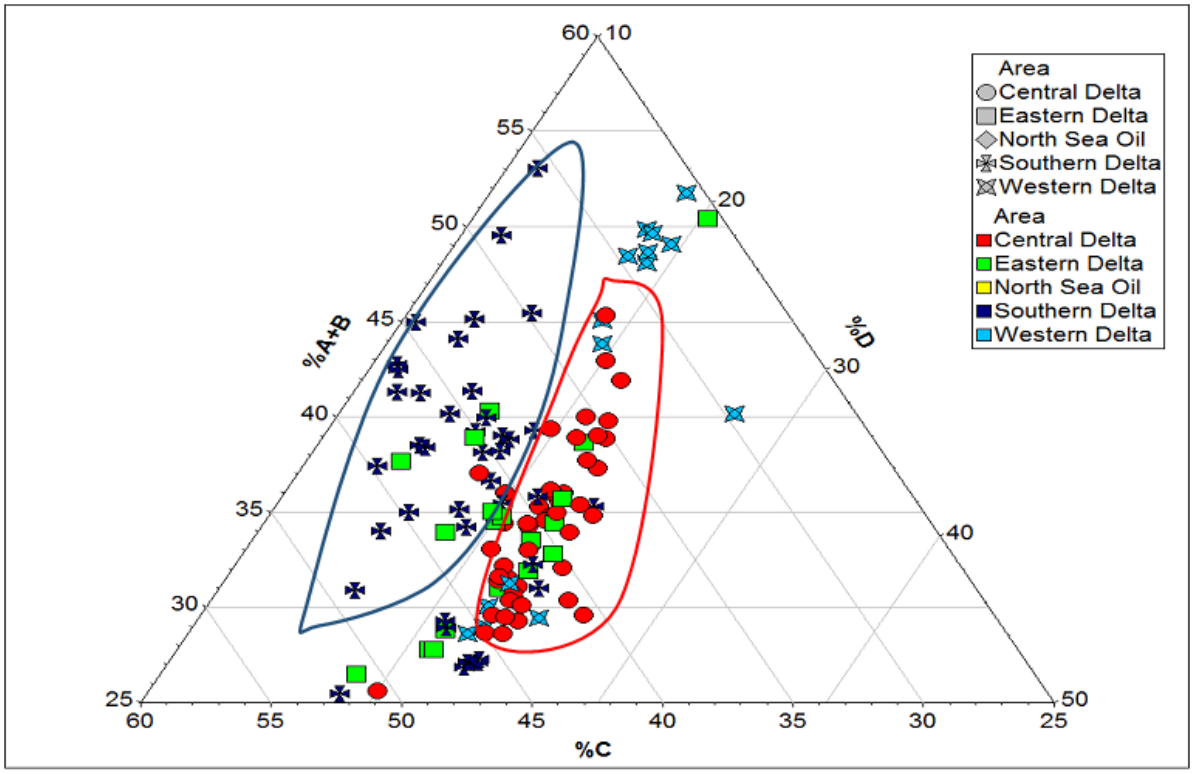

Figure 5.32b: Enlarged ternary plot of % A+B, C, D sesquiterpane data shown in figure 7.33a, showing the separation of the Southern Delta oil samples from the Central Delta oil samples; the Eastern Delta samples are possible a mixtures of oils from both other regions.

An unknown C_{29} triterpane (Peak A) from the *m/z* 191 (Figure 4.25), which has the same retention time as a C_{29} 25-norhopane, was seen to be present in all the Niger Delta oil samples and this peak can also be seen in the *m/z* 191 chromatograms shown in some earlier work (e.g. Eneogwe *et al*., 2002; Eneogwe & Ekundayo 2003; Sonibare *et al*., 2008; Samuel 2008; Samuel *et al*., 2009). The peak has not been identified, but has the same elution time C_{29} 25-norhopane when compared with a West. Shetland oil containing a 25-norhopanes (Figure 5.34a), and it was first thought was that it was a 25-norhopane, but when the *m/z* 177 was compared with the West. Shetland oil, those of the Niger Delta oils do not have the full series of 25-norhopanes peaks in the C_{30} to C_{34} range (Figure 5.33a). There are also small differences in the mass spectra of these two triterpanes (Figure 5.33b) and it is thought that the peak may be related to an oleanane-type triterpane.

A cross plot of oleanane index against the unknown C_{29} hopane/unknown C_{29} hopane + $C_{29}\alpha\beta$ hopane shows an almost perfect correlation between these two parameters, although the Southern Delta oil samples form a separate group from the other Niger Delta oil samples (Figure 6.33c). This result follows the same trends as the K index (Figure 5.30) and also the tricyclic terpanes index (Figure 5.29), which were proposed as possible source, environment of deposition and angiosperm input indicators (Samuel 2008; Samuel *et al*., 2009; Nytoft *et al*., 2009).

A cross plot of the unknown C_{29} hopane/unknown C_{29} hopane + $C_{29}\alpha\beta$ hopane against the C_{15} sesquiterpanes (A+B)/(A+B+C+D) (Figure 5.34) shows a positive correlation but, with a clear indication that the unknown C_{29} hopane/ unknown C_{29} hopane + $C_{29}\alpha\beta$ hopane ratio has a very high range of variation with level of biodegradation (Figure 5.34). This is also seen in figure (5.31) with the oleanane index and it is thought that these ratios can be used in biodegradation studies for unmixed oil especially the ternary plot of % A+B, C, D sesquiterpanes from *m/z* 193 mass chromatogram data (e.g. Figure 5.32).

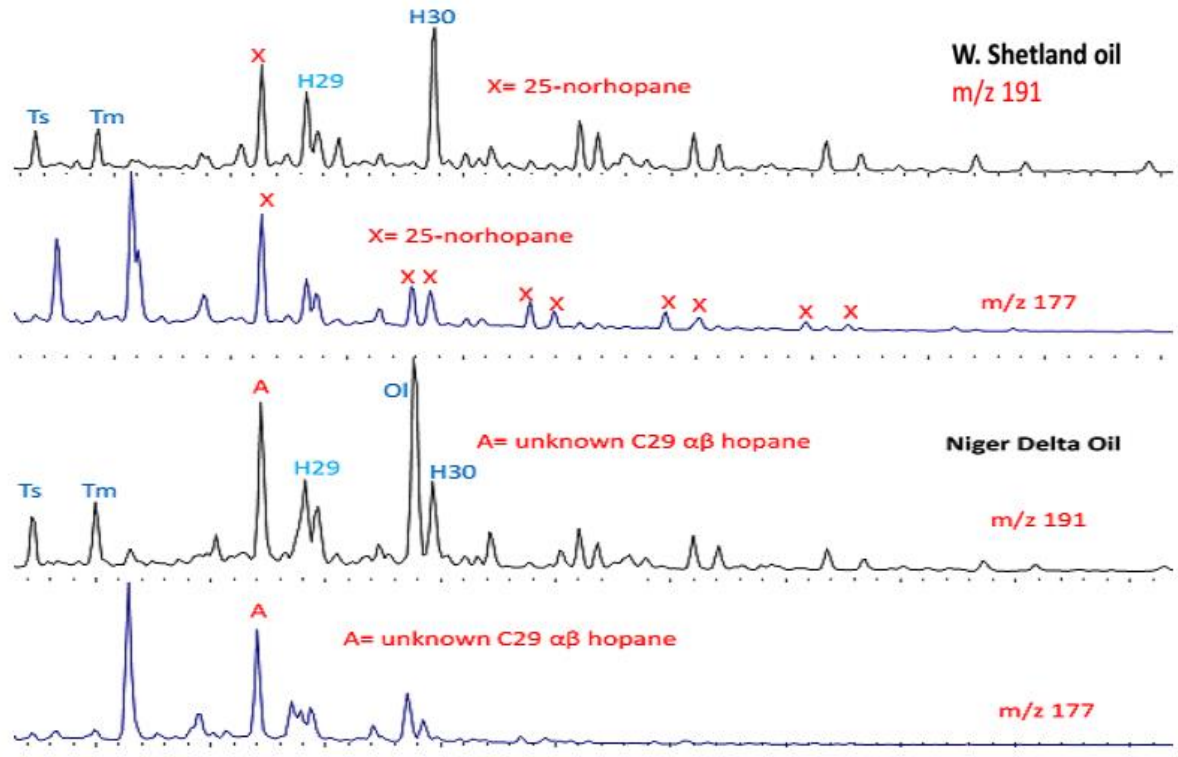

Figure 5.33a: Representative *m/z* 191 and 177 mass chromatograms for W. Shetland oil and Niger Delta oils showing a full range of 25norhopanes in the W. Shetland oil which are absent in the Niger Delta oil (OE083) in *m/z* 177. Note that peak A has the same elution time as the C_{29} 25-norhopane in the West Shetland.

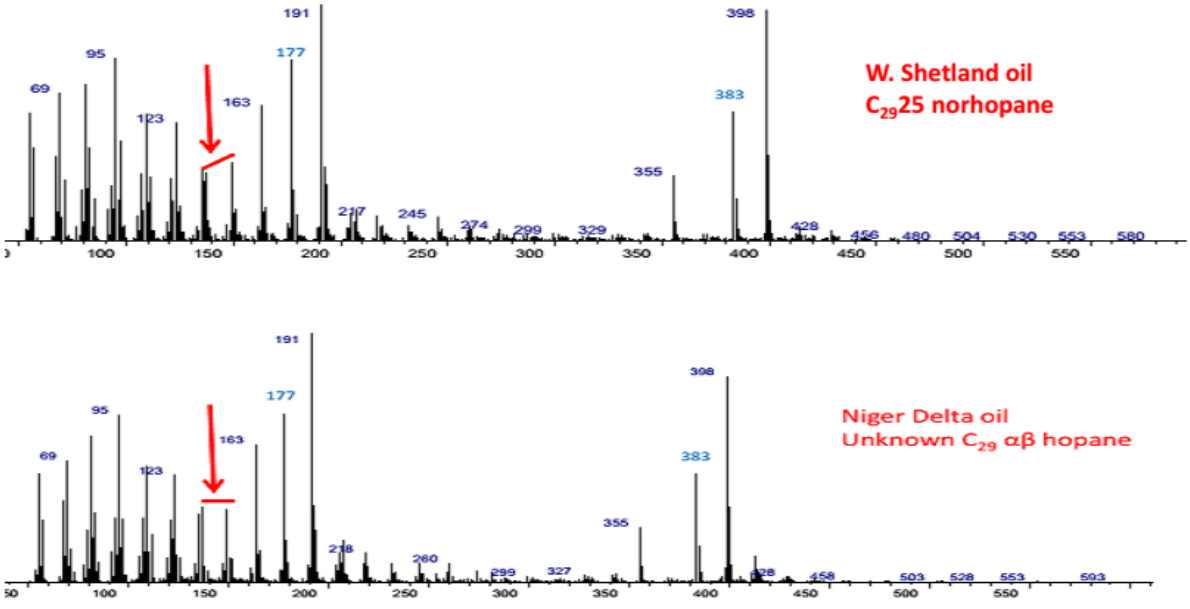

Figure 5.33b: Mass spectra of C_{29} 25-norhopane in West Shetland oil and an unidentified peak A from the Niger Delta oil OE083. The red arrow shows the only noticeable difference in the mass spectra

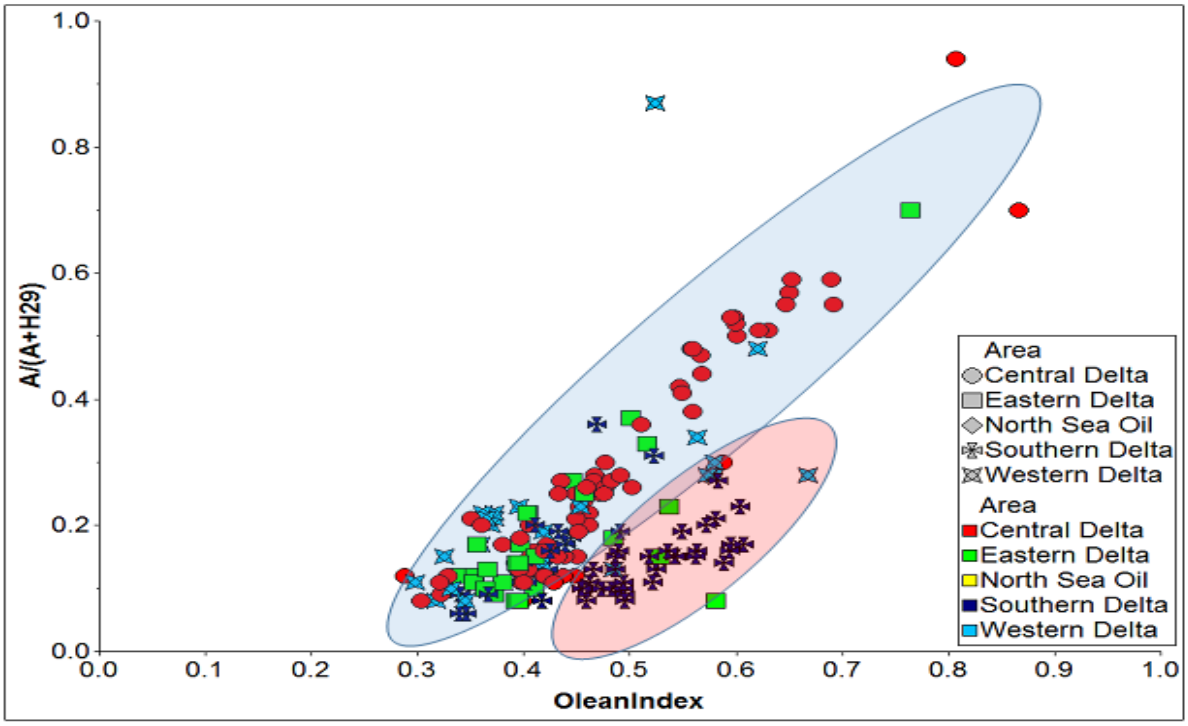

Figure 5.33c: Cross plot of oleanane index against (A)/(A+C29αβ hopane) showing a positive correlation between both parameters. Peak A is an unknown C_{29} hopane shown in *m/z* 191 mass chromatograms. Note the separation of the Southern Delta oils into a sub group.

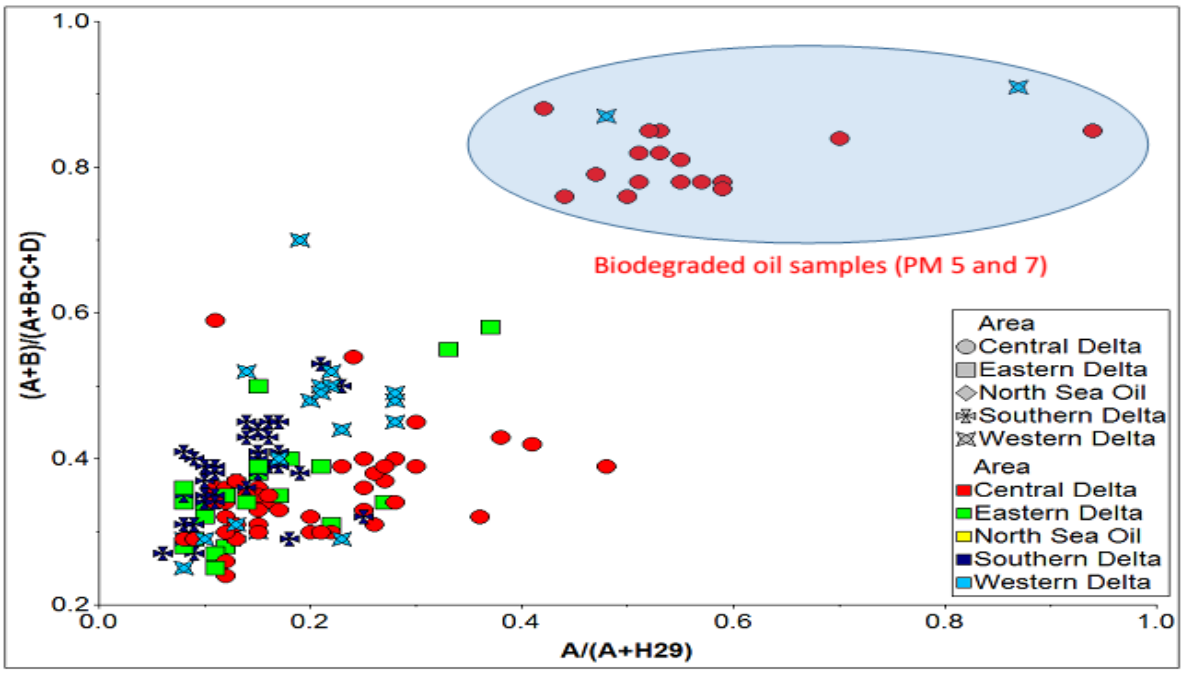

Figure 5.34: Cross plot of C_{15} sesquiterpanes (A+B)/(A+B+C+D) against A/A+C_{29}αβ hopane ratios showing elevated values in highly biodegraded oil samples because of the relatively high resistance to biodegradation of peaks (A+B) from the *m/z* 193 and peak A from *m/z* 191 mass chromatograms, respectively.

5.6.2 Thermal maturity

The thermal maturity parameters of oil samples calculated from molecular marker ratios have been shown to have several limitations, which include influence of limited ranges of validity, source/facies, deposition environment, mixing, effects etc., (Peters *et al*., 2005). It has also been noted that reduced concentrations of biomarker are an indication of high thermal maturity (e.g Mackenzie *et al*., 1985; Dahl *et al*., 1999). The 22S/(22S+22R) homohopane isomerisation maturity parameter is very popular and has been used for maturity interpretations in several Niger Delta studies (e.g Ekweozor & Udo 1987; Sonibare *et al*., 2008; Samuel *et al*., 2009; Lehne & Dieckmann, 2010). However, this index is only useful for immature to early mature oils (Peters *et al*., 2005) and the equilibrium has been known to occur at as low as 0.5% vitrinite reflectance in Mahakam Delta rocks (Schoell *et a*l., 1983), though fully isomerised homohopanes have also been found in immature rocks (Moldowan *et al*., 1982).. Nevertheless, values lower than 0.5 have also been reported in crude oil from the Gippsland Basin in Australia (Philip 1982) The calculated 22S/(22S+22R) homohopane isomerisation ratios for the Niger Delta oil samples do not show any correlation with other terpane maturity parameters and this might be an indication of mixing of oils of different thermal maturities.

The Ts/Ts+Tm ratio, although dependent on source, is valid from immature to post-mature maturity ranges (Moldowan *et al*., 1986) and is a generally reliable maturity indicator when dealing with same type of source e.g. shale facies or carbonate facies (McKirdy *et al*., 1983; Rullkotter *et al*., 1985; Peters *et al*., 2005). Based on this ratio it is indicated that the Niger Delta oil samples are of mid-mature (0.4 to 0.6 %VRo equivalent) and the North Sea oil plots in the same range (Figure 5.35). The C_{29}(Ts/Ts+Tm) which is complementary to the Ts/Ts+Tm ratio, gives the same indications that the samples are of mid-maturity; it should also be noted that all samples that plot above the North Sea oil in Figure 5.36, have been biodegraded to at least PM level 6 especially the Central Delta oils.

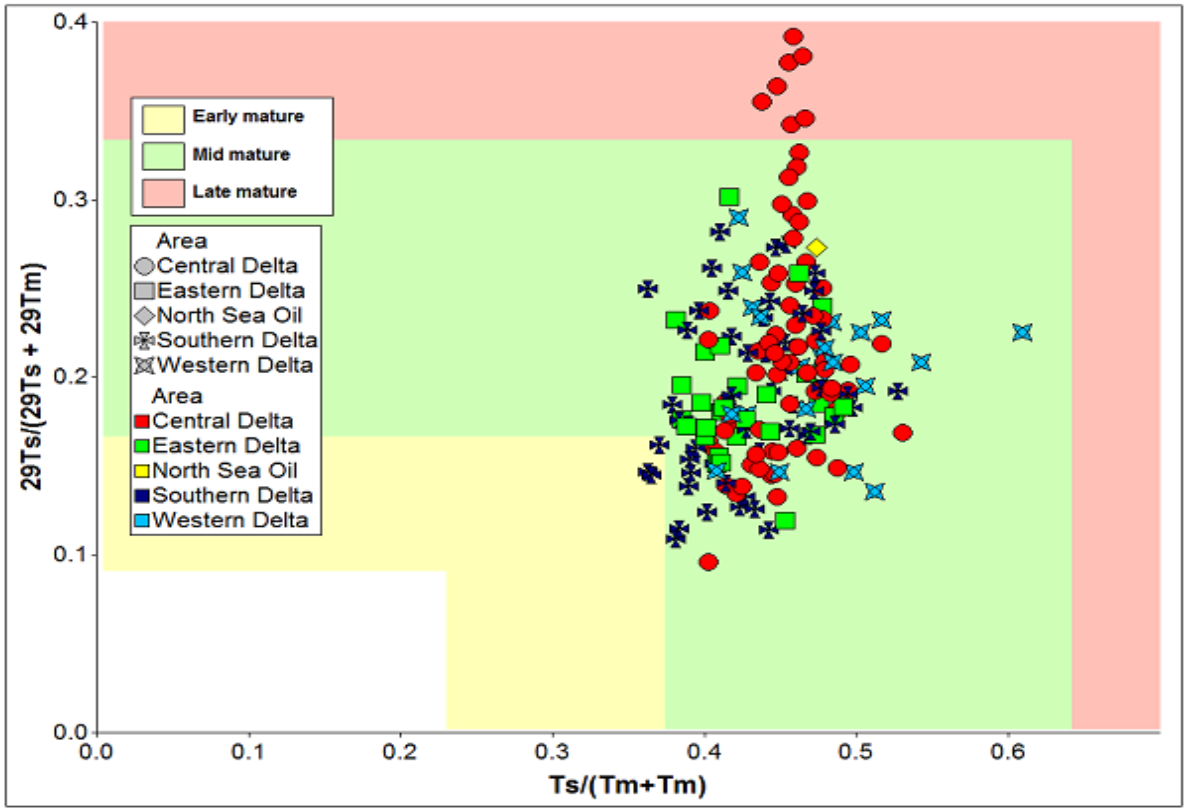

Figure 5.35: Plot of Ts/Ts+Tm against 29Ts/29Ts+29Tm hopane maturity parameters, showing that the samples are of mid oil window maturity. Note that all the Central Delta oil samples with apparent elevated maturity are biodegraded to at least PM 6. The North Sea oil enables comparison with a thermally mature, marine sourced oil. Interpretation overlay is from p:IGI 3.5 software.

While the Ts/Ts+Tm ratio indicates that the Niger Delta oil samples are of mid-maturity, with thermal maturities generally lower than the North Sea oil, the hopane/moretane and the diahopane/normoretane ratios, which are highly specific for immature to early oil generation (Seifert & Moldowan 1980; Mackenzie *et al*., 1980) shows that the Niger Delta oil samples are mainly of low thermal maturity and even lower than the North Sea oil (Figure 5.36). However, although these ratios have been shown to depend on source input/ depositional environment (Rullkotter & Marzi 1988), interpretations based on them correlate with other hopane and sterane thermal maturity ratios.

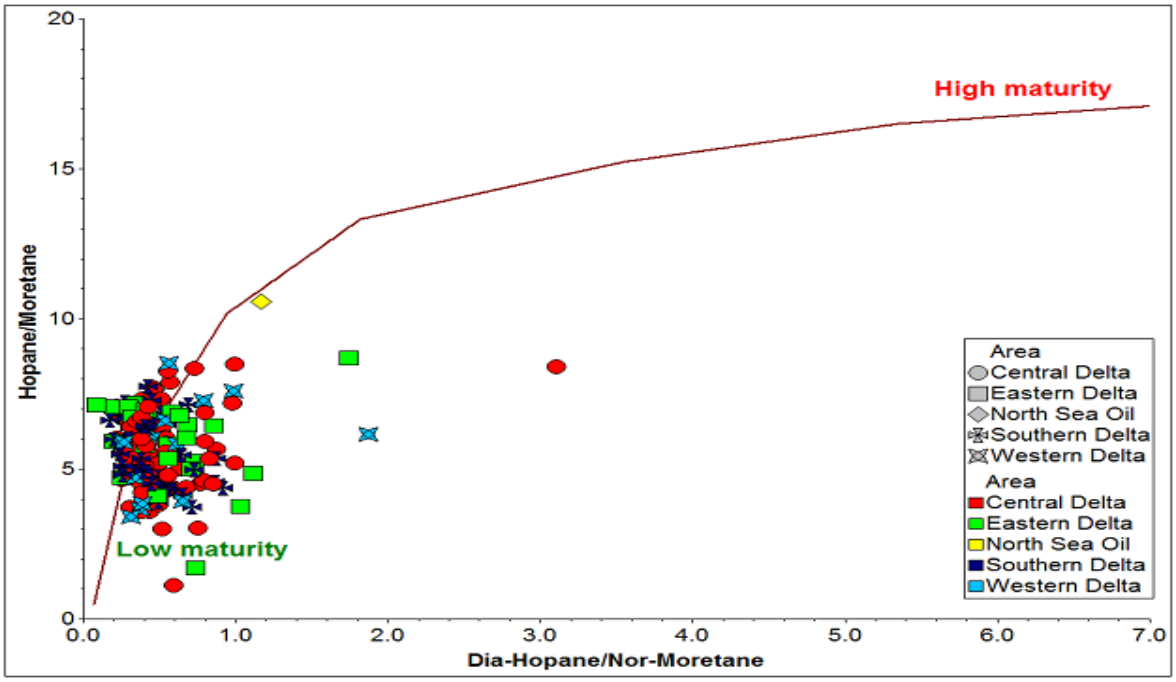

Figure 5.36: Plot of hopane/moretane against diahopane/normoretane hopane ratio maturity parameters. These indicate that most of the samples are of low maturity. Note the North Sea oil enables comparison with a thermally mature, marine sourced oil. Interpretation overlay from p:IGI 3.5 software.

5.6.3 Hopane hydrocarbon summary

Based on the results from the analyses of the hopane hydrocarbons, it can be summarised that:

1. The Niger Delta oil samples were sourced from a marine shale that was deposited in oxic/dysoxic environments.
2. Relatively very high oleanane contents in some Niger Delta oils can be as a result of biodegradation, because of their selective preservation in biodegraded oil.
3. Niger Delta oil samples that are late mature based on 29Ts/29Ts+29Tm hopane maturity parameter, are all biodegraded to about PM level 6.
4. The Southern Delta oil have elevated higher plant inputs than those from the other regions.
5. The Niger Delta oil sample analysed in this study are mainly of mid thermal maturity.

5.7 Conclusions

The complexity of the Niger Delta basin cannot be over-emphasised, with differing interpretations arrived at, based on the different component parts of oil analysed (Table 5.1). Unlike the North Sea oil analysed that yields a fairly consistent source and maturity interpretation (Table 5.1) no matter what hydrocarbon component was analysed. Conclusions based on the Niger Delta oil analyses are therefore also described and discussed under the following subheadings in order to give overviews of the oil geochemistry in this complex and dynamic basin.

Source kerogen type

The kerogen type of the Niger Delta oil varies and the results indicate the possibility of different kerogen types from Type II organic matter (based on diamondoid analyses) to Type II, II/III and III organic matter (based on gasoline range hydrocarbons and *n*-alkanes). Since high concentrations of diamondoids in hydrocarbon can only be sourced from thermally cracked oils, we can infer that the Niger Delta must have been charged multiple times, with at least one of the sources being from a relatively pure Type II organic matter, and the other sources being of variable kerogen compositions with possibilities of Type II, II/III and Type III organic matter.

Source environment of deposition

The variable environments of deposition present in the Niger Delta shows the dynamic nature of a paralic basin that has undergone multiple transgression and regression phases in its build-up. The Niger Delta oil samples shows that their sources were either deposited under relatively pure marine environments (based on diamondoid analyses) or marine/transition/terrigenous environments (based on light hydrocarbons, *n*-alkanes, aromatics, steranes and hopanes) in an oxic/dysoxic depositional environment. The incursion of ocean water into a transition/deltaic environment is known to always yields mixed kerogen Types, similar to what is observed in these results but the overwhelming

indications are that our initial Type II charge was sourced from only a marine facies. This implies that there was minimal influence of fresh water input when this formation was deposited and that it was at a period at the onset of formation of the delta.

It is therefore suggested that a Type II marine formation was deposited before the delta (sub delta), that it has its own petroleum system and that the present day Niger Delta just serves as an overburden to give the right burial depth/maturation conditions for petroleum generation and also contains reservoirs for the expelled oil. This Type II system is clearly different from the present under-compacted and over-pressured Akata formation/the lean Agbada petroleum systems, where the marine/transition/terrigenous deposition environment can be clearly seen.

Thermal maturity, cracking and reservoir mixing

Mixed thermal maturity signals from various hydrocarbon component parts of an oil generally points to mixing and sometimes to migration contamination. It is useful to compare the very good level of consistency in the North Sea oil hydrocarbon component results which is different from that seen in the Niger Delta oils. The apparent thermal maturity of the Niger Delta oils varies greatly based on the compound class and carbon number range of the parameters used for interpretation i.e. hopanes/steranes (low to mid maturity), alkylated naphthalene and phenanthrene aromatics (peak to late oil window), diamondoids (late oil window to early gas window), *n*-alkanes (early to mid-mature) and gasoline range (mid- mature).

In the case of a highly mature cracked oil mixed with a low maturity oil, it is expected that the highly mature cracked hydrocarbon will contribute a relatively higher percentage to the gasoline range hydrocarbons, light *n*-alkanes and two and three ringed aromatic hydrocarbon and minimal percentage to the higher weight *n*-alkanes ($>C_{25}$) including the biomarkers. Therefore results from the analyses of the higher molecular weight parts of the mixed oil will indicate that the oil is of low thermal maturity. Wilhelms & Larter (2004)

pointed out that biomarkers in a mixture of low and high maturity oils, a low mature oil comprising only 10% by volume of the mixture, will effectively mask the biomarkers in the mature oil which comprises 90% by volume, and it is believed that a similar effect is seen in the Niger Delta oil samples. However, in the Niger Delta oils, it is expected that the mature source contributes mainly to the gasoline range (normal mature to mature), aromatics (peak to late oil window) and nearly 100% contribution to the diamondoids hydrocarbon (late oil to early gas window) components.

It can be concluded that the Niger Delta oils studied must have had a least two pulses of charge, which were from a very mature Type II marine source rock that generated oil that was cracked and this mixed with a thermally mature oil of Type II/III source rock deposited in a paralic environment. Based on diamondoid concentrations, the highly mature cracked oil may have contributed up to 90% of the volume of hydrocarbons in some Central Delta fields and generally contributed more than 50% of the volume of hydrocarbons in many of the other fields around the Niger Delta that were analysed.

Biomarkers and *n*-alkanes in the mixed Niger Delta oil can show several orders of magnitude in concentration variation depending on the thermal maturity of the mixed oils and this can have an enormous influence on the interpretations made. However, light hydrocarbons and aromatics hydrocarbons may provide a better interpretation of the overall mixed oil, since they will be volumetrically important components of the mixed oil, whereas the diamondoids will mostly provide information on the highly matured cracked hydrocarbon component of the mixed oils.

Table 5.1: Summary of compound class parameter interpretations for the Niger Delta oil samples

Compound class parameters	Kerogen type	Deposition environment	Maturity	Mixing	Cracking
Light Hydrocarbon	Type II and II/III Type II	Mostly marine + terrigenous Marine	Mid-mature to mature Mature		
***n*-alkane/ isoprenoid**	Type III with some II/III Type II/III	Mainly oxic paralic delta Dysoxic	Immature to mature Mature		
Diamondoids	Type II Type II	Marine shale Marine	Late oil window to early gas window Peak oil window	Lightly to severely mixed no	Lightly to severely cracked no
Aromatics		Mainly marine with some terrigenous and possible lacustrine Marine	Peak to late oil window Peak oil window	Yes and very prevalent no	
Sterane		Open to shallow marine + Deltaic environment Open marine	Low maturity Mature		
Hopane		Marine shale Marine shale	Low maturity Mature		

Note: North Sea Oil-1 interpretation is in red

CHAPTER SIX

SECONDARY MIGRATION AND RESERVOIR ALTERATION

6.0 Introduction

Petroleum can only accumulate in a trap (stratigraphic or structural) after a deeply buried source rock that as attained sufficient burial depth and temperature, has generated and expelled hydrocarbons, which then migrate into a reservoir (Magoon & Dow, 1994). The essential elements of a petroleum system, which are source, reservoir, seal and overburden, have to be in place during trap formation and before the generation/expulsion/migration/accumulation of hydrocarbons (Peters *et al*., 2009). Magoon & Beaumont (2000) divided the level of certainty of a petroleum system into 3 possible subdivisions; [1] known (positive oil-source rock correlation), [2] hypothetical (absence of positive oil-source correlation) and [3] speculative (only limited geological/geophysical evidence). Several authors have tried to argue in favour of either one or combination of two or three possible level of certainty for the petroleum systems of the Niger Delta basin (Bustin, 1988; Haack *et al*., 2000; Eneogwe, 2004; Akinlua *et al*., 2006; Samuel *et al*., 2009).

This chapter investigates the possibilities of establishing the secondary migration pathway distance and the probable alteration processes that affected the Niger Delta oils either during migration or within the reservoir environment.

6.1 Secondary migration distance

Alkylated carbazoles and benzocarbazoles are two types of neutral nitrogen containing compounds which are often present in source rocks and crude oil (Li *et al*., 1995; Larter *et al*., 1996; Huang, 2003). Although in the previous chapter, the oil samples from the Niger Delta have been shown to be potentially mixtures of different oils with different thermal maturities (early/late/gas window mature hydrocarbon), the discussion of migration

distance presented here assumes similarity between the oil in terms of source facies, thermal maturity and mixing. The interpretation of molecular migration distance marker data is therefore very simplistic and prone to potentially significant error, however care has been taken to remove all samples that are biodegraded above PM level 3 from the migration distance discussion because of the potential effect of biodegradation.

The Niger Delta oil samples are characterised by very low carbazole concentrations (*cf*. Bennett *et al*., 2002). Benzo[a]carbazole + benzo[c]carbazole concentrations range from 0.1 to 1.2 ppm (Figure 6.1). In a study of oils from the Western Canada Basin, Larter *et al*., (1996) found that the concentration of benzocarbazoles decreases with increasing migration distance and if this interpretation basis is used for the Niger Delta oil (Figure 6.1) then the Western Delta oil samples, which are mostly devoid of carbazoles, must either have migrated over a longer distance or carbazoles were not present in the source rocks that produced these oils. Although Samuel *et al*., (2009) showed some positive correlation between the Western Delta oil samples and source rocks from the Dahomey Basin in the western part of Nigeria, with an average surface distance of about 400 km on the surface between these two locations, it is unproven that the Western Niger Delta oil has migrated over such a long distance.

The temperature of expulsion of hydrocarbons from different source rocks is dependent on the organic facies of the source, i.e. high temperature of expulsion for Type III and low temperature of expulsion for Type II (Pepper & Corvi 1995). The calculated temperature of expulsion of Niger Delta oil samples (120 to 142 ºC) shows that the lower the temperature of expulsion the shorter the possible migration distance and verse versa based on their negative correlation with the benzocarbazole ratio (Figure 6.2), this is of great importance because the temperature of expulsion has a positive correlation with depth of burial, which will have a positive correlation with distance to reservoir. Therefore those samples that have a low temperature of expulsion might have migrated over a shorter

distance to the reservoir than those samples that have a higher temperature of expulsion (Figure 6.2).

There is a possibility of two migration distance/expulsion temperature trends for the Niger Delta oil samples as shown in Figure 6.2, with the Southern Delta oils having a different trend to the Eastern Delta oil, which might be as a result of differences in rate of sedimentation and regional heat flow in those two regions.

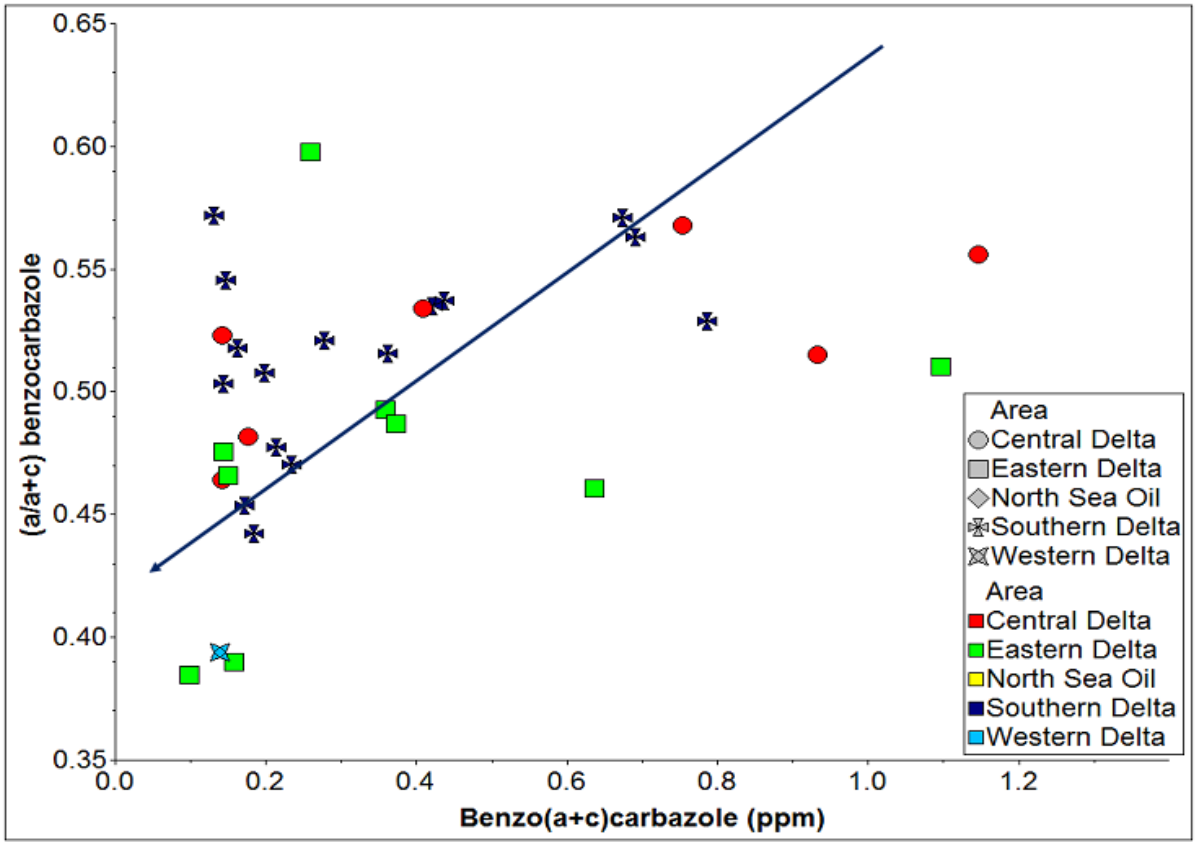

Figure 6.1: Plot of benzocarbazole [a]/([a]+[c]) ratio (BCR) against concentration of benzo(a) and benzo(c)carbazoles in the Niger Delta oil samples. The concentration of benzocarbazoles and BCR decreases with increase in migration distance.

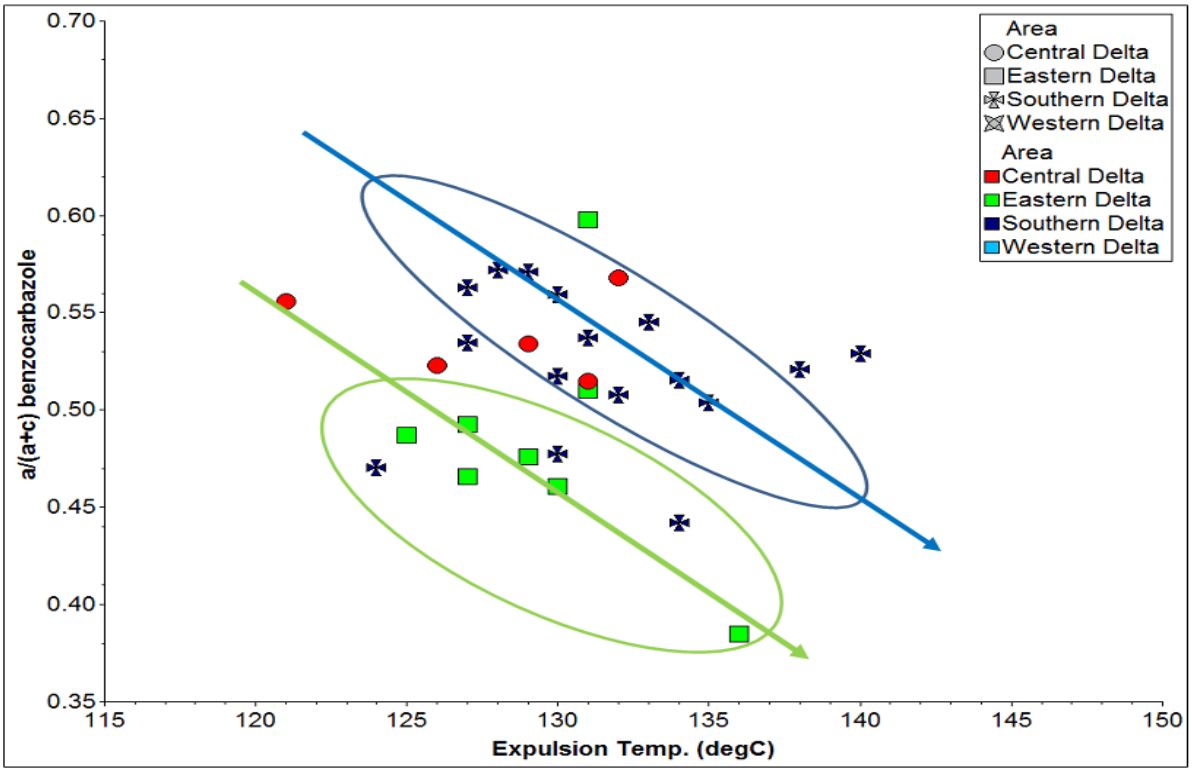

Figure 6.2: Plot of benzocarbazole ratios against calculated temperature of expulsion (ºC) in the oil samples showing a negative correlation between both parameters (note the two possible trends for the oil samples from the Southern and Eastern Delta).

With the alkylcarbazoles, the ratio of 1-methylcarbazole to 4-methylcarbazole (NH-partially shielded isomer/NH-exposed isomer) tends to increase with increasing migration distance (Li *et al*., 1997) and also the ratio of benzo[a]carbazole/benzo[a+c]carbazoles (BCR) tend to decrease with increase in migration distance (Li *et al*., 1995; 1997; Larter *et al*., 1996; Clegg *et al*., 1998; Bennett *et al*., 2002; Huang *et al*., 2003; Bechtel *et al*., 2013). A cross plot of these ratios (Figure 7.3) indicates that the Eastern Delta oil samples may have migrated a relatively longer distance than the Southern Delta oil samples (Figure 6.3).

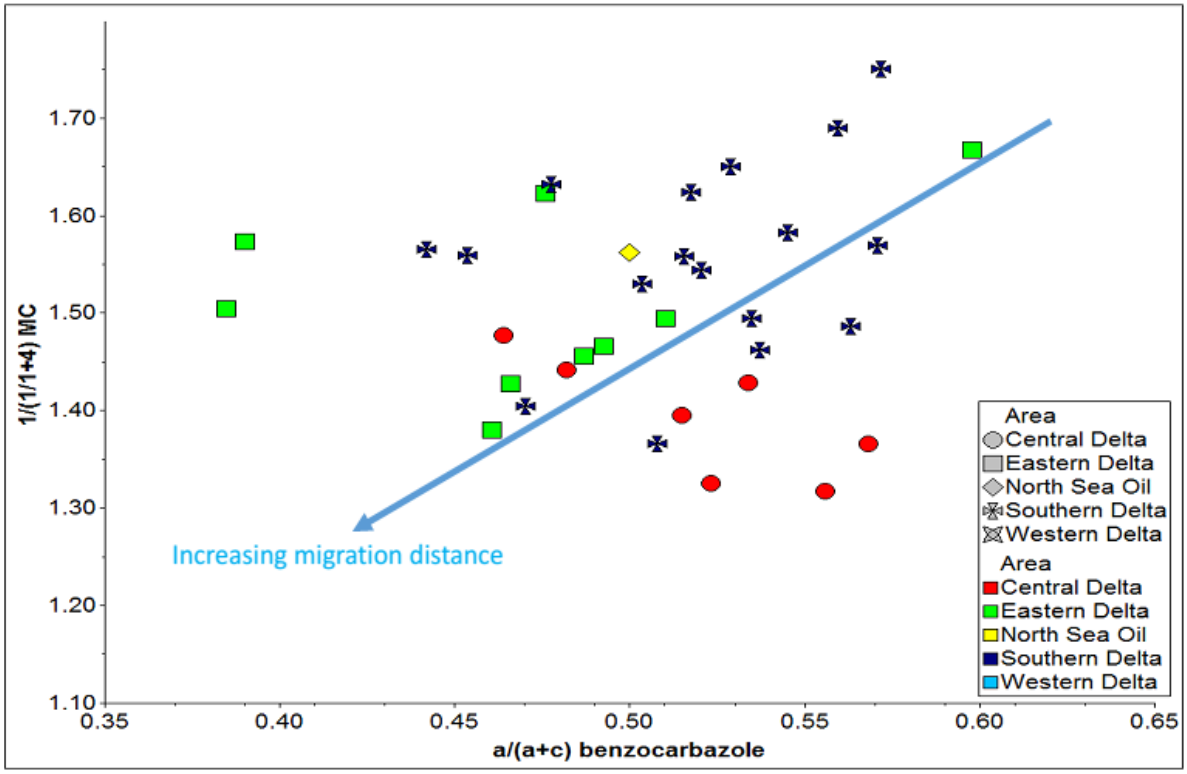

Figure 6.3: Plot of benzocarbazole ratios against the inverse of (1/1+4) methylcarbazole ratios, showing a weak migration distance trend.

The 3- + 4-methyldiamantane (MD) concentrations in the Niger Delta oil samples was shown to be related to the degree of thermal cracking and mixing of the oil samples in the Delta (see Chapter 6). There is a negative correlation between the the BCR and 3+4-MD concentration, which may suggest that the higher the propotion of highly mature oil in the mixture, the greater the migration distance and verse versa (Figure 6.4), although there is no established correlation of the BCR with other thermal maturity parameters in the Niger Delta oil samples. A high maturity oil is expected to have a low benzocarbazole concentration and BCR, therefore the addition of such oil to other oil would reduce the bezocarbazole concentration in the mixed oil.

The migration distance of Niger Delta oil samples cannot be meaningfully assessed on the basis of carbazole data due to the following factors:

1. Multiple contributing sources of the oils of the Niger Delta instead of similar source (cf. Larter *et al*., 1996; 1997).
2. The composition and nature of the carrier beds is not known.

3. Lack of migration pathway information (dispersed vs focus migration).
4. Mixture of different thermal maturities of oils in the Niger Delta (cf. Larter *et al*., 1996; 1997).
5. The possibility of different thermal maturity oils migrating through the same carrier beds in the Niger Delta.

Despite these shortcomings, the carbazole parameters may still help to give an insight into the relationship between these molecular migration distance indicators and other parameters in an effectively mixed petroleum system. Although the molecular migration tracers were first proposed more than a decade ago, secondary oil migration remain the least understood process in petroleum accumulation (Zhang *et al*., 2013).

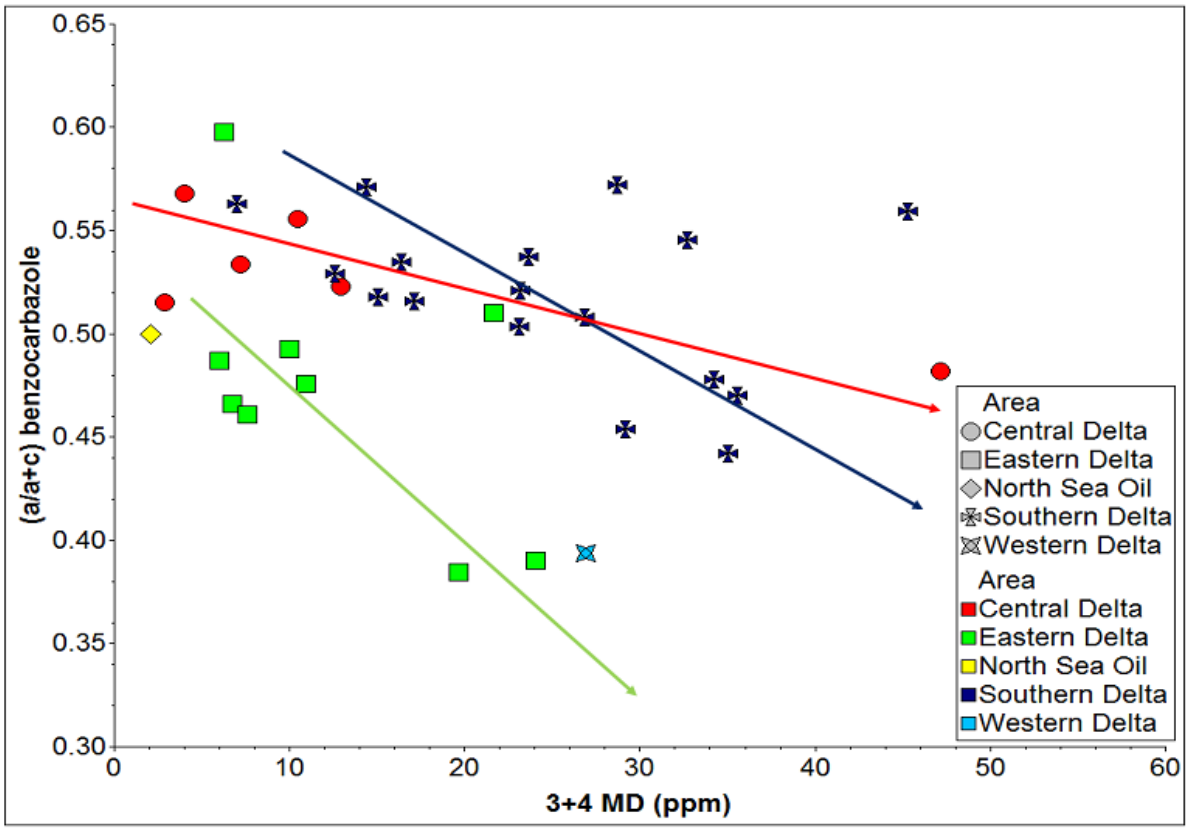

Figure 6.4: Plot of benzocarbazole ratio against 3+4 methyldiamantane concentration in the Niger Delta oil samples, showing a negative correlation between both parameters. Note the three possible trends for the oil samples from the Central, Southern and Eastern Delta.

6.1.1 Summary of secondary migration distance assessment

The assessment of secondary migration distance of the Niger Delta oil samples can be summarized as follows:

1. Western Delta oils are generally devoid of carbazoles; this may reflect either long distance migration or the absence of these compounds in the source rocks that produced the oil.
2. Eastern Delta oils have migrated over a longer distance than the Southern Delta oils based on results from the benzocarbazole ratio (BCR).
3. The higher the temperature of expulsion (as calculated from gasoline range hydrocarbons) the greater the apparent secondary migration distance.
4. The higher the ratio of 1/1+4-MC i.e (NH-shielded isomer/NH-exposed methylcarbazole isomers) the longer the apparent migration distance.
5. The higher the concentration of 3+4-MD in the oil samples, the greater the apparent migration distance, this might also be as a result of mixing of highly mature oils with low carbazole concentrations.

6.2 Biodegradation

Since there are several possible factors that control biodegradation in oil reservoirs (e.g. Head *et al*., 2003), and the effects of biodegradation on all compounds in oils are not fully known, this study will not only be focused on the commonly analysed compound classes, but also on some of the unknown peaks found in these Niger Delta samples. Notwithstanding that the oil samples studied are mixtures of hydrocarbons from different sources, reference will be made to the Peters and Moldowan (PM) biodegradation scale and or the Wenger biodegradation scale (Figure 6.5). The generally accepted hydrocarbon biodegradation sequence in oils is *n*-alkane and isoprenoids > monoaromatics

hydrocarbons > polyaromatic hydrocarbons and thioaromatic compounds > bicyclic sesquiterpanes > steranes > hopanes > diasteranes > pregnanes (Marcano *et al*., 2013).

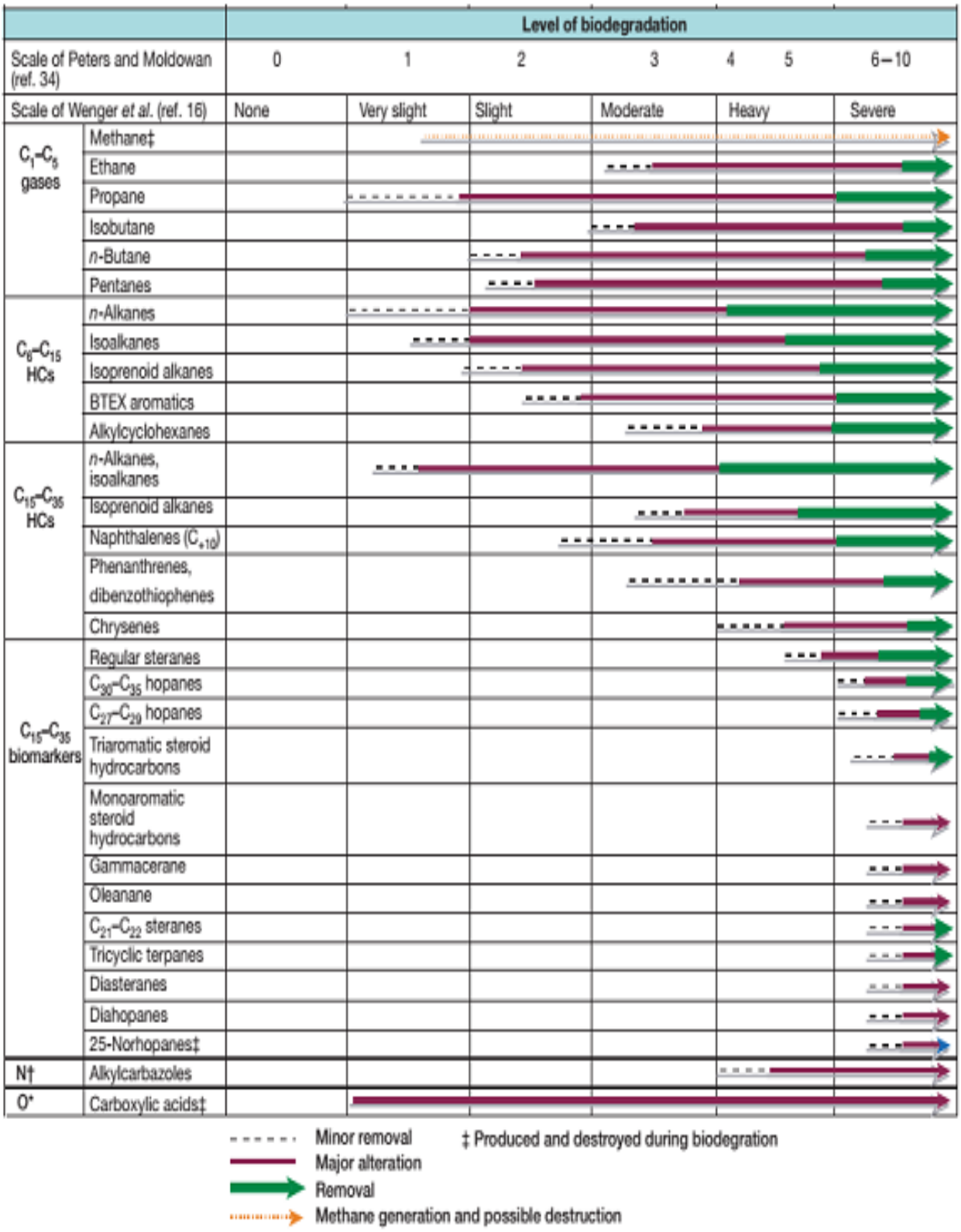

Figure 6.5: Schematic biodegradation of hydrocarbon effects (Head *et al*., 2003), showing the Peters & Moldowan (199)3 and Wenger *et al*. (2001).

6.2.1 Effect of reservoir depth on biodegradation in the Niger Delta oils

Although no actual reservoir depth information was available, the oil samples provided were described as from shallow reservoir (Short string) or deep reservoirs (long string) and they were selected from different wells around Niger Delta basin on the basis of both geographical location and relative depth. Biodegradation is known to either occur in reservoirs that have not been paleopasturised, where reservoir temperature is lower than 80 ºC (Larter *et al*., 2000), and fastest in close proximity to the oil water contact (Head *et al*., 2003). A quick look through the data set shows no consistent biodegradation relationships with reservoir depth, which does not have any relationship with any particular region. Those relationship included both decreases and increases in biodegradation level with reservoir depth and sometimes constant biodegradation levels with change in depth within a well

6.2.1.1 Decrease in biodegradation with reservoir depth.

Oil samples from several of the studied Niger Delta wells show a decrease in biodegradation with reservoir depth (Figure 6.6) and this is a prominent feature in the basin (Kolonic, 2014, personal communication). The most likely reason for this is that the shallow reservoirs have never been buried to the cut-off temperature for paleopasturisation to occur (cf. Larter *et al*., 2000) and there is also possibility that there is continual fresh charge to the deep reservoir. However, reservoir burial and charge history modelling would be needed to support this hypothesis. There are several biodegradation ranges observed within single wells, with some wells showing range from PM level 0 oil in the deep reservoir to PM level 6 in the shallow reservoir (e.g. samples OE015 and OE016), while others wells could contain PM level 5 oil in the deep reservoir and PM level 6 in shallow reservoir (e.g. samples OE099 and OE100) but the important factor here is that biodegradation is seen to be more at the sallower reservoir than the deep reservoir. However, no detailed depth information was provided for the oil samples.

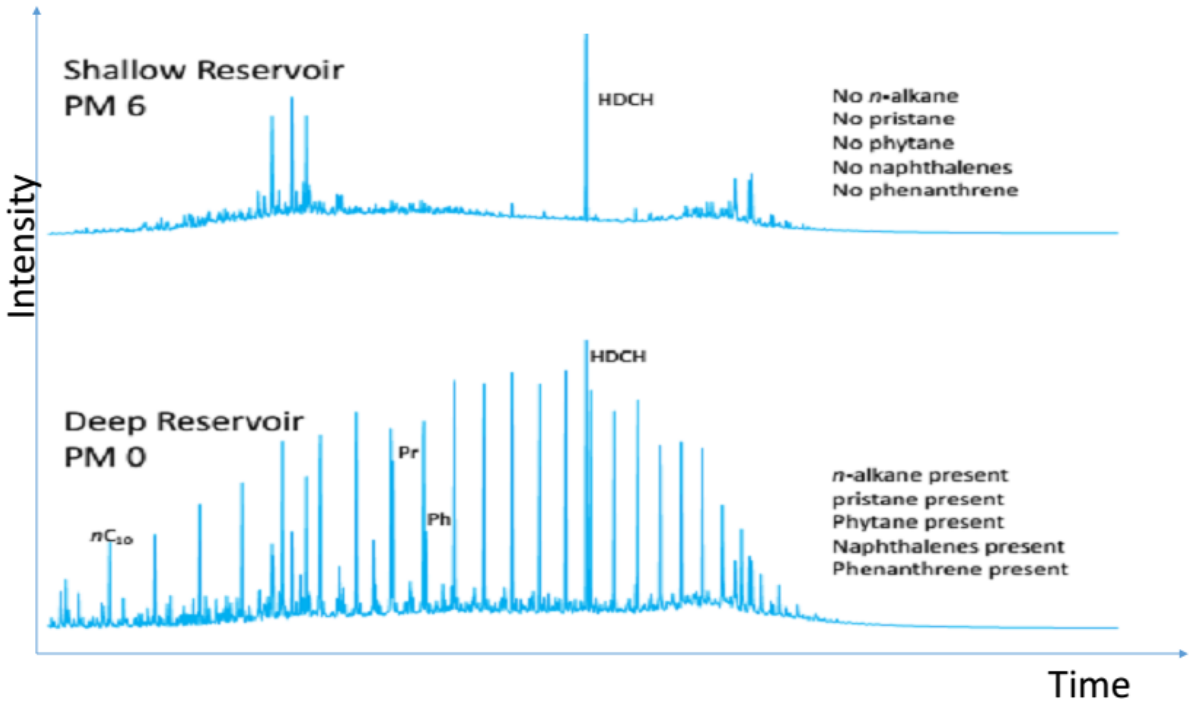

Figure 6.6: Variation in biodegradation within a well in Niger Delta showing reduction in biodegradation with reservoir depth (OEE97 and OEE98). HDCH is the added heptadecyclohexane internal standard.

6.2.1.2 Variation in oil biodegradation extent with reservoir depth.

The extent of oil biodegradation is often greater in shallower, cooler reservoirs and within a reservoir it often increases closer to the oil water contact zone because there will be availability of nutrients from the water to be used by the organisms in and around the oil water contact zone to degrade the hydrocarbon in the reservoir (Head *et al*., 2003). Amongst the Niger Delta samples analysed, several scenarios exist, with some wells showing a large difference in biodegradation level from PM 0 for the shallow reservoir to PM level 6 for deep reservoir, while others may just vary from PM level 1 to PM level 2 with differences in reservoir depth.

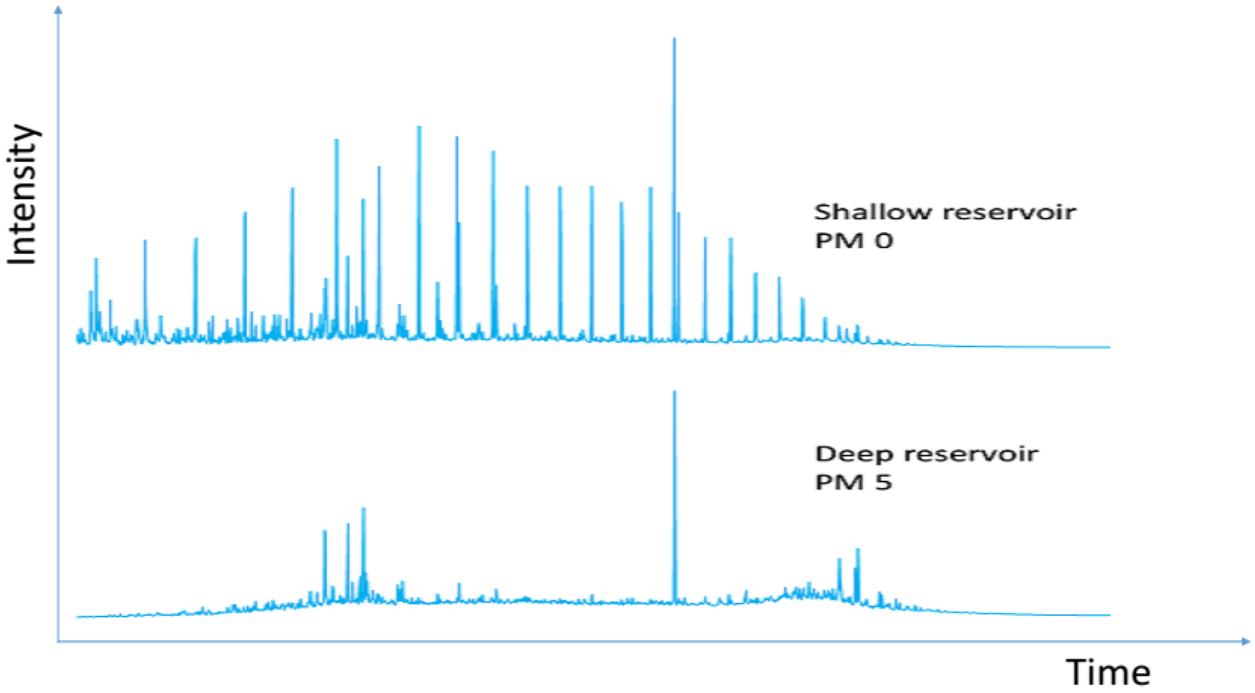

Figure 6.7: Variation in biodegradation within a well in Niger Delta showing progressive biodegradation with reservoir depth (OE073 and OE074). Note that the shallow reservoir is not biodegraded while the deep reservoir is biodegraded.

6.2.2 Effect of mild biodegradation on oil geochemical parameters and isotopic compositions

Samples from seventeen wells were selected from different oil fields across the Niger Delta basin to study the effect of mild biodegradation on molecular parameters and also isotopic values of individual *n*-alkanes. Two samples were selected from each well, one from a shallow reservoir one from a deeper reservoir (Figure 6.8).

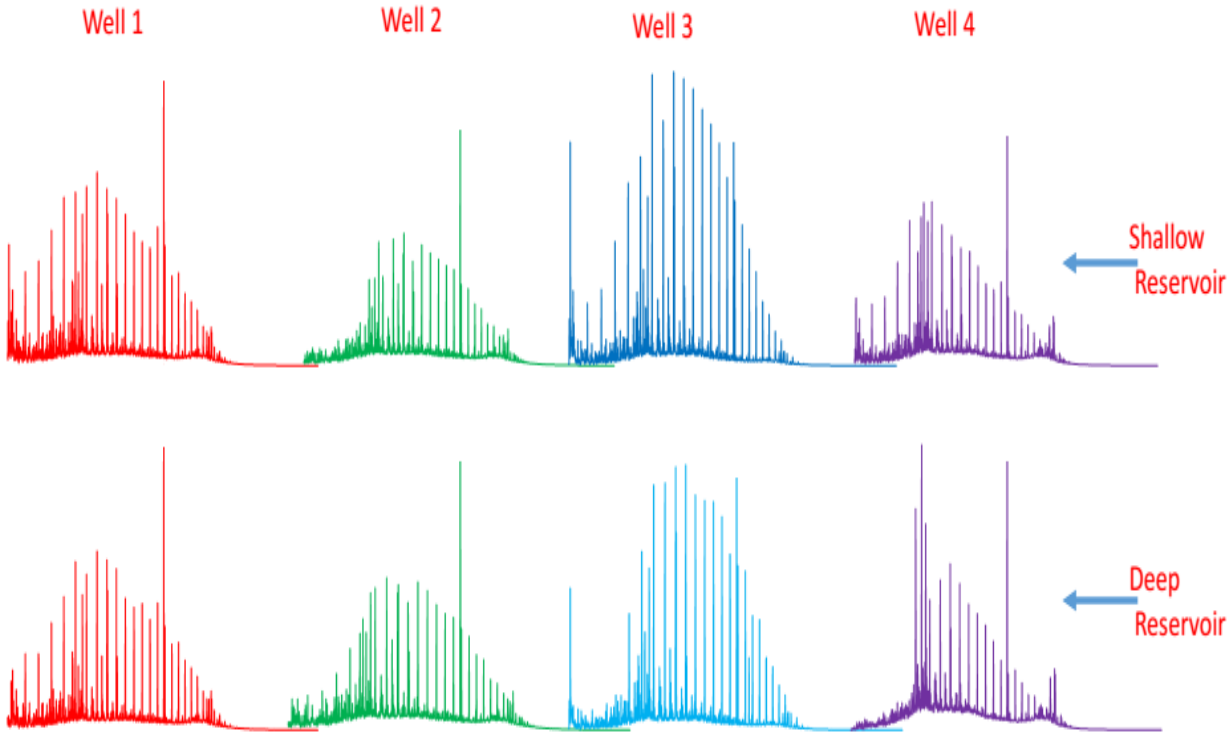

Figure 6.8: Representative gas chromatograms of saturated hydrocarbon fractions of selected oil samples from shallow and deep reservoir from different Niger Delta oil fields, showing non-biodegraded to slightly biodegraded oil samples (well 1 PM 0 to 0, well 2 PM 1 to 1, well 3 PM 0 to 1, well 4 PM 0 to 2).

Several geochemical parameters were measured and there was usually no variation in most geochemical parameters with either slight biodegradation or reservoir depth differences. The star plot in figure 6.9 shows some geochemical parameters which include the source/deposition environment parameters: Pr/Ph, $t_{19}/t_{19}+t_{23}$, oleanane index, $\%C_{29}$, %A+B, correlation parameter: Homohopane index, maturity parameters: CPI, 20(S/S+R), 22(S/S+R), Ts/Ts+Tm, calculated Rc, cracking and mixing: 3+4 MD concentrations and these parameters show no obvious variations with slight changes in level of biodegradation. The maturity and environment of deposition / source parameters show strong correlations for both the shallow and the deep reservoirs for all wells, with the only variation seen in well 4 for the calculated Rc value where the shallow reservoir appears more mature than the deep reservoir. This finding was not surprising because more mature hydrocarbons tend to fill the crest of the structure or fill a shallower reservoir, due to earlier filling of deeper

reservoirs with less mature oil. The concentrations of 3- + 4- MD (Figure 6.9), which are used as an indication of maturity, cracking and mixing of hydrocarbons (Dahl *et al*., 1999), show that the shallow reservoirs always have higher concentrations that the deep reservoirs. This indicates that although the high molecular weight biomarker source and maturity parameter are similar, the lower molecular weight diamondoids show variations within a well and the highly matured/cracked hydrocarbon charges are mostly concentrated in the shallow reservoirs of any well.

However, well four shows the opposite of this trend with the shallow reservoir having a lower diamondoid concentrations than the deeper reservoir. This reversal in well 4 cannot be explained by mass balance alone, i.e. although a change in biodegradation level from PM level 0 to PM level 2 might have concentrated the more resistant diamondoids in the deep reservoir, this would be insufficient to account for the observed values. Since, the gasoline range often makes up about 30% of oil composition (Hunt *et al*., 1980), therefore if these light end components were all lost then the diamondoids must have concentrated by about 30% and some *n*-alkane must have been lost also, this clearly does not account for the difference in diamondoid concentration from 26.8 to 62.8 ppm which is 134% increase. The observed 134% increase and the mass balance projection of between 30 to 60% increase are very different A possible explanation for these high diamondoid concentrations might be that the initial highly matured charge have been biodegraded to a higher extent than what is observed before mixing with a fresh, lower maturity charge which had a masking effect on the true state of the original oil or that the two reservoir are not in communication (reservoir compartmentalisation).

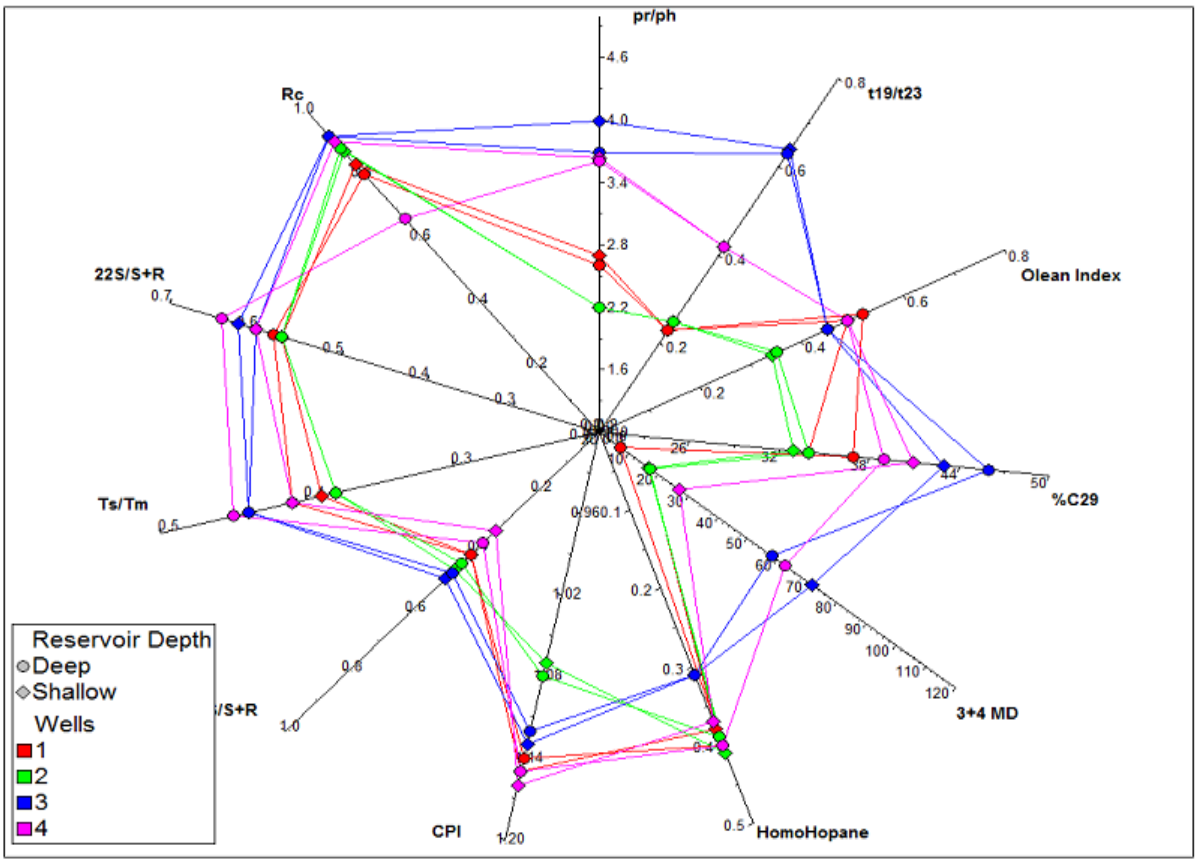

Figure 6.9: Star diagram of crude oil molecular marker parameters from representative wells from four different Niger Delta fields, also showing the relationships between shallow and deep reservoirs from them.

Compound specific isotope analysis of individual *n*-alkanes is a very useful tool for correlation of hydrocarbons and characterising mixed oils (Murray *et al*., 1993; Rooney *et al*., 1998; Curiale *et al*., 2005; Dawson *et al*., 2007; Aboglila *et al*., 2010) but biodegradation which is a very common secondary alteration process in most of the world's oil fields and can have a measurable effect on isotopic compositions of the gasoline range hydrocarbons (Huang *et al*., 1997) but does not usually have major effects on those of the > nC_{12} range (Huang et al., 1997; Mansuy *et al*., 1997). However, a significant increase in maturity have been shown to lead to enrichment in ^{13}C which might be as a result of release from components that are depleted in ^{13}C (Clayton, 1991; Dawson *et al*., 2007).

A careful study of the carbon isotopic composition of individual *n*-alkanes of the shallow and deep reservoired oils from the 17 wells gave similar result for all wells (Figure 6.10). The lighter *n*-alkanes ($\leq C_{21}$) of the shallow reservoired samples show enrichment in ^{13}C

which cannot be explained based on the biomarkers maturity parameters measured (Figure 6.9) as these parameters were similar in both shallow and deep reservoired oils. However, the shallow reservoired samples always showed elevated 3+4 MD concentrations, which indicates that there must have been a higher percentage of mixing of the highly mature charge in those shallow reservoirs.

The *n*-alkane isotopic inversion is prominent for the light ends (Figure 6.10), where the highly matured source must have contributed a higher percentage to the shallow reservoirs. These observations support the hypothesis of the prevalence of cracking and mixing in the Niger Delta basin, with the more mature hydrocarbons in the shallower reservoir having higher enrichment in ^{13}C which might be as a result of release from components that are depleted in ^{13}C generated from the highly matured source (e.g. Clayton 1991; Dawson *et al*., 2007).

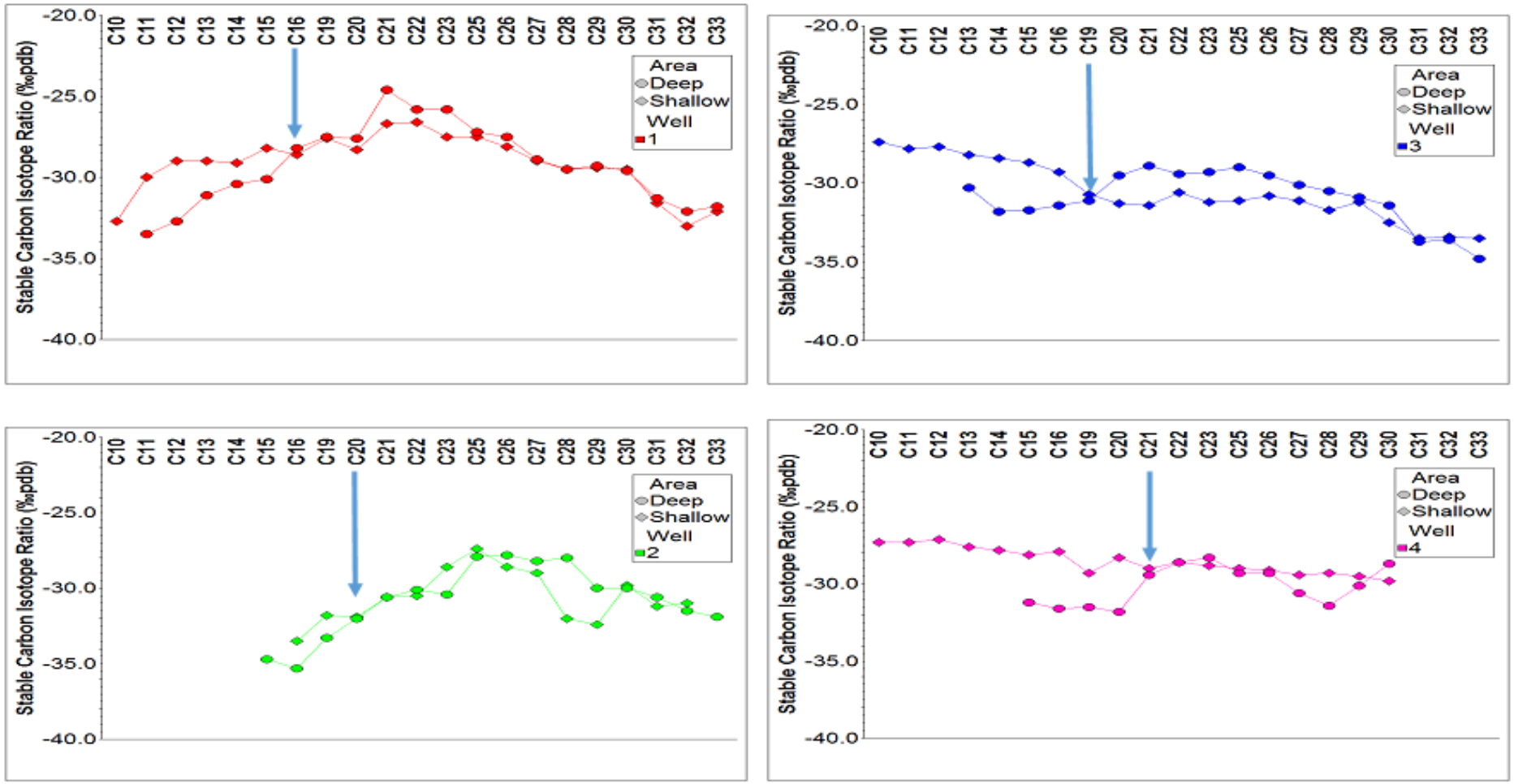

Figure 6.10: Representative *n*-alkane carbon isotope profiles of oils from 4 wells in the Niger Delta showing the trend for shallow and deep reservoirs. Note the isotopic cross over point of shallow and deep reservoirs for individual wells.

6.2.3 Effects of biodegradation on gasoline range hydrocarbons

It is usually difficult to assess the level of biodegradation of most oil samples that still have some parts of their light hydrocarbons. Thompson (1983) was able to show that oils with low heptane and isoheptane values must have been biodegraded and that as biodegradation increased, those values tended to 0. Although Thompson (1983) stated that oil samples with heptane ratios below 18% are biodegraded, the results from this present study show that some oil samples that appear non-biodegraded (PM level 0), have heptane ratio values of 12%. This latter observation is in agreement with the findings of Peters *et al*., (2005) though they believed that this was as a result of low maturity (Figure 6.11).

There is no sharp distinction of oil samples with different biodegradation levels on the Thompson plot (Figure 6.11). Some PM level 2 samples (possible mixed oils) plot in the region where the PM level 0 samples plot, but generally PM level 1 and level 2 samples plot towards the origin on the graph (Figure 6.11). The Thompson plot can only show early biodegradation levels in samples with gasoline range hydrocarbons and discrimination of biodegradation level between PM level 1 and PM level 2 is not really very possible and might depend on other parameters as PM level 1 and 2 plots in the same region. The extent of biodegradation of the oil samples, based on gasoline range parameters, do not show any particular trend with region or reservoir depth in the delta.

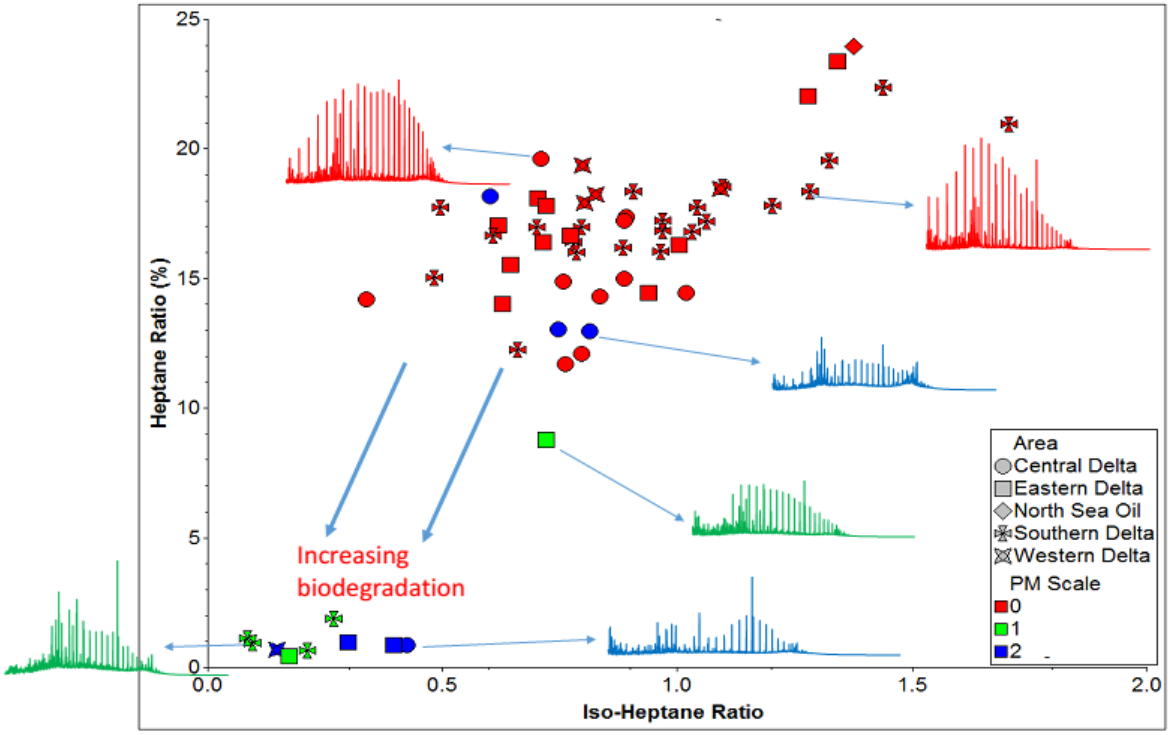

Figure 6.11: Plot of heptane versus isoheptane ratios of oils from the different regions of the Niger Delta showing biodegraded oil samples. Note the North Sea oil enables comparison with a non-biodegraded marine sourced oil. Modified after Thompson (1983).

6.2.4 Effects of biodegradation on *n*-alkanes and isoprenoid hydrocarbons

A cross-plot of Pr/*n*-C_{17} against Ph/*n*-C_{18} shows the susceptibility of the normal alkanes to biodegradation as against the isoprenoids. Non-biodegraded samples mostly have low Pr/*n*-C_{17} and Ph/*n*-C_{18} ratios (Figure 6.12) although there is no clear distinction between oil samples of PM level 0 and PM level 1, but as these ratios increase, the biodegradation level tends to increase up to PM level 3 (Figure 6.12).

The biodegradation level of the oil samples based on *n*-alkanes/isoprenoid hydrocarbons does not show any particular trend with region or reservoir depth. The p:IGI software overlay of biodegradation shows the onset of biodegradation based on the Pr/*n*-C_{17} ratio as 4 (Figure 6.12), but based on the results obtained from these Niger Delta oil samples it is clear that the onset of biodegradation should be around a value of 2 for the Pr/*n*-C_{17} and 1 for Ph/*n*-C_{18} ratios.

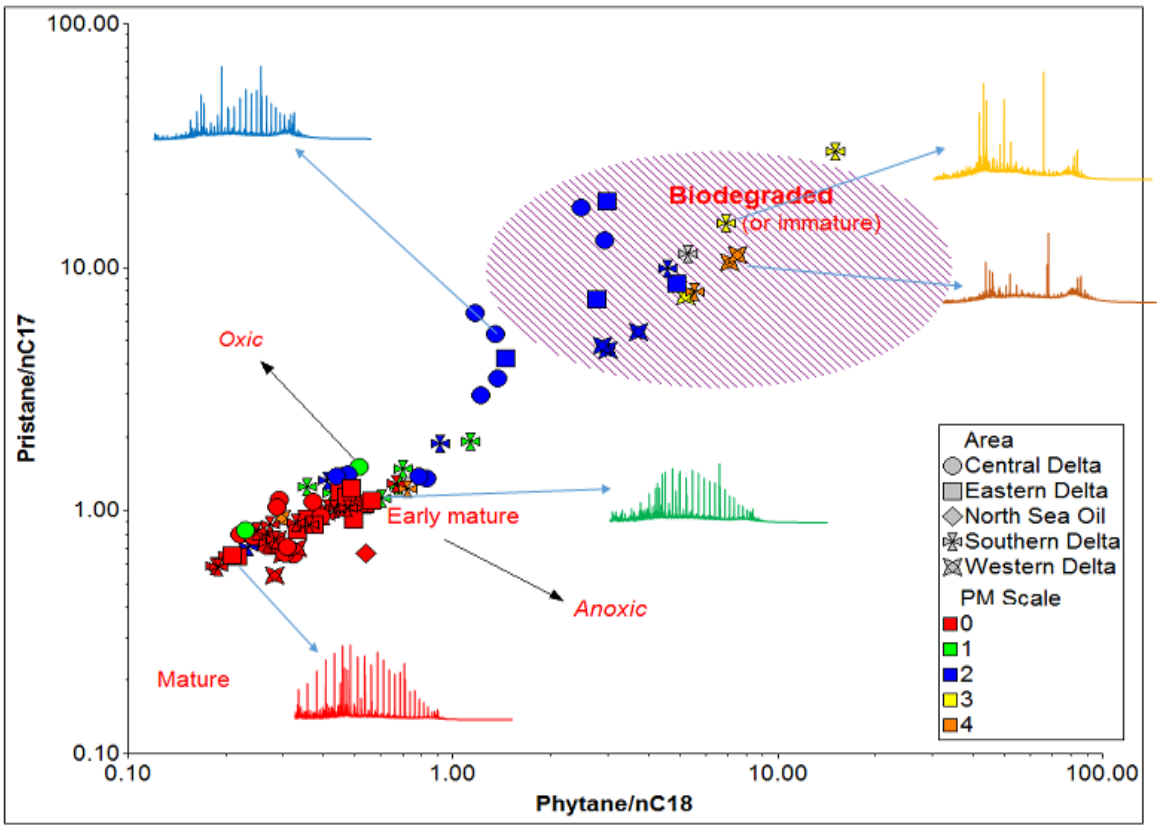

Figure 6.12: Cross-plot of Pr/*n*-C_{17} versus Ph/*n*-C_{18} showing biodegradation trends in Niger Delta oil samples. Note the North Sea oil enables comparison with a non-biodegraded marine sourced oil (modified after Shanmugam 1985). Overlay from p:IGI 3.5 software.

6.2.5 Effects of biodegradation on diamondoids hydrocarbon

The effects of biodegradation on gasoline range hydrocarbons, *n*-alkanes, isoprenoids, aromatics and biomarkers have been highly studied, while the effect of biodegradation on diamondoids hydrocarbon is much less studied. Grice *et al.* (2000) were able to show that the ratio of methyladamantane/adamantane (MA/AD) increases with an increase in biodegradation level, but in this present study there is no systematic increase in this MA/AD ratio with increase in biodegradation in the Niger Delta oil samples. A possible explanation for this is that the samples that have elevated MA/AD values but are of PM level 0 to 2 must have been mixtures of different charges of hydrocarbons, with the earlier charge having been severely biodegraded and the late charge not biodegraded (Grice *et al.*, 2000). The ratio of MA/*n*-C_{11} increases with increase in level of biodegradation (Figure 6.13) and this ratio is a good indicator of the level of biodegradation in the oil fields studied, as

indicated on the TIC of samples (Figure 6.13). This is because of the preferential degradation of *n*-alkanes as against the more resistant diamondoids, which normally leads to diamondoid enrichment in biodegraded oil (cf. Grice *et al*., 2000).

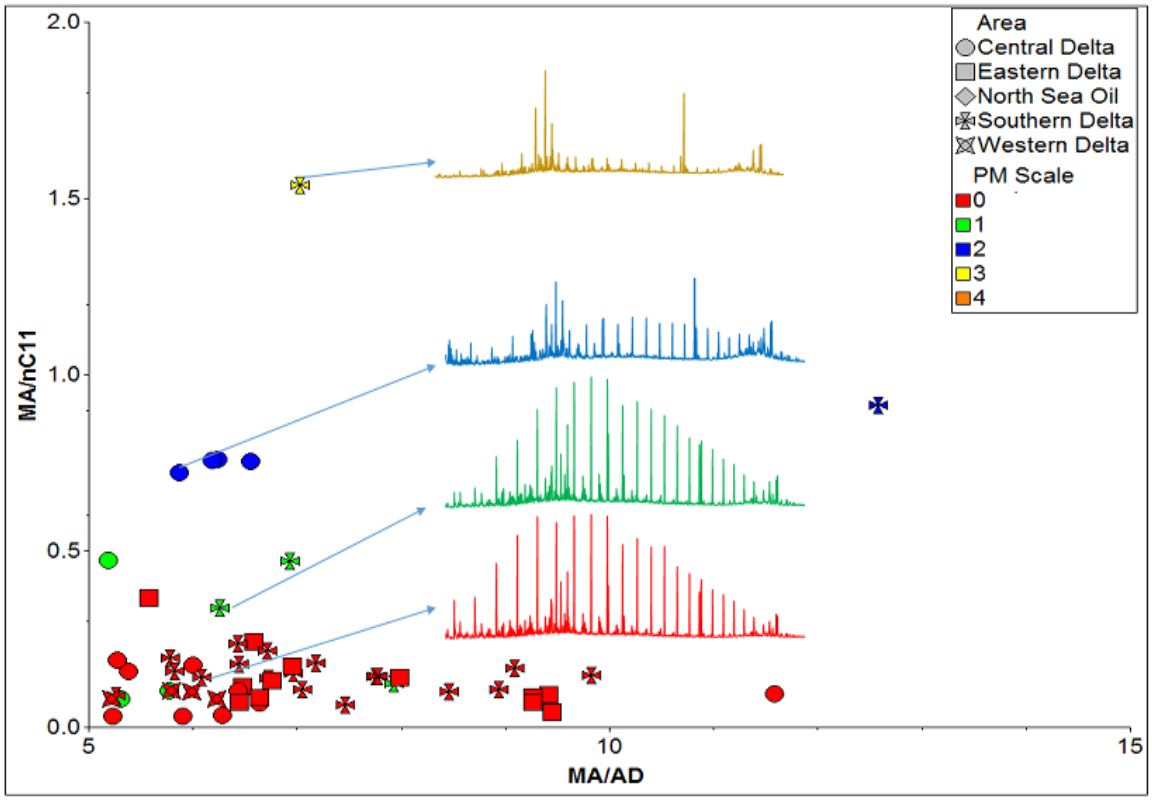

Figure 6.13: Cross-plot of methyladamantanes/*n*-C_{11} versus methyladamantanes/adamantane showing biodegradation trends in the Niger Delta oil samples (cf. Grice *et al*., 2000). High MA/AD values in PM level 0 samples might indicate mixing of highly biodegraded oil with a fresh charge.

6.2.6 Effects of biodegradation on aromatics hydrocarbon

There appear to be a complex interplay of different compound removal susceptibilities in the aromatic hydrocarbons of the Niger Delta oil samples analysed, though most of the aromatic compounds relatively remain unaltered until very high biodegradation levels. Some proposed biodegradation ratios in oils do not follow any reported trends for the Niger Delta e.g. 9-MP/1-MP (Bennett & Larter 2008); 3-MP/2-MP (Bennett *et al*., 2013). Those ratio neither increase nor decrease with the increasing level of biodegradation in these oil samples, but at PM level 6, the methylnaphthalenes get destroyed and at PM level 7 the methylphenanthrenes get removed (e.g. Figure 6.14).

There are no marked variations amongst aromatic compounds within the shallow and the deep reservoirs of individual wells and the only major effects come into play at extreme biodegradation levels where the aromatic compounds are destroyed (e.g. Figure 6.14). The interplay of multiple charge episodes and mixing, fill and spill, complex reservoir architecture, differential rates of biodegradation to rates of charge/recharging must have led to the complexities in the distributions of aromatic compounds observed.

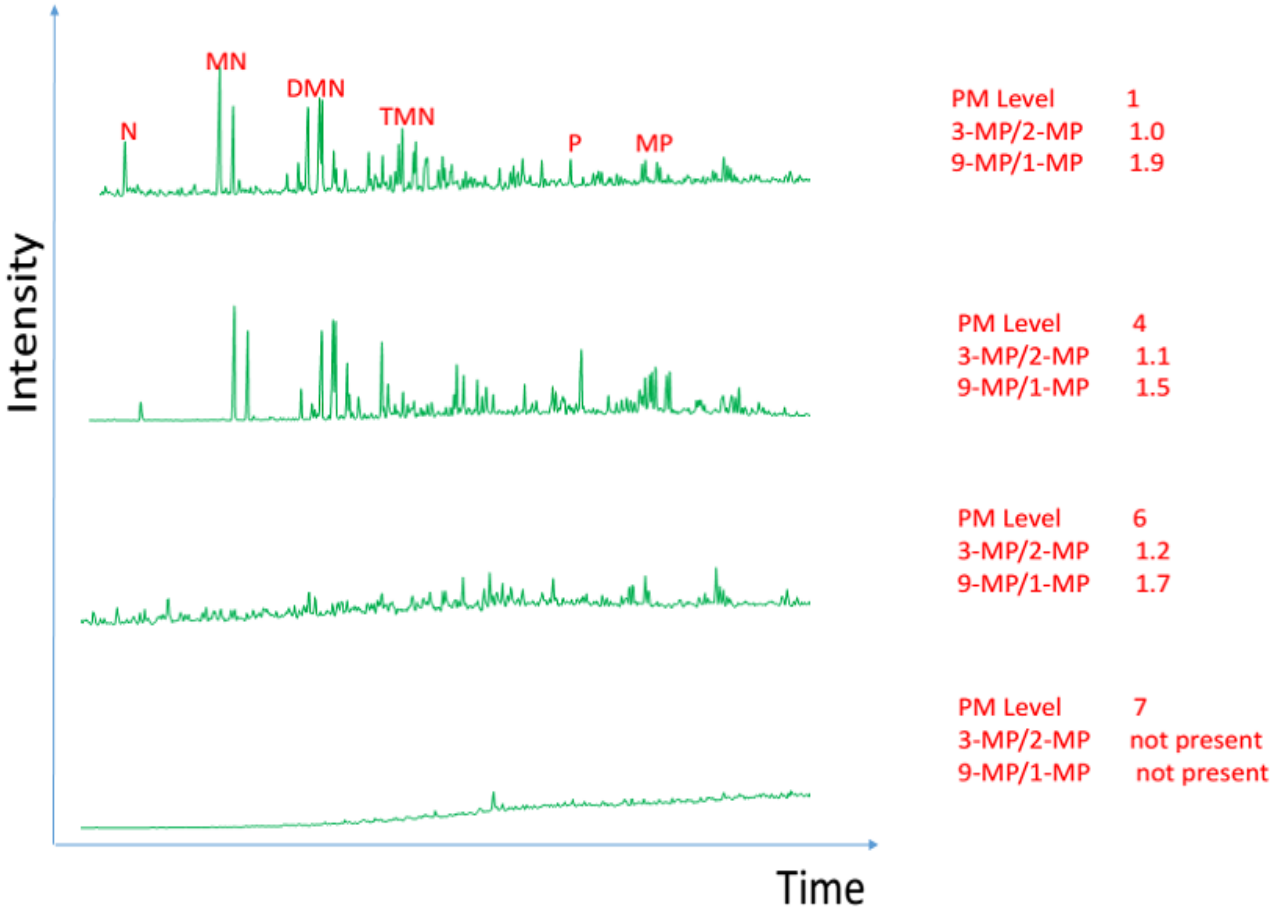

Figure 6.14: Representative total ion current (TIC) chromatograms of aromatic hydrocarbon fractions of Niger Delta oil samples showing relative biodegradation susceptibilities of different aromatic compounds (OE034, OE121, OE100 and OE035).

6.2.7 Effects of biodegradation on sterane biomarkers

The attack on the sterane distributions does not start until after PM level 5 when all the isoprenoids have been altered. At PM level 7 there is a clear attack on the regular steranes (Figure 6.15) and any ratio calculated from those samples will be potentially misleading,

but the diasteranes are more resistant to biodegradation than the regular steranes and they do not seem affected (Figure 8.15). The %$C_{27, 28, 29}$ ααα 20R steranes at very high biodegradation levels is unreliable and should not be used for interpretation (e.g. Figure 6.15), and the 20R isomers are relatively more susceptible to biodegradation than the 20S isomers of the $C_{27, 28, 29}$ ααα steranes as seen in the Niger Delta oil samples (cf. Peters *et al*., 2005).

At very high levels of biodegradation when the $C_{27, 28, 29}$ ααα 20R steranes are preferentially removed from oil samples, there could be a tendency to misinterpret source and maturity of the samples.

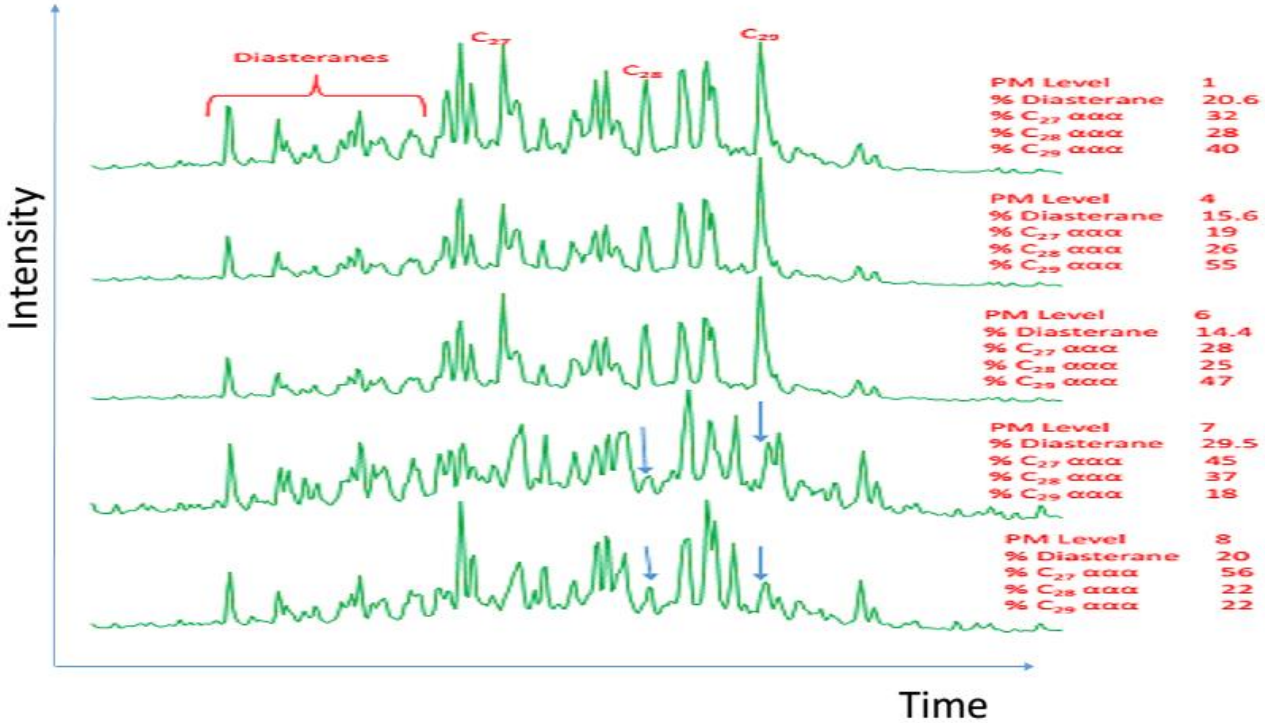

Figure 6.15: Representative *m/z* 217 mass chromatograms showing the distribution of the diasteranes and the regular steranes in the Niger Delta oil samples. Note the preferential removal of the $C_{27, 28, 29}$ ααα 20R steranes from the onset of PM level 7 and the selective preservation of the diasteranes (OE016, OE007, OE126, OE081 and OE038).

6.2.8 Effects of biodegradation on hopane biomarkers

The attack on and removal of hopane biomarkers only starts at around PM level 7/8 where the C_{30} to C_{35} 22S and 22R hopanes are removed. An obvious feature in the *m/z* 191 mass chromatograms of the Niger Delta oil samples is the relative enrichment of the unknown

C_{29} triterpane peak A which seems to be relatively resistant to biodegradation (Figure 6.16) and this peak stays relatively elevated even when other hopanes are depleted/destroyed. At these PM levels the relative abundances of oleanane also increase because of the relative removal of the C_{30} αβ hopane, which might lead to the reporting of anomalous oleanane index values of highly biodegraded oils (Figure 6.16). Peak A elutes around where the 25-norhopane is expected to elute but the mass spectra shows that they are different compounds though the compound can be useful when dealing with the degradation level of highly biodegraded oil samples. The Central Delta oil samples are much more biodegraded whereas the Southern Delta oil samples are least biodegraded based on peak A/ hopane ratio (Figure 6.17).

The seco-oleananes identifiable in the *m/z* 193 mass chromatograms can also be used for the assessment of very high biodegradation levels, with peak A+B showing resistance to biodegradation, whereas peaks C and peak D are preferentially biodegraded (Figure 6.16). The %A+B is positively correlated with oleanane index and at very high biodegradation (> PM 5) these peaks show elevated abundances relative to peaks C and D in the Niger Delta oil samples (Figure 6.16 & 6.18). Although C_{29} triterpane peak A and seco-oleanane peak A+B are useful to indicate heavily biodegraded oils, there is a high possibility that they are source specific and are also resistant to biodegradation (previous chapter, section 5.7.1).

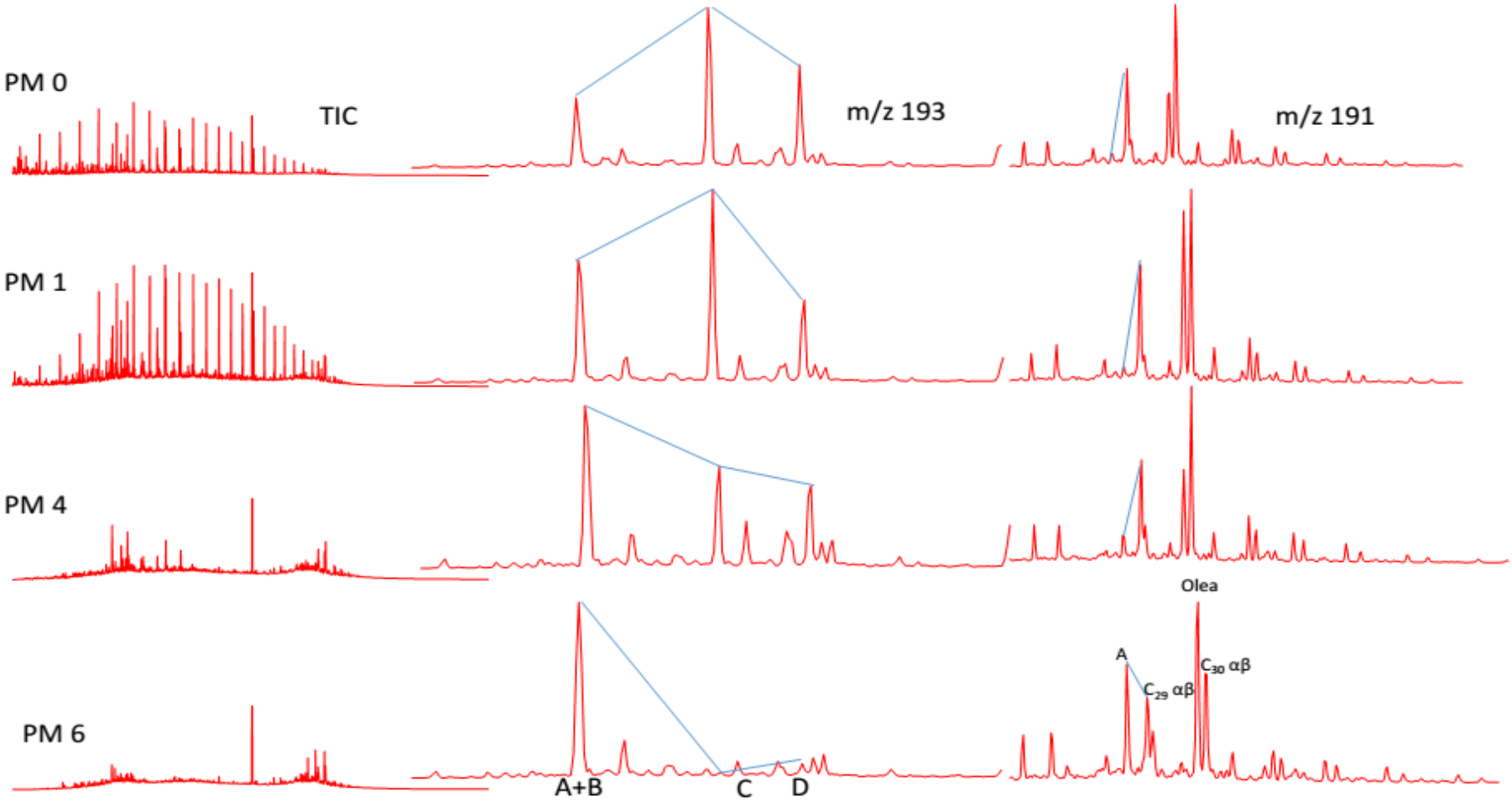

Figure 6.16: Representative total ion current (TIC), *m/z* 193 and 191 mass chromatograms displaying the distribution of the seco-oleananes and triterpanes in Niger Delta oil samples. Note the preferential enrichment (resistance to biodegradation) of seco-oleanane peak A+B (*m/z* 193) and triterpene peak A (*m/z* 191) and the preferential removal of peaks C and D (*m/z* 193).

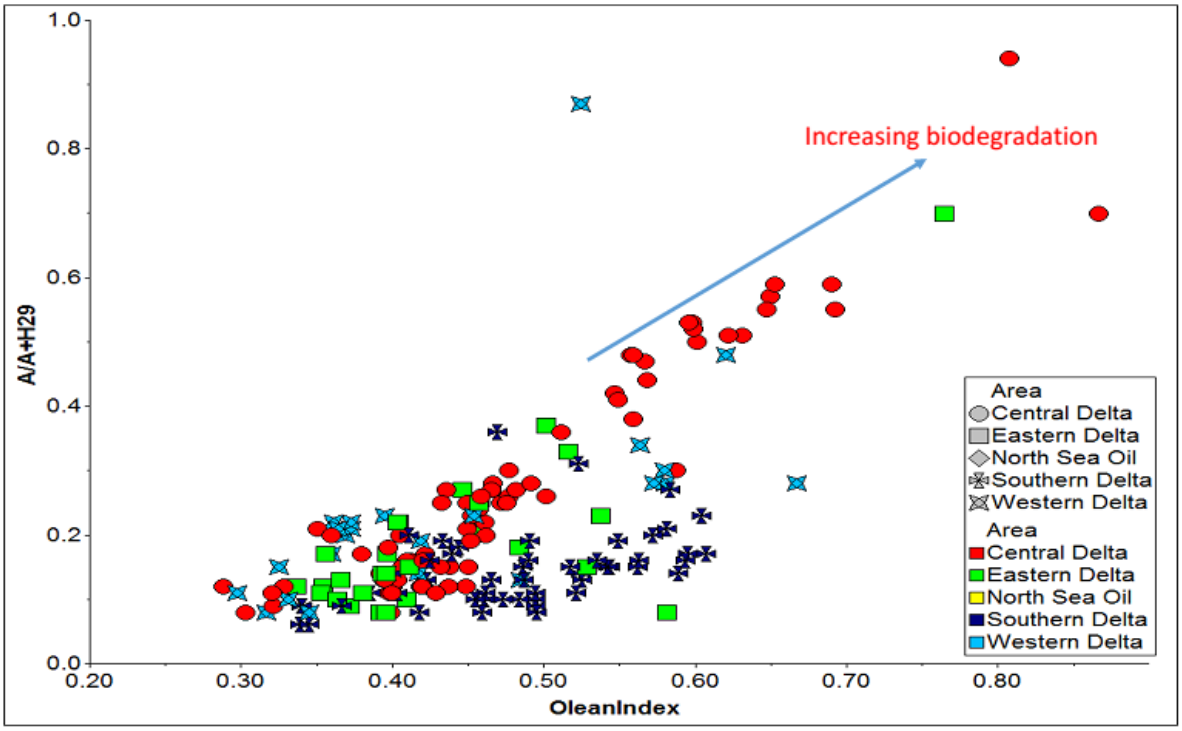

Figure 6.17: Cross-plot of oleanane index against A/A+C_{29} αβ hopane showing a positive correlation trend with biodegradation, especially after PM level 5.

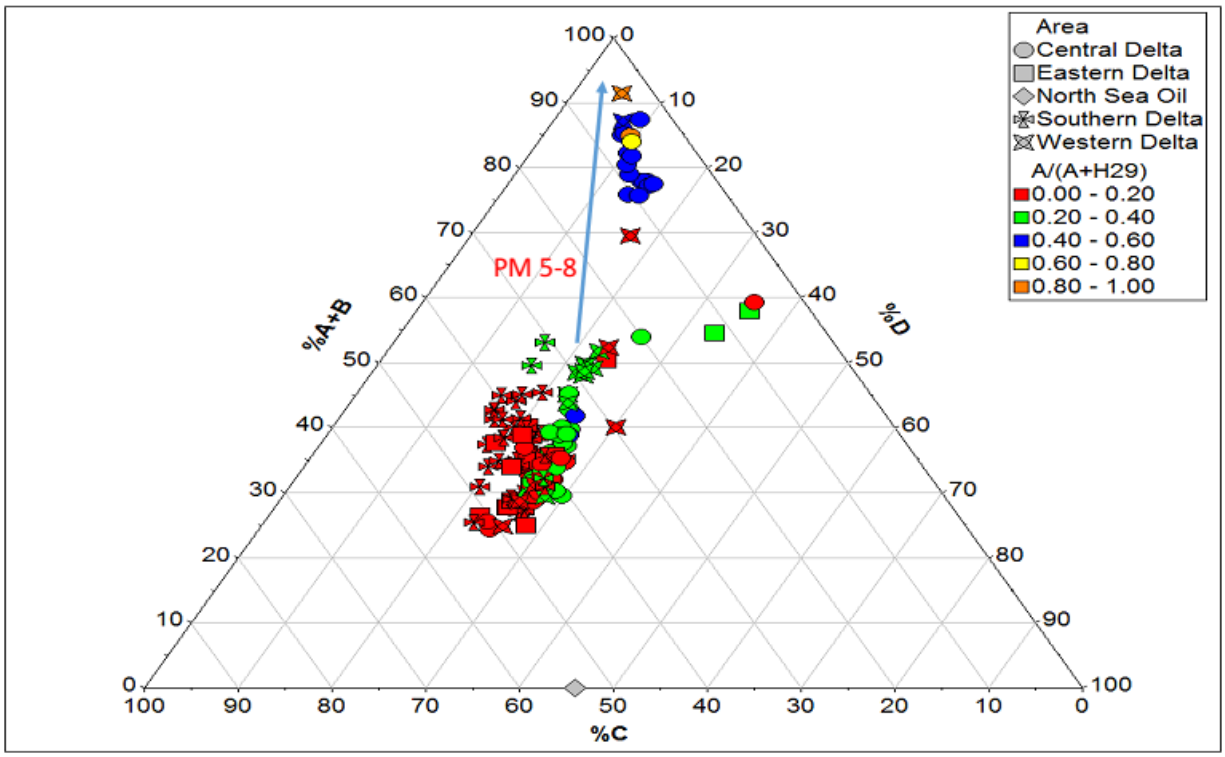

Figure 6.18: Ternary plot of %A+B, C%, D% showing increasing relative abundance of A+B after PM 5 in Niger Delta oil samples. Note the North Sea oil does not have peak A+B and there is possibility that peak seco-oleanane A+B (*m/z* 193) and unknown triterpane peak A (*m/z* 191) are related as they divide the Niger Delta oil samples into two sub-groups.

There is a positive correlation of %A+B (*m/z* 193), A/A+C_{29} αβ hopane (*m/z* 191) and oleanane index in the heavily degraded oil samples from the Niger Delta as seen from Figures 6.32; 6.35 & 6.17, but this positive correlation might break down when one consider any individual well with two extremes of biodegradation level in either the shallow reservoir or the deep reservoir, e.g. one reservoir with PM 0-1 and the other reservoir with PM 5-7. This may be due to the possible effect of mixing of a fresh charge with the biodegraded oil because even at high PM, some oils do not show much compositional variation to a PM level 0/1 oil sample from a different reservoir depth within the same well (Figure 6.19).

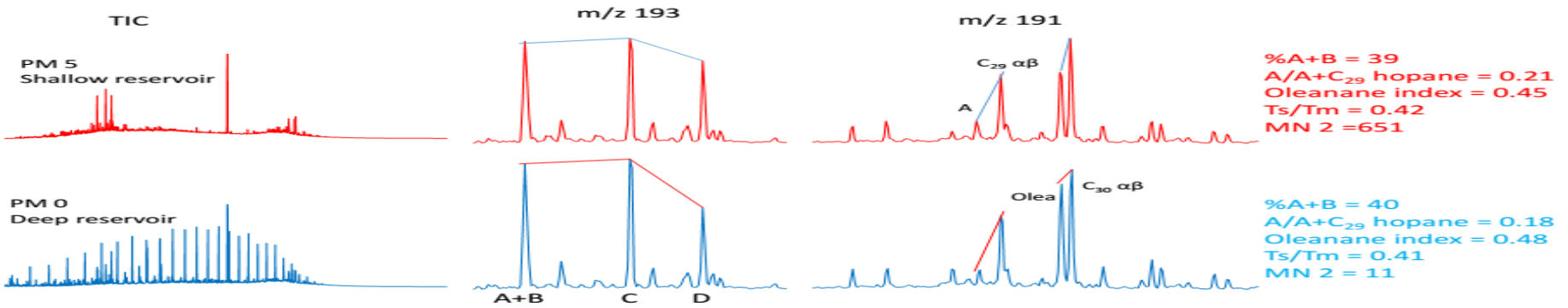

Figure 6.19: Representative TIC, *m/z* 193 and 191 mass chromatograms displaying the distribution of the seco-oleananes and hopanes in a Niger Delta well. Note the similarity in the *m/z* 193 peaks A+B and *m/z* 191 peak A and the prominent peak A in the undegraded and the degraded oil but there is a huge difference in MN 2 (MANCO number 2) (OE015 and OE016).

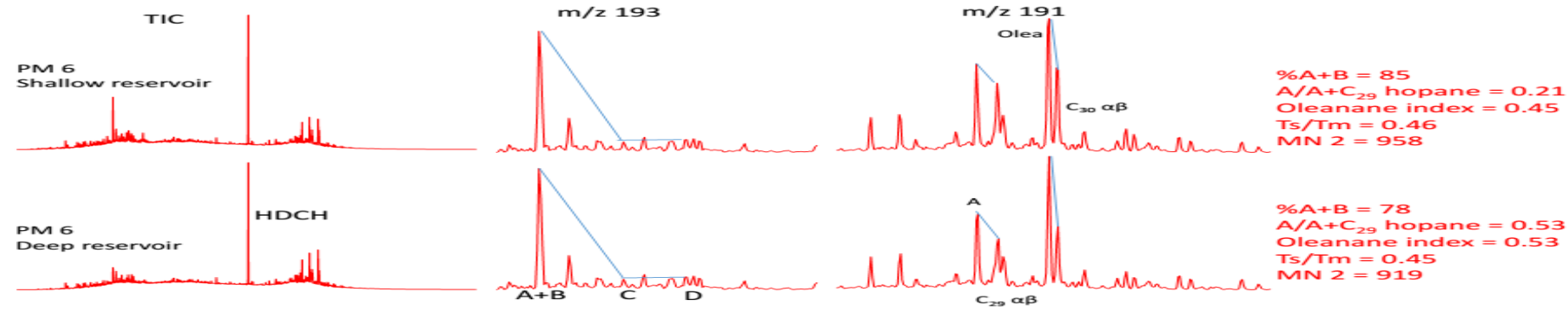

Figure 6.20: Representative TIC, *m/z* 193 and 191 mass chromatograms displaying the distribution of the seco-oleananes and hopanes in a Niger Delta well. Note the similarity in the *m/z* 193 peaks A+B and *m/z* 191 peak A in both biodegraded oils from the different reservoirs and also the similarity in the MN 2 (MANCO number 2) (OE007 and OE008).

6.3 Modular Analysis and Numerical Classification of Oil (MANCO biodegradation scale)

In a bid to improve the resolution of the various biodegradation scales (e.g. Volkman *et al*., 1983; Peters & Moldowan, 1993; Wenger *et al*., 2002; Peters *et al*., 2005), Larter *et al*., (2012) proposed the Modular Analysis and Numerical Classification of oil (MANCO) biodegradation scale which assigns a higher weight (vector/number) to compounds least susceptible to biodegradation by looking at a sequence of compounds in any oil sample.

Eleven compound classes were considered in the present work on the Niger Delta oils, and these were: class 0 (low molecular weight *n*-alkanes i.e. < nC_{15}), class 1 (high molecular weight *n*-alkanes i.e. > nC_{15}), class 2 (isoprenoid alkanes), class 3 (alkyltoluenes), class 4 (naphthalene and methylnaphthalenes), class 5 (dimethylnaphthalenes), class 6 (trimethylnaphthalenes), class 7 (methyldibenzothiophenes), class 8 (tetramethylnaphthalenes), class 9 (phenanthrene + methylphenanthrenes), class 10 (steranes). The 11 compound classes were then sub-grouped into 5 level for each compound class from 0 – 4, i.e. 0 (pristine), 1 (lightly degraded), 2 (moderately degraded), 3 (heavily degraded) and 4 (completely depleted). This gave 5 levels of degradation within each class of the 11 compound class (Larter *et al*., 2012).

The Manco number (MN2) is calculated based on the formula:

$$MN2 = \frac{[(\text{no of compound classes})+(\log_5(MN1)*(\text{scale maximum}-1))}{\text{No. of compound classes}}$$

Where:

No. of compound class = 0 - 10 (11 compound class)

Scale maximum = 1000

$MN1 = \sum (\text{class score}_i * 5^i)$

Where:

Class score= range from 0 to 4 (depending on level of compound degradation)

I= is the compound class (0 – 10).

The calculated MN2 reflects a higher number for the alteration of an increasingly resistant class, thereby providing non-linear increment with increase in degradation and highly influenced by the alterations in higher compound class (Larter *et al*., 2012). A pristine oil sample with score 0 for class 0 will give an MN2 value of undefined but this has been regarded as 0 in the present calculations and samples that also shows overwhelming indications of multiple oil charge history (biodegraded oil + fresh charge) were removed from the calculations because they will give misleading results (Figure 6.21).

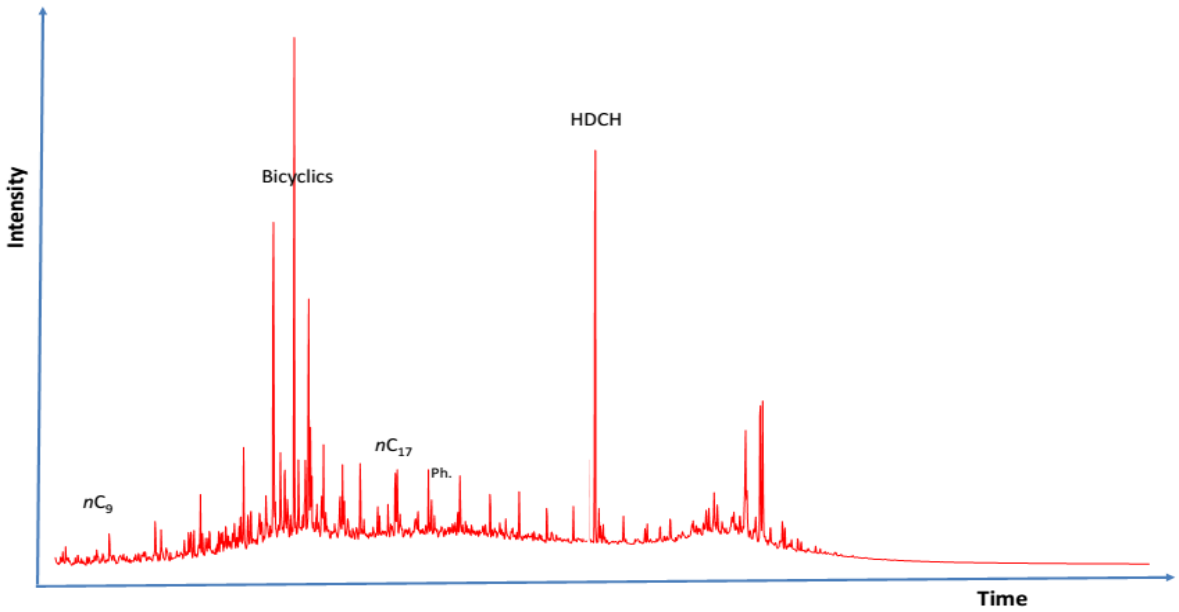

Figure 6.21: Representative TIC of an oil that had undergone multiple charge events. The elevated bicyclic peaks must have been from an early charge that has lost its pristane and phytane (PM 5) and a later charge that consist of full suite of *n*-alkanes. Note Pr and Ph are lower in concentration than the bicyclics and must have been from the later charge (OE128).

6.3.1 Comparison of Manco scale to PM scale.

The Manco scale has the big advantage that there is a possibility of a wide range of MN2 values in any PM level that is considered (Figure 6.22). For example, for the oil samples that have lost their *n*-alkanes but still possess isoprenoid alkanes, all those oils will be labelled PM level 4 based on Peters and Moldowan scale, but what the Manco scale have done is not to just stop at this stage but also to assign numbers for the stage of degradation of the alkyltoluenes, naphthalene, methynaphthalenes, dimethylnaphthalenes and trimethynaphthalenes that will be present in a PM 4 samples but might be degraded to different extents in different oils, thereby providing possible sub-divisions at any given PM level of biodegradation (Figure 6.22).

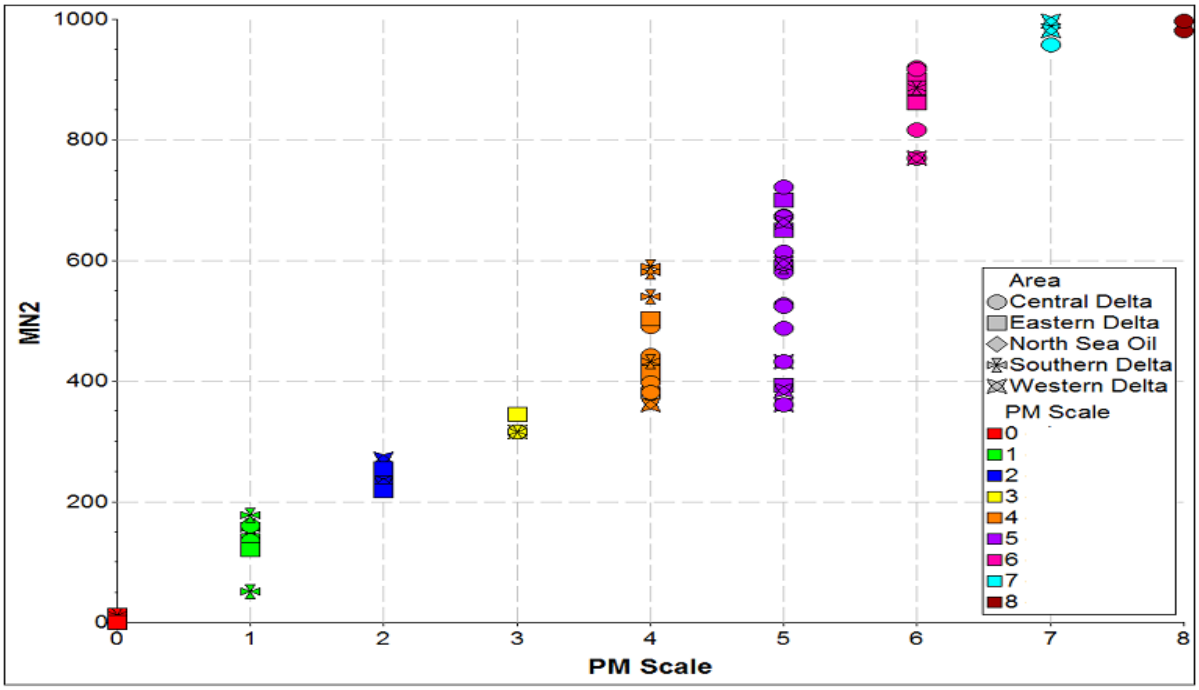

Figure 6.22: Cross-plot of Manco number 2 (MN2) against PM level of biodegradation of the Niger Delta oil samples, showing series of overlaps in MN2 of different PM levels of biodegradation. Note the range in MN2 for different PM levels.

Considering MN2 values of 350 to 600 (Figure 6.22), all PM level 4 (*n*-alkane absent + acyclic isoprenoid present) oil samples are in this range and most PM level 5 (*n*-alkane absent + acyclic isoprenoid absent) oil samples also falls in the same range. Therefore it can be pointed out that it is not just what is completely degraded that affects this but the

level (score) of degradation of compounds that are not completely degraded yet that matters in the computation of the MN2 number, as they are given a higher weight because their relative higher resistance to biodegradation. This same situation can be seen in PM level 7 and 8, where the MN2 number are similar and have same level of sterane attack, but at PM level 7 the homohopanes have not been removed but they are removed at PM level 8. It will be useful to consider the attack and removal of the C_{29} to C_{35} hopanes in the calculation of the MN2 value so as to be able to differentiate the MN2 values of PM 7 and PM 8, instead of ignoring the hopane degradation as proposed by Larter *et al*., (2012).

The inconsistencies in relative removal of compounds in an oil during biodegradation has been shown to be problematic for both biodegradation scales (Larter *et al*., 2012), while the effect of mixing and recharging of a biodegraded reservoir complicates any biodegradation study (Obermajer *et al*., 2004; Bennett & Larter 2008). Therefore as much information about the reservoir environment and its charge and thermal history as possible, should be considered in order to understand the biodegradation effects on this petroleum system.

6.3.2 Comparison of Manco scale with gasoline biodegradation parameters

The Thompson (1983) heptane ratio is a major parameter that is controlled by the biodegradation level in the gasoline range hydrocarbon of crude oils. As seen from figure 6.23, at a heptane ratio of around 12%, there is the onset of PM 1 level of biodegradation, although Thompson (1983) stated that oil samples with heptane ratio below 18% are biodegraded. It is obvious from figure 7.23 that PM level 1 samples have MN2 between 50 and 160 and PM level 2 samples have MN2 greater than 200.

The same relationship was observed with the isoheptane ratio and it can be concluded that the isoheptane ratio and heptane ratios, although are mainly used as a measure of oil maturity, they can also be used as a measure of the onset of biodegradation in any oil sample as these ratios show a correlation with the PM and Manco biodegradation scale at the onset

of biodegradation but might not be able to discriminate between PM level 1 and PM level 2 biodegradation.

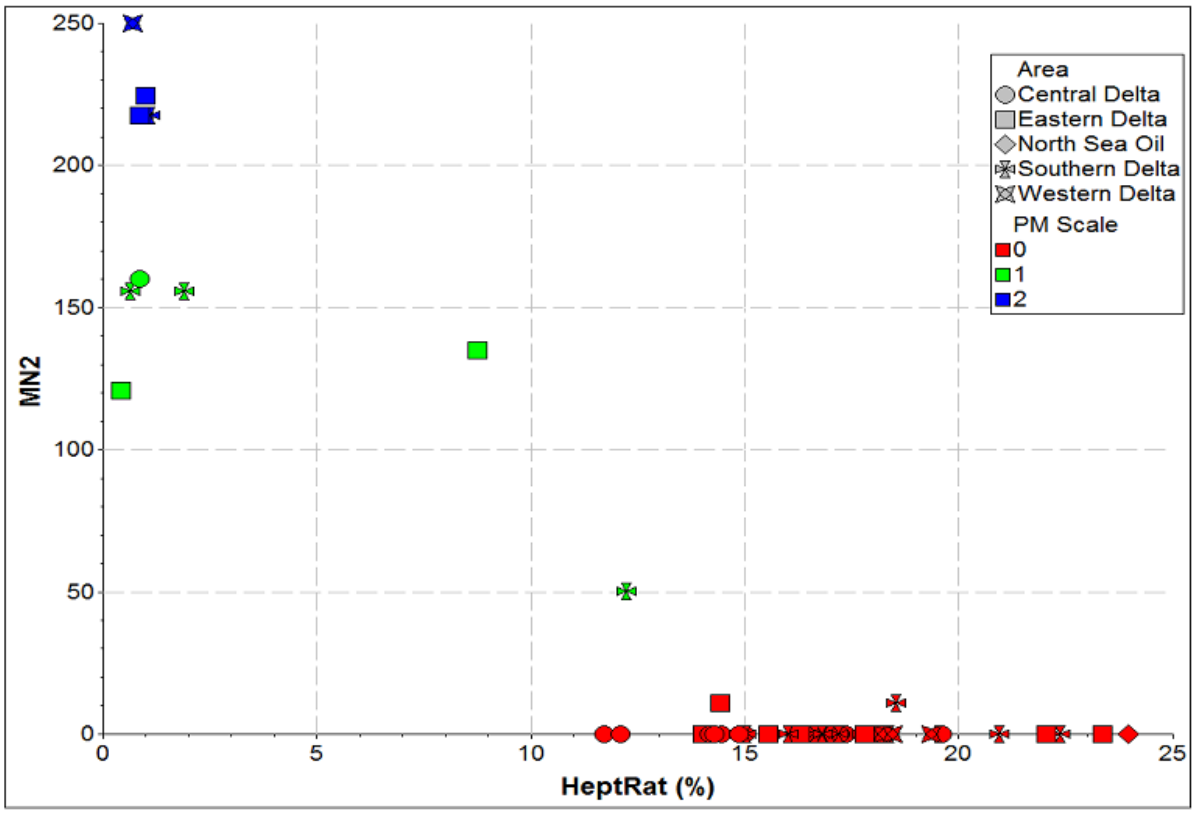

Figure 6.23: Cross-plot of Manco number 2 (MN2) against Heptane ratio. Note that with reduction in heptane ratio the MN2 increases.

6.3.3 Comparison of Manco scale with *n*-alkane and isoprenoid biodegradation parameters

The Pr/*n*-C_{17} against Ph/*n*-C_{18} ratios show the susceptibility of the normal alkanes to biodegradation as against that of the isoprenoids, because *n*-alkanes get removed from oils at PM level 4 whereas isoprenoids get removed at PM level 5. PM level 1 oil samples have an MN2 range of approximately 50 to 200 (Figure 6.24), although based on PM alone there exist no clear distinction between PM level 0 and 1 when comparing them based on the *n*-alkane/isoprenoid relationship. The PM level 2 oil samples have MN2 values above 200 but lower than 300 and PM level 3 oil samples usually have MN2 value above 300.

There is a no sharp distinction between PM level 0 and 1 and PM level 1 and 2 oil samples when comparing the relationship of the isoprenoids/*n*-alkanes values, but this can only be

valid up to PM level 3 when some *n*-alkanes are still present in the oil samples (Figure 6.24).

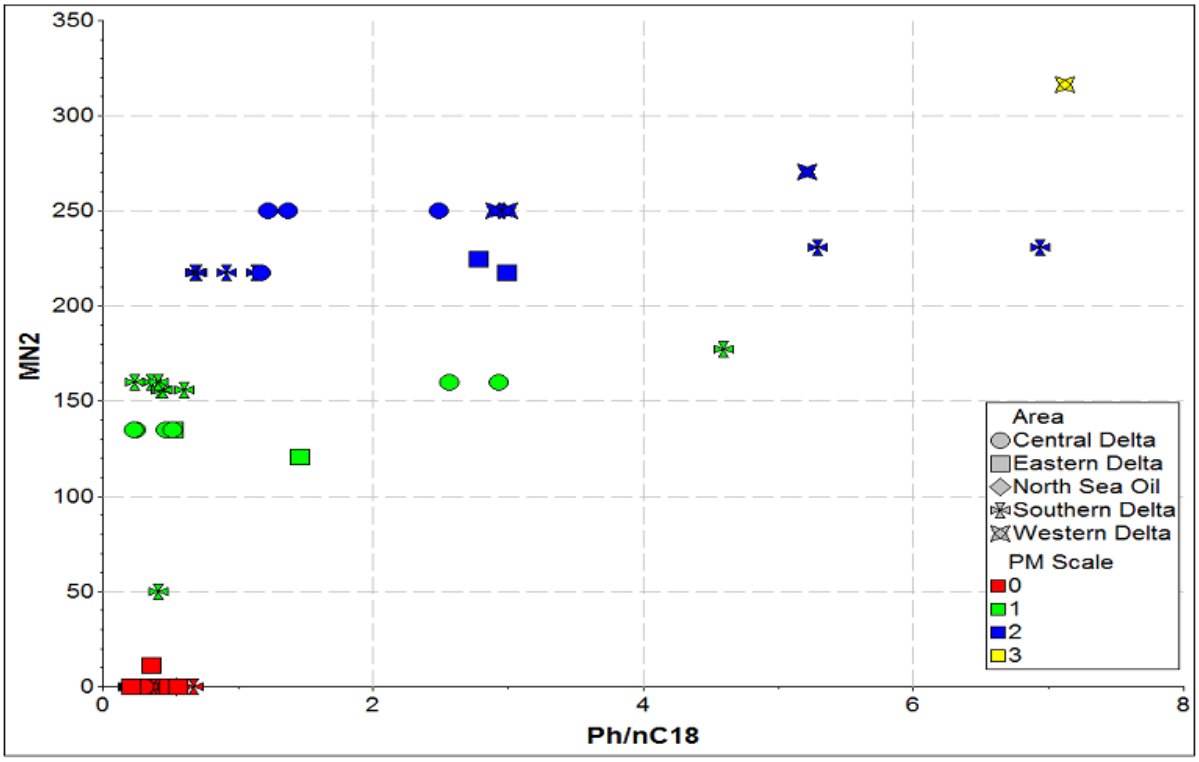

Figure 6.24: Cross-plot of Manco number 2 (MN2) against Ph/*n*C18 with PM level of biodegradation showing series of overlap in MN2 of different PM level of biodegradation. Note the range in MN2 for different PM levels.

6.3.4 Comparison of Manco scale with diamondoid biodegradation parameters

The ratio of MA/*n*-C_{11} increases with increase in biodegradation (Grice *et al.*, 2000) and when this ratio is compared to the MN2 there is a strong correlation but MA/n-C_{11} can only be calculated for oil samples with n-C_{11} and therefore at higher biodegradation levels where *n*-alkanes are absent, this ratio cannot be used. However, when the methyladamantane/adamantane (MA/AD) is considered, there is no striking relationship with either the PM biodegradation scale or the MN2 level, although Grice *et al.*, (2000) shows that MA/AD can be used as a pointer in biodegradation studies. A cross-plot of MA/*n*-C_{11} against MA/AD does not show any relationship (Figure 6.13), therefore the ratio MA/AD should be used with caution in biodegradation studies on Niger Delta oils.

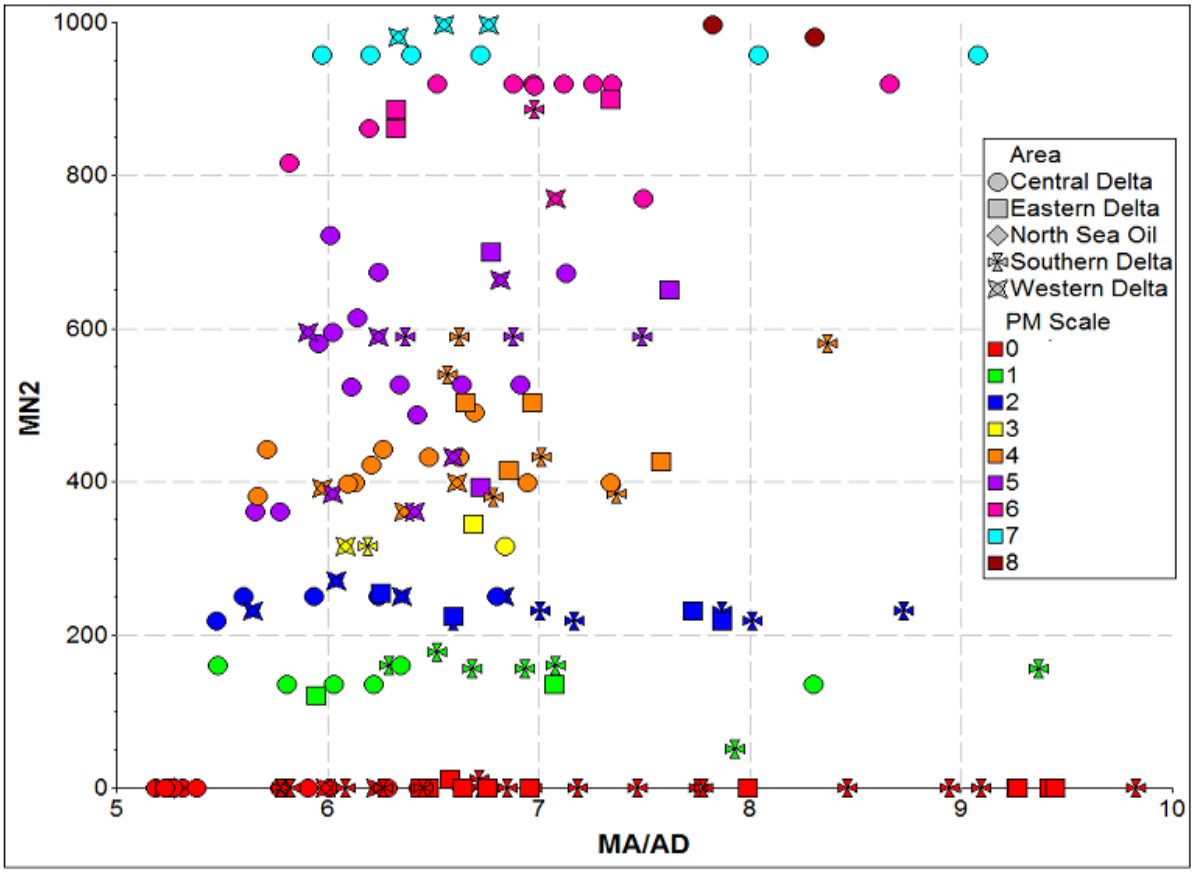

Figure 6.25: Cross-plot of Manco number 2 (MN2) against MA/AD with PM level of biodegradation showing series of overlap in MN2 of different PM level of biodegradation.

6.3.5 Comparison of Manco scale with aromatic biodegradation parameters

There is no clear relationship between the aromatic hydrocarbon distributions and the level of biodegradation. The ratio of 9-MP/1-MP (Bennett & Larter 2008; Larter *et al*., 2012); 3-MP/2-MP (Bennett *et al*., 2013) have been shown to be related to the level of biodegradation but when this ratios were considered for the Niger Delta oil samples, there was no sharp variation of these ratios with the level of biodegradation. The naphthalene concentrations in the oil samples seems to reduce with an increase in biodegradation (Figure 6.26) but even at low biodegradation levels, there are samples with low naphthalene concentrations.

The ratio 9-MP/1-MP which is known to increase at high level of biodegradation, does not show any specific pattern of variation with the MN2 values in the Niger Delta oil samples (Figure 6.27) and there is therefore a possibility of a complex interplay of multiple charge

episodes and mixing, fill and spill, complex reservoir architecture, differential rate of biodegradation to rate of charge/recharging, which could have led to these ratios not being consistent in the oil samples, because of the addition of fresh aromatic compounds to the oils while other aromatic compounds were been destroyed.

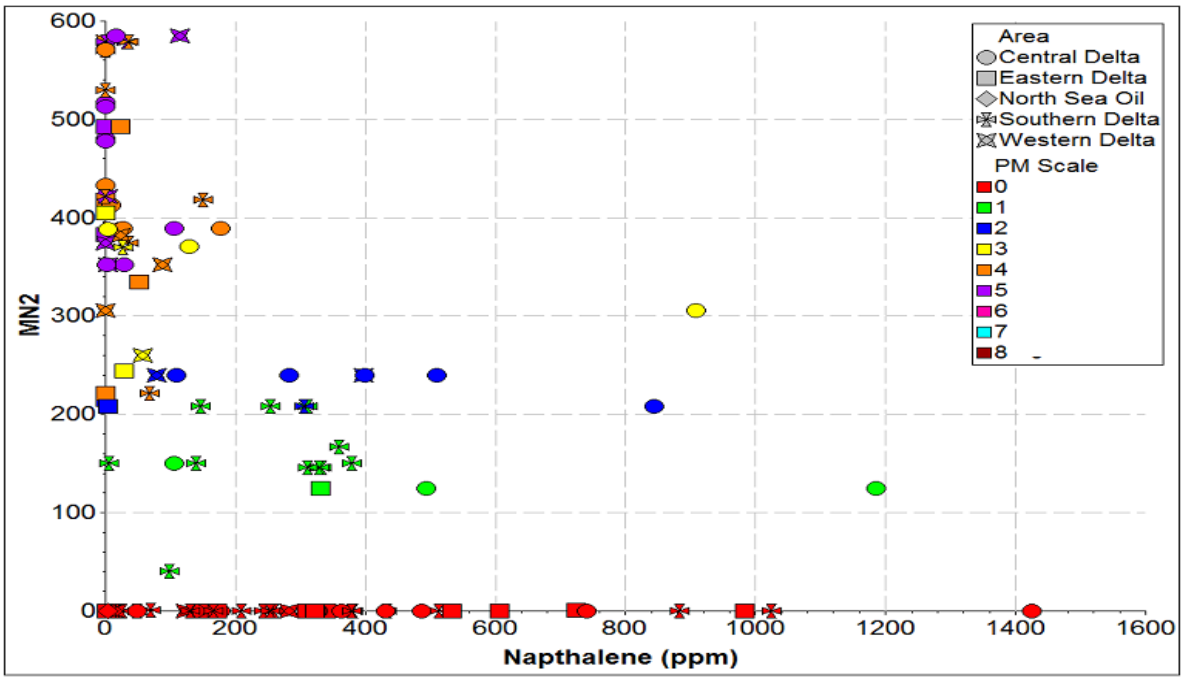

Figure 6.26: Cross-plot of Manco number 2 (MN2) against naphthalene concentration with PM level of biodegradation, showing series of overlap in MN2 of different PM level of biodegradation. Note the range in MN2 for different PM level.

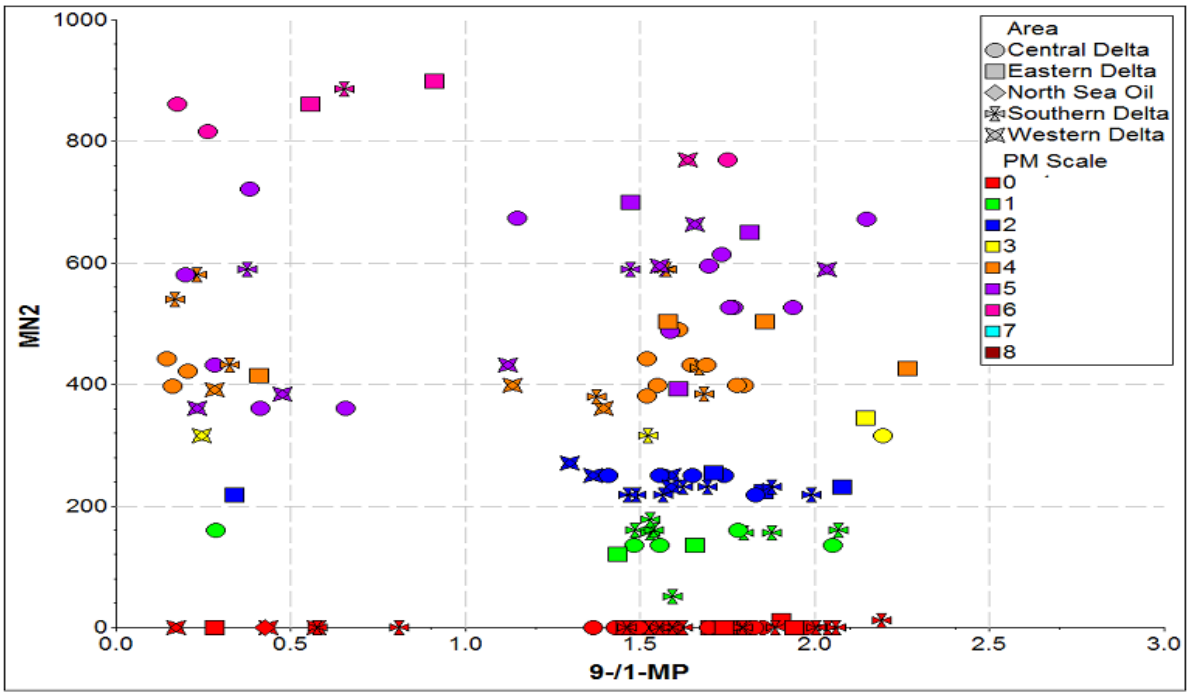

Figure 6.27: Cross-plot of Manco number 2 (MN2) against 9-/1-MP with PM level of biodegradation, showing series of overlap in MN2 of different PM level of biodegradation. Note the range in MN2 for different PM level.

7.3.6 Comparison of Manco scale with hopane biodegradation parameter

A clear feature in the *m/z* 191 mass chromatograms of the Niger Delta oil samples is the relative enrichment of the unknown C_{29} triterpane (peak A) which increases in biodegraded samples as it is relatively resistant to biodegradation and it stays relatively elevated when other hopanes are attacked (e.g. figure 6.34a). Oil samples at PM level 6 have MN2 values of between 600 and 960, and there is an obvious division of PM 6 into two sub-groups based on the MN2 values (Figures 6.28), samples that have MN2 values between 600 and 880 have relatively similar A/A+C_{30} αβ hopane ratios and most samples that have between MN2 values between 880 and 960 have elevated A/A+C_{30} αβ hopane ratios which shows that this ratio can be used to study biodegradation at very high degradation levels (PM level 6 and above).

The seco-oleananes from the *m/z* 193 mass chromatograms can also help to distinguish biodegraded oils at very high degradation levels (PM 6 and above). The %(Peak A+B)/Peak(A+B+C+D) shows a clear subdivision of oils of PM level 6, just as the Peak

A parameter showed previously, and this result can be used to subdivide PM level 6 biodegradation levels in oil samples that have peak A+B present in them (Figure 6.29).

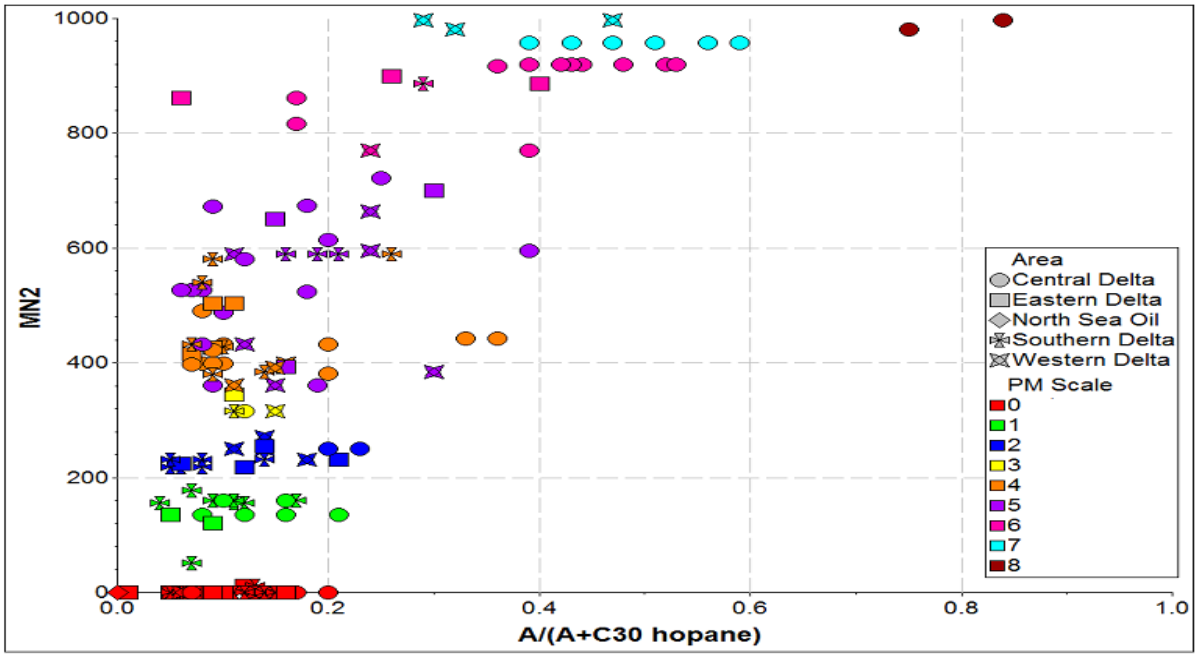

Figure 6.28: Cross-plot of Manco number 2 (MN2) against A/A+C30 hopane with PM level of biodegradation showing series of overlaps in MN2 values with different PM levels of biodegradation. Note the range in MN2 values for different PM levels.

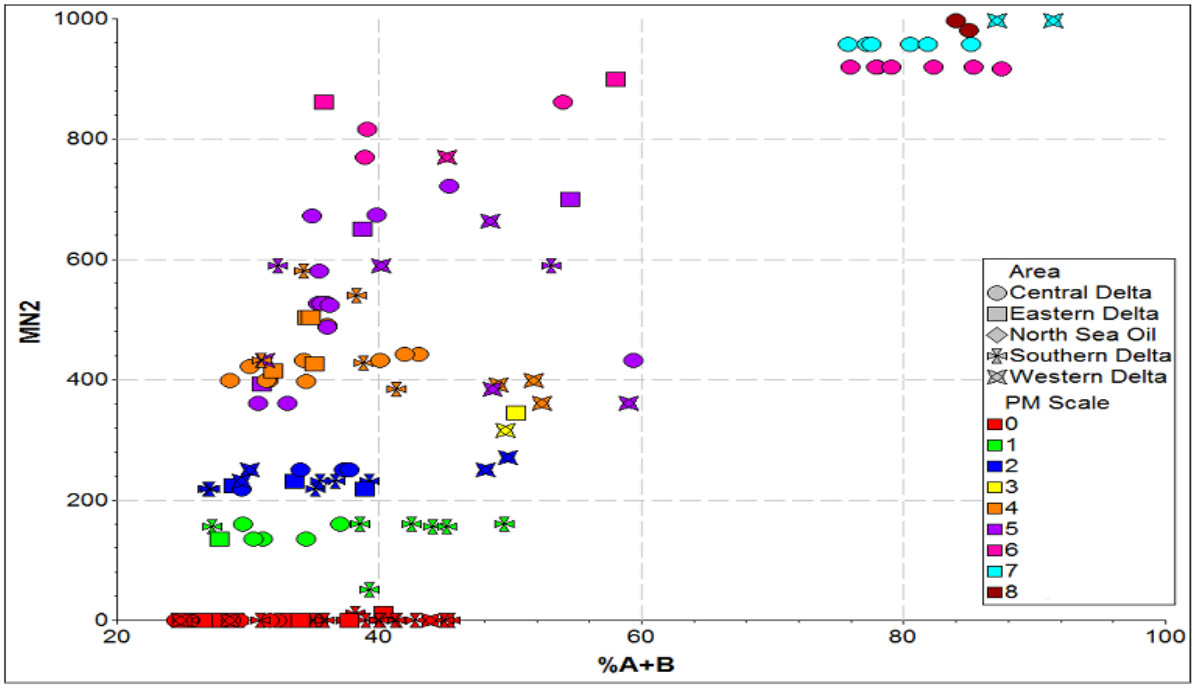

Figure 6.29: Cross-plot of Manco number 2 (MN2) against %A+B with PM biodegradation scale showing series of overlaps in MN2 values of different PM levels of biodegradation. Note the range in MN2 values for different PM levels.

6.3.7 Summary of biodegradation effects

The complex biodegradation scenarios found in the oil fields of the Niger Delta basin can be summarised as follows:

1. The central delta oil are most biodegraded whereas the southern delta oil are least biodegraded.
2. There is no obvious variation in most geochemical parameters with slight changes in the level of oil biodegradation within a well.
3. There is always a difference in the ^{13}C contents of *n*-alkanes lower than nC_{21} in oils of different reservoir depths within a well.
4. The *n*-alkane/acyclic isoprenoid alkane ratio can be a very good indicator of early biodegradation level in the Niger Delta oil samples.
5. The MA/AD diamondoid biodegradation parameter does not show any variations in the oil samples of Niger Delta probably because they are mixtures of multiple charges, whereas the MA/nC_{11} is a good indicator of early biodegradation.
6. There is no strong relationship of the aromatic biodegradation ratios with the level of biodegradation of the other Niger Delta oil hydrocarbons.
7. The unknown peak A (a C_{29} triterpane seen in the *m/z* 191 mass chromatograms) and peak A+B (seco-oleananes seen in the *m/z* 193 mass chromatograms) can be used for biodegradation studies of highly biodegraded Niger Delta oil samples.
8. The MANCO scale can potentially subdivide any single PM level of biodegraded oils, but often shows overlap in PM levels 4/5 and 7/8.
9. The interplay of multiple charge episodes and complex reservoir histories control the present day apparent level of biodegradation in the Niger Delta oils studied.

6.4 Evaporative fractionation

Gussow (1954) was the first to point out the possibility of having immature condensate which will be enriched with light aromatic compounds in the hydrocarbon gasoline range. Thompson (1987) used the term evaporative fractionation for the separation of gas from oil in the reservoir, which can be a continuous process with pressure reduction in the reservoir and this process is thought to be the origin of some condensates which are not formed by cracking of oil to gas.

Oil accumulation that has been continually washed by gas will generate two other types of hydrocarbon accumulations:

1. Gas condensates
2. Residual oil

The gas that fractionates an oil can be generated from a highly mature source rock or Type III source rock and/or cracking of oil to gas in deep reservoirs (Thompson 1987) and in the Niger Delta basin there is the possibility of several origins for such gases. The complex nature of deltaic settings (repetitive trap/seal sequences) with very thick overburden and rapid sedimentation often gives rise to overpressure and under compacted sequences which aid the formation of structures (e.g. folds/faults) that aid migration and remigration of hydrocarbons and have a very high possibility of resulting in fractionated hydrocarbon (Losh & Cathles, 2010), as in the case of Gulf Coast (Thompson, 1987) and this scenario is also possible for the Niger Delta basin which is a classical deltaic setting.

6.4.1 Fractionation from gasoline range hydrocarbons

The Niger Delta is an important gas basin with about 100 trillion cubic feet (15 billion barrels of oil equivalent) of recoverable gas in the basin (Tuttle *et al*., 1997). This basin's gas reserve is half of the oil reserve (Tuttle *et al*., 1997) and must have migrated either as a separate gas phase or dissolved gas in oil. There is a high possibility of migration and remigration of hydrocarbon in the basin due to the complex structuration and the large

connectivity of fractures and faulted formations due principally to the regional growth faults which developed because of the under-compacted and over-pressured Akata Formation (Tuttle *et al*., 1997; Haack *et al*., 2000).

A careful study of the whole oil chromatograms of the Niger Delta oil samples (Figure 6.30) indicates that there has been fractionation in most of the oil fields and this does not have any relationship with the reservoir depth (deep vs shallow) and their 3+4 MD concentrations. The concentration of aromatic compounds is seen to increase with increasing fractionation and there is also a relative reduction of *n*-alkanes with increasing fractionation as they must have been mobilised into the gas phase washing the oil column.

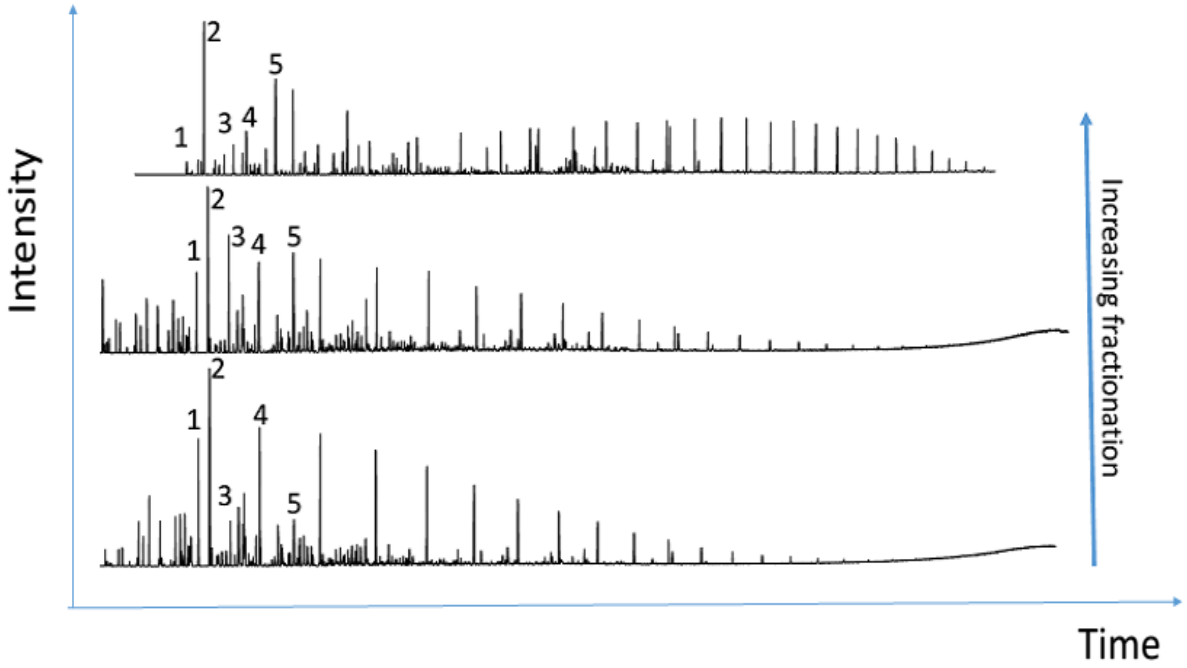

Figure 6.30: Representative whole oil chromatograms (for Niger Delta oil samples OE98, OE162, OE87) showing increasing fractionation. Note the relative enrichment of aromatic compounds and depletion of *n*-alkanes with increasing fractionation. The three Niger Delta oils shown do not appear to have been biodegraded and have nC$_{17}$ > pristane.
(1= *n*-heptane. 2= methylcyclohexane. 3= Toluene. 4= *n*-octane. 5= meta & para xylene).

The Thompson BF-diagram (Figure 6.31) shows that some of the Niger Delta oils analysed have been fractionated and the extent of fractionation is different for different reservoir and regions. The Central Delta oils show intense fractionation, with most of the samples from this region showing fractionation effects and some of the Southern Delta oils have also

been fractionated, although most of the samples from this region plot in the pristine oil zone of Figure 6.31. Some samples from the Eastern Delta have been fractionated but like those of the Southern Delta region, most of the oils from this region plot in the pristine oil zone. Only five samples were analysed from the Western Delta because most of the samples were biodegraded and have lost their *n*-alkanes, of these one was biodegraded and the other four were pristine oils (Figure 6.31) and these analyses indicate that the Western Delta region oils analysed have not suffered from reservoir fractionation, but this need to be re-evaluated by increasing the granularity of the sampling from this region to confirm the validity of these findings across the region.

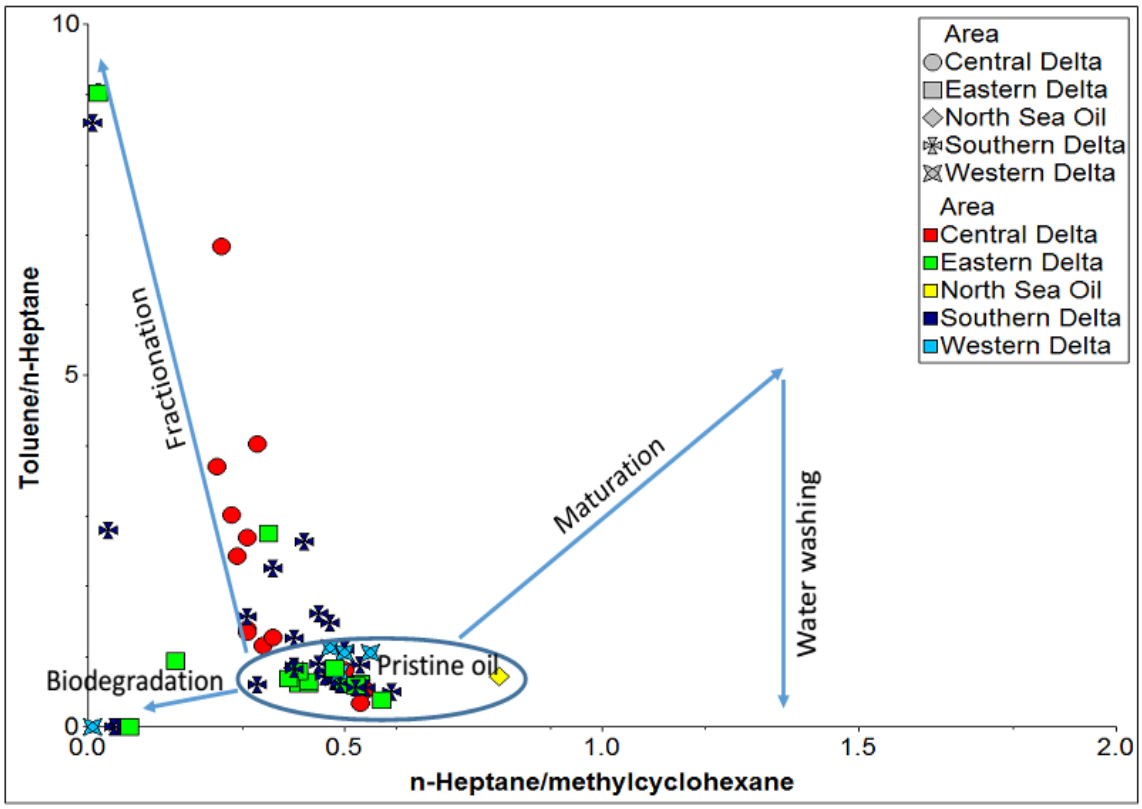

Figure 6.31: Plot of toluene/n-heptane (aromaticity ratio) and n-heptane/methylcyclohexane (paraffinity ratio) showing evaporative fractionation effects in the Niger Delta oil samples analysed. Fractionation is prevalent in Central Delta but very uncommon in Western Delta samples. Note the North Sea oil enables comparison with an unfractionated oil (after Thompson, 1987).

6.4.2: Fractionation model in Niger Delta.

Meulbrock *et al*., (1998) developed two models of gas washing in an oil field, with the possibility of the gas migrating from underneath the oil and washing the oil if there is sufficient time to equilibrate, or an oil phase migrating through a gas phase but moving slower than the gas (Figure 6.32). Both these two model scenarios may have been possible in the Niger Delta and might have enhanced the rate of fractionation in the basin, but the effect of spill and fill might have been the major cause of fractionation of these oils (Figure 6.33).

Oil that is generated early will fill the deepest reservoir which is closest to the source rocks i.e. trap 1 (Figure 6.33). Continued generation of oil will fill trap 1 up to the spill point and then spill into trap 2, and if there is generation of highly mature oil (late oil window and early gas window) as in the case of Niger Delta (see previous chapter section 5.4.3) these highly mature hydrocarbons (light oil and gas) will displace the initial oil in the reservoir and this can happen by the gas displacing the oil by moving as discrete phase up dip to the crest of the structure. This density driving mixing can easily lead to fractionation of any oil column if the reservoir has either low permeability or porosity, or both might be at play in the reservoir which will increase the residence time of the gas phase in the oil column which will in turn lead to more contact of both phases (England 1989).

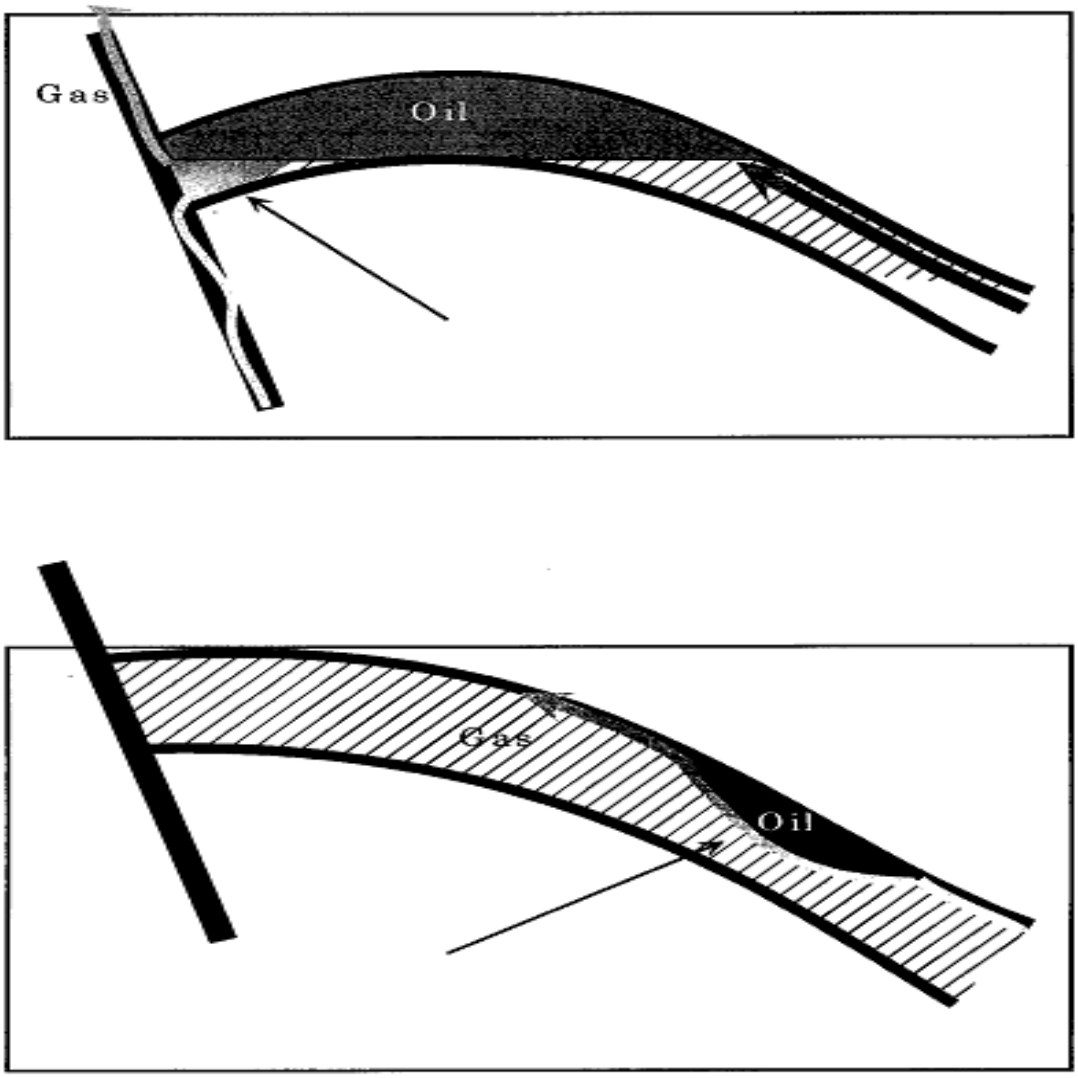

Figure 6.32: Two models of gas washing in an oil field (Meulbrock *et al.*, 1998). Arrow shows direction of movement of gas.

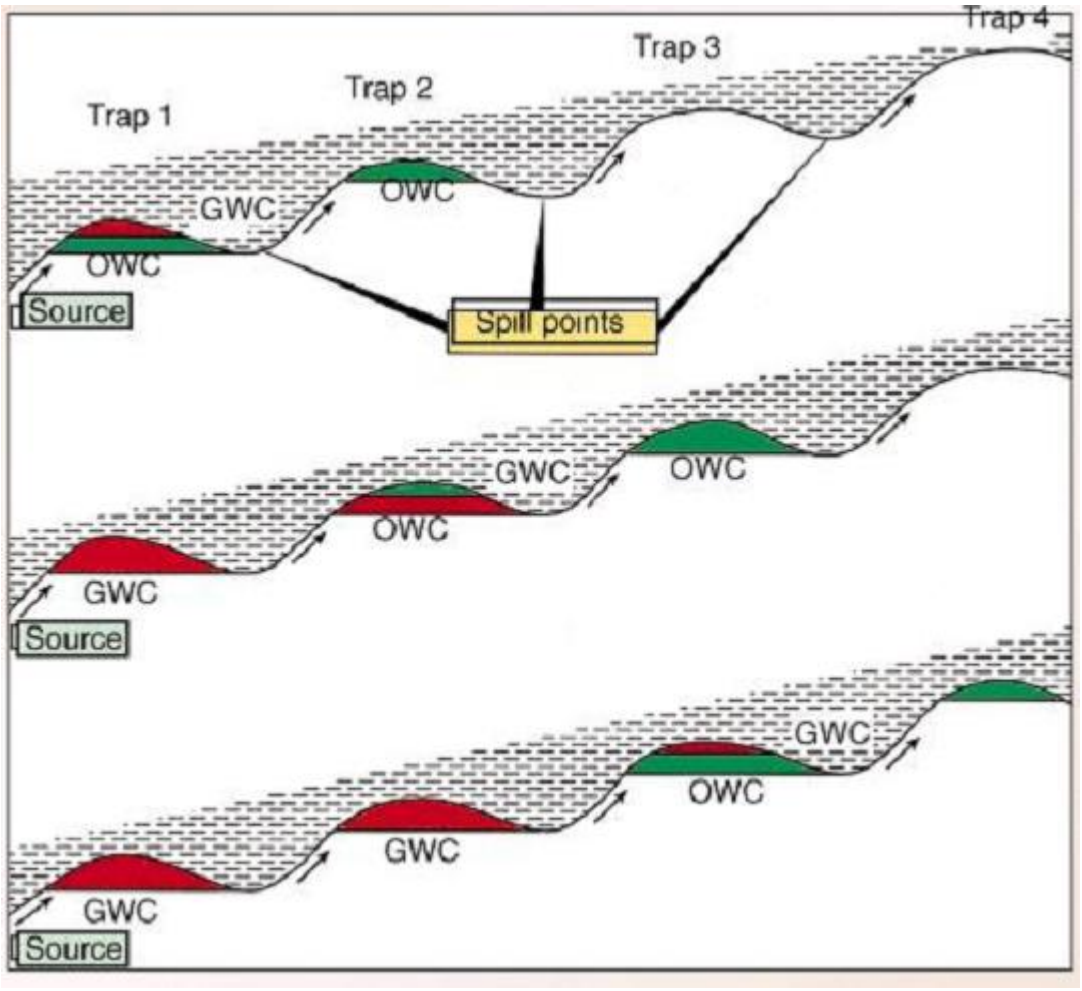

Figure 6.33: Model for Niger Delta oil fractionation as a result of continuous fill and spill events in the basin.

6.4.3 Summary of fractionation

The reservoir alteration of the Niger Delta oils by fractionation can be summarized as follows:

1. The Central Delta oils have been highly fractionated.
2. The Southern Delta oils have been fractionated to some extent.
3. There is a high possibility that the Western Delta oil are mostly pristine and have not been fractionated.
4. Fractionation in Niger Delta might be due to fill and spill mechanisms, where light oil tends to displace the initial reservoired oil.

6.5 Water washing

The preferential removal of light aromatic hydrocarbons relative to other fractions in the Niger Delta oil was studied based on two parameters Bz/cHx and Tol/mcHx. The oils used in the water washing studies were not biodegraded and they had all their light hydrocarbon contents intact/almost intact (PM level 0 to PM level 1) but there was preferential removal of benzene and toluene compared with the other fractions (Figures 6.34 & 6.35) in some samples. Based on this, a scheme was used to categorise the oil samples into groups of intense water washing; slight water washing and no water washing.

Water washing in the oils from the basin did not show any particular relationship with reservoir depth, but most oil samples that appeared water washed were also biodegraded to PM level 1and the oil samples from the Eastern Niger Delta had suffered more water washing than all the other part of the delta (Figure 6.34). Based on this it could be speculated that there may be more active hydrodynamic movement in the Eastern part of Niger Delta basin.

The continual removal of soluble hydrocarbon components by formation waters will lead to compositional heterogeneity even in genetically related hydrocarbons and could lead to false correlation results in basin studies. However, the abundances of benzene and toluene have been used as a separating factor between terrigenous sources and marine sources, as source rocks deposited in marine environment are known to be depleted in their toluene and benzene concentration compared to those of terrigenous origin (Leythaeuser *et al*., 1979a; 1979b; Odden *et al*., 1998). Therefore, there exist a possibility that the Eastern Niger Delta oil samples are mainly marine and their depletion in gasoline range aromatics is source dependent.

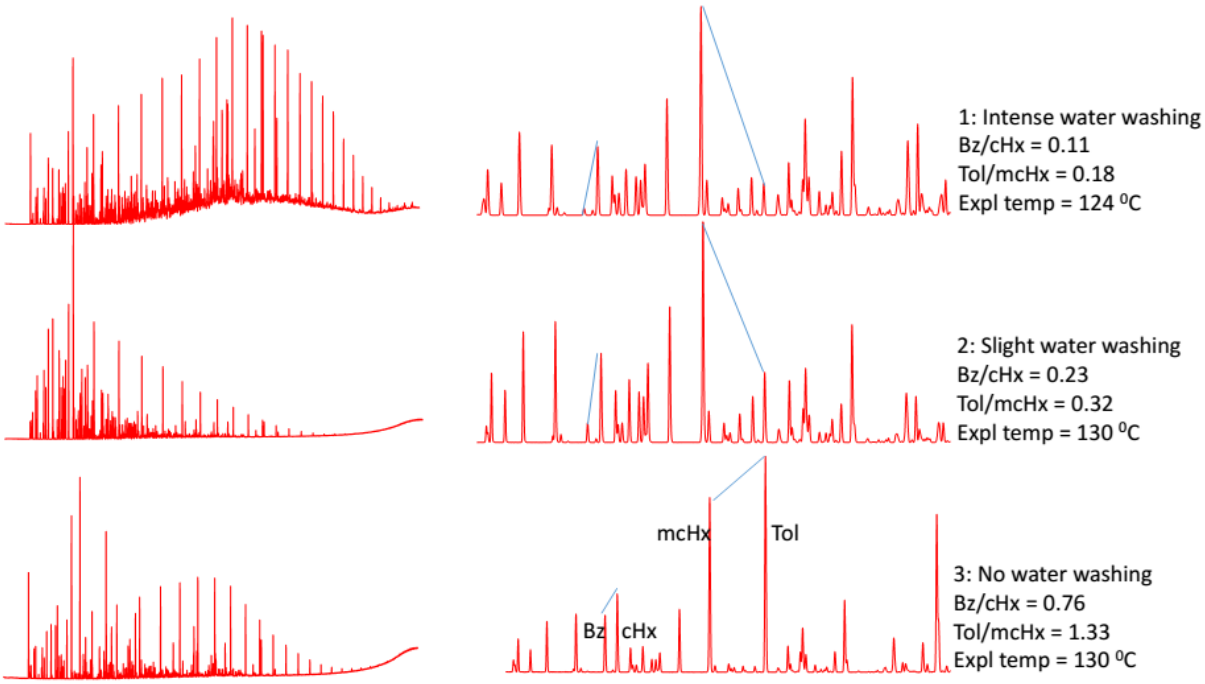

Figure 6.34: Representative whole oil gas chromatograms and partial chromatograms showing the effects of water washing on light hydrocarbons of non-biodegraded oil samples from the Niger Delta. Oil sample 1 may be a mixture of highly biodegraded oil with a non-biodegraded fresh charge with hump of unresolved complex mixture. Note the relative peak intensities of benzene, cyclohexane, methylcyclohexane and toluene (OE115, OE064 and OE039).

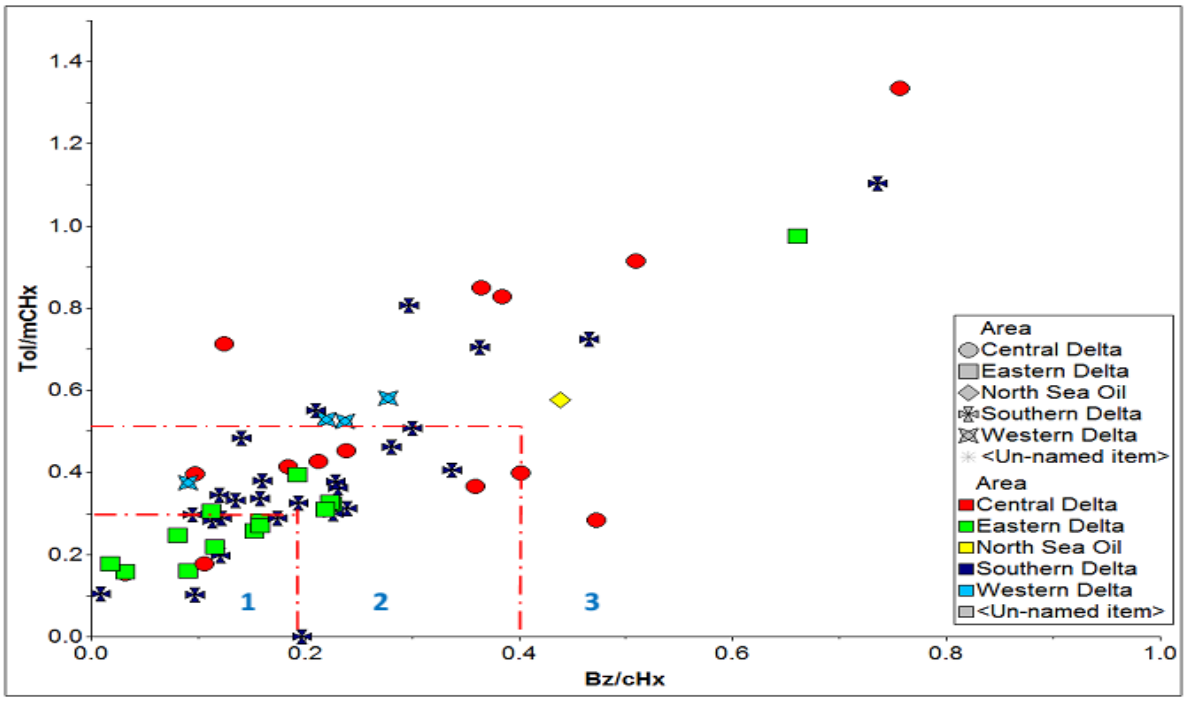

Figure 6.35: Cross plot of toluene/methyl cyclohexane against benzene/cyclohexane showing different intensities of water washing (1: intense water washing, 2: slight water washing, 3: no water washing) in Niger Delta oil samples. Sub divisions of water washing was arbitrarily set and the North Sea oil allows for comparison.

6.5.1 Summary of water washing

The reservoir alteration of the Niger Delta oils by water washing can be summarized as follows:

1. Water washing is not related to reservoir depth in the Niger Delta basin.
2. Most samples that show some indication of water washing have also been biodegraded to at least PM level 1.
3. The Eastern Niger Delta oil samples analysed are generally more water washed than those of the other region.
4. Depletion in aromatics might be as a result of source and not water washing.

CHAPTER SEVEN

OIL FAMILIES AND THEIR INFERRED SOURCE ROCKS

7.0 Introduction

Principal component analysis (PCA) which is tool used in chemometric analysis, helps to simplify complex data with large numbers of variables, into a new compressed variable while filtering out noise and data that show no relationships (e.g. Parfitt & Farrimond, 1998; He *et al*., 2012); variables that plot in same cluster hold similar interpretations and those that plots away from each other are either not related or negatively related (Gurgey, 2003). In addition to conventional molecular marker distribution measurements and parameters, the compound specific isotope analysis of *n*-alkanes is also a very useful tool for correlation of either oils to oils or oil to source rocks (e.g. Murray *et al*., 1993) and has proved extremely useful when dealing with comingled oil (Rooney *et al*., 1998; Peters *et al*., 2005). Carbon isotope ($^{13}C/^{12}C$) and hydrogen isotope (D/H) ratios have been used as a diagnostic tools in several geochemical studies (e.g. Murray *et al*., 1993; Rooney *et al*., 1998; Santos Neto & Hayes, 1999; Li *et al*., 2001; Schimmelmann *et al*., 2004; Pedentchouk *et al*., 2004; 2006; Sun *et al*., 2005) for either finding a positive or negative correlations among oil and their probable source rocks, while anomalies seen in isotopic signatures can help unravel new petroleum systems and exploration targets (Summons *et al*., 1998).

7.1 Oil to oil correlation

The correlation parameters considered in this work are those that mainly reflect organic matter source input, however some of them are also affected by thermal maturity, biodegradation etc., and their effects are considered during the interpretation. PCA is used for oil to oil correlation and the first two principal components (i.e. PC1 and 2) are the main ones considered as they contain the greatest percentage variance and highest Eigenvalues of any of the studied data. The interpretation follows the same format that was used in chapter 6, i.e. by consideration of each the molecular composition classes of the oil studied

(i.e. gasoline range, *n*-alkanes, diamondoids, aromatics, sterane and hopane biomarkers); sub-groupings are also considered based on their maturity as different compositional classes or molecular weight ranges sometimes indicate different levels of thermal maturity. This approach helps to minimize the effect of intense mixing from oils of different thermal maturities and source deposition environments that is prevalent in the Niger Delta basin. Compound specific isotope analysis of *n*-alkanes is also used for attempting to correlate the Niger Delta oils and well cuttings samples analysed, into families.

7.1.1 Thermally cracked oil families

Thermal maturity results from diamondoid hydrocarbons indicate that the Niger Delta oils analysed are of very high thermal maturity with %VRo equivalent of 1.1 to 1.6%, (Chapter 5, and Figure 5.15) which corresponds to late oil window to early gas window maturity and indicates that they had suffered from thermal cracking. The diamondoid results also indicated that the oils were derived from a Type II marine source (Chapter 5, and Figure 5.14). The PCA of the diamondoid hydrocarbon distributions is also used to help to unravel the number of oil families that are possible in these thermally cracked oil contributions (see below).

7.1.1.1 Correlation from diamondoid hydrocarbons

A total of 180 oil samples and 18 diamondoid hydrocarbon parameters were used for the PCA, although 8 parameters (MAI, MDI, EAI-1, EAI-2, DMAI-1, DMAI-2, TMAI-1, and TMA1-2) were rejected because they only contributed to noise in the data and did not show any particular trends. The oil samples showed different ranges of biodegradation but despite this all of the oil samples were used for the PCA, since they all contained appreciable quantities of diamondoids.

The loadings plot (Figure 7.1) shows division of the 10 accepted diamondoid hydrocarbon parameters into 3 groups, with group 1 made up of the following parameters; MA/EA, MA/DMA, MA/TMA, MA/TeMA, DMA/TMA, TA/TeMA, TMA/TMA, which are

mainly used for correlation purposes. The group 2 diamondoid hydrocarbon parameters are**;** MD/D, MA/AD and these two parameters can be used for correlation purposes but have been shown to be susceptible to biodegradation (Grice *et al*; 2000). The diamondoid hydrocarbon parameter in group 3 is TeMA/TeMA, and although this is a correlation parameter, it plots on its own and it was not clear if it was affected by some secondary alteration process, or that its use as a correlation parameter might be of limited significance in the Niger Delta oils.

The loadings and scores plots of the diamondoid hydrocarbon parameters (Figures 7.1 & 7.2) indicates that all the Niger Delta oil samples are genetically related. All the samples in family A1 show elevated MA/EA (Wang *et al*., 2006; Yang *et al*., 2006), MA/DMA (de Araujo *et al*., 2012), MA/TMA (de Araujo *et al*., 2012), MA/TeMA (de Araujo *et al*., 2012), DMA/TMA (de Araujo *et al*., 2012), TA/TeMA (de Araujo *et al*., 2012), TMA/TMA (Wang *et al*., 2006; de Araujo *et al*., 2012) values, and these have been shown (Chapter 7, Section 7.4.2, and Figure 7.14) that they are all indicative of a Type II marine source rock. It is thus highly possible that the cracked hydrocarbons in Niger Delta are of the same family (A1).

The other samples that plot outside the group A1 have elevated MD/D (3.3 to 4.9) and MA/AD (10.9 to 33.5) values which indicates that they have been highly biodegraded (Grice *et al*., 2000) when compared with those that plot within family A1 with different ranges of MD/D (1.56 to 3.39) and MA/AD (5.18 to 8.73) values. Diamondoid hydrocarbons therefore show that these Niger Delta hydrocarbons are potentially mixtures, where the main contributory source is thought to be from thermally cracked oil. This highly mature Type II marine source must have been of regional extent and must have been buried to a deeper depth than the other sources in the Delta. The PCA helps to reveal that the thermally cracked oils are genetically related and belong to the same family (Figure 7.2) based on their diamondoids signature.

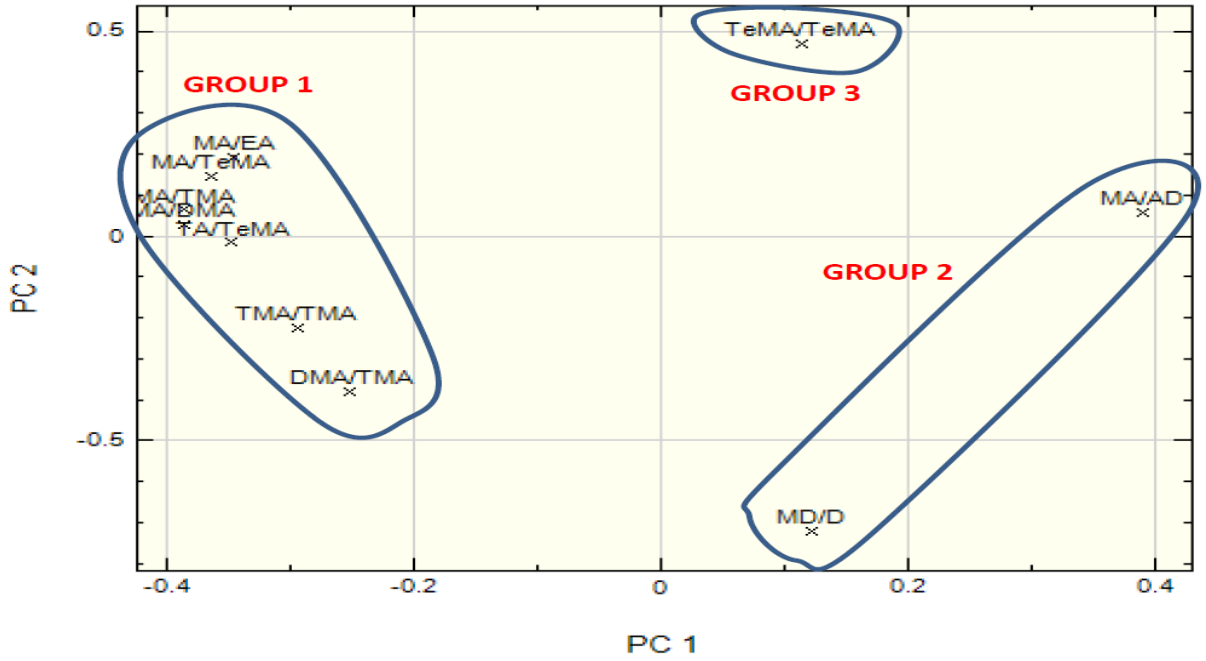

Figure 7.1: Loadings plot of first (63% of the variance) and second (14% of the variance) principal components of diamondoid hydrocarbon parameters showing the relationships between parameters used.

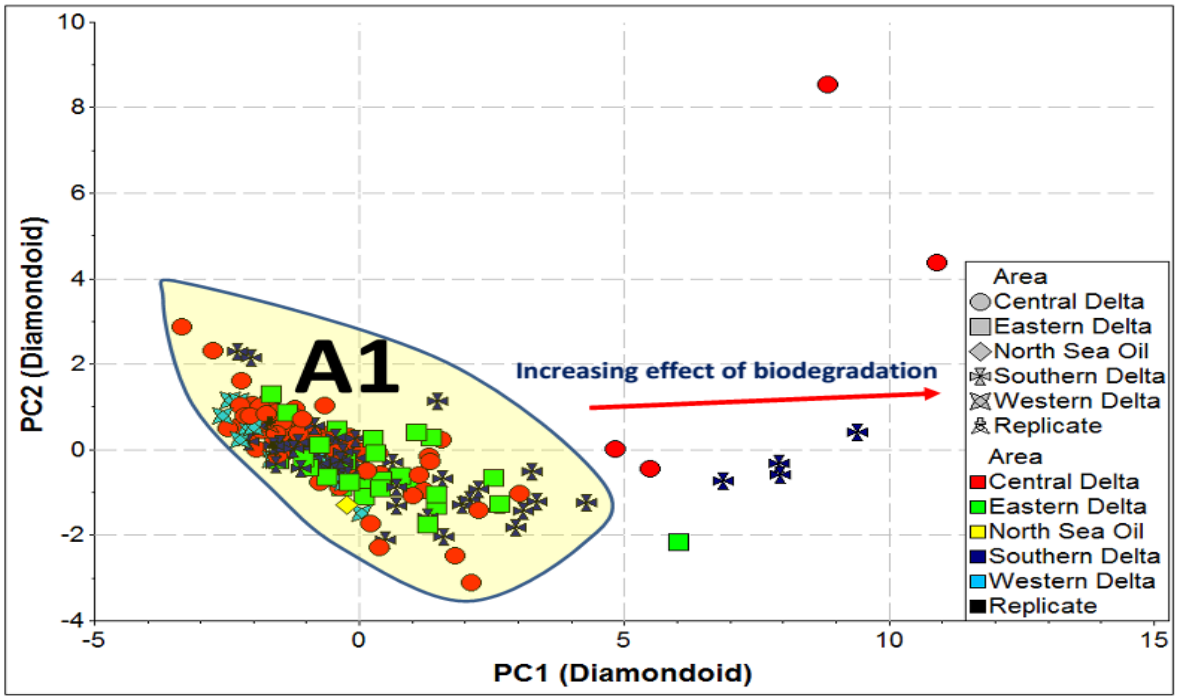

Figure 7.2: PCA scores plot of diamondoid hydrocarbon parameters for the first two principal components showing genetic relationships among the 180 Niger Delta oils analysed. Note the North Sea oil enables comparison with a known marine sourced oil. Data from replicate oil analyses plot almost on top of each other validating the significance of the experimental results.

7.1.2 Thermally mature oil families

Thermal maturity results from the gasoline range and aromatic hydrocarbons (Chapter 5, Section 5.2.3 & 5.5.2, Figures 5.19) indicates that the Niger Delta oils analysed were from a thermally mature Type II marine source with some terrigenous input. The PCA of the gasoline range and aromatic hydrocarbons helps to unravel the number of families that are possible in these highly mature oil contributions.

7.1.2.1 Correlation from gasoline range hydrocarbons

A total of 58 oil samples and 25 gasoline range hydrocarbon parameters were used for the gasoline range PCA. Of these 10 gasoline hydrocarbon parameters (P3/N2, 22/24dmP, 11/1c3dmP, P2/3mH, e/11dmcP, dmc/dmP, Bz/cH, mcH/cH, nC$_7$/nC$_6$ and Tol/Bz) were rejected because they only contributed noise in the data and they did not show any particular trend.

The loadings plot shows division of the 15 accepted gasoline range hydrocarbon parameters into 4 groups (Figure 7.3) with group 1 made up of the following gasoline range hydrocarbon parameters: mcP/nC$_6$ which is the ratio of methylcyclopentane/n-hexane (Mango 1997), mcH/nC$_7$ which is the ratio of methylcyclohexane/n-heptane (Mango 1997), dmcP/mH which is the ratio of 1-trans-3-dimethylcyclopentane/3-methylhexane (Mango 1997). All three ratios are used for fingerprinting and reservoir characterisation studies but are strongly affected by water washing and biodegradation (Mango, 1997).

The group 2 gasoline hydrocarbon parameters are**:** C$_7$Naph which is the ratio of C$_7$ naphthenes/total C$_7$ hydrocarbons (p:IGI, 2004), cP/bcC$_7$ which is the ratio of cyclopentylheptanes/branched +cyclic C$_7$ hydrocarbons (Mango, 1997; ten Haven, 1996), and N15/N16 which is the ratio of cyclopentanes/cyclohexyls (Mango, 1997; ten Haven, 1996). All the gasoline range hydrocarbon parameters in this group are mainly used for oil to oil correlation studies and are not affected by any secondary alteration process because of their relative high resistance to these alteration process (Mango, 1997; ten Haven, 1996).

The gasoline hydrocarbon parameters in group 3 are; HeptRat (Thompson 1979; 1983), P1/hept (Mango, 1997; ten Haven, 1996; Thompson, 1979; Philippi, 1975), IsohepRat (Thompson, 1979; 1983), C_7Paraf (p:IGI, 2004), P2/Hept (Mango, 1997; ten Haven, 1996; Thompson, 1979; Philippi, 1975) and b/bcC_7 (Mango, 1997; ten Haven, 1996). Although the gasoline range hydrocarbon parameters in this group are thermal maturity indicators, they can also be used to infer source deposition environment of hydrocarbons (p:IGI, 2004). The group 4 gasoline range hydrocarbon parameters are cH/bcC_7 which is the ratio of C_7 cyclohexyl/branch+cyclic C_7 hydrocarbons (Mango, 1997; ten Haven, 1996), Tol/mcH which is the ratio of toluene/methylcyclohexane (Mango, 1997), C_7Arom which is the ratio of C_7 Aromatics/total C_7 hydrocarbons (p:IGI,, 2004) and are all used for correlation and reservoir characterisation studies (ten Haven, 1996; Mango, 1997; p:IGI, 2004).

The loadings and scores plots of the light hydrocarbon parameters (Figure 7.3 & 7.4) help divide the Niger Delta hydrocarbons into 2 main families (i.e. Families A2 and B2). Family A2 samples have elevated values of C_7Naph (56.6 to 57.4) (p:IGI, 2004) as compared to family B2, cP/bcC_7 (0.29 to 0.48) (Mango, 1997; ten Haven, 1996), N15/N16 (0.19 to 0.43) (Mango, 1997; ten Haven, 1996) and are defined as having increasing marine input and they also have lower values of cH/bcC_7 (0.55 to 1.33) (Mango, 1997; ten Haven, 1996), Tol/mcH (0.22 to 0.31) (Mango, 1997), C_7Arom (6.46 to 11.7) (p:IGI, 2004, 2004). Most family A2 oils are from the Eastern, Western and Southern Delta regions and they also have relatively lower Pr/Ph and higher nC$_{17}$/nC$_{27}$ ratios when compared with the Central Delta oil samples (Figure 8.4a & 8.4b).

The family B2 oil samples have elevated values of cH/bcC_7 (1.8 to 4.35) (Mango, 1997; ten Haven, 1996) as compared to family B1, Tol/mcH (0.43 to 1.79) (Mango, 1997), C_7Arom (19.06 to 48.19) (p:IGI, 2004). The family B2 also have lower values of C_7Naph (37.8 to 56.5) (p:IGI, 2004), cP/bcC_7 (0.12 to 0.25) (Mango, 1997; ten Haven 1996), N15/N16 (0.06 to 0.17) (Mango, 1997; ten Haven, 1996) and can be interpreted as having

increased terrigenous input. This group is mainly made up of Central Delta oils, which also have high Pr/Ph and very low nC_{17}/nC_{27} ratios (Figure 7.4a & 7.4b) and are believed to be mainly sourced from mixed Type II/III organic matter facies.

Although there are two broad families (Family A2 and B2) on the plot in Figure 7.4a, some samples plot outside the two groups and they have elevated values of mcP/nC_6 (4.2 to 15.1) (Mango, 1997), mcH/nC_7 (27.4 to 114.7) (Mango, 1997), dmcP/mH (2.41 to 4.82) (Mango, 1997). All these oil samples have been biodegraded to some extent and these parameters show elevated values due to the higher resistance of methylcyclopentane, methylcycclohexane and 1-trans-3-dimethylcyclopentane, all of which are used as numerators in calculating the ratios when compared to denominators of those parameters which are; n-hexane, n-heptane and 3-methylhexane, that are relatively easier to degrade.

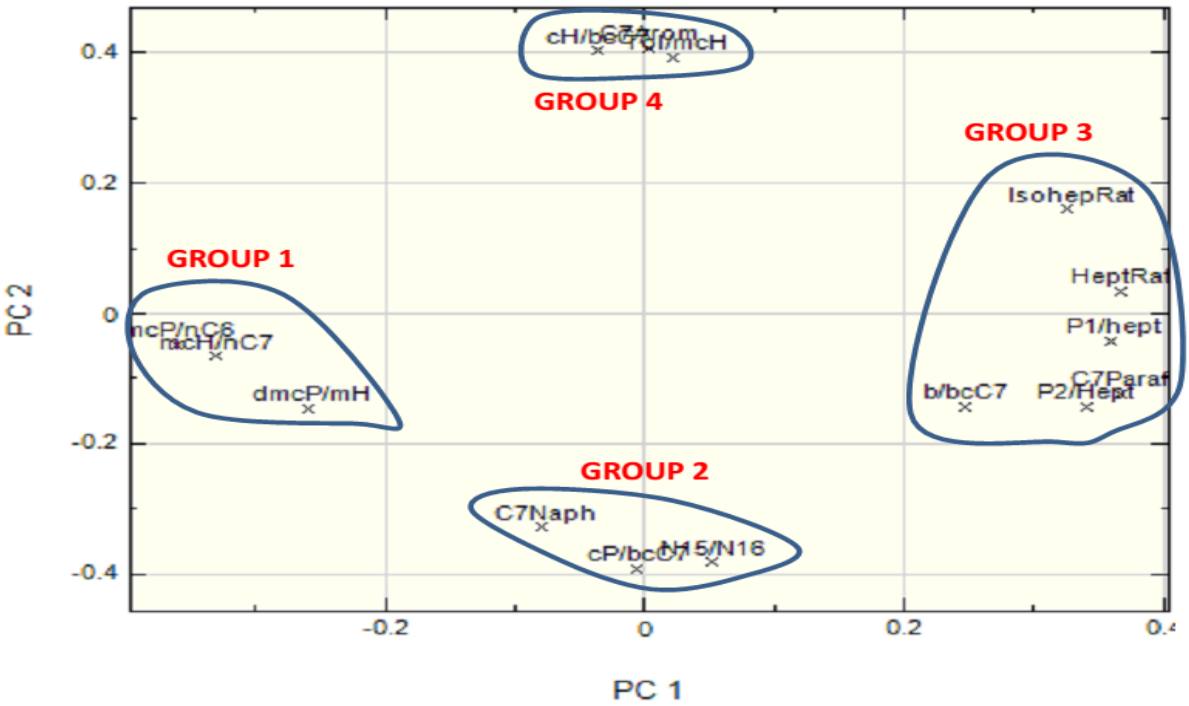

Figure 7.3: Loadings plot of PC 1 (43% of the variance) and PC 2 (34% of the variance) of the gasoline range hydrocarbon parameters. Note the 4 possible groupings of the parameters.

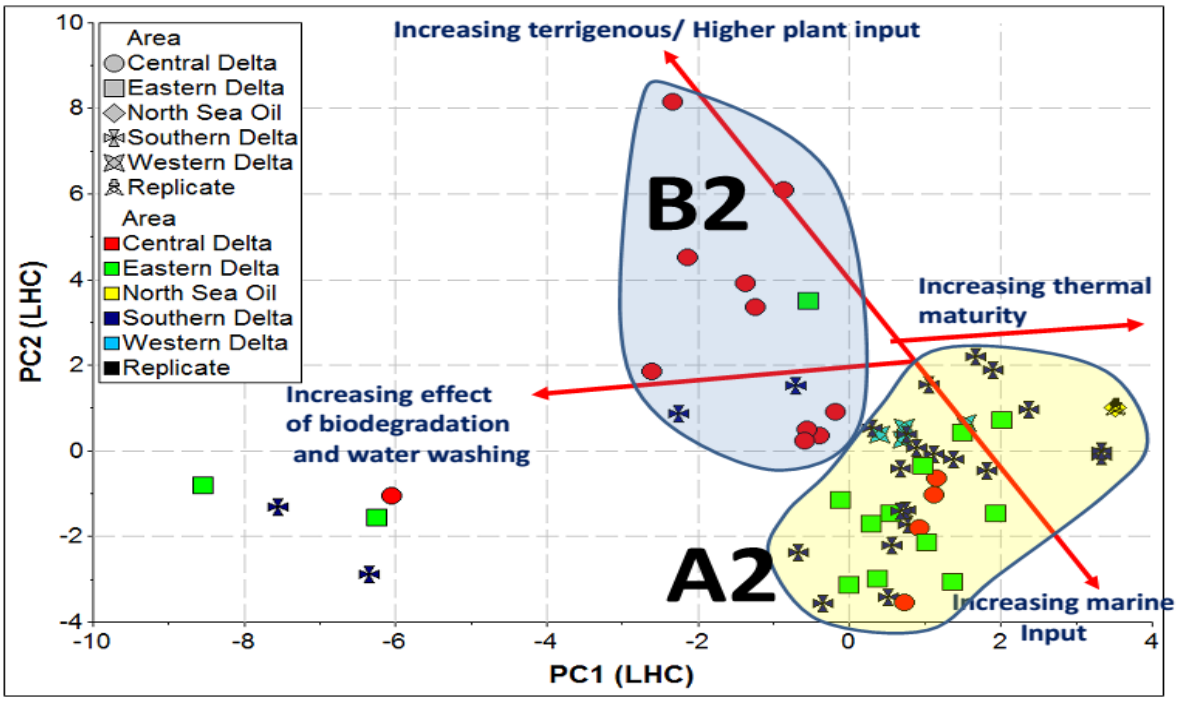

Figure 7.4a: Scores plot of gasoline range hydrocarbon parameters for the first two principal components showing relationships among the 58 Niger Delta oils analysed. Note the North Sea oil enables comparison with a known marine sourced oil.

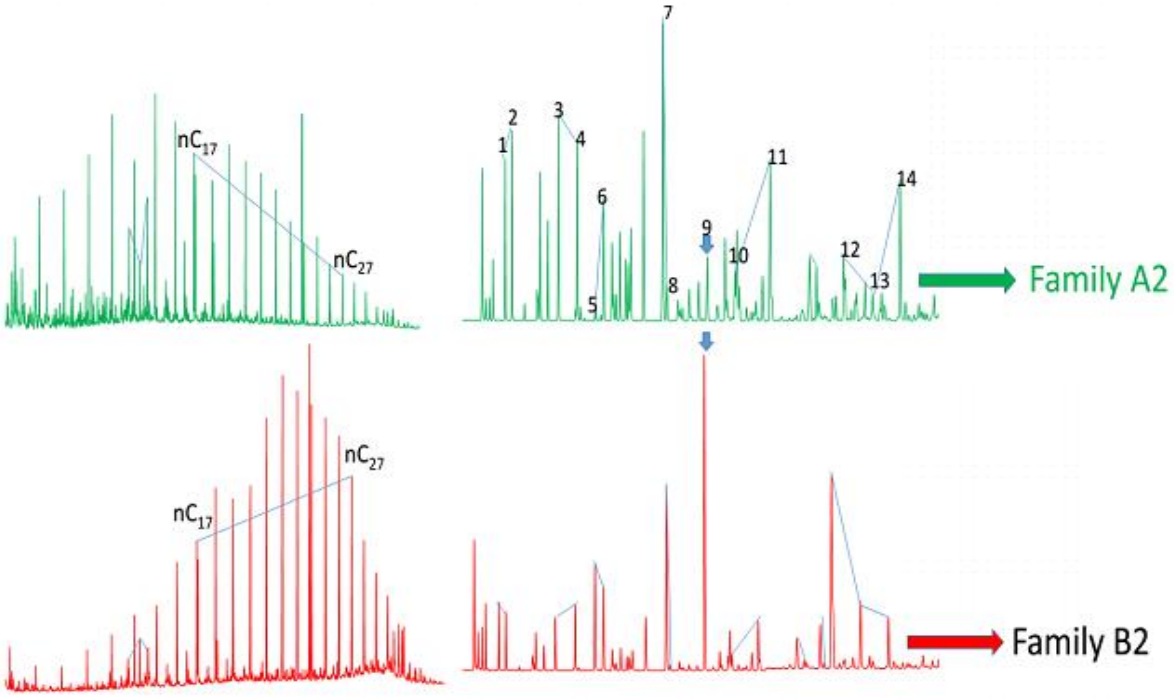

Figure 7.4b: Representative saturated hydrocarbon fraction gas chromatograms showing *n*-alkanes and partial whole oil GC-MS TIC chromatogram showing the distribution of light hydrocarbons of representative oils OE092 and OE117 from Families A2 and B2, respectively. Note the differences in the relative peak intensities.

1= iso-pentane (C_5 mono-branched). 2= n-pentane (C_5 straight). 3= n-hexane (C_6 straight). 4= methylcyclopentane (C_6 cyclo). 5= benzene (C_6 aromatic). 6= cyclohexane (C_6 cyclo). 7= methylcyclohexane (C_7 cyclo). 8= 1-cis-2-dimethylcyclopentane (C_7 cyclo). 9= toluene. 10= 3-methylheptane. 11= n-octane. 12= meta & para xylene. 13= ortho xylene. 14= n-nonane.

7.1.2.2 Correlations from aromatic hydrocarbons

A total of 156 oil samples and 11 aromatic hydrocarbon parameters were used for the aromatic hydrocarbon PCA, although 5 aromatic hydrocarbon parameters (MNR, DMN, MPR, MAS (21+22/total), MAS 29(S/S+R)) were rejected because they only contributed noise in the data and did not show any particular trends.

The loadings plot shows division of the 6 accepted aromatic hydrocarbon parameters into 3 groups (Figure 9.5) with group 1 made up of the following aromatic hydrocarbon parameters: MP(3+2/9+1), MPI-1, MPI-2 and Rc (Ro<1.35) which are mainly used for thermal maturity assessment. The group 2 aromatic hydrocarbon parameter is TAS 27 (Peters *et al*., 2005) and it plots away from the group 3 parameter which is TAS 28 (Peters *et al*., 2005) and these two parameters can be used for correlation purposes, although they have different significances. The TAS 27 which is TAS (27/26+27+28), is related to the St28iso (C_{28} αββ S+R) parameter and the TAS 28 which is TAS (28/26+27+28) is related to the St29iso (C_{29} αββ S+R) parameter (p:IGI, 2004).

The loadings and scores plots of the aromatic hydrocarbon parameters (Figure 7.5 & 7.6a) helps divide the Niger Delta oils into 2 main families (i.e. Families A2 and B2). Family A2 samples have elevated TAS 27 values (36.3 to 48.32) which is related to the C_{28} αββ (S+R) parameter and are reported as indicating marine input (Peters *et al*., 2005). Most of the Eastern Delta oils plot in this region, while the family B2 samples have elevated TAS 28 (47.06 to 56.4) values which indicates terrigenous/ land plant input (Peters *et al*., 2005) as they have been compared with the C_{29} αββ (S+R) parameter; most samples from the Central Delta plot in this family. Family A2 samples also have lower Pr/Ph and higher nC_{17}/nC_{27} ratios, whereas Family B2 has higher Pr/Ph and lower nC_{17}/nC_{27} ratios as shown by their chromatograms (Figure 7.6b).

The Western Delta and Southern Delta oil samples plot mainly with family A2 but increasingly mixed with family B2 and there is no clear distinction between these two

families. The grouping looks rather different to the light hydrocarbon groupings possibly because of the different numbers of samples used for the PCA, while it may also be due the effects of mixing proportions on individual compounds in the light hydrocarbon range, which may be different to that in the range of the aromatic hydrocarbons analysed.

The aromatic maturity parameters used MPR (3+2/9+1); MPI-1 (Radke & Welte, 1983; Radke et al; 1986), MPI-2 (Radke et al., 1986) and Rc (Ro<1.35) (Radke & Welte, 1983)], do not have a great influence on discriminating the oil samples as shown by the scores plot (Figure 7.6a).

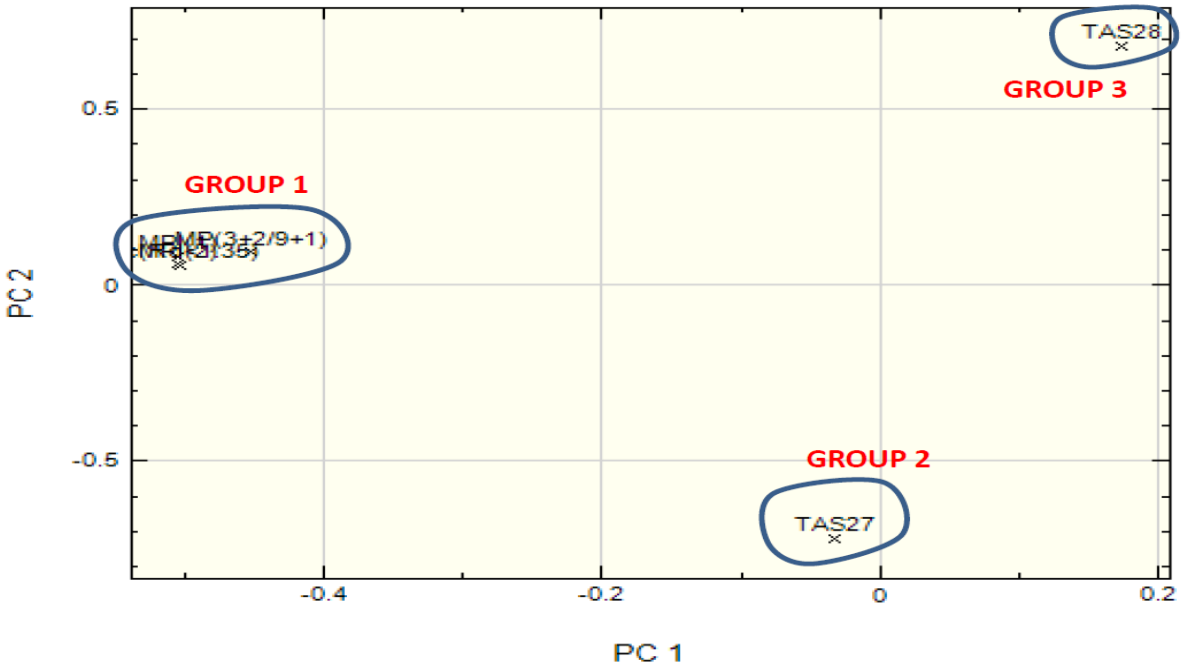

Fig 7.5: Loadings plot of first (63% of the variance) and second (32% of the variance) principal components of aromatic hydrocarbon parameters showing the relationships between parameters used.

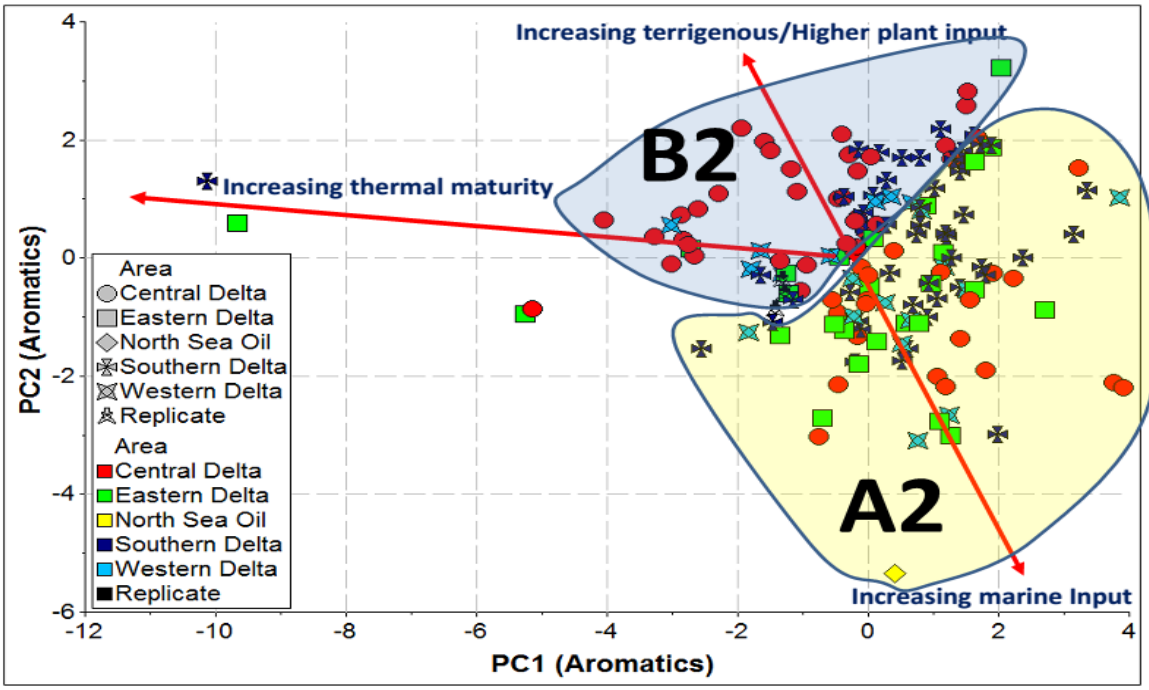

Fig 7.6a: Scores plot of aromatic hydrocarbon parameters for the first two principal components showing relationships among the 156 Niger Delta oil samples analysed. Note the North Sea oil enables comparison with a known marine sourced oil.

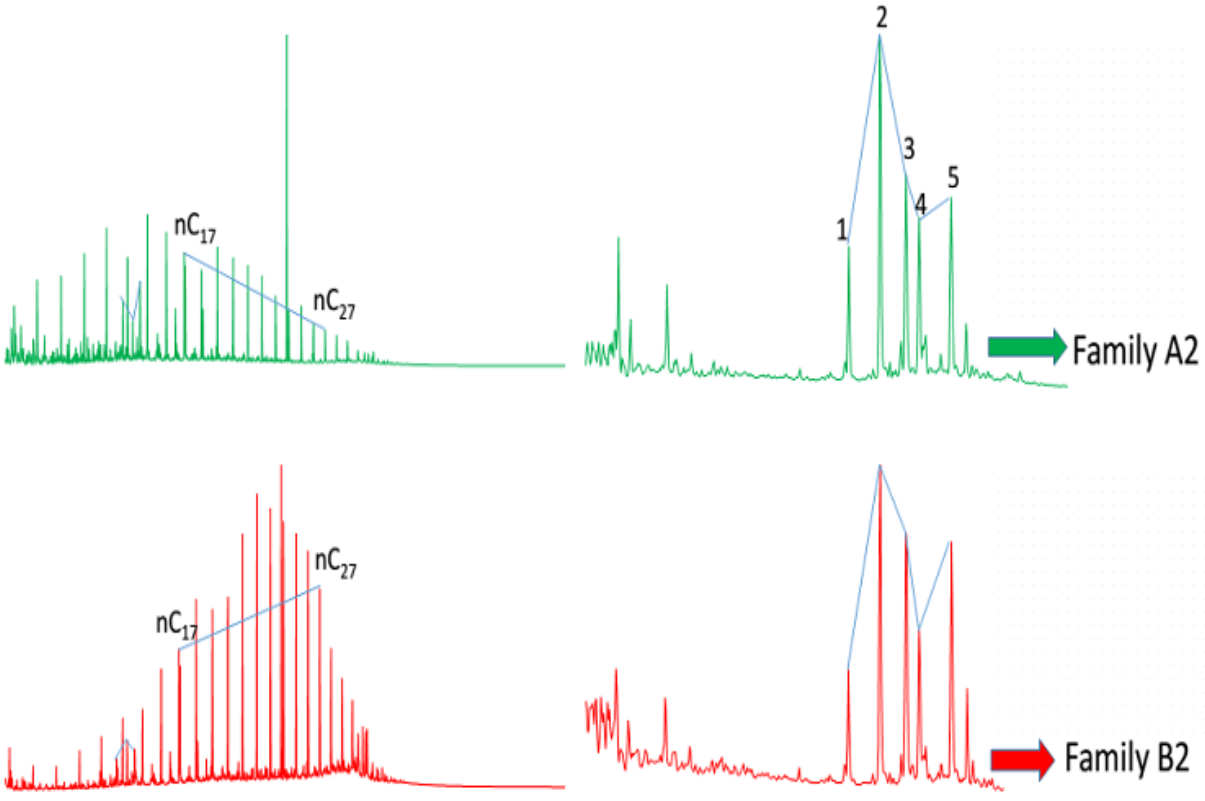

Figure 7.6b: Representative saturated hydrocarbon fraction gas chromatograms showing *n*-alkanes and partial aromatic hydrocarbon fraction *m/z* 231 mass chromatograms showing the distributions of triaromatic steroids from representative oils OE092 and OE117 from Families A2 and B2, respectively Note the differences in relative peak intensities.
1= C_{26} 20S tri-aromatic. 2= C_{26} 20R + C_{27} 20S tri-aromatic. 3= C_{28} 20S tri-aromatic. 4= C_{27} 20R tri-aromatic. 5= C_{28} 20R tri-aromatic.

7.1.3 Early mature oil families

Thermal maturity assessments from sterane and hopane biomarkers indicate that the Niger Delta oils are of early maturity (Chapter 5, Sections 5.6.3; 5.7.2 and Figures 5.24; 5.37), sourced from shales (Chapter 5, Section 5.7.1 and Figure 5.28) that were mainly deposited in a shallow marine depositional settings with high deltaic influence (Chapter 5, Section 5.6.2 and Figure 5.22). The PCA of the sterane and hopane biomarkers will help to unravel the number of families that are possible in the early mature oil contributions.

7.1.3.1 Correlation from sterane biomarkers

A total of 178 oil samples and 12 sterane hydrocarbon parameters were used for the sterane PCA, although four sterane hydrocarbon parameters (pregnanes, DiaSt, St29(S/S+R), St29(I/I+R)) were rejected because they only contributed noise in the data and did not show any particular trends in those parameters which are mainly used as thermal maturity indicators.

The loadings plot shows division of the 8 accepted sterane hydrocarbon parameters into 4 groups (Figure 7.7), with group 1 made up of the 28St217 i.e. C_{28} ααα 20R/$C_{27\text{-}29}$ ααα 20R measured from *m/z* 217 mass chromatograms (Huang & Meinschein, 1979; Peters *et al*., 2005), St28iso i.e. C_{28} αββ (20S+20R)/$C_{27\text{-}29}$ αββ (20S+20R) sterane parameter (measured from *m/z* 218 mass chromatograms) which show increasing diatom input and is specific for marine depositional environment sourced oils (Huang & Meinschein, 1979; Peters *et al*., 2005). The group 2 diagnostic sterane hydrocarbon parameters are**;** 27St217 i.e. C_{27} ααα 20R/$C_{27\text{-}29}$ ααα 20R *m/z* 217 (Huang & Meinschein 1979; Peters *et al*., 2005), St27iso i.e. C_{27} αββ (20S+20R)/$C_{27\text{-}29}$ αββ (20S+20R) from *m/z* 218 (Huang & Meinschein, 1979; Volkman et al., 1998; Peters *et al*., 2005), and they indicate increased plankton and algal sources of hydrocarbons. The group 3 sterane parameters are; 30St217 i.e. C_{30} ααα 20R/$C_{27\text{-}30}$ ααα 20R *m/z* 217 (Moldowan *et al*., 1990), St30iso i.e C_{30} αββ (20S+20R)/)/$C_{27\text{-}30}$ αββ

(20S+20R) from *m/z* 218 (Moldowan *et al*., 1990), and are indicators of marine OM contribution, however this group plots close to the group 4 sterane parameters which are: 29St217, i.e. C_{29} ααα 20R/$C_{27\text{-}29}$ ααα 20R from the *m/z* 217 mass chromatograms (Huang & Meinschein 1979 Peters *et al*., 2005), St29iso i.e. C_{29} αββ (20S+20R))/$C_{27\text{-}29}$ αββ (20S+20R) from the *m/z* 218 mass chromatograms (Huang & Meinschein 1979; Peters *et al*., 2005), and are used as indicators of terrigenous/land plant input.

The loadings and scores plot of the sterane hydrocarbon parameters (Figure 7.7 & 7.8a) helps divide the Niger Delta oil samples into 2 main families (i.e. families A3 and B3), the family A3 samples have elevated 28St217; St28iso (33.09 to 37.68), 27St217; St27iso (26.2 to 33.67) (Huang & Meinschein, 1979; Peters *et al*., 2005) and those parameters indicate that sources of family A3 oil samples were deposited in a marine environment but either not an open marine one as in the case of the North Sea oil, or have had input from land plant material. This family is mainly made up of samples from the Eastern Delta and some samples from the Southern Delta and Western Delta region.

The family B3 is subdivided into two sub families i.e. family B3A and family B3B. The family B3A oil samples have elevated 29St217; St29iso (39.8 to 43.96) (Huang & Meinschein 1979; Peters *et al*., 2005) and they indicate terrigenous input, with high Pr/Ph ratios, whereas the family B3B have elevated 30St217; St30iso (0.35 – 0.41) (Moldowan *et al*., 1990) and have lower values of St29iso compared to the family B3A oils (Figure 8.7, 8.8a & 8.8b). The Central Delta oil samples have elevated C_{29} steranes (Chapter 5, Section 5.6.2, and Figure 5.21) and this shows that they are mainly of terrigenous origin or have high contributions from land plants. The Central Delta oil samples are mainly in family B3A with some in family B3B, while the Western and Southern Delta oil samples are mainly of family B3B although they have relatively elevated C_{29} steranes and 30St217 and St30iso (Moldowan et al., 1990) parameter values which are indications of marine OM contribution. In summary, the Eastern Delta oil samples are mainly of marine origin, while

the Central Delta oil samples comprise of substantial amounts of terrigenous OM. The oil from the other two regions (Western Delta and Southern Delta) oils are mainly mixed, with input from both marine and terrigenous sources.

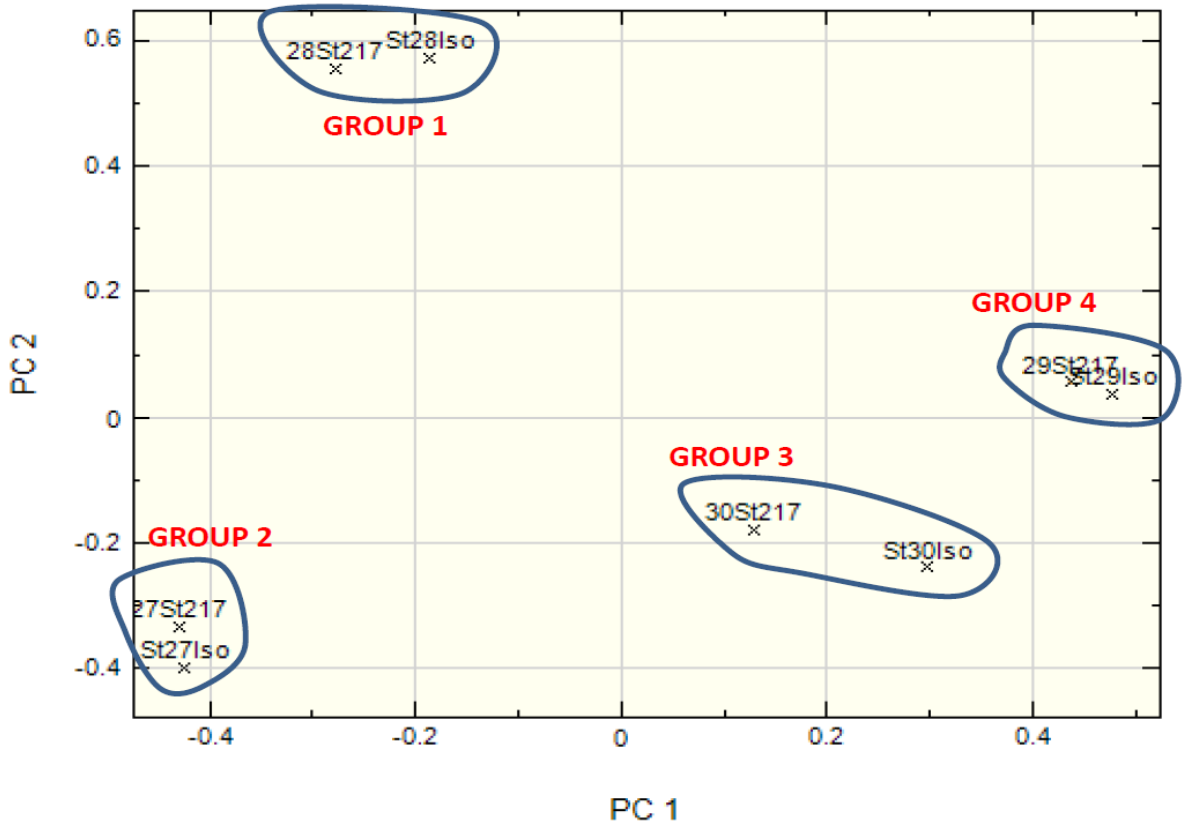

Figure 7.7: Loadings plot of first (50% of the variance) and second (19% of the variance) principal components of sterane hydrocarbon parameters showing relationships between parameters.

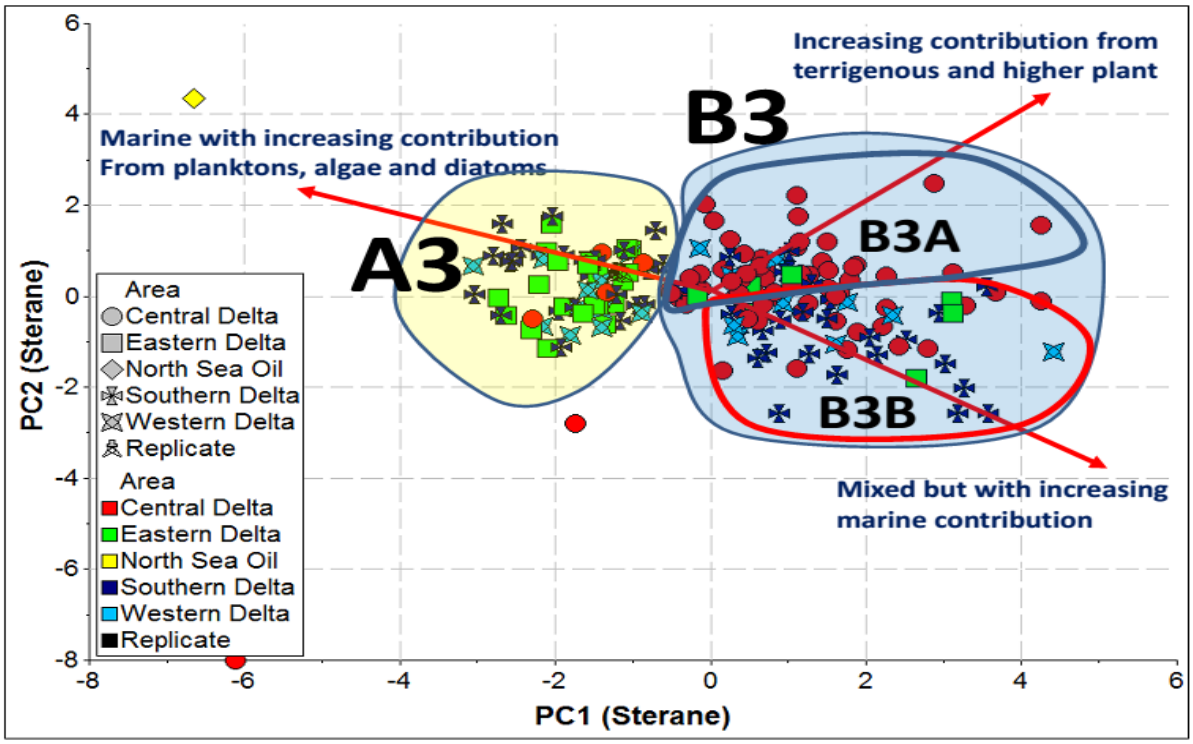

Fig 7.8a: Scores plot of sterane hydrocarbon parameters for the first two principal components showing relationships among the 178 Niger Delta oil samples analysed. Note the North Sea oil enables comparison with a known marine sourced oil.

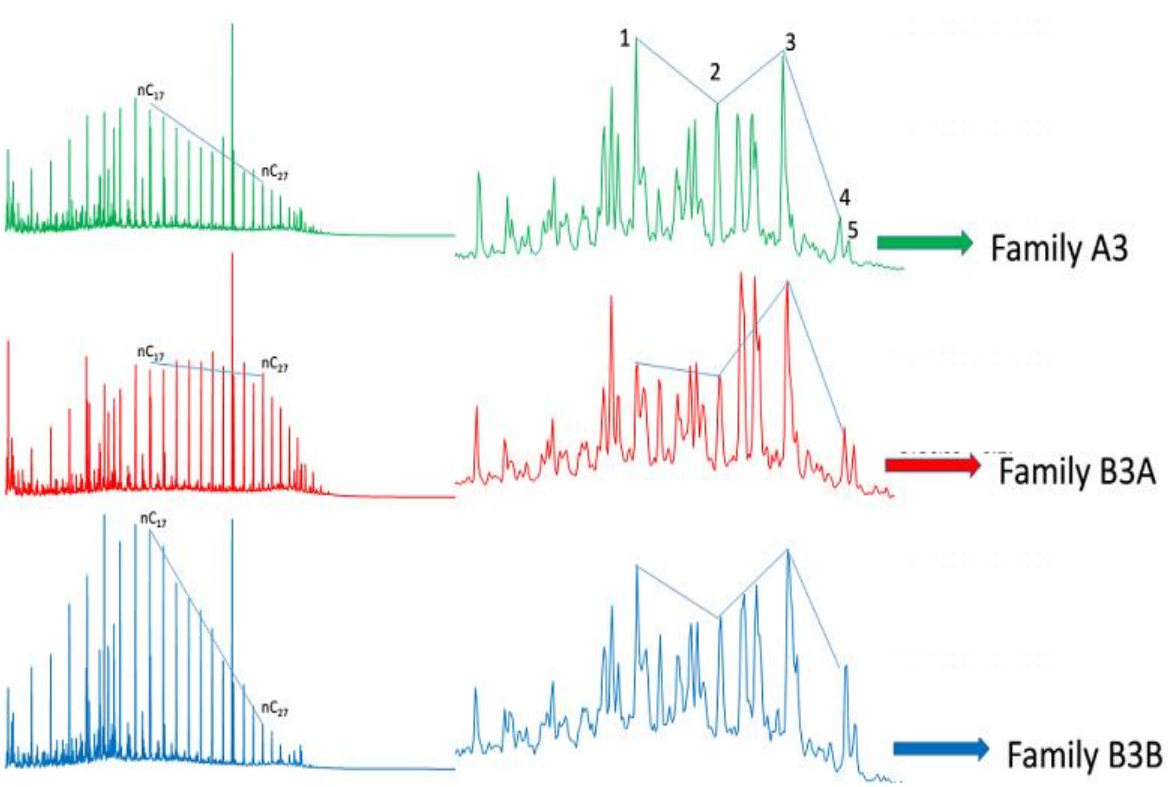

Figure 7.8b: Representative gas chromatograms of saturated hydrocarbon fractions showing *n*-alkanes and partial *m/z* 217 mass chromatograms showing the distributions of steranes of representative oils OE023, OE055 and OE091 from families A3, B3A and B3B, respectively. Note the differences in relative peak intensities.

1= C_{27} 5α(H),14α(H),17α(H) (20R). **1=** C_{28} 5α(H),14α(H),17α(H) (20R). **3=** C_{29} 5α(H),14α(H),17α(H) (20R). **4=** C_{30} 5α(H),14β(H),17β(H) (20R). **5=** C_{30} 5α(H),14β(H),17β(H) (20S).

7.1.3.2 Correlations from hopane biomarkers

A total of 179 oil samples and 19 hopane hydrocarbon parameters were used for the hopane PCA, although 11 hopane hydrocarbon parameters (t20/t21, t26/t25, t20-t26/T30H, Tri/Tetra, 31Hops, Hop/Mor, Dia/NorM, 29Ts/29Tm, Hop30/29, HomoHop, Hop34/35) were rejected because they only contributed noise in the data and did not show any particular trends.

The loadings plot shows division of the 8 accepted sterane hydrocarbon parameters into 4 groups (Figure 9.9), with group 1 made up of the t_{23}/T30H which is a correlation parameter (Seifert & Moldowan, 1978; AquinoNeto *et al*., 1983; De Grande *et al*., 1983) and group 2 made up of Tetra/Hop which is known to show the presence of coal in source rocks (Philp & Gilbert, 1986; Killops *et al.,* 1994) and is used for correlation in oil samples, although is affected by biodegradation and thermal maturity (Peters & Moldowan, 1983). The group 3 parameters are made up of t_{19}/t_{21+23} which can indicate deltaic source depositional environments (Zumberge, 1987; Rooney *et al*., 1998; Peters *et al*., 2005; He *et al*., 2012), and OleanIndex which indicates higher plant input (Ekweozor & Telnaes, 1990), 29Hop which can indicate source depositional environment (Ourisson et al 1987; Killops *et al.*, 1998). The group 4 parameters can be source depositional environment indicators but they mostly find use as thermal maturity indicators and these include: Ts/Ts+Tm (Seifert & Moldowan 1978; Moldowan *et al.*, 1986), Hop32 (S/S+R) (Seifert & Moldowan 1986), 30 Hops (Ourisson *et al*., 1987; Killops *et al*., 1998).

The loadings and scores plot of the hopane hydrocarbon parameters (Figure 7.9 & 7.10) enables division of the Niger Delta oils into 2 main families (i.e. families A3 and B3). The family A3 samples have elevated t_{23}/T30H (0.05 to 0.12) parameter values (Seifert & Moldowan 1978; AquinoNeto et al., 1983; De Grande et al., 1983) which is indicative of a marine source environment and this family is mainly made up of oil samples from the Eastern, Southern and Western Delta region.

The family B3 samples have elevated t_{19}/t_{23} parameter values (0.51 to 0.73) (Zumberge, 1987; Rooney *et al*., 1998; Peters *et al*., 2005; He *et al*., 2012), which is indicative of a deltaic source depositional environment and OleanIndex (Ekweozor & Telnaes, 1990) which indicates higher plant input, and this family is mainly made up of samples from the Central Delta, however some oil samples from the Western and Southern Delta also plot in this region.

Although the Tetra/Hop parameter (Peters & Moldowan 1983) is commonly used as a source indicator, elevated values of this parameter signifies intense biodegradation because of the relative susceptibility of C_{30} αβ hopane to biodegradation when compared with the tetracyclics (t_{28} (S+R), t_{29} (S+R)). Most of the oil samples that plot along this trend line are from the Central Delta region which are of PM level 4 to 8 and have high Tetra/Hop ratios (0.08 to 0.41), whereas all the other oil samples have Tetra/Hop values from 0.05 to 0.07.

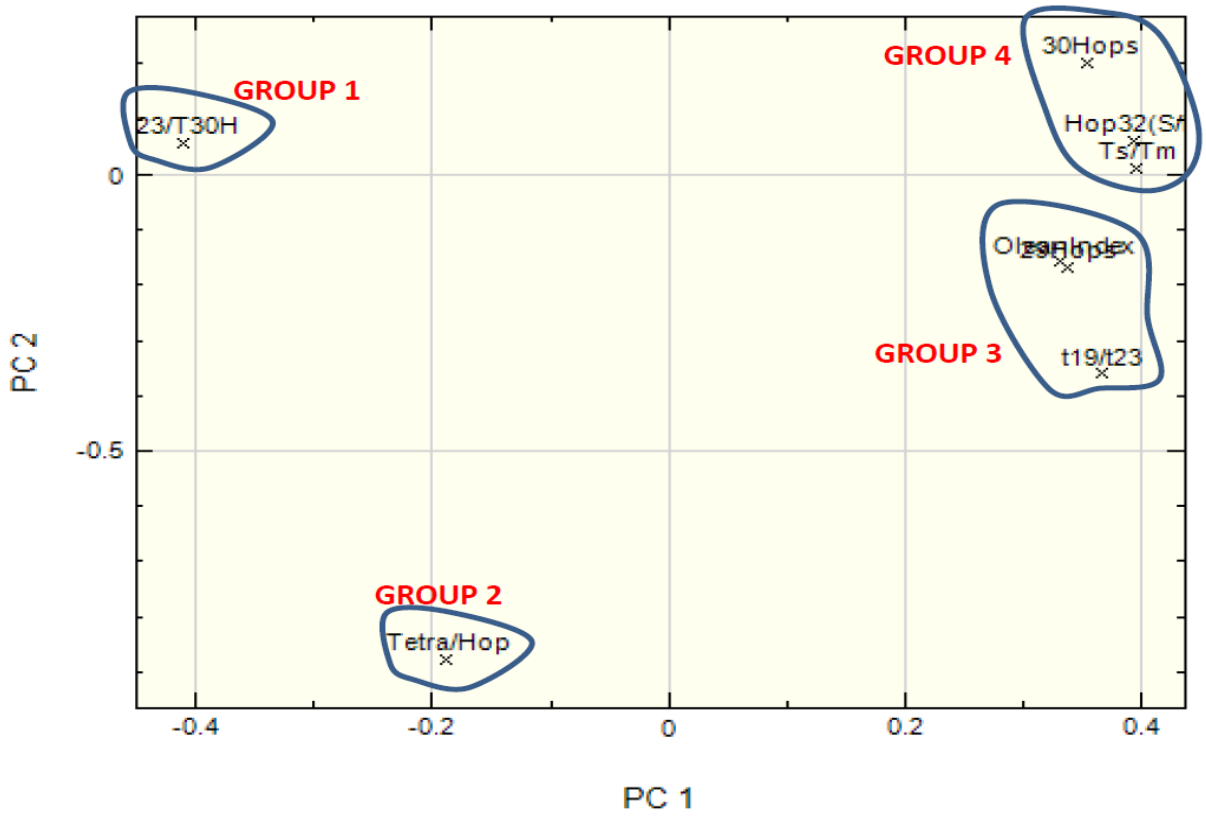

Figure 7.9: Loadings plot of first (73% of the variance) and second (12% of the variance) principal components of hopane hydrocarbon parameters showing the relationships between parameters.

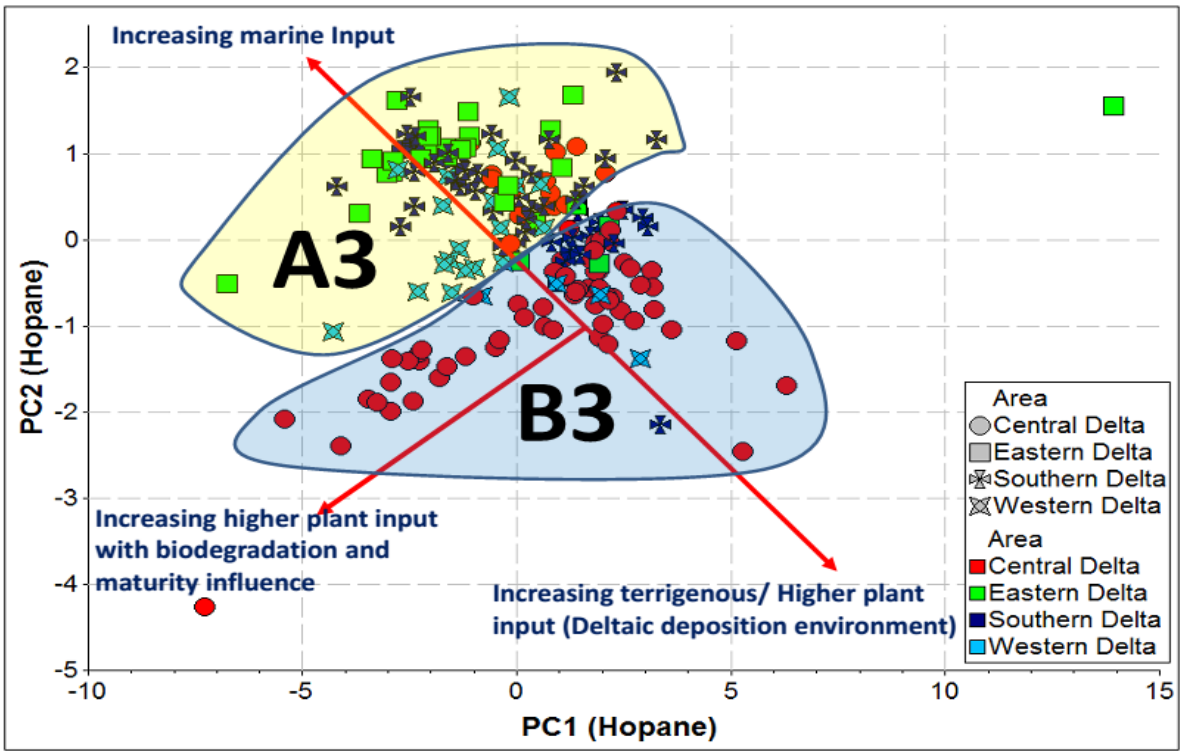

Figure 7.10: Scores plot of hopane hydrocarbon parameters for the first two principal components showing the relationships among the 179 Niger Delta oil samples analysed. Note the North Sea oil was not included because of the absence of some studied hopane peaks.

7.1.4 Correlations from compound specific isotope analysis

The plot (Figure 7.11) of the stable carbon $\delta^{13}C$ against stable hydrogen δD isotopic ratios of the *n*-alkane peaks (nC_{12}, nC_{19}, nC_{27}, nC_{28}) in the samples analysed shows the possibility of differentiating the lighter ends (nC_{12}, nC_{19}) of the Western Delta oil samples from the other samples because in this range they are isotopically heavier than the other oil samples, although nC_{19} components from the Southern Delta oils do not correlate well with the other oil samples. There is also the possibility that two groups exist within the Southern Delta oils (Figure 7.11) but it is not clear if this is due to factors such as the differential fractionation of the hydrogen isotope with the formation water during migration or different maturation processes in that part of the basin (Pedentchouk et al., 2004; 2006).

The higher molecular weight *n*-alkanes (nC_{27}, nC_{28}) do not show significant differences between the different oils and this might mean that the components within this range are related, unlike the lighter ends which show significant variations. However, the Western

Delta oils may have a significant component from a different source compared with the rest of oils, possibly from marine derived organic matter which is seen to be enriched in ^{13}C and ^{2}H in comparison with the other oils, and this makes the $\delta^{13}C$ and δD values from these oils more positive (Figure 7.11). This is consistent with the interpretation that there is enrichment of marine sourced organic matter in the lighter range due to the contribution from thermally cracked marine Type II organic matter, as indicated from the diamondoid analysis. However, there also exists the possibility that the Western Delta oils might have undergone a different maturation (higher maturity?) history, so that a significant proportion of *n*-alkanes in the short and mid-chain range underwent more extensive fractionation, leading to their more positive $\delta^{13}C$ and $\delta^{2}H$ values. The reason for the more positive δD value is not as clear and it could, for example, indicate that fractionation due to bond breaking of ^{13}C-^{12}C vs ^{12}C-^{12}C may be a more important process than the ^{2}H-^{1}H vs ^{1}H-^{1}H exchange with formation waters (N. Pedentchouk, personal communication 2015).

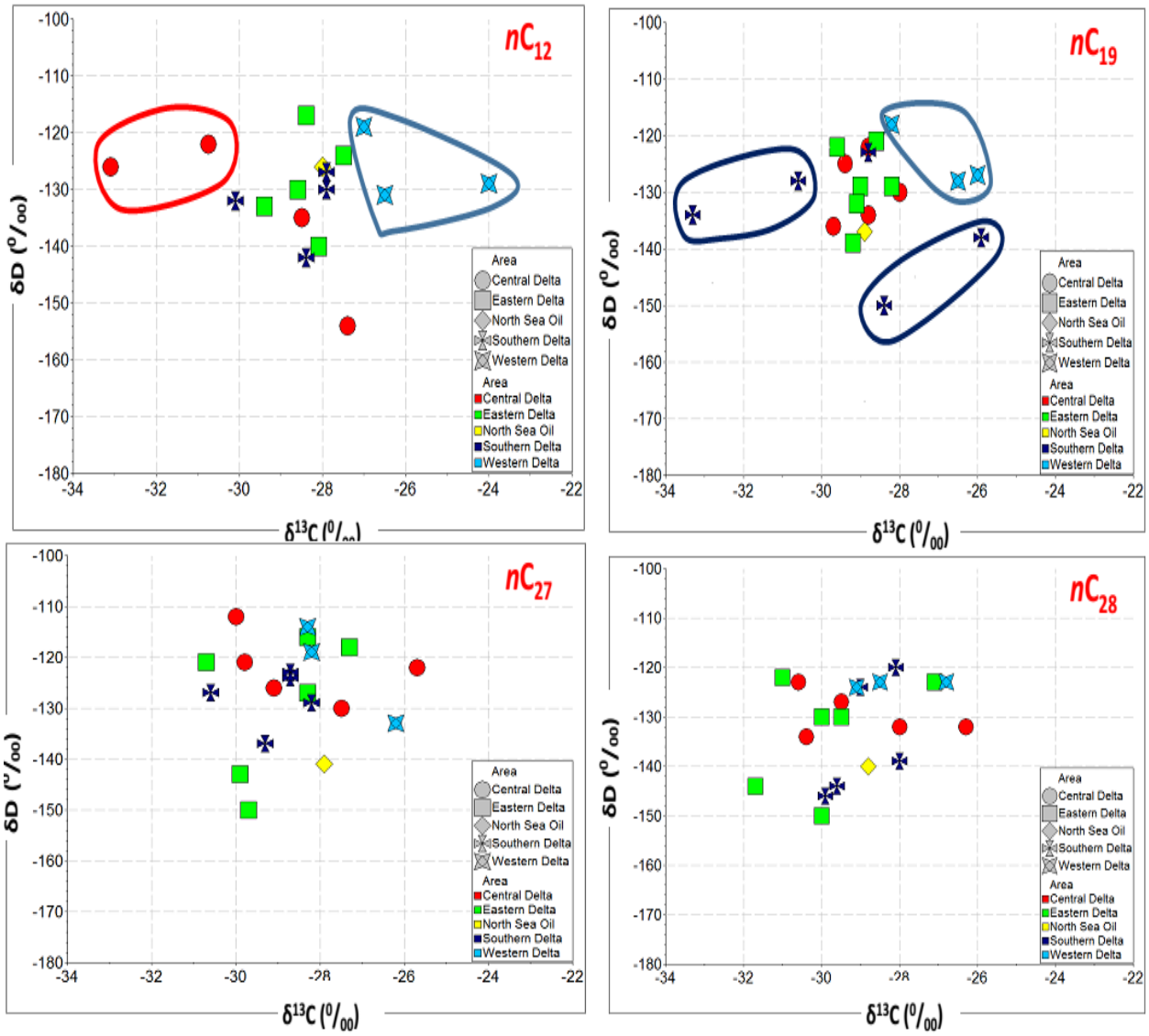

Figure 7.11: Plot of δD against $\delta^{13}C$ of selected *n*-alkanes ($nC_{12, 19, 27, 28}$) in the Niger Delta oil samples analysed, showing differences in the lighter *n*-alkane carbon isotopic values. (Standard error, in permil, at nC_{12} for δD = ±4.9, $\delta^{13}C$ =±0.09, Standard error at nC_{19} for δD = ±0.9, $\delta^{13}C$ =±0.09, Standard error at nC_{27} for δD = ±3.3, $\delta^{13}C$ =±0.38, Standard error at nC_{28} for δD = ±2.8, $\delta^{13}C$ =±0.42).

7.3 Oil to source rock correlation

An oil-source rock correlation can be seen as a study that tries to establish a genetic relationship between an oil which was derived in whole or part from an oil prone source rock that must have a comparable chemical/geochemical (elemental, molecular and isotopic) and geological (basin formation, sediments transportation, deposition, compaction, fluid flow, heat flow) relationship with the said oil (Curiale, 2008). Although

there appear appreciable improvement in geochemical oil source correlation techniques since some of the first work by Hunt *et al*. (1954), there still remain a lot of uncertainties in defining the geological influences in a successful oil-source correlation study and these uncertainties can be as a result of our limited knowledge of fine scale vertical and lateral variability in the depositional system of source and reservoir rocks (Keller & Macquaker, 2001; Barker *et al*., 2001).

Despite all these potential problems associated with oil-source rock correlation, the importance of any oil-source rock correlation cannot be overemphasized as a possible oil-source rock correlation study is better than one without any possible correlation established (Peters *et al*., 2005).

7.3.1 Correlation from diamondoids hydrocarbon

A total of 180 oil samples and 21 well cuttings extracts were used for the diamondoid hydrocarbon PCA. The loadings plot (Figure 7.12) shows the division of the 9 diamondoid hydrocarbon parameters into 3 groups. Group 1 is made up of the following diamondoid hydrocarbon parameters; MA/EA (Wang *et al*., 2006; Yang *et al*., 2006), MA/DMA (de Araujo *et al*., 2012), MA/TMA (de Araujo *et al*., 2012) (de Araujo *et al*., 2012), MA/TeMA (de Araujo *et al*., 2012), and TA/TeMA (de Araujo *et al*., 2012) which are mainly parameters used for correlation purposes. The group 2 parameter is**;** MA/AD and this parameter can be used for correlation purpose but has been shown to be susceptible to biodegradation (Grice *et al*; 2000). The parameters in group 3 are TMA/TMA, TeMA/TeMA, although these are usually correlation parameters (e.g. Wang *et al*., 2006; de Araujo *et al*., 2012), they plot away from other correlation parameters in group 1 and it is not clear if they may have been affected by secondary alteration process or if their use as correlation parameters may be of limited value in the Niger Delta oils.

The loadings and scores plot of the diamondoid hydrocarbons (Figure 7.12 & 7.13) helps to show that all the Niger Delta oil samples are genetically related and are very different

from the well cuttings extracts. All the oil samples are characterised by elevated MA/EA (Wang *et al*., 2006; Yang *et al*., 2006), MA/DMA, MA/TMA, MA/TeMA and TA/TeMA values (de Araujo *et al*., 2012). It is possible to conclude from the PCA (Figure 9.13) that the thermally cracked hydrocarbons may be genetically related and that they are very different from the extracts of the well cuttings, although correlation of multiple sourced oils and mixed hydrocarbons with multiple thermal maturity levels as seen in the Niger Delta basin, is known to introduce significant compositional variabilities within the trapped hydrocarbon (Seifert et al., 1979; Peters *et al*., 1989; Chen *et al*., 2003a,b). It is interesting to note that on this plot, the North Sea oil diamondoid source data appears similar to that of the Niger Delta oil samples (Figure 7.13).

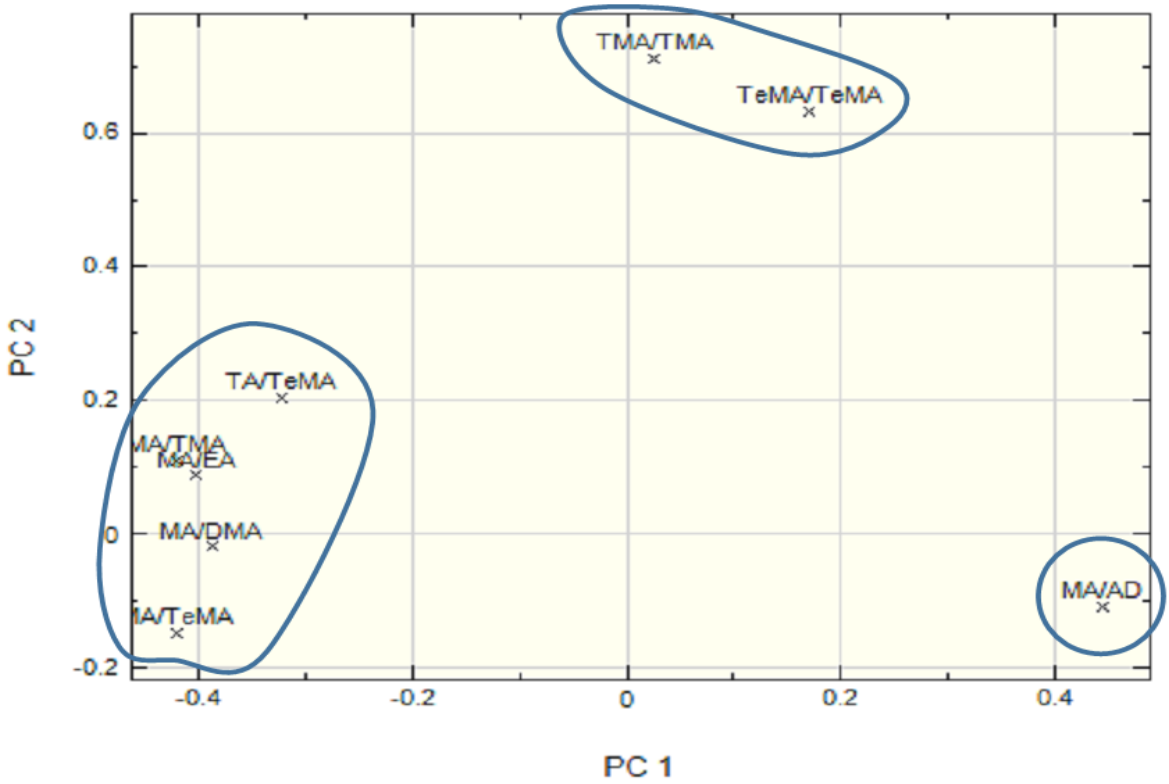

Figure 7.12: Loadings plot of the first (61% of the variance) and second (21% of the variance) principal components of the diamondoid hydrocarbon parameters, showing the relationship between parameters used.

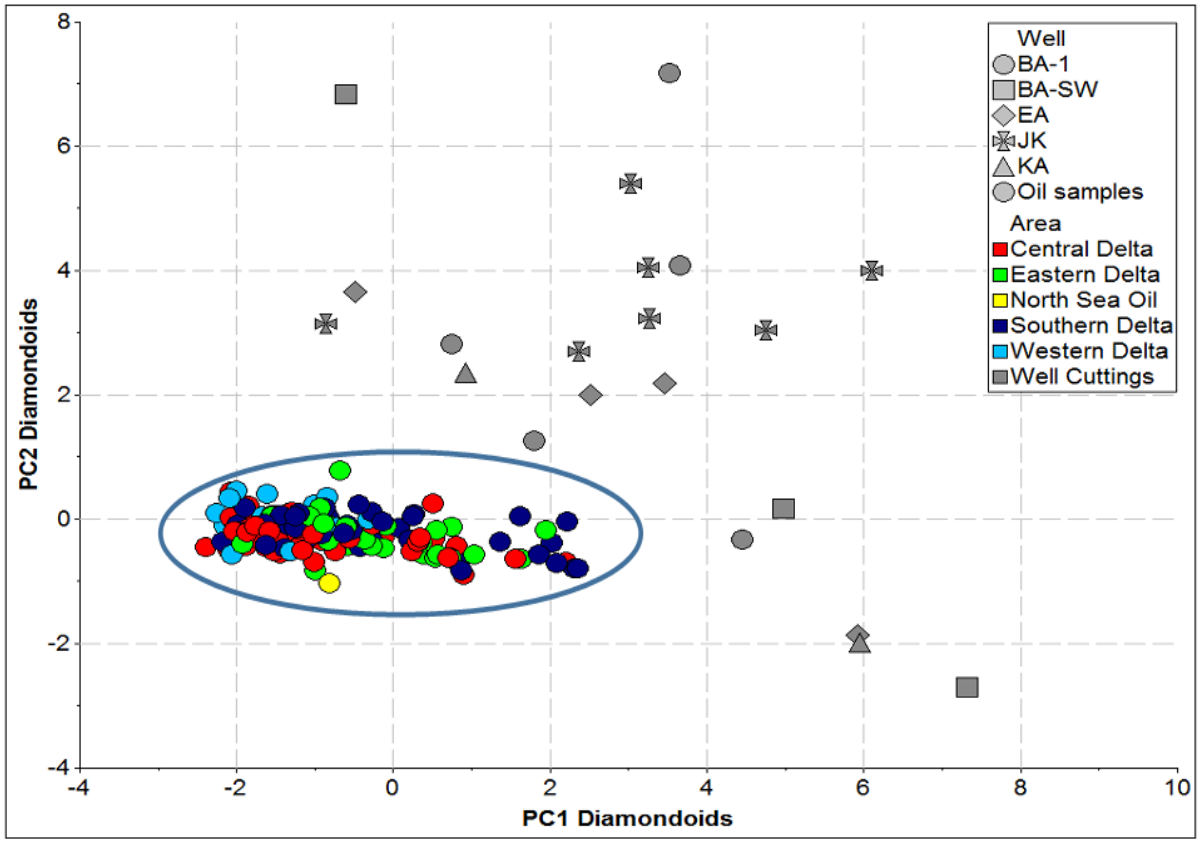

Figure 7.13: Scores plot of the diamondoid hydrocarbon parameters for the first two principal components showing the relationships among the 180 Niger Delta oil and well cuttings samples. Note the Niger Delta oil hydrocarbons are possibly from the same or similar source rock which is different to the well cutting samples. The North Sea oil enables comparison with a known marine sourced oil.

7.3.2 Correlations from sterane/hopane biomarkers

The steranes/17α-hopanes ratio, as measured from *m/z* 217 and 191 mass chromatograms is a ratio of the regular steranes to the 17α-hopanes i.e. [$C_{27\text{-}29}$ ααα(20S+20R) + $C_{27\text{-}29}$ αββ(20S+20R) steranes]/[$C_{29\text{-}30}$ αβ + $C_{31\text{-}C33}$ αβ(22S+22R) hopanes]. This ratio can indicate the relative eukaryotic/prokaryotic OM inputs to the source rock i.e. [(algae + higher plant)/bacteria] (Peters et al., 2005). Increased thermal maturity may increase this ratio (Seifert & Moldowan, 1978) but related oils with different thermal maturities are known to have the same trend line (Peters et al., 2005).

Based on a plot of the steranes/17α-hopanes ratio against %C_{29}αββ (20S+20R)/ $C_{27\text{-}29}$αββ (20S+20R) sterane (Figure 7.14), it is possible to see that the Niger Delta oils are not related with the source rock cuttings samples from wells KA and JK, but that they may be

related to those cutting samples from wells EA, BA-1 and BA-SW. Cuttings samples from well EA have elevated %St29Iso values and very low sterane/hopane ratios, and they have similarities to the family B3B oil samples that have relatively abundant C_{29} and C_{30} steranes, which might indicate a mixing of marine and terrigenous sourced OM (Moldowan et al., 1990).

Cuttings samples from wells BA-1 and BA-SW show good correlations with the Central Delta oil samples (Figure 7.14) which are mainly oils with relatively increased terrigenous input (Figures 7.8a & 7.10) even though those cuttings have been shown to contain mainly Type II kerogen. Since the sterane/hopane ratio is known to increase with increase in thermal maturity (Seifert & Moldowan, 1978), one could speculate that at a higher thermal maturities, the cuttings samples from wells BA-1 and BA-SW might show a better correlation with oil samples from the Eastern Delta which show a more marine source signature.

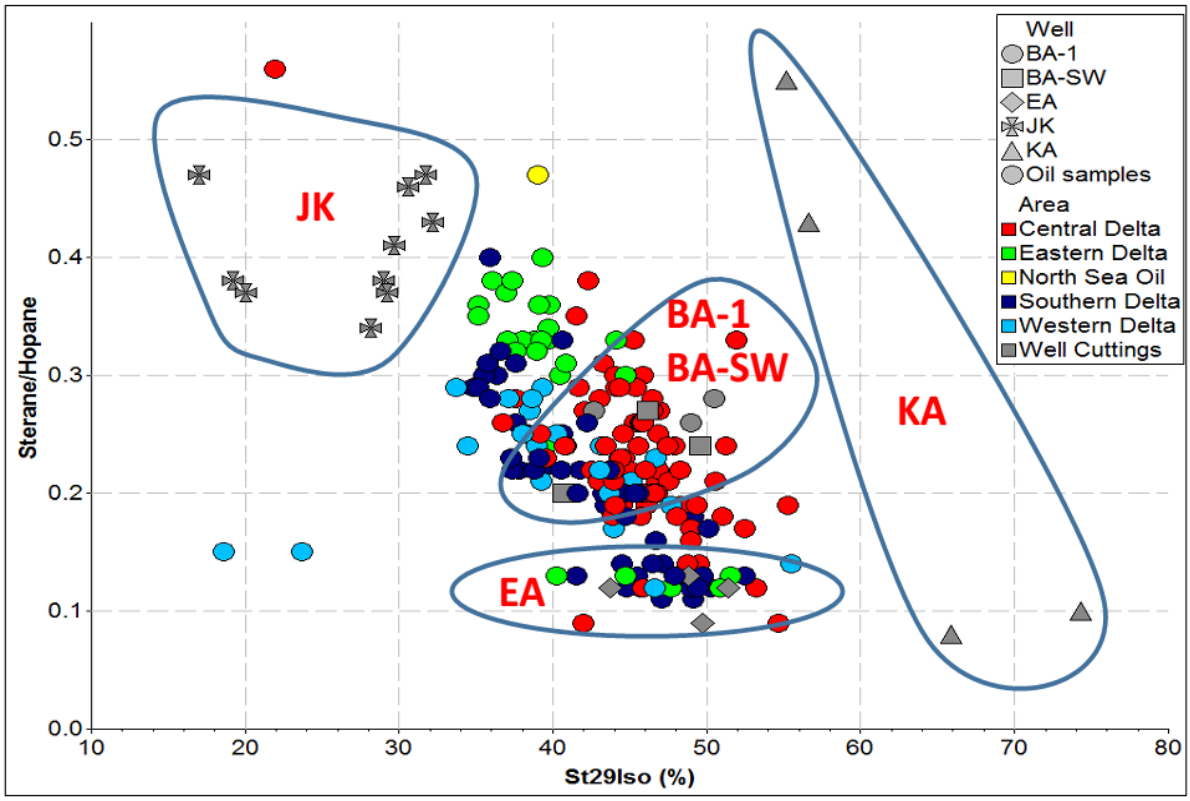

Figure 7.14: Cross plot of steranes/17α-hopanes against %St29Iso values showing some possible correlations between the Niger Delta oil samples and the well cutting samples. Note the cutting samples from wells JK and KI do not show any relationships with the oil samples.

7.3.3 Correlations from compound specific isotope analyses of *n*-alkane

The plot of carbon $\delta^{13}C$ against hydrogen δD isotopic ratios of selected *n*-alkane peaks (nC_{15}, nC_{16}, nC_{22}, nC_{23}) show the possibility of differentiating the lighter ends (nC_{15}, nC_{16}) of the oil samples from those of the well cuttings samples (Figure 9.15). The cuttings samples are depleted in ^{13}C and ^{2}H at the lighter end and this indicates the likelihood that these well cutting samples are not genetically related to those of the oil samples light end (Figure 9.15).

The higher molecular weight oil *n*-alkanes (nC_{22}, nC_{23}) might possibly be related to those hydrocarbons found in the cuttings samples from well BA-1, EA and KA (Figure 8.15) although it is not clearly understood how thermal maturation and the mixing of oils sourced from different facies would affect these results. Cuttings samples from wells JK and BA-SW do not show any correlation with the *n*-alkanes from the oil samples either at the lighter ends or the heavier ends (Figure 7.15). The non-correlation of the hydrocarbons in the cuttings samples from well BA-SW might be attributed to enrichment in deuterium because the well cuttings had similar $\delta^{13}C$ values as most of the oil samples, and the possibility exists that the differences in the hydrogen isotope values might have been due to fractionation effects between D and H in formation waters (N. Pedentchouk, personal communication 2015).

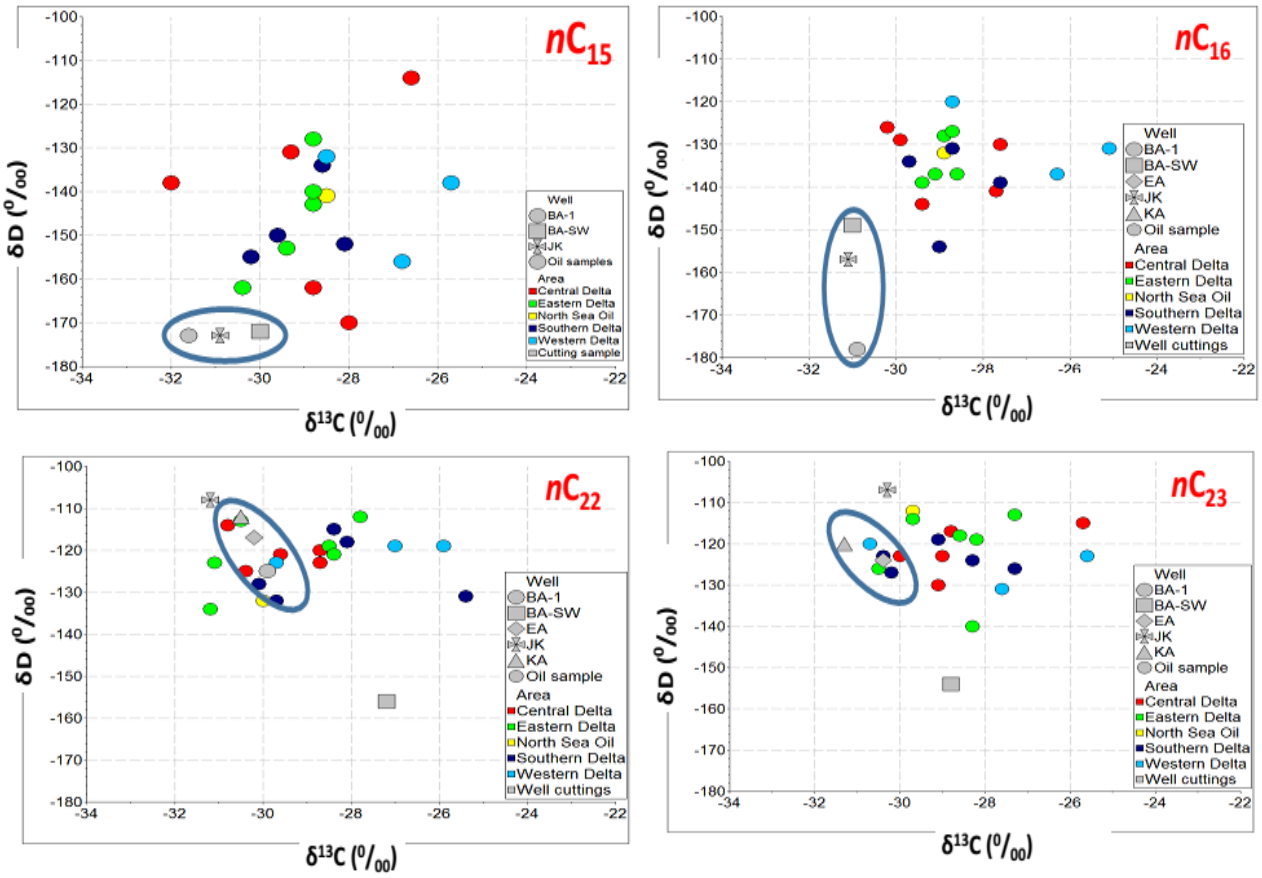

Figure 7.15: Plot of δD against $\delta^{13}C$ of selected *n*-alkanes (nC_{15}, nC_{16}, nC_{22}, nC_{23}) in the Niger Delta oils and well cuttings samples analysed, showing differences in the lighter *n*-alkane carbon isotopic values and some similarities in the higher molecular weight *n*-alkane carbon values. (Standard errors, in permil for nC_{15} for δD = ±6.5, δ13C =±0.09, nC_{16} for δD = ±1.5, $\delta^{13}C$ =±0.21, nC_{22} for δD = ±1.8, $\delta^{13}C$ =±0.24, nC_{23} for δD = ±1.3, $\delta^{13}C$ =±0.18).

7.4 Summary

This chapter highlights the existence of possible oil families in the Niger Delta basin, although the complex structuration of the basin might have contributed to the intense mixing of different thermal maturity oils which complicates the interpretation of the geochemical data from the samples analysed. The main findings of this chapter can be summarised as:

1. Principal component analysis of correlation parameters from diamondoids in the Niger Delta oils analysed reveals that they are from similar sources and thus were assigned as of the same family (Family A1) and also that they do not show any relationship with the well cuttings samples extracts analysed. The diamondoids represent a thermally over-mature (cracked hydrocarbons) part of the oils.

2. Principal component analysis of gasoline range and aromatic hydrocarbons reveals that the Niger Delta oil samples are potentially mixtures, with oil samples from the Central Niger Delta (Family B2) showing relatively increased terrigenous input and less marine input, while those from the other regions have more marine input and less terrigenous input (Family A2). These gasoline range and aromatic hydrocarbons represent a thermally mature portion of the mixed oil.
3. Principal component analysis of hopane and steranes (representing a low thermal maturity portion of the oils) reveals that the Niger Delta oil can also be divided into two families, with family A3 having more marine contribution while family B3 have more terrigenous contribution.
4. It may be possible to subdivide Family B3 into two sub-groups (i.e. B3A having relatively higher terrigenous contribution and Family B3B having relatively higher marine input).
5. The hydrocarbons in cuttings samples from wells JK and KA do not show any relationship with those in the Niger Delta oils analysed. However, cutting samples from wells BA-1, BA-SW and EA show some correlations with the oil samples based on hopane and sterane biomarkers.
6. Compound specific isotope analysis ($\delta^{13}C$ and $\delta^{2}H$) of *n*-alkanes indicates that the light ends of the Western Delta oil samples, although of marine source, might have a different source from those in oils from the other regions; however, the higher molecular weight *n*-alkanes have similar values and thus may be related.
7. The well cuttings samples extracts appear not to be related with the lighter end *n*-alkanes of the Niger Delta oil samples but those of cuttings samples from wells BA-1, EA and KA are similar to those in the higher molecular weight components in the oils.

CHAPTER EIGHT
OVERALL CONCLUSIONS

The overall aim of this project is to gain a better understanding of the Niger Delta petroleum system with a view to predicting the source of the hydrocarbons found in the basin and ultimately be able to predict the likely mixing percentages of high maturity sourced oils with those of lower thermal maturity and how this mixing may change across the regions of the delta. In order to achieve these aims, several objectives were targeted which included: inferring the organic facies and depositional environments of source rocks of the Niger Delta Basin based on the geochemistry of a large data set of oil samples; predicting the percentage contribution of the highly matured deep source to the Tertiary reservoired hydrocarbons; determination of the possible migration distances and alteration processes that affected the produced oil samples and also to assess the source potential of transgressive shales of the Niger Delta Basin based on the available well cutting samples. In order to achieve the overall aims of the project a total of 50 well cuttings samples from 6 exploratory wells and 180 oil samples from 40 oil fields, were used for this project.

8.1 Source depositional environment and thermal maturity

There is huge complexity in the Niger Delta Basin petroleum systems based on the contradictory geochemical results generated from the Niger Delta oils analysed, as indicated by the differences in the thermal maturity depending on the compound class/molecular weight range of the hydrocarbons in the oils that were studied. These thermal maturity measurements indicated that there has been at least two possible charges in the oils studied from the basin. These consisted of a highly mature and cracked charge possibly coming from a sub-delta (deep Cretaceous) source as indicated by the diamondoid hydrocarbon analyses and a peak mature charge contribution from a source that has not been buried as deeply as the highly mature charge (Figure 8.1) as indicated by results from the gasoline range and aromatic hydrocarbons. The highly mature early charge was sourced

from a Type II kerogen deposited in a marine environment and was of late oil window maturity to early gas window maturity, with the oil having been thermally cracked. The peak oil window maturity charge appears to have been sourced from shales containing Type II kerogen deposited in marine environment with various proportion of terrigenous input depending on proximity to land (i.e. mixed Type II/III), with the Central and Southern Delta regions having the highest terrigenous inputs compared with the other parts of the delta.

The Niger Delta oils are potential mixtures of oils from a wide range of thermal maturities, which have been contributed to by different source facies. In these mixed oils, the first charge, which is the thermally cracked oil sourced from a marine sourced Type II kerogen, is thought to have a regional extent, based on the strong relationships of the different oils from the PCA of diamondoid parameters. The second charge of thermally mature oil is shown to be differentiated by the level of terrigenous input into the marine organic matter (i.e. Type II/III facies) with possibility of a wide spectrum of terrigenous input depending on the region of the delta.

Based on the PCA results, it is possible to conclude that the highly mature charge was generated from a Type II, sub-delta source which is of regional extent and which was responsible for a high proportion of the oil in the Niger Delta that has migrated into the Tertiary reservoirs of the Agbada Formation. The mature charge must have been from the thick Akata Formation that was deposited during the rapid prograding sedimentation in the Delta and the low thermal maturity signature seen in the hydrocarbons of this basin is mainly from migration contamination and/or signatures picked from the transgressive shale streaks that are present in the Tertiary Agbada Formation reservoirs.

Compound specific isotope ($\delta^{13}C$ and δD) analysis of *n*-alkanes indicates that the light ends of the Western Delta oil samples, although mostly marine organic matter derived, might have a different source from the other regions, but that the higher molecular weight *n*-alkanes have similar carbon isotopic values to those of the other regions. The differences

in the compositions of the Niger Delta oils analysed reflect variations in source depositional environments, source organic matter input and thermal maturity, the mixing proportions of different charges and reservoir alteration processes that affected these oils.

8.2 Thermal cracking and mixing

The thermal cracking of hydrocarbons is a function of temperature, which is primarily dependent on depth of burial (and thermal gradient) and with the maximum baseline concentration for diamondoids (3+4 MD) in oils and source rocks that have not undergone cracking, set at 10 ppm (based on large data set of samples worldwide), it can be concluded that the Niger Delta hydrocarbons are mixtures of thermal cracked hydrocarbons with those of uncracked ones because of the elevated concentrations of diamondoids (3+4 MD), which are as high as 100 pm in some samples and generally higher than 10 ppm.

An oil with a diamondoid (3+4 MD) concentration of 20 ppm would have been mixed in a 50:50 ratio of cracked to uncracked oil (with a baseline of 10 ppm) while a concentration of 100 ppm would have had 90 percent contribution from the cracked source and 10 percent from the uncracked source (chapter 5, section 5.3.3) Biodegradation and evaporative fractionation, which can lead to over-estimation of diamondoid concentrations, was not considered during this calculation, but the concentrations of diamondoids in these fluids generally points to a source that has been intensely cracked.

The extent of cracking in the oils is seen to be related to the basin architecture, since the Eastern Delta region, which has low sediment thicknesses, has oils with lower cracking index values than those from the other parts of the delta with thicker sediment thicknesses. The oils from the Central Niger Delta which have mostly received a higher proportion from the sub-delta charge, as seen from the diamondoid based cracked oil charge map (Figure 5.16), have also received oils that have more terrigenous input due to the source region proximity to land and land-plants (Figure 5.23). The elevated diamondoid concentrations

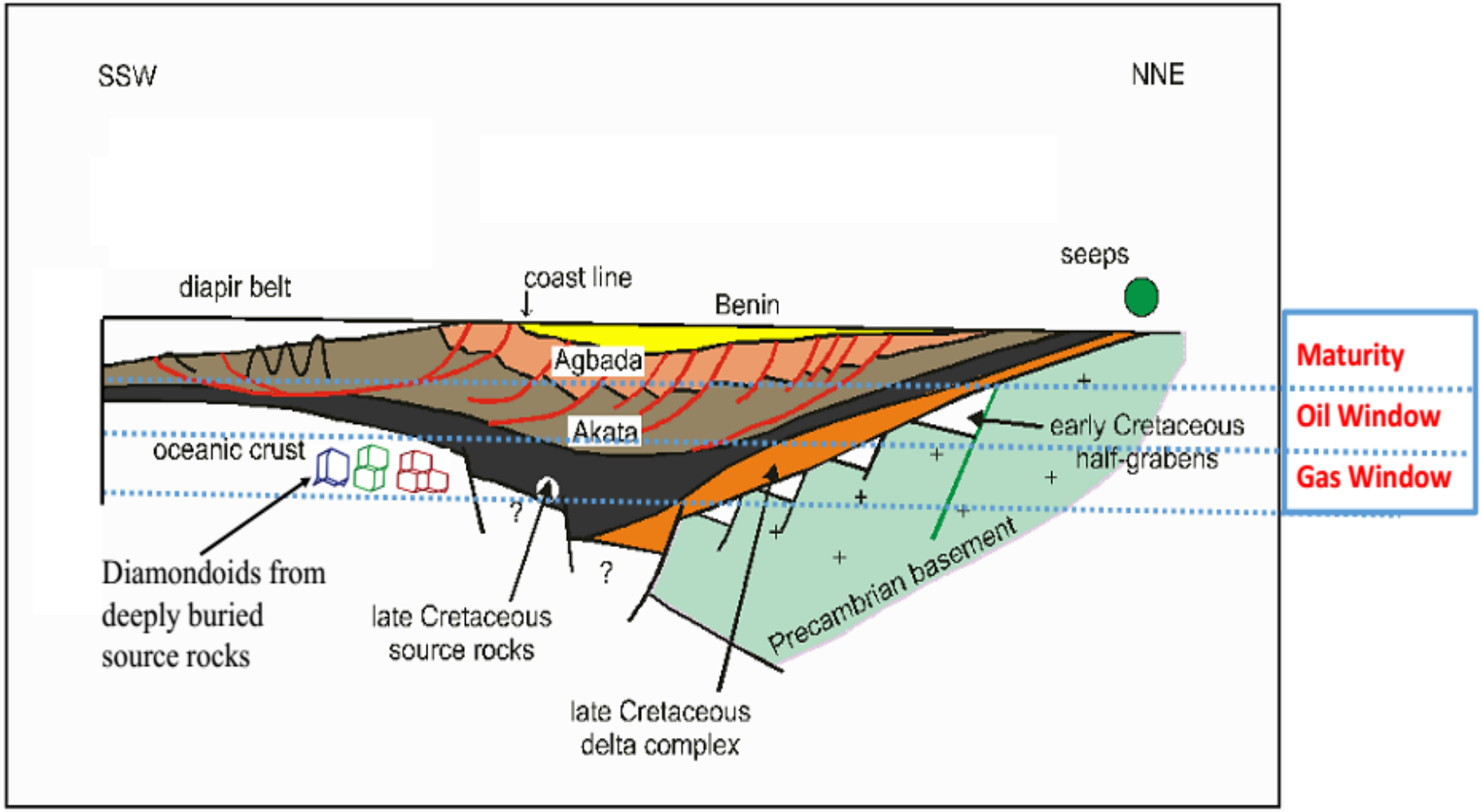

Figure 8.1: A cross section of the Niger Delta Basin (NNE to SSW) showing the different formations (modified after Thomas, 1985) and their proposed regional thermal maturities relating to oil and gas generation. Note that localised thermal gradient hotspots were not considered and that diamondoids are mainly contributed from the deeply buried sub-delta source rock.

are believed to be coming from the marine Type II sub-delta source that has been deeply buried in the basin (Figure 8.1). The Tertiary reservoired hydrocarbons in Niger Delta Basin are derived from multiple source rocks, though this is also true for most prolific oil and gas regions of the world today. However, in the case of the Niger Delta Basin, the most important petroleum source must be biomarker depleted as indicated by the elevated diamondoid concentrations which reveal high thermal cracking.

8.3 Source potential of the Niger Delta transgressive shales

Assessment of cuttings samples showed that those from well BA-1 recovered from depths of 3.1 to 3.4 km contained Type II kerogen, deposited in a shallow marine environment, with good potential to generate hydrocarbons but that they were thermally immature. Therefore, although this depth interval from this well might have not contributed to the oil in the basin, deeper intervals in this well might be in the oil window and will have generated oil and some gas. The samples from well BA-SW recovered from depths of 3.9 to 4.1 km contained Type II kerogen, deposited in a shallow marine environment, with fair potential to generate hydrocarbon and the samples from well BA-SW were thermally immature based on sterane isomerisation and have not contributed to the oil reservoired in the Tertiary Niger Delta.

Cuttings samples from wells EA (1.2 – 2.3 km), KA (2.1 – 3 km), KI (2.5 – 2.7 km) contained Type III kerogens deposited in deltaic settings, with poor to good potential to generate hydrocarbons These particular samples were immature and thus would not have contributed to the Niger Delta oil accumulations, but with the right thermal maturity had potential to generate gas and some oil. Cuttings samples from well JK recovered from depths of 1 to 4 km contained Type II kerogen deposited under open marine environments and had fair to excellent potential to generate hydrocarbons and were in the oil window maturity range. However, the cuttings samples from this well had been heavily

contaminated with what appeared to be an oil based drilling fluid and so the cuttings geochemical results from this well could be misleading.

The hydrocarbons in the cuttings samples from wells JK and KA do not show any genetic relationships with the Niger Delta oils, but those of the cutting samples from wells BA-1, BA-SW and EA do show some correlations with the oils based on hopane and sterane biomarkers. Thus, if these intervals penetrated in the wells were buried to the appropriate depth to be thermally mature enough to have expelled, hydrocarbons, they could have contributed to the oil charge sourced from the intra-delta shales. However there is also the possibility that the relationship between the well cuttings and the oil samples just point to the source of the migration contamination seen in these fluids. Compound specific isotope (δD and $\delta^{13}C$) analysis of light-end *n*-alkanes below nC_{16}, showed that the well cuttings samples were not related to those of the oils and this molecular range is thought to be mainly contributed by the cracked oil of the deeply buried, sub-delta, Type II source and also that these are different to the hydrocarbons from the source rocks in the intra-delta wedge.

8.4 Secondary migration and alteration processes

The Tertiary reservoired oils in the Niger Delta are believed to have migrated from source rocks within the vicinity of the delta (either sub-delta or intra-delta) and the indications from the carbazole and phenol analyses are that the Western Delta oils might have migrated over a longer distance than those from the other regions, whereas the Southern Delta oils might have migrated over the shortest distance. This information has possible implications for future exploration activities, as new exploration targets might be located on migration pathways. It was generally found in the oils that the higher the calculated temperature of expulsion (which is also a function of the organofacies type) and 3+4 MD concentration, the longer the relative migration distance. However, inferences drawn on migration distance need to be treated cautiously because of the multiple contributory sources and

different thermal maturities of these sources, which could affect these migration parameters.There exists the possibilities of complex biodegradation/gas washing/water washing scenarios in the oils of the Niger Delta basin and this might be as a result of the prevailing reservoir physiochemical conditions and multiple charging episodes in the various sub-basins that was controlled by the complex structuration in the basin. Generally, the Southern Delta oils are least biodegraded while the Central Delta oils are mostly biodegraded, with the slight changes in biodegradation level within a well not having a significant effect on the calculated geochemical parameters and interpretations based on them.

The *n*-alkane/acyclic isoprenoid alkane ratio can be a very good indicator of early biodegradation level in the Niger Delta oil samples analysed, whereas the MA/AD diamondoid biodegradation parameter does not show any variations in the Niger Delta oil samples. There is also no strong relationship of the aromatic biodegradation ratios with the level of biodegradation measured based on the aliphatics fraction of the Niger Delta oils. The unknown peak A (a C_{29} triterpane seen in the *m/z* 191 mass chromatograms) and unknown peak %A+B (thought to be a bicyclic seco-oleanane seen in the *m/z* 193 mass chromatograms) can be used for biodegradation assessment of these heavily biodegraded oil samples. The MANCO scale of Larter *et al*., (2012) is useful for potentially sub-dividing any PM level of oil biodegradation, but in the oils from this study there is potential overlap in them at PM levels 4/5 and 7/8 it is not clear if this overlap will be present in oil from other basins.

The complex trapping system in the Niger Delta basin with repetitive trap/seal sequences in the Agbada Formation might have been responsible for the intense fractionation/gas washing in the Central Delta region oils. The Southern Delta region oils have also been fractionated to some extent, although the Western Delta oils are more pristine and do not appear to have been fractionated. However, oil fractionation in the Niger Delta might also

be controlled by the fill and spill mechanism, where light oil tends to displace the initial reservoired oil. Gas washing also is consistent with the premise that Niger Delta oil are mixtures of highly mature and less mature oils, which might be as a result of early gas window mature oil migrating through oil of lower thermal maturity.

Apart from alteration as a result of gas washing, there is also the possibility of water washing in the Niger Delta oils and this does not appear to be related to reservoir depth but may be somehow related to depth of basement, as most of the Eastern Niger Delta oil samples have suffered from intense water washing, whereas the other regions appear to have been only slightly water washed but this is inconclusive as the light aromatics parameters are source dependent.

8.5 Implications for petroleum exploration and production

The current work has been able to show that a sub-delta Type II marine source has contributed mainly late oil window to early gas window maturity oil to the Niger Delta Tertiary reservoired oils, with the charge from the sub-delta generally of highest proportion in the potentially mixed oils in the basin. The cracked source is a marine Type II (sub-delta) while the second less mature source is a Type II/III facie (i.e. marine Type II with varying percentage of terrigenous Type III input). The Central and Southern Delta oils have a higher terrigenous input than those of the Eastern and Western Deltas. It should also be noted that all the samples that show a high terrigenous input, also always have some marine signature, and there is a clear indication that there is a mixed facies of algal and terrigenous input, with bacteria reworking, deposited in a marine setting.

The timing of oil generation is controlled by the sediment thicknesses in the delta, which was mainly controlled by accommodation space and basin structure, thus the Central Delta area should have been charged before the other areas and with the depth-to-basement information in the delta, we can predict fluid type that will probably be encountered in the

deeper reservoirs i.e. in high pressure /high temperature (HP/HT) reservoirs mainly in proven areas of the delta. There also exists the possibility to explore more in deeper waters and outer fold belt regions of the delta (deep offshore), but success in this region will be dependent on regional migration of hydrocarbons, as source rocks will thin out in this region and the timing of structure formation might be recent compared to the time of hydrocarbon generation in the basin centre. It can be concluded that the HP/HT reservoirs in proven areas will also hold oil/gas based on the fact that they are closest to the source that has produced a greater proportion of the Niger Delta oil, however drilling deeper in the delta will be challenging because of the following factors;

1. Reduction in reservoir porosity and permeability based on higher compaction and cementation of the reservoirs.
2. Problems from over-pressure during drilling.
3. Production of multiple phase fluid with pressure released during production.
4. Problems with scaling and mineral deposits in production pipes due to pressure release.
5. The greatest singular problem will be trap integrity as there will be increased possibility of seal breaching when the formation pressure is equivalent to fluid pressure.

8.6 Future work

Follow-up work in this basin should be able to answer the following questions but this will depend on the availability of relevant data and background information. These questions should be able to address issues around thermal maturity, migration, cracking and mixing, reservoir alteration and reservoir presence.

8.3.1 Thermal maturity;

1. Does shoreline progradation play a very important part in source rock maturity in the delta?
2. Was the Cretaceous sourced oil reservoired in deep reservoirs and the present delta merely serves as overburden in maturing the source and cracking the reservoired oil after subjection to a deeper burial?
3. Will PY-GCMS of immature Cretaceous source rock indicate the possibility of thermal maturity history of this formation?
4. Would the Cameroon volcanism have contributed to the heating of sources and reservoirs in the Niger Delta Basin?

8.3.2 Migration;

1. Has there been a time where the present over-pressured and under-compacted Akata formation might have served as a good migration route or as a seal that later failed due to increasing lithostatic and hydrostatic pressure in the basin?
2. If migration of the highly mature charge has travelled through the Akata formation, what role will the migrating fluid play in increasing the expulsion efficiency of the formation as an important source?
3. If the first charge was stored in deeper reservoirs what triggered the breaching of the seals in these deep reservoirs or was it all about fill and spill mechanism?

8.3.3 Cracking and mixing;

1. Did cracking occur in the reservoir or source, and if both, what are the proportions and which is more important source of the highly cracked oil?
2. What proportion of methane will be formed during expulsion at the gas window; also oil to gas cracking and biodegradation of the oil?
3. How to quantify different charges that might have been biodegraded to different levels?

4. Can mixing curves be effectively generated for non-degraded, end -member oils?

8.3.4 Reservoir alteration;

1. How do diamondoid and biomarker concentrations vary with biodegradation levels?
2. Can oil quality and volumetric be predicted based on probable reservoir information?

8.3.5 Reservoirs;

1. Is there a possibility of highly fractured and weathered basement reservoirs in the Niger Delta?

REFERENCES

Aboglila, S., Grice, K., Trinajstic, K., Dawson, D., & Williford, K.H. 2010. Use of biomarker distributions and compound specific isotopes of carbon and hydrogen to delineate hydrocarbon characteristics in the East Sirte Basin (Libya). Organic Geochemistry. 41, 1249–1258.

Aitken C. M., Jones D. M., & Larter S. R. 2004. Anaerobic hydrocarbon biodegradation in deep subsurface oil reservoirs. Nature. 431, 291–294.

Aitken, C., Brown, A., Gray, N., Rowan, A., Head, I., Jones, M. & Larter, S.R., 2007. Anaerobic hydrocarbon degradation in petroleum reservoirs and methane generation. In: Farrimond, P. (Ed.), 23rd International Meeting on Organic Geochemistry, Book of Abstracts. European Association of Organic Geochemists, Torquay, England, p. 833.

Akinlua A, Ajayi T.R, Jarvie D.M & Adeleke B.B. 2005. A re-appraisal of the application of Rock-Eval pyrolysis to source rock studies in the Niger Delta. Petroleum Geology. 28. 39- 48.

Akinlau A, Ajayi T.R & Adeleke B.B. 2006. Niger Delta oil geochemistry: Insight from light hydrocarbons. Petroleum science and engineering. 50. 308-314.

Akinlua A & Ajayi T.R. 2009. Geochemical characterisation of Niger Delta oils. Petroleum Geology. 34. 373-382.

Akinlua A & Torto N. 2011. Geochemical evaluation of Niger Delta sedimentary organic rocks: a new insight. Earth Science. 100. 1401-1411.

Alexander R., Kagi. R & Woodhouse G.W. 1981. Geochemical correlation of Windalia oil and extract of Winning Group (Cretaceous) potential source rocks, Barrow Subbasin, Western Australia. American Association of Petroleum Geologists. 65. 235-250.

Alexander, R., Kagi, R.I., Rowland, S.J., Sheppard, P.N., & Chirila, T.V., 1985. The effects of thermal maturity on distribution of dimethylnaphthalenes and trimethylnaphthalenes in some ancient sediments and petroleums. Geochimica et Cosmochimica Acta 49. 385-395.

Alexander, R., Bastow, T.P., Fisher, S.J., & Kagi, R.I., 1995. Geosynthesis of organic compounds. II - Methylation of phenanthrene and alkylphenanthrenes. Geochimica et Cosmochimica. Acta 59. 4259-4266.

Aquino Neto, F. R., Albrecht J.M, Restle A, Connan J & Albrecht P, 1983, Occurrence and formation of tricylic terpanes in sediments and petroleums: in M. Bjorøy, (Ed.), Advances in Organic Geochemistry 1981, John Wiley and Sons Ltd, 659-667.

Avbovbo, A.A., 1978. Tertiary lithostratigraphy of Niger Delta. American Association of Petroleum Geologists. 62. 295–300.

Azevedo, D.A., Tamanqueira, J.B., Dias, J.C.M., Carmo, A.P.B., Landau, L & Gonçalves, F.T.T. 2008. Multivariate statistical analysis of diamondoid and biomarker data from Brazilian Basin oil samples. Fuel. 87. 2122–2130.

Barker, C.E., Pawlewicz, M., & Cobabe, E.A., 2001. Deposition of sedimentary organic matter in blacks shale facies indicated by the geochemistry and petrography of high-resolution samples, Blake Nose, western North Atlantic. In: Western North Atlantic Palaeogene and Cretaceous Palaeoceanography. Geological Society, London. 183. 49–72.

Baskin, D.K. 1997. Atomic H/C Ratio of Kerogen as an Estimate of Thermal Maturity and Organic Matter Conversion. American Association of Petroleum Geologists. 81. 1437-1450.

Bastow, T.P., Alexander, R., Sosrowidjojo, I.B., & Kagi, R.I., 1998. Pentamethylnaphthalenes and related compounds in sedimentary organic matter. Organic Geochemistry 28. 585-595.

Baudouy, S., & Legorjus, C., 1991, Sendji field—People's Republic of Congo, Congo Basin, in Foster, N.H., and Beaumont, E.A., eds., Treatise of petroleum geology, Atlas of oil and gas fields—Structural traps V: Tulsa, Okla., American Association of Petroleum Geologists. 121–149.

Beach, F., Peakman, T.M, Abbott G.D., Sleeman R., & Maxwell J.R, 1989, Laboratory thermal alteration of triaromatic steroid hydrocarbons: Organic Geochemistry. 14. 109-111.

Bechtel A, Gratzer R, Linzer H.G, & Sachsenhofer R. F. 2013. Influence of Migration distance, maturity and facies on the stable isotopic composition of alkanes and on carbazole distribution in oils and source rocks of the Alpine Foreland Basin of Austria. Organic Geochemistry. 62. 74-85.

Beka, F. T., & Oti, M. N., 1995, The distal offshore Niger Delta: frontier prospects of a mature petroleum province, in, Oti, M.N., and Postma,G., eds., Geology of Deltas: Rotterdam. 237-241.

Bellingham P, Connors C, Haworth R, Radovich B & Danforth A, 2014. The Deepwater Niger Delta: An Underexplored World-Class Petroleum Province. GeoExPro. 55-56.

BeMent. W. O., Levey, R. A. & Mango, F. D. 1995. The temperature of oil generation as defined with C_7 chemistry maturity parameter (2,4-DMP/2,3-DMP ratio). In

Organic Geochemistry: Developments and Applications to Energy, Climate, Environment and Human History. J. 0. Grimalt and C. Dorronsoro (Eds.) 505-507.

Bernard, F.P., & Connan, J., 1992. Indigenous microorganisms in connate waters of many oilfields: a new tool in exploration and production techniques. Society of Petroleum Explorationist. 24811. In: 67th Annual Technical Conference and Exhibition of the Society of Petroleum Engineers, Washington, DC, 467–476.

Bekins, B. A., Hostettler, F. D., Herkelrath, W. N., Delin, G. N., Warren, E., & Essaid, H. I., 2005. Progression of methanogenic degradation of crude oil in the subsurface. Environmental Geosciences, 12, 139-152.

Bennett, B., Chen, M., Brincat, D., Gelin, F.J.P., & Larter, S.R., 2002. Fractionation of benzocarbazoles between source rocks and petroleums. Organic Geochemistry. 33. 545–559.

Bennett, B., & Larter, S.R., 2008. Biodegradation scales: applications and limitations. Organic Geochemistry. 39. 1222–1228.

Bennett, B., Adams, J.J., Gray, N.D., Sherry, A., Oldenburg, T.B.P., Huang, H., Larter, S.R., & Head, I.M., 2013. The controls on the composition of biodegraded oils in the deep subsurface – Part 3. The impact of microorganism distribution on petroleum geochemical gradients in biodegraded petroleum reservoirs. Organic Geochemistry. 56. 94–105.

Bilotti, F., & Shaw, J.H., 2005. Deep-water Niger Delta fold and thrust belt modelled as a critical-taper wedge. The influence of elevated basal fluid pressure on structural styles. American Association of Petroleum Geologists. 89. 1475–1491.

Boll, M., Fuchs, G., & Heider, J., 2002. Anaerobic oxidation of aromatic compounds and hydrocarbons. Current Opinion in Chemical Biology. 6. 604-611.

Bray, E. E., & Evans,E.D. 1961. Distribution of n-paraffins as a clue to the recognition of source beds. Geochimica et Cosmochimica Acta. 22. 2-15.

Brooks, P.W., Fowler, M.G., & Macqueen, R.W., 1988. Biological marker and conventional organic geochemistry of oil sands/heavy oils, Western Canada Basin. Organic Geochemistry. 12. 519–538.

Brownfield, M.E., & Charpentier, R.R., 2006. Geology and total petroleum systems of the West-Central Coastal Province (7203), West Africa: U.S. Geological Survey Bulletin 2207-B, 52p.

Burke, K.C., 1972. Longshore drift, submarine canyon and submarine fans in development of Niger delta. American Association of Petroleum Geologists. 56. 1975-1983.

Burnham A. K. & Braun R. L. 1990. Development of a detailed model of petroleum formation, destruction and expulsion from lacustrine and marine source rocks. Organic Geochemistry. 16. 27-40.

Blanc, P., & Connan, J. 1992. Origin and occurrence of 25-norhopanes: a statistical study: Organic Geochemistry. 18. 813-829.

Bustin, R.M., 1988. Sedimentology and characteristics of dispersed organic matter in Tertiary Niger Delta. Origin of source rocks in deltaic environments. American Association of Petroleum Geologists. 72. 277–298.

Canipa-Morales N K, Galan-Vidal C A, & Guzman-Vega M A. 2003. Effect of evaporation on C_7 light hydrocarbon parameters. Organic Geochemistry. 34. 813 -826.

Chen, J. Fu, Sheng G, Liu D, & Zhang J. 1996. Diamondoid hydrocarbon ratios: Novel maturity indices for highly mature crude oils, Organic Geochemistry. 25. 179–190.

Chen, J, Liang, D, Wang, X, Zhong, N, Song, F, Deng, C, Shi, X, Tao, J, & Xiang, S, 2003a. Mixed oils derived from multiple source rocks in the Cainan oilfield, Junggar Basin, Northwest China; Part I: genetic potential of source rocks, features of biomarkers and oil sources of typical crude oils. Organic Geochemistry 34. 889–909.

Chen, J, Deng, C, Digang, L, Wang, X, Zhong, N, Song, F, Shi, X, Tao, J, & Xiang, S, 2003b. Mixed oils derived from multiple source rocks in the Cainan oilfield, Junggar Basin, Northwest China; Part II, Artificial mixing experiments on typical crude oils and quantitative oil–source correlation. Organic Geochemistry. 34. 911–930.

Christie O.H.J. 1992. Multivariate methodology in petroleum exploration. A geochemical software package. Chemometric and Intelligent Laboratory System. 14. 319-329.

Christie O.H.J. Esbensen K Meyer T. & Wold S. 1984. Aspect of pattern recognition in organic geochemistry. Organic Geochemistry. 6. 889-891.

Chukwu G.A. 1991. The Niger Delta complex basin: Stratigraphy, structure and hydrocarbon potential. Petroleum Geology. 14. 211–220.

Chung H.M, Rooney M.A, Toon M.B, & Claypool, G.E. 1992. Carbon isotope composition of marine crude oil. American Association of Petroleum Geologists. 76. 1000-1007.

Clayton J.L. King J.D. Threlkeld C.N. Vueletich A. 1987. Geochemical correlation of Palaeozoic oils, Northern Denver Basin – implication for exploration. American Association of Petroleum Geologists. 71. 103-109.

Clayton, C.J., 1991. Effect of maturity on carbon isotope ratios of oils and condensates. Organic Geochemistry. 17. 887-899.

Clegg, H., Wilkes, H. & Horsfield, B. 1997. Carbazole distributions in carbonate and clastic source rocks. Geochimica et Cosmochimica Acta. 61. 5335-5345.

Clegg, H., Horsfield, B., Wilkes, H., Sinninghe Damsté, J.S. & Koopmans, M.P. 1998a. Effect of artificial maturation on carbazole distributions, as revealed by the hydrous pyrolysis of an organic-sulphur-rich source rock (Ghareb Formation, Jordan), Organic Geochemistry. 29. 1953-1960.

Clegg, H., Wilkes, H., Oldenburg, T., Santamaría-Orozco, D. & Horsfield, B. 1998b. Influence of maturity on carbazole and benzocarbazole distributions in crude oil and source rocks from the Sonda de Campeche, Gulf of Mexico. Organic Geochemistry. 29. 183-194.

Connan, J., 1984. Biodegradation of crude oils in reservoirs. In: Brooks, J., Welte, D. (Eds.), Advances in Petroleum Geochemistry I. Academic Press, London. 299.

Cornford, C. 1998. Source rocks and hydrocarbons of the North Sea. In: Glennie, K.W. (ed.) Petroleum Geology of the North Sea (4th edn). Blackwell Science Limited. Oxford. 376–462.

Cornford, C., J. Morrow, A., Turrington, A, Miles, J.A & Brooks, J. 1983. Some geological controls on oil composition in the UK. North Sea, in J. Brooks, (ed.), Petroleum Geochemistry and Exploration of Europe. Geological Society Special Publication. 12. 175-194

Cornford, C., Needham, C.E.J. & Walque, L. de 1986. Geochemical habitat of North Sea oils and gases. In: Spencer, A.M. (ed.) Habitat of Hydrocarbons on the Norwegian Continental Shelf. Norwegian Petroleum Society. Graham & Trotman, London, 39–54.

Cornford, C., Burgess, C., Gliddon, T. & Kelly, R. 2001. Geochemical truths in large data sets -II: Risking petroleum systems. In: 20th International Meeting on Organic Geochemistry. Abstracts. 322-323.

Corredor, F., Shaw, J.H., & Bilotti, F., 2005. Structural styles in the deep-water fold and thrust belts of the Niger Delta. American Association of Petroleum Geologists. 89. 753–780.

Coward, M.P., Purdy, E.G., Ries, A.C., & Smith, D.G., 1999. The distribution of petroleum reserves in basins of the South Atlantic margins; in Cameron, N.R., Bate, R.H., & Clure, V.S., (eds.), The oil and gas habitats of the South Atlantic: Geological Society of London Special Publication 153. 101–131.

Curiale J.A., Sperry, S.W., 2000. An isotope-based oil–source rock correlation in the Camamu Basin, offshore Brazil. In: Proceedings Volume of the 6th Latin

American Congress on Organic Geochemistry. Revista Latino Americana de Geoquimica Organica. 4. 51–64.

Curiale, J.A., & Bromley, B.W., 1996. Migration of petroleum into Vermilion 14 field, Gulf Coast, USA — molecular evidence. Organic Geochemistry. 24. 563–579.

Curiale, 1., Morelos, 1., Lambiase, J. & Mueller, W. 2000. Brunei Darussalem-characteristics of selected petroleums and source rocks. Organic Geochemistry. 31. 1475-93.

Curiale, l.A. 2002. A review of the occurrences and causes of migration contamination in crude oils. Organic Geochemistry. 33. 1389-1400.

Curiale J.A., Decker J.D. & Lin R. 2005. Isotopic and molecular characteristics of Miocene-reservoired oils of the Kutei Basin, Indonesia, Organic Geochemistry. 36. 405–424.

Curiale, J. A., 2008, Oil-source rock correlations - Limitations and recommendations. Organic Geochemistry.39. 1150-1161.

Dahl, J.E., Moldowan, J.M., Peters, K.E., Claypool, G.E., Rooney, M.A., Michael, G.E., Mello, M.R. & Kohnen, M.L. 1999. Diamondoid hydrocarbons as indicators of natural oil cracking. Nature. 399. 54–57.

Dawson, D., Grice, K., Wang, S.X., Alexander, R., & Radke, J., 2004. Stable hydrogen isotopic compositions of hydrocarbons in torbanites (Late Carbonifierous to Late Permian) deposited under various climatic conditions. Organic Geochemistry. 35. 189–197.

Dawson, D., Grice, K., & Alexander, R., 2005. Effect on maturation on the indigenous dD signatures of individual hydrocarbons in sediments and crude oils from the Perth Basin (Western Australia). Organic Geochemistry. 36. 95–104.

Dawson, D., Grice, K., Edwards, D.S., & Alexander, R., 2007. The effect of source and maturity on the stable isotopic compositions of individual hydrocarbons in sediments and crude oils from the Vulcan Sub-basin, Timor Sea, Northern Australia. Organic Geochemistry. 38. 1015–1038.

De Araujo, P.L.B., Mansoori, G.A., & Araujo, E.S. 2012. Diamondoids: Occurrence in fossil fuels, applications in petroleum exploration and fouling in petroleum production. A review paper. Oil Gas and Coal Technology. 5. 316-367.

De Grande, S. M. B., F. R. Aquino Neto, F.R & Mello, M.R. 1993. Extended tricyclic terpanes in sediments and petroleums. Organic Geochemistry. 20. 1039-1047.

De Hemptinne J.C, Peumery R, Ruffier-Meray V, Moracchini G, Naiglin J. Carpentier B, Oudin J.L, & Connan J. 2001. Compositional changes resulting from the water-washing of a petroleum fluid. Petroleum Science and Engineering. 29. 39–51.

Didyk, B. M., Simoneit, B.R.T, Brassell, S.C & Eglinton, G 1978. Organic geochemical indicators of paleoenvironmental conditions of sedimentation. Nature. 272. 216-222.

Doust, H., & Omatsola, E., 1990. Niger Delta. In: Edwards, J.D., & Santogrossi, P.A. (Eds.), Divergent/Passive Margin Basins, American Association of Petroleum Geologists Memoir 44. 239–248.

Dzou, L. I. and Hughes, W. B. 1993. Geochemistry of oils and condensates, k field, offshore Taiwan: a case study in migration fractionation. Organic Geochemistry. 20. 437-462.

Edwards, J.D., & Santogrossi, P.A., 1990. Summary and conclusions. In: Edwards, J.D., & Santogrossi, P.A., (eds.) Divergent/Passive Margin Basins, American Association of Petroleum Geologists Memoir 48. 239-248.

Ejedawe, J.E., Coker, S.J., Lambert-Aikhionbare, D.O., Alofe, K.O., & Adoh, F.O., 1984. Evolution of oil-generative window and oil and gas occurrence in Tertiary Niger Delta basin. American Association of Petroleum Geologists. 68. 1744– 1751.

Ekweozor, C.M., Okogun, J.I., Ekong, D.E.U., & Maxwell, J.R., 1979. Preliminary organic geochemical studies of samples from the Niger Delta (Nigeria): Analysis of crude oils for triterpanes. Chemical Geology. 27. 11–28.

Ekweozor, C.M., & Okoye, N.V., 1980. Petroleum source-bed evaluation of the Tertiary Niger Delta. American Association of Petroleum Geologists. 64. 1251– 1259.

Ekweozor, C.M., & Daukoru, E.M., 1984. Petroleum source bed evaluation of the Tertiary Niger Delta-reply. American Association of Petroleum Geologists. 68. 390–394.

Ekweozor C.M, & Udo O.T. 1988. The oleananes: origin, maturation and limit of occurrence in Southern Nigeria sedimentary basins. Advances in organic geochemistry. 13. 131-140.

Ekweozor, C. M., & Telnaes, N. 1989, Oleanane parameter: verification by quantitative study of the biomarker occurrence in sediments of the Niger Delta. In: B. Durand, & F. Behar, (eds.) Advances in Organic Geochemistry. 401-415.

Ekweozor, C. M., & Daukoru, E.M, 1994, Northern delta depobelt portion of the Akata-agbada(!) petroleum system, Niger Delta, Nigeria, in, Magoon, L.B., and Dow, W.G., eds., The Petroleum System--From Source to Trap, American Association of Petroleum Geologists Memoir 60. 599-614.

Eneogwe C, Ekundayo O, & Patterson B. 2002. Source-derived oleanenes identified in Niger Delta oils. Petroleum Geology. 25. 83-95.

Eneogwe C., & Ekundayo O. 2003. Geochemical correlations of crude oil in the NW Niger Delta, Nigeria. Petroleum Geology. 26. 95-103.

England, W. A. & Mackenzie, A. S. 1989. Some aspects of the organic geochemistry of petroleum fluids. Geologische Rundschau 78. 291-303.

Espitalie, J., Madec, M., Tissot, B., Menning, J. J., & Leplat, P., 1977. Source rock characterization methods for petroleum exploration. Offshore Technology. 3. 439-444.

Evamy, B.D., Kamerling, P., Knaap, W.A., Molloy, F.A., & Rowlands, P.H., 1978. Hydrocarbon habitat of Tertiary Niger Delta. American Association of Petroleum Geologists. 62, 277–298.

Fadahunsi, O., Lawrence, S.R., Richards, M., & Bray, R., 2004. Plays, traps and petroleum systems in the Deepwater Niger Delta. In: Nigerian Association of Petroleum Explorationists/American Association of Petroleum Geologists Regional West Africa Deepwater Conference, Abuja, Nigeria.

Fang., C. Xiong., Y. Li., Y. Liu., C. Zhang., H Adedosu., T.A. & Peng., P 2013. The origin and evolution of adamantanes and diamantanes in petroleum. Geochemica et Cosmochimca Acta. 120. 109-120

Frost, B.R., 1997. A Cretaceous Niger Delta Petroleum System. In: Extended Abstracts, Petroleum Systems of the South Atlantic Margin. American Association of Petroleum Geologists Research Symposium. 16-19.

Grantham, P.J., 1986. Sterane isomerization and moretane/hopane ratios in crude oils derived from Tertiary source rocks. Organic Geochemistry. 9. 293–304.

Gratzer, R.A., Bechtel, A., Sachsenhofer, R.F., Linzer, H.G., Reischenbacher, D., & Schulz, H.M., 2011. Oil–oil and oil–source rock correlations in the Alpine Foreland Basin of Austria: insights from biomarker and stable carbon isotope studies. Marine Petroleum Geology. 28. 1171–1186.

Goossens, H., de Leeuw, J.W. Schenck, P.A & Brassell, S.C 1984. Tocopherols, likely precursors of pristane in the ancient sediments and crude oils. Nature. 312. 440-442.

Grice, K., Alexander, R., & Kagi, R.I., 2000. Diamondoid hydrocarbon ratios as indicators of biodegradation in Australian crude oils. Organic Geochemistry. 31. 67–73.

Gurgey K. 2002. An attempt to recognise oil populations and potential source rocks types in Paleozoic sub- and Mesozoic-Cenozoic supra-salt strata in the southern margin

of the Pre-Caspian Basin, Kazakhstan Republic. Organic Geochemistry. 33. 723-741.

Gussow, W. C. 1954. Differential entrapment of oil and gas: a fundamental principle. American Association of Petroleum Geologists. 38. 816-853.

Haack, R.C., Sundararaman, P., & Dahl, J., 1997. Niger Delta Petroleum System, in, Extended Abstracts, American Association of Petroleum Geologists /ABGP Hedberg Research Symposium, Petroleum Systems of the South Atlantic Margin. Rio de Janeiro, Brazil.

Haack, R.C., Sundararaman, P., Diedjomahor, J.O., Xiao, H., Gant, N.J., May, E.D., & Kelsch, K., 2000. Niger Delta petroleum systems, Nigeria. In: Mello, M.R., Katz, B.J. (Eds.), Petroleum Systems of the South Atlantic Margins. American Association of Petroleum Geologists Memoir 73. 213-231.

He. M, Moldowan. J.M, Rovenskaya. A.N, & Peters, K.E. 2012. Oil families and their inferred source rocks in the Barents Sea and Northern Timan-Pechora Basin, Rusia. American Association of Petroleum Geologist. 96. 1121-1146.

Head, I.M., Jones, D.M., & Larter, S.R., 2003. Biological activity in the deep subsurface and the origin of heavy oil. Nature. 426. 344–352.

Hill, R. J., Jarvie, D. M. Zumberge, J. Henry, M & Pollastro, R. M. 2007. Oil and gas geochemistry and petroleum systems of the Fort Worth Basin. American Association of Petroleum Geologists. 91. 445 – 473.

Hoffmann C.F, Mackenzie A.S, Lewis C.A, Maxwell J.R, Oudin L.L, Durand B. & Vandenbroucke M. 1984. A biological marker studies of coals, shales and oils from the Mahakam Delta, Kalimanta, Indonesia. Chemical Geology. 42. 1-23.

Horsfield, B., Schenk, H. J., Mills, N. & Welt. D. H. 1992. An investigation of the in-reservoir conversion of oil to gas: Compositional and kinetic findings from closed-system programmed-temperature pyrolysis. Organic Geochemistry. 19. 191-204.

Horstad I. Larter S.R. Dypvik H. 1990. Degradation and maturity controls on oil field petroleum column heterogeneity in the Gullfaks Field, Norwegian North Sea. Organic Geochemistry. 16. 497-510.

Horstad I, larter S.R, Mills N 1991. A quantitative model of biological petroleum degradation within the Brent Group reservoir in the Gullfaks Field, Norwegian North Sea.Organic Geochemistry. 19. 107–117.

Hospers, J., 1965, Gravity field and structure of the Niger Delta, Nigeria, West Africa: Geological Society of America. 76. 407–422.

Huang, W. Y., & Meinschein, W.G. 1979. Sterols as ecological indicators. Geochimica et Cosmochimica Acta. 43. 739-745.

Huang, D., Zhang, D., Li, J., Huang, X., Zhou, Z., 1989. The tertiary oil source correlation in Qaidam Basin. Acta Sedimentologica Sinica 7. 1–14.

Huang. D. li J. & Zhang D. 1990. Maturation sequence of continental crude oil in hydrocarbon basins in China and its significance. Organic Geochemistry. 16. 521-529.

Huang, D.F., Liu, B.W., Wang, T.D., Xu, Y.C., Chen, S.J., & Zhao, M.J., 1999. Genetic type and maturity of Lower Paleozoic marine hydrocarbon gases in the eastern Tarim Basin. Chemical Geology. 162. 65–77.

Huang, Y., Freeman, K.H., Wilkin, R.T., Arthur, M.A. & Jones, A.D. 2000. Black Sea chemocline oscillations during the Holocene: molecular and isotopic studies of marginal sediments. Organic Geochemistry. 31. 1525-1531.

Huang, H., Ren, F.X., & Larter, S.R., 2002. Influence of biodegradation on benzocarbazole distributions in reservoired oils. Chinese Science. 47. 1734–1739.

Huang, H., Bowler, B.F.J., Zhang, Z., Oldenburg, T.B.P., & Larter, S.R., 2003. Influence of biodegradation on carbazole and benzocarbazole distributions in oil columns from the Liaohe Basin, NE China. Organic Geochemistry. 34. 951–969.

Hughes W.B. Holba A.G, Mueller D.E. & Richardson J.S. 1985. Geochemistry of greater Ekofisk crude oils. In: Geochemistry in exploration of the Norwegian Shelf. Thomas B.M (ed). Graham and Trotman, London. 75-92.

Hughes, W.B. & Dzou, L.I.P. 1995. Reservoir overprinting of crude oils. Organic Geochemistry. 23. 905-914.

Hunt, J.M., Stewart, F., & Dickey, P.A., 1954. Origin of hydrocarbons of Uinta Basin, Utah. American Association of Petroleum Geologists. 1671- 1698.

Hunt, J. M., Huc, A.Y & Whelan, J.K. 1980. Generation of light hydrocarbons in sedimentary rocks. Nature. 288. 688-690.

Hunt, J. M. 1996. Petroleum Geochemistry and Geology. W.H. Freeman, New York, 2nd edition. 437p.

Jobson, A., Cook, F.D. & Westlake, D.W.S., 1972. Microbial utilisation of crude oil. Applied Microbial. 23. 1082-1089.

Jobson, A.M., Cook, F.D., & Westlake, D.W.S., .1979. Interaction of aerobic and anaerobic bacteria in petroleum biodegradation. Chemical Geology. 24. 355-366.

Jones, D.M., Head, I.M., Gray, N.D., Adams, J.J., Rowan, A.K., Aitken, C.M., Bennett, B.,Huang, H., Brown, A., Bowler, B.F.J., Oldenburg, T., Erdmann, M., & Larter,

S.R., 2008. Crude-oil biodegradation via methanogenesis in subsurface petroleum reservoirs. Nature. 451. 176–180.

Kaplan, A., Lusser, C.U., & Norton, I.O., 1994. Tectonic map of the world, panel 10: Tulsa, American Association of Petroleum Geologists, scale 1:10,000,000

Keller M.A. & MacQuaker J.H.S. 2001. High resolution analysis of petroleum source potential and lithofacies of lower Cretaceous mudstone core pebble shale unit and GRZ of Hue Shale, Mikkelsen Bay state no 1 well, North Slope Alaska. In: Petroleum plays and system in the national petroleum reserve-Alaska. Houseknecht. D.W (Ed). Society of Economic Palaeontologists and Mineralogists. Tulsa. Oklahoma. 37-56.

Kramer R. 1998. Chemometrics techniques for quantitative analysis. Marcel Dekker, New York.

Knox, G.J., & Omatsola, E.M., 1989. Development of the Cenozoic Niger Delta in terms of the 'Escalator Regression' model and impact on hydrocarbon distribution. In: van der Linden, W.J.M., Cloetingh, S.A.P.L., Kaasschieter, J.P.K., van der Graff W.J.E., Vandenberghe, J., van der Gun, J.A.M. (Eds.). Proceedings KNGMG Symposiums on Coastal Lowlands, Geology and Geotechnology. 181–202.

Kruge M.A. 2000. Determination of thermal maturity and organic matter type by principal component analysis of the distribution of polycyclic aromatic compounds. Coal Geology. 43. 27-51.

Killops, S. D., & Killops, V.J. 1993. An introduction to organic geochemistry. Harlow, Longman Scientific and Technical.

Killops, S.D., Woolhouse, A.D., Weston, RJ. & Cook, R.A.1994. A Geochemical Appraisal of Oil Generation in the Taranaki Basin, New Zealand. American Association of Petroleum Geologists Bulletin. 78. 1560-1585.

Killops, S. D., Funnell, R.H. Suggate, R.P. Sykes, R. Peters, K.E. Walters, C. Woolhouse, A.D Weston, R.J & Boudou, J.P 1998. Predicting generation and expulsion of paraffinic oil from vitrinite-rich coals. Organic Geochemistry. 29. 1-21.

Kulke, H., 1995. Nigeria. In: Kulke, H. (Ed.), Regional Petroleum Geology of the World. Part II: Africa, America, Australia and Antarctica. Gebru Borntraege Berlin, 143–172.

Lafargue, E. & Thiez, P.L. 1996. Effect of water washing on light end compositional heterogeneity. Organic Geochemistry. 24. 1141-1150.

Lafargue, E. & Barker, C. 1988. Effect of water washing on crude oil compositions. American Association of Petroleum Geologists. 72. 263— 276.

Lambert-Aikhionbare, D.O., & Ibe, A.C., 1984. Petroleum source-bed evaluation of the Tertiary Niger Delta: Discussion. American Association of Petroleum Geologists. 61. 961–981.

Larter, S., & Mills, N., 1991. Phase-controlled molecular fractionations in migrating petroleum charges. In: England, W., & Fleet, A. (Eds.). Petroleum Migration. Geological Society London Special Publication. 59. 137–147.

Larter, S. R. and A. C. Aplin, 1995, Reservoir geochemistry: methods, application and opportunities, in J. M. Cubitt and W. A. England, eds, The geochemistry of reservoirs. 86, 5 — 32.

Larter, S.R., Bowler, B.F.J., Li, M., Chen, M., Brincat, D., Bennett, B., Noke, K., Donohoe, P., Simmons, D., Kohnen, M., Allan, J., Telnæs, N. & Horstad, I. 1996. Molecular indicators of secondary oil migration distances. Nature. 383. 593-597.

Larter, S.R., Bowler, B.F.J., Clarke, E., Wilson, C., Moffat, B., Bennett, B., Yardley, G., & Carruthers, D., 2000. An experimental investigation of geochromatography during secondary migration of petroleum performed under subsurface conditions with a real rock. Geochemical Transactions. 9. 1-7.

Larter, S.R., Wilhelms, A., Head, I., Koopmans, M., Aplin, A., Di Primio, R., Zwach, C., Erdmann, M., & Telnaes, N., 2003. The controls on the composition of biodegraded oils in the deep subsurface: Part 1 - Biodegradation rates in petroleum reservoirs. Organic Geochemistry. 34. 601–613.

Larter, S.R., Huan, H., Adams, J., Bennett, B., Jokanola, O., Oldenburg, T., Jones, M., Head, I., Riediger, C., & Fowler, M., 2006. The controls on the composition of biodegraded oils in the deep subsurface: Part II – Geological controls on subsurface biodegradation fluxes and constraints on reservoir-fluid property prediction. American Association of Petroleum Geologists. 90. 921–938.

Larter, S.R., Adams, J., Gates, I.D., Bennett, B., & Huang, H., 2008. The origin, prediction and impact of oil viscosity heterogeneity on the production characteristics of tar sand and heavy oil reservoirs. Journal of Canadian Petroleum Technology. 47. 52–61.

Larter, S., Huang, H., Adams, J., Bennett, B., & Snowdon, L.R., 2012. A practical biodegradation scale for use in reservoir geochemical studies of biodegraded oils. Organic Geochemistry. 45. 66–76.

Lehne E & Dieckmann. 2010. Improved understanding of mixed oil in Nigeria based on pyrolysis of asphaltenes. Organic Geochemistry. 41. 661-674.

Lehner, P., & De Ritter, P.A.C., 1977. Structural history of Atlantic margin of Africa. American Association of Petroleum Geologists. 61. 961–981.

Leythaeuser, D., R. G. Schaefer, C. Cornford, & B. Weiner, 1979a. Generation and migration of light hydrocarbons (C_2-C_7) in sedimentary basins. Organic Geochemistry. 1. 191-204.

Leythaeuser, D., R. Schaefer, G & Weiner, B. 1979b. Generation of low molecular weight hydrocarbons from organic matter in source beds as a function of temperature and facies. Chemical Geology. 25. 95-108.

Leythaeuser, D. & Ruckheim, J. 1989. Heterogeneity of oil composition within a reservoir as a reflection of accumulation history. Geochimica et Cosmochimica Acta. 53. 2119-2123.

Li, M., Larter, S.R., Stoddart, D. & Bjorøy, M. 1995. Fractionation of pyrrolic nitrogen compounds in petroleum during migration: derivation of migration-related geochemical parameters. In: Cubitt, J.M. and England, W.A. (Eds.). The Geochemistry of Reservoirs. Geological Society of London. 103-123.

Li, M., Yao, H., Stasiuk, L.D., Fowler, M.G. & Larter, S.R. 1997. Effect of maturity and petroleum expulsion on pyrrolic nitrogen compound yields and distributions in Duvernay Formation petroleum source rocks in central Alberta, Canada, Organic Geochemistry. 26. 731-744.

Li, J., Paul, P., Cui, M., 2000. Methyldiamantane index (MDI) as a maturity parameter for lower Palaeozoic carbonate rocks at high maturity and over-maturity. Organic Geochemistry. 31. 267–272.

Li M., Huang Y. S., Obermajer M., Jiang C., Snowdon L. R., and Fowler M. G. 2001. Hydrogen isotopic composition of individual n-alkanes as a new approach to petroleum correlation: case studies from the Western Canada Sedimentary Basin. Organic Geochemistry. 32. 1387-1399.

Li S. Pang X. Li M. & Jin Z. 2003. Geochemistry of petroleum systems in the Niuzhaung South Slope of Bohai Bay Basin – part 1: source rock characterisation. Organic Geochemistry. 34. 389-412.

Li X, Zhang G, & Zhang Y. 2007. Analysis on upstream developing trend of multinational petroleum corporations. Petroleum Exploration and Development. 34. 19-22.

Lijmbach G.W.M. 1975. On the origin of petroleum. Proceeding of the 9th world petroleum congress. 2. 357-369.

Liu J, Pan X, Ma J, Tian Z, Chen Y, & Wan L. 2008. Petroleum geology and resources in West Africa: An overview. Petroleum Exploration and Development. 35. 378-384

Lloyds R.M. 1966. Oxygen isotope enrichment of sea water by evaporation. Geochemica et Cosmochimica Acta. 30. 801-834.

Losh, S., Cathles, L., & Meulbroek, P., 2002. Gas washing of oil along a regional transect, offshore Louisiana. Organic Geochemistry. 33. 655–663.

Losh, S., Cathles, L., 2010. Phase fractionation and oil-condensate mass balance in the South Marsh Island Block 208–239 area, offshore Louisiana. Marine and Petroleum Geology 27. 467–475.

Mackenzie, A. S., 1984, Applications of biological markers in petroleum geochemistry. In: J. Brooks, and D. Welte, (Eds.). Advances in Petroleum Geochemistry. Academic Press. 115-214.

Mackenzie A. S., Brasell S. C., Eglinton G. & Maxwell J. R. 1982. Chemical fossils: the geological fate of steroids. Science. 217. 491-504.

Mackenzie A.S. & Mckenie D. 1983. Isomerization and aromatization of hydrocarbons in sedimentary basins formed by extension. Geology. 120. 417-528.

Mackenzie A.S. Rullkotter J. Welte D.H. & Mankiewicz P. 1985. Reconstruction of oil formation and accumulation in the North Slope, Alaska, using quantitative gas chromatography-mass spectrometry. In: Alaska North Slope oil/source rock correlation study. Magoon L.B. & Claypool G.E. (Eds). American Association of Petroleum Geologists. Tulsa. Oklahoma. 319-377.

Mackenzie, A. S., & T. M. Quigley. 1988. Principles of geochemical prospect appraisal. In: E. A. Beaumont, & N. H. Foster, (Eds.), Geochemistry. Treatise of Petroleum Geology. American Association of Petroleum Geologists. 231-248.

Magoon, L.B. & Dow, W.O. 1994. The Petroleum System. In: Magoon, L.B. & Dow, W.G. (Eds.). The Petroleum System-From Source to Trap, American Association of Petroleum Geologists Memoir. 60. 3-24.

Magoon, L.B. & Beaumont, E.A. 1999. Petroleum systems. In: Beaumont, E.A & Foster, N.H. (Eds.), Handbook of Petroleum Geology: Exploring/or oil and Gas Traps, American Association of Petroleum Geologists. Washington DC. 31-34.

Magoon, L.B. & Dow, W.G. 2000. Mapping the petroleum· system – an investigative technique to explore the hydrocarbon fluid system. In: Mello, M.R & Katz, B.l. (Eds.), Petroleum Systems of South Atlantic margins, American Association of Petroleum Geologists Memoir. 73. 53-68.

Mango, F. D., 1997. The light hydrocarbons in petroleum: a critical review. Organic Geochemistry. 26. 417-440.

Mango, F. D., Hightower. J. W. & James, A. T. 1994. Role of transition-metal catalysis in the formation of natural gas. Nature. 368. 536-538.

Marcano N. Larter S, & Mayer B. 2013. The impact of severe biodegradation on the molecular and stable (C, H, N, S) isotopic compositions of oils in the Alberta Basin, Canada. Organic Geochemistry. 59. 114–132.

Martin W. Gierl A. & Saelter H. 1989. Molecular evidence of pre-Cretaceous angiosperm origins. Nature. 339. 46-48.

Mansuy, L., Philp, R.P., Allen, J., 1997. Source identification of oil spills based on isotopic composition of individual components in weathered oil samples. Environmental Science and Technology. 31. 3417-3425.

McCaffrey M.A. Moldowan J.M. Lipton P.A. Summons R.E. Peters K.E. Jeganathan A. & Watt. D.S. 1994. Paleoenvironment implication of novel C_{30} sterane in Precambrian to Cenozoic age petroleum and bitumen. Geochemica et Cosmochimica Acta, 58. 529-532.

McHargue, T.R., 1990, Stratigraphic development of proto-South Atlantic rifting in Cabinda, Angola—A petroliferous lake basin, in Katz, B.J., ed., Lacustrine basin exploration case studies and modern analogues. American Association of Petroleum Geologists Memoir. 50. 307–326.

McKirdy D.M. Aldrige A.K & Ypma P.J.M. 1983. A geochemical comparison of some crude oil from Pre-Ordovician carbonate rocks. In: Advances in organic geochemistry. Bjoroy. M. Albrecht C., Conford C. (Eds). John Wiley & Sons. New York. 99-107.

McNeil, R. I. & BeMent, W. O. 1996. Thermal stability of hydrocarbons: Laboratory criteria and field examples. Energy & Fuels 10. 60-67.

Mello, M. R., Telnaes, N. Gaglianone, P.C. Chicarelli, M.I. Brassell, S.C. & Maxwell, J.R. 1988. Organic geochemical characterisation of depositional palaeoenvironment of source rocks and oils in Brazilian marginal basins. Advances in Organic Geochemistry. 13. 31-46.

Meulbroek, P., Cathles, L., Whelan, J., 1998. Phase fractionation at South Eugene Island Block 330. Organic Geochemistry 29, 223–239.

Moldowan, J. M., Seifert, W.K & Gallegos, E.J. 1985. Relationship between petroleum composition and depositional environment of petroleum source rocks. American Association of Petroleum Geologists. 69. 1255-1268.

Moldowan, J. M., Sundararaman, P, & Schoell, M. 1986. Sensitivity of biomarker properties to depositional environment and/or source input in the Lower Toarcian of SW. Germany. 10. 915-926.

Moldowan J. M. and Fago F. J. 1986. Structure and significance of a novel rearranged monoaromatic steroid hydrocarbon in petroleum. Geochimica et Cosmochimica Acta. 50. 343-351.

Moldowan, J. M., Fago, F., Lee, C.Y., Jacobson, S.R., Watt, D.S., Slougui, N., Jeganathan, A. & Young, D.C. 1990. Sedimentary 24-n-propylcholestanes, molecular fossils diagnostic of marine algae. Science. 247. 309-312.

Moldowan, J. M., Lee, C. Y. Watt, D.S. Jeganathan, A. Slougui, N.E & Gallegos, E.J. 1991. Analysis and occurrence of C_{26} -steranes in petroleum and source rocks: Geochimica et Cosmochimica Acta. 55. 1065-1081.

Moldowan J.M. Dahl J. Huizinga B.J. Fago F.J. Hickey L.J. Peakman T.M. & Taylor D.W. 1994. The molecular fossil record of oleanane and its relation to angiosperm. Science. 265. 268-271.

Moldowan, J.M., Zinniker, D., Dahl, J., Denisevich, P., Moldowan, S., Bender, A.A., Barbanti, S.M., Mello, M.R., 2010. Determination and quantification of petroleum mixtures. American Association of Petroleum Geologists Annual Convention and Exhibition. New Orleans, Louisiana.

Morgan R. 2003. Prospectivity in ultra-deep water: the case for petroleum generation and migration within the outer parts of the Niger Delta apron. (In) Authur T.J, MacGregor D.S, Cameron N.R (Eds) Petroleum Geology of Africa: new themes and developing technologies. Geological society special publication. 207. 151-164.

Murray, A.P., Summons, R.E., Bradshaw, J., & Pawih, B., 1993. Cainozoic oil in Papua New Guinea: evidence from geochemical analysis of two newly discovered seeps. In: Carman, G.J., Carman, Z. (Eds.), Petroleum Exploration and Development in Papua New Guinea: Proc. 2nd Papua New Guinea Petroleum Convention. PNG Chamber of Mines and Petroleum. 489-498.

Murray A.P, Summoms R.E, Boreham C.J, & Dowling L.M. 1994. Biomarker and n-alkane isotope profiles for Tertiary oils: relationship to source rocks depositional setting. Advances in organic geochemistry. 22. 521-542.

Murray, A. P., Sosrowidjojo, I. B., Alexander, R., Kagi, R. I., Norgate C. M. & Summons R. E. 1997. Oleananes in oils and sediments: Evidence of marine influence during early diagenesis. Geochimica et Cosmochimica Acta. 61. 1261-1276.

Nasir S. & Fazeelat T. 2013. Diamondoid hydrocarbon as maturity indicators for condensates from Southern Indus Basin. Pakistan. Chemistry. 1-10.

Nwachukwu, S.O., 1972. The tectonic evolution of the southern portion of the Benue Trough, Nigeria: Geology Magazine.109. 411-419.

Nwachukwu, J.I., & Chukwura, P.I., 1986. Organic matter of Agbada Formation, Niger Delta, Nigeria. American Association of Petroleum Geologists 70, 48– 55.

Nytoft, H.P., Samuel, O.J., Kildahl-Andersen, G., Johansen, J.E., & Jones, M., 2009. Novel C_{15} sesquiterpanes in Niger Delta oils: structural identification and potential application as new markers of angiosperm input in light oils. Organic Geochemistry 40. 595-603.

Obaje, N.G., 2009. Geology and Mineral Resources of Nigeria. Springer-Verlag, Dordrecht, Heidelberg, London, New York.

Obermajer, M., Osadetz, K.G, Fowler, M.G., Li, M., & Snowdown, L.R., 2004. Variable alteration in heavy crude oilof west-central Saskatchewan, Canada. Organic Geochemistry. 35. 469-491.

Odden, W., Patience, R.L & van Graas, G.W. 1998. Application of light hydrocarbons (C_4-C_{13}) to oil/source rock correlations: a study of the light hydrocarbon compositions of source rocks and test fluids from offshore Mid-Norway: Organic Geochemistry. 28. 823-848.

Oluwole, A.F., Adegoke, O.S., & Kehinde, L.O. 1985. Chemical composition of bitumen extracts from Nigerian tar sands. In 3rd. International UNITAR/UNDP Heavy Crude & Tar Sand conf., Long Beach, CA, USA. 1, 373-379.

Orr, W. L., 1986. Kerogen/asphaltene/sulphur relationships in sulphur-rich Monterey oils. In: Leythaeuser, D & Rullkotter J. (Eds). Advances in organic geochemistry. Pergamon. Oxford. 499-516.

Ourisson, G., Rohmer, & Poralla, K. 1987. Prokaryotic hopanoids and other polyterpenoid steroid surrogates. Microbiology. 41. 301-333.

Palmer S.E. 1993. Effect of biodegradation and water washing on crude oil composition. In: Organic geochemistry. Engel M.H & Macko S.A (Eds). Plenum Press. New York. 511-533.

Pang, X., Li, M., Li, S., & Jin, Z., 2003. Geochemistry of petroleum systems in the Niuzhuang South Slope of Bohai Bay Basin. Part 2: Evidence for significant contribution of mature source rocks to ‘‘immature oils” in the Bamianhe field. Organic Geochemistry 34. 931–950.

Parfitt M. and Farrimond P. 1998. The Mupe Bay oil seep: A detailed organic geochemical study of a controversial outcrop. In: Underhill J.R. (Ed.) "Development, Evolution and Petroleum Geology of the Wessex Basin". Geological Society Special Publication. 133. 387-397.

Pasley, M.A., Wilson, E.N., Abreu, V.A., Brandão, M.G.P., & Telles, A.S., 1998. Lower Cretaceous stratigraphy and source rock distribution in pre-salt basins of the South Atlantic—Comparison of Angola and Southern Brazil: American Association of Petroleum Geologists Bulletin. 82. 1949.

Pedentchouk, N., Freeman, K.H., & Harris, N.B., 2006. Different response of delta D values of n-alkanes, isoprenoids, and kerogen during thermal maturation. Geochimica et Cosmochimica Acta. 70, 2063–2072.

Pedentchouk, N., Freeman, K.H., Harris, N.B., Cliffird D.J, & Grice K. 2004. Sources of alkylbenzenes in Lower Creataceous lacustrine source rocks. West African rift basins. Organic Geochemistry. 35. 33-45.

P:igi geochemical manual. 2004. The program for integrated geochemical interpretation. Integrated geochemical interpretation limited. Devon. UK.

Peters, K. E., 1986, Guidelines for evaluating petroleum source rock using programmed pyrolysis: American Association of Petroleum Geologist. 70. 318-329.

Peters, K.E., Moldowan M., Schoell, M. & Hempkin, W.B. 1986. Petroleum isotopic and biomarker composition related to source rock organic matter and depositional environment. Organic Geochemistry. 10. 17-27.

Peters, K. E., Moldowan, J.M & Sundararaman, P. 1990. Effects of hydrous pyrolysis on biomarker thermal maturity parameters: Monterey Phosphatic and Siliceous members. Organic Geochemistry. 15. 249-266.

Peters, K. E., & Moldowan, J. 1991. Effects of source, thermal maturity, and biodegradation on the distribution and isomerization of homohopanes in petroleum. Organic Geochemistry. 17. 47-61.

Peters, K.E., & Moldowan, J. 1993. The Biomarker Guide. Interpreting Molecular fossils in Petroleum and Ancient Sediments. Patience-Hall, Englewood Cliffs, New Jersey.

Peters, K. E., Kontorovich, A.E. Moldowan, J.M. Andrusevich, V.E. Huizinga, B.J. Demaison, G.J & Stasova, O.F. 1993. Geochemistry of selected oils and rocks from the central portion of the West Siberian Basin, Russia: American Association of Petroleum Geologists. 77. 863–887.

Peters, K. E., & Cassa, M.R. 1994, Applied source rock geochemistry, in L. B. Magoon and W. G. Dow, eds., The petroleum system: From source to trap: American Association of Petroleum Geologists Memoir 60. 93–120.

Peters, K.E.,Kontorovich, A.E. Huizinga, B.J. Moldowan, J.M & Lee, C.Y. 1994. Multiple oil families in the West Siberian Basin: American Association of Petroleum Geologists. 78. 893–909.

Peters K.E. Cunningham A.E. Walters C.C. Jiang J. & Zhaoan F. 1996a. Petroleum systems in the Jiangling-Dangyang area, Jiangham Basin, China. Organic Geochemistry. 24. 1035-1060.

Peters K.E. Moldowan J.M. McCaffery M.A & Fago F.J. 1996b. Selective biodegradation of extended hopanes of 25-norhopanes in petroleum reservoirs. Insights from molecular mechanics. Organic Geochemistry. 24. 765-783.

Peters K.E. Fraser T.H. Amris W. Rustanto B. & Hermanto E. 1999. Geochemistry of crude oil from Eastern Indonesia. American Association of Petroleum Geologists. 83. 1927- 1942.

Peters K.E. Snedden J.W. Sulaeman A. Sarg J.F. & Enrico R.J. 2000. A new geochemical-stratigraphic model for the Mahakam Delta. And Makassar slope. Kalimantan, Indonesia. American Association of Petroleum Geologists. 84. 12-44.

Peters, K.E. & Fowler, M.G., 2002. Applications of petroleum geochemistry to exploration and reservoir management. Organic Geochemistry 33. 5–36.

Peters, K.E., Walters, C.C & Moldowan, J.M. 2005a. The Biomarker Guide: Biomarkers and Isotopes in Environment and Human History, 2nd edition: Cambridge University Press, United Kingdom, 1. p. 471.

Peters, K.E., Walters, C.C & Moldowan, J.M. 2005b. The Biomarker Guide: Biomarkers and Isotopes in Petroleum Exploration and Earth History, 2nd edition: Cambridge University Press, United Kingdom, v. 2, p. 1155.

Peters, K. E., Ramos, L.S. Zumberge, J.E. Valin, Z.C. Scotese, C.R. & Gautier, D.L. 2007. Circum-Arctic petroleum systems identified using decision-tree chemometrics: American Association of Petroleum Geologists. 91. 877–913.

Peters, K.E., Schenk, O & Wygrala, B. 2009. Exploration paradigm shift: The dynamic petroleum system concept. Swiss Bulletin of Applied Geology. 14. 65-71.

Pepper, A.S. & Corvi, P.l. 1995. Simple kinetic models of petroleum formation. Part III: modelling an open system. Marine and Petroleum Geology. 12. 417-403.

Philip R.P & Gilbert T.D. 1982. Unusual distribution of biological markers in an Australian crude oil. Nature. 299. 245-247.

Philip R.P & Gilbert T.D. 1986. Biomarker distributions in Australian oils predominantly derived from terrigenous source material. Organic Geochemistry. 10. 73-84.

Philippi, G. T., 1975. The deep subsurface temperature controlled origin of the gaseous and gasoline-range hydrocarbons of petroleum: Geochimica et Cosmochimica Acta. 39. 1353-1373.

Quigley, T. M. & Mackenzie, A. S. 1988. The temperature of oil and gas formation in the subsurface. Nature. 333. 549-552.

Radke, M., Welte, D.H. & Willsch, H. 1982. Geochemical study on a well in Western Canada Basin: relation of the aromatic distribution pattern to maturity of organic matter: Geochimica et Cosmochimica Acta. 46. 1-10.

Radke, M., & Welte, D.H. 1983. The Methylphenanthrene Index (MPI): a maturity parameter based on aromatic hydrocarbons, in M. Bjorøy, (Ed), Advances in Organic Geochemistry. 504-512.

Radke, M., Leythaeuser, D. & Teichmuller, M 1984, Relationship between rank and composition of aromatic hydrocarbons for coals of different origins, in E. A. Baker., (ed.), Advances in Organic Geochemistry. 423-430.

Radke, M., Welte, D.H. & Willsch, H. 1986. Maturity parameters based on aromatic hydrocarbons: influence of the organic matter type, in D. Leythaeuser, and J. Rullkötter, (Eds). Advances in Organic Geochemistry. 51- 64.

Radke, M., 1987, Organic geochemistry of aromatic hydrocarbons, in J. Brooks, and D. Welte., eds., Advances in Petroleum Geochemistry. 141-207.

Radke, M., Willsch, H & Teichmuller, M. 1990. Generation and distribution of aromatic hydrocarbons in coals of low rank: Organic Geochemistry. 15. 539-564.

Radke, M., Rullkoetter, J., Vriend, S.P., 1994. Distribution of naphthalenes in crude oils from the Java Sea: source and maturation effects. Geochimica et Cosmochimica Acta. 58. 3675-3689

Radke, J., Bechtel, A., Gaupp, R., Puttmann, W., Schwark, L., Sachse, D., Gleixner, G., 2005. Correlation between hydrogen isotope ratios of lipid biomarkers and sediment maturity. Geochimica et Cosmochimica Acta. 69. 5517–5530.

Rangel A. Parra P & Nino C. 2000. The La Luna formation: chemostratigraphy and organic facies in the Middle Magdalene Basin. Organic Geochemistry. 31. 1267-1284.

Reijers T. J. A. 2011. Stratigraphy and sedimentology of the Niger Delta. Geologos 17. 133-162.

Rooney M.A, Vuletich A.K, & Griffith C.E. 1998. Compound-specific isotope analysis as a tool of characterising mixed oil: an example from the West of Shetlands area. Organic geochemistry. 29. 241-254.

Rullkotter J. Spiro B. Nissenbaum A. 1985. Biological marker characteristics of oils and asphalts from carbonate source rocks in a rapid subsiding graben, Dead Sea, Israel. Geochemica et Cosmochimica Acta. 49. 1357-1370.

Rullkötter, J., & Marzi, R. 1988. Natural and artificial maturation of biological markers in Toarcian shale from northern Germany, in L. Mattavelli and L. Novelli (Eds.), Advances in Organic Geochemistry. 639-645.

Samuel, O.J., 2008. Molecular and isotopic constraints on oil accumulations in Tertiary deltas. Unpublished PhD thesis, Newcastle University, England, 380p.

Samuel, O., Jones, D.M., Cornford, C., 2007. Intra-Delta versus Sub-Delta Sourcing of Petroleum - a Global Review. American Association of Petroleum Geologists Search and Discovery. 1-7.

Samuel, O.J., Cornford, C., Jones, M., Adekeye, O.A., & Akande, S.O., 2009. Improved understanding of the petroleum systems of the Niger Delta Basin, Nigeria. Organic Geochemistry. 40. 461–483.

Samuel O. Kildahl-Andersen G. Nytoft H.P. Johansen J.E. Jones. M. 2010. Novel tricyclic and tetracyclic terpanes in Tertiary deltaic oils: Structural identification, origin and application to petroleum correlation. Organic Geochemistry 41. 1326–1337.

Santos N.E.V, & Hayes J.M, 1999. Use of hydrogen and carbon isotope characterising oil from the Pontiguar Basin (Onshore), North-eastern Brazil. American Association of petroleum geologist. 83. 496-518.

Scanlan, R. S., & Smith, J.E. 1970. An improved measure of the odd-even predominance in the normal alkanes of sediment extracts and petroleum. Geochimica et Cosmochimica Acta. 34. 611-620.

Schiefelbein, C. F., Zumberge, J.E. Cameron, N.C. & Brown, S.W. 1999. Petroleum Systems in the South Atlantic margins. In: Cameron, N.R, Bate R.H & Clure, V.s (eds) The Oil and Gas Habitats of the South Atlantic. Geological Society of London, Special Publications. 153. 169-179.

Schiefelbein, C. F., Zumberge, J.E. Cameron, N.C & Brown, S.W. 2000. Geochemical comparison of crude oil along the South Atlantic margins, in M. R. Mello and B. J. Katz, eds., Petroleum systems of South Atlantic margins: American Association of Petroleum Geologists Memoir 73. 15–26.

Schimmelmann A, Sessions A.L, Boreham C.J, Edwards D.S, Logan G.A, & Summons R.E. 2004. D/H ratio in terrestrial sourced petroleum systems. Organic Geochemistry. 35. 1169-1195.

Schoell, M., Teschner, M., Wehner, H., Durand, B. & Oudin, J.L.1983. Maturity related biomarker and stable isotope variations and their application to oil source rock correlation in the Mahakam Delta, Kalimantan. In: Bjomy, M. (ed.), Advances in Organic Geochemistry 1981, Chichester, Wiley, pp. 156-163.

Schoell, M., Durand, B. & Oudin, J. L. 1985. Migration of oil and gas in the Mahakam Delta, Kalimantan: evidence and quantitative estimate from isotope and biomarker studies. In 14th Indonesian Petroleum Association Convention Proceedings 2. Indonesian Petroleum Association, Jakarta, 49-56.

Schulz, L.K., Wilhelms, A., Rein, E. & Steen, A.S. 2001. Applications of diamondoids to distinguish source rock facies. Organic Geochemistry. 32. 365–375.

Seifert, W. K., & Moldowan, J.M. 1978. Applications of steranes, terpanes and monaromatics to the maturation, migration and source of crude oils: Geochimica et Cosmochimica Acta. 42, p. 77-95.

Seifert, W.K., & Moldowan, J.M. 1979. The effect of biodegradation on steranes and terpanes in crude oils, Geochimica et Cosmochimica Acta. 43. 111-126.

Seifert, W. K., & Moldowan, J.M 1980. The effect of thermal stress on source rock quality as measured by hopane stereochemistry, in A. G. Douglas, and J. R. Maxwell, eds., Advances in Organic Geochemistry 1979, Proc. 9th International Organic Geochemistry Meeting. Newcastle-upon-Tyne. Oxford, Pergamon, 229-237.

Seifert, W. K., & Moldowan, J.M. 1981. Paleoreconstruction by biological markers: Geochimica et Cosmochimica Acta. 45. 783-794.

Seifert W.K. Moldowan J.M & Demison G.J. 1984. Source correlation of biodegraded oils. Organic Geochemistry. 6. 633-643.

Seifert, W. K., & Moldowan, J.M. 1986. Use of biological markers in petroleum exploration, in R. B. Johns, ed., Biological Markers in the Sedimentary Record, Elsevier. 261-290.

Shacklenton N.J 1968. Depth of pelagic foraminifera and isotopic changes in Pleistocene oceans. Nature. 218. 79-80

Shanmugam, G. 1985. Significance of coniferous rain forests and related organic matter in generating commercial quantities of oil, Gippsland Basin, Australia. American Association of Petroleum Geologists. 69.1241–1254.

Short, K.C., & Stauble, A.J., 1967. Outline of geology of Niger Delta. American Association of Petroleum Geologists. 51. 761–779.

Smith B.N, & Epstein S. 1970. Biogeochemistry of the stable isotope of hydrogen and carbon in salt marsh biota. Plant physiology. 46. 738-742.

Smith, M., & Bend, S. 2004. Geochemical analysis and familial association of Red River and Winnipeg reservoired oils of the Williston Basin, Canada: Organic Geochemistry. 35. 443-452

Summons, R. E., & Capon, R.J. 1988. Fossil steranes with unprecedented methylation in Ring-A: Geochimica et Cosmochimica Acta. 52. 2733-2736.

Summons, R. E., & Capon, R.J. 1991. Identification and significance of 3B-ethyl steranes in sediment and petroleum: Geochimica et Cosmochimica Acta. 55. 2391-2395.

Summons, R.E., Bradshaw, M., Crowley, J., Edwards, D.S., George, S.C., Zumberge, J.E., 1998. Vagrant oils: geochemical signposts to unrecognised petroleum systems. In: Purcell, P.G., Purcell, R.R. (Eds.). The Sedimentary Basins of Western Australia 2. Proceedings of Petroleum Exploration Society of Australia Symposium, Perth, 1998. 169–184.

Sun, Y., Chen, Z., Xu, S., and Cai, P. 2005. Stable carbon and hydrogen isotopic fractionation of individual n-alkanes accompanying biodegradation: evidence from a group of progressively biodegraded oils. Organic Geochemistry. 36. 225–238.

Sofer, Z. & Gat, J. R. 1975. The isotope composition of evaporating brines: effect on the isotope activity ratio in saline solutions. Earth and Planetary Science Letters 26. 179-186.

Sonibare, O., Alimi, H., Jarvie, D. & Ehinola, O.A. 2008. Origin and Occurrence of Crude Oil in the Niger Delta, Nigeria. Petroleum Science and Engineering. 61. 99-107.

Silverman, S.R. 1965. Migration and segregation of oil and gas. In: Fluids in Subsurface Environments. (eds). A., Young & G. E. Galley. American Association of Petroleum Geologists. 53-65.

Stacher, P., 1995. Present understanding of the Niger Delta hydrocarbon habitat, in, Oti, M.N., and Postma, G., (Eds) Geology of Deltas. Rotterdam. 257-267.

Teisserence P & Villemine J. 1990. Sedimentary basin of Garbon – Geology and oil systems. In: Edwards J.D (ed) Divergent/Passive Margin Basins. American Association of Petroleum Geologists. 48. 117-199.

ten Haven, H. L., de Leeuw, J.W. Peakman, T.M. & Maxwell, J.R. 1986. Anomalies in steroid and hopanoid maturity indices. Geochimica et Cosmochimica Acta. 50. 853-855.

ten Haven, H. L., de Leeuw, J.W, Rullkötter, J. & Sinninghe-Damsté, J. 1987. Restricted utility of the pristane/phytane ratio as a palaeoenvironmental indicator. Nature. 330. 641-643.

ten Haven, H. L., 1996. Applications and limitations of Mango's light hydrocarbon parameters in petroleum correlation studies. Organic Geochemistry. 24. 957-976.

Thomas, D. 1995. Exploration gaps exist in Nigeria's prolific delta. Oil and Gas. 93. 66-71.

Thompson, K. F. M., 1979, Light hydrocarbons in subsurface sediments: Geochimica et Cosmochimica Acta. 43. 657-672.

Thompson, K. F. M., 1983, Classification and thermal history of petroleum based on light hydrocarbons: Geochimica et Cosmochimica Acta. 47. 303-316.

Thompson, K. F. M., 1987. Fractionated aromatic petroleums and the generation of gas condensates. Organic Geochemistry. 11. 573-590.

Thompson, K. F. M., 1988, Gas-condensate migration and oil-fractionation in deltaic systems. Petroleum Geology. 5. 237-246.

Thompson, K.F.M., Kennicutt, M. & Brooks, J.M. 1990.Classification of offshore Gulf of Mexico oil and Gas Condensates. American Association of Petroleum Geologists. 74. 187-198.

Tissot, B.P. & Welte, D.H. 1984. Petroleum Formation and Occurrence. Springer-Verlag, New York, 699.

Tuttle, W.L.M, Brownfield, E.M. & Charpentier, R.R. 1999. The Niger Delta Petroleum System. Chapter A: Tertiary Niger Delta (Akata-Agbada) Petroleum System, Niger Delta Province, Nigeria, Cameroon and Equatorial Guinea, Africa. U.S. Geolgical Survey, Open File Report. 99-50H. http://pubs.usgs.gov/of/1999/ofr-99-0050/OF99-50H/OF99-50H.pdf.

van Aarssen, B.G.K., Bastow, T.P., Alexander, R., & Kagi, R.I., 1999. Distribution of methylated naphthalenes in crude oils: indicators of maturity, biodegradation and mixing. Organic geochemistry. 30. 1213–1227.

van Graas G.W, Gilje A.E, Isom T.P & Tau L.A. 2000. The effects of phase fractionation on the composition of oils, condensates and gases. Organic Geochemistry 31. 1419- 1439.

Volkman, J.K., Alexander, R., Kagi, R.I., Woodhouse, G.W., 1983. Demethylated hopanes in crude oils and their applications in petroleum geochemistry. Geochimica et Cosmochimica Acta. 47. 785–794.

Volkman, J.K., Alexander, R., Kagi, R.I., Rowland, S.J., & Sheppard, P.N., 1984. Biodegradation of aromatic hydrocarbons in crude oils from the Barrow Subbasin of Western Australia. Organic Geochemistry. 6. 619–632.

Volkman, J. K. & Maxwell, J.R, 1986. Acyclic isoprenoids as biological markers, in R. B. Johns (Eds) Biological Markers in the Sedimentary Record. Elsevier. 1-42.

Volkman, J.K., Barrett, S.M., Blackburn, S.I., Mansour, M.P., Sikes, E.L. & Gelin, F. 1998. Microalgal biomarkers: a review of recent research developments. Organic Geochemistry. 29. 1163-1179.

Wang D. 2007. The consumption of oil and gas in China will be up to 65×10^6 t in 2010. Petroleum Exploration and Development, 2007, 34(1): 82.

Wang, Z., Yang, C., Hollebone, B. & Fingas, M. 2006. Forensic fingerprinting of diamondoids for correlation and differentiation of spilled oil and petroleum products. Environmental Science and Technology. 40.5636–5646.

Waples, D.W., 2000. The kinetics of in-reservoir oil destruction and gas formation: constraints from experimental and empirical data, and from thermodynamics. Organic Geochemistry. 31. 553–575

Weber, K. J. 1971. Sedimentological aspects of oil-fields in the Niger Delta. Geologie. 50. 559-576.

Weber, K.J., & Daukoru, E.M., 1975. Petroleum geology of the Niger Delta. In: Proceedings of the Ninth World Petroleum Congress, Geology. 2. Applied Science Publishers Limited, London. 210–221.

Weber, K.J., 1987, Hydrocarbon distribution patterns in Nigerian growth fault structures controlled by structural style and stratigraphy: Petroleum Science and Engineering, 1, 91-104.

Wei, Z., Moldowan, J.M. & Paytan, A. 2006. Diamondoids and molecular biomarkers generated from modern sediments in the absence and presence of minerals during hydrous pyrolysis. Organic Geochemistry. 37. 891–911.

Wei, Z., Moldowan, J.M., Peters, K.E., Wang, Y. & Xiang, W. 2007. The abundance and distribution of diamondoids in biodegraded oils from the San Joaquin Valley: implications for biodegradation of diamondoids in petroleum reservoirs. Organic Geochemistry. 38. 1910–1926.

Welte, D.H., Horfield, B., Barker, D.R., 1997. Petroleum and Basin Evolution. Springer, New York, 535.

Wenger, L.M., Davis, C.L., & Isaksen, G.H., 2002. Multiple controls on petroleum biodegradation and impact on oil quality. Society of Petroleum Explorationist. Reservoir Evaluation and Engineering 5. 375–383.

Whiteman, A., 1982, Nigeria: Its Petroleum Geology, Resources and Potential: London, Graham and Trotman, 394.

Wilhelms, A.S., & Larter, S.R. 1994. Origin of tar mats in petroleum reservoirs. Part II: formation mechanisms for tar mats. Marine and Petroleum Geology, 11 (1994). 442–456

Wilhelms, A., Larter, S.R., Head, I., Farrimond, P., di Primio, R., & Zwach, C., 2001. Biodegradation of oil in uplifted basins prevented by deep-burial sterilization. Nature. 411. 1034–1037.

Wilhelms A & Larter S, 2004. Shaken but not always stirred. Impact of petroleum charge mixing on reservoir geochemistry. In CUBITT, J. M., ENGLAND, W. A. & LARTER, S. (eds) 2004. Understanding Petroleum Reservoirs." Towards an Integrated Reservoir Engineering and Geochemical Approach. Geological Society, London, Special Publications, 237. 27-35.

Worden R.H & Smalley P.C. 1996. H_2S producing reactions in deep carbonate gas reservoirs: Khuff Formation Abu Dhabi. Chemical Geology. 133. 157-177.

Xiong Y, Geng A, Pan C, Liu D, & Peng P. 2005. Characterisation of the hydrogen isotopic composition of individual n-alkanes in terrestrial source rocks. Applied geochemistry. 20. 455-464.

Yang, C., Wang, Z.D., Hollebone, B.P., Peng, X., Fingas, M. & Landriault, M. 2006. GC/MS quantitation of diamondoid compounds in crude oils and petroleum products. Environmental Forensics. 7. 377–390.

Zhang, C., Zhao, H., Mei, B., Chen, M., Xiao, Q., & Wu, T., 1999. Effect of biodegradation on carbazole compounds in crude oils. Oil and Gas Geology. 20. 341–343.

Zhang S, Huang H 2005. Geochemistry of Palaeozoic marine petroleum from the Tarim Basin, NW China. Part 1. Oil family classification. Organic Geochemistry. 36. 1204–1214.

Zhang, C., Huang, H.P., Xiao, Z.Y., & Liang, D.G., 2005. Geochemistry of Palaeozoic marine petroleum from the Tarim Basin, NW China: Part 2. Maturity assessment. Organic Geochemistry 36, 1215–1225.

Zhang, L., Li, M.,Wang, Y., Yin, Z., Zhang,W., 2013. A novel molecular index for secondary oil migration distance. Nature. 3. 1-8.

Zhao X, Jin Q, Jin F, Ma P, Wang Q, Wang J, Ren C, & Xi Q. 2013. Origin and accumulation of high-maturity oil and gas in deep parts of the Baxian Depression, Bohai Bay Basin, China. Petroleum Science. 10. 303-313.

Zumberge J.E & Ramos S. 1996. Classifications of crude oil based on genetic origin using multivariate modelling techniques. Australian Geological Convention. 13. Canberra. Australia.

Zumberge J.E 1987. Prediction of source rocks characteristics based on terpane biomarkers in crude oil: a multivariate statistical approach. Geochimica et Cosmochimica Acta. 51. 1625-1637.